TEXAS ★ STATE UNIVERSITY ®

The rising STAR of Texas

TxDOT Report 0-7017-1

Investigating the Use of Rapid Setting Hydraulic Cements (RSHCs) for Structural Applications

Texas State University, Department of Engineering Technology; San Marcos, Texas
Dr. Federico Aguayo
Dr. Anthony Torres (PI)
Dr. Ikechukwu K. Okechi
Laura Velandia
Deep Kotadiya
Debo Brata Paul Argha
Dr. Tijani Mohammed

Technical Report Documentation Page

1. Report No. FHWA/TX-24/0-7017-1	2. Government Accession No.	3. Recipient's Catalog No.
4. Title and Subtitle Investigating the Use of Rapid Setting Hydraulic Cements (RSHCs) for Structural Applications		5. Report Date Submitted: May 2024
		6. Performing Organization Code
7. Author(s) Federico Aguayo, https://orcid.org/0000-0001-8153-3121 Anthony Torres, https://orcid.org/0000-0001-5060-3203 Ikechukwu K. Okechi, Laura Velandia, Deep Kotadiya, Debo Brata Paul Argha, Tijani Mohammed		8. Performing Organization Report No. 0-7017
9. Performing Organization Name and Address Texas State University San Marcos, TX 78666		10. Work Unit No. (TRAIS)
		11. Contract or Grant No. 0-7017
12. Sponsoring Agency Name and Address Texas Department of Transportation Research and Technology Implementation Division 125 E. 11th Street Austin, TX 78701		13. Type of Report and Period Covered Technical Report September 2020 – December 2023
		14. Sponsoring Agency Code
15. Supplementary Notes Project performed in cooperation with the Texas Department of Transportation and the Federal Highway Administration.		

16. Abstract

Construction and replacement of infrastructure assets results in costly road closures. Rapid setting hydraulic cements (RSHCs), like calcium sulfoaluminate (CSA) cement and calcium aluminate cement (CAC), can dramatically reduce the time needed for construction. These cements are beginning to gain the attention of various stakeholders in the cement and concrete industry owing to their remarkable properties and notably lower carbon footprint compared to ordinary portland cement (OPC) and other traditional infrastructure materials. Currently, the use of CSA and CAC cement is often limited to rapid repair applications and other special applications where their exclusive qualities are required. The primary goal of the work outlined in this report is to demonstrate the use of RSHCs for use in structural applications. This study showed that RSHC concrete can be designed to meet structural class specifications in terms of fresh (i.e., workability and working time) and hardened properties (early- and/or later-age strength). All RHSCs mixtures, when evaluated under accelerated carbonation, showed significantly lower carbonation resistance when compared to OPC at an equivalent w/c ratio and curing age. When the RHSCs mixtures were evaluated for natural concrete carbonation outdoors in Texas, the performance of RSHCs was dependent on exposure type. Samples placed outdoors and exposed to precipitation had a markedly higher resistance to carbonation compared to samples placed in sheltered conditions. Regarding corrosion potential, all RSHC mixtures, with the exception of a few CSA cement types corrosion potential appears to be comparable to OPC after 3 years of exposure. Bulk-chloride diffusion test showed that these cements had much lower chloride binding capacity compared to CAC and OPC systems. Despite these results more information is still needed to fully understand the performance of RSHC in various durability-related distresses. In particular, more work is needed to understand their potential implication in chloride- and carbonation-induced corrosion. While many RSHCs showed potential in being capable of meeting durability performance, time is still needed to discern their behavior in these conditions, especially under long-term service conditions (i.e., cracked and carbonated RSHC concrete). Nonetheless, opportunities may arise for some RSHCs to be used in targeted structural applications that can achieve durability requirements.

17. Key Words Concrete, Cement, Durability, Structures, Sustainability	18. Distribution Statement No restrictions. This document is available to the public through the National Technical Information Service, Alexandria, Virginia 22312; www.ntis.gov.		
19. Security Classif. (of report) Unclassified	20. Security Classif. (of this page) Unclassified	21. No. of pages TBD [Total count excl. cover]	22. Price

Form DOT F 1700.7 (8-72) Reproduction of completed page authorized

Investigating the Use of Rapid Setting Hydraulic Cements (RSHCs) for Structural Applications

By
Dr. Federico Aguayo
Texas State University

Dr. Anthony Torres
Texas State University

Dr. Ikechukwu K. Okechi
Texas State University

Laura Velandia
Texas State University

Deep Kotadiya
Texas State University

Debo Brata Paul Argha
Texas State University

and

Dr. Tijani Mohammed
Texas State University

Report 0-7017-1
Project 0-7017
Project Title: Use of Rapid Setting Hydraulic Cements (RSHCs) for Structural Applications

Disclaimers

Author's Disclaimer: The contents of this report reflect the views of the authors, who are responsible for the facts and the accuracy of the data presented herein. The contents do not necessarily reflect the official view or policies of the Federal Highway Administration or the Texas Department of Transportation (TxDOT). This report does not constitute a standard, specification, or regulation.

Patent Disclaimer: There was no invention or discovery conceived or first actually reduced to practice in the course of or under this contract, including any art, method, process, machine manufacture, design or composition of matter, or any new useful improvement thereof, or any variety of plant, which is or may be patentable under the patent laws of the United States of America or any foreign country.

Engineering Disclaimer

NOT INTENDED FOR CONSTRUCTION, BIDDING, OR PERMIT PURPOSES.

Research Supervisor: Anthony Torres

Acknowledgments

TABLE OF CONTENTS

LIST OF FIGURES

LIST OF TABLES

LIST OF ACRONYMS

ACI   American Concrete Institute

AFt   Ettringite

AFm   Monosulfate

ASR   Alkali-Silica Reactivity

C/S   Cement to Sand Ratio

CAC   Calcium Aluminate Cement

CH   Calcium Hydroxide

CSA   Calcium Sulfoaluminate Cement

DEF   Delayed Ettringite Formation

HRWR   High-Range Water-Reducing

OPC   Ordinary Portland Cement

RCPT   Rapid Chloride Permeability Test

RSHC   Rapid Setting Hydraulic Cement

TxDOT   Texas Department of Transportation

W/C   Water-to-Cement Ratio

XRD   X-Ray Diffraction

XRF   X-Ray Fluorescence

CHAPTER 1: INTRODUCTION AND SCOPE

1.1 INTRODUCTION

Construction of most infrastructure assets is a lengthy process, with time to completion typically stated in years. Factors which influence this time includes, among others, mobilization of the contractor, site preparation, construction method, lead time for ordering parts, materials, and supplies, sub-contractor availability, sequence of tasks, and weather. Rapid construction considers each factor individually to determine how it's time to complete can be shortened and how that will influence other factors and ultimately the entire construction schedule. For cast-in-place concrete construction, placement of reinforcement, placement of formwork, and strength development of the concrete all take time. Shortening the time to develop strength in concrete is commonly addressed by using high-early portland cement with a relatively high quantity of binder and dosage of set-accelerator admixtures. On the other hand, fabrication, delivery, and assembly of precast structural elements can also serve as an alternative to speeding up the construction operation. Regardless of option, ordinary portland cement (OPC) is normally the choice of binder for producing these concretes. However, alternative cementitious materials (ACMs) like calcium sulfoaluminate (CSA) cement and calcium aluminate cement (CAC) are beginning to gain the attention of stakeholders in the cement and concrete industry owing to their remarkable properties and often noted lower carbon footprint with respect to OPC and other traditional infrastructure materials.

Currently, the use of CSA and CAC cement is limited to rapid repair applications and other special applications where their exclusive qualities are required. Although there are hardly any records of their use in new structural applications, recent advances in these cements have shown great potential to be successfully used in producing structural-grade concrete. A good illustration will be the possibility of harnessing their rapid strength gain abilities in reducing the duration of in-situ concrete activities during construction, thereby reducing construction project delivery time. However, the lack of long-term durability performance data of their use in concrete in various environmental conditions has deterred their adoption for use in new structural applications compared to OPC. This indicates the need to evaluate their short and long-term durability performance as it relates to key durability issues associated with reinforced concrete.

This report summarizes the findings from TxDOT Project 0-7017, *Use of Rapid Setting Hydraulic Cements (RSHCs) in Structural Applications.* This project, funded by the Texas Department of Transportation (TxDOT), was aimed at evaluating and determining whether rapid setting cements, such as CSA, CAC, and blended systems of OPC with CSA and/or CAC can be effectively, efficiently, and safely

utilized as structural building materials for highway and transportation infrastructure. To partly fill this gap and begin to encourage the use of RSHCs in structural applications, this research provides profound insights into the fresh, hardened, as well as short- and long-term durability performance as it applies to reinforced concrete structures. This report summarizes the overall results from this comprehensive research project, which includes experimental work on a variety of RSHCs formulations exposed under lab and field conditions within Texas. The generated data serves as a guide for the safe and effective use of these cements systems, especially in structural applications.

1.2 SCOPE OF PROJECT

There are a variety of rapid setting cement systems available with a range of different formulations. This research, however, was limited to ettringite-based cement systems (e.g., CSA and CAC) either as the primary binder (i.e., pure cement), or a blend with portland cement and/or other mineral additives. As such, characterizing the short- and long-term performance of CSA and CAC based cement systems forms the basis of the project. The scope of the project is outlined below:

- To optimize RSHC concrete mixture proportions for structural class concrete as described in TxDOT ITEM 421 specifications.
- To focus on key material and durability properties that are relevant for the design of structural class concrete as described in TxDOT ITEM 421 specifications.
- To determine the effectiveness and robustness of current laboratory test methods to predict field performance of RSHCs, especially since these may not be suitable for RSHC systems.
- To link lab results with corresponding field specimens and testing.

1.3 REPORT OUTLINE

This report is based on the Master of Science theses of Velandia, L., Kotadiya, D., Argha, D., and Doctor of Philosophy dissertation of Okechi. I.K all of which are under Texas State University embargo hold until the publication of this document. The project findings are organized into the following chapters.

- **Chapter 1** presents an introduction and outline of this report.

- **Chapter 2** presents a history and background of RSHCs and their blended systems.

- **Chapter 3** presents the materials used in the laboratory and field-testing programs.

- **Chapter 4** presents a preliminary experimental investigation of RSHC mortars and concretes.

- **Chapter 5** presents the experimental investigation of the early- and later-age mechanical properties of concrete produced with RSHCs and blended systems.

- **Chapter 6** presents accelerated carbonation testing of RSHCs and blended systems focusing on the effect of curing and permeability.

- **Chapter 7** presents accelerated carbonation testing of RSHCs and blended systems focusing on the effect of relative humidity and CO_2 concentration.

- **Chapter 8** presents the results of natural carbonation of concrete produced with RSHCs and blended systems and exposed in central Texas.

- **Chapter 9** presents the results of chloride-ion induced corrosion of concrete produced with RSHCs and blended systems.

- **Chapter 10** presents the results of marine exposure conditions on concrete produced with RSHCs and blended systems.

- **Chapter 11** presents the alkali-silica reactivity and delayed ettringite formation results of concrete produced with RSHCs and blended systems RSCHs.

- **Chapter 12** presents the value of research (VoR) for the project.

- **Chapter 13** presents final project conclusions and future work.

CHAPTER 2: BACKGROUND ON RSHCS AND BLENDED SYSTEMS

2.1 INTRODUCTION

ASTM C1600 "Standard Specification for Rapid Hardening Hydraulic Cement" [1] is the primary standard for RSHCs, which specifies the compressive strength requirement of cements including ultra-rapid hardening (URH), very rapid hardening (VRH), medium rapid hardening (MRH) and general rapid hardening (GRH) cements. Details regarding the strength criteria with limits on setting time and drying shrinkage used in ASTM C1600 are shown in the Table 2.1. An industry standard often applied to rapid set concrete is to attain a compressive strength of 20.5MPa (3,000 psi) in three hours, but it is not specifically stated in ASTM C1600. Based on the compressive strength, drying shrinkage, and setting time data, ASTM C1600 will classify these RSHCs differently.

Table 2.1: ASTM C1600 cement specification [1]

TABLE 1 Standard Physical Requirements
(must be reported on manufacturer's certification)

	Cement Type				
	URH	VRH	MRH	GRH	RH-CAC
Minimum Compressive Strength (see Section 9 for procedures), min, MPa [psi]					
1½ h	21 [3000]	12 [1700]	...	...	6 [800]
3 h	28 [4100]	15 [2200]	10 [1500]	7 [1000]	20 [2900]
6 h	...	...	14 [2000]	10 [1500]	28 [4100]
1 day	35 [5100]	24 [3500]	17 [2500]	14 [2000]	34 [4900]
7 days	41 [6000]	28 [4100]	28 [4100]	24 [3500]	...
28 days	57 [8300]	35 [5100]	31 [4500]	28 [4100]	...
Converted	n/a^B	n/a^B	n/a^B	n/a^B	34 [4900]
Maximum Drying Shrinkage, %					
7 days	0.06	0.06	0.08	0.10	0.10
28 days, air storage	0.07	0.07	0.09	0.12	0.12
Minimum Time of Final Set C191 Apparatus					
Minutes^A	10	10	10	10	10
Maximum Autoclave, expansion %	0.8	0.8	0.8	0.8	0.8

^{A} The initial setting time typically ranges from 10 to 45 min for rapid hardening cements of various types and composition.
^{B} Requirement is not applicable to this cement type.

While ASTM C1600 is often specified for rapid hardening cements, it does have some limitations: These guidelines are mainly for rapid repair purpose but not for large structural scale usage whose requirements can be different. The specific limitations include the following:

a) **High water to cement ratio (W/C):** According to the ASTM C1600 specification, the amount of mixing water for compressive strength specimens should be such that it can produce a flow of 110 ± 5 as specified in ASTM C109 "Standard Test Method for Compressive Strength of Hydraulic Cement Mortars (Using 2-in. or [50-mm] Cube Specimens)" [2]. Generally, rapid setting and hardening cements require a high amount of water to produce the required flow. Consequently, the high-water dosage can lead to significant dilution effects and slower strength developments than what would be normally anticipated in a concrete mixture. For instance, some Calcium sulfoaluminate cements may requires a high W/C ratio (1:1), which results in significantly lower compressive strengths.

b) **Workability/Flowability:** The water content required to achieve standard flow varies widely among different RSHCs, making it difficult to compare mixture performance directly. Additionally, the workability/flow is often short-lived making it difficult to cast the number of specimens required for testing.

c) **Varying cement to sand ratio (C/S):** For the drying shrinkage test, ASTM C1600 specifies testing to follow ASTM C596 "Standard Test Method for Drying Shrinkage of Mortar Containing Hydraulic Cement"[3], where the required c/s ratio is 1:2. However, for the compressive strength test, ASTM C1600 refers to ASTM C109 where the c/s ratio requirement is 1:2.75.

2.2 CALCIUM ALUMINATE CEMENT (CAC)

2.2.1 Background and History

In the mid-1800s, it was realized that alumina-rich cements had inherently excellent cementing properties. However, the development of modern CACs is largely credited to Jules Bied through his work at the J. & A. Pavin de Lafarge Company in Le Teil, France, and the first patent for the manufacturing process of CAC was created in 1908 [4]. This cement showed excellent performance in sulfate resistance; it also hardened much more rapidly compared to OPC. The material was made available to the general public under the name of 'Ciment Fondu Lafarge' (CFL) [5, 6]

A vast market for using CAC in prestressed concrete was established in the 1950s and 1960s in the UK. However, the conversion process of CAC that causes strength reduction was discovered in the 1970s because of three structural collapses and since then, CAC has been prevented in structural applications and was only used in other niche applications such as repair of concrete structures.

CAC is produced by heating suitable proportions of fusing limestone and bauxite together. CAC is more expensive than OPC since Bauxite, which is rich in aluminum oxides, is costly. CACs are graded in terms

of their alumina content, which can range from 35 to 80%, but the standard grade of CAC contains approximately 36 to 42% Al_2O_3 [6]. CFL was known for its rapid hardening characteristics and its ability to be placed in harsh sulfate environments [7]

2.2.2 Hydration of CAC

The hydration of CAC systems is significantly different from ordinary portland cement (OPC) because it is mainly dependent on the temperature history during hydration [6]. The CAC systems lose strength over time due to "conversion". During the hydration of CAC at ambient temperatures, metastable hydrates (CAH_{10}) and (C_2AH_8) are formed but these metastable hydrates will convert to thermodynamically more stable C_3AH_6 and AH_3 hydrates, either over time or an increase in hydration temperature. Scrivener [6] summarized the hydration process shown in the Equations 2.1 to 2.4 below:

$$CA + 10H \rightarrow CAH_{10} \qquad\qquad 2.1$$

$$2CA + 11H \rightarrow C_2AH_8 + AH_3 \qquad\qquad 2.2$$

$$2CAH_{10} \rightarrow C_2AH_8 + AH_3 + 9H^* \qquad\qquad 2.3$$

$$3C_2AH_8 \rightarrow 2C_3AH_6 + AH_3 + 9H^* \qquad\qquad 2.4$$

*   Conversion reactions

This conversion process leads to an increase in porosity which can cause significant strength loss for CAC concrete [6]. Since the metastable hydrates convert to stable hydrates, some water may be released during the conversion process. This water can be recombined to form additional hydration products, resulting in a slight strength regain. However, the strength is almost never full regained and often specification require that the design strength be based on the converted strength (i.e., lower strength at conversion). The CAC conversion and strength development over time is illustrated in Figure 2.1.
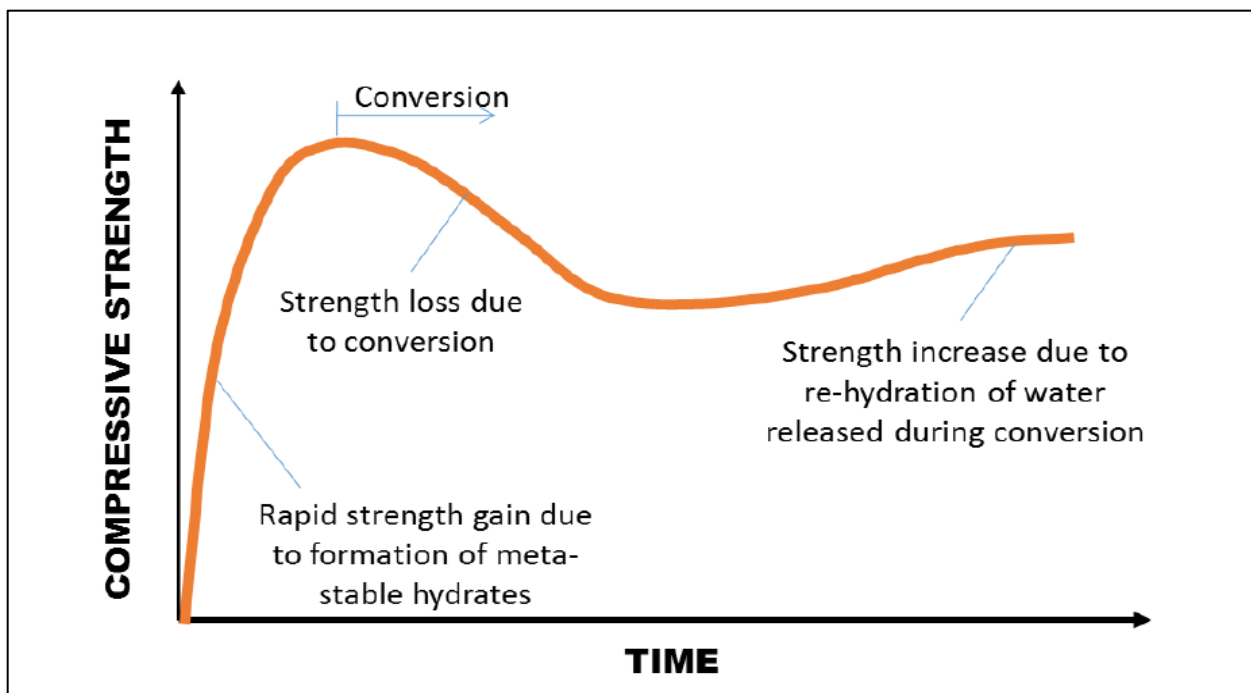
Figure 2.1: Strength development curve of CAC conversion [6]

Conversion has the largest impact on CAC concrete when produced with W/C ratios greater than 0.5. From the study by [6], it is revealed that W/C below 0.4 significantly decreased the volume loss because water takes up less space.

Conversion can be detrimental if it is not taken seriously, but it can be avoided with the addition of OPC, calcium sulfate (C$\bar{\text{S}}$), and supplementary cementitious materials (SCMs) [8].

2.2.3 Applications of CAC Concrete

CAC concrete has several unique characteristics that make it suitable for certain specialty applications. These characteristics include:

- Rapid hardening characteristics and similar setting time when compared to OPCs [9].
- Resistance to abrasion and impact when mixed with appropriate aggregates.
- Having an ability to withstand low temperatures during the time of placing and usage.
- Having an ability to endure repeated heating to high temperatures and refractory concretes [10].
- In a blended system with OPC, calcium sulfate, or both, CAC can form ettringite which is advantageous for controllable setting, hardening and shrinkage compensation.

CAC concretes exhibit an increased abrasion resistance which makes them very durable in highly abrasive environments including the spillway of dams, sections of roadway subjected to heavy wear, and industrial floors [4]. Since CACs are expensive, typically they are not used in applications where OPC concretes could satisfy the need. At an equivalent W/C, OPC concrete strength is typically higher than that of CAC after conversion [11]. Instead, they are more often used in specialized applications where the benefits of CACs listed above can be utilized.

2.3 CALCIUM SULFOALUMINATE CEMENTS (CSA)

2.3.1 Background and History

CSAs are manufactured primarily from calcium sulfate, limestone, and bauxite. Ye'elimite ($C_3A_3\bar{S}$) is the main constituent of CSA cements, normally accounting for 30-70%. In the 1960s, Ye'elimite was introduced as a cementitious phase and Alexander Klein from the University of California, Berkeley [10] patented Ye'elimite. It has an expansive or shrinkage compensating ability in addition to serving as a cementitious cement. This active compound in CSA cement is also known as "Klein's compound" [12, 13]

The firing temperature required to produce CSA clinker is 1250°C, which is 200°C lower than that used for portland cement clinker. This clinker is easier to grind [14] compared to portland cement clinker. As a result, CSA cements can be considered as a low-CO_2 alternative to OPC. [15]

In addition to ye'elimite, CSA cements are also composed of belite (C_2S) and anhydrite or gypsum. Normally, 15-25% of gypsum is interground with the clinker, which is used to achieve an optimum setting time, strength development and volume stability. The amount and reactivity of the added calcium sulfate is a key factor of the hydration of CSA.

CSA cements can harden very rapidly (often within 10-20 minutes) but the set time can be controlled using a set retarder, typically citric acid. CSA and CSAB (calcium sulfoaluminate-belite) both contain ye'elimite, but pure CSA systems often contain a higher ye'elimite type. CSAB contains a greater quantity of belite (C_2S), which enables the hydrated paste to continue to gain strength in the later age after the initial hydration. CSA and CSAB cements are often used in self-leveling screeds, as well as in repairs due to the fast hardening and expansive ability of certain formulations of the material. Controlling dimensional stability is a significant concern associated with the use of CSA and CSAB cements. The variance in ye'elimite, gypsum content, and curing conditions can result in expansive behavior [16]. Moffat [17] completed a study where two CSAs were evaluated. Namely, a higher ye'elimite type and a

belite type. Type K is another type of cement that is rich in aluminum and may contain anhydrite or gypsum and, in some cases, free lime.

2.3.2 Hydration of CSA

The hydration of tetracalcium trialuminate sulfate ($C4A3\overline{S}$) is primarily dependent on the presence of calcium sulfate and/or calcium hydroxide. The pure material ($C4A3\overline{S}$) and water hydrate to form monosulfate ($C4A\overline{S}H12$), and aluminium hydroxide (AH3) as shown in Equation 2.5 ([18-22].

$$C4A3\overline{S} + 18H \rightarrow C4A\overline{S}H12 + AH3 \text{ (monosulfate formation)} \qquad 2.5$$

The addition of calcium hydroxide (CH) and gypsum ($C\overline{S}H2$) results in the formation of ettringite ($C6A\overline{S}H32$) and monosulfate, if the molar ratio is at least 1:2. This is the most common reaction, which dominates the early stages of hydration. The reaction is shown in Equation 2.6:

$$2C4A3\overline{S} + 2C\overline{S}H2 + 52H \rightarrow C6A\overline{S}H32 + C4A\overline{S}H12 + 4AH3 \qquad 2.6$$

(ettringite and monosulfate formation)

If the level of calcium sulfate is too low for a complete conversion of aluminium oxide required for the continued hydration of ettringite, ettringite will convert to monosulfate ($C4A\overline{S}H12$), which is shown in the equation below:

$$C6A\overline{S}H32 + AH3 \rightarrow C4A\overline{S}H12 + 2H \text{ (monosulfate formation)} \qquad 2.7$$
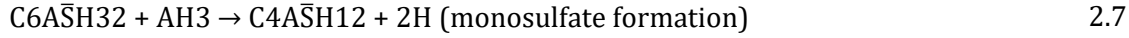
Generally, several hydraulic phases are found in CSA cements. Compared to other phases like C2S, C4AF or CA, C4A3S is more reactive. CSA cements react faster in comparison to OPC, and within 2 to 24 hrs. the majority of the hydration heat evolution occurs.

2.3.3 Application of CSA

CSA cements can be a replacement of OPC in the construction industry in certain cases. For airport concrete runaways rehabilitation, CSA cements have gained attraction since they have a very short setting time (20 minute) and excellent durability characteristics. Another advantage of CSA is that due to the rapid setting characteristics, CSA is also advantageous in airports or high traffic highways where

construction interruptions affect the normal functionality process and result in significant cost. In addition, for tunneling and underground construction projects, CSA is advantageous. CSA cements are also used in prestressed concrete because they can minimize prestressing loss associated with shrinkage when OPC is utilized. CSA concrete are very resistant to freeze-thaw attack and other chemical attacks like sulfate attack; it also showed improved dimensional stability [13].

In China, CSA cements are used as a cement for concrete bridges, leakage and seepage prevention, precast concrete, and low temperature construction. Moreover, due to their low pH, low porosity, and the ability of ettringite formation, the blending system of CSA and OPC are receiving increasing attention in hazardous waste encapsulation [23-26]. In the UK, there is a long history of using CSA type cements mainly in the mining industry [27].

2.4 BLENDED CAC AND CSA SYSTEMS

2.4.1 CAC Based Blended System

This section discusses the CAC based blended cements. In this system, within the first few hours of hydration, high early strength is achieved because of the rapid formation of ettringite. In OPC systems, ettringite is only a minor constituent but the mineral is abundant in blended systems composed of CAC, CSO4 and OPC. High early strength is possible in plain CAC with the addition of accelerator but due to the conversion phenomenon a later age strength loss is common. A blended system (OPC-CAC) also results in high early strength. However, little later age strength gain is often observed due to the "blocking ettringite" formed around unhydrated C3S that prevents further hydration. The addition of calcium sulfate ($C\bar{S}$) to form a ternary system results in high early strength by the formation of ettringite within the first few hours of hydration and significant later age strength gain due to the OPC hydration [17].

2.4.2 Binary Blended System of CAC + OPC

CAC cannot generate ettringite like CSA cement does during its hydration process. Hence CAC is usually mixed with calcium sulfate ($C\bar{S}$) or OPC as a binary cementitious system. In the OPC/CAC blending system, the formation of ettringite will hinder the hydration of OPC, resulting in lower strength development. According to [28], this delay is produced by the ettringite layer which covers the surface of unhydrated OPC grains. This barrier layer slows down the hydration as water and ions need to diffuse to reach to the grains [29].

Ettringite is the hydration product of OPC, produced primarily as an interaction between C3A and gypsum reaction. In a binary blending system of OPC/CAC, ettringite can be formed within a very short period of hydration through the following reactions (Equation 2.8 and 2.9):

$$CA + 3C\bar{S}H2 + 2C + 26H \rightarrow C6A\bar{S}H32 \qquad\qquad 2.8$$

$$C3A + 3C\bar{S}H2 + 26H \rightarrow C6A\bar{S}H32 \qquad\qquad 2.9$$

The early strength gain of this binary blending system is attributed to these two reactions [30]. The OPC is the primary source of sulfate and CAC provides the aluminates. The availability of sulfate and aluminates governs the formation of ettringite.

A study was completed by Gu et al. [28] on three pastes with different OPC/CAC ratios. They investigated the ettringite formation, early strength development, and delayed hydration of OPC of the binary blend system. They found that in blended systems containing 92.5%/7.5% (OPC/CAC) paste, a small amount of ettringite formation is evident from both SEM and XRD tests. However, the strength development from the contribution of minor amounts of ettringite was low. In the 80%/20% (OPC/CAC) blend, a large amount of needle-like ettringite crystal is evident in both SEM and XRD results. In the 20%/80% (OPC/CAC) blend, XRD and SEM failed to identify any ettringite crystals. Since there was not enough sulfate available in the system, the hydration and strength development were similar to the pure CAC paste. The study concluded that the 80%/20% blend has the highest early strength among the three pastes and ettringite formation contributes to the early strength.

2.4.3 Binary Blended System of CAC/Anhydrite (C$\bar{S}$)

CAC can be used in combination with different calcium sulfate sources. Monocalcium aluminate from CAC and sulfate from anhydrite react to form ettringite (Equation 2.10) which plays the key role in the rapid strength development and expansive behavior [31].

$$3CA + 3C\bar{S} + 38H \rightarrow C6A\bar{S}3H32 + 2AH3 \qquad\qquad 2.10$$

[32] investigated the influence of the CAC/anhydrite ratio and the W/C ratio on the hydration kinetics. He observed that a reduction in the extent of hydration happened at the lower W/C ratio because of insufficient water for completing the hydration and/or the filling of space by hydrates. Other findings from this study are that when the binary system of CAC/anhydrite has a weight ratio of 1, ettringite and

AH3 are the main hydration products. When a ratio of 2.3 (CAC/anhydrite) was used, in the early age, ettringite, AH3 and monosulfate were present, and at the later age stratlingite was also present in the system.

2.4.4 Ternary Blended System (OPC+CAC+CSA)

The ternary blend composition can be two types, as shown in Figure 2.2. The systems in zone 1 are rich in OPC (typically more than 70 percent) and are used in rapid repair applications as well as shrinkage compensation due to the relatively low amount of calcium sulfate. The systems in zone 2, where CAC and $C\bar{S}$ from CSA are the main constituents, have very fast hardening kinetics, self-drying capacity, and size variation characteristics. They are used in applications such as self-levelling screeds, tile adhesives and rapid repair mortars [33]. The composition of the ternary blending system in this study falls in Zone 1 shown in Figure 2.2.
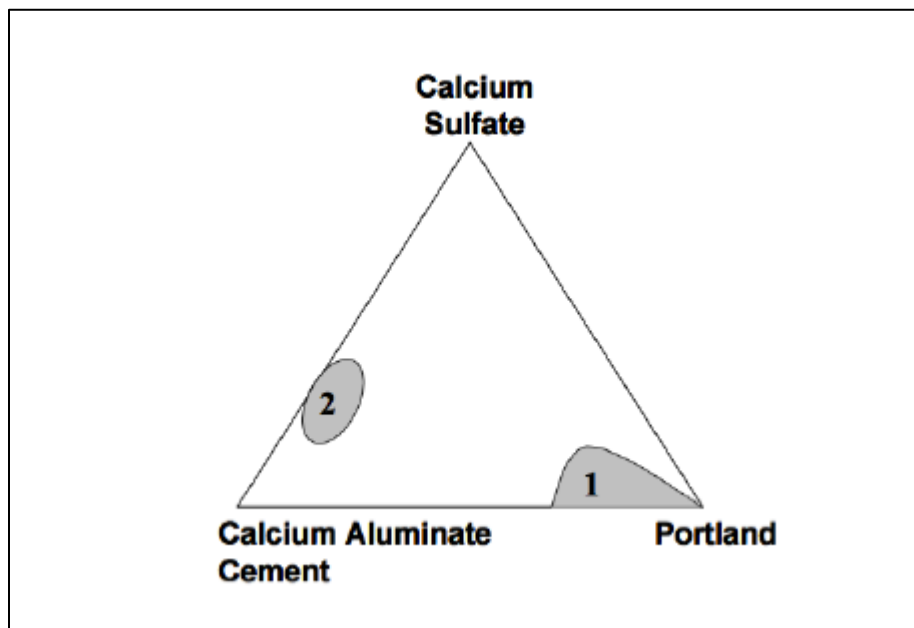
Figure 2.2: Ternary diagram depicting composition of CAC:OPC:C$\bar{S}$ blends [33]

For the hydration of CAC ternary-based systems, the formation of metastable hydrates is prevented because of the addition of $C\bar{S}$ from CSA and rapid formation of ettringite. This phenomenon eliminates the downside of strength loss in pure CAC systems due to conversion. The reaction of monocalcium aluminate and calcium sulfate leads the hydration of this system as presented in Equations 2.11 and 2.12 [10, 33]. It results in the formation of ettringite, and amorphous aluminum hydroxide.

$$3CA + 3C\bar{S}Hx + (38 - 3x)\ H \rightarrow C3A.3C\bar{S}.H32 + 2AH3 \qquad\qquad 2.11$$

$$3CA + 9C\bar{S}Hx + 6CH + (90-9x)\ H \rightarrow 3C3A \cdot 3C\bar{S} \cdot H32 \qquad\qquad 2.12$$
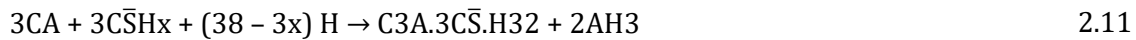
Where $x = 0$ for anhydrite, $x = 0.5$ for hemihydrate and $x=2$ for gypsum.

The addition of calcium hydroxide results in ettringite as the only hydration product [34]. Ettringite forms in the bulk of the paste and is not at the surface of the C3A grain. This is a key factor for the early strength of the systems.

The incorporation of $C\bar{S}$ in CSA decreases the set time of these materials. According to [35], if the amount of calcium sulfate is lower than the required amount for all CA to react, after the depletion of calcium sulfate, calcium monosulfate will start to form as a result of the interaction between ettringite and unreacted tricalcium aluminate (C3A). This is shown in Equation 2.13:

$$3C3A \cdot 3C\bar{S}.H32 + 2C3A + 4H \rightarrow 3C3A \cdot C\bar{S} \cdot H12 \qquad\qquad 2.13$$

Another recent study by [36] investigated the strength development of ternary blends containing CSA, CAC and OPC. They concluded that the incorporation of CAC-OPC into CSA accelerates the setting time of ternary blends and the strength continues to increase with time. Another finding from their study is that the amount of ettringite in ternary blends at 2 hr. is higher than that of CSA, resulting in the high early strength.

In literature [37], the hydration of OPC was studied thoroughly in the formation of C-S-H, CH and other minor constituents such ettringite (AFt) and monosulfate (AFm) as presented below:

$$C3S + (y + 1.3)\ H \rightarrow C1.7SHy + 1.3H \qquad\qquad 2.14$$

$$C2S + (y + 0.3)\ H \rightarrow C11.7SHy + 0.3H \qquad\qquad 2.15$$

$$C3A + 3C\bar{S}Hx + (32-3x)\ H \rightarrow C3A \cdot 3C\bar{S} \cdot H32 \qquad\qquad 2.16$$

$$3C4AF + 12C\overline{S}Hx + (134-12x)\ H \rightarrow 4C3(A,F)\cdot 3C\overline{S}\cdot H32 + 2(A,F)H3 \qquad 2.17$$
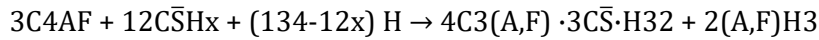
A comparison of strength gain curves of the CAC systems and OPC concrete is depicted in Figure 2.3.
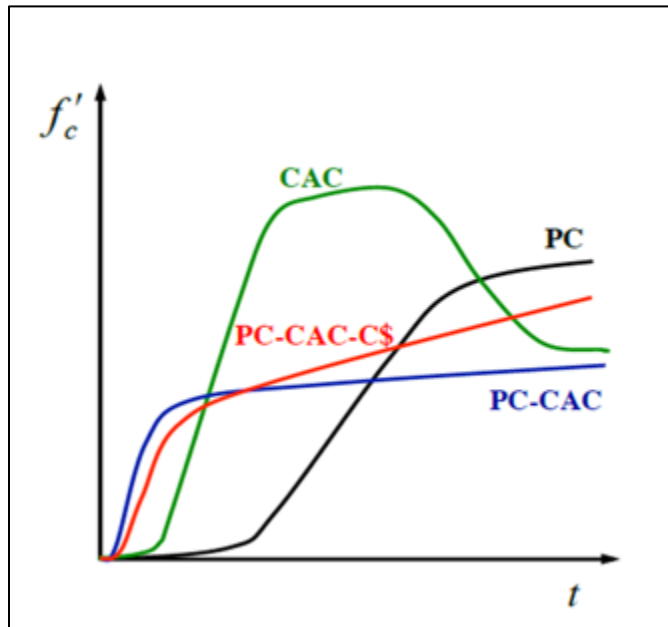
Figure 2.3: Strength development of a ternary based system (Scrivener, 2014)

2.4.5 Ternary Blended System (OPC+CAC+C$\overline{S}$)

The influence of calcium sulfate on the hydration of OPC-CAC mixtures has been investigated by different authors. It is well known that CAC is added into OPC to accelerate the setting time [38]. However, the replacement of OPC with CAC has a downside of decreasing later age compressive strength due to: [39]

$$3CA + 12H \rightarrow C3AH6 + 2AH3 \qquad 2.18$$
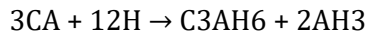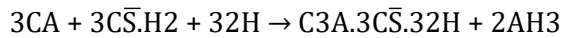
$$3CA + 3C\overline{S}.H2 + 32H \rightarrow C3A.3C\overline{S}.32H + 2AH3 \qquad 2.19$$

To improve the later age strength, the use of chemical additives is common, especially calcium sulfate (in the forms of anhydrite C$\overline{S}$, gypsum C$\overline{S}$.H2 or hemihydrate C$\overline{S}$H1/2) [40]. With the presence of calcium sulfate, the hydration of CAC changes from Equation 2.18 to Equation 2.19, leading to the rapid formation of ettringite and amorphous AH3 [41]. The hydration of this ternary system is complex because

every material has its own reaction. Ettringite is the main phase of this ternary system. It is the key factor of controlling the setting rate of highly reactive aluminate phases such as tricalcium aluminate (C3A) in OPC and monocalcium aluminate (CA) in CAC, which react with calcium sulfate. This way the later strength is enhanced [42, 43]. The influence of calcium sulfate on the hydration process in OPC/CAC blending system has been studied by [44]. The authors found that the OPC/CAC blend without any incorporation of calcium sulfate exhibits extremely slow hydration kinetics during the first two days, which is consistent with the findings from [28, 45]. This long dormant period may be defined as a surface coverage of the clinker grains by early hydration that impedes further OPC hydration. By adding calcium sulfate, the hydration can be accelerated, although the setting time is prolonged. Another important finding from this study is that the incorporation of calcium sulfate improves the compressive strength at all curing ages.

2.4.6 CSA Based Ternary Blended System (OPC+CSA+C$\overline{S}$)

The CSA/OPC and incorporation of anhydrite (C$\overline{S}$) to form ternary blended systems have been studied recently to understand the physico-chemical properties of CSA/OPC cements for use in concrete structures. C3S, C2S, C3A and C4AF are the four main phases of OPC clinker and C$\overline{S}$ is added to the system to control setting time. Early hydration is mainly dominated by C3S and C3A while C2S hydrates slower and helps develop the later age properties [46]. The hydration scheme can be subdivided into early hydration, where ettringite and AH3 are the main hydrates, and C4AHX, C2ASH8, C-S-H, monosulphate hydrates form at later stages. From the study of [47], the AFt-formation (Equation 2.20) occurs during the first hydration phase. In the second hydration stage, the OPC clinker starts to react and C3S can be consumed by Equation (2.21 & 2.22), resulting in producing stratlingite or C-S-H in association with portlandite (CH).

$$C4A3\overline{S} + 2C\overline{S} + 38H \rightarrow C3A.3C\overline{S}.H32 + 2AH3 \hspace{3cm} 2.20$$

$$C3S + AH3 + 6H \rightarrow C2ASH8 + CH \hspace{3.5cm} 2.21$$

$$C3S + 3.7\ H \rightarrow CSH1.7 + 2CH \hspace{4cm} 2.22$$

From this study, the early hydration reaction generates high early strength up to ~8 MPa measured at 6 hours up to 7 day. The CSA clinker mainly reacts and the C4A3$\overline{S}$ concentration decreases and reaches a

very low value by 28-day. After 7 days, C3S from the OPC begins to hydrate and generates C2ASH8 and C-S-H. On the other side, AFt reacts with other phases to generate monosulphoaluminate. At day 28, the hydrates present in the mix are AFt, C4AHX, monosulphoaluminate, hemicarbonate, monocarbonate and stratlingite. The authors concluded that the CSA clinker was mainly responsible for the early mechanical properties and the later age strength gain was due to OPC.

Another study by [48], investigated the replacement of OPC with CSA by 10%. The results showed a predominant hydration of C4A3$\overline{S}$ at the early age, which reduced the initial setting time, but it also led to the delayed hydration of C3S. The authors also observed that the addition of C$\overline{S}$ to the CSA/OPC blend mitigated the ettringite formation at early stages but allowed more ettringite formation after a few hours of hydration. The authors concluded that hydration of C4A3$\overline{S}$ and formation of ettringite are responsible for setting of cement while the major strength giving phase is C-S-H that is developed from the hydration of C3S. This is consistent with the findings of [47].

From the study by [47], the CSA/OPC blending system exhibited compressive strength of 20 MPa after 1 day of hydration, even though the hydration of OPC was delayed. A high amount of CSA (20-30%) in the CSA-OPC blending system with the addition of C$\overline{S}$ supplemented the required sulfate for ettringite stabilization, which is responsible for high compressive strength at 1 day.

In summary, the hydration kinetics for the formation of ettringite in CSA-OPC blended systems is similar to that for CAC-OPC blends where early hydration is dominated by the formation of ettringite [49].

2.4.7 Application of Blended Systems

Both CAC and CSA are high in manufacturing cost compared to OPC. However, blended systems containing CAC, CSA and OPC provide a cement with multiple positive aspects such as rapid hardening abilities, reduced manufacturing cost and reduced carbon footprint. The application of these blended systems is popular not only due to rapid hardening but also impermeability, low pH, and high corrosion resistance [50]. These blended systems lean towards OPC have a good malleability and appealing features of high sulfate resistance and rapid setting and strength grain.

2.5 INFLUENCE OF CURING TEMPERATURE ON BLENDED SYSTEMS

Curing temperature is an important factor on the cement hydration kinetics [51]. Phase assemblages and the spatial distribution of hydration products change with varying temperature. The dissolution behavior of calcium sulfate varies significantly with temperature. The solubility of calcium sulfate and ettringite increases with the increase of temperature [52]. Above 70°C, the formed ettringite becomes less

thermodynamically stable than monosulfate (AFm), resulting in the conversion from ettringite to AFm. This phenomenon is also known as a prerequisite for concrete deterioration caused by delayed ettringite formation (DEF) [53]. In practice, rapid hardening mortars are frequently used in many applications such as night repairs (at temperature below 20°C) and winter constructions [54], but not much work has been done to quantify the hydration kinematics of a ternary blend system at low temperature. A study completed by [53] on the hydration mechanisms of a ternary system at 0°C, 10°C, 20°C, and 40°C revealed that calcium sulfoaluminate based phases are the main hydration products. Increasing temperature results in faster conversion from ettringite to monosulfate, and stratlingite (C2ASH8) is also observed in the paste at 40°C. Another finding from this study is that the increased temperature significantly accelerates the compressive strength gain at day 1, but temperature has less influence on the strength development after day 3. [55] investigated the formation of ettringite and hydration kinetics in a ternary blend system at lower temperatures of 0°C, 5°C, 10°C, and 20 °C. The results reveal that, with the increase of temperature, both initial and final setting times are shortened, and the compressive and flexural strengths are also increased. Another finding from this study is that paste incorporated with anhydrite sets more quickly and the effect of increasing temperature on final setting time is more pronounced compared with hemihydrate. Mortar with anhydrite behaves differently. It achieves higher strength between 0°C and 10 °C but lower strength at 20 °C compared with hemihydrate.

2.6 COMPARISON OF OPC, CAC, AND CSA

Table 2.2 compares OPC with CAC and CSA that are explored in this study in terms of properties, composition, energy use, CO2 emissions and performance.

Table 2.2: A comparison of OPC, CAC and CSA

	Portland Cement	Calcium Aluminate Cement	Calcium Sulfoaluminate Cement
Primary Phases	C_3S	CA	$C_4A_3\bar{S}$, C_2S, $C\bar{S}$
Hydrates	C-S-H, CH, AFt, AFm	CAH_{10} (metastable), C_2AH_8 (metastable), C_3AH_6, AH_3	AFt, AH_3, AFm, C_2ASH_8, C–S–H
Raw material CO2 (g/g)	C_3S=0.578	CA=0.279	$C_4A_3\bar{S}$= 0.216, C_2S = 0.511

primary phase [56]			
Clinkering temperature	~1450 °C	~1450 °C	1250 °C
Advantages	Standard compositions	Rapid strength, sulfate resistant, No ASR	Rapid Strength, Low energy, less shrinkage
Disadvantages	High energy, Low early strength,	Later age strength reduction due to Conversion	Expensive, durability performance has been proven

2.7 WATER REDUCING ADMIXTURES

2.7.1 Background

The purpose of using superplasticizing and/or water reducing admixtures is to increase the workability without increasing the water content of concrete, or to reduce the water content without decreasing the slump. As water reducers reduce the water content, it effectively reduces the water to cement ratio of the concrete, which results in improved strength and durability. Normally, three types of water reducers are available: Normal (conventional) water reducers, mid-range water reducers, and high range water reducers. A HRWR can reduce the water content up to 12% to 40%. The reduced water cement ratio can produce concrete with (i) compressive strength greater than 70 MPa, (ii) increased early strength gain, (iii) reduced chloride ion penetration [57, 58]

2.7.2 Composition of Water Reducing Admixtures

The underlying chemistry of water-reducing admixtures attributes to lignosulfonates, hydroxycarboxylic acid, hydroxylated polymers, salts of melamine formaldehyde sulfonates or naphthalene formaldehyde sulfonic acids, and polycarboxylates. Since the 1930s, the use of organic materials to reduce the water content or increase the fluidity of concrete has been common. The development of high range water reducers in the late 1980s has brought a new dimension in this technology, and the technology is based on polycarboxylates [57].

2.7.3 Mechanisms of Water Reducers

Electrostatic and steric repulsive forces lead the functionability of water reducers as a cement dispersant. The surface charges on the cement particles are neutralized by the acidic group within the polymer [59-62]. The acidic group gets attached to the positive ions on the cement particle surfaces. These ions create a bond with the polymer and provide the cement with a minimal negative charge that will create a layer on the surface. This negative charge and layer of absorbed compounds create a combination of electrostatic and steric repulsion forces among individual cement particles that will help disperse them, and thus the water tied up in agglomerations to reduce the viscosity of the paste and concrete. The dosage, sequence of addition, and molecular weight are the key factors that define the effectiveness of water reducers [57].

2.7.4 Polycarboxylate Technology

Polycarboxylate technology derivatives are the newest generation and the most effective HRWRs. These polymers have a main carbon chain with carboxylate groups and polyethylene oxide (PEO) side chains. Another advantage of the polycarboxylate technology is that the number of carboxylate groups and the number and length of PEO side chains can be adjusted to alter the properties of the plasticizer [63].

In this study, Sika ViscoCrete - 4100 was used as a HRWR. It is a polycarboxylate polymer-based technology which meets the requirement for ASTM C494. Sika 4100 does not contain formaldehyde, calcium chloride or any other chlorides. It can reduce the water content up to 40% at high dosages. It is also effective in providing plasticity of the concrete and extending workability time during hot weather when slump loss can be a major issue.

2.7.5 Effect of Water Reducers on Calcium Aluminate Cement

CACs are typically harsher than OPCs, making them difficult to finish. Moreover, concrete mixtures with CACs have a higher fine to coarse aggregate ratio to improve finishability, which can increase the water/workability demand. From the study of [64], calcium lignosulfonate can improve the workability of CAC without extending the setting time or entraining much air when used in low dosages.

[65] investigated the effects of poly-carboxylate based superplasticizers (dosages from 0.05% to 0.40% based on the cement weight) on workability and time until the heat of hydration starts. From this study, a slump greater than 150mm was achieved in CAC with a W/C 0.30 and a dosage of 0.1-0.2% of poly-carboxylate superplasticizer.

2.7.6 Effect of Water Reducers on CSA Cement

A recent study by [66] completed an experiment performed with aliphatic water reducing agent (AP), polycarboxylic acid water reducing agent (PC) and melamine water reducing agent (MA) to investigate the fluidity, setting time and hydration process in ferrite rich calcium sulfoaluminate cement. The authors noticed that without any water reducing agents, the CSA paste could hardly flow. The addition of the water reducer improved the fluidity, and the PC had a better dispersion capacity compared to AP and MA. This study also investigated the effect of water reducers on setting time, and they found that PC was able to extend the initial and final setting times significantly. With the dosage of 2.5% for the PC case, initial and final setting times of paste were 6.08 hours and 7.16 hours, which was considerably higher than the other two water reducing agent. From this study, the PC water reducing agent delayed immensely the hydration rate and ettringite formation.

Another study completed by [67] investigated the compatibility between a polycarboxylate (PC) water reducer and belite rich sulfoaluminate cement and is mainly focused on setting time and hydration properties. The authors found that if the PC dosage is more than 0.075% (by the cement weight), PC could have a retarding effect and the initial setting time was extended from 18 mins to 72 mins. Moreover, the dosages greater than 0.075% reduced the one-day compressive strength. The most important result from this study is that when the cement contains 0.075% of PC, the strength of cement paste at 28 days increased remarkably.

2.8 SET CONTROLLING ADMIXTURES

2.8.1 Set Retarders

RSHCs are of great interest to the future of evolving infrastructures due to their inherent advantage of fast-setting. However, the disadvantage of RSHCs is that their fast-setting may lead to reduced window time for concrete placement.

Among the chemical admixtures used as retarders, the salts of lignosulfonic acid and hydroxylated carboxylic acids, and carbohydrates such as sucrose, glucose, polymers, and sodium gluconate are very common and effective to extend the setting time for hydraulic cement hydration. Citric acid, tartaric acid, and various phosphorous such as nitrilotris, methelyne triphosphonate are also used as set retarders for cement hydration [68, 69]. The impacts of retarders include:

- Impact of retarders on silicates
- Impact of retarder on hydration

- Interaction of retarders with aluminates

The development of alternative cementitious cements requires further attention of hydration mechanisms and kinetics since new cements come with new need [8]. Chemical admixtures such as set retarders are very common in using at a small dosage since they have the potential to alter the cement's hydration process, cement chemistry and cement's performance.

Ettringite based cements set very fast. Citric acid is commonly used as a set retarder to control the workability and setting time of the cement. Moreover, citric acid can also change the phase assemblage of the cement, which results in an increase in the compressive strength of the cement up to 45% [70].

Citric acid is known to retard the dissolution and formation of phases in multiple ways: 1) By forming complexes with dissolved Ca ions in the pore solution, it can lower their availability to participate in hydration. However, this mechanism is not strong enough to describe the retardation process. 2) By getting absorbed on the cement grains, citric acid can form a protective layer, resulting in preventing their dissolution. 3) By retarding the nucleation and growth of ettringite crystals in the pore solution, it delays the hydration process.

2.8.2 Effect of Citric Acid on Calcium Sulfoaluminate Cement

For larger scale placements, retardation of the CSA reactions is needed, and citric acid is considered as the primary set retarder for CSA cements. In a recent study by [71], the authors investigated the use of citric acid with CSA cements by tracking the effects of dosage on phase development, hydration, setting time and compressive strengths of the resulting concrete. The key contribution from this study is that, up to a 2% by mass of cement dosage, citric acid can effectively extend the initial and final setting times without compromising the compressive strength. However, citric acid was found to be more effective at delaying hydration of belite rich CSA compared to conventional CSA mixtures. Cumulative heat measurements from the isothermal calorimetry test revealed that despite citric acid delayed the hydration process, it did not reduce the total hydration of the CSA systems. Another recent work, completed by [72], also found that, with the citric acid dosage of 0.75% to 1.5% by weight of the cement, an initial setting time greater than 60 minutes and a final setting time greater than 120 minutes can be achieved in high belite based CSA cements. Cheung and Zou [68, 69] investigated the mechanism of citric acid on delaying CSA hydration. The authors found that the formation of complex between calcium and citrate in the solution that are absorbed on the solid surface extended the $C_4A_3\bar{S}$, anhydrite and AFt nucleation.

2.8.3 Effect of Citric Acid on Calcium Aluminate Cement

[73] observed from the study that citric acid is an effective set retarder for CACs when CACs are used in concrete mixture. The authors suggested that an amorphous protective gel coating can be formed around the cement grains, which inhibits the CAC hydration until the citrate from the citric acid is precipitated. [74] investigated the effect of citric acid on the hydration of OPC-CAC blending system. They found that the compressive and flexural strengths of the OPC-CAC blended cement were reduced with the addition of citric acid. They also noticed that 1% of citric did not reduce the compressive strength up to 28 days compared to the mix without any citric acid. However, at higher dosages the citric acid blocked the dissolution of cement hydrates and impeded the hydration process.

2.9 SET ACCELERATOR

2.9.1 Background

A set accelerating admixture speeds up the rate of hydration and strength development of concrete at an early age. Calcium chloride ($CaCl_2$) is a common set accelerator that has been used over many decades. It is very effective in non-reinforced concrete. However, its dosage is limited to 2% or less (by mass of cement) for reinforced concrete, as chlorides will accelerate corrosion of reinforcement [57].

As such, non-chloride containing accelerators have gained popularity. Organic compounds such as triethanolamine (TEA) and inorganic salts such as sodium and calcium salts of formate, nitrate and nitrite are often used [57]. However, inorganic salts seem to be less effective compared to calcium chloride, so higher dosages compared to calcium chloride are needed.

2.9.2 Set Accelerator on CAC

For CACs, solutions of sodium, potassium, and calcium hydroxides as well as sodium and potassium carbonates are common accelerators [64], but lithium salts are the most used form of set accelerators for CACs. Lithium salts can reduce the set times to just a few minutes with a minimal addition (e.g., 0.1% of the cement weight). However, the CHRYSO group has recently been found to be an effective set accelerator for CAC concrete in the industry.

2.9.3 Set Accelerator on CSA

Lithium salts, including Li-containing aluminum hydroxide, can accelerate the hydration of CSA as well as CAC [75]. The use of lithium salts promotes the amorphous aluminum hydroxide formation, which speeds up the hydration process of cements [76]. A recent study completed by [77] explored the effect of

lithium salts on setting time, mechanical strength, and heat release of CSA cement where different proportions of gypsum are incorporated. The results revealed that the addition of Li_2CO_3 significantly accelerates the early hydration and decreases the setting time, and the effect has no relation with the amount of gypsum added to the cement. Another significant finding from this study is that the addition of Li_2CO_3 does not alter the hydration product but inhibits $C4A3\bar{S}$ hydration of CSA at day 1 when 10% gypsum is incorporated, while the presence of Li_2CO3 accelerates the precipitation of ettringite after one day of hydration.

2.9.4 Effects of Set Accelerator on Concrete Properties

The main objective of a set accelerator is to reduce both initial and final setting times. The admixture dosage, composition, and time of addition all play a defining role in early age strength development. However, using a higher dosage of set accelerator has some downside such as an increase in drying shrinkage, rapid stiffening, corrosion of reinforcement, and later age strength loss [78].

2.10 REFERENCES

[1]   *ASTM C1600M-19 Standard Specification for Rapid Hardening Hydraulic Cement*, ASTM International, 2019. [Online]. Available: https://compass.astm.org/document/?contentCode=ASTM%7CC1600_C1600M-19%7Cen-US

[2]   *ASTM C109-21 Standard Test Method for Compressive Strength of Hydraulic Cement Mortars (Using 2-in. or [50-mm] Cube Specimens)*, ASTM International, 2021.

[3]   *ASTM C596-23 Standard Test Method for Drying Shrinkage of Mortar Containing Hydraulic Cement*, ASTM International, 2023.

[4]   A. Bentivegna, "Multi-Scale Characterization, Implementation, and Monitoring of Calcium Aluminte Cement Based Systems (Dissertation). Austin, TX: The University of Texas at Austin.," Dissertation 2012. The University of Texas at Austin.

[5]   P. Hewlett and M. Liska, *Lea's chemistry of cement and concrete*. Butterworth-Heinemann, 2019.

[6]   K. Scrivener and A. J. A. c. t. Capmas, "Calcium aluminate cements," pp. 1-31, 2003.

[7]   K. Scrivener, "100 years of calcium aluminate cements," in *Proceedings of International Conference on Calcium Aluminate Cements*, 2008, pp. 3-6.

[8]   J. H. Ideker, C. Gosselin, and R. J. C. i. Barborak, "An alternative repair material," vol. 35, no. 4, pp. 33-37, 2013.

[9]   K. L. Scrivener, "HISTORICAL AND PRESENT DAY APPLICATION OF CALCIUM ALUMINATES CEMENTS," 2001: INTERNATIONAL CONFERENCE ON CALCIUM ALUMINATE CEMENT.

[10]   I. Odler, "Special inorganic cements, Modern Concrete Technology 8, E&FN," ed: Taylor & Francis Group, 2000.

[11]   J. H. Ideker, "Early-Age Behaviour of Calcium Aluminate Cement Systems (Dissertation). Austin, TX: The University of Texas at Austin.," 2008.

[12]   P. Arjunan, M. R. Silsbee, and M. R. Della, "Sulfoaluminate-belite cement from low-calcium fly ash and sulfur-rich and other industrial by-products," *Cement and Concrete Research,* vol. 29, no. 8, pp. 1305-1311, 1999/08/01/ 1999, doi: https://doi.org/10.1016/S0008-8846(99)00072-1.

[13]   M. C. G. Juenger, F. Winnefeld, J. L. Provis, and J. H. Ideker, "Advances in alternative cementitious binders," *Cement and Concrete Research,* vol. 41, no. 12, pp. 1232-1243, 2011/12/01/ 2011, doi: https://doi.org/10.1016/j.cemconres.2010.11.012.

[14]   L. Zhang and F. J. A. i. c. r. Glasser, "Hydration of calcium sulfoaluminate cement at less than 24 h," vol. 14, no. 4, pp. 141-155, 2002.

[15]   G. Bernardo, A. Telesca, and G. L. Valenti, "A porosimetric study of calcium sulfoaluminate cement pastes cured at early ages," *Cement and Concrete Research,* vol. 36, no. 6, pp. 1042-1047, 2006/06/01/ 2006, doi: https://doi.org/10.1016/j.cemconres.2006.02.014.

[16]   L. E. Burris, P. Alapati, R. D. Moser, M. T. Ley, N. Berke, and K. E. Kurtis, "Alternative cementitious materials: challenges and opportunities," in *International Workshop on Durability and Sustainability of Concrete Structures, Bologna, Italy*, 2015.

[17]   E. Moffatt, "Durability of Rapid-set (ettringite based) Concrete," Dissertation 2016. University of New Brunswick.

[18]   F. Winnefeld, S. J. J. o. t. a. Barlag, and calorimetry, "Calorimetric and thermogravimetric study on the influence of calcium sulfate on the hydration of ye'elimite," vol. 101, no. 3, pp. 949-957, 2010.

[19]   F. Hanic, I. Kaprálik, A. J. C. Gabrisová, and c. research, "Mechanism of hydration reactions in the system C4A3S☐CS☐CaO☐H2O referred to hydration of sulphoaluminate cements," vol. 19, no. 5, pp. 671-682, 1989.

[20]   M. Palou, J. J. J. o. T. A. Majling, and Calorimetry, "Hydration in the system C 4 A 3‾ SC‾ SH 2-CH-H," vol. 46, no. 2, pp. 557-563, 1996.

[21]   J. T. Song and J. F. J. J. o. t. A. C. S. Young, "Direct synthesis and hydration of calcium aluminosulfate (Ca4Al6O16S)," vol. 85, no. 3, pp. 535-539, 2002.

[22]   I. Kaprálik, F. J. C. Hanic, and C. Research, "Phase relations in the subsystem C4A3S☐CSH2☐CH☐H2O of the system CaO☐Al2O3☐CS☐H2O referred to hydration of sulphoaluminate cement," vol. 19, no. 1, pp. 89-102, 1989.

[23]   F. P. Glasser, L. J. C. Zhang, and C. Research, "High-performance cement matrices based on calcium sulfoaluminate–belite compositions," vol. 31, no. 12, pp. 1881-1886, 2001.

[24]   Y. Wang and M. J. W. C. Su, "The third cement series in China," vol. 25, no. 8, pp. 6-10, 1994.

[25]   W. Lan and F. J. A. i. c. r. Glasser, "Hydration of calcium sulphoaluminate cements," vol. 8, no. 31, pp. 127-134, 1996.

[26]   J. Sharp, C. Lawrence, and R. J. A. i. C. R. Yang, "Calcium sulfoaluminate cements—low-energy cements, special cements or what?," vol. 11, no. 1, pp. 3-13, 1999.

[27]   A. J. P. o. t. C. Brown, "Application of calcium sulfoaluminate cements in the 21st century," pp. 1773-8, 2000.

[28]   P. Gu, J. J. Beaudoin, E. G. Quinn, and R. E. J. A. c. b. m. Myers, "Early strength development and hydration of ordinary Portland cement/calcium aluminate cement pastes," vol. 6, no. 2, pp. 53-58, 1997.

[29]   S. Zhang *et al.*, "Effect of calcium sulfate type and dosage on properties of calcium aluminate cement-based self-leveling mortar," vol. 167, pp. 253-262, 2018.

[30]   R. Mangabhai, *Calcium Aluminate Cements: Proceedings of a Symposium dedicated to HG Midgley, London, July 1990*. CRC Press, 1990.

[31]   F. Glasser, L. Zhang, and Q. Zhou, "Reactions of aluminate cements with calcium sulphate," in *International conference on calcium aluminate cements*, 2001, pp. 551-564.

[32]   G. Le Saôut, B. Lothenbach, P. Taquet, H. Fryda, and F. J. A. i. c. r. Winnefeld, "Hydration of calcium aluminate cement blended with anhydrite," vol. 30, no. 1, pp. 24-36, 2018.

[33]   S. Lamberet, "Durability of Ternary Binders Based on Portland Cement, Calcium Aluminate Cement and Calcium Sulfate. Ph.D. thesis, École Polytechnique Fédérale de

Lausanne, Lausanne, Switzerland," 2005.

[34]   P. K. J. J. o. t. A. C. S. Mehta, "Effect of lime on hydration of pastes containing gypsum and calcium aluminates or calcium sulfoaluminate," vol. 56, no. 6, pp. 315-319, 1973.

[35]   J. Bizzozero, C. Gosselin, and K. L. Scrivener, "Expansion mechanisms in calcium aluminate and sulfoaluminate systems with calcium sulfate," *Cement and Concrete Research,* vol. 56, pp. 190-202, 2014/02/01/ 2014, doi: https://doi.org/10.1016/j.cemconres.2013.11.011.

[36]   J. Zhang, G. Li, X. Yang, S. Ren, and Z. Song, "Study on a high strength ternary blend containing calcium sulfoaluminate cement/calcium aluminate cement/ordinary Portland cement," *Construction and Building Materials,* vol. 191, pp. 544-553, 2018/12/10/ 2018, doi: https://doi.org/10.1016/j.conbuildmat.2018.10.040.

[37]   K. L. Scrivener, "The development of microstructure during the hydration of Portland cement," Imperial College London (University of London), 1984.

[38]   L. Amathieu, T. A. Bier, and K. Scrivener, "Mechanisms of set acceleration of Portland cement through CAC addition," in *International conference on calcium aluminate cements*, 2001, pp. 303-317.

[39]   P. Garces, E. Garcia Alcocel, and C. J. Z. i. Garcia Andreu, "Hydration characteristics of high alumina cement," vol. 51, no. 11, pp. 646-649, 1998.

[40]   P. Gu and J. J. J. o. m. s. l. Beaudoin, "Lithium salt-based additives for early strength-enhancement of ordinary Portland cement-high alumina cement paste," vol. 16, no. 9, pp. 696-698, 1997.

[41]   J. Bizzozero, C. Gosselin, K. L. J. C. Scrivener, and C. Research, "Expansion mechanisms in calcium aluminate and sulfoaluminate systems with calcium sulfate," vol. 56, pp. 190-202, 2014.

[42]   J. Kighelman, K. Scrivener, and R. Zurbriggen, "Effect of the mix binder system on the hydration of self-leveling compounds," in *16th international conference on building materials*, 2006.

[43]   I. Odler, J. J. C. Colán-Subauste, and C. Research, "Investigations on cement expansion associated with ettringite formation," vol. 29, no. 5, pp. 731-735, 1999.

[44]   L. Xu, P. Wang, G. J. J. o. t. a. Zhang, and calorimetry, "Calorimetric study on the influence of calcium sulfate on the hydration of Portland cement–calcium aluminate cement mixtures," vol. 110, no. 2, pp. 725-731, 2012.

[45]   P. Gu and J. J. J. o. m. s. Beaudoin, "A conduction calorimetric study of early hydration of ordinary Portland cement/high alumina cement pastes," vol. 32, no. 14, pp. 3875-3881, 1997.

[46]   H. Taylor, "Cement chemistry, London," ed: Thomas Telford, 1997.

[47]   L. Pelletier, F. Winnefeld, B. J. C. Lothenbach, and C. Composites, "The ternary system Portland cement–calcium sulphoaluminate clinker–anhydrite: hydration mechanism and mortar properties," vol. 32, no. 7, pp. 497-507, 2010.

[48]   S. Park, Y. Jeong, J. Moon, and N. J. J. o. B. E. Lee, "Hydration characteristics of calcium sulfoaluminate (CSA) cement/portland cement blended pastes," vol. 34, p. 101880, 2021.

[49]   R. Lute, "DURABILITY OF CALCIUM-ALUMINATE BASED BINDERS FOR RAPID REPAIR APPLICATIONS, Dissertation, The University of Texas at Austin," 2016.

[50]   K. Kurtis, P. Alapati, and L. J. P. R. Burris, "Alternative Cementitious Materials: An Evolution or Revolution?," vol. 83, no. 3, 2019.

[51]   B. Lothenbach, F. Winnefeld, C. Alder, E. Wieland, P. J. C. Lunk, and C. Research, "Effect of temperature on the pore solution, microstructure and hydration products of Portland cement pastes," vol. 37, no. 4, pp. 483-491, 2007.

[52]   B. Lothenbach, T. Matschei, G. Möschner, F. P. J. C. Glasser, and C. Research, "Thermodynamic modelling of the effect of temperature on the hydration and porosity of Portland cement," vol. 38, no. 1, pp. 1-18, 2008.

[53]   L. Xu, K. Wu, C. Rößler, P. Wang, H. J. C. Ludwig, and C. Composites, "Influence of curing temperatures on the hydration of calcium aluminate cement/Portland cement/calcium sulfate blends," vol. 80, pp. 298-306, 2017.

[54]   E. Sakai, Y. Nikaido, T. Itoh, M. J. C. Daimon, and c. research, "Ettringite formation and microstructure of rapid hardening cement," vol. 34, no. 9, pp. 1669-1673, 2004.

[55]   L. Xu, P. Wang, G. J. C. Zhang, and B. Materials, "Formation of ettringite in Portland cement/calcium aluminate cement/calcium sulfate ternary system hydrates at lower temperatures," vol. 31, pp. 347-352, 2012.

[56]   E. J. C. Gartner and C. research, "Industrially interesting approaches to "low-CO2" cements," vol. 34, no. 9, pp. 1489-1498, 2004.

[57]   S. H. Kosmatka, W. C. Panarese, and B. Kerkhoff, *Design and control of concrete mixtures*. Portland Cement Association Skokie, IL, 2002.

[58]   P. K. Mehta and P. J. Monteiro, *Concrete microstructure, properties and materials*. 2017.

[59]   V. S. Ramachandran, V. Malhotra, C. Jolicoeur, and N. Spiratos, "Superplasticizers: properties and applications in concrete," 1998.

[60]   M. Collepardi and M. J. S. P. Valente, "Recent developments in superplasticizers," vol. 239, pp. 1-14, 2006.

[61]   D. Whiting and W. Dziedzic, "Effects of conventional and high-range water reducers on concrete properties," 1992.

[62]   A. C. I. Committee, "Admixtures for Concrete," *ACI Journal Proceedings,* vol. 51, no. 10, 10/1/1954, doi: 10.14359/11670.

[63]   M. Thomas and L. J. C.-R. C. Wilson, Portland Cement Association, Skokie, IL, "Admixtures for use in concrete," 2002.

[64]   T. D. Robson, *High-alumina cements and concretes*. Contractors Record, 1962.

[65]   H. Fryda, V. Gachet, and P. J. S. P. Bost, "Interaction of superplasticizers with calcium aluminate cements," vol. 195, pp. 91-100, 2000.

[66]   C. Huang, Z. Cheng, J. Zhao, Y. Wang, and J. J. C. Pang, "The influence of water reducing agents on early hydration property of ferrite aluminate cement paste," vol. 11, no. 7, p. 731, 2021.

[67]   B. Ma, M. Ma, X. Shen, X. Li, X. J. C. Wu, and B. Materials, "Compatibility between a polycarboxylate superplasticizer and the belite-rich sulfoaluminate cement: Setting time and the hydration properties," vol. 51, pp. 47-54, 2014.

[68]   D. Zou, Z. Zhang, and D. Wang, "Influence of citric acid and sodium gluconate on hydration of calcium sulfoaluminate cement at various temperatures," *Construction and Building Materials,* vol. 263, p. 120247, 2020/12/10/ 2020, doi: https://doi.org/10.1016/j.conbuildmat.2020.120247.

[69]   J. Cheung, A. Jeknavorian, and L. Roberts, "Impact of admixtures on the hydration kinetics of Portland cement (in Cement and Concrete Research 41 (12): 1289–1309," ed, 2011.

[70]   H. Nguyen *et al.*, "Ettringite-based binder from ladle slag and gypsum–The effect of citric acid on fresh and hardened state properties," vol. 123, p. 105800, 2019.

[71]   L. E. Burris, K. E. J. C. Kurtis, and C. Research, "Influence of set retarding admixtures on calcium sulfoaluminate cement hydration and property development," vol. 104, pp. 105-113, 2018.

[72]   A. Prasanth, "MULTISCALE INVESTIGATION OF ALTERNATIVE CEMENTITIOUS MATERIAL SYSTEMS," Dissertation 2020. Georgia Institute of Technology.

[73]   S. Rodger, D. J. C. Double, and C. Research, "The chemistry of hydration of high alumina cement in the presence of accelerating and retarding admixtures," vol. 14, no. 1, pp. 73-82, 1984.

[74]   G. Kastiukas, X. Zhou, J. Castro-Gomes, S. Huang, M. J. C. Saafi, and B. Materials, "Effects of lactic and citric acid on early-age engineering properties of Portland/calcium aluminate blended cements," vol. 101, pp. 389-395, 2015.

[75]   D. Damidot, A. Rettel, and A. J. A. i. C. R. Capmas, "Action of admixtures on Fondu cement: Part 1. Lithium and sodium salts compared," vol. 8, no. 31, pp. 111-119, 1996.

[76]   C. C. D. Coumes, M. Dhoury, J.-B. Champenois, C. Mercier, D. J. C. Damidot, and C. Research, "Physico-chemical mechanisms involved in the acceleration of the hydration of calcium sulfoaluminate cement by lithium ions," vol. 96, pp. 42-51, 2017.

[77] Y. Shen, W. Zhang, P. Wang, X. Chen, H. J. J. o. T. A. Zhu, and Calorimetry, "Influence of lithium salt on the performance of calcium sulfoaluminate cement," vol. 147, no. 4, pp. 3043-3051, 2022.

[78] H. B. J. C. Lackey, Concrete and Aggregates, "Factors affecting use of calcium chloride in concrete," vol. 14, no. 2, 1992.

CHAPTER 3: MATERIALS

The materials used throughout this project including cements, aggregates, and admixtures (mineral and chemical) are summarized in the sections below. While this chapter is intended to provide an overall discussion on the materials used and their chemical/physical properties, specific materials and mixture proportions used in each experimental program are described in subsequent chapters.

3.1 CEMENTS

In this project, a total of 10 rapid setting hydraulic cements (RSHCs) were investigated. The majority of RSCHs were either a calcium aluminate (CAC) or calcium sulfoaluminate cement (CSA) as the primary base binder, with several of them produced as either a pure/straight cement system, or a proprietary blended product containing other supplementary cementing materials and/or mineral admixtures (e.g., water reducer, retarder, etc.) to enhance fresh and hardened properties. All proprietary blends of CAC and CSA cements with other powder materials was carried out during cement production by the manufacturer.

Additionally, two laboratory blends of either CAC or CSA combined with a local Type I/II cement prior to the process of mixing concrete were also investigated. The blended CSA binder, designated as CSA-OPC2, contained a mixture of calcium sulfoaluminate in which the main phases were ye'elimite and calcium sulfate (CSA1) blended with a Type I/II cement procured locally in central Texas at a 25% replacement level (by total mass). Similarly, the blended CAC binder, designated as CAC-OPC2, utilized a combination of calcium aluminate cement and calcium sulfate at a ratio of 2.2:1. This blend was then combined with a Type I/II cement at a 25% replacement level. It should be noted that the proprietary blend cement, CAC-B1, is an equivalent ternary system to CAC-OPC1 containing equal parts of calcium aluminate, calcium sulfate, and Type I/II. However, the type I/II used in the proprietary blend was from a different source procured by the manufacturer, and all constituents were blended during cement production. The reason for investigating both proprietary and laboratory blended RSHC systems was to provide a performance comparison between each variation depicting what is often done in current practice in the field with CAC and CSA cements.

Finally, besides CACs and CSAs, three ASTM C150 [1] portland cements procured locally in central Texas were chosen for this study including a high-early strength Type III for comparison to the RSHCs.

Table 3.1 outlines all the cements investigated in this study along with their cement identification (ID) codes, followed by a short description. The ID codes was developed to facilitate the identification of the different binder types tested under the experimental investigation described in this Final Report. Unless

otherwise noted in a specific section or chapter, these IDs are used throughout the Final Report. Table 3.2 outlines the chemical composition of all the cements investigated in this study given by X-ray fluorescence (XRF) analysis. Please note the following information on the cements:

- XRF analysis was performed by TxDOT at the Cedar Park Campus to obtain the chemical composition of each RSHC.
- All proprietary blended products containing other additives were interground during cement production and used in their final dry form during mixing.
- The proprietary blended cement designated as CAC-B1* is calcium aluminate and calcium sulfate blend intended to be used in combination with a locally available portland cement to produce a rapid setting ternary system (CAC-OPC2). This combination is equivalent to the lab blend designed as CAC-B1 with the exception that the portland cement was added at the time of mixing and not at the production plant.
- The equivalent alkali content (Na_2O_e) for RSHCs was calculated using the same expression for equivalent alkalis in portland cement ($\%Na_2O + 0.658*\%K_2O$).
- The chemical composition of both laboratory blends (CAC-OPC2 & CSA-OPC2) is based on a weighted average of the combination of constituents used (i.e., 75% Type I/II and 25% RSHC).

Table 3.1: Cement types, IDs, and Descriptions

Cement or Blend Type	Cement ID	Cement Category	Description
Straight Cements	OPC1	Portland	Type I OPC, high C_3A, high alkali, used only in ASR testing
	OPC2	Portland	Type I/II OPC, moderate C_3A, and low alkali
	OPC3	Portland	High-early strength Type III OPC
	CAC	Calcium Aluminate	100% Plain CAC, main phase monocalcium aluminate
	CSA1	Calcium Sulfoaluminate	100% Plain CSA, main phases ye'elimite and calcium sulfate
	CSA2	Calcium Sulfoaluminate	100% Plain CSA, main phases belite, ye'elimite and calcium sulfate
Proprietary Blended Cements	CAC-B1	Calcium Aluminate	Ternary blend of CAC, calcium sulfate, and Type I/II
	CAC-B1*	Calcium Aluminate	Binary system of CAC and calcium sulfate and used in combination with a local Type I/II to produce laboratory ternary blend (CAC-OPC2)
	CAC-B2	Calcium Aluminate	Blend of CAC and fly ash
	CSA-B1	Calcium Sulfoaluminate	Proprietary pre-blend of CSA with mineral admixtures (powder additives)
	CSA-B2	Calcium Sulfoaluminate	Proprietary pre-blend of CSA with mineral admixtures (powder additives)
	PCSA1	Calcium Sulfoaluminate	Proprietary pre-blend not reported by manufacturer
	PCSA2	Calcium Sulfoaluminate	Proprietary pre-blend not reported by manufacturer
Lab Blends	CAC-OPC2	Calcium Aluminate with portland cement	A lab blended cement containing 25% of a calcium aluminate/calcium sulfate blend (CAC-B1*) and 75% of OPC2
	CSA1-OPC2	Calcium sulfoaluminate with portland cement	A lab blended cement containing 25% of CSA1 and 75% of OPC2

Table 3.2: Chemical composition of all sets of cement in this study

Cement Type	Cement ID	SiO$_2$	Al$_2$O$_3$	Fe$_2$O$_3$	CaO	MgO	SO$_3$	Na$_2$O	K$_2$O	Na$_2$O$_e$	LOI
Pure Cements	OPC1	19.60	5.19	2.06	64.01	1.12	3.86	0.12	0.91	0.72	3.80
	OPC2	21.06	4.02	3.19	63.91	1.08	2.89	0.14	0.61	0.53	2.29
	OPC3	19.67	5.34	1.76	63.41	0.99	5.27	0.10	0.44	0.39	4.06
	CAC	4.34	38.65	15.09	38.37	0.39	0.16	0.05	0.14	0.14	1.55
	CSA1	9.07	21.61	2.26	45.26	0.94	20.26	0.07	0.30	0.27	1.05
	CSA2	20.56	16.14	1.35	45.31	1.23	14.73	0.77	0.72	1.24	4.74
Proprietary Blended Cements	CAC-B1	13.46	12.23	2.67	56.65	2.86	9.90	0.20	0.79	0.72	1.21
	CAC-B1*	2.93	31.12	1.25	40.57	0.33	21.08	0.14	0.19	0.27	1.90
	CAC-B2	12.71	32.94	12.95	35.09	1.79	0.84	0.50	0.24	0.65	1.23
	CSA-B1	13.63	15.82	0.75	51.28	1.14	16.62	0.29	0.62	0.69	3.06
	CSA-B2	14.72	14.37	1.22	53.85	1.23	14.40	0.10	0.59	0.49	3.39
	PCSA1	17.38	11.06	2.98	55.82	1.25	10.68	0.43	0.52	0.77	2.26
	PCSA2	20.14	15.73	3.52	43.90	1.55	12.88	0.59	0.52	0.93	1.95
Lab Blends	CAC-OPC2	16.53	10.79	2.71	58.07	0.89	7.43	0.14	0.50	0.47	2.19
	CSA1-OPC2	18.06	8.42	2.96	59.25	1.04	7.23	0.12	0.53	0.47	1.98

Table 3.3 shows the particle diameters, in micrometers, corresponding to the 10%, 50%, and 90% values of the cumulative particle size distribution curve. These values are denoted as d_{10}, d_{50}, and d_{90}. Finally, the particle size distribution curves for all cements can be seen in Figure 3.1

Table 3.3: Particle diameters given by laser PSD analysis

Cement ID	d_{10} (µm)	d_{50} (µm)	d_{90} (µm)
OPC1	2.1	12.6	42.0
OPC2	2.0	10.7	27.0
OPC3	1.8	9.5	24.0
CAC	3.4	15.2	40.8
CSA1	1.7	8.5	37.0
CSA2	1.7	9.8	33.0
CAC-B1	2.6	12.9	42.1
CAC-B1*	2.4	15.1	47.5
CSA-B1	1.4	8.5	28.9
CSA-B2	1.6	9.2	29.0
PCSA1	1.8	8.9	33.9
PCSA2	2.1	11.2	45.4
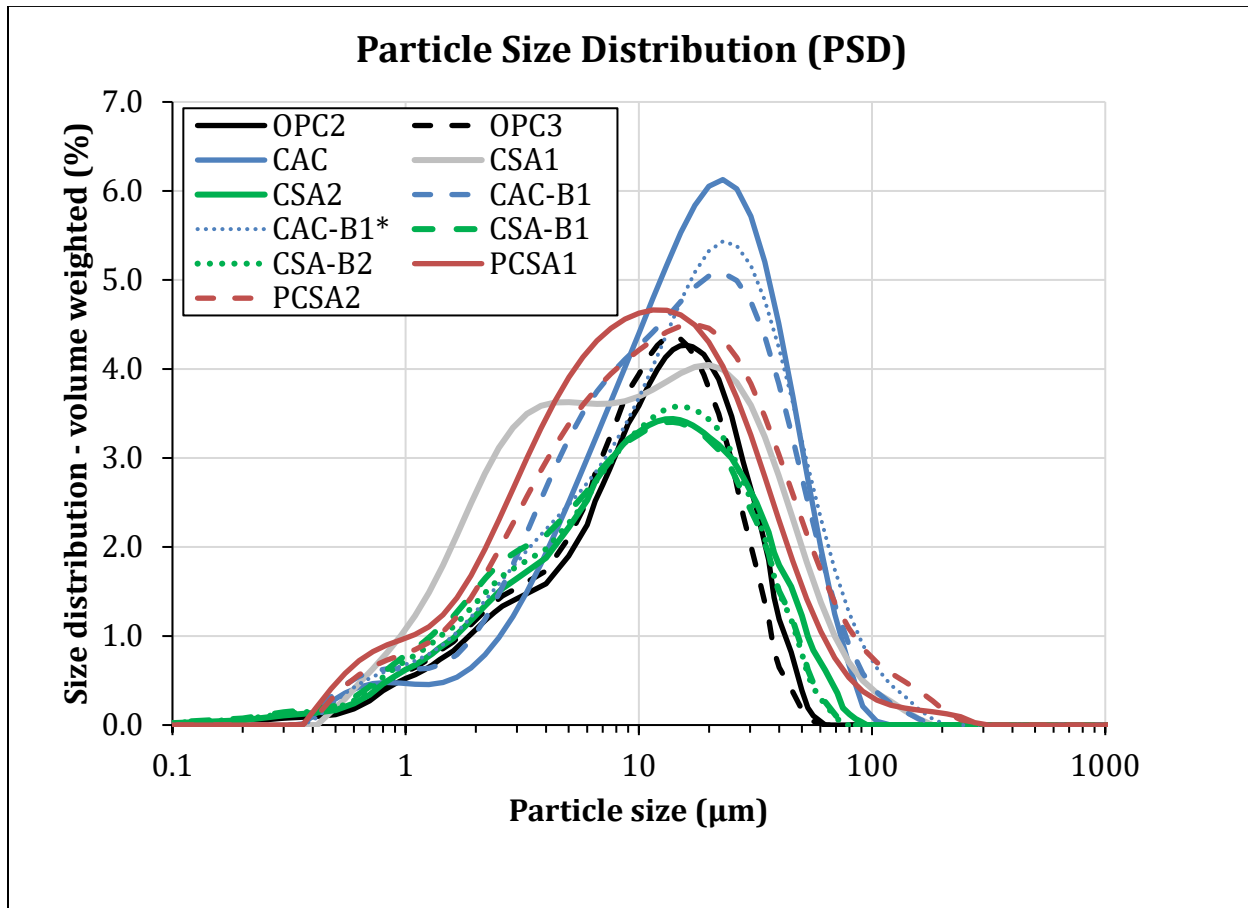
Figure 3.1: Particle size distribution of cements.

3.2 AGGREGAATES

Different types of fine and coarse aggregates were used to complete the research described in the Final
Report. The selection of aggregate was dependent on the specific test and/or intended research objective.
All aggregates met the requirements specified in ASTM C33 [2].

3.2.1 Fine Aggregates

A total of four fine aggregates were used in the project with the majority of concrete mixtures using a
single source natural river sand obtained in central Texas (FA1). This aggregate is classified as being
relatively innocuous with regards to alkali silica reactivity (ASR) and delayed ettringite formation (DEF)
and thus, was used in concrete to assess mechanical properties and durability testing not involving
aggregate reactivity (e.g. corrosion and carbonation). On the other hand, three fine aggregates with
varying levels of reactivity with regards to ASR and DEF (FA2, FA3, and FA4) were included for

aggregate reactivity testing (i.e., ASR and DEF). Table 3.4 provides information on the physical properties for each fine aggregate type.

3.2.2 Coarse Aggregate

A single crushed limestone (CA) procured locally in central Texas was used in all concrete testing that is reported in this Final Report. The limestone conformed to a size 67 grading requirements established in ASTM C33 [2]. Table 3.4 provides the physical properties of the coarse aggregate.

Table 3.4: Aggregate Properties and Testing

Aggregates	Absorption Capacity	Specific Gravity (SSD)	Description	Experimental Work Performed
CA	2.66	2.56	Crushed Limestone Rock	All Concrete Testing
FA1	2.59	0.56	Natural River Sand	Mechanical/Durability Testing
FA2	1.62	2.68	Natural River Sand	ASR/DEF
FA3	1.87	2.48	Natural River Sand	ASR/DEF
FA4	3.89	2.55	Manufactured Limestone Sand	ASR/DEF

3.2.3 Standardized Graded Sand

Preliminary testing of various RSCHs and blends to optimize fresh and hardened properties were done on cementitious mortars. While some mortar specimens were fabricated using a natural river sand (FA1), majority of mixtures and test results described in the Final Report were done using a graded standard Ottawa sand meeting the requirements for ASTM C778 "Standard Specification Standard Sand" [3].

3.3 ADMIXTURES

Several admixtures were used in this study extensively including liquid and powder-based products, to increase the flow and extend the working period for all RSHCs mixtures. The admixtures as well as their description and potential outcome are listed in Table 3.5. It should be noted that all admixtures used throughout the program were dosed based on a percentage of cement weight for each mixture. Specific details on total amount used are described in subsequent chapters.

Table 3.5: Admixture Description and Uses

Admixture	Description	Potential Outcome
Water Reducer	Polycarboxylate high-range water reducer	Increase workability for low W/C mixtures
Accelerator	Non-chloride accelerator	Accelerate the setting time and increases early age strength of OPC mixtures
Accelerator	Lithium sulfate accelerator	Accelerate the setting time and increases early age strength of CAC mixtures
Retarder	Citric acid powder	Delay the setting time of CAC, CSA, and blended systems of OPC with CSA and/or CAC

3.4 REFERENCES

[1] *ASTM C150M-19 Standard Specification for Portland Cement*, ASTM International, 2019. [Online]. Available: https://compass.astm.org/document/?contentCode=ASTM%7CC0150_C0150M-19%7Cen-US

[2] *ASTM C33M-18 Standard Specifications for Concrete Aggregates*, ASTM International, 2018. [Online]. Available: https://compass.astm.org/document/?contentCode=ASTM%7CC0033_C0033M-18%7Cen-US

[3] *ASTM C778-17 Standard Specification for Standard Sand*, ASTM International, 2017.

CHAPTER 4: EXPERIMENTAL INVESTIGATION OF RAPID SETTING HYDRAULIC CEMENT MORTARS

4.1 INTRODUCTION

The experimental work described in this chapter aims to investigate the material behavior of various RSHC mortars including both fresh and hardened properties. A primary focus in this experimental work was to optimize material combination for developing RSHC concrete mixtures. Specifically, the focus and objective were to optimize workability, setting time and gain insight as to early-age strength development of RSHC mixtures.

To characterize material behavior for each RSHC, testing as specified in ASTM C1600 "Standard Specification for Rapid Hardening Hydraulic Cements" [1] was followed to inform a baseline reference of performance of each RSHC. Thereafter, variations in cement and sand (c/s) content, chemical/mineral admixture doses, and water to cement (W/C) ratio were also investigated to evaluate material robustness and the influence of these on early-age performance. Various tests were employed to characterize performing of RSHC mortars including mortar flow, compressive strength of cube specimens, drying shrinkage, isothermal calorimetry, and mini-slump. Thereafter, the experimental data collected from the mortar experimental program helped to inform an experimental matrix of RSHC concretes which was predominately used throughout the project.

4.2 RESULTS AND DISCUSSION

4.2.1 Determination of Flow

This section describes how the flow test was performed and the trial batching used to assess the impact of the amount of water needed to reach the specified flow in ASTM C109 [2]. The flow table test was performed for each RSHC to obtain a flow value of 110 ± 5. The flow test was performed following ASTM C1437 "Standard Test Method for Flow of Hydraulic Cement Mortar" [3] by varying the water content through trial-and-error. Thereafter, the same mixtures were investigated with a constant W/C ratio, but a HRWR was used to adjust the mortar flow until the specified flow value (110 ± 5) was achieved. Additionally, the impact of two different cement to sand (c/s) contents on the flow was investigated. Lastly, the impact of standard Ottawa sand as compared to the use of conventional concrete sand (natural river sand) on the flow was investigated. Table 4.1 shows the different mixture proportions of the trial batch flow tests.

Table 4.1: Quantities of materials for trial batches

Mixture Series	c/s ratio	W/C ratio	Cement (g)	Fine Aggregate Sand (g)	Water (g)	HRWR (%weight of cement)	Aggregate Type
1	1:2.75	varies	340	935	Required for flow	N/A	Natural River Sand (FA1)
2	1:2	varies	340	680	Required for flow	N/A	Natural River Sand (FA1)
3	1:2.75	0.485	340	935	165	Required for flow	Natural River Sand (FA1)
4	1:2.75	0.485	340	935	165	Required for flow	Standard graded Ottawa Sand
5	1:2.75	0.350	340	935	119	Required for flow	Natural River Sand (FA1)

4.2.2 Influence of C/S content on RSHC Mortar Flow (Mixture Series 1 & 2)

Flow value at different c/s ratios was determined, and Table 4.2 shows the results of W/C ratio required for every RSHC at different c/s ratio

Table 4.2: Flow value at two different c/s ratio of 1:2.75 and 1:2

Cement	W/C (c/s = 1:2.75)*	W/C (c/s = 1:2)**
CAC	0.52	0.38
CSA1	1.00	0.88
CSA2	0.50	0.36
CAC-B1	0.53	0.38
CSA2-B1	0.51	0.35
CSA2-B2	0.63	0.51
PCSA1	0.51	0.37
PCSA2	0.50	0.35
CSA1-OPC2	0.54	0.41
CAC-OPC2	0.50	0.38

*Started the flow test with W/C ratio 0.485 and then increased incrementally

** Started the flow test with W/C ratio 0.350 and then increased incrementally

From Table 4.2, the c/s ratio of 1:2.75 required higher amounts of water compared to the c/s ratio of 1:2 for all the RSHCs and blends investigated. Most of the cement's W/C ratio was between 0.5 to 0.6 when c/s ratio was 1:2.75, except that of CSA1. CSA1 required the highest amount of water to achieve a flow value of 110 ± 5 for both mixtures.

4.2.3 Influence of Fine Aggregate Type on RSHC Mortar Flow (Mixture Series 3 & 4)

Table 4.3 shows the amount of HRWR required to reach the flow of 110 ± 5 as specified by ASTM C1600.

Table 4.3: Amount of HRWR flow requirements for both Ottawa sand and river sand

Cement	Amount of HRWR (%weight of cement)	
	Standard Ottawa Sand	Natural River Sand (FA1)
CAC	3.0%	1.0%
CSA1	7.5%	3.0%
CSA2	2.0%	0.75%
CAC-B1	6.0%	1.5%
CSA2-B1	6.0%	1.5%
CSA2-B2	7.5%	1.75%
PCSA1	7.0%	1.5%
PCSA2	5.0%	0.75%
CSA1-OPC2	6.0%	1.5%
CAC-OPC2	7.5%	2.0%

* c/s ratio 1:2.75, W/C ratio 0.350 for both standard Ottawa sand and river sand

Table 4.3 shows that the amount of HRWR varied significantly for river sand and standard Ottawa sand. Most of the cements required 1% - 2% HRWR when mixed with river sand except CSA1, in which it required 3% of HRWR. On the other hand, mixtures with standard Ottawa sand containing CSA1, CSA2-B2, and CAC-OPC2 required 7.5% of HRWR. It is likely that the contributing factors to these variations are the particle size distribution and fineness of the river sand and Ottawa sand.

4.2.4 Influence of W/C Ratio on RSHC Mortar Flow (Mixture Series 3 & 5)

In addition to the aforementioned tests, the influence of W/C ratios on the requirement of HRWR to achieve the required flow values were investigated. The results are shown in Table 4.4.

Table 4.4: Comparison of required amount of HRWR at two different W/C ratio

Cement	Ottawa Sand Amount of HRWR (%cement by mass) (W/C = 0.350) *	Ottawa Sand Amount of HRWR (% cement by mass) (W/C = 0.485) *
CAC	3.0%	1.5%
CSA1	7.5%	4.5%
CSA2	2.0%	0.5%
CAC-B1	6.0%	0.75%
CSA2-B1	6.0%	1.5%
CSA2-B2	7.5%	1.0%
PCSA1	7.0%	2.0%
PCSA2	5.0%	0.5%
CSA1-OPC2	6.0%	1.0%
CAC-OPC2	7.5%	1.5%

* c/s ratio was 1:2.75 for both cases

The results from Table 4.4 indicates that as W/C increased the required amount of HRWR decreased, which is expected. Like all other flow test results, CSA1 required a high amount of HRWR to achieve the flow, since this cement is extremely fast setting. For the remaining cements, the required amount of HRWR was in between 0.5%-2%.

4.3 ISOTHERMAL CALORIMETRY

4.3.1 Background

For OPCs, the heat evolution normally continues for several days. If SCMs are added to the mixture, this duration may change. For RSHCs, the heat evolution generally occurs within 24 hours. The isothermal calorimetry test can help find the following parameters for different mixtures: 1) time to peak heat - the time at which the maximum point on the heat of hydration curve is reached, 2) the peak heat flow, and 3) total cumulative heat evolved - the area underneath the heat of hydration curve. The time to peak heat

flow gives an idea at which the material begins to develop mechanical properties or final setting time. Comparing this point can determine the "time window" that a material can be placed in the field. The total cumulative heat shows the total amount of energy the cement experiences during hydration, which can infer the temperature change of the structures built with the cement.

Isothermal calorimeters are normally temperature-controlled chambers that have a thermostat and heating and cooling fan to maintain the isothermal testing conditions. There are multiple small cells inside of the chamber and an aluminum mass is normally used in these chambers. These cells can be called as thermal heat sinks and cementitious samples are placed here in closed vials. These heat sinks are used to direct the heat flow outward through the bottom of the chamber by a Peltier solid state active heat pump. The isothermal calorimetry was used extensively in this study to investigate the time and shape of heat flow curves generated from the hydration of different sets of cement. The difference in the curves is noticeable with the addition of chemical admixtures (e.g., accelerators and retarders) at different dosages [4]. To evaluate the effect of curing temperature on hydration process, the isothermal calorimetry test was performed at 23°C and 38°C.

A total of seven different experimental mixtures were performed for all RSHCs and blends. The first mixture series were performed without any admixtures and using a W/C to obtain a flow value of 110 ± 5 as determined by varying the water content through trial-and-error (Table 4.2). Additionally, a c/s of 1:2.75 was used as prescribed in ASTM C109. The mixture proportions for the first mixture series are provided in Table 4.5 below.

Table 4.5: Mixture proportion of isothermal calorimetry test of the first mixture series

Cement	W/C	Cement (g)	Water (g)	Sand (g)
CAC	0.52	300	156	825
CSA1	1.00	300	300	825
CSA2	0.50	300	150	825
CAC-B1	0.53	300	159	825
CSA2-B1	0.51	300	153	825
CSA2-B2	0.63	300	189	825
PCSA1	0.51	300	153	825
PCSA2	0.50	300	150	825
CSA1-OPC2	0.54	300	162	825
CSA1-OPC2	0.50	300	150	825

The second series included the use of set control admixtures (retarder) and high-range water reducing (HRWR) agent to determine their impact on rate of hydration. In the second mixture series, a required

amount of HRWR was added to achieve a mortar flow value of 110 ± 5 (Table 4.3). Thereafter, citric acid was administered in the third and fourth mixture series in 0.5% incremental dosages (by weight of cement). Mixture proportion for these mixtures is presented in Table 4.6.

Table 4.6: Mixture proportion of isothermal calorimetry test with admixtures

Cement	W/C	HRWR (%weight of cement)	Set Retarder (% weight of cement)	Cement (g)	Water (g)	Sand (g)
CAC	0.35	3.0%	0%, 0.5%, 1.0%	300	105	825
CSA1	0.35	7.5%	0%, 0.5%, 1.0%	300	105	825
CSA2	0.35	2.0%	0%, 0.5%, 1.0%	300	105	825
CAC-B1	0.35	6.0%	0%, 0.5%, 1.0%	300	105	825
CSA2-B1	0.35	6.0%	0%, 0.5%, 1.0%	300	105	825
CSA2-B2	0.35	7.5%	0%, 0.5%, 1.0%	300	105	825
PCSA1	0.35	7.0%	0%, 0.5%, 1.0%	300	105	825
PCSA2	0.35	0.75%	0%, 0.5%, 1.0%	300	105	825
CSA1-OPC2	0.35	1.5%	0%, 0.5%, 1.0%	300	105	825
CSA1-OPC2	0.35	1.5%	0%, 0.5%, 1.0%	300	105	825

4.3.2 Heat Flow (mW/g) of Samples

The heat flow measurement is the most common method to assess the hydration process of different mixtures. The heat flow sensors located underneath each sample record the heat flow. The sensors work by recording the voltage of the difference in heat across one known sensor, which is directly below the sample, and another sensor in an ambient condition. This voltage is then converted to a power normally in milliwatts (mW). This power reading is then normalized per gram of the sample material. Heat flow curves generated by isothermal calorimetry for different cements generally are characterized by an initial peak due to material dissolution, followed by an induction period and then a single sharp peak that occurs within the first hours of hydration that indicates the massive precipitation of hydrates. The first peak due to dissolution was not recorded in this study because it took five minutes (or less) after mixing for all the mixtures to transfer the sample to vials.

4.3.3 Isothermal Calorimetry Test at 23°C

The results of the isothermal calorimetry tests for the straight CSA1 mixtures are shown in Figure 4.1 and Table 4.7.
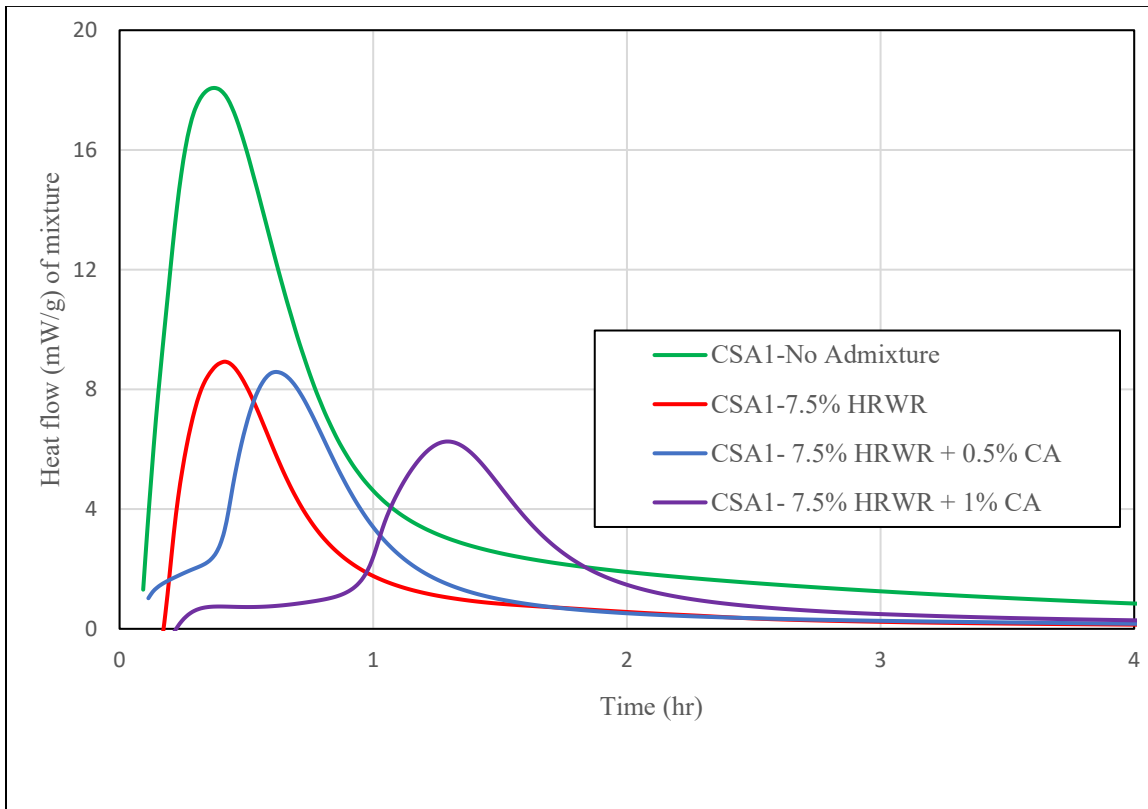
Figure 4.1: Isothermal Calorimetry Test of CSA1 at 23°C

Table 4.7: Peak heat flow and time until peak heat flow for CSA1

Mixture No.	Temperature	Avg. Peak Heat Flow (mW/g of mixture)	Avg. Time until Peak Heat Flow (h)
CSA1-No Admixture	23°C	17.97	0.343
CSA1-7.5% HRWR	23°C	8.88	0.43
CSA1-7.5% HRWR+0.5% CA	23°C	8.56	0.63
CSA1-7.5% HRWR+1% CA	23°C	6.25	1.29

Figure 4.1 and Table 4.7 illustrate that without any set control admixtures CSA1 produces high amounts of heat within a short period. However, with the addition of HRWR and set retarder, the peak heat flow decreases and the average time to reach the peak heat flow increases. The highest dormant period of 90 minutes was achieved for CSA1 with an addition of 1% set retarder. From Table 4.7, the peak heat flow was not affected much with an addition of set retarder when compared to the mixture with HRWR only.

The results of the isothermal calorimetry tests for the straight CSA2 mixtures are shown in Figure 4.2 and Table 4.8.

41
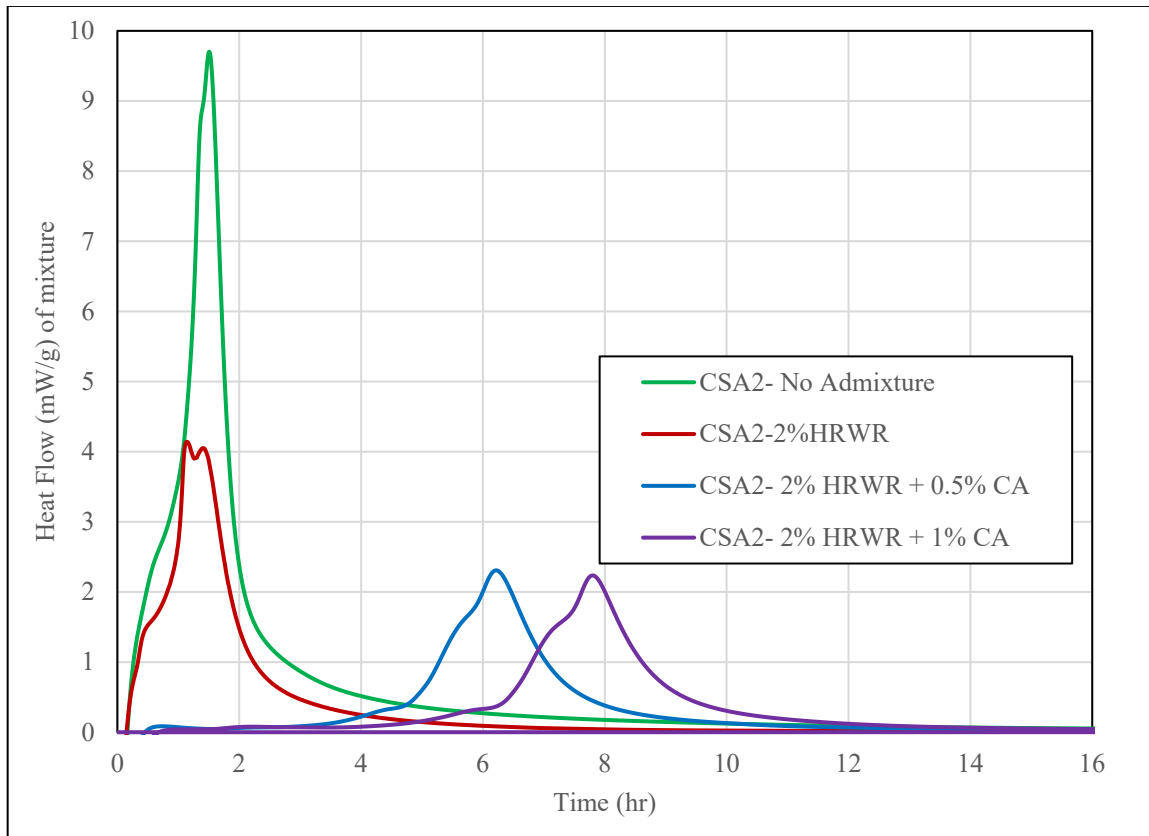
Figure 4.2: Isothermal Calorimetry Test of CSA2 at 23°C

Table 4.8: Peak heat flow and time until peak heat flow for CSA2

Mixture No.	Temperature	Avg. Peak Heat Flow (mW/g of mixture)	Avg. Time until Peak Heat Flow (h)
CSA2-No Admixture	23°C	9.63	1.48
CSA2-2% HRWR	23°C	4.12	1.12
CSA2-2% HRWR+0.5% CA	23°C	2.29	6.26
CSA2-2% HRWR+1% CA	23°C	2.29	7.85

From Figure 4.2 and Table 4.8, a six-to-seven-hour dormant period was achieved with the addition of HRWR and the set control admixtures. The peak heat flow was reduced up to 50% with an addition of 0.5% set retarder. However, with 1% set retarder, the peak heat flow remained the same. Table 4.8 also shows that without any set control admixtures the average time to reach the peak flow is very fast (within an hour and half). Based on the results, CSA2 may be more suitable for mass concrete infrastructures over OPC due to its lower peak heat flow and a dormant period of six hours.

The results of the isothermal calorimetry tests for the CSA2-B1 are shown in Figure 4.3 and Table 4.9.
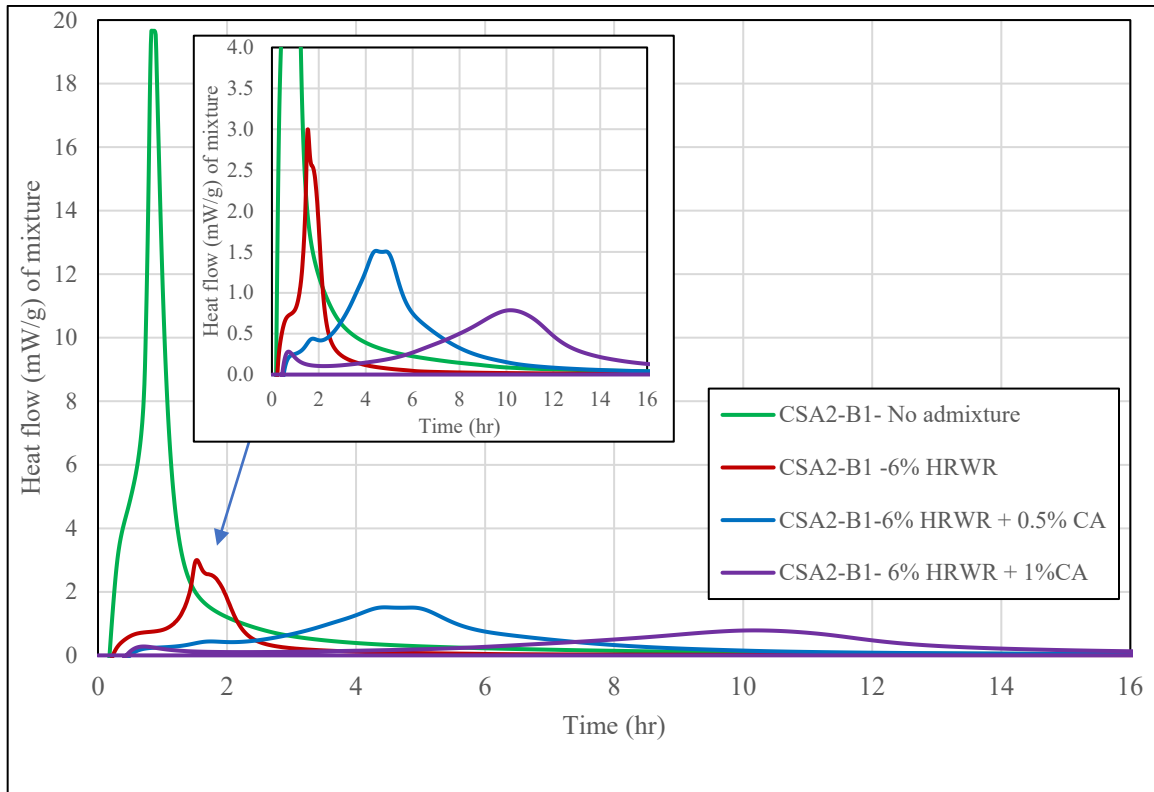
Figure 4.3: Isothermal Calorimetry Test of CSA2-B1 at 23°C

Table 4.9: Peak heat flow and time until peak heat flow for CSA2-B1

Mixture No.	Temperature	Avg. Peak Heat Flow (mW/g of mixture)	Avg. Time until Peak Heat Flow (h)
CSA2-B1-No Admixture	23°C	19.65	0.82
CSA2-B1-6% HRWR	23°C	2.95	1.51
CSA2-B1-6% HRWR+0.5% CA	23°C	1.51	4.72
CSA2-B1-6% HRWR+1% CA	23°C	0.76	10.58

From Figure 4.3 and Table 4.9, the result clearly depicts that like the other two CSA cements, the average peak heat flow of CSA2-B1 is very high and the average time to obtain the peak heat flow is very short, without any set control admixtures. However, with an addition of HRWR and set retarder, the peak heat flow decreased up to one sixth when compared to the case without any admixtures. It is also found that with 0.5% set retarder the average time to obtain the peak heat flow is 4.72 hours, while with 1% set retarder the value is 10.58 hours.

The results of the isothermal calorimetry tests for the CSA2-B2 are shown in Figure 4.4 and Table 4.10.

43
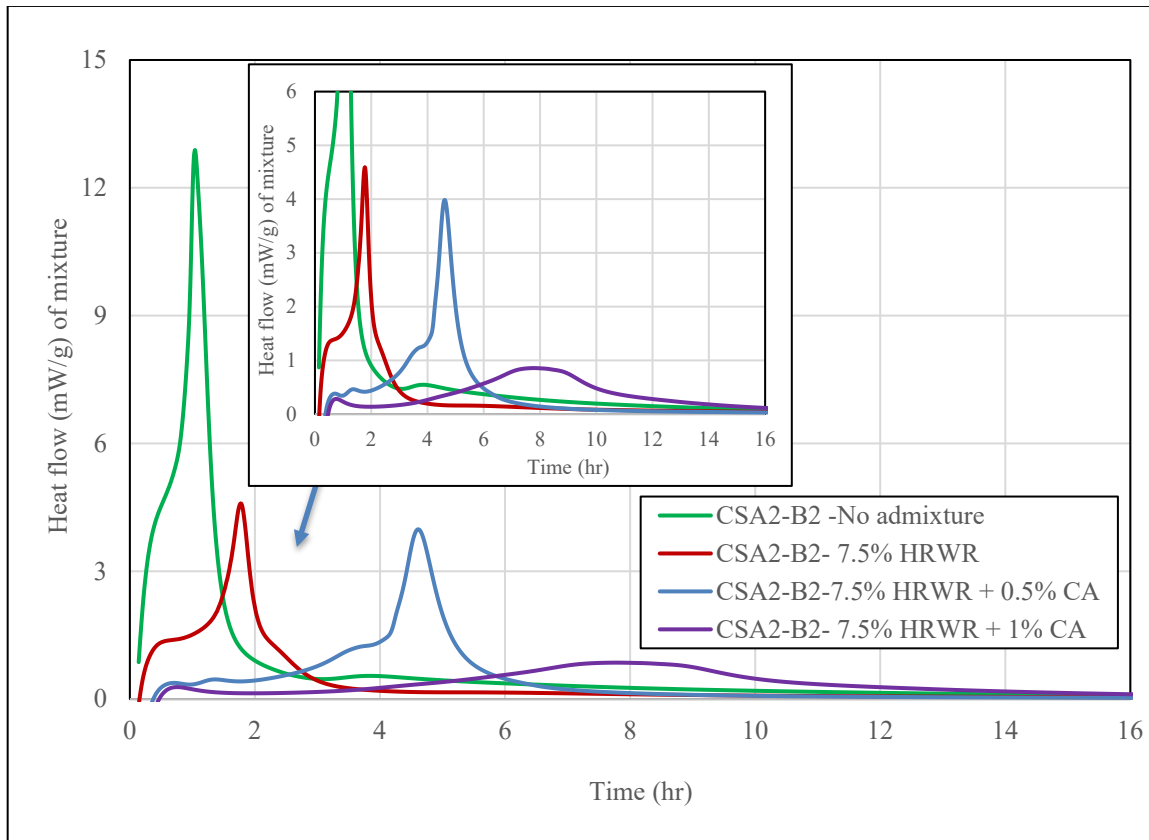
Figure 4.4: Isothermal Calorimetry Test of CSA2-B2 at 23°C

Table 4.10: Peak heat flow and time until peak heat flow for CSA2-B2

Mixture No.	Temperature	Avg. Peak Heat Flow (mW/g of mixture)	Avg. Time until Peak Heat Flow (h)
CSA2-B2-No Admixture	23°C	12.73	1.02
CSA2-B2-7.5% HRWR	23°C	4.59	1.77
CSA2-B2-7.5% HRWR+0.5% CA	23°C	3.95	4.64
CSA2-B2-7.5% HRWR+1% CA	23°C	0.85	7.85

CSA2-B2 is a proprietary blended cement. From Figure 4.4 and Table 4.10, the mixture with HRWR and 0.5% of set retarder performed better than all other mixtures (based on peak heat flow and time until peak heat flow), where the set retarder effectively extended the dormant period up to 4.64 hours.

The results of the isothermal calorimetry tests for the laboratory blend CSA cement (CSA1-OPC2) mixtures are shown in Figure 4.5 and Table 4.11.
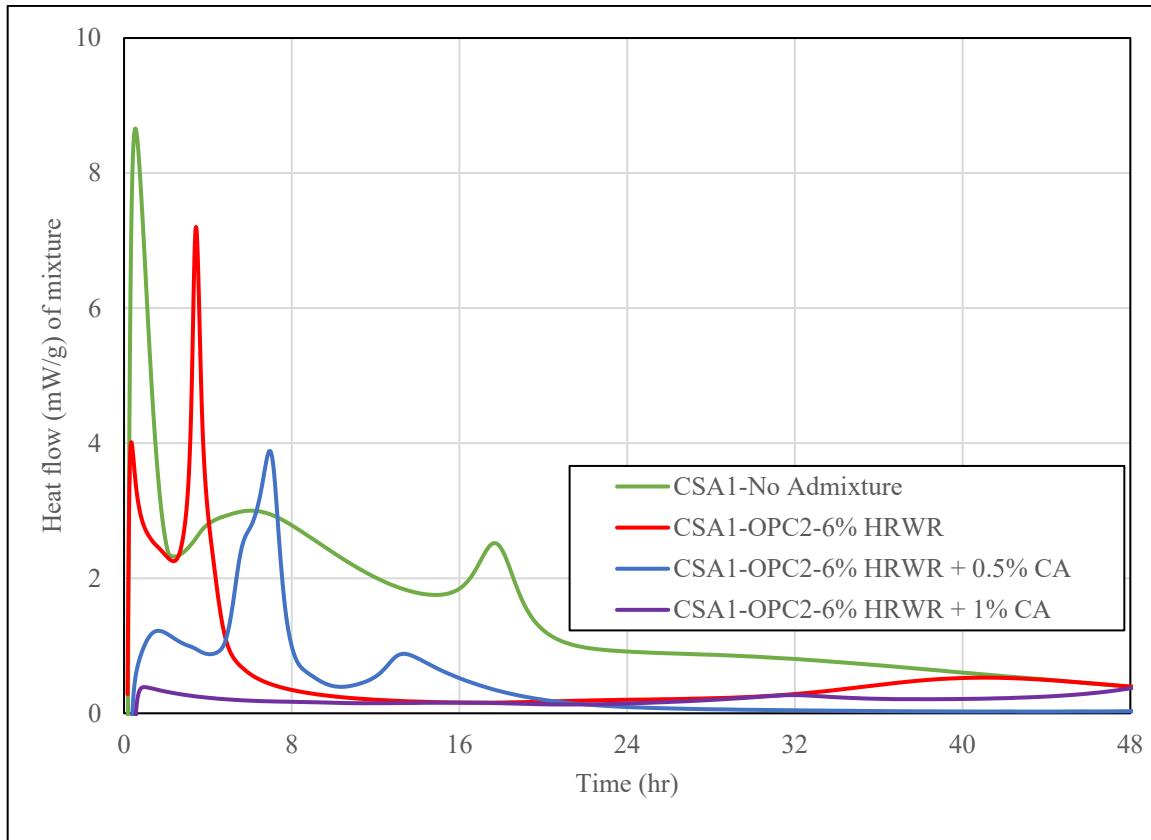
Figure 4.5: Isothermal Calorimetry Test of CSA1-OPC2 at 23°C

Table 4.11: Peak heat flow and time until peak heat flow for CSA1-OPC2

Mixture No.	Temperature	Avg. Peak Heat Flow (mW/g of mixture)	Avg. Time until Peak Heat Flow (h)
CSA1-OPC2-No Admixture	23°C	0.357	2.096
CSA1-OPC2-7.5% HRWR	23°C	3.43	1.82
CSA1-OPC2-7.5% HRWR+0.5% CA	23°C	0.93	6.98
CSA1-OPC2-7.5% HRWR+1% CA	23°C	0.146	51.02

Recall that the CSA1-OPC2 system is a lab blended cement containing 25% CSA and 75% OPC2. From Figure 4.5 and Table 4.11, the set control admixture affected the hydration process adversely. With an addition of 1% set retarder, the dormant period was extended out to over 51 hours which essentially did not set at all. On the other hand, with 0.5% set retarder the dormant period was only 7 hours indicating the very high sensitivity of the mixture to citric acid. Additionally, a secondary peak is also noticeable in most of the CSA-OPC2 mixtures. This second peak is likely attributed from the hydration of calcium

silicates in the ordinary portland cement in the blend. However, the timing and amount of heat release is very sensitive to the amount and type of admixture included in the mixture.

The results of the isothermal calorimetry tests for the PCSA1 are shown in Figure 4.6 and Table 4.12.
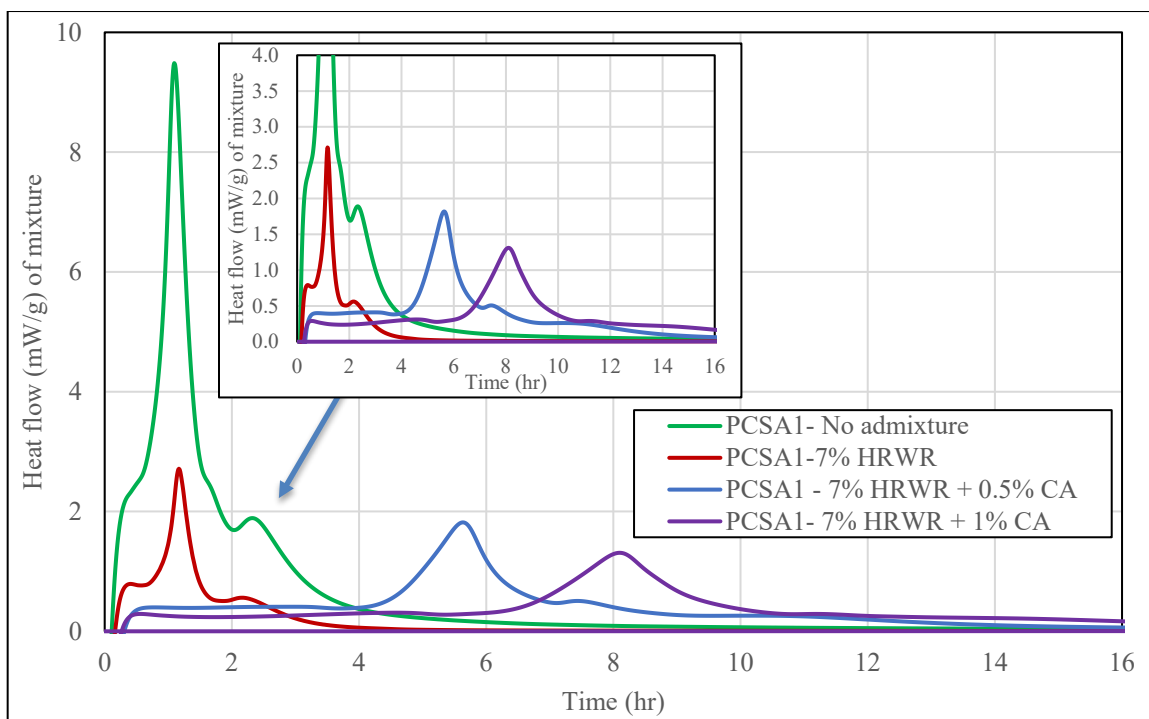
Figure 4.6: Isothermal Calorimetry Test of PCSA1 at 23°C

Table 4.12: Peak heat flow and time until peak heat flow for PCSA1

Mixture No.	Temperature	Avg. Peak Heat Flow (mW/g of mixture)	Avg. Time until Peak Heat Flow (h)
PCSA1-No Admixture	23°C	9.05	1.05
PCSA1-7% HRWR	23°C	2.81	1.21
PCSA1-7% HRWR+0.5% CA	23°C	1.79	5.69
PCSA1-7% HRWR+1% CA	23°C	1.31	8.08

PCSA1 is another proprietary RSHC blend. From Figure 4.6 and Table 4.12, the addition of HRWR and citric acid slowed the hydration process down. Citric acid effectively extended the average peak heat flow up to 5.69 hours with 0.5% addition and 8.08 hours with 1% addition. The results also illustrate that without any set retarder the average time for peak heat flow is 1.21 hours.

The results of the isothermal calorimetry tests for the PCSA2 mixtures are shown in Figure 4.7 and Table 4.13.
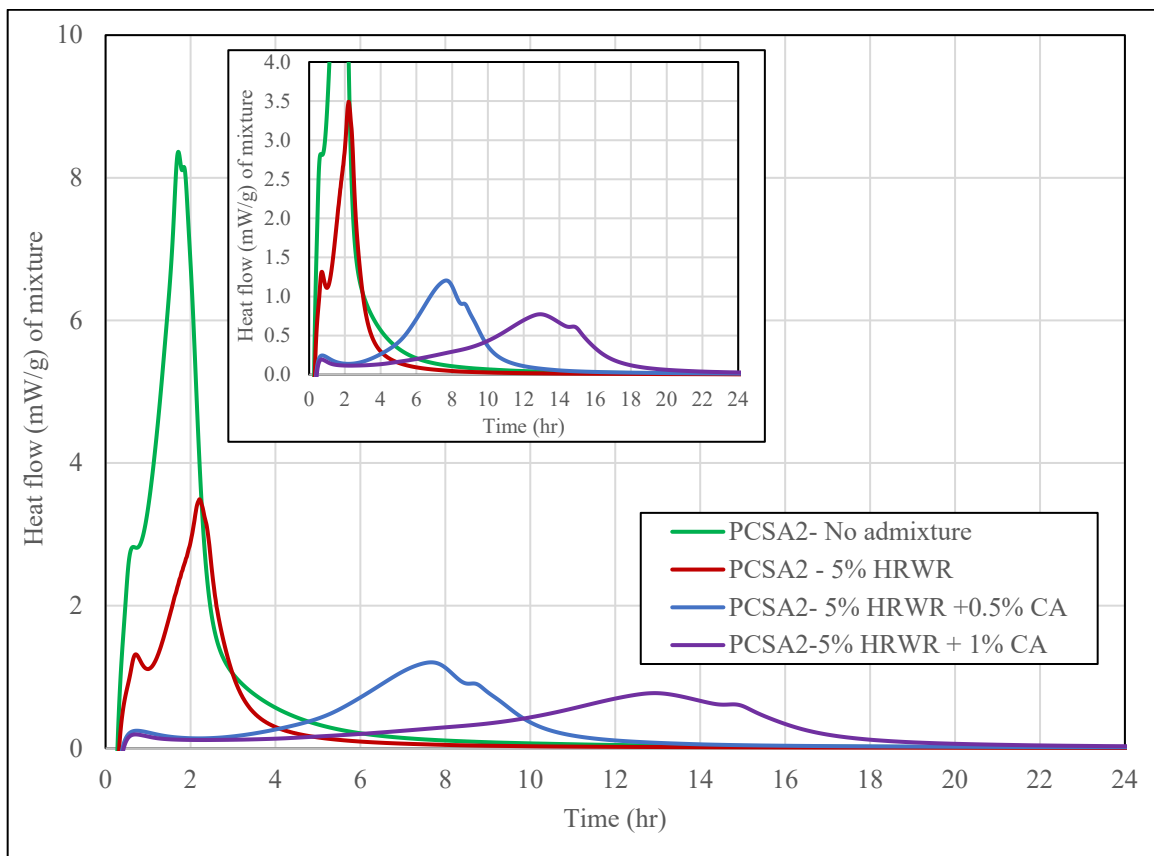
Figure 4.7: Isothermal Calorimetry Test of PCSA2 at 23°C

Table 4.13: Peak heat flow and time until peak heat flow for PCSA-2

Mixture No.	Temperature	Avg. Peak Heat Flow (mW/g of mixture)	Avg. Time until Peak Heat Flow (h)
PCSA2-No Admixture	23°C	8.12	1.66
PCSA2-5% HRWR	23°C	3.6	2.21
PCSA2-5% HRWR+0.5% CA	23°C	1.21	7.63
PCSA2-5% HRWR+1% CA	23°C	0.76	13.19

The test results from Figure 4.7 and Table 4.13 indicate that high dosage set retarder affected the PCSA2 hydration process negatively. With an addition of 1% set retarder, the average time for peak heat flow was extended up to 13.19 hours. It was also observed that HRWR did not affect the hydration time to a great degree. The results also illustrate that an average time to peak heat flow of 7.63 hours, suggesting a proper induction period was possible with an addition of 0.5% citric acid.

The results of the isothermal calorimetry tests for the CAC-B1 mixtures are shown in Figure 4.8 and Table 4.14.
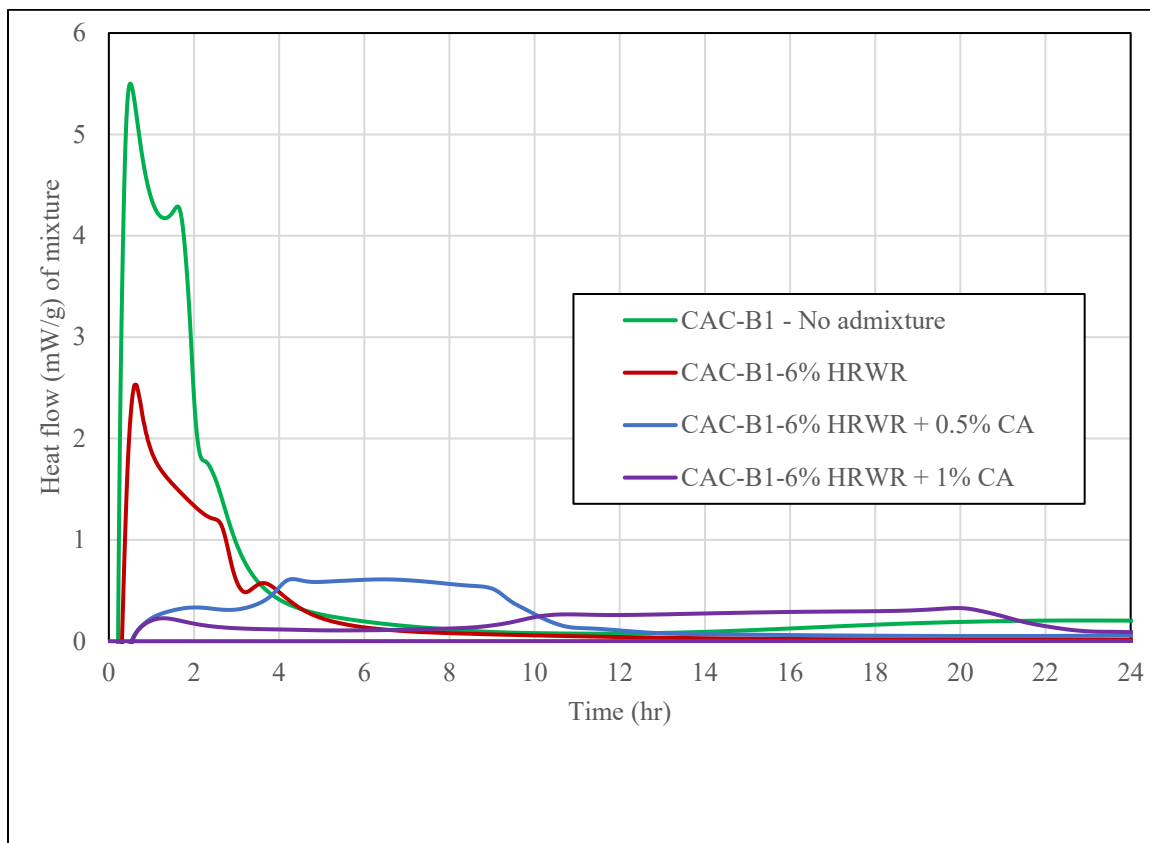
Figure 4.8: Isothermal Calorimetry Test of CAC-B1 at 23°C

Table 4.14: Peak heat flow and time until peak heat flow for CAC-B1

Mixture No.	Temperature	Avg. Peak Heat Flow (mW/g of mixture)	Avg. Time until Peak Heat Flow (h)
CAC-B1-No Admixture	23°C	5.28	0.43
CAC-B1-6% HRWR	23°C	2.84	0.57
CAC-B1-6% HRWR+0.5% CA	23°C	0.59	4.17
CAC-B1-6% HRWR+1% CA	23°C	0.31	20.56

Recall that CAC-B1 mixture is a proprietary ternary blended system consisting of CAC, calcium sulfate, and portland cement. From the Figure 4.8 and Table 4.14, the addition of HRWR did not affect the time of the peak heat flow. However, with an addition of 1% set retarder, the average time of the peak heat flow was extended up to 20.56 hours. The potency of high dosage citric acid is quite evident in the CAC-

B1 cement. The mixture with an addition of 0.5% set retarder performed better than other four mixtures based on induction period and peak heat flow.

The results of the isothermal calorimetry tests for the CAC-OPC2 mixtures can be seen in Figure 4.9 and quantified in Table 4.15.
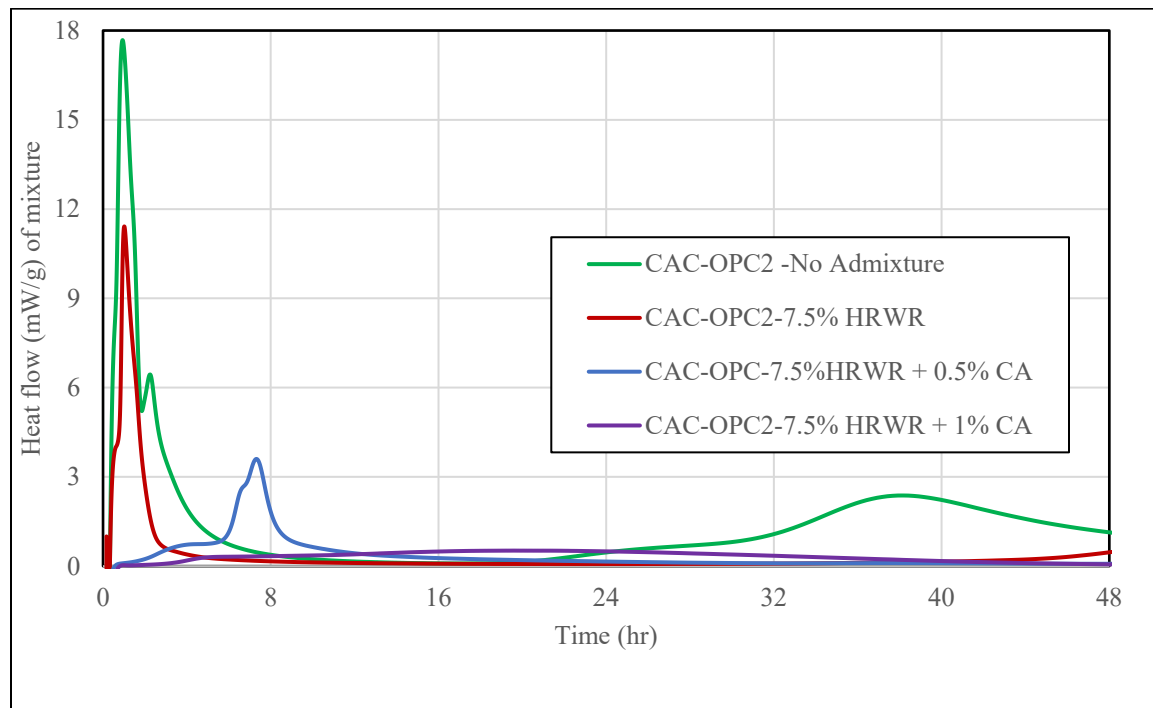
Figure 4.9: Isothermal Calorimetry Test of CAC-OPC2 at 23°C

Table 4.15: Peak heat flow and time until peak heat flow for CAC-OPC2

Mixture No.	Temperature	Avg. Peak Heat Flow (mW/g of mixture)	Avg. Time until Peak Heat Flow (h)
CAC-OPC2-No Admixture	23°C	4.38	0.95
CAC-OPC2-7.5% HRWR	23°C	2.79	1.01
CAC-OPC2-7.5% HRWR+0.5% CA	23°C	0.907	7.42
CAC-OPC2-7.5% HRWR+1% CA	23°C	0.12	56.62

Recall that CAC-OPC2 is a laboratory blended cement containing 25% CAC and 75% OPC2. The results indicate that with an addition of 1% set retarder the average time for peak heat flow was extended up to 56.62 hours. With 0.5% set retarder the time for peak heat flow was 7.42 hours.

The results of the isothermal calorimetry tests for straight CAC1 mixtures are shown in Figure 4.10.
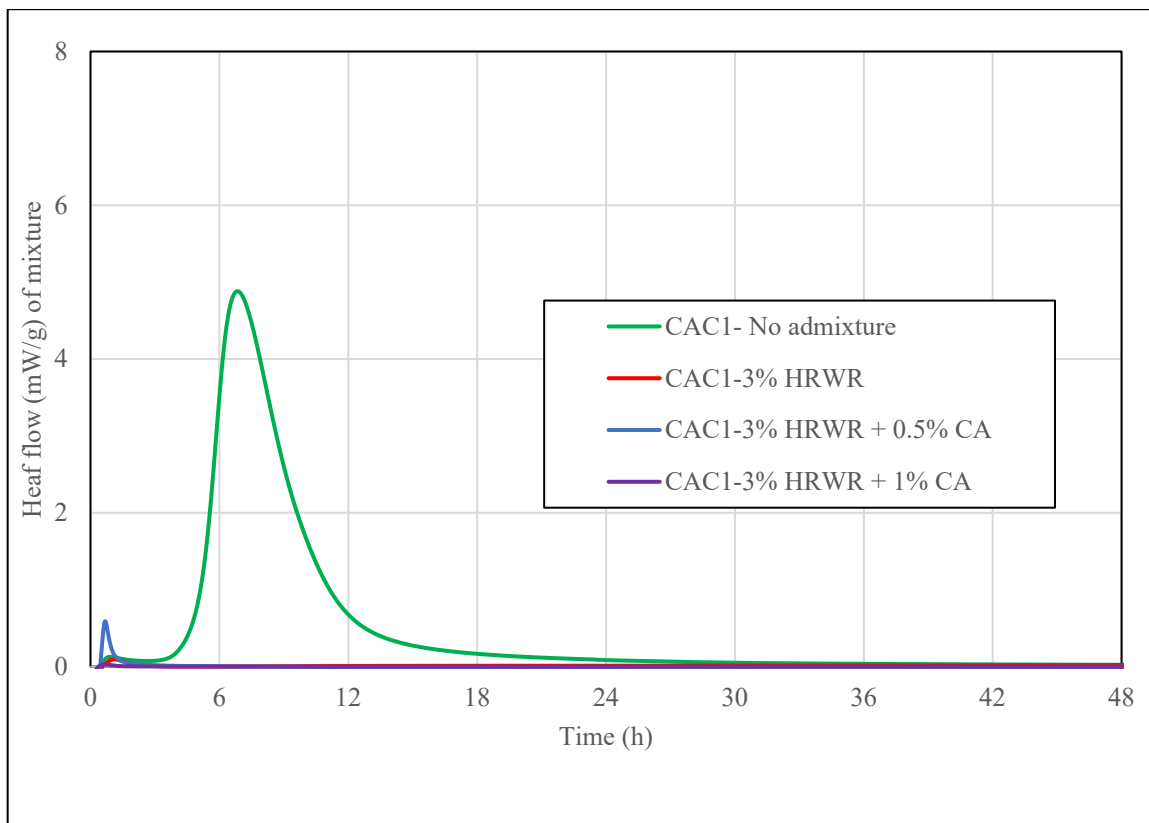
Figure 4.10: Isothermal Calorimetry Test of CAC at 23°C

From Figure 4.10, the results are different than expected since there is little heat flow from the mixtures containing citric acid. With no admixtures, CAC hydration process was fast, but admixtures terminated the hydration process up to 48 hours. Set control admixtures HRWR and citric acid were found to adversely affect the hydration process of CAC cements.

In conclusion, with the addition of HRWR and set retarder, the peak heat flow and hydration process were delayed and diminished for all RSHCs. The admixture affect is more significant for CACs compared to CSA based cements. The set retarder significantly reduced the peak heat flow for the laboratory blended cements that contain 75% OPC2. The peak heat flow of the CSA cement systems was higher compared to the CAC systems. Among five different types of CSA cements investigated, CSA2 appears to be best cement option for large scale construction given its satisfactory heat of hydration performance.

4.3.4 Isothermal Calorimetry Test at 38°C

In order to investigate the impact of curing temperatures on the heat of hydration, the isothermal calorimetry test was performed at 38°C with and without any set retarder. The results for all the RSHCs and blends are shown in Figures 4.11, 4.12 and Table 4.16.
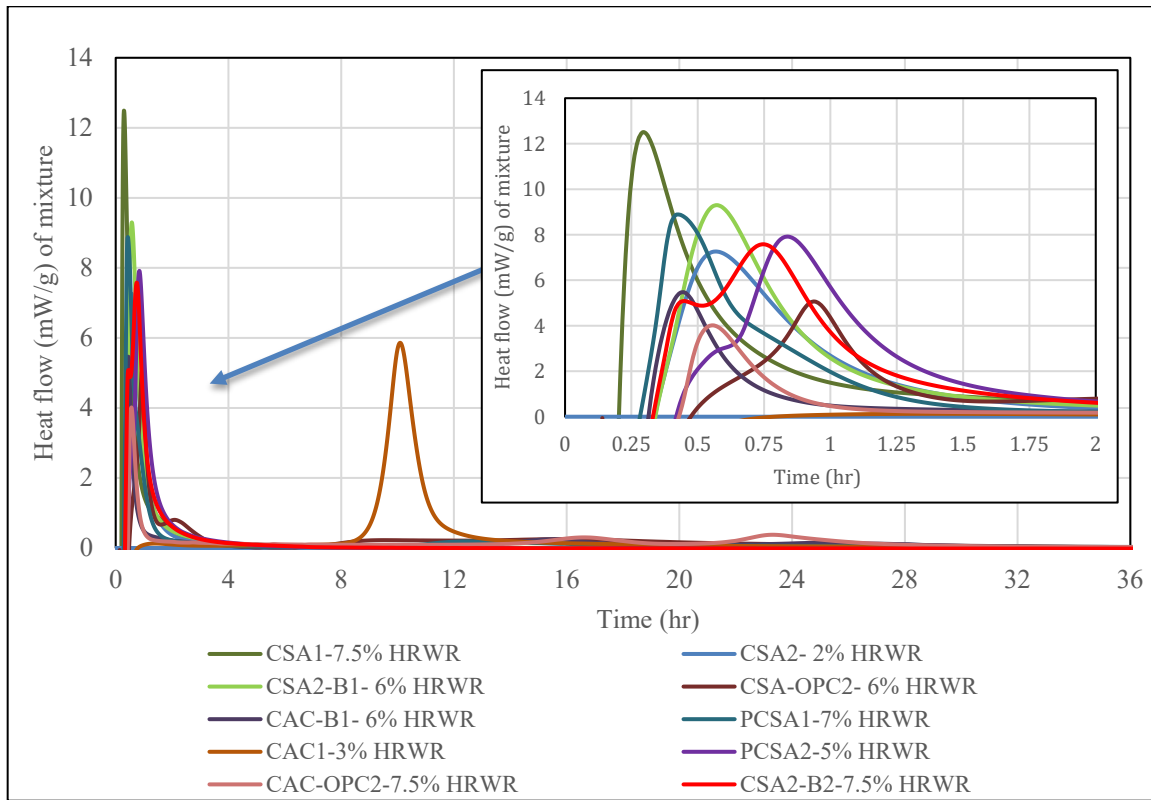
Figure 4.11: Isothermal calorimetry test for all cements at 38°C
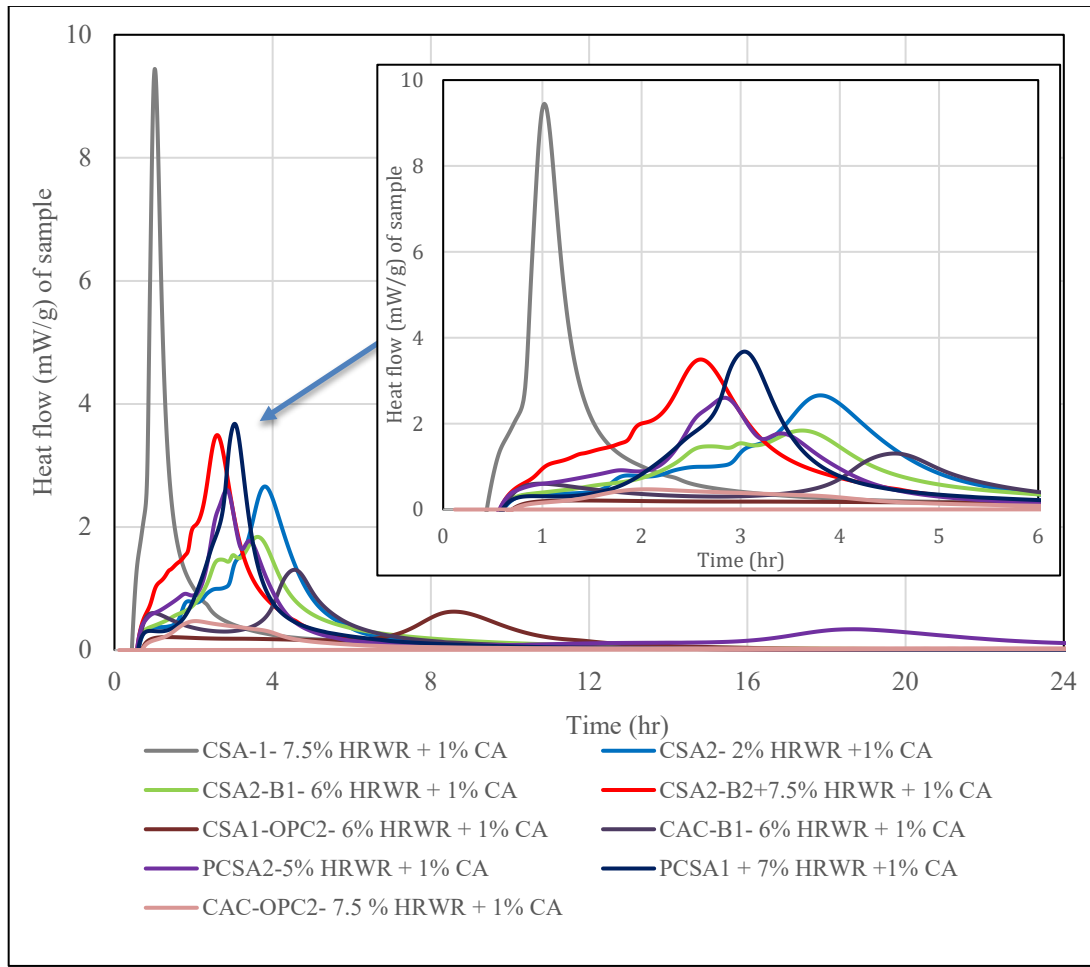
Figure 4.12: Isothermal Calorimetry test for all cements at 38°C with 1% set retarder

Table 4.16: Peak heat flow and time until peak heat flow for all cements at 38°C

Cement	Without any set retarder		With 1% set retarder	
	Avg. Peak Heat Flow (mW/g of mixture)	Avg. Time until Peak Heat Flow (hour)	Avg. Peak Heat Flow (mW/g of mixture)	Avg. Time until Peak Heat Flow (h)
CSA1	12.41	0.31	9.39	1.03
CSA2	7.25	0.57	2.65	3.79
CSA2-B1	9.29	0.57	1.82	3.69
CSA2-B2	11.44	0.31	3.48	2.62
CSA1-OPC2	5.06	0.94	0.62	8.68
PCSA1	8.88	0.43	3.65	2.79
PCSA2	7.88	0.82	2.54	3.01
CAC-B1	5.43	0.43	1.3	4.53
CAC-OPC2	3.95	0.57	Did not set	Did not set

The results show that at 38°C without any set retarder, the average time of peak heat flow is less than 1 hour for all the cements. This confirms that the reaction rate is very fast compared to the curing temperature of 23°C. However, 1% set retarder did not affect the average peak heat flow significantly for CSA and CSA2-B2. For CSA2, the time extended approximately 4 hours. The set retarder did not adversely affect the CSA1-OPC2 blended cement like it did at 23°C. The average time for peak heat flow for CAC-OPC2 was 0.57 hour. However, with an addition of 1% set retarder, no peak was observed within 48 hours of hydration time of CAC-OPC2. Figure 4.12 illustrates that the average time for peak heat flow for CAC was extended up to 10 hours when there is no set retarder. This implies that the effect of HRWR is quite significant in both curing temperatures investigated for CACs. The results also showed that the average peak heat flow for all the cements except CSA1 was reduced considerably with 1% set retarder. Table 4.16 clearly illustrates that the reaction rate was lower for both the CSA and CAC systems that contain set retarders.

4.3.5 Isothermal Calorimetry Test at Different c/s Ratio

In order to investigate the impact of the amount of sand used on the heat of hydration, additional samples with a c/s ratio of 1:2 were investigated. This was done to determine if the additional sand in the sample would affect the heat of hydration due to an increase in nucleation sites for hydration products. The results are shown in Figure 4.13 and Table 4.17.
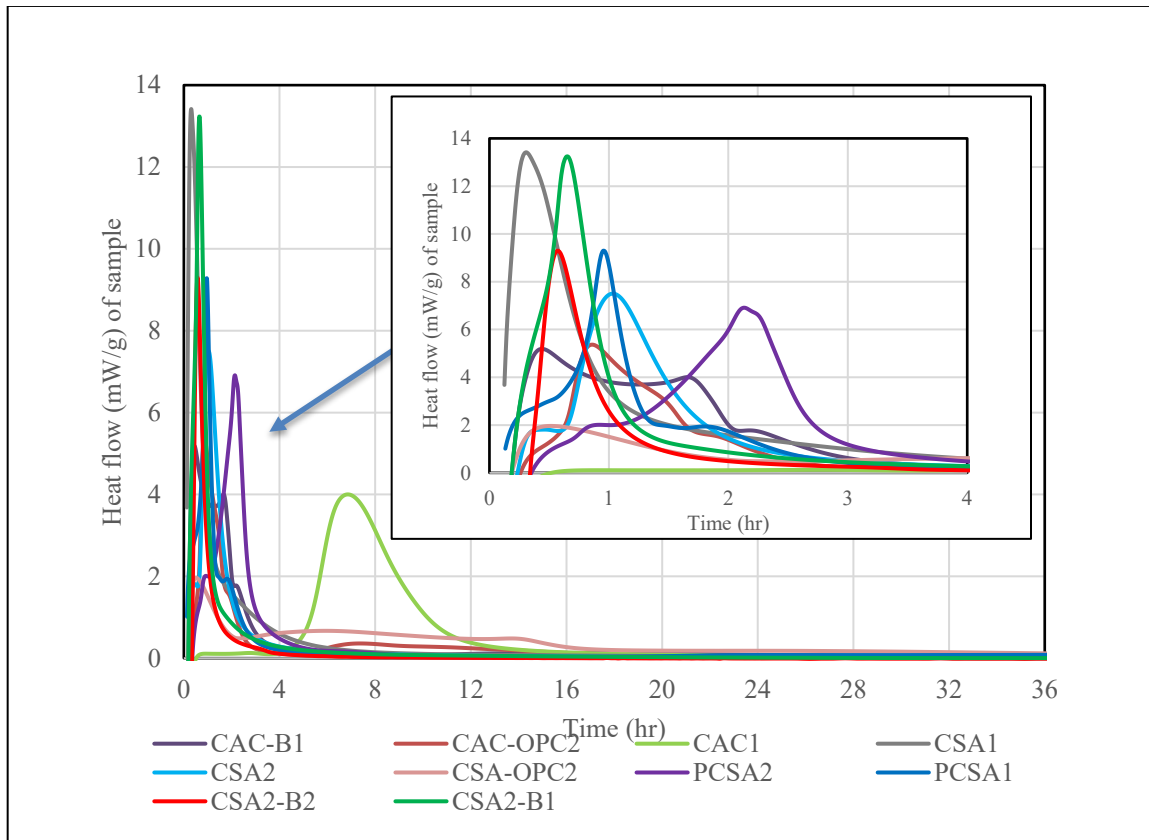
Figure 4.13: Isothermal Calorimetry test at c/s ratio 1:2

Table 4.17: Peak heat flow and time until peak heat flow for all cements at c/s ratio 1:2

Cement	Avg. Peak Heat Flow (mW/g of mixture)	Avg. Time until Peak Heat Flow (h)
CSA1	13.35	0.36
CSA2	7.42	0.99
CSA2-B1	13.23	0.67
CSA2-B2	9.71	0.54
CSA-OPC2	1.95	0.46
PCSA1	9.07	0.98
PCSA2	6.91	2.31
CAC-B1	5.06	0.48
CAC-OPC2	5.27	0.90

The isothermal calorimetry test was performed at a c/s ratio of 1:2 with a varying water content to achieve the specified flow without any set control admixture. Here, the power reading is normalized per gram of the sample material. For an equal comparison with other mixtures having a c/s of 1:2.75, the values were multiplied by 1.375 (= 2.75/2). From the results, the induction period was extended when less sand was included in the mixture.

4.4 COMPRESSION TEST

To assess the compressive strength of the RSHCs and blends, mortar mixtures (cement, fine aggregate, and water) were prepared following the procedure in ASTM C109[2]. ASTM C109 specifies mixture proportions for casting 50 mm mortar cube samples for determining compressive strength. The mixture proportions are based on an OPC at a W/C = 0.485 and a c/s ratio of 1:2.75. Table 4.18 provides the basic mixture proportions as described in ASTM C109 for casting 18 cubes. ASTM C109 also specifies that the amount of mixing water for mixtures other than OPC (i.e., rapid setting cements) will be such that to produce a flow of 110 ± 5 following ASTM C1437. Four different experimental mix matrixes were considered for all RSHCs and blends.

Table 4.18: Quantities of materials for batch for cube compression test

W/C = 0.485 for OPC2 c/s = 1:2.75	
Number of specimens	18 Cubes
Cement	1480 g
Sand	4070 g
Water (for OPC2)	718 g

The first mixture series were designed at a c/s ratio of 1:2.75 and a varying water content for RSHCs and blends. Mixture proportions are presented in Table 4.19. The required water amount was obtained from the previously completed flow test (see Table 4.2). No admixtures (i.e., HRWR or set controlling) were added in the mixtures. The compressive strength was performed at the ages of 1.5 hours, 3 hours, 6 hours, 24 hours, 7 days and 28 days.

Table 4.19: Mixture proportions of cube compression test for the first mixture series

Cement	W/C to achieve mortar flow of 110 ± 5	Cement (g)	Water (g)	Sand (g)
CAC	0.52	1480	770	4070
CSA1	1.00	1480	1480	4070
CSA2	0.50	1480	740	4070
CAC-B1	0.53	1480	784	4070
CSA2-B1	0.51	1480	755	4070
CSA2-B2	0.63	1480	932	4070
PCSA1	0.51	1480	755	4070
PCSA2	0.50	1480	740	4070
CSA1-OPC2	0.54	1480	799	4070
CSA1-OPC2	0.50	1480	740	4070

The results of the mortar cube compressive strength tests including the resulting W/C for each mixture is presented in Figure 4.14.
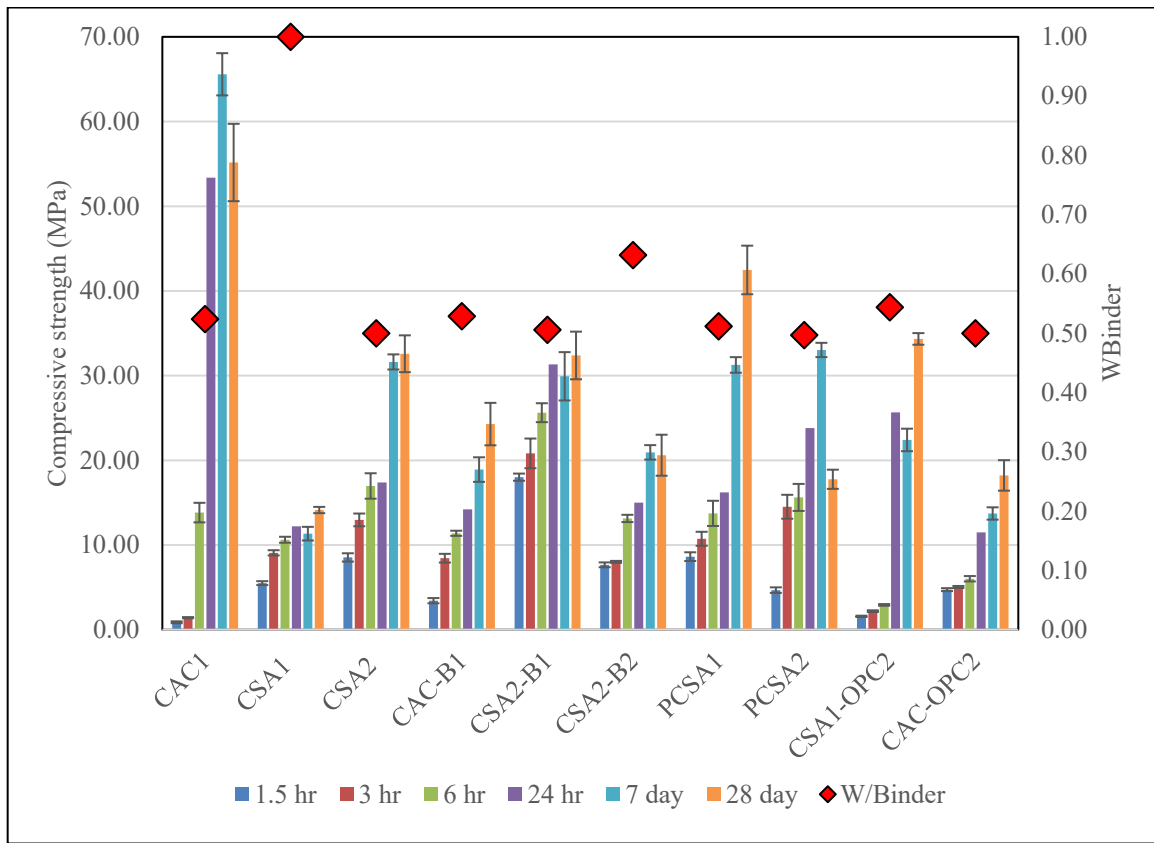
Figure 4.14: Compressive strength of all the cements at different curing ages

The first set of mixtures were performed without adding any set control admixtures. The W/C varied for each cement (shown in Figure 4.14) because the required amount of water is different for each cement to achieve the specified mortar flow value from ASTM C109[2]. Figure 4.14 also shows the difference in early age strength gain of different RSHCs. Without any admixture and within six hours of hydration, almost all the rapid setting cements achieved more than 10 MPa in compressive strength. Though CSA1 is a very fast setting cement, with a W/C ratio of 1.00 the early age strength gain was relatively lower than other rapid setting cements. The straight CAC cement early age strength gain was higher than any other cements, which was approximately 65.50 MPa. The two laboratory blended cements behaved similarly to OPC2 since 75% of the cementitious material is OPC2. Another important finding from the test results is that the 28-day strength was lower for CAC1 likely due to the potential of conversion common in CACs.

The second mixture series were designed at a cement to sand ratio (c/s) of 1:2 and a varying water content required to achieve the flow outlined in ASTM C1437. Table 4.20 represents the mixture proportions of the second mixture series. The required water amount was obtained from the previously completed flow test (see Table 4.2), and the W/C ratio was also presented for each RSHCs and blends in Table 4.20. The compressive strength was performed at the ages of 1.5 hours, 3 hours, 6 hours, 24 hours, 7 days, and 28 days.

Table 4.20: Mixture proportions of cube compression test for the second mixture series

Cement	W/C to achieve mortar flow of 110 ± 5	Cement (g)	Water (g)	Sand (g)
CAC	0.38	1480	562	2960
CSA1	0.88	1480	1302	2960
CSA2	0.36	1480	533	2960
CAC-B1	0.38	1480	562	2960
CSA2-B1	0.35	1480	518	2960
CSA2-B2	0.51	1480	755	2960
PCSA1	0.37	1480	548	2960
PCSA2	0.35	1480	518	2960
CSA1-OPC2	0.41	1480	607	2960
CSA1-OPC2	0.38	1480	562	2960

The results of the mortar cube compressive strength tests of the second mixture series are shown in Figure 4.15.
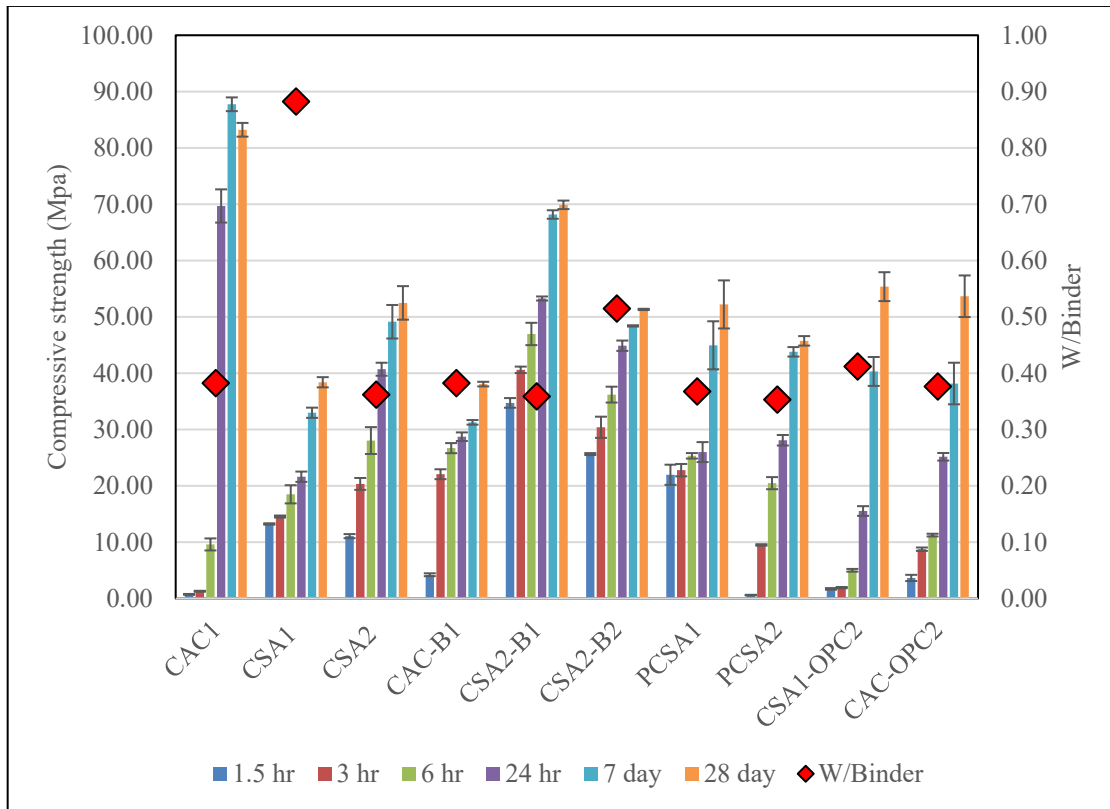
Figure 4.15: Compressive strength of all the cements at different hydration period

The results show that since the water requirement was lower compared to the first series, the compressive strength was higher for all RSHCs and blends in the second mixture series at all curing ages. CAC1 achieved approximately 70 MPa in compressive strength within 24 hours of hydration time. After 7 days of hydration, the strength reached 90 MPa. However, the 28-day strength was lower for CAC1 likely attributed to conversion. Just like in Series 1, CSA1's later age strength was lower compared to other CSA based cements because of the high W/C ratio of 0.88. Again, the results highlight the negative impact of high water requirement on compressive strength for these fast setting cements to achieve the specified flow. The CSA2 results were also consistent in terms of the strength gain. CSA2-B1's early age strength was the highest among all RSHCs and blends. Within 1.5 hours of hydration, CSA2-B1 was able to achieve a compressive strength of 35 MPa. CSA2-B2 was also able to achieve a high strength having more than 30 MPa by 1.5 hours of hydration. Between PCSA1 and PCSA2, PCSA2's early age strength gain was lower. Within 1.5 hour of hydration time, PCSA1 achieved more than 20 MPa in compressive strength. Another CAC mortar - CAC-B1- also achieved a high strength. The difference between CAC and CAC-B1 is that at an early age of 3 hours, CAC was not able to gain strength but CAC-B1 was able to gain strength of 22 MPa. Two laboratory blend RSHCs behaved similarly in terms of early age strength

gain. However, later age strength was high because 75% of the blend is OPC2 and between two laboratory blended RSHCs, CSA1-OPC2 later age strength is higher than CAC-OPC2.

As previously stated, additional sets of tests were performed on the samples whose W/C was held constant as 0.35 but the amount of HRWR varied to meet the flow requirement. The third and fourth mixture series were performed with set control admixtures at a fixed W/C 0.35 and c/s of 1:2.75 along with the HRWR dosage determined from the flow test (see Table 4.4). In the third mixture series, no citric acid was added. However, citric acid was administered at a dosage of 0.5% of cement weight in the fourth mixture series. Table 4.21 shows the mixture proportions with required amount of HRWR for each RSHCs and blends. The compressive strength was determined at the ages of 1.5 hours, 3 hours, 6 hours, 24 hours, 7 days and 28 days.

Table 4.21: Mixture proportions for cube compression test with set control admixtures

Cement	W/C	HRWR (% weight of cement)	Set Retarder (% weight of cement)	Cement (g)	Water (g)	Sand (g)
CAC	0.35	3.0%	0%, 0.5%	1480	518	4070
CSA1	0.35	7.5%	0%, 0.5%	1480	518	4070
CSA2	0.35	2.0%	0%, 0.5%	1480	518	4070
CAC-B1	0.35	6.0%	0%, 0.5%	1480	518	4070
CSA2-B1	0.35	6.0%	0%, 0.5%	1480	518	4070
CSA2-B2	0.35	7.5%	0%, 0.5%	1480	518	4070
PCSA1	0.35	7.0%	0%, 0.5%	1480	518	4070
PCSA2	0.35	0.75%	0%, 0.5%	1480	518	4070
CSA1-OPC2	0.35	1.5%	0%, 0.5%	1480	518	4070
CSA1-OPC2	0.35	1.5%	0%, 0.5%	1480	518	4070

The results of the mortar cube compressive strength tests of the third mixture series with HRWR are shown in Figure 4.16.
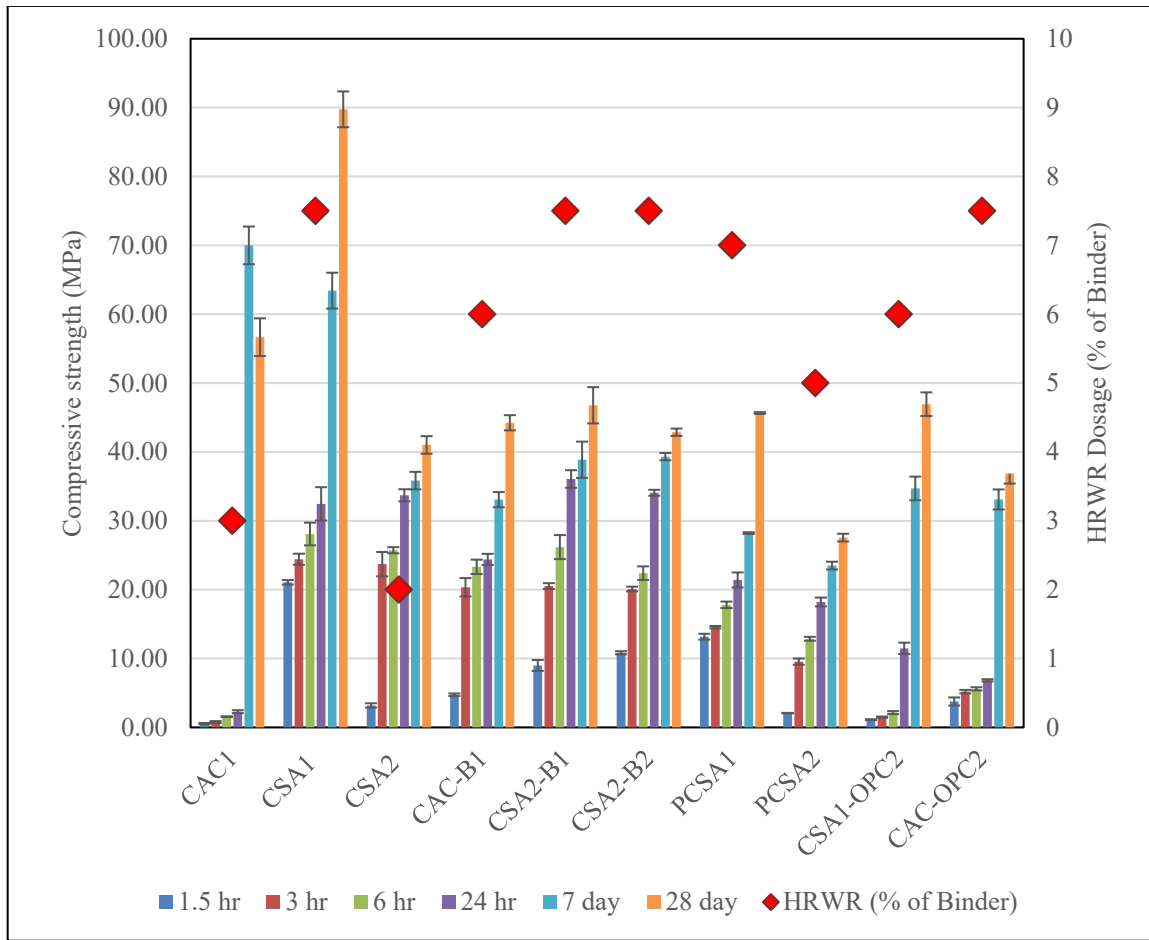
Figure 4.16: Compressive strength of all the cements with HRWR

The early age strength of CAC1 was severely negatively affected with the addition of HRWR. From the results, CAC's strength was high at 7-day and 28-day but almost non-existent prior to that. The straight CSA1 mixture had a high early age strength gain due to the low W/C ratio of 0.350 with required amount of HRWR, when compared to the W/C ratio of 1.0 and W/C ratio of 0.880 observed in the first and second mixture series, respectively. Within 90 minutes of hydration CSA1 achieved a compressive strength of 20 MPa. There was a sharp rise in compressive strength at 28 days (88 MPa). The CSA2's strength data was also consistent. The CSA2 blended mixtures (CSA2-B1 and CSA2-B2) achieved high strength. However, the addition of HRWR decreased the strength of the two CSA2 blended mixtures. PCSA1 and PCSA2 also gained a high early strength, and the dosage of HRWR did not affect the strength gain too much. From Figure 4.16, at the six hours of hydration, most of the CSA based cements achieved around 20 MPa in compressive strength. In addition, the CAC based cement blend, CAC-B1, also gained a high early age strength. The two laboratory-based RSHCs, CAC-OPC2 and CSA1-OPC2, along with the straight CAC did not gain any early age strength.

The impact of 0.5% set retarder was also investigated following the mixture proportions in Table 4.21, and the results are shown in Figure 4.17. The compression test was conducted at 8 hours, 24 hours, 3 days, 7 days, 28 days, and 56 days.
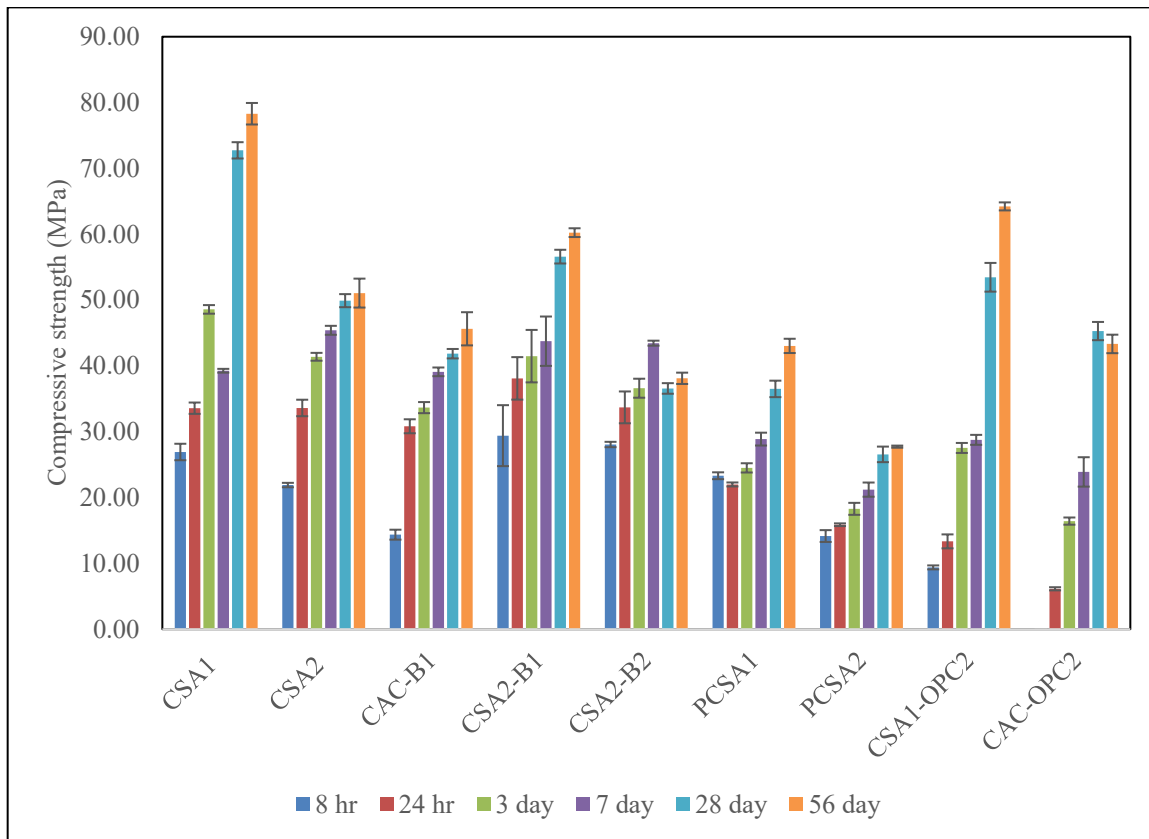
Figure 4.17: Compressive strength of all the cements with 0.5% set retarder

As observed in Figure 4.17, citric acid was not found to negatively affect the compressive strength of any of the RSHCs and blends investigated in this study. The compressive strength of CSA2 increased in both early and later ages with the addition of citric acid as a set retarder compared to the case without any citric acid. The compressive strength of CSA1 was not affected by citric acid. CSA2-B2 also experienced strength gain with citric acid. Two proprietary blended cements had higher strength with the addition of citric acid. Citric acid did not affect the later age strength of the cements either. Laboratory blended RSHCs also experienced strength gain at later ages with an incorporation of 0.5% of citric acid. CAC cement with citric acid was not tested since HRWR was found to adversely affect the hydration process and addition of citric acid will further the delay the hydration process.

4.5 DRYING SHRINKAGE

For each mixture, six mortar prisms were casted, and the dimension of the prism were 25 x 25 x 285 mm. All prisms were allowed to cure for 24 hours under wet burlap and plastic. Following, the prisms were cured for an additional period of 48 hours in saturated limewater solution (3 gm lime per liter of water). After curing for 72 hours (24 hours under burlap followed by 48 hours in limewater), immediately the initial (zero day) reading was taken using the length comparator. The reading was taken quickly so that the prisms did not dry while in the lab environment. Once the reading had been recorded for all prisms, each prism was placed in a walk-in environmental chamber that was conditioned at 23°C and 50% RH. The length change readings were taken at 4, 7, 11, 14, 18, 25, and 28 days. Three different experimental mix matrixes were performed for all the RSHCs and blends.

The first mixture series for drying shrinkage test were designed at a c/s of 1:2.75 and a varying water content for each set of RSHCS and blends. Mixture proportions are presented in Table 4.22. The required water amount was obtained from the previously completed flow test of each cement and is also presented in Table 4.22. No admixture was added in mixtures.

Table 4.22: Mixture proportion for drying shrinkage test for the first mixture series

Cement	W/C to achieve mortar flow of 110 ± 5	Cement (g)	Water (g)	Sand (g)
CAC	0.52	800	416	2200
CSA1	1.00	800	800	2200
CSA2	0.50	800	400	2200
CAC-B1	0.53	800	424	2200
CSA2-B1	0.51	800	408	2200
CSA2-B2	0.63	800	504	2200
PCSA1	0.51	800	408	2200
PCSA2	0.50	800	400	2200
CSA1-OPC2	0.54	800	432	2200
CSA1-OPC2	0.50	800	400	2200

The results of the drying shrinkage tests for the first mixture series are shown in Figure 4.18.
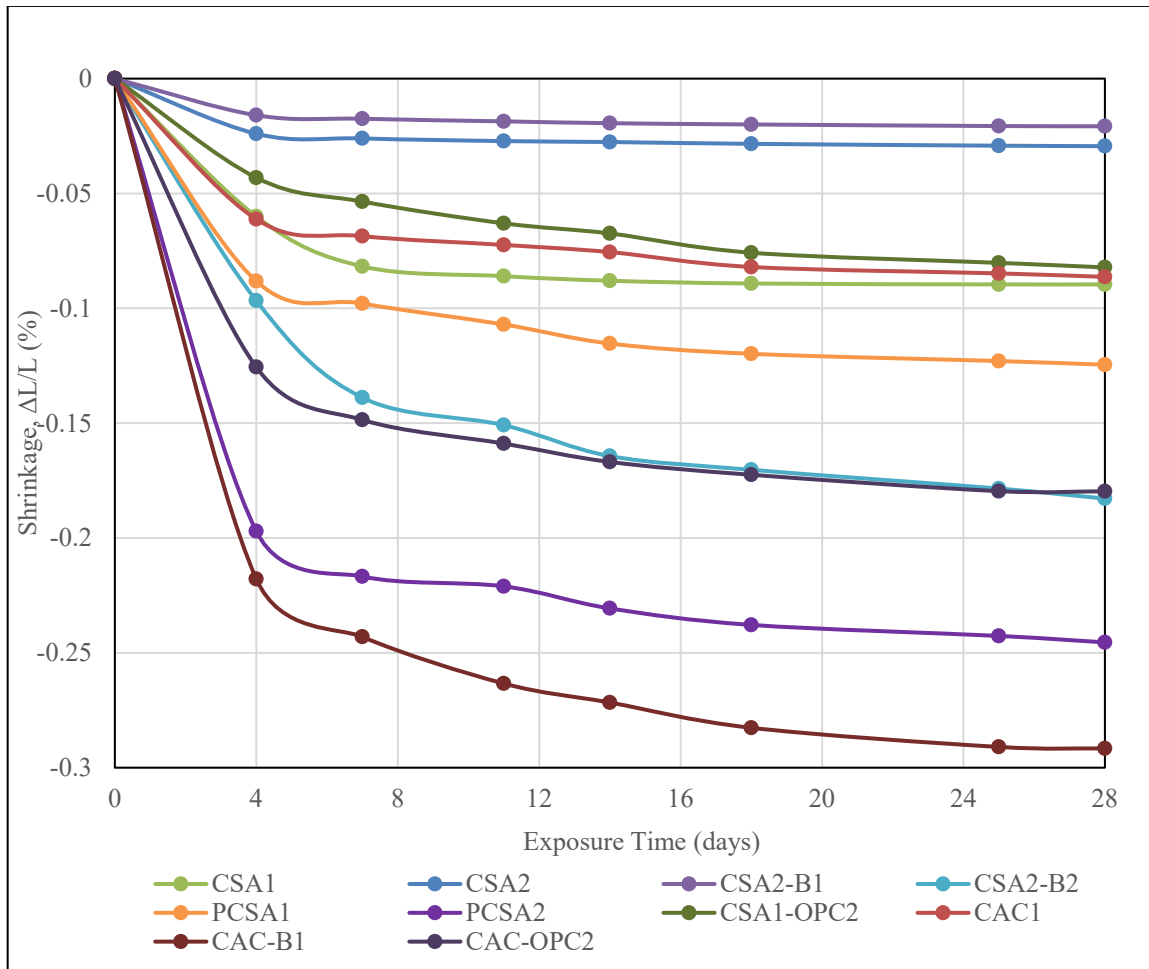
Figure 4.18: Drying shrinkage test for all the cements of the first mixture series

Since this mixture design has a significantly high amount of W/C for all the cements, at the early age the shrinkage was considerably high for all the cements. From Figure 4.18, CSA2-B1 had the least amount of shrinkage whereas the shrinkage of CAC-B1 was very high. CSA1 required a high amount of water for flow which also resulted in high shrinkage at initial ages. Low shrinkage was observed in CSA2 mixtures. Between two proprietary blended cements, a lower shrinkage value was observed for PCSA1. The shrinkage was low in CSA1-OPC2 compared to CAC-OPC2.

The second mixture series were designed at a c/s of 1:2 and a varying water content required to achieve the flow as outlined in ASTM C1437. No admixture was added in the samples. Table 4.23 presents the mixture proportions of these mixtures and the W/C ratio for each RSHCs and blends.

Table 4.23: Mixture proportion for drying shrinkage test for the second mixture series

Cement	W/C to achieve mortar flow of 110 ± 5	Cement (g)	Water (g)	Sand (g)
CAC	0.38	800	304	1600
CSA1	0.88	800	704	1600
CSA2	0.36	800	288	1600
CAC-B1	0.38	800	304	1600
CSA2-B1	0.35	800	280	1600
CSA2-B2	0.51	800	408	1600
PCSA1	0.37	800	296	1600
PCSA2	0.35	800	280	1600
CSA1-OPC2	0.41	800	328	1600
CSA1-OPC2	0.38	800	304	1600

The results of the drying shrinkage tests of the second mixture series are shown in Figure 4.19.
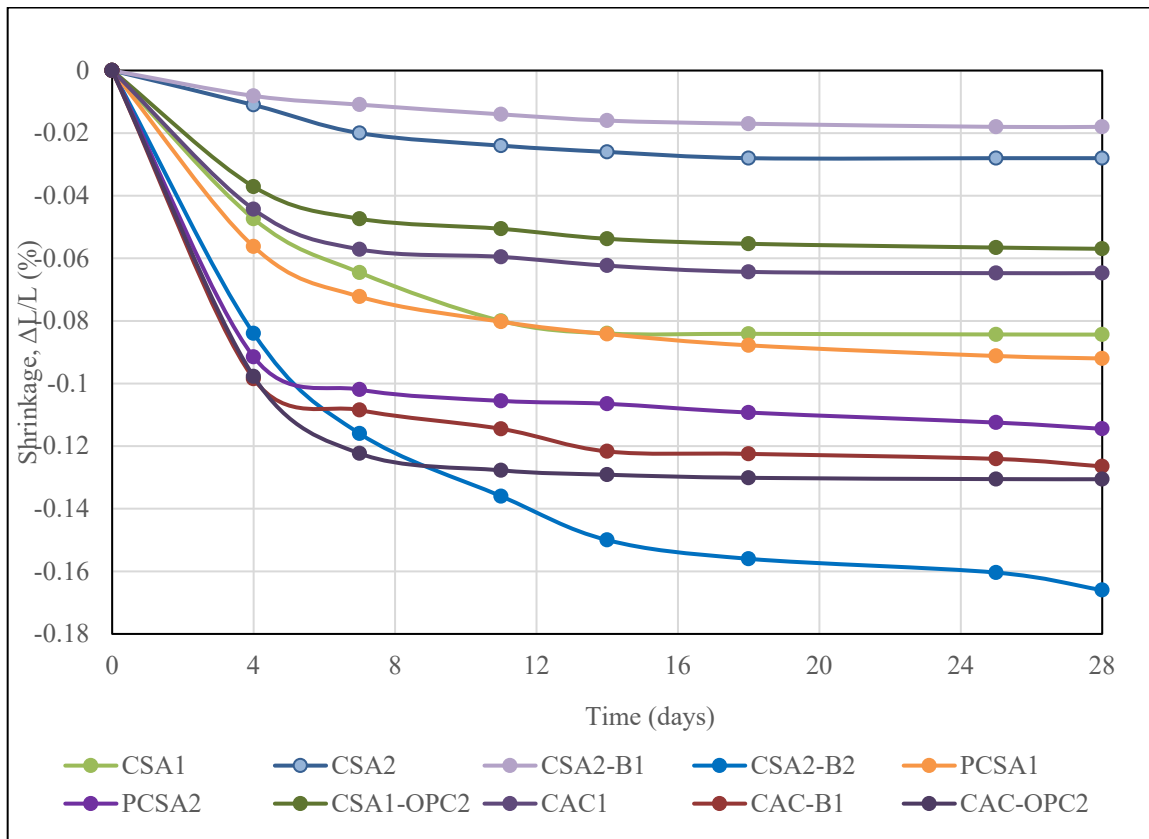
Figure 4.19: Drying shrinkage test for all the cements for the second mixture series

The drying shrinkage result was different for the second mixture series where W/C is lower for all the cements. Since the water content was lower, the early age shrinkage was lower compared to the first mixture series. The lowest amount of shrinkage was observed for CSA2-B1, whereas CSA-B2 had the

highest shrinkage, as shown in Figure 4.19. Significant shrinkage was also observed for CAC-B1 and CAC-OPC2. Between PCSA1 and PCSA2, PCSA1 experienced lower shrinkage. CSA2 did not experience much shrinkage. The shrinkage was lower for CSA1 as less amount of water was added in the mixture to achieve the required flow.

As previously stated, an additional set of tests were performed in which the W/C and c/s were held constant but the amount of HRWR varied until the ASTM C1600 flow was achieved for each set of cement. Table 4.24 presents the mixture proportions of the third mixture series and along with the required HRWR for each RSHCs and blends.

Table 4.24: Mixture proportion for drying shrinkage test for the third mixture series

Cement	W/C	HRWR (% weight of cement)	Cement (g)	Water (g)	Sand (g)
CAC	0.35	3.0%	800	280	4070
CSA1	0.35	7.5%	800	280	4070
CSA2	0.35	2.0%	800	280	4070
CAC-B1	0.35	6.0%	800	280	4070
CSA2-B1	0.35	6.0%	800	280	4070
CSA2-B2	0.35	7.5%	800	280	4070
PCSA1	0.35	7.0%	800	280	4070
PCSA2	0.35	0.75%	800	280	4070
CSA1-OPC2	0.35	1.5%	800	280	4070
CAC-OPC2	0.35	1.5%	800	280	4070

The results of the drying shrinkage tests of the third mixture series are shown in Figure 4.20.
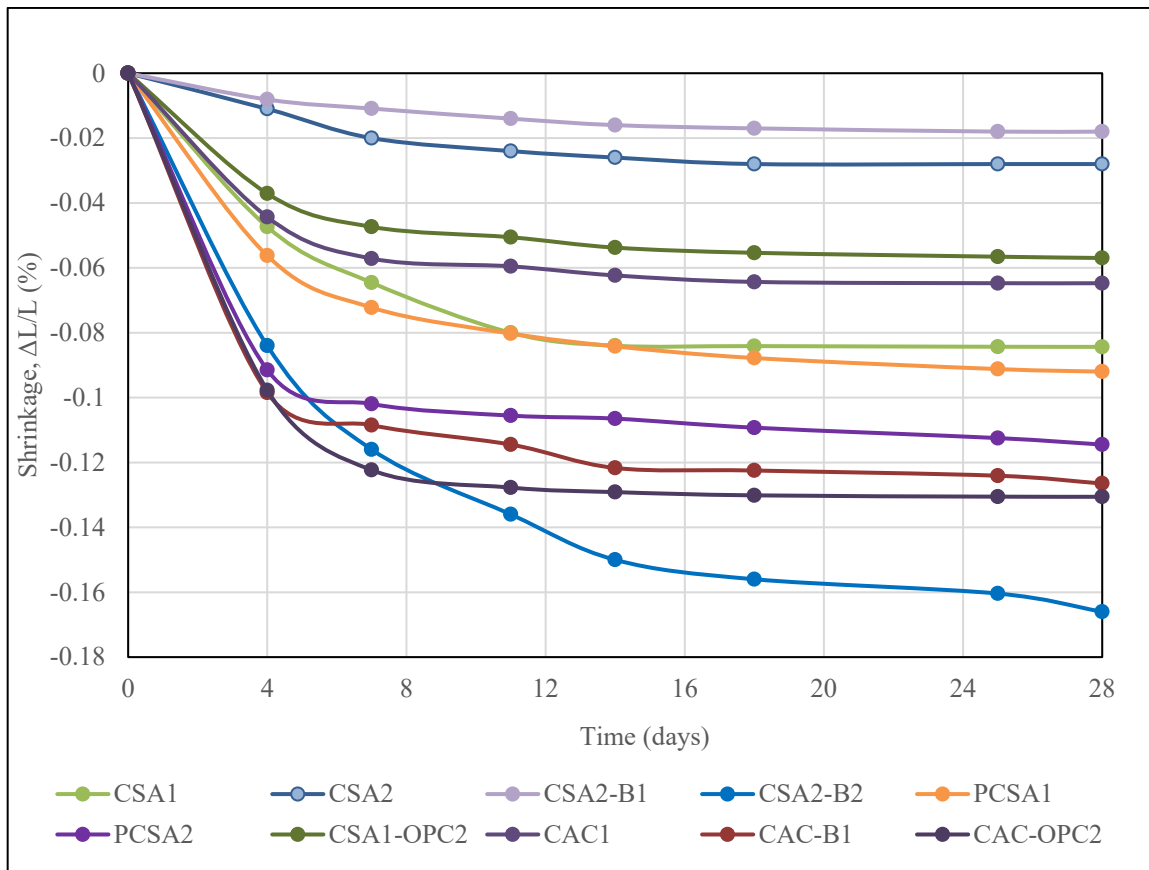
Figure 4.20: Drying shrinkage test for all the cements for the second mixture series

The third mixture series of drying shrinkage test contained HRWR and had a fixed W/C ratio of 0.35. The CSA based cement with HRWR had lower shrinkage since a less amount of water was added in the mix. The early age shrinkage of CSA1, PCSA1, PCSA2, CSA2, and CSA2-B1 was very low compared to the previous two sets of mixtures except CSA2-B2. The CAC based system (CAC1, CAC-B1 and CAC-OPC2) had high shrinkage. Among all four cements, CAC1 had the lowest shrinkage.

4.6 MINI-SLUMP TEST

A mini-slump cone can be used to evaluate the influence of set control admixtures on the workability/flowability of cement mortars. The loss of flow over time can be measured by performing the test at different time intervals. The mini-slump test on cement mortar mixes was performed using a small sample size. Therefore, it was rapid and required less effort and materials than the conventional slump test method. The mini-slump test was performed in this study to measure the influence of set control admixtures on flowability. Figure 4.21 shows the dimension of the mini-slump cone used for this study. The mini-slump cone used in this research has the top and base diameters of 50 mm and 100 mm

respectively. The height of the cone is 151 mm. Three different mixtures were taken into consideration for all the cements. The test was performed at 5, 15, 30, 45, 60, 80, 100, 120, 140 and 160 minutes since the start of hydration.
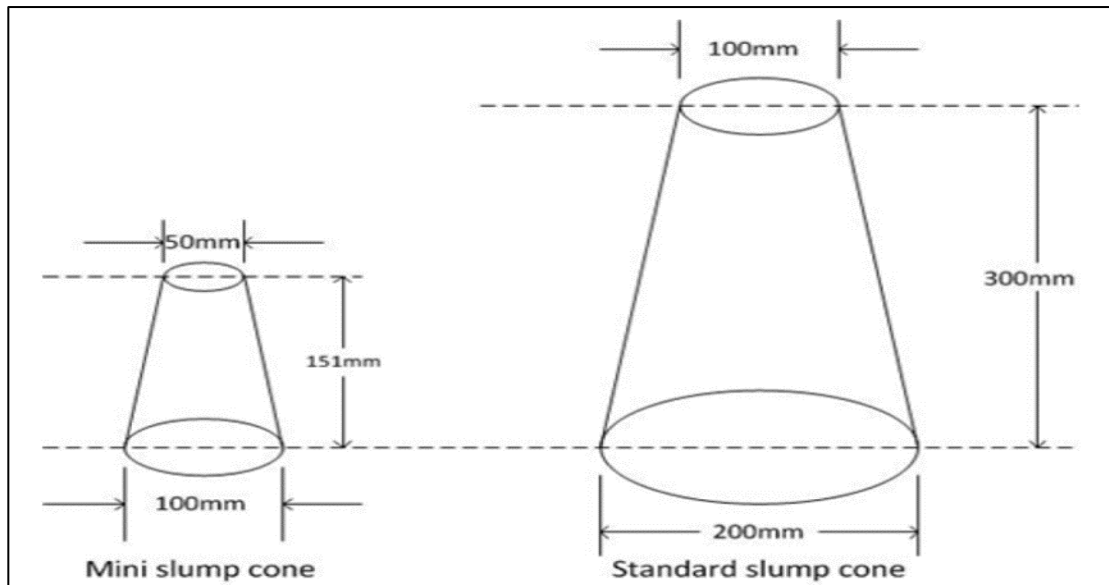
Figure 4.21: Mini-slump cone and standard slump cone [5]

Table 4.25 shows the mixture proportions of the mini-slump cone test with a constant W/C of 0.35, c/s of 1:2.75 and the amount of HRWR required to reach the flow of 110 ± 5. In the first mixture, citric acid was not added. However, the citric acid dosage was administered in two increments by weight of cement - 0.5% in the second mixture and 1.0% in the third mixture.

Table 4.25: Mixture proportions for mini-slump cone test

Cement	W/C	HRWR (%weight of cement)	Set Retarder (% weight of cement)	Cement (g)	Water (g)	Sand (g)
CAC	0.35	1.0%	0%, 0.5%, 1.0%	400	140	1100
CSA1	0.35	3.0%	0%, 0.5%, 1.0%	400	140	1100
CSA2	0.35	0.75%	0%, 0.5%, 1.0%	400	140	1100
CAC-B1	0.35	1.5%	0%, 0.5%, 1.0%	400	140	1100
CSA2-B1	0.35	1.5%	0%, 0.5%, 1.0%	400	140	1100
CSA2-B2	0.35	1.75%	0%, 0.5%, 1.0%	400	140	1100
PCSA1	0.35	1.5%	0%, 0.5%, 1.0%	400	140	1100
PCSA2	0.35	0.75%	0%, 0.5%, 1.0%	400	140	1100
CSA1-OPC2	0.35	1.5%	0%, 0.5%, 1.0%	400	140	1100
CAC-OPC2	0.35	2.0%	0%, 0.5%, 1.0%	400	140	1100

Figure 4.22 to Figure 4.28 show the mini-slump cone test of each RSHC. All of these figures are plotted one after another to depict the effect of set retarder at different dosages on flowability/workability of cement mortar. Insights into the usage of RSHCs and blends in larger scale applications may be obtained from the following figures. Figure 4.22 presents the flow as a function of time for CSA1.
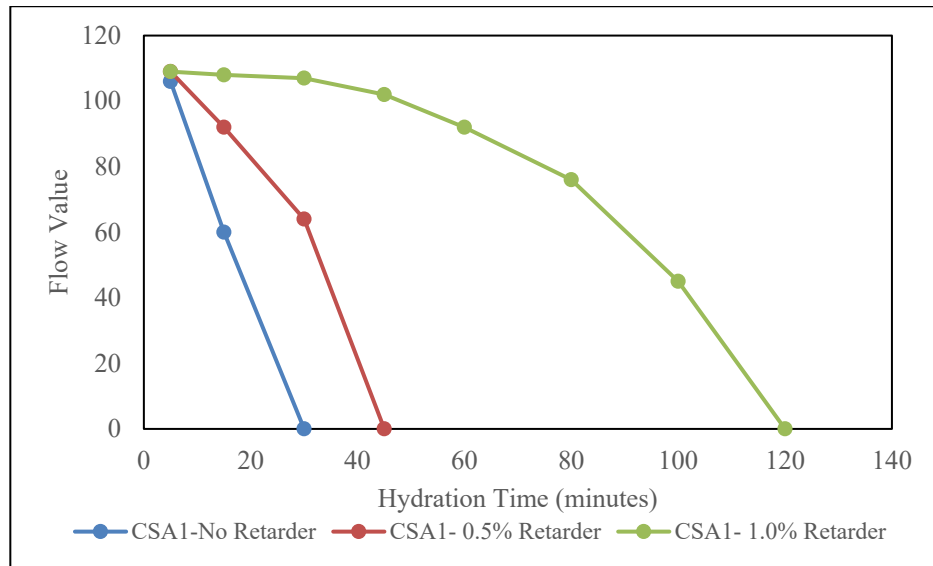
Figure 4.22: Flow as a function of time for CSA1

From Figure 4.22, without any retarder, CSA1 lost its flowability within 30 minutes. With an addition of 0.50% set retarder, the flow was retained up to 45 minutes. Therefore, no significant change was observed in flow with an addition of 0.5% set retarder. However, at the dosage of 1.0% set retarder, a significant increase in time to retain flowability was observed until 120 minutes. Figure 4.23 presents the flow as a function of time for CSA2.
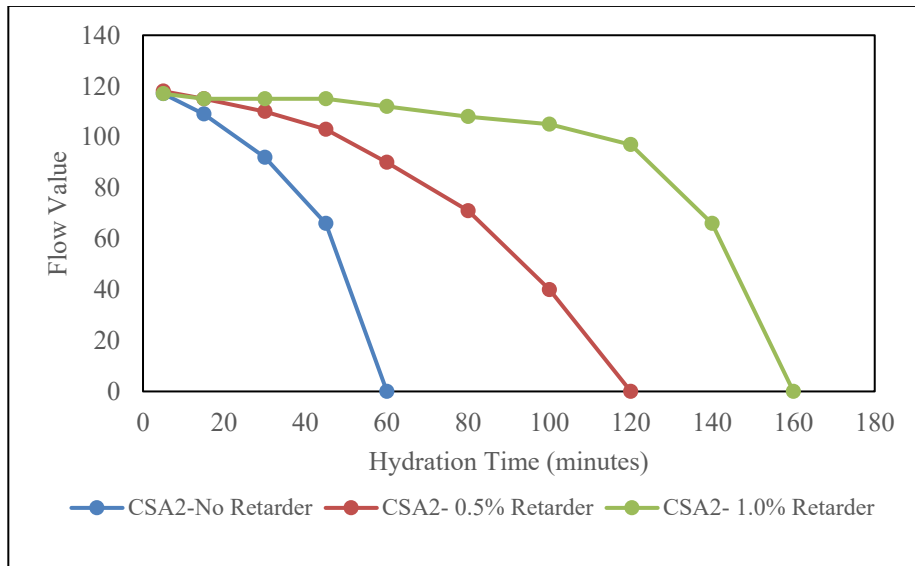
Figure 4.23: Flow as a function of time for CSA2

Figure 4.23 reveals that without any retarder CSA2 retained its flow till 60 minutes. Addition of 0.50% set retarder was very effective to retain the flow up to 120 minutes. The dosage of 1.0% set retarder was also effective to maintain the flowability but later (after 140 minutes of hydration) the flowability dropped significantly. Figure 4.24 presents the flow as a function of time for CSA2-B1.
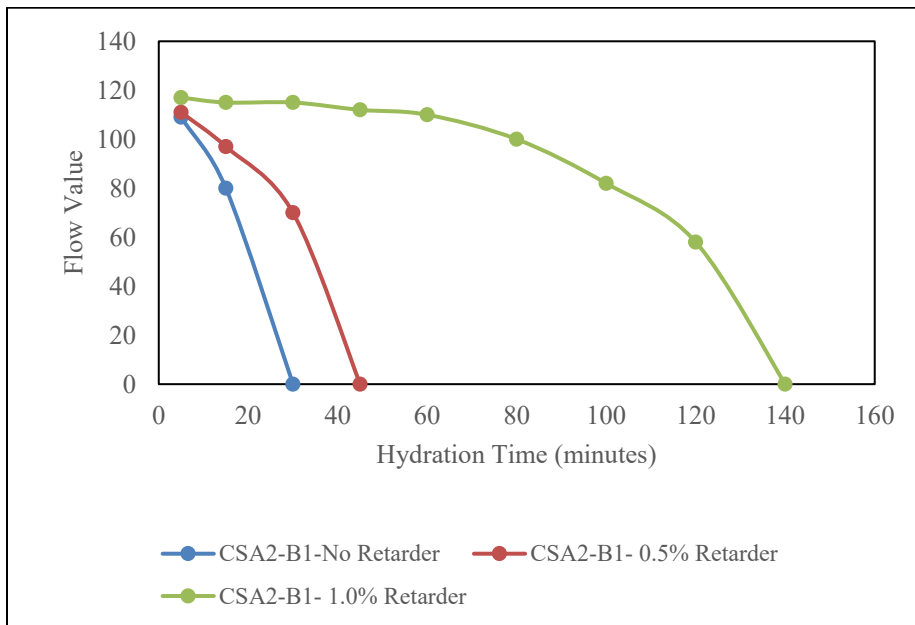
Figure 4.24: Flow as a function of time for CSA2-B1

For CSA2-B1, the flow retention capability was very low even with an incorporation of 0.50% set retarder. 0.5% retarder was not effective for CSA2-B1, as shown in Figure 4.24. However, with an addition of 1.0% set retarder, flowability was retained till 140 minutes of hydration time. Figure 4.25 presents the flow as a function of time for CSA2-B2.
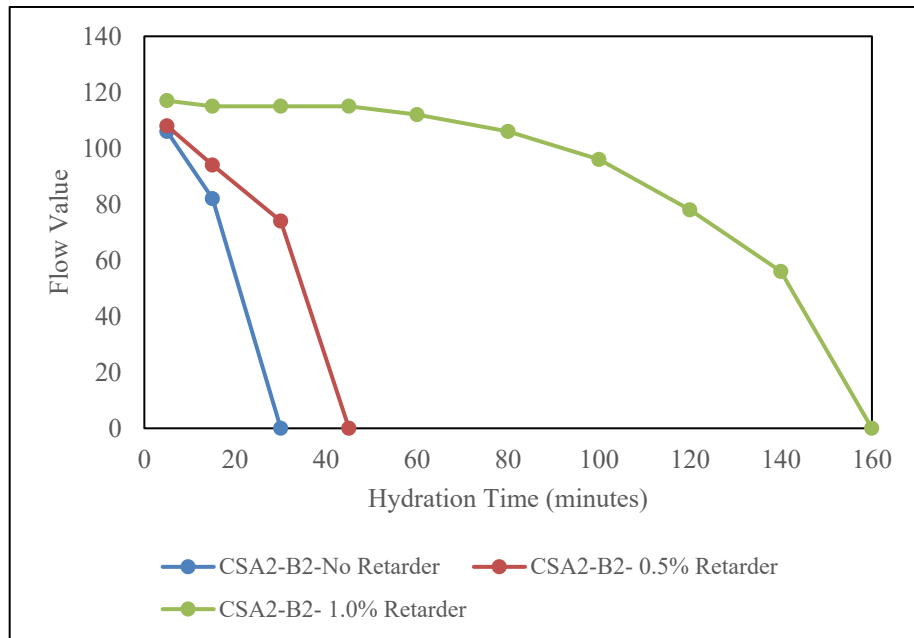
Figure 4.25: Flow as a function of time for CSA2-B2

From Figure 4.25, CSA2-B2 had no flow after 30 minutes and with an addition of 0.50% set retarder flow was retained till 45 minutes. Therefore, addition of 0.50% set retarder was not found to be effective. However, incorporation of 1.0% set retarder was found to be very effective. Figure 4.26 presents the flow as a function of time for PCSA1.
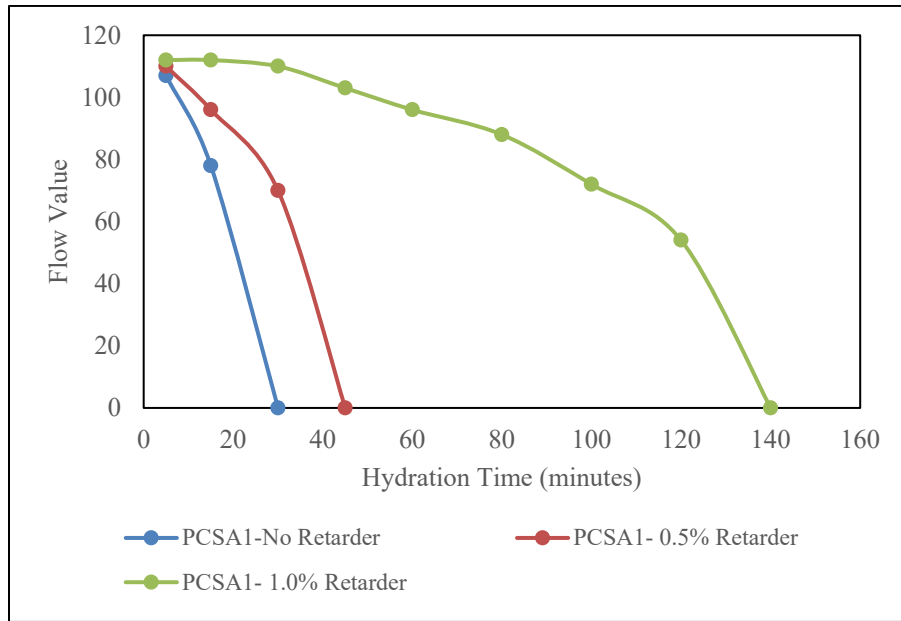
Figure 4.26: Flow as function of time for PCSA1

Figure 4.26 shows that PCSA1 was not able to retain its flow till 30 minutes without any retarder or 45 minutes with an addition of 0.50% set retarder. However, PCSA1 mixtures showed significant improvement in flow retaining with an addition of 1.0% set retarder till 140 minutes. Figure 4.27 presents the flow as a function of time for PCSA2.
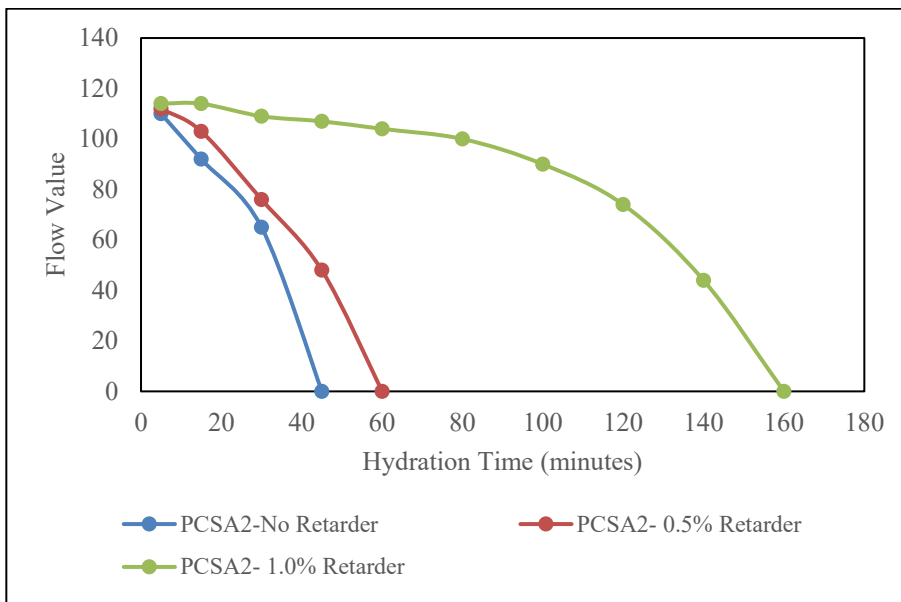
Figure 4.27: Flow as a function of time for PCSA2

71

From Figure 4.27, 1.0% set retarder was able to retain the flow of PCSA2 untill 160 minutes of hydration time and the minimum standard of flow of 105 can be achieved till 60 minutes. On the other hand, 0.5% set retarder was not effective to hold the flowability of PCSA2 mixture. Figure 4.28 presents the flow as a function of time for CAC-B1.
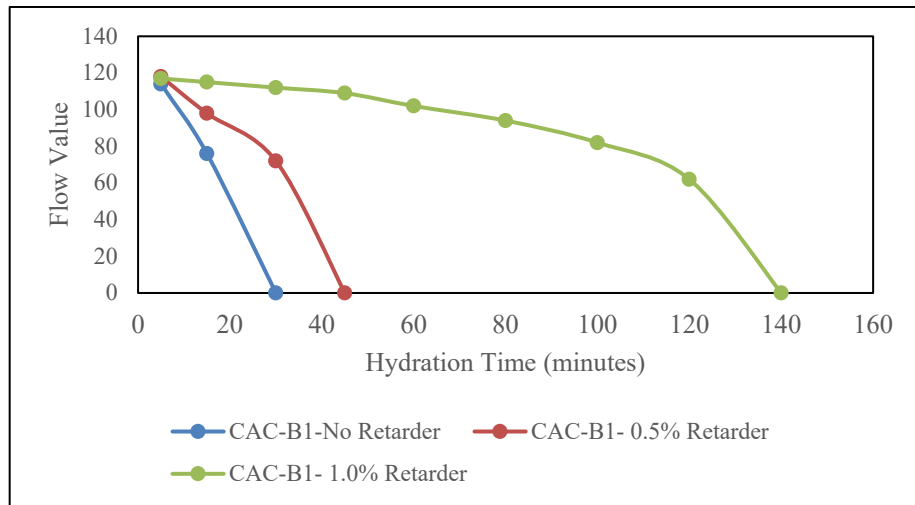
Figure 4.28: Flow as a function of time for CAC-B1

Figure 4.28 illustrates that CAC-B1 was set within 30 minutes without any set retarder and incorporation of 0.5% set retarder extended the flowability up to 45 minutes. On the other hand, addition of 1.0% set retarder was found to be very effective to retain the flow till 140 minutes of hydration time. Figure 4.29 presents the flow as a function of time for CAC-OPC2.
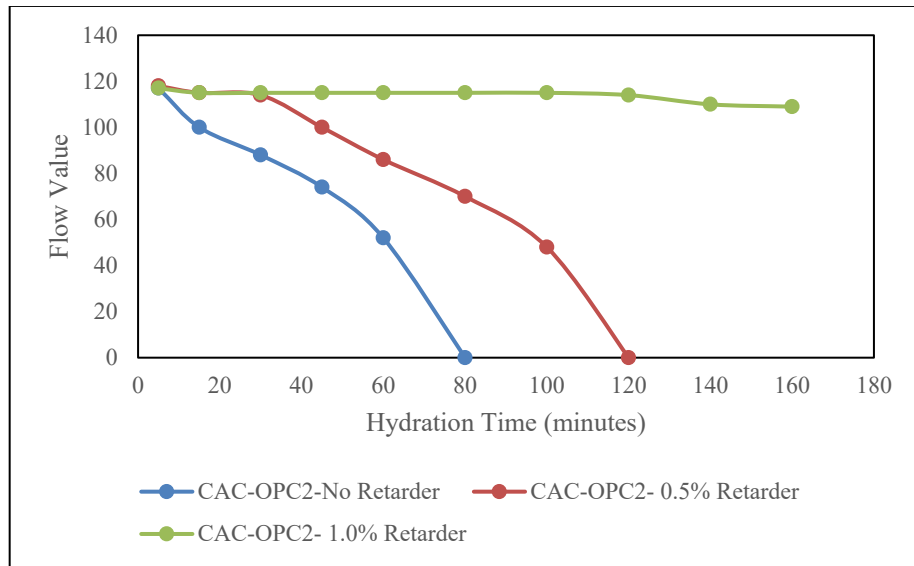
Figure 4.29: Flow as a function of time for CAC-OPC2

CAC-OPC2 is a laboratory blended cement containing 25% CAC and 75% OPC2. Figure 4.29 illustrates that without any set retarder this blended cement was able to hold till 80 minutes. The results also indicate that incorporation of 0.5% set retarder was effective to retain the flow up to 120 minutes. On the other hand, an addition of 1.0% set retarder extensively delayed the setting time. Figure 4.30 presents the flow as a function of time for CSA1.
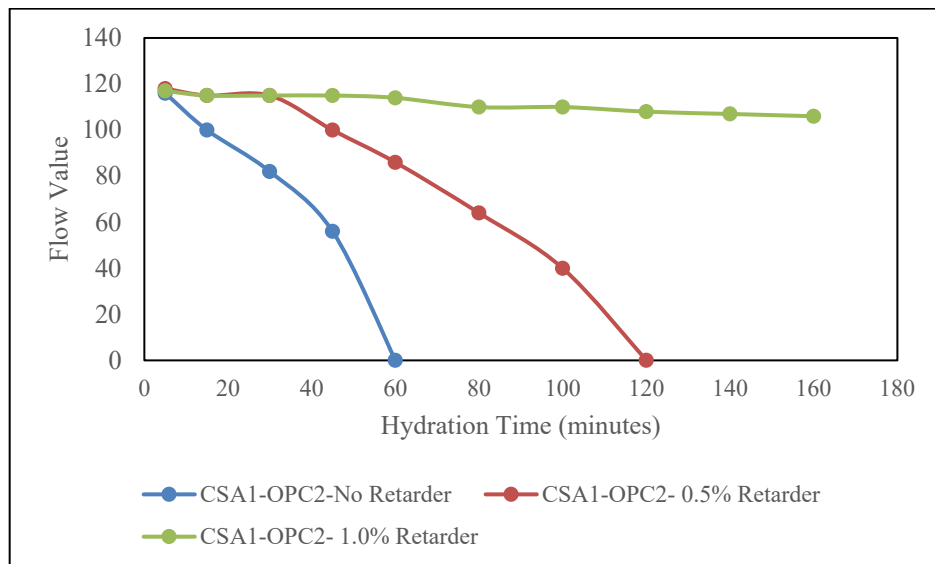
Figure 4.30: Flow as a function of time for CSA1-OPC2

The CSA1-OPC2 system is another lab blended system containing 25% CSA1 and 75% OPC2. Figure 4.30 depicts that even without set retarder this blended system had a high flow retainability, and with an incorporation of 0.5% set retarder, the flow was observed till 120 minutes of hydration process. However, addition of 1.0% set retarder delayed the setting time and almost no change of flow was observed up to 160 minutes of hydration time.

4.7 DEVELOPING RSHC CONCRETE MIXTURES

Besides RSHC mortars, included in Chapter 4 was a small experimental program on translating the information learned from the RSHC mortar testing to that of concrete produced with RCHCs and blended systems. Therefore, concrete mixtures with satisfactory performance were developed using a combination of isothermal calorimetry test, flow test, cube compression test, and mini slump test to link cement characteristics, admixture type and dosage to early age behavior. Since each cement behaves differently from other cements, the required admixture dosage was also different for different cements. Table 4.26 summarizes the mixture proportion of all the concrete mixtures produced in this chapter. The technical criteria for concrete performance defined in this experimental program was to achieve a slump rbetween 125 mm to 175 mm and a minimum 24-hour compressive strength of 27.5 MPa.

Table 4.26: Mixture proportion of concrete mixture

Cement ID	W/C	Cement kg/m³	Rock (SSD) kg/m³	Sand (SSD) kg/m³	Water kg/m³	Admixture Dosage (% weight of cement)	
						Retarder	HRWR
CSA1	0.38	390	1113	695	148	2.0%	4.5%
CSA2	0.38	390	1113	695	148	0.5%	0.50%
CAC-B1	0.38	390	1113	695	148	0.5%	2.00%
CSA2-B1	0.38	390	1113	695	148	1.0%	2.25%
CSA2-B2	0.38	390	1113	695	148	0.5%	2.50%
CAC1*	0.38	390	1113	695	148	0.5%	2.50%
CSA-OPC2	0.38	390	1113	695	148	0.5%	1.00%
CAC-OPC2	0.38	390	1113	695	148	0.5%	1.00%

*A set accelerator was added to CAC1 concrete at a dosage of 1.5% weight of the cement

CSA1 required the highest amount of HRWR and CSA2 required the least. For the rest of the cements, the required amount of HRWR varied from 0.5% - 2%. The set retarder dosage was also high for CSA as the mortar results showed it sets extremely fast. CSA2-B1 was very fast setting and required 1% set retarder. For the rest of the mix, 0.5% set retarder was added. As CAC hydration was affected adversely by the addition of HRWR and set retarder, a set accelerator was added for CAC. Initially, the dosage of GCX-500 was 0.5% but it took more than 24 hours to set. Therefore, after several trial and error, with a

1.5% dosage of the GCX, the CAC concrete achieved the desired set time requirement. Compressive Strength was measured on three concrete cylinders of dimensions 100 mm x 200 mm. The measurements were made at the ages of 1, 3, 7 and 28 days. The results are shown in Table 4.27 and Figure 4.30.

Table 4.27: Slump and 24 hours compressive strength of the RSHCs and blends

Cement	Concrete Slump (mm)	Compressive Strength at 24 hours (MPa)
CAC	140	32.7
CSA1	140	44.8
CSA2	152	38.4
CAC-B1	140	28.0
CSA2-B1	140	47.7
CSA2-B2	152	46.2
CSA1-OPC2	152	21.2
CAC-OPC2	165	18.2

From the results, all RSHC samples except CAC-OPC2, CSA1-OPC2 achieved the early age workability and strength criteria. For the CSA mixture, a high dosage of HRWR and set retarder was added, and the 24-hr. compressive strength was similar to the other CSA based concrete. CSA2-B1 gained the highest strength among all the concrete within 24 hours. The other two CAC based concrete (CAC, CAC-B1) also achieved the required strength. For the two laboratory blend cements, however, the 24 hours strength was less than 27.5 MPa. This is because 75% of these two cements were OPC2 which diluted the compressive strength substantially. In addition, the HRWR and set retarder, the hydration process of the two-laboratory blend RSHCs delayed extensively. Nonetheless, to compare performances between mixtures the same binder content and W/C were used for all concrete mixtures.
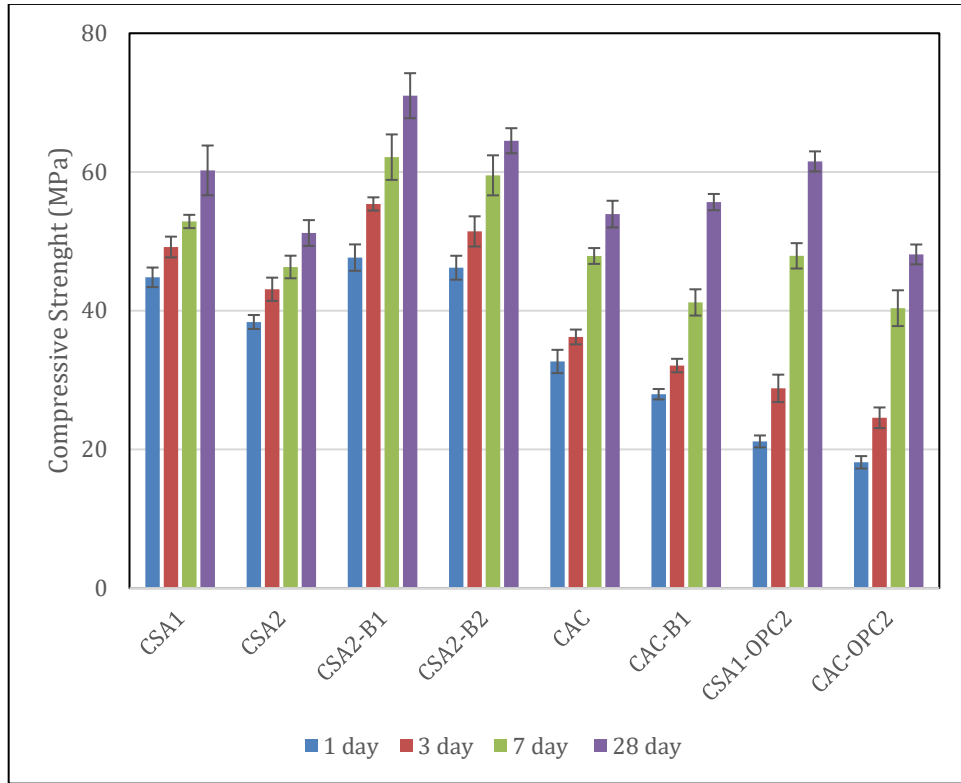
Figure 4.31: Concrete compressive strength at different ages

With a high dosage of set retarder and HRWR, CSA1 strength was similar to all other CSA based cements. For the CSA2, the strength gain was very steady, which may be attributed to higher amount of belite. Although the set control admixtures affected CAC mortar hydration process adversely, with an addition of high dosage of set accelerator, the CAC concrete initial strength gain was high. For the CAC-B1, later age strength gain was also high. CAC-OPC2 and CSA1-OPC2 behaved like an OPC2, and the early age strength was very low compared to the other cements, but the later age strength gain was high.

In addition to compressive strength data the permeability of the produced concrete was determined via a bulk resistivity test. Therefore, the bulk resistivity test was performed at 28 days and Table 4.28 shows the test results.

Table 4.28: Bulk Resistivity Test of RSHCs and blends

Cement	Bulk Resistivity (ohm.m)	Permeability Indicator Result (Potential Chloride Penetration)
CAC	468.15	Very low
CSA1	500.32	Very low
CSA2	104.39	Low
CAC-B1	97.39	Moderate
CSA2-B1	379.66	Very low
CSA2-B2	169.21	Low
CSA1-OPC2	62.15	High
CAC-OPC2	50.08	High

From the resistivity result, the majority of rapid setting mixtures showed low to very low permeability range with the exception of CAC-B1. Pure rapid setting cements CAC and CSA1 showed a very low permeability (i.e., potential chloride penetration) based off their bulk resistivity value. On the other hand, CSA2 had a dramatically lower bulk resistivity at only 104 ohm-m and only narrowly achieved a low permeability rating. This is likely attributed to the lower ye'elimite and higher belite (C_2S) content in this particular system (i.e., calcium sulfoaluminate belite cements) leading to a slower rate in strength development and densification of the microstructure. Though in the CSA mix design a high amount of HRWR and set retarder was added, the chloride penetration rate is very low. In the blended systems, the resistivity results varied significantly depending on cement and blend type, especially if they were blends produced in the lab (CSA1-OPC2 & CAC-OPC2). For example, CSA2-B1 and CSA2-B2 showed a relatively fast and high compressive strength development while also measuring very low permeability. On the other hand, CAC based blends such as CAC-B1 only measured a moderate permeability value. For the blended systems produced in the lab such as CSA1-OPC2 and CAC-OPC2, the resistivity results were dramatically lower only measuring a bulk resistivity of 62 ohm-m and 50 ohm-m, respectively. Interestingly, the lab blended systems are very similar in replacement contents as those in the proprietary blends (75% OPC and 25% RSHC) however, they are not intergrinded which may have been the reason for the lower results.

4.8 CONCLUSIONS

The objective of this experimental work was to characterize and document the early age properties of several RSHCs and their blended systems. Specifically, the influence of set control admixtures dosages on the flowability, heat of hydration, compressive strength, and early-age shrinkage of a variety of RSHCs and their blended systems was investigated. The primary contribution of this work is to provide insight into the early age behavior of various RSHCs and blended RSHCs systems. Concrete mixtures with satisfactory performance can be developed by using a combination of isothermal calorimetry, the peak

heat flow, mortar compressive strength and flow tests to link cement characteristics, admixture type, and dosage to early age behavior. This will benefit researchers and end-users by providing much needed information regarding the proper dosage of HRWR and set retarder to RSHCs in structural applications.

The key findings and contributions from the study are summarized below:

- Citric acid was found to be effective in extending the hydration process for all RSHCs. However, citric acid was found to adversely delay the hydration of CAC compared to CSA at similar dosages.
- Citric acid was not found to negatively affect compressive strength and even it increased the later age compressive strength for most RSHCs.
- Curing isothermally at 23°C with 0.5% dosage of citric acid and curing isothermally at 38°C with 1.0% dosage citric acid were able to extend the working time of most RSHCs without impacting the early- and later-age strengths.
- HRWR was successful to reduce the amount of water required to achieve the desirable flow. CAC based RSHCs required less amount of HRWR compared to CSA based RSHCs.
- Effect of HRWR is more evident in CAC based system compared to CSA based system in terms of early age compressive strength.
- Curing isothermally at temperature of 23°C, the effect of HRWR is prominent in the context of reducing peak heat flow and extending the time for peak heat flow for all RSHCs.
- Drying shrinkage measurements using HRWR demonstrated that CAC based system (CAC1, CAC-B1 and CAC-OPC2) had high shrinkage.
- Among all RSHCs, CAC1 and the laboratory blended RSHCs (CSA1-OPC2 and CAC-OPC2) were all negatively affected with the addition of HRWR and the set retarder in terms of hydration and early age hardened properties.
- Other than CAC-OPC2 and CSA1-OPC2, all the concrete mixtures with RSHCs achieved the required early age properties in terms of slump, compressive strength, and permeability.
- Among all RSHCs, set control admixtures (at a dosage of 2% HRWR and 0.5 % set retarder) were effective for CSA2. It delayed the hydration period in every case which was compatible for practical usage of CSA2 in large infrastructure, without compromising important hardened properties or adversely affecting the hydration process.

4.9 REFERENCES

[1]   *ASTM C1600M-19 Standard Specification for Rapid Hardening Hydraulic Cement*, ASTM International, 2019. [Online]. Available: https://compass.astm.org/document/?contentCode=ASTM%7CC1600_C1600M-19%7Cen-US

[2]   *ASTM C109-21 Standard Test Method for Compressive Strength of Hydraulic Cement Mortars (Using 2-in. or [50-mm] Cube Specimens)*, ASTM International, 2021.

[3]   *ASTM C1437-20 Standard Test Method for Flow of Hydraulic Cement Mortar*, ASTM International, 2020.

[4]   A. Bentivegna, "Multi-Scale Characterization, Implementation, and Monitoring of Calcium Aluminte Cement Based Systems (Dissertation). Austin, TX: The University of Texas at Austin.," Dissertation 2012. The University of Texas at Austin.

[5]   Q. Jia *et al.*, "Effects of fine content, binder type and porosity on mechanical properties of cemented paste backfill with co-deposition of tailings sand and smelter slag," *Electron. J. Geotech. Eng,* vol. 21, pp. 6971-6988, 2016.

CHAPTER 5: FRESH AND HARDENED PROPERTIES OF RAPID SETTING HYDRAULIC CEMENT CONCRETE SYSTEMS

5.1 INTRODUCTION

Starting from the 1980s, major advances in understanding the hydration and material characterization of cementitious materials took place [1]. Soon after, the increase in the use of supplementary cementitious materials (SCMs) and the raise of major chemical admixtures allowed the production of highly flowable concrete with a relatively low water-to-binder ratio [1]. As a result of the combined effects of such special additives and admixtures, the use and implementation of concrete structures started to face a rapid growth due to the relative ease in procurement of portland cement and the implementation of concrete structures. About a few decades after this sustained growth, concrete structures face major structural deficiencies mainly due to durability issues (e.g., carbonation and chloride induced corrosion, freeze thawing), as well as overpassing their designed life expectancy. This can be seen from the recent report card published by the American Society of Civil Engineers (ASCE) that claimed a nearly 231,000 bridges in all 50 U.S. states are structurally deficient and require about $125 billion immediate investment in repair and rehabilitation practices [2].

The heavy cost and major socio-ecological implications of reconstructing rebuilding major structures such as bridges and dams has caused a significant amount of research and development to take place in repair and rehabilitation of concrete structures. In that respect, a variety of cementing materials and binding agents including various polymer binders, such as epoxy [3] and polyester [4], alkali-activated materials[5], biologically induced binders (e.g., bio-cementation [6]) and rapid setting hardening cements (RSHCs) such as Type III Portland cement [7], calcium sulfoaluminate (CSA) [8]and calcium aluminate CAC [9] cement have been researched.

Although certain techniques, such as the use of polymer binders are relatively inseparable from rehabilitation practices, their relatively low thermal performance and often higher likelihood of experiencing delamination is a cause for concerns. Similarly, alkali-activated materials' significant variation in strength values and their relatively high porosity, as well as biologically induced binding systems' lack of ease in applications, is considered to be a relatively incompatible means for repair of structural components [10]. From this perspective and unlike other binding systems, the discovery and use of rapid hardening binders started at 1900s with the early intention of developing sulfate resistant

cement [11]. The later commercialization of CACs in Europe and England during the 1910s and 1920s were the initial stages of developing rapid hardening cements [11, 12]. Although CACs became very popular after their commercialization and used in numerous precast and refractory applications, they were found to experience a specific strength loss over time when exposed to sufficient moisture and moderate to high temperatures[13, 14]. This caused a few major structural failures and resulted in CACs being banned for use of the main structural applications during 1970s [12]. Followed by this, for the purpose of making shrinkage resistant and self-stressing cements [15], rapid hardening CSA cements have been developed [16].

In general, due to the significantly high strength gain rate of CSA (almost twice of Portland cement [17]), dense micro structure and low hydration pH, and high impermeability, CSA cements have found a variety of applications specifically in rehabilitation practices where serviceability of the infrastructural components is of major consideration. This includes precast and repair materials, as well as many marine applications [15], [18]. In addition to the benefits of CSA cements, as noted by Pimraksa et al. [15], CSA produces only one third CO_2 when compared to Portland cement. The raw meal for CSA production in known to be made of bauxite, limestone, clay, and smaller quantity of other minerals, such as gypsum or anhydrite at 1250-1350°C in rotary kilns [19]. The main minerals in CSA clinker, as noted by Ref. [20], are belite and ye'elimite with other minor phases such as gehlenite, perovskite, ferrite, mayenite and anhydrite. Ye'elimite, is considered to increase the early strength gain of CSA cements but it can affect the calcination process, requiring a higher temperature for the production of CSA. As a result, a variety of blended cements with various contents of belite ($Ca_2.SiO_4$), ye'elimite ($Ca_4.(AlO_2)_6.SO_4$) and alite ($3CaO·SiO_2$), have been practiced (e.g., [21, 22]) only to find that a higher belite content can reduce the sintering temperature considerably [23]. Although the exact values reported can be different, earlier studies (e.g., [24, 25]) have reported that the inclusion of higher content of belite reduces the temperatures from ~1450°C to ~1200°C in the calcination process of cement production which translates into ~30% lower CO_2 production [26].

In either case, however, the use of CSA can often pose some challenges due to its rapid hardening that does not allow sufficient working time. To address this, previous studies (e.g., [26]) have studied the effect of various phases on the speed of hydration and reported that depending on the raw material used in the production of CSA cements, the clinker can contain various content of minor phases resulting in variation of hardening duration [27]. It was further reported that increasing the belite (C_2S) content can reduce the initial setting time [28] and densify the microstructure [29]. According to Winnefeld and Lothenbach [27] and Seo et al. [30], the hydration of belite containing cements leads to formation of strätlingite and C-S-H, at later ages and to some extend resembles portland cement's hydration.

In general, it is known that belite is impure dicalcium silicate (Ca_2SiO_4) that is one of the key minerals (along with alite) that controls the setting time and strength development of commonly used cements [31, 32]. It is extensively used in the production of portland cement, but since it has lower reactivity than alite, its use is generally in lower quantity than alite [31], [32]. In turn, as reported by Refs. [21], ye'elimite is the main hydrating phase in CSA cements that can significantly affect the early strength gain rate. Based on this, numerous studies have evaluated the various ratios of chemical composition for early microstructural development. Ref.[33], for instance, studied the hydrothermal calcination of high belite CSA cements synthesized with industrial byproducts, such as Al-rich sludge, lignite fly and bottom ash as well as flue gas desulfurization gypsum. In their analyses, the hydration reaction was studied based on mechanical properties and microstructural analysis. Yet, only one type of CSA cement was used with a single variable of gypsum content and no comprehensive use of commercially available products have been evaluated. Similarly, Li et al. [34]and Lu et al. [22] studied the synthesis of belite, ye'elimite, ternesite and alite clinker to provide optimum ratio of the mentioned phases that result in lower sintering temperatures. Although a comprehensive microstructural analysis is conducted in these studies and belite's effect is favorably noted, the early hardening temperature, setting time and other physico-mechanical properties are not evaluated. Numerous other studies such as, Galluccio et al. [23], Negrao et al. [35], Coumes et al. [36]and He et al. [37]also examined the use of optimum raw meals for the production of CSA cements but mostly reported microstructural development phases.

In summary, the majority of studies in this area have only focused on the materials science and microstructural development of such blended systems, mostly to evaluate the hydration process and no study to date have evaluated the hardening and maturity of commercially available, blended, as well as lab blended products. In other words, for the actual use of RSHCs and their on-site application, it is very plausible that the contractors rely mostly on the available cements in the market or attempt to simply blended those in various quantities with portland cement which results in each binder from specific manufacturer have a different chemical composition and early reaction behavior. For this purpose and to fill this research gap, in this study, a thorough understanding of fresh and hardened properties on a variety of RSHC concretes was performed. Further information regarding the experimental program and tests conducted can be found in the following sections.

5.2 EXPERIMENTAL

5.2.1 Materials

In this study, thirteen cements were evaluated which included OPC, CSA, and CAC cements. A description of these cements and their chemical compositions are shown in Tables 5.1 and 5.2, respectively. Also, in Table 5.1, the terms CSA ye'elmite cement and CSA belite cement were used to indicate the main phases in the CSA cements. The phase compositions for the CSA cements in Table 6.1 were calculated using modified Bogue equations adapted from Iacobescu et al. [38].

Table 5.1: Description of cements

Cement Category	Cement Type	Description
Pure Cements	OPC2	OPC Type I/II
	OPC3	OPC Type III
	CAC	Standard CAC cement
	CSA1	CSA Ye'elmite cement (40% Ye'elmite and 26% belite)
	CSA2	CSA belite cement (58% belite and 30% ye'elmite)
Proprietary Blended Cements	CAC-B1	CAC blend with OPC
	CAC-B2	CAC blended with set accelerating admixture
	CSA-B1	CSA belite cement (39% belite and 30% ye'elmite)
	CSA-B2	CSA belite cement (42% belite and 27% ye'elmite)
	PCSA1	CSA blend with OPC
	PCSA2	CSA blend with OPC and Fly ash
Lab Blends	CAC-OPC2	CAC blend with OPC
	CSA1-OPC2	CSA blend with OPC

Table 5.2: Chemical composition of the individual cement

Cement Type	Cement ID	SiO_2	Al_2O_3	Fe_2O_3	CaO	MgO	SO_3	Na_2O	K_2O	Na_2O_e	LOI
Pure Cements	OPC2	21.06	4.02	3.19	63.91	1.08	2.89	0.14	0.61	0.53	2.29
	OPC3	19.67	5.34	1.76	63.41	0.99	5.27	0.10	0.44	0.39	4.06
	CAC	4.34	38.65	15.09	38.37	0.39	0.16	0.05	0.14	0.14	1.55
	CSA1	9.07	21.61	2.26	45.26	0.94	20.26	0.07	0.30	0.27	1.05
	CSA2	20.56	16.14	1.35	45.31	1.23	14.73	0.77	0.72	1.24	4.74
Proprietary Blended Cements	CAC-B1	13.46	12.23	2.67	56.65	2.86	9.90	0.20	0.79	0.72	1.21
	CAC-B2	12.71	32.94	12.95	35.09	1.79	0.84	0.50	0.24	0.65	1.23
	CSA-B1	13.63	15.82	0.75	51.28	1.14	16.62	0.29	0.62	0.69	3.06
	CSA-B2	14.72	14.37	1.22	53.85	1.23	14.40	0.10	0.59	0.49	3.39
	PCSA1	17.38	11.06	2.98	55.82	1.25	10.68	0.43	0.52	0.77	2.26
	PCSA2	20.14	15.73	3.52	43.90	1.55	12.88	0.59	0.52	0.93	1.95
Lab Blends	CAC-OPC2	16.53	10.79	2.71	58.07	0.89	7.43	0.14	0.50	0.47	2.19
	CSA1-OPC2	18.06	8.42	2.96	59.25	1.04	7.23	0.12	0.53	0.47	1.98

Other materials used in this study were a grade 67 limestone rock, siliceous river sand, a liquid polycarboxylate-ether-based superplasticizer, and a set retarder, citric acid, which was used for slump control and delay setting to allow time for mixing and casting of RSHCs. A few mixtures, namely OPC2, OPC3, and CAC required the use of a set accelerator for increasing the speed of hydration.

5.2.2 Test Matrix

Based on the observation made in the mortar phase study, it was evident that the setting time and flowability of each rapid setting binder was particularly sensitive to the amount of admixture dosage. Additionally, the aggregate type and proportions had significant impacts. Fortunately, the preliminary evaluations on mortar helped to inform mixture proportions that would be most convenient and appropriate for structural class concrete in Texas. The final admixture dosages shown in Table 5.3 are based on a percent mass of total binder (Cement and/or RSHC) in the concrete mixture. In general, the dosage for set retarder and HRWR was 0.5% and 1.0% by mass on average, respectively.

A total of 23 concrete mixtures were include in this experimental program. As shown in Table 5.3, the mixtures include total cement contents of 446 kg/m^3 (752 lb/yd^3) and 390 kg/m^3 (658 lb/yd^3) using a W/CM ratio of 0.35 and 0.40, respectively. The only exception was cement CAC-B2 which had a W/CM ratio of 0.32 based on manufacturers recommendation. It should be noted that CAC-B2 was only included in this experimental program and not in the durability testing program. This was primarily due to its volatility in mechanical strength development and characteristic.

For all mixtures, the grade 67 limestone coarse aggregate and natural river sand were incorporated with a coarse to fine aggregate ratio kept constant at 60/40. For mixtures with a W/CM ratio of 0.40, the coarse aggregate fraction was 1072 kg/m^3 (1807 lb/yd^3) and the fine aggregate fraction was 715 kg/m^3 (1205 lb/yd^3). For mixtures with a W/CM ratio of 0.35, the coarse aggregate fraction was 1045 kg/m^3 (1762 lb/yd^3) and the fine aggregate fraction was 697 kg/m^3 (1174 lb/yd^3).

Table 5.3: Concrete mixture proportions – Mass in kg/m^3 (note 1 kg/m^3 = 1.69 lb/yd^3)

Cement Type	W/CM	RSHC Binder $kg/m^3(lb/yd^3)$	OPC2 Lab Blend $kg/m^3(lb/yd^3)$	Set Accelerator (% weight of cement)	Set Retarder (% weight of cement)	HRWR (% weight of cement)
OPC2	0.35	446 (752)	-	3.0		1.00
OPC3	0.35	446 (752)	-	3.0		1.00
CAC	0.35	446 (752)	-	1.75	0.50	-
CSA1	0.35	446 (752)	-	-	1.00	1.75
CSA2	0.35	446 (752)	-	-	0.75	-
CAC-B1	0.35	446 (752)	-	-	0.50	0.75
CAC-B2	0.32	446 (752)	-	-	1.00	-
CSA-B1	0.35	446 (752)	-	-	0.50	0.75
CSA-B2	0.35	446 (752)	-	-	0.50	0.75
PCSA1	0.35	446 (752)	-	-	0.25	0.50
PCSA2	0.35	446 (752)	-	-	0.25	0.50
CAC-OPC2	0.35	111.5 (188)	334.5 (564)	-	0.50	0.75
CSA1-OPC2	0.35	111.5 (188)	334.5 (564)	-	0.25	0.75
CAC	0.40	390 (658)	-		0.25	-
CSA1	0.40	390 (658)	-	-	1.00	1.75
CSA2	0.40	390 (658)	-	-	0.50	-
CAC-B1	0.40	390 (658)	-	-	0.25	1.00
CSA-B1	0.40	390 (658)	-	-	0.25	0.50
CSA-B2	0.40	390 (658)	-	-	0.25	0.50
PCSA1	0.40	390 (658)	-	-	0.25	0.50
PCSA2	0.40	390 (658)	-	-	0.25	0.50
CAC-OPC2	0.40	97.5 (164.5)	292.5 (493.5)	-	0.25	0.75
CSA1-OPC2	0.40	97.5 (164.5)	292.5 (493.5)	-	0.25	0.75

5.2.3 Sample Preparation and Testing Program

To fully elucidate the mechanical behavior of RSHC concretes, a comprehensive testing program was initiated to evaluate the early- and later-age properties of each mixture exposed to a variety of controlled laboratory conditions. Specifically, three series of testing programs were performed. The first series included performing a full suite of fresh and hardened property tests on all RSCH concretes under

standard lab temperature conditions of 73 °F (23 °C). The second series included a temperature robustness testing program in which compressive strength development was evaluated at 50 °F (10 °C) and 100 °F (38 °C) to understand the sensitivity of RSHCs to various climatic conditions available in Texas. Finally, the third series focused on evaluating RSHC systems containing CAC as a primary component in the binder for the potential of strength reduction (i.e., conversion). This section outlines the experimental procedures and series of tests performed on each RSHC mixture.

5.2.3.1 Fresh concrete properties

In the first series of RSHC mixtures that were tested at 73 °F (23°C), slump, unit weight, and air content were recorded. These tests followed the following ASTM standards:

- Slump: ASTM C143 [39]
- Unit Weight: ASTM C138 [40]
- Fresh Air Content: ASTM C231 [41]

Besides the most common fresh concrete property tests, the setting time for each RSHC concrete was measured as per ASTM C143 [42]. Two time-of-set specimens were made. These specimens were fabricated using ink cans that were 5 in. (125 mm) high with a 6 in (150 mm) diameter.

Finally, to evaluate the temperature development and hydration characteristic of RSCHs, temperature sensor was embedded into large concrete blocks at the moment of casting. The sensors monitored the temperature rise in each RSHC concrete stored under controlled laboratory conditions 73 °F (23°C) for a period of 24-48 hrs.

5.2.3.2 Hardened properties

In the first series of RSHC mixtures that were tested at 73 °F (23°F), a total of thirty-one 100 mm x 200 mm (4 in x 8 in) cylinders were cast and cured following the requirements of ASTM C192 to obtain samples for mechanical property testing. Twenty-seven cylinders were tested in accordance with ASTM C39 [43] to obtain the compressive strength of each mixture at 3, 6, 8, and 24 hr as well as 3, 7, 28, 91, and 365 days. Four of the twenty-seven cylinders that were cast to obtain the compressive strength were first used to obtain the modulus of elasticity of each concrete mixture at 7 and 28 days in accordance with the procedure described in ASTM C469 [44]. Additionally, four cylinders were used to obtain the splitting tensile strength of each mixture at 1 and 28 days, in accordance with the requirement specified in ASTM C496 [45]. Finally, four concrete beams measuring 500 mm x 150 mm x 150 mm (20 in 6 in x 6in) were used to obtain the flexural strength of each mixture at 28 days, in accordance with the

requirement specified in ASTM C78 [46]. It should be noted that due to the rapid setting characteristic of each RSHC, flexural beams were cast and tested using a separate batch from the previously described cylinders for mechanical strength testing.

Besides mechanical testing, transport properties were also evaluated for each RSHC including bulk resistivity (ASTM C1876) [47] rapid chloride penetration testing (ASTM C1202) [48], and water sorptivity testing (ASTM C1585) [49].

5.2.3.3 Temperature robustness testing

The temperature robustness testing program included ten concrete mixtures cured at "high" and "low" temperatures to examine the mechanical performance sensitivity of each RSHC at extreme temperatures. Some binders, such as calcium sulfoaluminate, have been known to be more sensitivity to temperature than other binder systems. On the other hand, previous literature has suggested that CAC can be placed at low temperature with little reduction in strength [11, 50]. However, there is little data available for many newly developed RSHCs tested at various temperature extremes, especially when proportioned as structural based concrete mixtures.

The research team elected to test a subset of mixtures from the initial series test matrix (see Table 5.4). Specifically, ten RSCH mixtures were cast for the temperature robustness testing program with a total cement content of 446 kg/m^3 (752 lb/yd^3) and using a W/CM ratio of 0.40 (CAC-B2 was not included in this experimental program). For all mixtures in this testing program, a limestone coarse aggregate and natural river sand was incorporated with a coarse to fine aggregate ratio kept constant at 60/40.

For the temperature robustness program, all the mixing materials were measured and stored in an environmental chamber at the specified temperature for 24 hrs before mixing time. This step ensured that all of the materials were at the specified temperature before mixing and casting. The specimens were mixed and cast in the mixing room which is kept at standard temperature of 73 °F (23 °C). Immediately after being cast, all samples were placed back into the environmental chamber for 24 hrs after the time of casting. The research team cast a total of twenty-two 100 mm x 200 mm (4 in x 8 in) cylinders for compressive, tensile and modulus testing. Each mixture's compressive strength was measured at 3, 6, 8 and 24-hr intervals as well as 7 and 28-day after casting for comparison to the compressive strengths measured at ambient 73 °F temperature. It should be noted that due to their rapid hardening characteristics, the admixture dosages for each mixture in the temperature robustness testing program was modified based on the research team's best judgement to achieve suitable working time till hardening. Thus, not all admixture dosages were equivalent for each mixture at the different curing temperatures.

Table 5.4: Temperature Robustness Testing Program Matrix – Mass in kg/m³ (note 1 kg/m³ = 1.69 lb/yd³)

Cement Type	W/CM	RSHC Binder kg/m³(lb/yd³)	OPC2 Lab Blend kg/m³(lb/yd³)
CAC	0.35	446 (752)	-
CSA1	0.35	446 (752)	-
CSA2	0.35	446 (752)	-
CAC-B1	0.35	446 (752)	-
CSA-B1	0.35	446 (752)	-
CSA-B2	0.35	446 (752)	-
PCSA1	0.35	446 (752)	-
PCSA2	0.35	446 (752)	-
CAC-OPC2	0.35	111.5 (188)	334.5 (564)
CSA1-OPC2	0.35	111.5 (188)	334.5 (564)

5.2.3.4 CAC Conversion Testing

A total of six calcium aluminate cement (CAC) based mixtures were cast in this series to identify the potential for strength reduction (i.e., conversion) during hydration. Each mixture consisted of three CAC binder: Pure CAC (CAC1), a preblended ternary blend of CAC, calcium sulfate, and ordinary Portland cement (CAC-B1), and lab blend of CAC, calcium sulfate, and a local ordinary portland cement from Texas (CAC-OPC2). Table 5.5 shows the six mixture proportions for each type of CAC binder.

In order to evaluate the potential for conversion in each CAC binder system, fifteen 100 mmx 200 mm (4 in x 8 in) cylinders were cast and cured at elevated temperatures to trigger the process of converting the metastable phases to stable phases. Samples were initially cast and allowed to cure at an ambient laboratory temperature of 23 °C (73 °F) for a period of 24 hrs. Thereafter, samples were demolded and placed into a heated curing tank maintained at 50 °C (122 °F). Compressive strength of each mixture were monitored and measured at 1 day (prior to transferring to heated bath), and 3, 7, 28, and 91 day of curing in 50 °C (122 °F).

Table 5.5: Temperature Robustness Testing Program Matrix – Mass in kg/m³ (note 1 kg/m³ = 1.69 lb/yd³)

Cement Type	W/CM	RSHC Binder kg/m³(lb/yd³)	OPC2 Lab Blend kg/m³(lb/yd³)
CAC	0.35	446 (752)	-
CAC-B1	0.35	446 (752)	-
CAC-OPC2	0.35	111.5 (188)	334.5 (564)
CAC	0.40	390 (658)	-
CAC-B1	0.40	390 (658)	-
CAC-OPC2	0.40	97.5 (164.5)	292.5 (493.5)

5.3 RESULTS AND DISCUSSIONS

5.3.1 Fresh Properties of RSHC Concretes

5.3.1.1 Slump, unit weight, and air content

Tables 5.6 and 5.7 summarizes the fresh property results (slump, fresh density, and air content) for all concrete mixtures at a cement binder content of 446 kg/m³ (752 lb/yd³) and 390 kg/m³ (658 lb/yd³), respectively. Given the need for designing mixtures for structural applications, a target slump ranging between 75-230 mm (3-9 in) was set for all mixtures. The majority of mixtures were able to achieve a slump greater than 75 mm (3 in). While a few mixtures showed a slump that exceeded 230 mm (9 in), they did not display any sign of segregation or impact their rapid setting and strength characteristics. Interestingly, it was observed that mixtures having a slump greater than 150 mm (6 in) resulted in some of the best strength development between all mixtures. On the other hand, while some did not reach the minimum target slump, they were still suitable for fabricating test specimens using a mechanical vibrating table. With respect to measured fresh density and air content, all results showed typical ranges for non-air entrained concrete.

Table 5.6: Fresh properties result for 446 kg/m³ cement binder

Cement Type	Cement ID	Slump mm (in)	Unit weight kg/m³ (lb/ft³)	Air content (%)
Straight Cement	OPC2	130 (5.0)	2394 (149.5)	1.1
	OPC3	90 (3.5)	2369 (147.9)	2.0
	CAC1	40 (1.5)	2357 (147.1)	0.5
	CSA1	230 (9.0)	2316 (144.6)	1.8
	CSA2	>230 (>9.0)	2350 (146.7)	3.2
Proprietary Cement	CAC-B1	180 (7.0)	2365 (147.6)	2.4
	CAC-B2	100 (4.0)	2356 (147.1)	4.0
	CSA-B1	>230 (>9.0)	2375 (148.3)	4.0
	CSA-B2	90 (3.5)	2425 (151.4)	1.1
	PCSA1	230 (9.0)	2320 (144.8)	1.3
	PCSA2	>230 (>9.0)	2345 (146.4)	1.4
Lab Blended Cement	CAC1-OPC2	60 (2.5)	2386 (149.0)	2.3
	CSA1-OPC2	130 (5.0)	2394 (149.5)	2.3

Table 5.7: Fresh properties result for 390 kg/m³ cement binder

Cement Type	Cement ID	Slump mm (in)	Unit weight kg/m³ (lb/ft³)	Air content (%)
Straight Cement	CAC1	75 (3.0)	2407 (150.3)	1.6
	CSA1	13 (0.5)	2397 (149.6)	0.8
	CSA2	230 (9.0)	2372 (148.1)	2.8
Proprietary Cement	CAC-B1	13 (0.5)	2409 (150.4)	2.1
	CSA-B1	215 (8.5)	2359 (147.3)	2.7
	CSA-B2	50 (2.0)	2395 (149.5)	2.5
	PCSA1	200 (8.0)	2408 (150.3)	1.9
	PCSA2	200 (8.0)	2402 (149.9)	2.4
Lab Blended Cement	CAC1-OPC2	90 (3.5)	2388 (149.1)	2.5
	CSA1-OPC2	40 (1.5)	2361 (147.4)	2.4

5.3.2 Setting time of RSCH Concrete

Figures 5.1-5.3 show the time of setting for straight RSHCs, proprietary, and lab blended cement mortar at a cement binder of 446 and 390 kg/m³, respectively. The setting time of OPC2 and OPC3 are included in all three figures, making it the base parameter for comparing setting times with different cement types.

Additionally, the dashed lines represent the initial (500 psi) and final (4,000 psi) setting values for concrete according to the time-of-set penetrometer test.

The results show the variation in achieving the initial and final setting time for each binder. In comparing the setting time of rapid setting cements with OPC mixtures, there is noticeable differences in which the time between initial and final set is reached. It should be noted that both OPC mixtures (OPC2 and OPC3) were also combined with a set accelerator in order to attain rapid setting characteristics (see Table 5.3). With the exception of CAC1, all RSHC mixtures including OPC3 showed a faster onset of hardening achieving initial and final set quicker than OPC2. Each mixture showed a relatively gradual progression to initial set with a sudden rapid hardening to final set almost immediately; CAC was dosed with a higher than needed citric acid retarder which is likely the reason for the slower hydration and setting time observed. Interestingly, CSA mixtures (straight and proprietary blends) showed the fastest setting of all cements but had some of the highest slump values (see Tables 5.4 and 5.5). In addition, these cements measured some of the highest strengths at early ages (< 1 day).

With regards to cement content, majority of mixtures with lower cement showed a slight delay, or longer time to achieve initial set. Nonetheless, once initial set was achieved the rapid hardening to final set was almost immediately unlike the more gradual rise in OPC2. The lab blends performed similarly to OPC2 with a more graduate rate to initial and final set however, this was highly dependent on the type of binder and amount of admixture used in the mix.
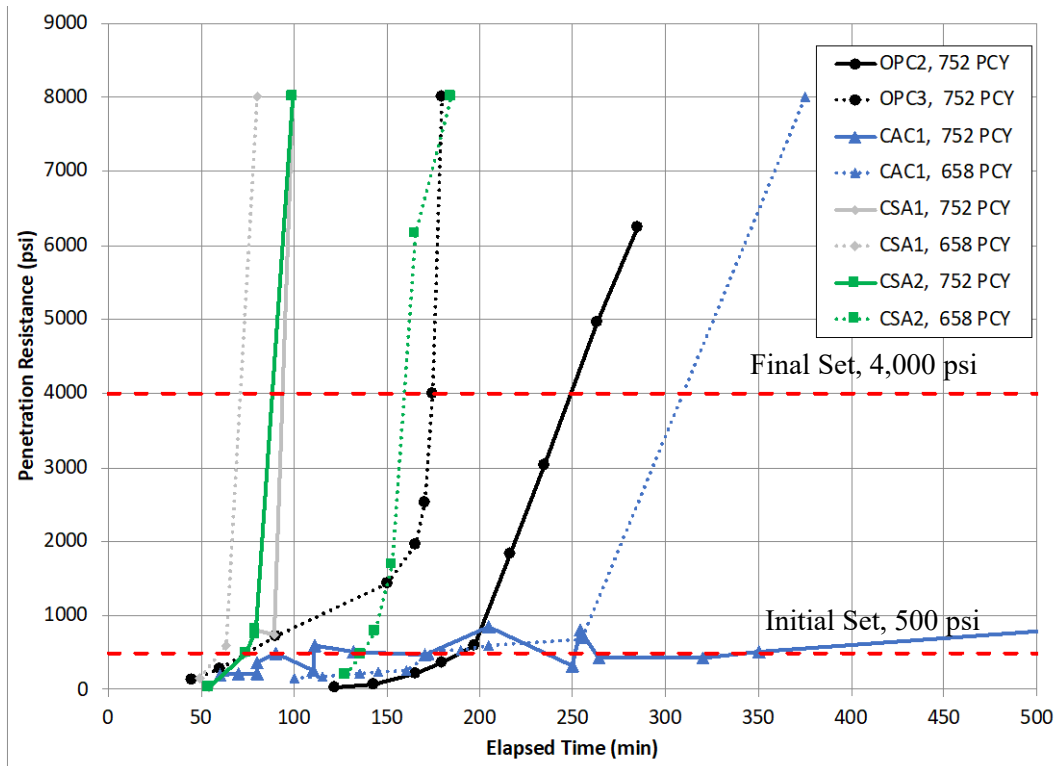
Figure 5.1: Setting time of straight cement mortar
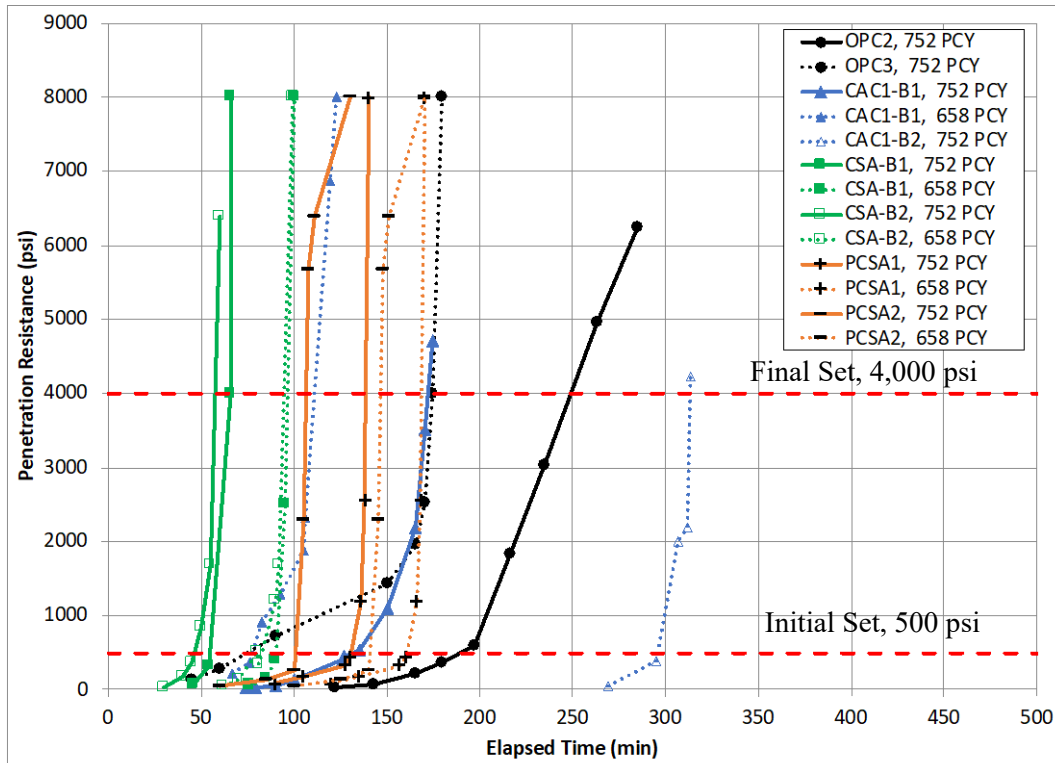
Figure 5.2: Setting time of proprietary cement mortar

92
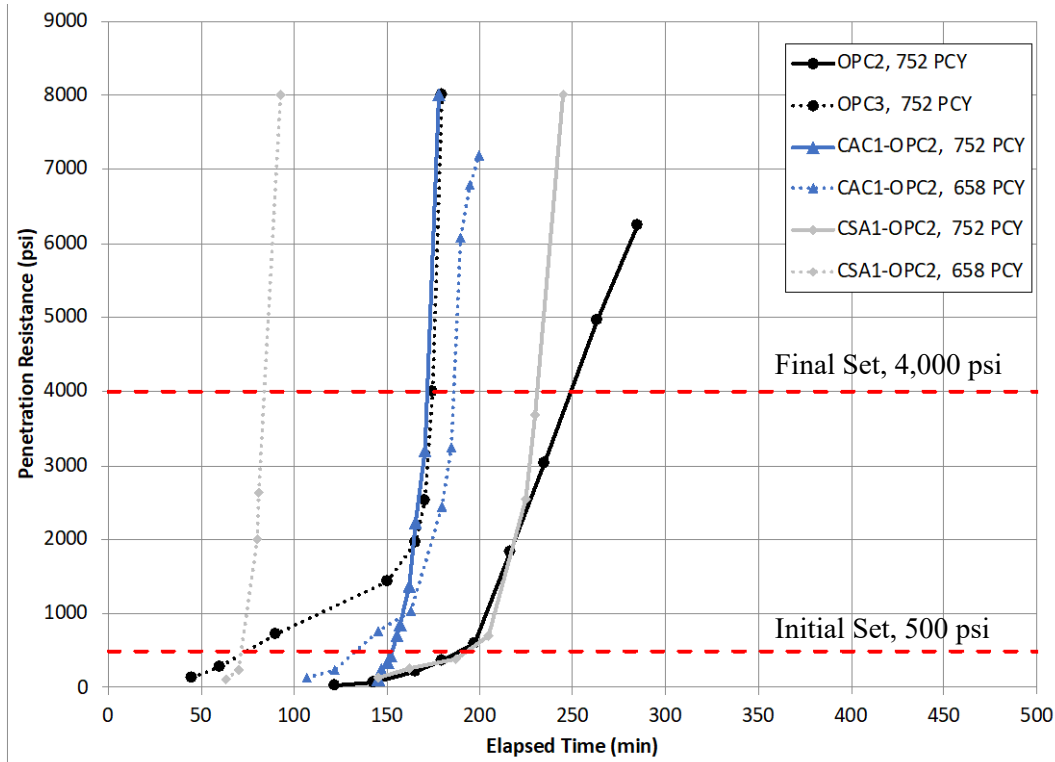
Figure 5.3: Setting time of lab-blended cement mortar

5.3.3 Hydration of RSHC Concrete

Figure 5.4 shows the time-temperature history for concrete mixtures at 752 PCY and at a W/CM of 0.35. Additionally, Table 5.8 summarizes the maximum peak temperature and the time at which the maximum temperature was measured in each RSCH concrete. The time-temperature history for each mixture was captured through the use of an embedded sensor. Each sensor monitors and records temperature as well as humidity for an indefinite period and transmits the data collected via Bluetooth. The sensors were embedded in the large concrete exposure blocks (16 x 16 x 16 in.) intended for evaluating long-term alkali silica reactivity (ASR) (see Chapter 11). In order to transmit the data via Bluetooth, each sensor was required to be embedded at a depth not to exceed 3 inches. Unfortunately, the sensor did not work in three of the RSHC mixtures (CSA2, PCSA2, and CAC-OPC2).

From the results, CSA1 showed the fastest onset of reactivity generating the thermal curve within minutes of hydration. The results agree with the measured setting time in which CSA1 had the fastest setting time of all mixtures. When compared to other RSHCs, the majority see similar behavior with a rapid acceleration and deceleration of the thermal curve once the hardening phase begins with a few exceptions including PCSA1 and CAC-B1. On the other hand, OPC1 showed a much longer lag and delay in reaching the peak heat of the curve. In addition, the dissipation of the peak heat temperature was much

longer in OPC1. However, with the exception of CAC1, the maximum measured peak heat did not vary significantly between rapid setting cements and OPC1 with most not exceeding 135 °F (57 °C). What is interesting to observe is the marked reduction in total peak heat for blended system incorporating OPC2 (CSA-OPC2 and CAC-B1). It should be noted that while CSA-B2 and PCSA1 showed a noticeable reduction in their peak heat, it is unknown if this is due to being blended with OPC or other constituents in the proprietary system.
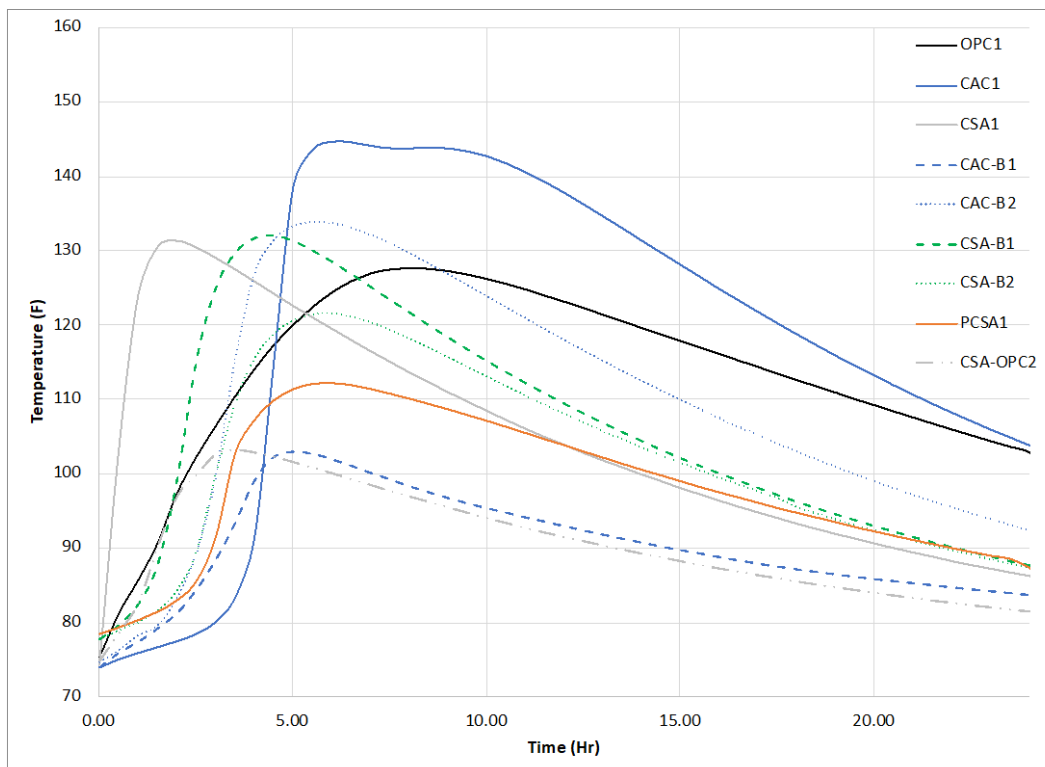
Figure 5.4: Time-Temperature History for RSHC concretes

Table 5.8: Temperature Profile of RSHC Concretes

Cement ID	Peak Temp, °F(°C)	Time to Peak Temp (Hr)
OPC2	128 (53)	8
CAC1	145 (63)	6
CSA1	131 (55)	2
CAC-B1	103 (39)	5
CAC-B2	134 (57)	5.5
CSA-B1	132 (56)	4.5
CSA-B2	122 (50)	6
PCSA1	112 (44)	6
CSA-OPC2	103 (39)	3.5

5.4 HARDENED PROPERTIES

5.4.1 Compressive Strength

Figures 5.4-5.6 shows the compressive strength of straight, proprietary, and lab blended cement, respectively. Each figure is further subdivided by breaking down the compressive strengths of each mixture at early-ages ($\leq$ 24-hours)and later-ages ($\geq$ 3-days). Additionally, in each figure both the water-to-cement ratio and total binder content are shown to illustrate the results between both sets of RSHC mixtures. Finally, in all figures OPC2 and OPC3 are included as a reference for comparing strengths between portland cements and RSHC concretes.

From Figure 5.4a, it is clear that all RSCHs showed a much faster onset of strength development in comparison to OPC2 and OPC3. For example, both CSA1 and CSA2 had a minimum compressive strength of 3,000 psi by 6 hrs regardless of binder content and W/C. In fact, CSA1 and CSA2 measured a compressive strength greater than 5,000 psi by 3 hrs when using a higher binder content and lower W/C. Whereas OPC3 did not achieve this magnitude of strength until 24 hrs of curing age. On the other hand, CAC1 did not produce any measurable strength until 24 hrs likely due to its sensitivity to the set retarder (citric acid) used in the mixture. This was particularly common in all CAC mixtures throughout the experimental program. The results also show the impact of using a high water to cement ratio (0.40) in which as expected, a marked strength

reduction was observed in all the mixtures. Nonetheless, CSA1 and CSA2 were still capable of producing more than 5,000 psi by 24 hrs of curing.

In regard to strengths at later ages (> 24 hrs), it is interesting the see that very little measurable compressive strength is observed in RSCH concretes between 1 and 28 days of curing. In fact, both OPC2 and OPC3 measured a compressive strength higher than all RSCH concrete by 91 days of curing. Nonetheless, all RSCHs did continue to show some strength gain up to 1 year of age.
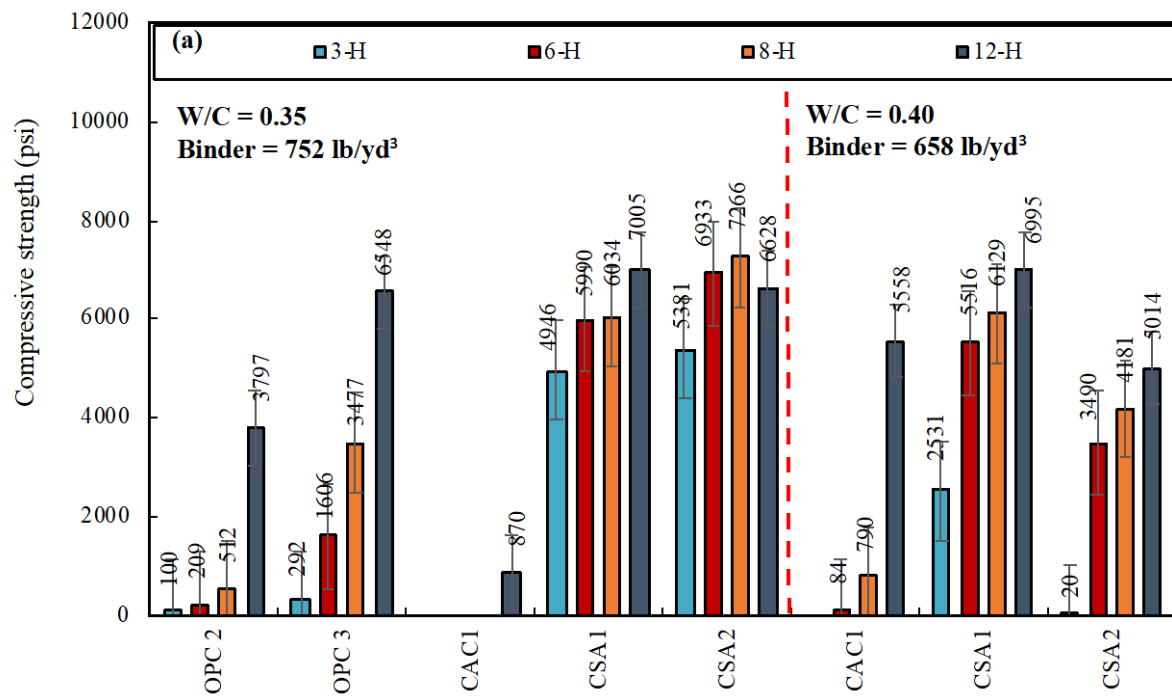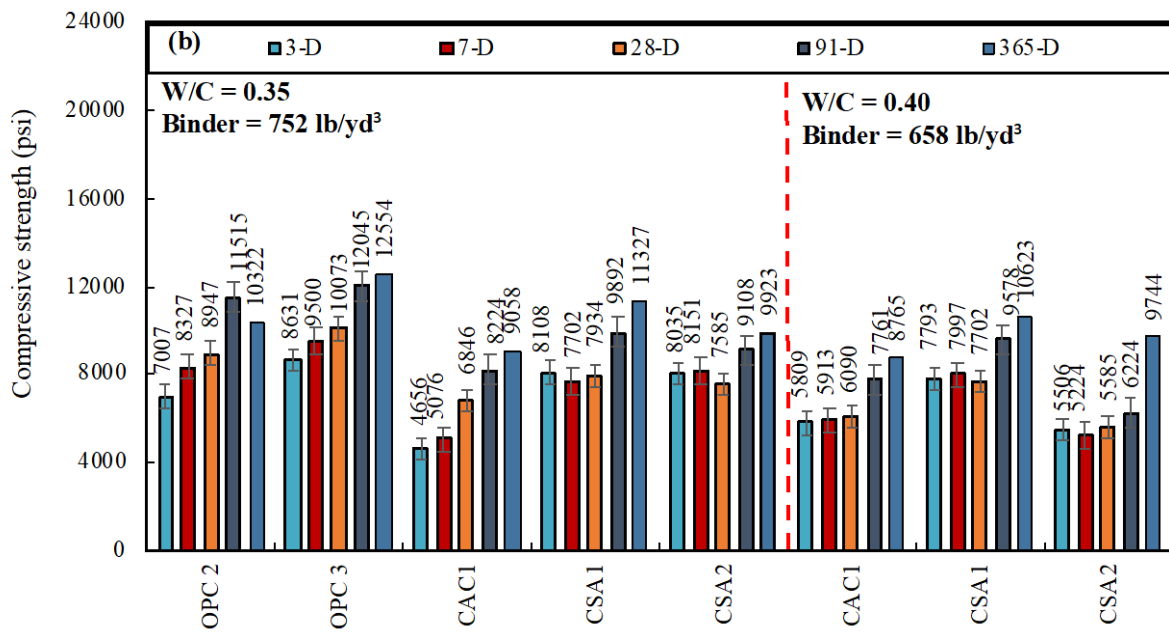
Figure 5.5: Concrete compressive strength of straight cements at (a) early curing ages and (b) later curing ages

Figure 5.6 shows the compressive strength plotted as a function of age for all proprietary cements. The same trends in mechanical strength can be observed: 1) RSHC concrete exhibited a faster onset of strength at early ages (< 24hrs); 2) Higher strengths were observed in mixtures using a high binder content (752 lb/yd³) and lower water to cement ratio (0.35); and 3) RSHC concrete exhibited lower or equal strengths to OPC2 and OPC3 with the exception of CSA-B1 which had the highest compressive strength of all mixtures at over 15,000 psi by 1 year of curing age. In the case of binder type and mechanical strength performance, CAC-B1 and CAC-B2 still exhibited a slower strength development in comparison to their CSA counterparts. Additionally, PCSA1 and PCSA2 are proprietary blend products and the ratios of components contained in them is unknown making it difficult to determine the impact of their strength development.
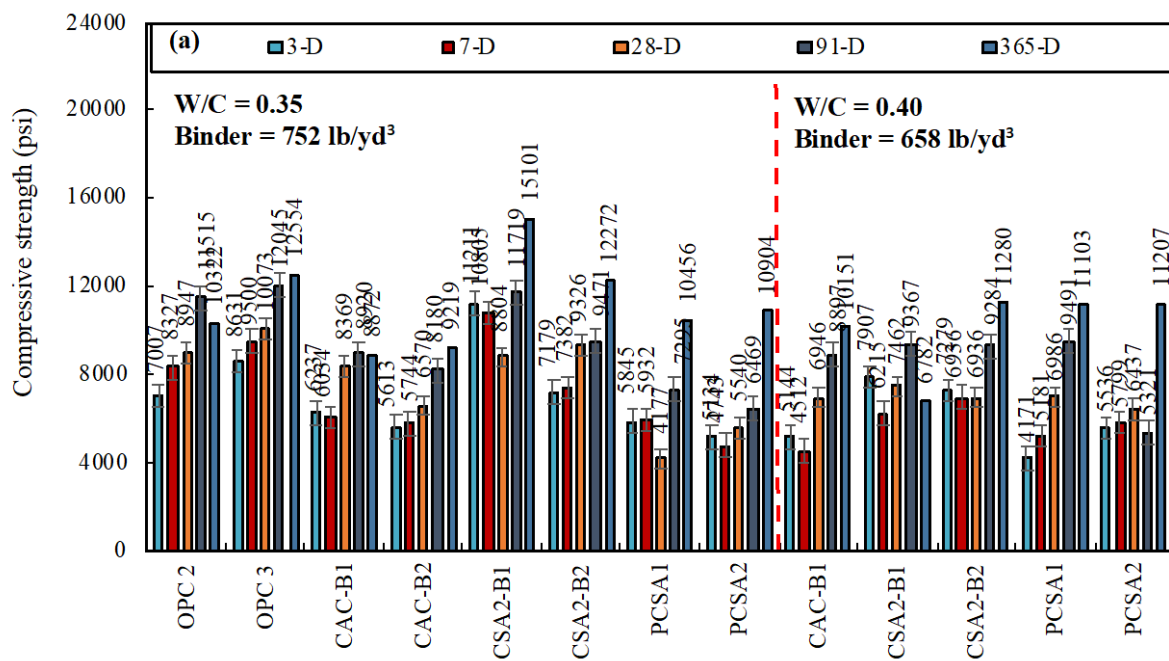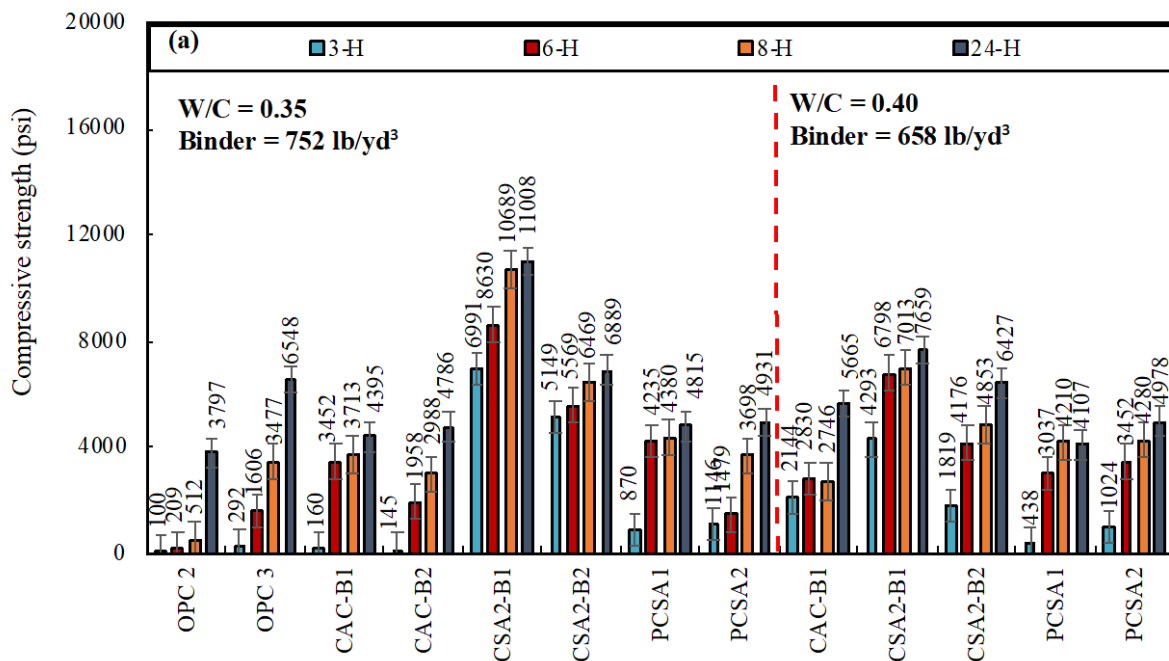
Figure 5.6: Concrete compressive strength of proprietary cements at (a) early curing ages and (b) later curing ages

Figure 5.7 shows the compressive strength plotted as a function of age for all lab blended cements. As a reminder, these blends were combined with a Type I/II cement at a 25% replacement level by mass. The lab blended mixtures observed some of the lowest and most gradual compressive strengths. Clearly, the blended system showed a dilution impact on the compressive strength, achieving only about 33% of the 1-day strength as the pure system. Nonetheless, the results shows there continues to be noticeable increases in strength with time with the blended system now achieving equivalent strength to that of other RSHC concrete by 28-days of curing age. It is worth noting that these mixtures showed a very similar behavior when evaluated using mortar cubes (see Chapter 3).
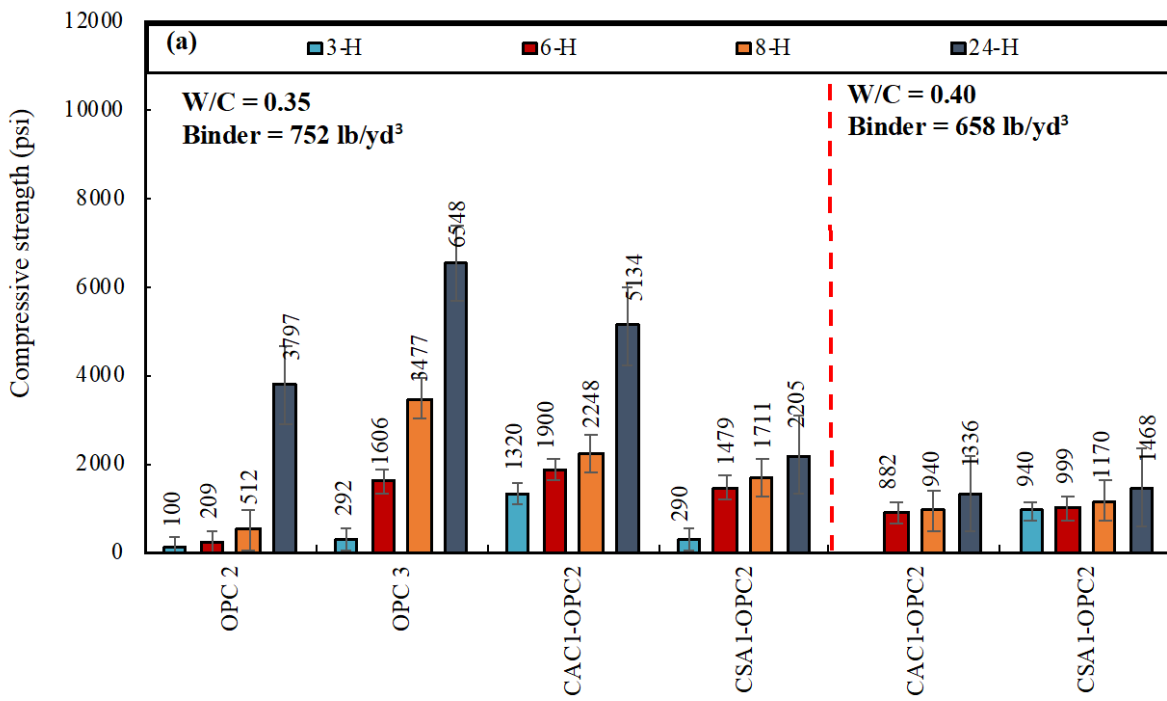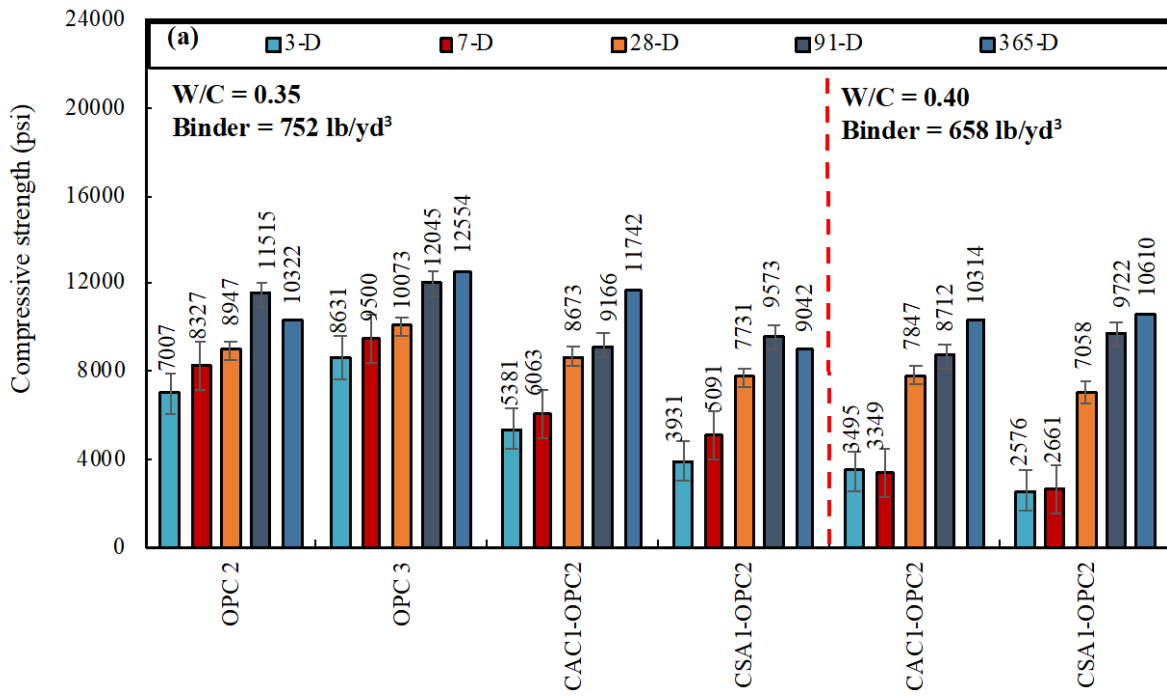
Figure 5.7: Concrete compressive strength of lab blended cements at (a) early curing ages and (b) later curing ages

5.4.2 Splitting Tensile Strength

Figure 5.8 shows the splitting tensile strength at 1d and 28d age for all RSCHs concretes. Additionally, the results in figure are subdivided between 752 and 658 lb/yd^3 binder content. In general, no clear trends were observed in the splitting tensile strength of RSHC concretes. Most RSCHs exhibited either equal or lower splitting tensile strengths than OPC2 and OPC3. What is interesting to note however, while majority of RSHC concretes did not exhibit any substantial increase in splitting tensile strength between 1 and 28 days of curing age, mixture comprised of OPC, including lab blended cements did see a substantial increase. For example, CAC1-OPC2 and CSA1-OPC2 both showed more than a 150% increase in their splitting tensile strength between 1 and 28 days. This is likely attributed to the silicate phases available in the higher amount of OPC of the blend.
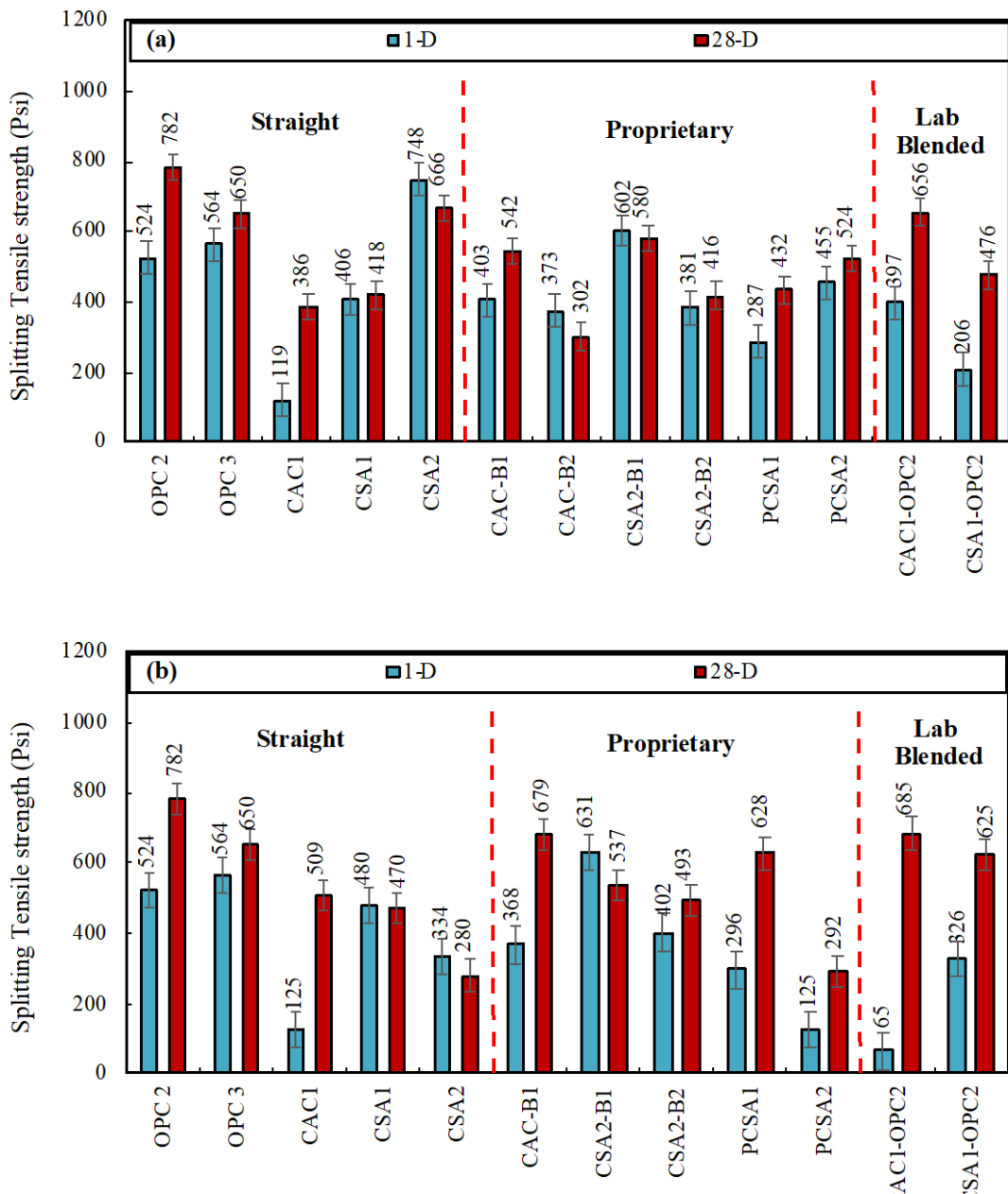
Figure 5.8: Splitting tensile strength of RSCH concretes using a) 752 lb/yd³ and b) 658 lb/yd³ total binder content

Figure 5.9 shows the ratio of splitting tensile strength to compressive strength at 1 and 28 days for all RSCH concretes. Across the board, the tensile to compressive strength ratio was on average 8.4% and 7.3% for 1 and 28 days of curing age. This was generally in agreement with OPC2 and OPC3 as well.
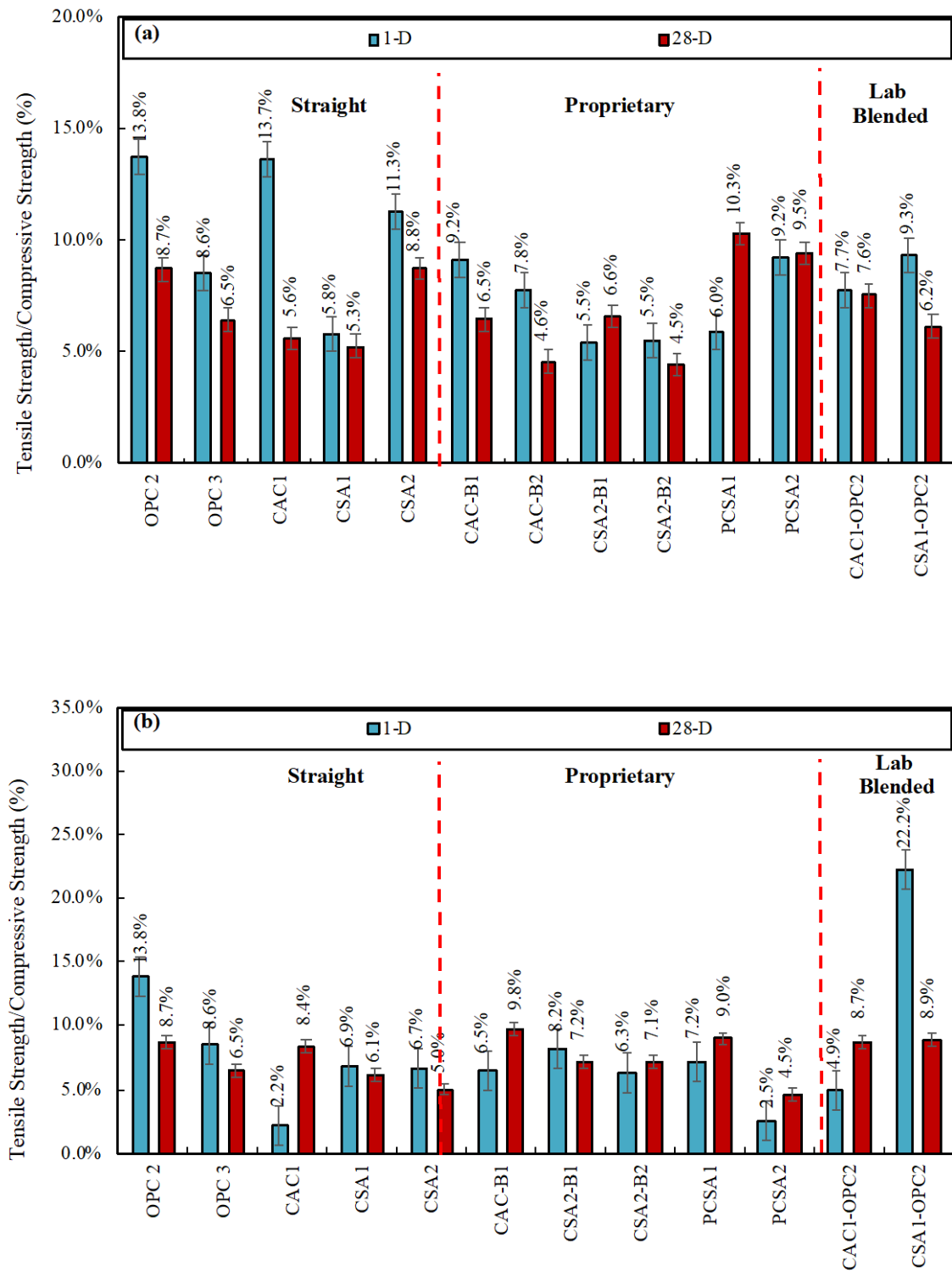
Figure 5.9: Splitting tensile strength to compressive strength ratio of RSCH concretes using a) 752 lb/yd³ and b) 658 lb/yd³ total binder content

5.4.3 Flexural Strength

Figure 5.10 shows the modulus of rupture (MOR) results for all RSCH concretes at 7 and 28 days of curing. Results below were only taken on mixtures comprised of a total binder content of 752 lb/yd^3 and a W/C of 0.35. Unlike the splitting tensile strength, some noticeable increase in strength is observed between 7 and 28 days. Additionally, some of the highest observed MOR strengths were PCSA2 which had one of the lowest splitting tensile strengths. Some of this could be attributed to the proprietary blend of the binder than may enhance the flexural strength. In general, the MOR for all concretes did not show a substantial difference between cement type or cement system.
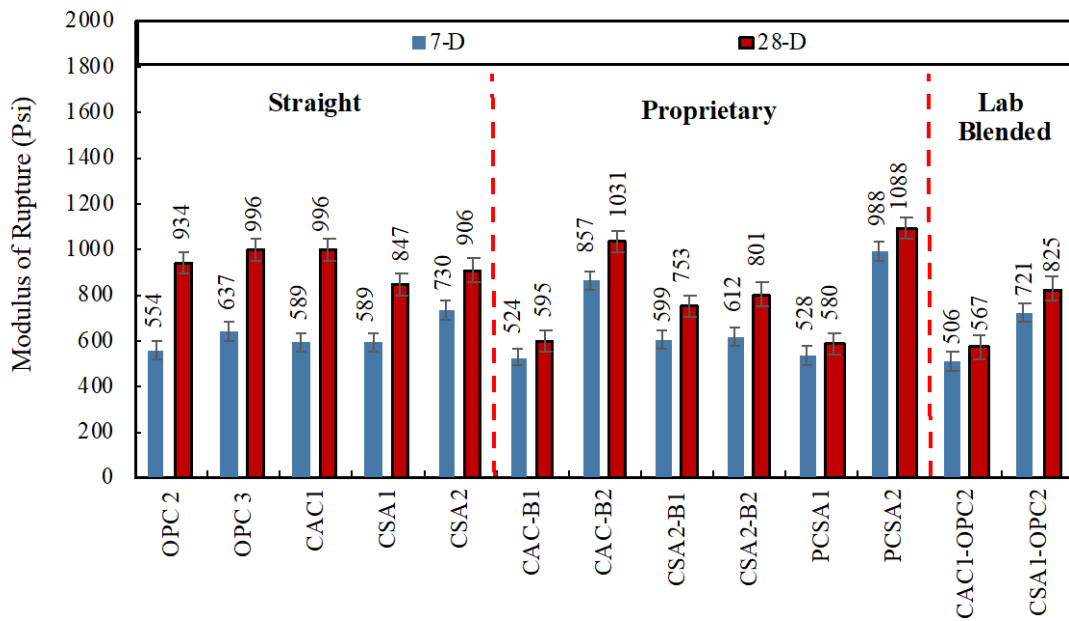
Figure 5.10: Flexural strength of RSCH concretes at 7 and 28 days of curing

5.4.4 Elastic Modulus

Figure 5.11 shows the results of modulus of elasticity for all concretes at 7 and 28 days. Whereas OPC2 and OPC3 showed an abrupt increase in stiffness between 7 and 28 days of curing, majority of RSHCs mixtures did not experience an increase in modulus. Additionally, very little difference were observed between the two cement contents.
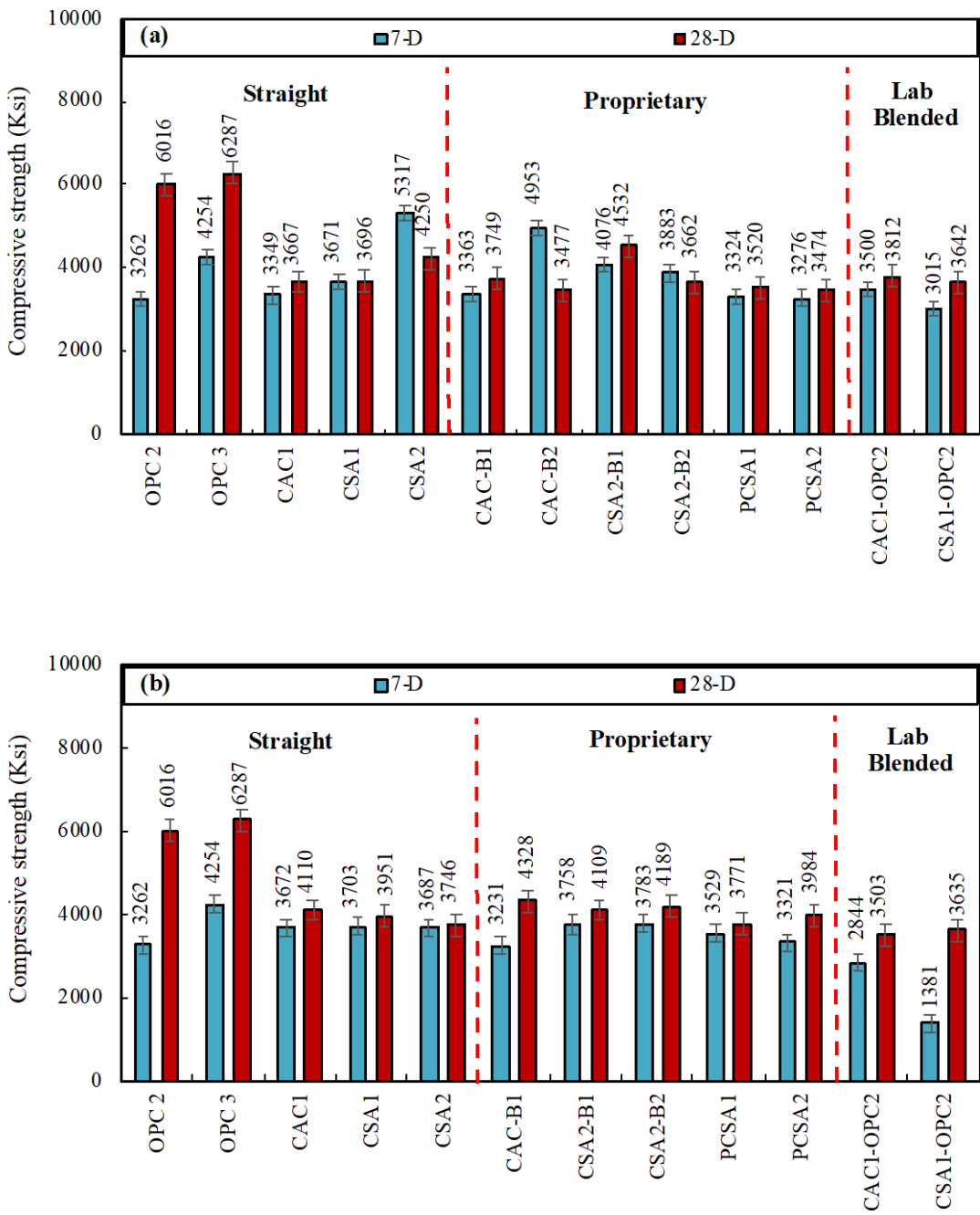
Figure 5.11: Modulus of elasticity of RSCH concretes using a) 752 lb/yd³ and b) 658 lb/yd³ total binder cement

The structural building code, ACI 318 [51], allows the use of an empirical equation to predict the modulus of elasticity of normal weight concrete. This equation was used to predict the elastic modulus based on the 7 and 28 day compressive strength. Figure 5.12 shows the ratio of predicted to experimental

elastic modulus at 7 and 28 days for all RSHC concretes. Please note that a ratio of 1.0 means that the predictive equation is accurate and a ratio below 1.0 would be a conservative prediction of modulus of elasticity in terms of structural design. In the majority of mixtures, the ratios range from 0.87 to 1.5 with a few outliers above this value. Generally, mixtures using a lower binder content (658 lb/yd^3) tended to observe closer to predicted values than those at the higher binder content (752 lb/yd^3). This likely due to the higher cement content contributing to a much faster onset of strength development. Nonetheless, the number of mixes that observed a ratio of less than 1 were few, indicating the empirical equation from ACI may not accurately represent the elastic modulus of RSHC type concrete. More work is needed to understand how the modulus is impacted by the structural class type of mixtures used in this experimental work.
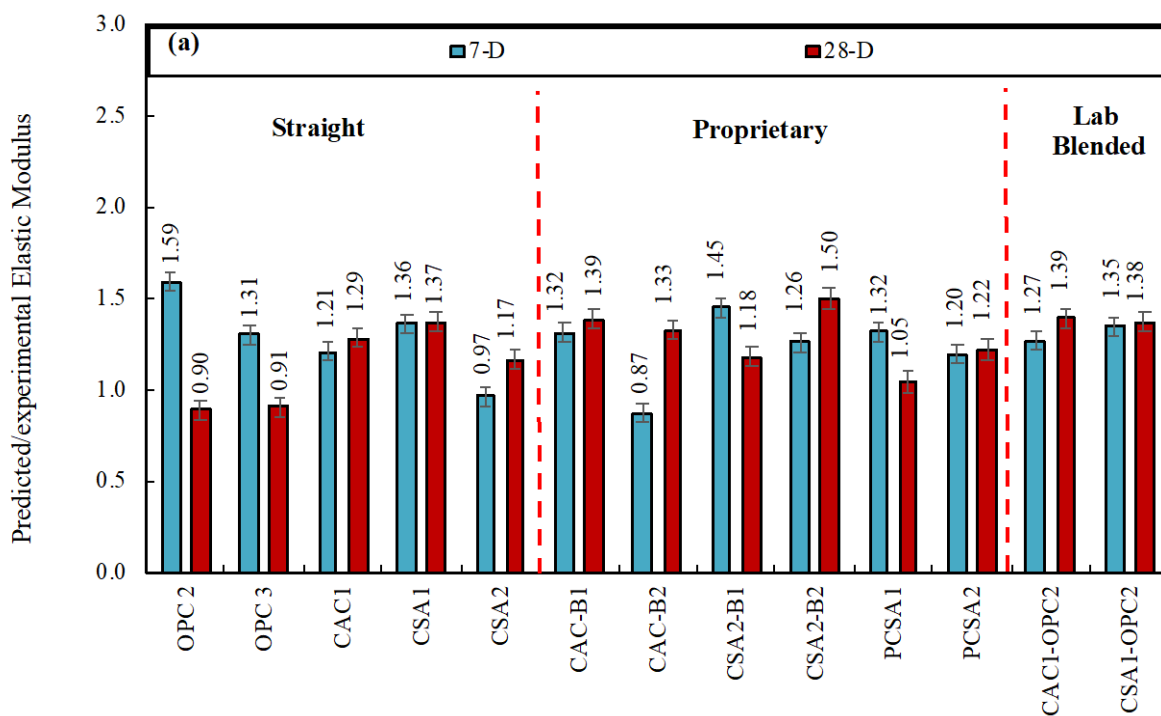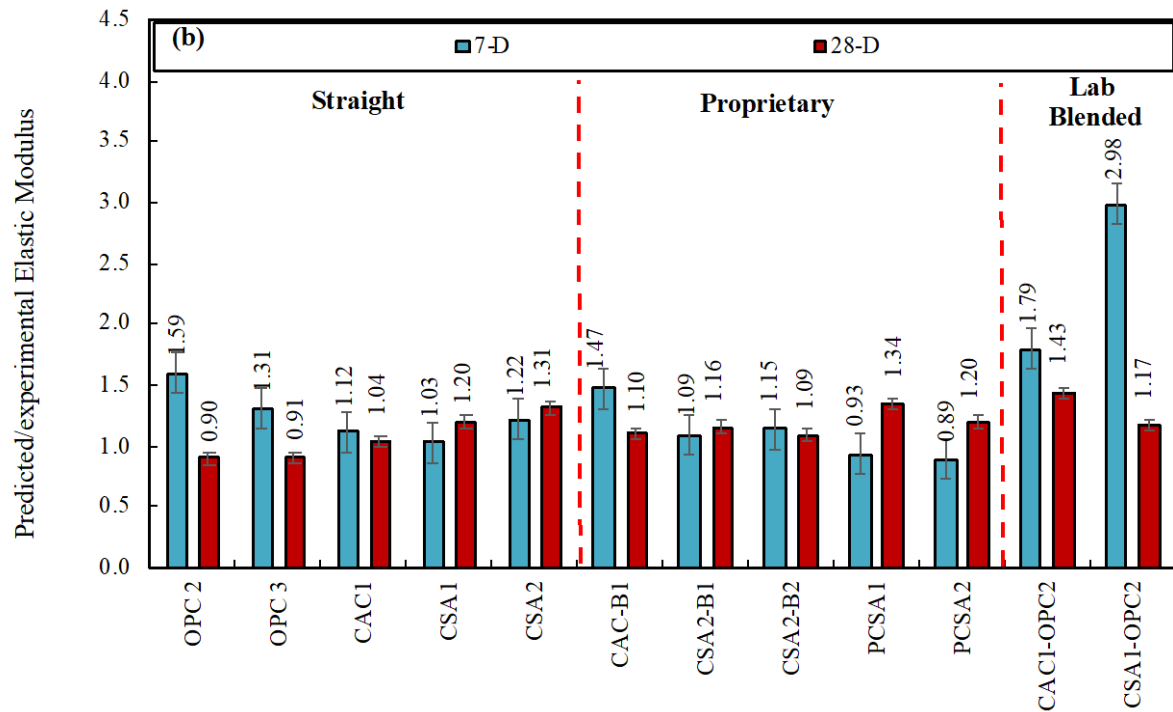
Figure 5.12: Ratio of predicted to experimental elastic modulus of RSCH concretes using a) 752 lb/yd³ and b) 658 lb/yd³ total binder cement

5.4.5 Drying Shrinkage

Concrete prisms were produced to determine the drying shrinkage of the RSHC mixtures in accordance with ASTM C157[52] . Changes to the ASTM standard procedure were implemented due to the rapid hydration of these specimens. The specimens were cast and cured for 6 and 24 hrs and quickly moved directly into the environmental chamber. This was done because of the rapid hydration of these systems and to match what would be done in the field for rapid turnaround. The environmental chamber was kept at 73 °F (23 °C) and 50% RH. The drying shrinkage results for all the concrete prism prepared are shown in Figures 5.13-5.16.

When comparing the RSCH systems to OPC2 and OPC3, there were few binders that observed less shrinkage however, no particular system did better. In other words, regardless of being CAC, CSA, or PCSA, some binder types showed higher shrinkage. Straight cement sample with 658 lb/yd³ cement binder has less shrinkage than those made at 752 lb/yd³ cement binder. Proprietary cement CAC1 B1 shows extreme shrinkage at both 6h and 1d cure. PCSA1 shows more shrinkage when demolded at 1d.

Lab blended cement CAC1-OPC2 shows lesser shrinkage when demolded at 6h, CSA1 OPC2 shows almost identical drying shrinkage whether demolded at 6h or 1d.
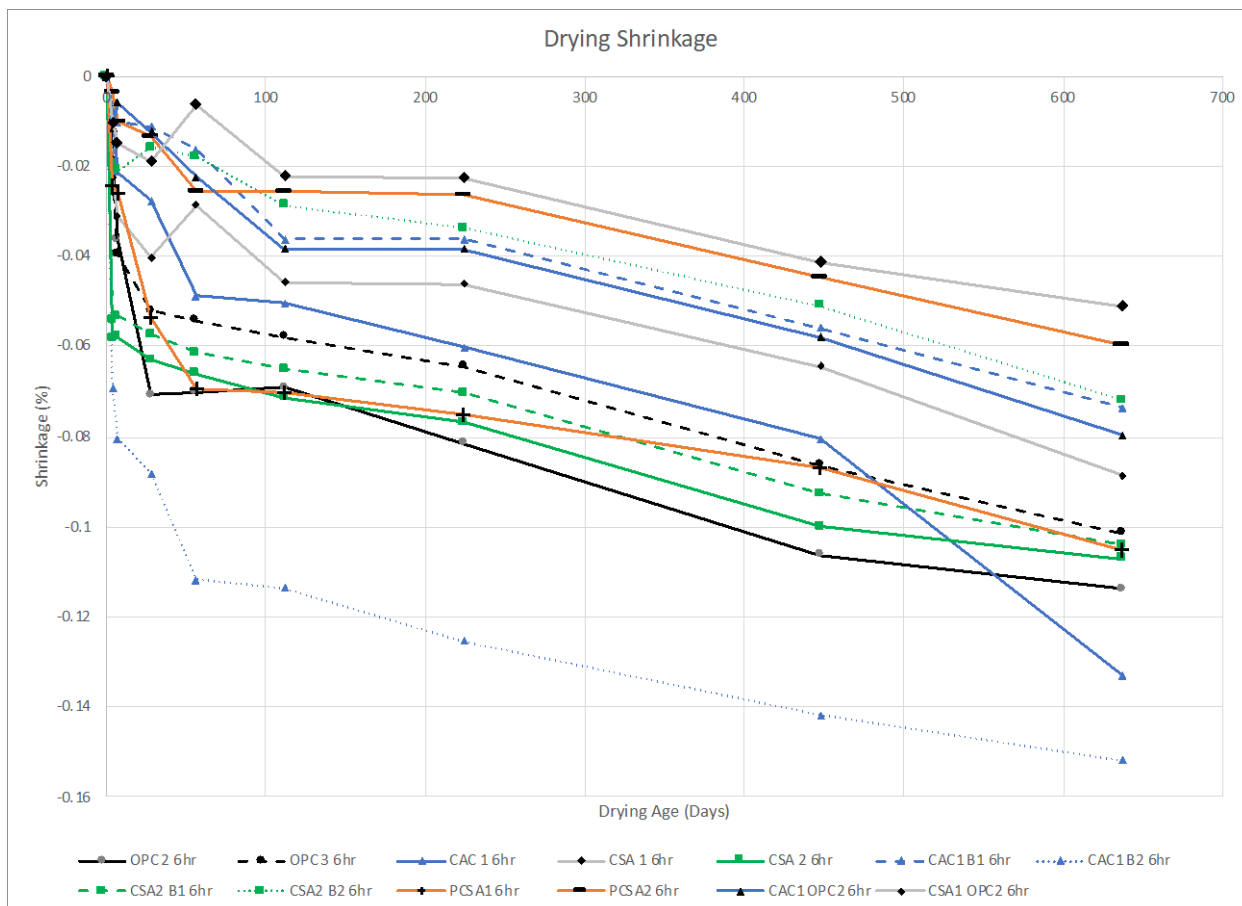
Figure 5.13: Drying shrinkage of prism demolded at 6h at 446 kg/m^3 cement binder
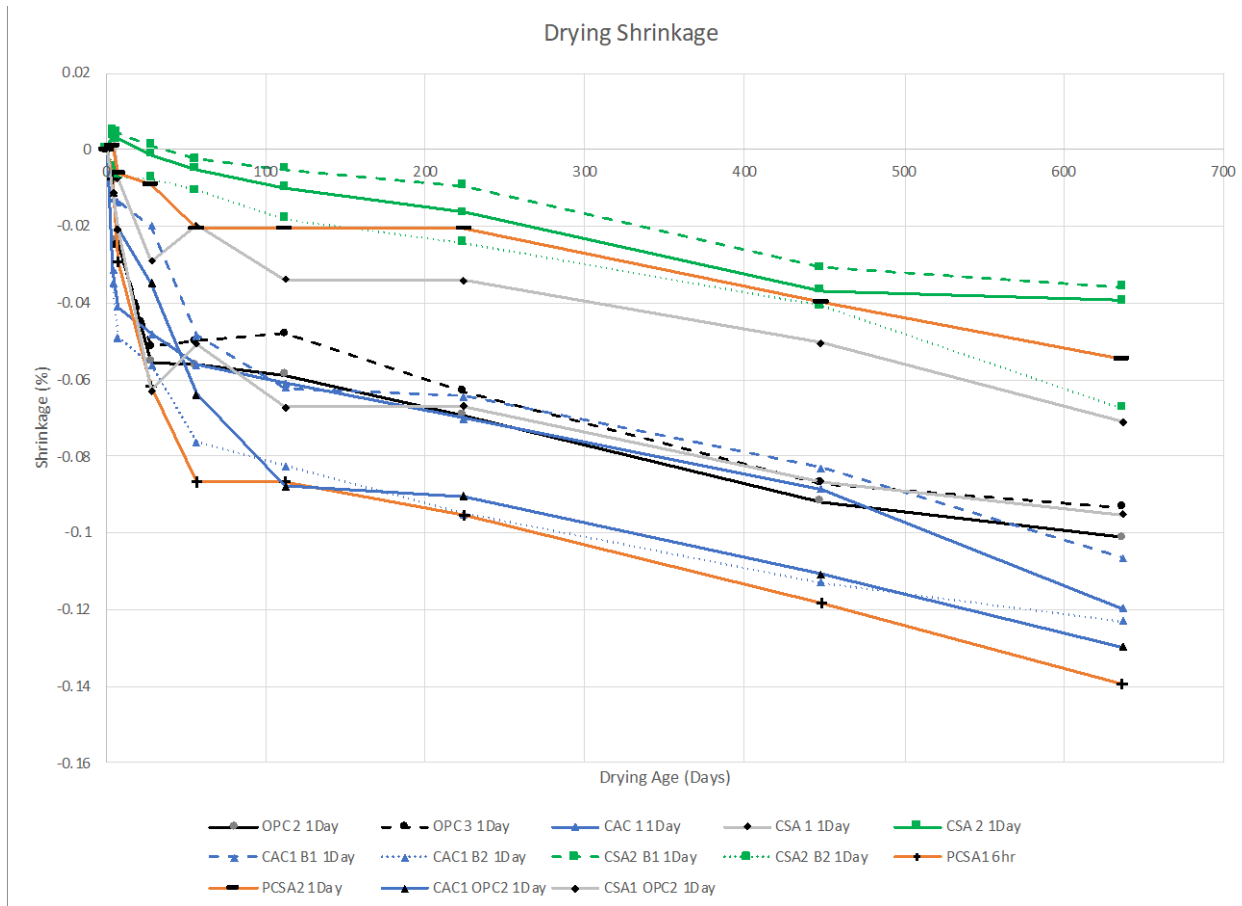
Figure 5.14: Drying shrinkage of prism demolded at 1d at 446 kg/m3 cement binder
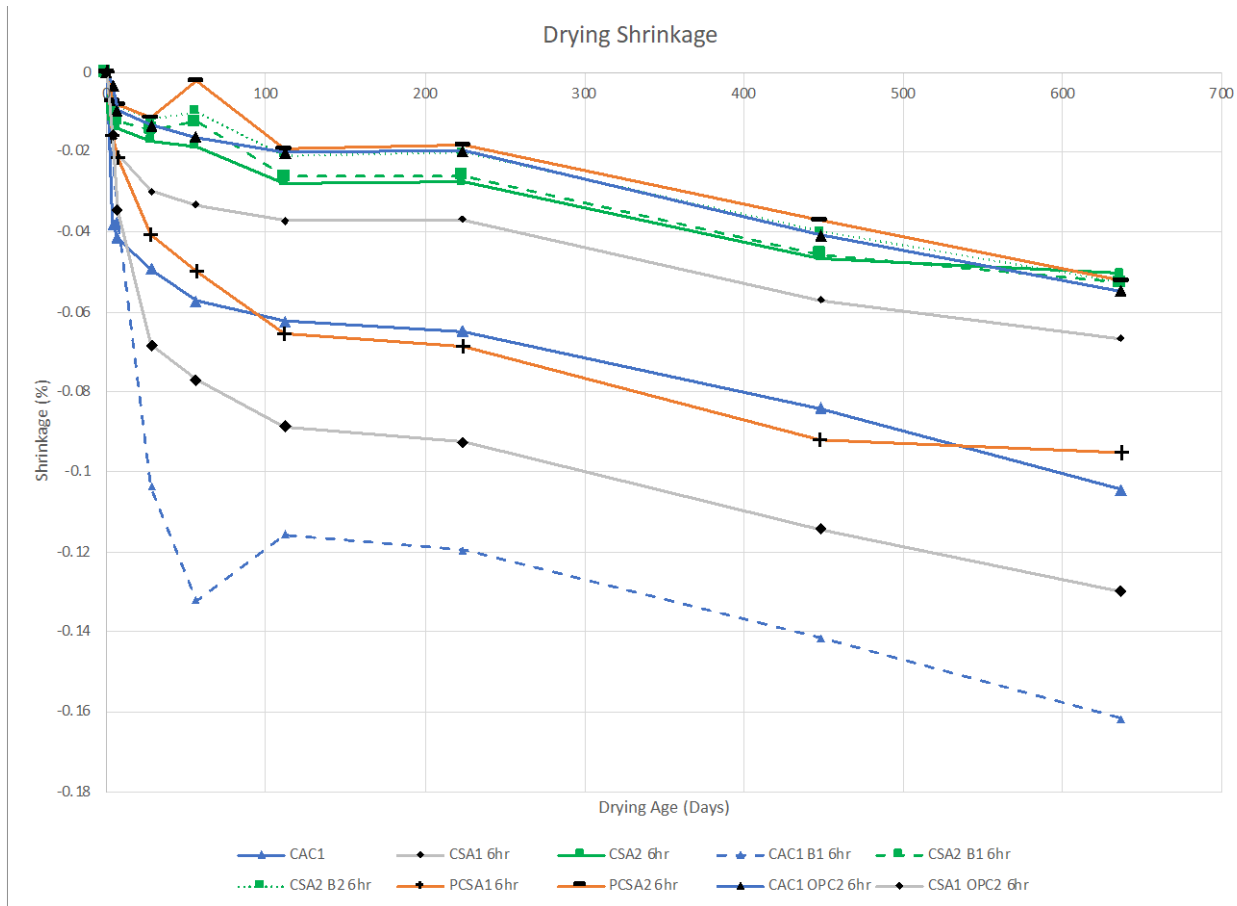
Figure 5.15: Drying shrinkage of prism demolded at 6h at 390 kg/m^3 cement binder
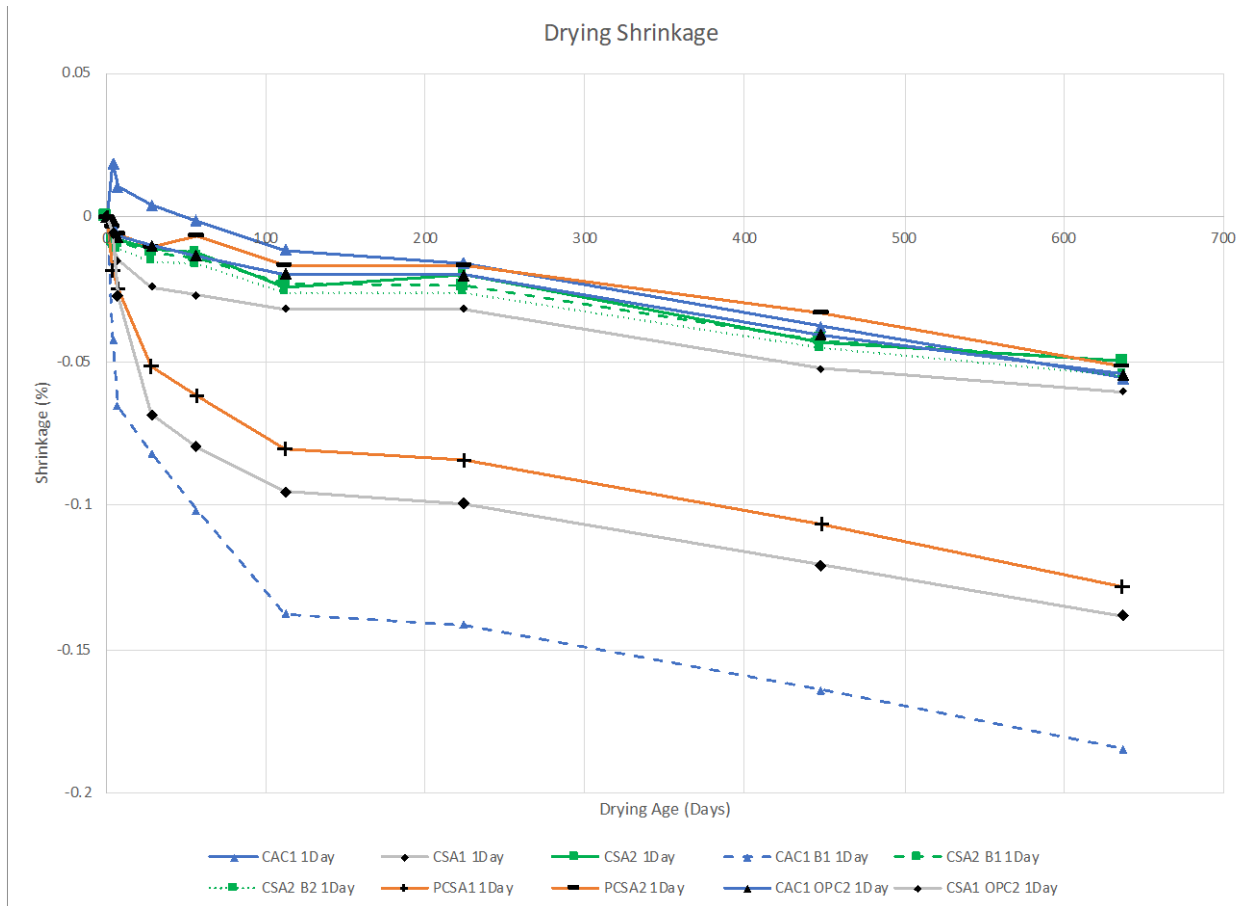
Figure 5.16: Drying shrinkage of prism demolded at 1d at 390 kg/m3 cement binder

5.4.6 Transport Properties

Water sorptivity testing was performed on each RSHC mixture as per ASTM C1585[49] . The initial and secondary absorption rates for each mixture are summarized Figure 5.17 with the performance of each mixture illustrated in Figures 5.18-5.20. With the exception of CSA1 and CSA2, OPC based binders showed a lower absorption rate compared to all other RSHC mixtures. Interestingly, CSA2 showed some of the lowest chloride concentration at the surface and highest diffusion coefficients which does not appear to agree with the low absorption values measured using ASTM C1585. The results appear to indicate the severity of these binding severely lacking the ability to bind chloride upon prolonged exposure. On the other hand, CSA2-B1 and CSA2-B2 showed some of the highest initial and secondary absorption rates. Additionally, CAC1 also showed high absorption rates which may be attributed to the conversion process that may have been triggered during the conditioning of the sample increasing the porosity. In general, the absorption rates vary widely across all RSCH mixtures and don't appear to agree with the diffusion coefficient rates as determined in chloride penetration testing.

110

Table 5.9 summarizes the bulk resistivity and RCPT measurements 100 x 200 mm (4 x 8 inches) concrete cylinders produced with the RSHCs. The bulk resistivity samples were cured in a curing room at 23°C and 100%RH and were tested on days 56. The samples were tested in a saturated surface dry state with the Gamry instrument using the Electrochemical Impedance Spectroscopy (EIS) technique. To aid the analysis, reference will be made to Table 5.8, which shows the equivalent bulk electrical resistivity ranges to the coulomb ranges prescribed in ASTM C 1202 for determining chloride penetrability.

Comparing CSA1 with other cements, CSA1 showed the highest resistivity. This is due to its high ye'elmite content resulting in rapid strength and microstructural development. Based on the high resistivity value of CSA1, it could be considered as having a very low chloride penetrability following the information in Table 5.8. The pure CSA2 cement did not exhibit as high resistivity as CSA1 due to its high belite content compared to ye'elmite. However, based on its resistivity values, it can be considered as having moderate chloride penetrability. Other CSA-based cements (CSA-B1, CSA-B2, PCSA1, and CSA1-OPC2) exhibited resistivity that placed them in the category of very low to moderate chloride penetrability. Despite the outstanding performance attributed to CSA1, CSA2, CSA-B1, and CSA-B2 from bulk electrical resistivity assessment, their performance seems not to be consistent with that from the chloride penetration test. This is because bulk electrical resistivity measurements are designed to determine concrete permeability, not chloride binding capacity, which is also an important determinant of chloride penetrability.

With regard to rapid chloride penetration testing (RCPT), RCPT values for RSHCs mixtures typically showed a lower permeability rating as compared to those measured for bulk resistivity. However, it should be noted that for bulk resistivity testing the conditioning of the sample has a large influence on the measured value. The samples measured in this study were all done following the "bucket" method in which all samples were fully submerged in water immediately after being removed from the curing room, and thereafter dried to SSD prior to being measured.
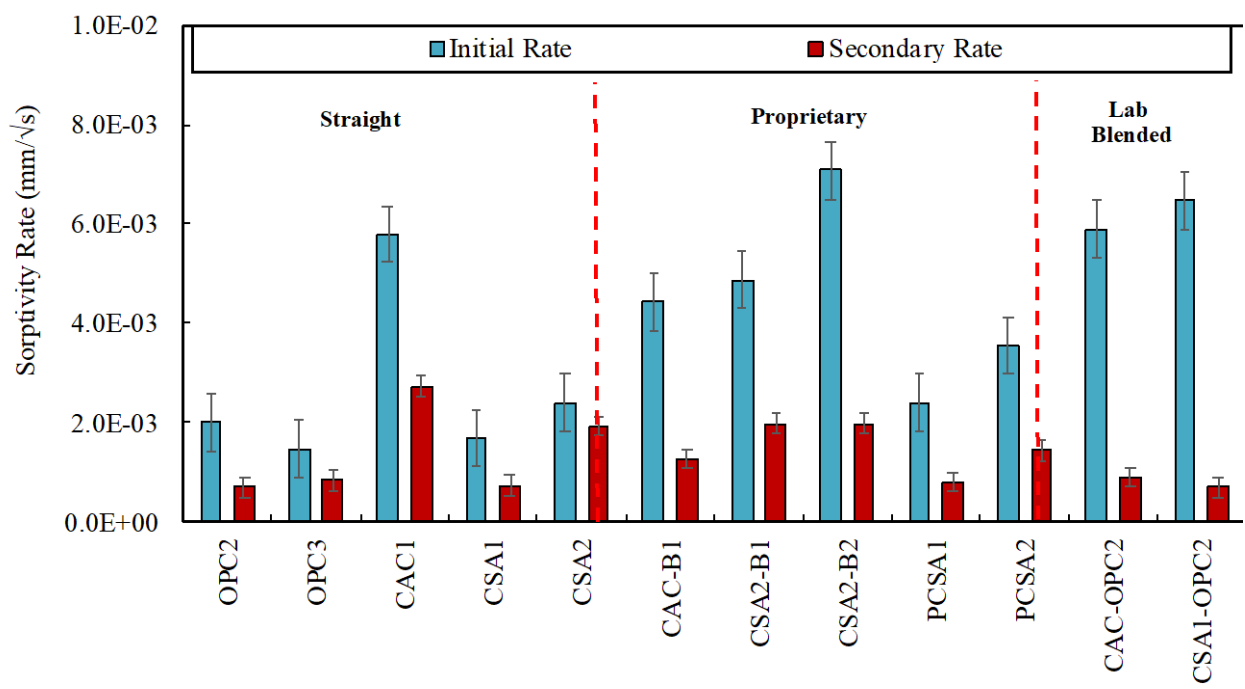
Figure 5.17: Initial and secondary sorptivity rates for various RSHC concretes
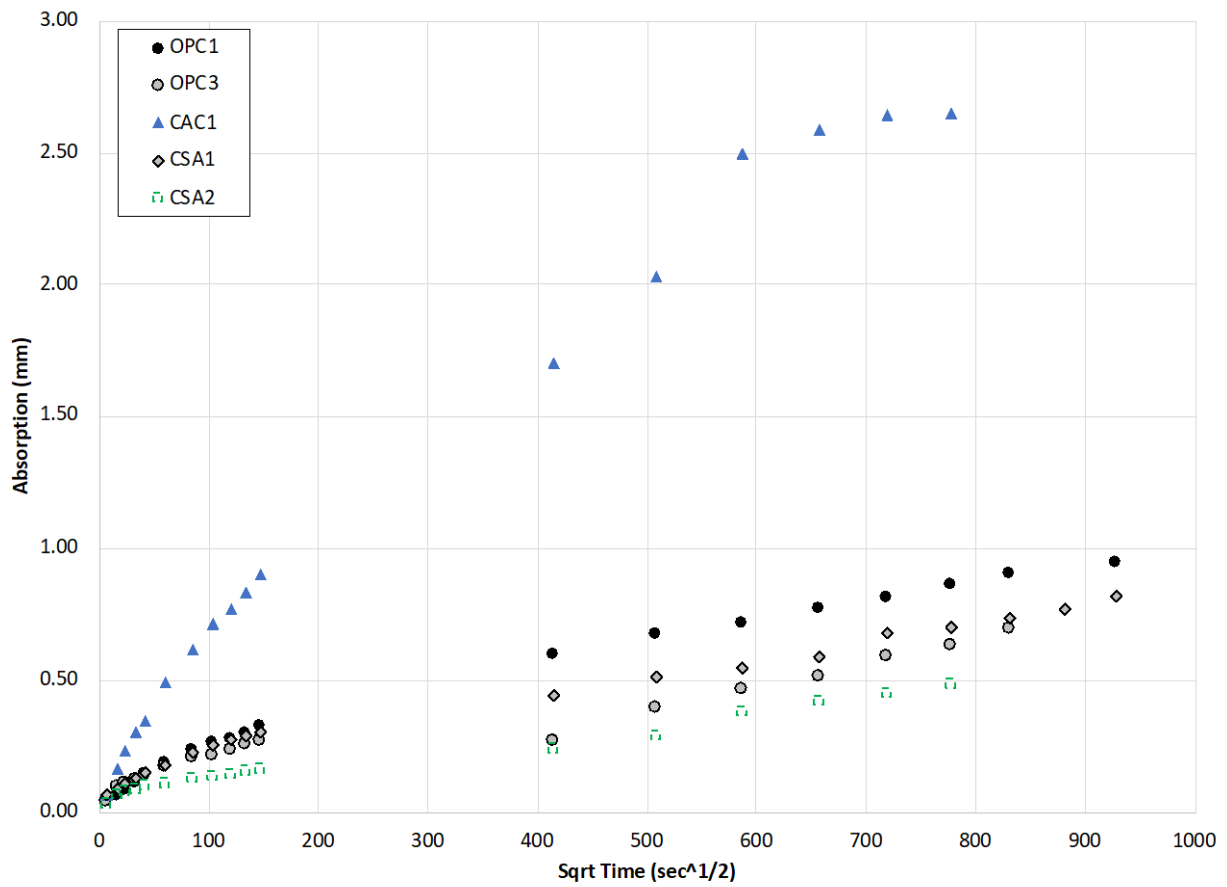
Figure 5.18: Sorptivity results for straight cements
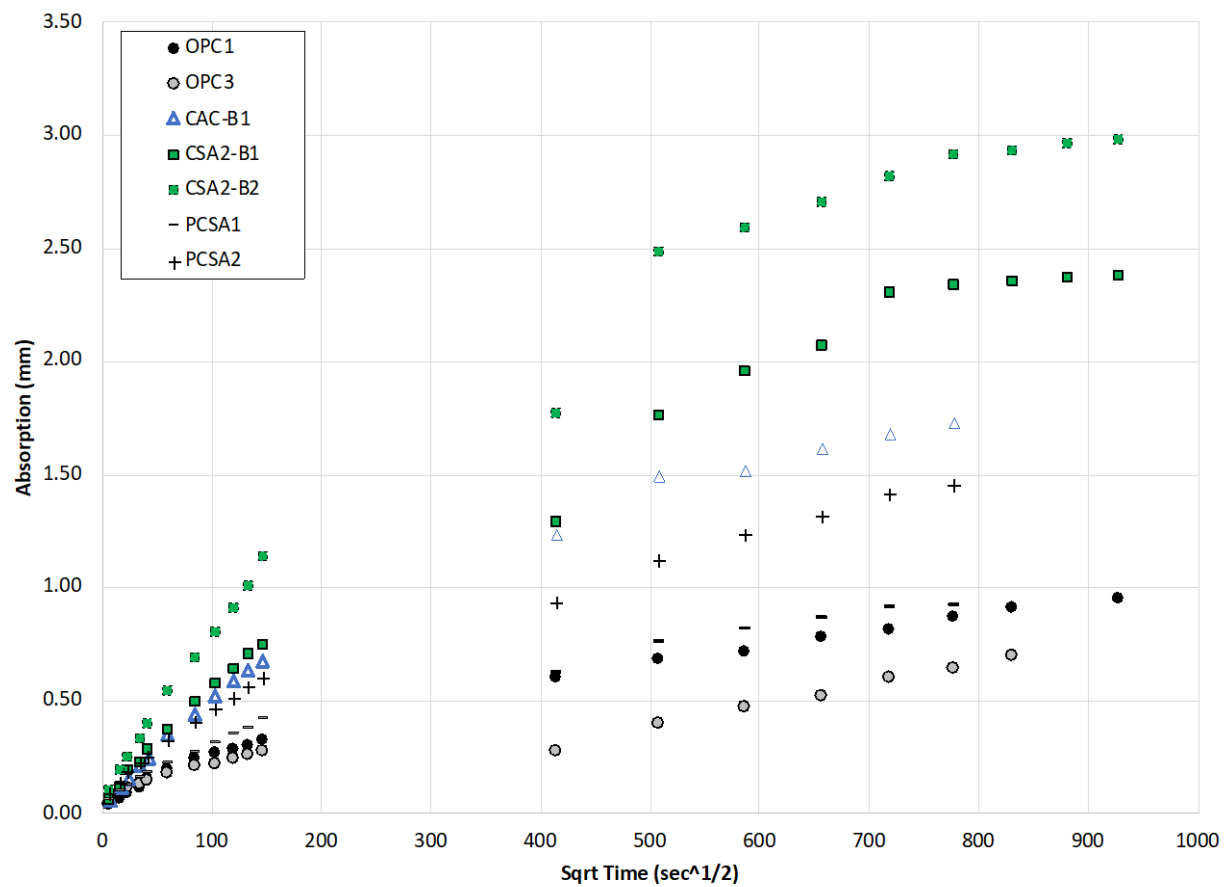
Figure 5.19: Sorptivity results for proprietary cements
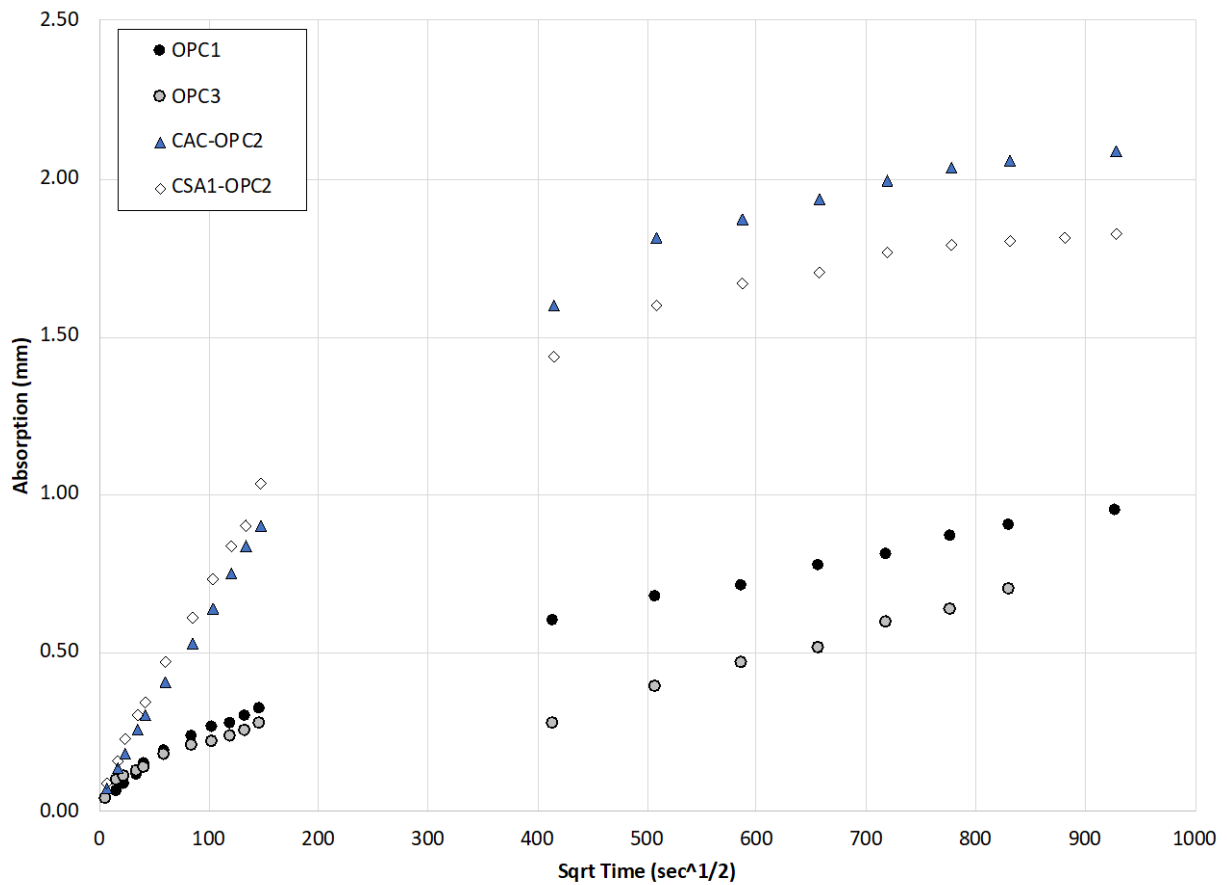
Table 5.9: Sorptivity results for lab blended cements

Chloride Penetration	Bulk Electrical Resistivity (ohm-m)	Rapid Chloride Permeability Charge Passed (Coulombs)
High	<50	>4000
Moderate	50 – 100	2000-4000
Low	100 – 200	1000-2000
Very Low	200 – 2000	100-1000
Negligible	>2000	<100

Table 5.10: Summary of transport property testing results

Cement Type	Cement ID	56 Days	Chloride Penetration per ASTM C1202	56 Days	Chloride Penetration per ASTM C1876	Agreement Between Test Methods
			Charge Passed (Coulombs)		**Bulk Resistivity (ohm.m)**	
Straight Cements	OPC2	1127	Low	51	Moderate	Don't Agree
	OPC3	2371	Moderate	71	Moderate	Agree
	CAC	543	Very Low	237	Very Low	Agree
	CSA1	354	Very Low	1128	Very Low	Agree
	CSA2	928	Very Low	86	Moderate	Don't Agree
Proprietary Blends	CAC-B1	1105	Low	82	Moderate	Don't Agree
	CSA2-B1	1543	Low	137	Low	Agree
	CSA2-B2	1269	Low	120	Low	Agree
	PCSA1	971	Very Low	131	Low	Don't Agree
	PCSA2	998	Very Low	126	Low	Don't Agree
Lab Blend Cements	CAC-OPC2	1010	Low	79	Moderate	Don't Agree
	CSA1-OPC2	3798	Moderate	87	Moderate	Agree

5.5 TEMPERATURE ROBUSTNESS TESTING PROGRAM

5.5.1 Compressive Strength

Figures 5.17-5.24 summarizes the compressive strength results for the temperature robustness testing program. For ease of reference, the research team has grouped the following figures between the different binder types used in this program. Namely, the groups are divided by CAC1, CSA1, CSA2, and PCSA2. Additionally, strength results are divided by early-age strengths (24 hrs) and later-age strength (> 24 hrs). Finally, OPC2 and OPC3 compressive strength results are added in for reference.
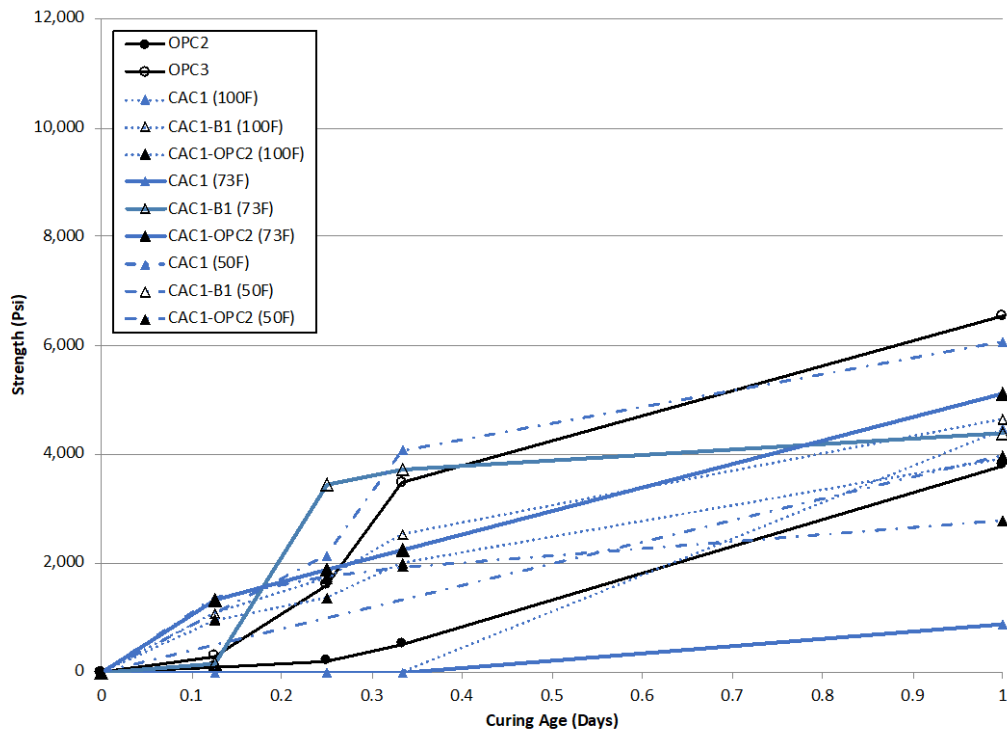
Figure 5.20: Compressive strength comparison at various curing regimes of CAC binders up to 24 hrs
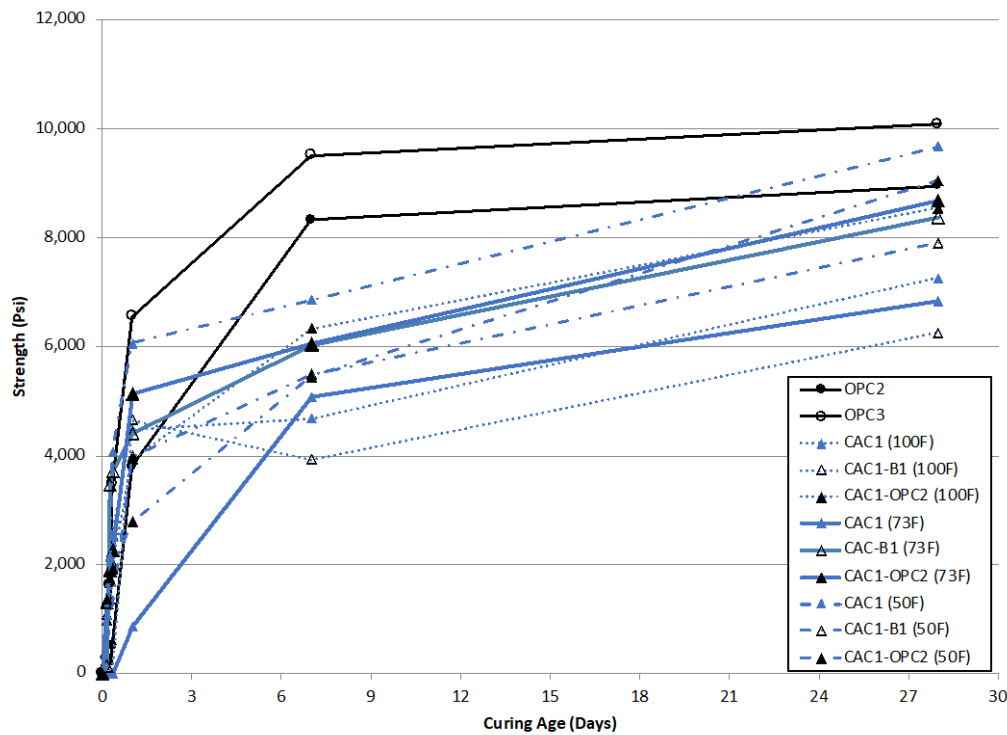
Figure 5.21: Compressive strength comparison at various curing regimes of CAC binders up to 28 days

117
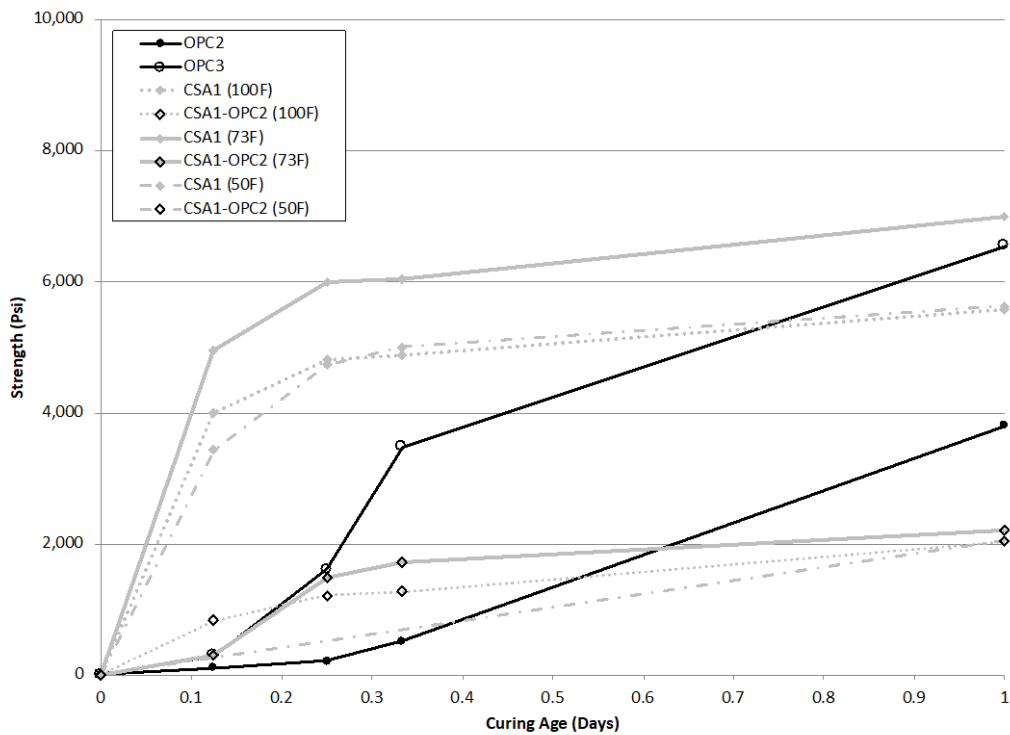
Figure 5.22: Compressive strength comparison at various curing regimes of CSA1 binders up to 24 hrs
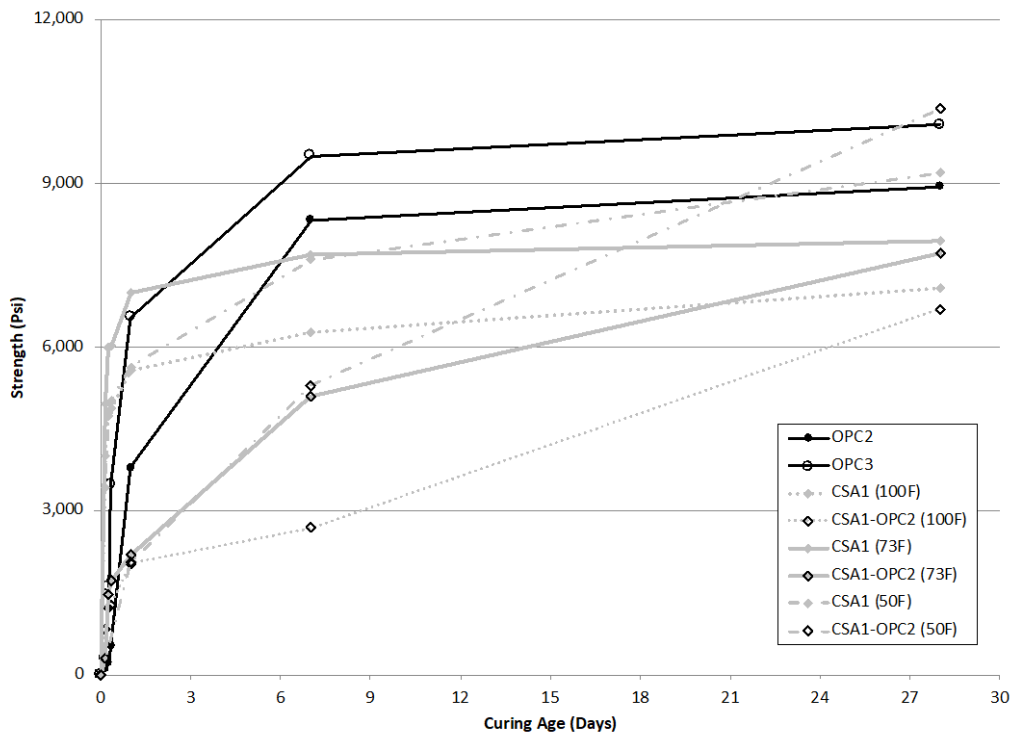
Figure 5.23: Compressive strength comparison at various curing regimes of CSA1 binders up to 28 days

118
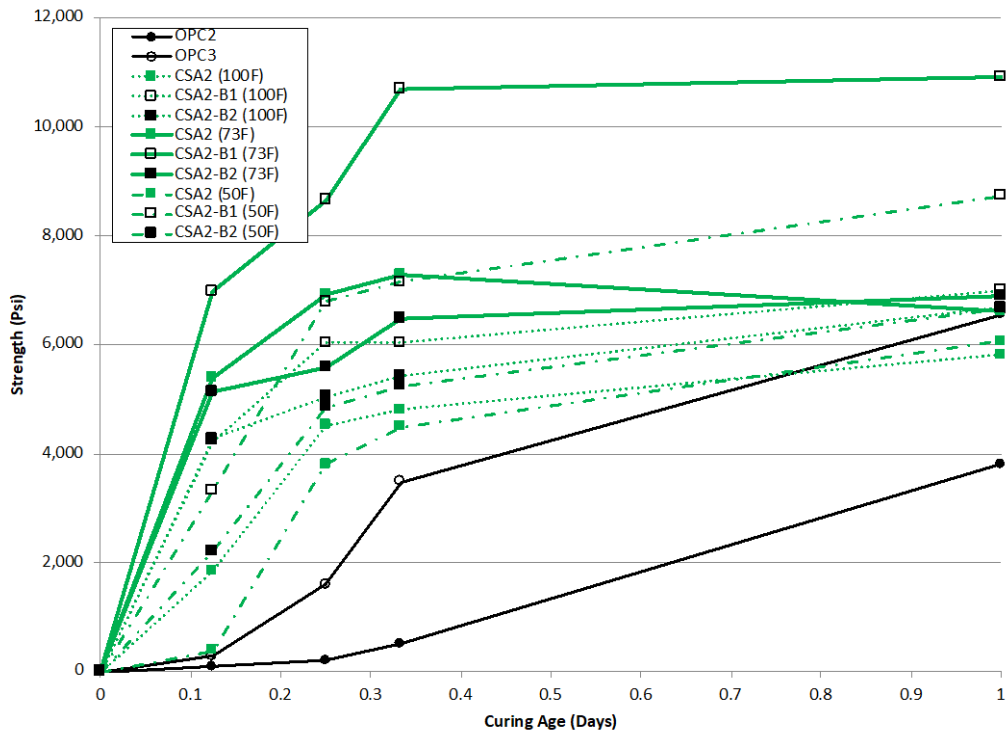
Figure 5.24: Compressive strength comparison at various curing regimes of CSA2 binders up to 24 hrs
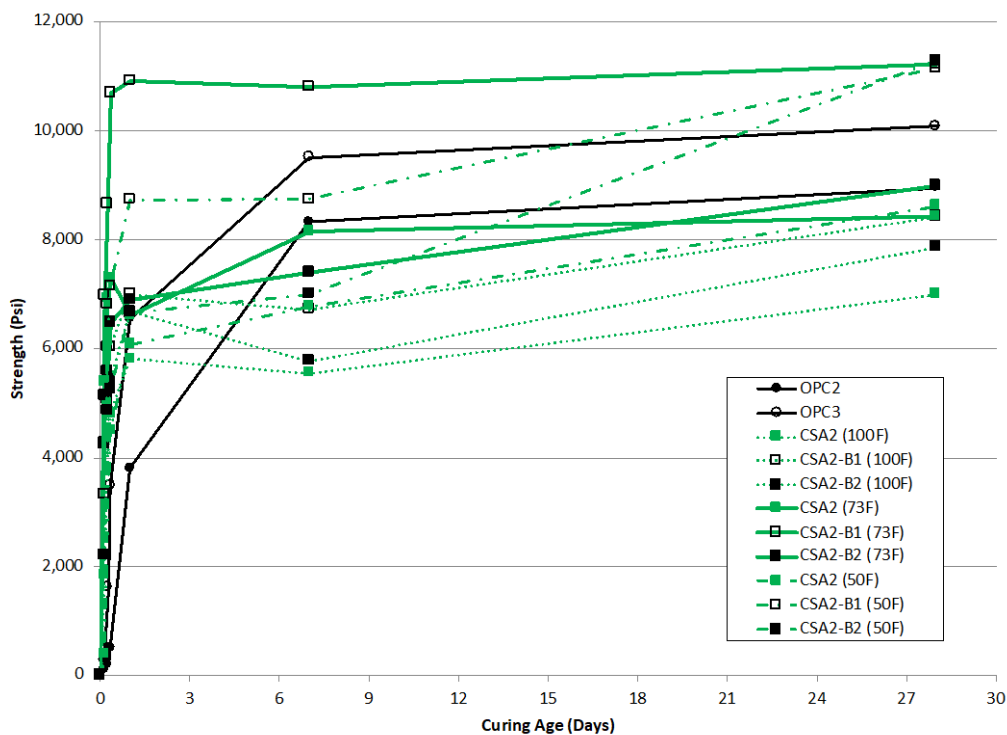
Figure 5.25: Compressive strength comparison at various curing regimes of CSA2 binders up to 28 days

119
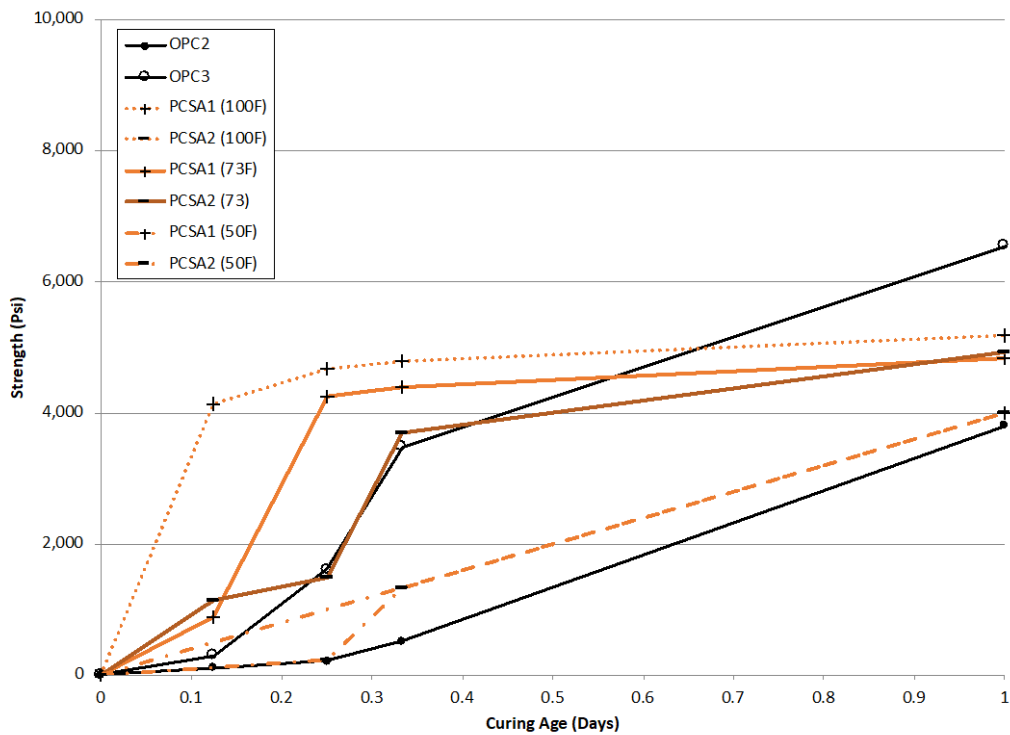
Figure 5.26: Compressive strength comparison at various curing regimes of PCSA binders up to 24 hrs
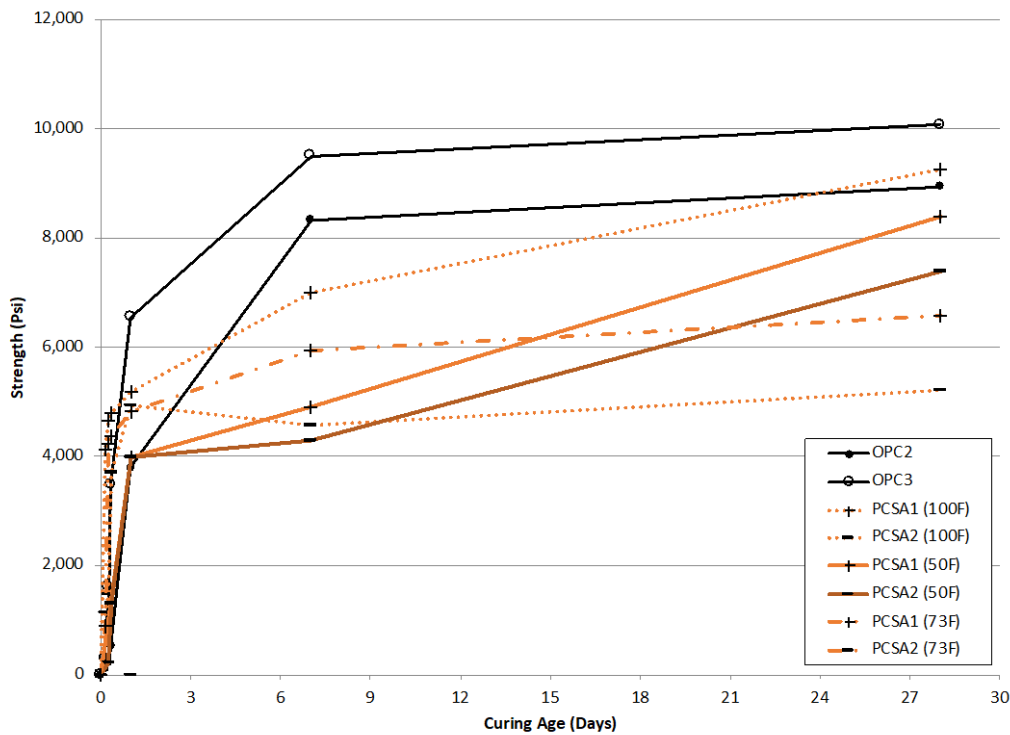
Figure 5.27: Compressive strength comparison at various curing regimes of PCSA binders up to 28 day

Figures 5.29-31. summarizes the 6 and 24 hr and 1-day compressive strength for all mixtures at each various curing temperature (50 °F, 73 °F, and 100 °F). It is interesting to note that based on the data obtained, most mixtures did not show much of an impact on their compressive strength from the cooler or hotter temperatures. In fact, most mixtures showed a higher compressive strength when cured at ambient 73 °F temperature. However, CAC1 did show a high compressive strengths at 50 °F than 100 °F which could be attributed to the conversion that CAC normally experiences at elevated temperatures. On the other hand, compressive strengths became higher for those mixtures cured at 50 °F after 28 days of curing.
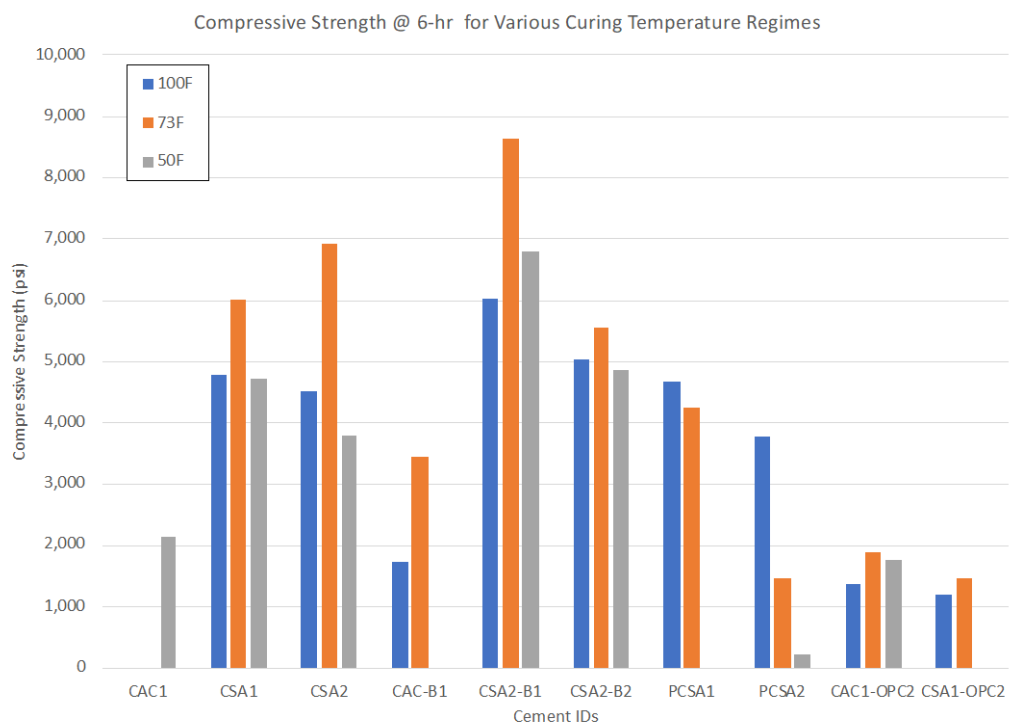
Figure 5.28: Summary of compressive strengths at various curing regimes of RSCH concrete at 6 hrs
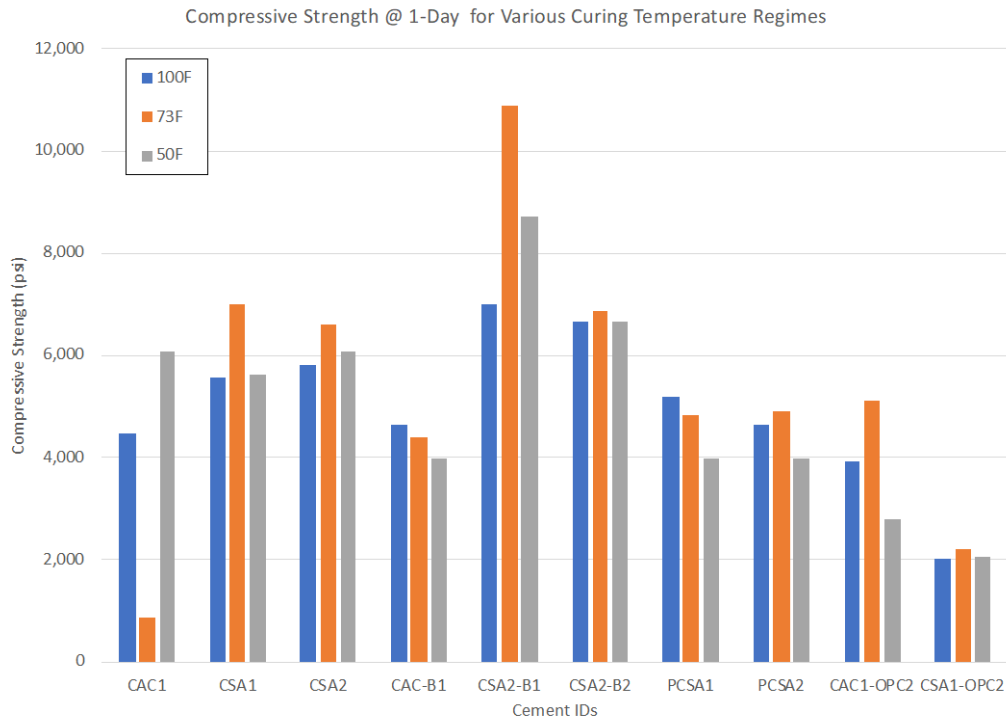
Figure 5.29: Summary of compressive strengths at various curing regimes of RSCH concrete at 24 hrs
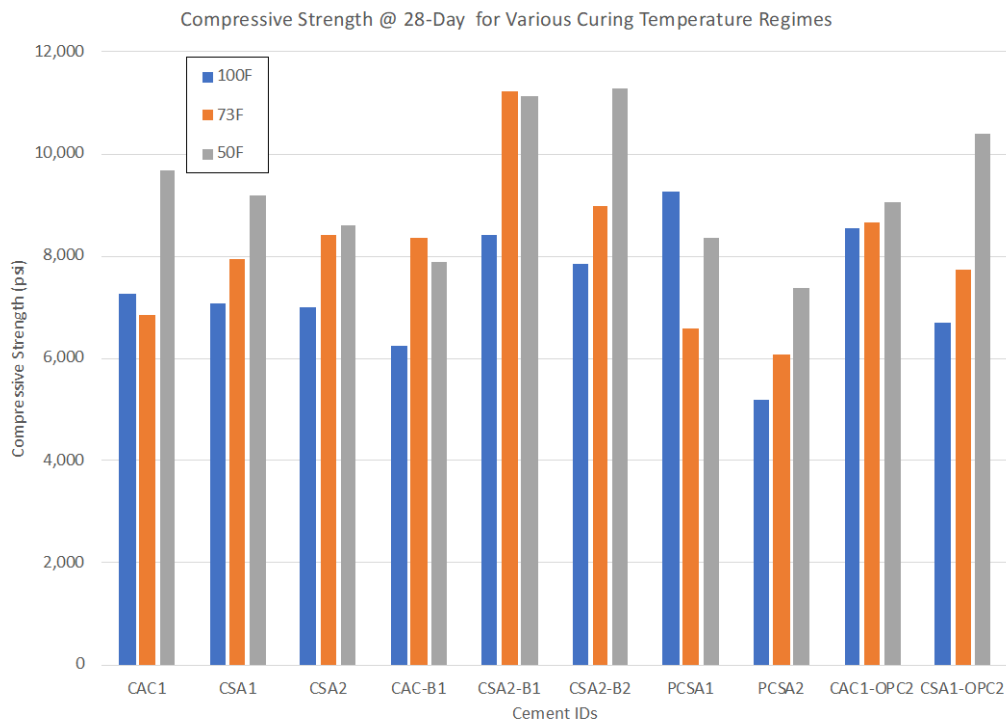
Figure 5.30: Summary of compressive strengths at various curing regimes of RSCH concrete at 28 hrs

122

5.6 CAC CONVERSION TESTING PROGRAM

5.6.1 Compressive Strength

The results show that in all the CAC mixtures cast, the only mixture to show any strength reduction was CAC. It is worth noting that a larger strength decrease was noted in the CAC mixture with a lower water to cement ratio (W/C = 0.35) and high cement content (752 lb/yd3) which is consistent with literature. In all blended based CAC mixtures, no strength reduction is observed up to 91 days. It is also worth noting that all CAC blended mixtures showed a high compressive strength compared to CAC beyond 7 days of curing.
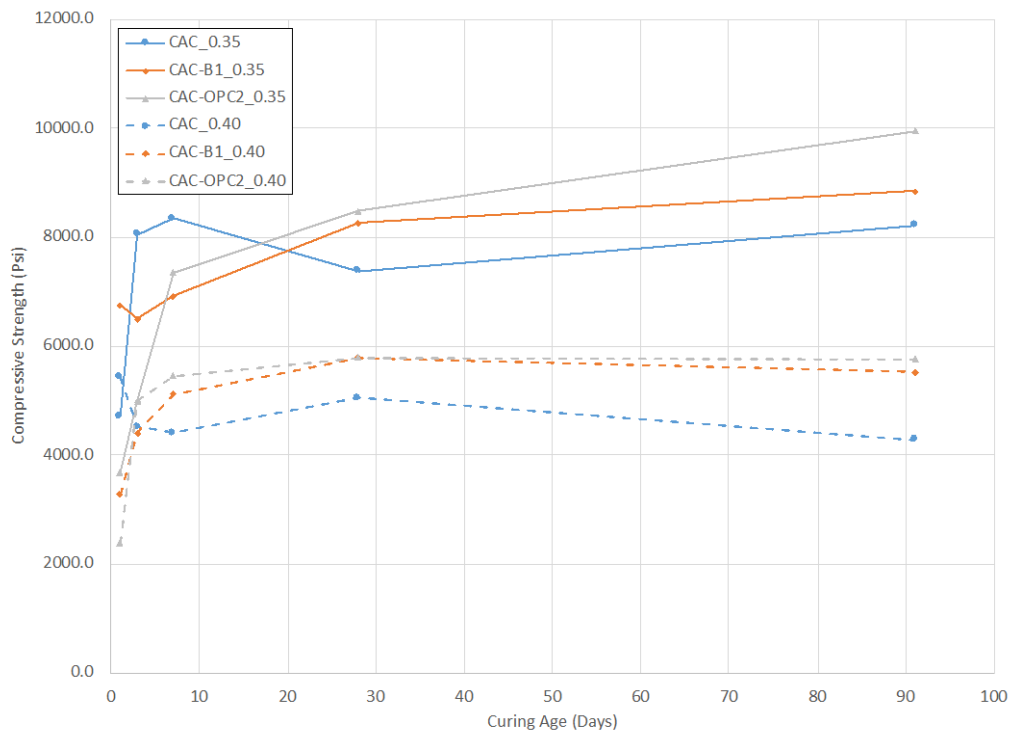
Figure 5.31: Compressive strength of CAC conversion testing

5.7 CONCLUSIONS

The key findings from the study are summarized below:

- Fresh property testing including slump, unit weight, and air content for all RSHCs show similar performance to that of OPC system.

- Cement compositions, including proprietary blends and lab-blended mixes, demonstrate varied setting characteristics influenced by factors such as cement content, type of binder, and admixture usage.

- Despite some exceptions, such as OPC1 exhibiting prolonged lag and dissipation of peak heat, the majority of RSHCs and OPC1 exhibit comparable maximum peak temperatures, suggesting similar overall heat generation characteristics, while blended systems incorporating OPC2 display a notable reduction in total peak heat, underscoring the potential impact of blending on thermal behavior.

- The analysis of compressive strength across different cement types highlights the rapid onset of strength development in rapid setting hydraulic cements (RSHCs) compared to ordinary Portland cements (OPC2 and OPC3) at early ages, with some exceptions such as CAC1 exhibiting delayed strength development attributed to its sensitivity to set retarder.

- While RSHC concretes generally demonstrate lower strengths compared to OPC2 and OPC3 at later ages (> 24 hrs), they continue to exhibit gradual strength gain up to 1 year of age. Notably, proprietary blends and lab-blended cements show varying degrees of strength development, with proprietary blends often exhibiting faster strength development than lab-blended mixtures due to their optimized formulations.

- The analysis of splitting tensile strength across rapid setting hydraulic cements (RSHCs) reveals varied trends, with most RSHC concretes exhibiting either equal or lower splitting tensile strengths compared to ordinary Portland cements (OPC2 and OPC3). However, mixtures comprised of OPC, including lab-blended cements, show substantial increases in splitting tensile strength between 1 and 28 days, likely attributed to the availability of silicate phases in higher OPC content blends.

- The tensile to compressive strength ratio remains consistent across the board and comparable to OPC2 and OPC3. Modulus of rupture (MOR) results exhibit some increase between 7 and 28 days, with notable strengths observed in certain proprietary blends. Modulus of elasticity analysis, however, indicates deviations from predicted values, particularly in mixtures with higher binder content, suggesting that empirical equations may not accurately represent the elastic modulus of RSHC concrete, emphasizing the need for further research in this area.

- Water sorptivity and bulk resistivity testing provide valuable insights into the permeability and chloride penetrability of rapid setting hydraulic cement (RSHC) mixtures. While OPC-based binders generally exhibit lower absorption rates, the results demonstrate significant variability across RSHC mixtures, with some showing unexpectedly high absorption rates, potentially attributed to factors such as binder composition and degree of hydration.

- The discrepancy between bulk resistivity and rapid chloride penetration testing (RCPT) results highlights the complexity of evaluating concrete permeability and chloride penetrability. While bulk resistivity assessments suggest favorable resistance to chloride penetration for certain RSHC mixtures like CSA1, CSA2, CSA-B1, and CSA-B2, RCPT results indicate lower permeability ratings. Understanding these discrepancies requires considering factors such as sample conditioning methods and the distinction between concrete permeability and chloride binding capacity. Further research is needed to refine testing methodologies and accurately assess the durability performance of RSHC mixtures.

- The compressive strength results from the temperature robustness testing program provide insights into the performance of different binder types under varying curing conditions. Despite the temperature variations (50 °F, 73 °F, and 100 °F), most mixtures exhibit consistent or even higher compressive strengths when cured at ambient temperature (73 °F). However, CAC1 demonstrates higher strengths at lower temperatures (50 °F), potentially due to the conversion process typical of CAC binders at elevated temperatures.

- The investigation into calcium aluminate cement (CAC) mixtures reveals that while pure CAC mixtures experience some strength reduction, particularly noticeable with lower water-to-cement ratios and higher cement content, blended CAC mixtures show no strength reduction up to 91 days of curing. This highlights the potential benefits of blending CAC with other materials, which not only mitigates strength reduction but also results in higher compressive strengths compared to pure CAC beyond 7 days of curing.

5.8 REFERENCES

[1]   A. E. Naaman; K. Wille, "The Path to Ultra-High Performance Fiber Reinforced Concrete (UHPFRC)," in *Third International Symposium on UHPC*, 2012, pp. 3-15.
[2]   A. S. o. C. E. (ASCE), "A comprehensive assessment of America's infrastructure, 2021 report card," [Online], 2021. [Online]. Available: https://infrastructurereportcard.org/
[3]   A. Kumar, "A Review on Epoxy and Polyester Based Polymer Concrete and Exploration of Polyfurfuryl Alcohol as Polymer Concrete," *Journal of Polymer,* vol. 2016, pp. 1-13, 2016, doi: 10.1155/2016/7249743.
[4]   J. M. L. D. Reis, "Effect of temperature on the mechanical properties of polymer mortars," *Materials Research,* vol. 15, no. 4, pp. 645-649, 2012, doi: 10.1590/S1516-14392012005000091.
[5]   M. N. V. M. Taghvaee, "Alkali-Activated Materials and Geopolymer: a Review of Common Precursors and Activators Addressing Circular Economy," *Circ. Econ. Sustainability,* 2021, doi: 10.1007/s43615-021-00029-w.
[6]   M. N. T. O. A. Gholampour, "A systematic review of bacteria-based self-healing concrete: Biomineralization, mechanical, and durability properties," *Journal of Building Engineering,* vol. 49, 2022, doi: 10.1016/j.jobe.2022.104038.

[7]   C. K. Y. L. T. Pheeraphan, "Microwave curing of Portland cement concrete: experimental results and feasibility for practical applications," *Construction and Building Materials,* vol. 9, no. 2, pp. 67-73, 1995, doi: 10.1016/0950-0618(94)00001-I.

[8]   J. P. J. Ambroise, "New applications of calcium sulfoaluminate cement," *Cement and COncrete Research,* vol. 34, no. 4, pp. 671-676, 2004, doi: 10.1016/j.cemconres.2003.10.019.

[9]   D. Torréns-Martín; L. Fernández-Carrasco; M. T. Blanco-Varela, "Conduction calorimetric studies of ternary binders based on Portland cement, calcium aluminate cement and calcium sulphate," *journal of thermal analysis and calorimetry,* vol. 114, no. 2, pp. 799-807, 2013, doi: 10.1007/s10973-013-3003-9.

[10]   T. O. M. Nodehi, A. Gholampour, T. Mohammed, and X. Shi, "The effect of curing regimes on physico-mechanical, microstructural and durability properties of alkali-activated materials: A review," *Construction and Building Materials,* vol. 321, 2022, doi: 10.1016/j.conbuildmat.2022.126335.

[11]   A. Bentivegna, "Multi-Scale Characterization, Implementation, and Monitoring of Calcium Aluminte Cement Based Systems (Dissertation). Austin, TX: The University of Texas at Austin.," Dissertation 2012. The University of Texas at Austin.

[12]   M. R.J., *Calcium Aluminate Cements*. CRC Press, 1990.

[13]   G. Y. Y. Zhang, W. Gu, D. Ding, L. Chen, and L. Zhu, "Conversion of calcium aluminate cement hydrates at 60°C with and without water," *Journal of American Ceramic Society,* vol. 101, no. 7, pp. 2712-2717, 2018, doi: 10.1111/jace.15505.

[14]   E. G. C. Gosselin, and K. Scrivener, "Influence of self heating and Li2SO4 addition on the microstructural development of calcium aluminate cement," *Cement and Concrete Research,* vol. 40, no. 10, pp. 1555-1570, 2010, doi: 10.1016/j.cemconres.2010.06.012.

[15]   K. P. a. P. Chindaprasirt, "Sulfoaluminate cement-based concrete," *Elsevier Ltd,* 2018.

[16]   G. Habert, "Assessing the environmental impact of conventional and "green" cement production," 2013.

[17]   K. P. S. Ioannou, L. Reig, and K. Quillin, "Preliminary investigation of artificial reef concrete with sulphoaluminate cement, marine sand and sea water," *Construction and Building Materials,* vol. 211, pp. 837-846, 2019, doi: 10.1016/j.conbuildmat.2019.03.272.

[18]   N. B. M. Q. Zhou, and M. Hayes, "Preliminary investigation of artificial reef concrete with sulphoaluminate cement, marine sand and sea water," *Construction and Building Materials,* vol. 211, pp. 837-846, 2019, doi: 10.1016/j.conbuildmat.2019.03.272.

[19]   N. B. M. Q. Zhou, and M. Hayes, "An alternative to Portland Cement for waste encapsulation-The calcium sulfoaluminate cement system," *Journal of Hazard Material* vol. 136, no. 1 Special Issue, pp. 120-129, 2006, doi: 10.1016/j.jhazmat.2005.11.038.

[20]   Z. Y. F. Song, F. Yang, Y. Lu, and Y. Liu, "Microstructure of amorphous aluminum hydroxide in belite-calcium sulfoaluminate cement," *Cement and Concrete Research,* vol. 71, no. 1-6, 2015, doi: 10.1016/j.cemconres.2015.01.013.

[21]   F. W. M. Ben Haha, and A. Pisch, "Advances in understanding ye'elimite-rich cements," *Cement and Concrete Research,* vol. 123, 2019, doi: 10.1016/j.cemconres.2019.105778.

[22]   Z. Y. X. Lu, S. Wang, P. Du, C. Li, and X. Cheng, "Study on the preparation and properties of belite-ye'elimite-alite cement," *Construction and Building Materials,* vol. 182, pp. 399-405, 2018, doi: 10.1016/j.conbuildmat.2018.06.143.

[23]   T. B. S. Galluccio, and H. Pöllmann, "Maximization of the reuse of industrial residues for the production of eco-friendly CSA-belite clinker," *Construction and Building Materials,* vol. 208, pp. 250-257, 2019, doi: 10.1016/j.conbuildmat.2019.02.148.

[24]   J. K. L. Barcelo, G. Walenta, and E. Gartner, "Cement and carbon emissions," *Materials and Structures,* vol. 47, no. 6, pp. 1055-1065, 2014, doi: 10.1617/s11527-013-0114-5.

[25]   T. S. a. P. Sulovský, "Active low-energy belite cemen," *Cement and Concrete Research,* vol. 68, pp. 203-210, 2015, doi: 10.1016/j.cemconres.2014.11.004.

[26] J. S. M. Zajac, F. Bullerjahn, and M. Ben Haha, "Effect of retarders on the early hydration of calcium-sulpho-aluminate (CSA) type cement," *Cement and Concrete Research,* vol. 84, pp. 62-75, 2016, doi: 10.1016/j.cemconres.2016.02.014.

[27] F. W. a. B. Lothenbach, "Hydration of calcium sulfoaluminate cements — Experimental findings and thermodynamic modelling," *Cement and Concrete Research,* vol. 40, no. 8, pp. 1239-1247, 2010, doi: 10.1016/j.cemconres.2009.08.014.

[28] A. S. D. Jansen, J. Neubauer, D. Ectors, and F. Goetz-Neunhoeffer, "Studies on the early hydration of two modifications of ye'elimite with gypsum," *Cement and Concrete Research,* vol. 91, pp. 106-116, 2017, doi: 10.1016/j.cemconres.2016.11.009.

[29] C. W. H. Y. Jeong, S. C. Chun, and J. Moon, "The effect of water and gypsum content on strätlingite formation in calcium sulfoaluminate-belite cement pastes," *Construction and Building Materials,* vol. 166, pp. 712-722, 2018, doi: 10.1016/j.conbuildmat.2018.01.153.

[30] J. H. S. S. P. S. K. N. Y. H. K. Lee, "Local Al network and material characterization of belite-calcium sulfoaluminate (CSA) cements," *Materials and Structures,* vol. 55, 2019, doi: 10.1617/s11527-021-01842-3.

[31] A. A. A. Cuesta, and M. A. G. Aranda, "Belite cements and their activation," *Cement and Concrete Research,* vol. 140, 2021, doi: 10.1016/j.cemconres.2020.106319.

[32] A. K. Chatterjee, "High belite cements—Present status and future technological options: Part I," *Cement and Concrete Research,* vol. 26, no. 8, pp. 1213-1225, 1996, doi: 10.1016/0008-8846(96)00099-3.

[33] C. S. P. A. Rungchet, P. Chindaprasirt, and K. Pimraksa, "Synthesis of low-temperature calcium sulfoaluminate-belite cements from industrial wastes and their hydration: Comparative studies between lignite fly ash and bottom ash," *Cement and Concrete Composites,* vol. 83, pp. 10-19, 2017, doi: 10.1016/j.cemconcomp.2017.06.013.

[34] D. J. W. Li, F. Shi, X. Huang, X. Ji, and S. Ma, "Study on the synthesis of belite-ye'elimite-ternesite clinker," *Construction and Building Materials,* vol. 319, 2022, doi: 10.1016/j.conbuildmat.2021.126022.

[35] H. P. L. B. A. Negrão, and M. L. da Costa, "Clinkering design of sulfobelite cements using clay overburden residue from bauxite mining," *Advances in Cement Research,* pp. 1-15, 2022, doi: 10.1680/jadcr.21.00118.

[36] O. F. C. Cau Dit Coumes, P. Antonucci, J.-B. Champenois, D. Lambertin, and A. Mesbah, "Design of self-desiccating binders using CSA cement: influence of the cement composition and sulfate source," *Advances in Cement Research,* vol. 31, no. 4, pp. 178-194, 2019, doi: 10.1680/jadcr.18.00100.

[37] R. L. W. He, Y. Zhang, and D. Nie, "Synergistic use of electrolytic manganese residue and barium slag to prepare belite- sulphoaluminate cement study," *Construction and Building Materials,* vol. 326, 2022, doi: 10.1016/j.conbuildmat.2022.126672.

[38] R. I. Iacobescu, Y. Pontikes, D. Koumpouri, and G. Angelopoulos, "Synthesis, characterization and properties of calcium ferroaluminate belite cements produced with electric arc furnace steel slag as raw material," *Cement and Concrete Composites,* vol. 44, pp. 1-8, 2013.

[39] *ASTM C143-20 Standard Test Method for Slump of Hydraulic-Cement Concrete*, ASTM International, 2020.

[40] *ASTM C138-18 Standard Test Method for Density (Unit Weight), Yield, and Air Content (Gravimetric) of Concrete*, ASTM International, 2018.

[41] *ASTM C231-17a Standard Test Method for Air Content of Freshly Mixed Concrete by the Pressure Method*, ASTM International, 2017.

[42] ASTM International, "ASTM C403-16 Standard Test Method for Time of Setting of Concrete Mixtures by Penetration Resistance," 2016.

[43] *ASTM C39-21 Standard Test Method for Compressive Strength of Cylindrical Concrete Specimens*, ASTM International, 2021.

[44]   *ASTM C469 Standard Test Method for Static Modulus of Elasticity and Poisson's Ratio of Concrete in Compression*, ASTM International, 2014.

[45]   *ASTM C496 Standard Test Method for Splitting Tensile Strength of Cylindrical Concrete Specimens*, ASTM International, 2017.

[46]   ASTM International, "ASTM C78 - 18 Standard Test Method for Flexural Strength of Concrete (Using Simple Beam with Third-Point Loading)," 2018.

[47]   *ASTM C1876-23 Standard Test Method for Bulk Electrical Resistivity or Bulk Conductivity of Concrete*, ASTM International, 2023.

[48]   *ASTM C1202-22 Standard Test Method for Electrical Indication of Concrete's Ability to Resist Chloride Ion Penetration*, ASTM International, 2022.

[49]   *ASTM C1585-20 Standard Test Method for Measurement of Rate of Absorption of Water by Hydraulic-Cement Concretes*, ASTM International, 2020.

[50]   M. Dornak, J. Zuniga, A. Garcia, T. Drimalas, and K. J. Folliard, "Development of Rapid, Cement-Based Repair Materials for Transportation Structures," 2015.

[51]   *ACI 318-19: Building Code Requirements and Commentary*, A. C. Institute, 2019.

[52]   *ASTM C157-17 Standard Test Method for Length Change of Hardened Hydraulic-Cement Mortar and Concrete*, ASTM International, 2017.

CHAPTER 6: ACCELERATED CARBONATION TESTING (EFFECT OF CURING AND PERMEABILITY)

6.1 INTRODUCTION

The durability of concrete depends greatly on its permeability to external agents that are perceived as harmful. Among the durability issues that occur in hydraulic-cement concrete is carbonation caused by the reaction between permeated carbon dioxide (CO_2) from the atmosphere and hydration products such as calcium hydroxide (CH) [1]. The carbonation rate is essentially controlled by the reserve of CH and by the diffusion process of CO_2 [2]. In ordinary portland cement (OPC) concrete, the amount of CH produced from its hydration accounts for 20-25% of the total hydration products [1]. The CH combined with other alkalis, such as sodium hydroxide (NaOH) and potassium hydroxide (KOH), resulting from hydration, produces a concrete pH of 13-14 [1]. This high alkalinity plays an important role in reinforced concrete by forming a passive protective film around steel reinforcement bars, which prevents them from being attacked by chemicals [1, 3, 4]. Extreme levels of carbonation could deplete the passive film protection on steel reinforcement in reinforced concrete hence exposing the steel to corrosion [5]. The carbonation process of OPC produces $CaCO_3$, which results in an increase in the solid volume of concrete by approximately 11%, coupled with an overall reduction in porosity [1, 3, 4]. Carbonation seems to be more pronounced in concrete produced with CAC, CSA cement, and other ettringite-based systems. This is due to their lower alkalinity or lack of CH compared to OPC. Although the alkaline contents of these cements are lower than that of OPC, they still have enough alkalinity to ensure the formation of a passive film on steel reinforcement for protection against corrosion [6]. Due to the absence of CH, ettringite-based binders carbonate significantly faster than OPC and may suffer an increase in porosity and significant loss of strength as ettringite converts to solids, which are far less dense [5].

In concrete, the depth of carbonation depends on its permeability, which is determined by its porosity and pore structure [7]. The curing of concrete, among other factors, can enhance the hydration of cement in the presence of water and a favorable temperature, thereby reducing its porosity and permeability. [8, 9]. While curing is important for strength development and microstructural improvement, curing conditions such as temperature, relative humidity, and curing duration are also equally important.

The external relative humidity (RH) of concrete is a strong determining factor in the continuance of hydration in concrete since the hydration process reduces its internal relative humidity. A decrease in internal RH below 80% can halt the hydration process, hence stalling the microstructural and strength

development of concrete [9, 10]. If adequate curing is not provided, this reduction in internal RH could occur in concrete produced at low water-cement ratios (W/C) and in concrete produced with rapid hardening cements, such as calcium sulfoaluminate (CSA) cement and calcium aluminate cement (CAC) [9, 10]. In CAC concrete, however, the internal relative humidity can increase as the metastable hydrates (CAH_{10} and C_2AH_8) are converted to stable hydrates (C_3AH_6 and AH_3) thus sustaining further hydration [11]. A good recommendation will be to ensure that the concrete surface stays fully saturated throughout the curing period to avoid jeopardizing the final properties of the concrete [9, 10].

Temperature is another factor that can influence the hydration of cement during curing. At low temperatures, the hydration reaction occurs at a very low rate, especially in OPC-based concrete, and can prolong the development of strength and microstructure. In such situations, additional heat may be provided via heaters or steam to maintain a favorable temperature to achieve adequate curing in less time [7]. It is also possible to use CAC and CSA cements at low temperatures due to the heat generated during their hydration, which can accelerate strength development and reduce the curing time [7, 11]. At high temperatures, the rate of hydration increases resulting in early strength gain and the development of microstructure. However, curing at high temperatures can reduce the later strength of concrete due to the weak zones formed in concrete by the nonuniform distribution of hydration products [10]. The effect of high temperature curing might be more pronounced for concrete incorporating CSA or CAC because of the heat generated during their hydration [11-13]. Although for CAC concrete, curing at higher temperatures can enable the fast attainment of the minimum converted strength which is the recommended design strength for CAC concrete [11]. To ensure that the final properties of concrete are not affected by temperature changes, measures have to be taken to ensure a favorable temperature is maintained during curing.

The duration of curing is also vital in ensuring that concrete attains its specified strength. The ACI standard practice for curing concrete (ACI 308) recommends 7 days of moist curing at temperatures above 5°C (40°F) for structural concrete or the time required to attain 70% of the designed flexural or compressive strength, whichever is greater [7, 14]. At low temperatures, the low rate of hydration necessitates an extension of curing duration beyond the recommended 7 days of moist curing [7]. In the case of rapid-hardening cement concrete such as CAC and CSA-based concrete, adequate curing can be achieved in less time [7, 11].

Several research investigations have been carried out to ascertain the effect of curing conditions on the microstructural development and permeability of concrete produced with PC and other alternative cementitious materials. Liu et al. [8] investigated the effect of curing conditions such as the curing time,

curing humidity, and curing temperature on the permeability of concrete with high-volume mineral admixtures. The results showed a decrease in water absorption, capillary water absorption, sorptivity coefficient, electric flux, and carbonation depth due to the combined effect of longer standard curing time, higher curing humidity, and a suitable curing temperature. Balayssac et al. [15] investigated the effect of curing on the carbonation of concrete produced with PC, slag cement, and cement with 25% limestone filler. The results showed that samples exhibited increased resistance to carbonation as the curing time increased. Lin et al. [13] investigated the effect of curing temperature and relative humidity on the hydrates and porosity of CSA. The results showed that curing at low temperatures and high RH favored the formation of ettringite hence reducing the total porosity of CSA. Whereas the formation of monosulfoaluminate and aluminum hydroxide was favored as the curing temperature and RH increased. Linglin et al. [16] investigated the effects of curing temperature on the hydration of ternary binders involving OPC, CAC, and calcium sulfate (anhydrite and hemihydrate) at a mass ratio of 22.5: 51.7: 25.8, respectively. The curing was done at 0, 10, 20, and 40°C. The results showed that the main hydration product is related to CSA-based phases. However, as the curing temperature increases, there is a fast conversion from ettringite to monosulfate for those mixes containing the anhydrite form of calcium sulfate. This was also followed by the formation of the CAC hydrates C_2AH_8 and AH_3. Also, at higher temperatures, they observed a coarser pore size for mixes containing anhydrite, while those containing hemihydrate had finer pore sizes.

The focus of this chapter is to investigate the effect of curing and permeability on the accelerated carbonation of concrete produced using CSA, CAC, and blended systems of OPC with CSA and OPC with CAC.

6.2 EXPERIMENTAL

6.2.1 Materials

This study involves testing various cement systems categorized as pure cements (i.e., cements that are not blended with any other material), proprietary blends (i.e., cements pre-blended with other materials during production), and lab blends (i.e., laboratory blended cements, 25% CAC + 75% OPC and 25% CSA + 75% OPC). The reason for the various categories is to depict the current practice in the use of CAC and CSA cements. Due to the high cost of pure CAC and CSA cements, (i.e., CAC and CSA cements that are not blended with any other materials), their use is currently limited to niche areas where their special qualities are required [17, 18]. However, there are also cases where CAC and CSA cements

are blended with OPC to accelerate the hydration of OPC and reduce the high cost of using CAC and CSA cements only [4, 11, 19, 20]. CAC and CSA cements are also blended with supplementary cementitious materials (SCM) such as fly ash to improve their durability performance and with other chemical admixtures that are used to control their workability [17-19]. The blending of CAC and CSA cements with other materials such as OPC, SCMs, and other chemical admixtures is usually carried out during cement production or in the process of mixing concrete. Therefore, including the proprietary blended and laboratory blended cement categories in this study was reasonable. The 25%/75% proportion for the laboratory blended cements was adopted because it was the optimum blend that satisfied both economy and mechanical performance. A description of these cements and their chemical compositions are shown in Tables 6.1 and 6.2, respectively. In Table 6.1, the controls OPC Type I/II (labeled as OPC2) and OPC Type III (labeled as OPC3) were used due to their different rates of hydration and strength development. OPC Type III has finely ground cement particles, which hydrate faster than OPC Type I/II and thereby show greater strength and microstructural development at an early age [10]. Also, in Table 6.1, the terms CSA ye'elmite cement and CSA belite cement were used to indicate the main phases in the CSA cements and to assess the impact of the hydration rate of these phases and their hydration products on the carbonation resistance of the CSA cements. The ye'elmite phase is responsible for rapid early strength gain and microstructural development in CSA cements, while the belite phase is responsible for later strength gain and microstructural development in CSA cements [21, 22]. The phase compositions for the CSA cements in Table 6.1 were calculated using modified Bogue equations adapted from Iacobescu et al. [22].

Table 6.1: Description of cements

Cement Category	Cement Type	Description
Pure Cements	OPC2	OPC Type I/II
	OPC3	OPC Type III
	CAC	Standard CAC cement
	CSA1	CSA Ye'elmite cement (40% Ye'elmite and 26% belite)
	CSA2	CSA belite cement (58% belite and 30% ye'elmite)
Proprietary Blended Cements	CAC-B1	CAC blend with OPC
	CAC-B2	CAC blended with set accelerating admixture
	CSA-B1	CSA belite cement (39% belite and 30% ye'elmite)
	CSA-B2	CSA belite cement (42% belite and 27% ye'elmite)
	PCSA1	CSA blend with OPC
	PCSA2	CSA blend with OPC and Fly ash
Lab Blends	CAC-OPC2	CAC blend with OPC
	CSA1-OPC2	CSA blend with OPC

Table 6.2: Chemical composition of the individual cement

Cement Type	Cement ID	SiO_2	Al_2O_3	Fe_2O_3	CaO	MgO	SO_3	Na_2O	K_2O	Na_2O_e	LOI
Pure Cements	OPC2	21.06	4.02	3.19	63.91	1.08	2.89	0.14	0.61	0.53	2.29
	OPC3	19.67	5.34	1.76	63.41	0.99	5.27	0.10	0.44	0.39	4.06
	CAC	4.34	38.65	15.09	38.37	0.39	0.16	0.05	0.14	0.14	1.55
	CSA1	9.07	21.61	2.26	45.26	0.94	20.26	0.07	0.30	0.27	1.05
	CSA2	20.56	16.14	1.35	45.31	1.23	14.73	0.77	0.72	1.24	4.74
Proprietary Blended Cements	CAC-B1	13.46	12.23	2.67	56.65	2.86	9.90	0.20	0.79	0.72	1.21
	CAC-B2	12.71	32.94	12.95	35.09	1.79	0.84	0.50	0.24	0.65	1.23
	CSA-B1	13.63	15.82	0.75	51.28	1.14	16.62	0.29	0.62	0.69	3.06
	CSA-B2	14.72	14.37	1.22	53.85	1.23	14.40	0.10	0.59	0.49	3.39
	PCSA1	17.38	11.06	2.98	55.82	1.25	10.68	0.43	0.52	0.77	2.26
	PCSA2	20.14	15.73	3.52	43.90	1.55	12.88	0.59	0.52	0.93	1.95
Lab Blends	CAC-OPC2	16.53	10.79	2.71	58.07	0.89	7.43	0.14	0.50	0.47	2.19
	CSA1-OPC2	18.06	8.42	2.96	59.25	1.04	7.23	0.12	0.53	0.47	1.98

Other materials used in this study are well-graded limestone rocks, siliceous river sand, a liquid polycarboxylate-ether-based superplasticizer, and a set retarder, citric acid, which was used for slump control and to delay setting and allow time for mixing and casting. A total of 16 cement mixtures were used for this study. Practically all mixtures were produced with a total cement content of 446 kg/m^3 (752 lb/yd^3) and a W/CM ratio of 0.35. However, there were a few exceptions where the total cement content was increased to 502 kg/m^3 (846 lb/yd^3) to ascertain its effect in the study and where it was decreased to 390 kg/m^3 (658 lb/yd^3) and W/CM ratio of 0.38 based on manufacturers recommendation. The total cement content of 502 kg/m^3 (846 lb/yd^3) and 390 kg/m^3 (658 lb/yd^3) were represented in this study as 846PCY and 658PCY, respectively. The "PCY" stands for pounds per cubic yard. Table 6.3 shows the concrete mixture proportions and compressive strengths on days 1, 7, and 28.

Table 6.3: Concrete mixture proportions and compressive strengths

Cement Type	W/CM	Total Binder Kg/m^3(lb/yd^3)	Replacement Level of Cement with Second Cement Blend (% of Control Cement Type by Mass)		Strength MPa (PSI)		
			Control Binder	Type I/II	1-Day	7-Day	28-Day
OPC2	0.35	446 (752)	100%	-	41 (6005)	60 (8746)	69 (10003)
OPC3	0.35	446 (752)	100%	-	54 (7868)	67 (9785)	76 (10954)
CAC	0.35	446 (752)	100%	-	29 (4269)	41 (5982)	51 (7353)
CSA1	0.35	446 (752)	100%	-	51 (7409)	60 (8692)	65 (9454)
CSA2	0.38	390 (658)	100%	-	36 (5291)	42 (6034)	44 (6370)
CSA2	0.38	446 (752)	100%	-	41 (6011)	46 (6605)	49 (7040)

CAC-B1	0.35	446 (752)	100%	-	39 (5698)	47 (6876)	60 (8726)
CAC-B1	0.35	502 (846)	100%	-	36 (5157)	42 (6032)	58 (8374)
CAC-B2	0.30	446 (752)	100%	-	27 (3960)	38 (5539)	47 (6873)
CSA-B1	0.38	390 (658)	100%	-	56 (8082)	59 (8519)	58 (8405)
CSA-B2	0.38	390 (658)	100%	-	36 (5158)	40 (5755)	45 (6559)
PCSA1	0.35	446 (752)	100%	-	36 (5165)	50 (7322)	64 (9293)
PCSA2	0.35	446 (752)	100%	-	27 (3874)	26 (3829)	27 (3962)
CAC-OPC2	0.35	446 (752)	25%	75%	22 (3185)	50 (7265)	64 (9251)
CSA1-OPC2	0.35	446 (752)	25%	75%	11 (1549)	48 (6964)	60 (8761)
CSA1-OPC2	0.35	502 (846)	25%	75%	17 (2490)	54 (7871)	67 (9768)

6.2.2 Sample Preparation

Three concrete prisms of dimension 100 x 100 x 350 mm (4 x 4 x 14 in) and eight concrete cylinders of dimension 100 x 200 mm (4 x 8 in) were produced for each of the mixtures in Table 6.3. The samples were cured with wet burlap and plastic sheet covers. Out of the three prisms, one was cured for 4-6 hours before demolding. Though the target curing period was 4 hours, the PC concrete and some of the CAC concrete did not achieve the final set until 6 hours. The remaining two concrete prisms were cured for 24 hours before demolding. However, one of the 24-hour cured prisms was transferred into a curing room at 23°C (73°F) and 100% RH for an additional 6 days of curing after demolding. The concrete prisms (4 hours, 24 hours, and 7 days cured prisms) were placed in a drying room at 23°C (73°F) and 50% RH after curing for 14 days before accelerated carbonation exposure. This was to reduce the level of saturation from curing that could hinder the carbonation process as well as to more easily maintain the RH within the chamber. Following a 24-hour cure, the concrete cylinders were demolded and moved to the aforementioned curing room for further curing.

6.2.3 Testing

The accelerated carbonation exposure was carried out in a sealed chamber fitted with equipment such as a dehumidifier for maintaining RH, a CO_2 cylinder to supply CO_2, CO_2 monitors to regulate the supply of CO2, and an internal sensor to monitor the RH of the system. Figure 6.1 shows the accelerated carbonation chamber.

134

Figure 6.1: Accelerated carbonation chamber

The concrete prisms were exposed to accelerated carbonation at 1% CO_2 concentration and 57% RH for 105 days. However, carbonation depth measurements were carried out before exposure and then on days 28, 56, 63, 70, and 105. In order to measure the carbonation depth, a 50 mm (2-inch) thick sample was cut out of the concrete prism and then sprayed with phenolphthalein to reveal carbonated (colorless) and uncarbonated (purple color) regions. The exposed surface of the cut concrete prism was coated with carbonation-resistant paint and returned to the accelerated carbonation chamber. Measurements were taken with the aid of a steel scale (0.5 mm accuracy) by measuring the distance from the edge of the sample to the point where the uncarbonated (purple color) region begins on the sample. This was done on five different points on each of the four edges of the sample. However, there was a 25 mm (1 inch) offset from the corners to avoid any "corner effects" of CO_2 ingression during measurements. The final carbonation depth was the average depth measured from all four edges. Figure 6.2 illustrates the carbonation depth measurement procedure.
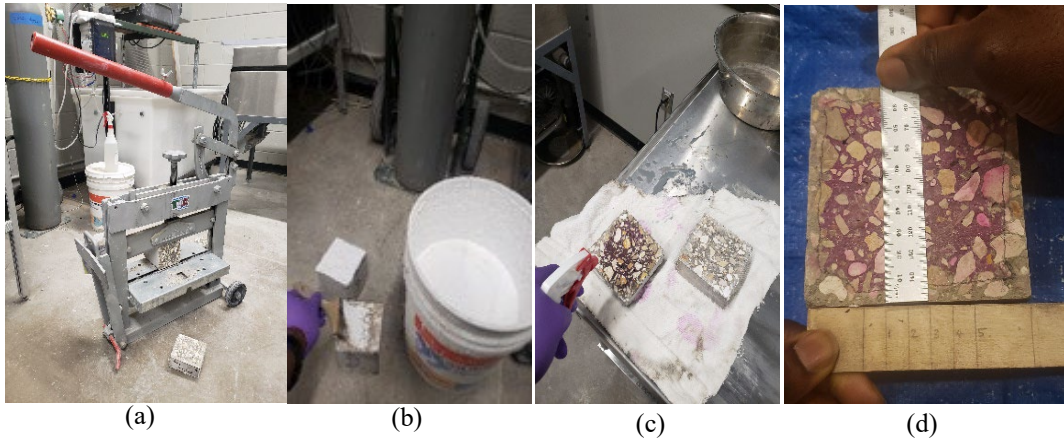
Figure 6.2: Carbonation depth measurement procedure. (a) cutting out the 50 mm thick sample, (b) coating the exposed surface of the concrete prism with carbonation-resistant paint, (c) spraying the 50 mm cut sample with phenolphthalein, (d) measurement with steel scale

Six concrete cylinders out of the eight produced were used for the compressive strength test. Two cylinders were tested from each concrete mixture on days 1, 7, and 28. The results of the compressive strength test are shown in Table 6.3. In order to ascertain the permeability of the mixtures as their microstructure develops due to curing, bulk electrical resistivity measurements were carried out on the remaining two concrete cylinders on days 1, 7, 28, 56, and 91. The impedance measurement was done with Gamry testing equipment and software using the Electrochemical Impedance Spectroscopy (EIS) technique. In order to carry out this test at each stipulated age of curing, the concrete cylinder samples were submerged in water immediately after being removed from the curing room and remained submerged until the testing time. This was to ensure that the samples were in a saturated state before the test. Two concrete cylinder samples were tested for each mixture at a stable room temperature (23°C). The impedance measurement was carried out three times on each sample. During the test, a sample is removed from the water and wiped with a dry cloth to remove any excess surface moisture. Afterward, the sample was placed between two conductive plates in a way that it made contact with the plates via a damp sponge. The conductive plates were connected to the Gamry equipment, which aided the impedance measurement. Figure 6.3 shows the bulk electrical resistivity measurement setup.
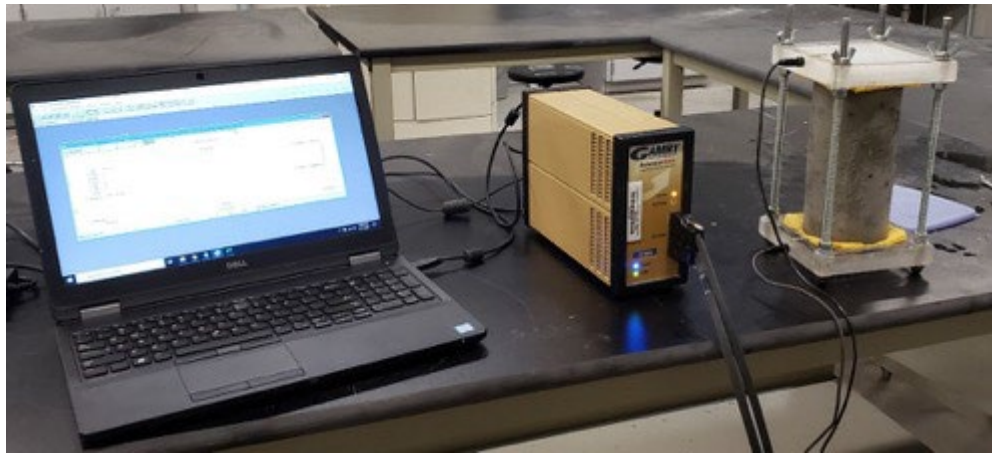
Figure 6.3: Bulk electrical resistivity measurement setup

The final impedance was obtained by calculating the average of the three measurements on each sample and then the average of the two samples representing each mixture. Resistivity (ρ) was determined with equation 6.1, where Z is the measured impedance, A is the cross-sectional area of the sample, and L is the length or height of the sample.

$$\rho = \frac{zA}{L}$$
Eq. 6.1

6.3 RESULTS

6.3.1 Accelerated Carbonation

Figures 6.4 and 6.5 show the accelerated carbonation depth on day 28 and day 105, respectively. In order to aid the analysis of both figures, the dashed line was added to indicate an assumption of 25 mm (1 inch) concrete cover thickness. Also, Figure 6.6 shows the carbonation coefficient of the cement mixtures. The carbonation coefficient was determined using the square root of time model, which is one of several models used in predicting carbonation depth in concrete. The square root of time model postulates that the depth of carbonation over time is proportional to the square root of time [23]. This is illustrated in Equation 6.2 as follows:

X_f is the final carbonation depth, X_i is the initial carbonation depth, t is the exposure time, and K_c is the carbonation coefficient or carbonation rate.

$$X_f - X_i = K_c \times t^{1/2}$$
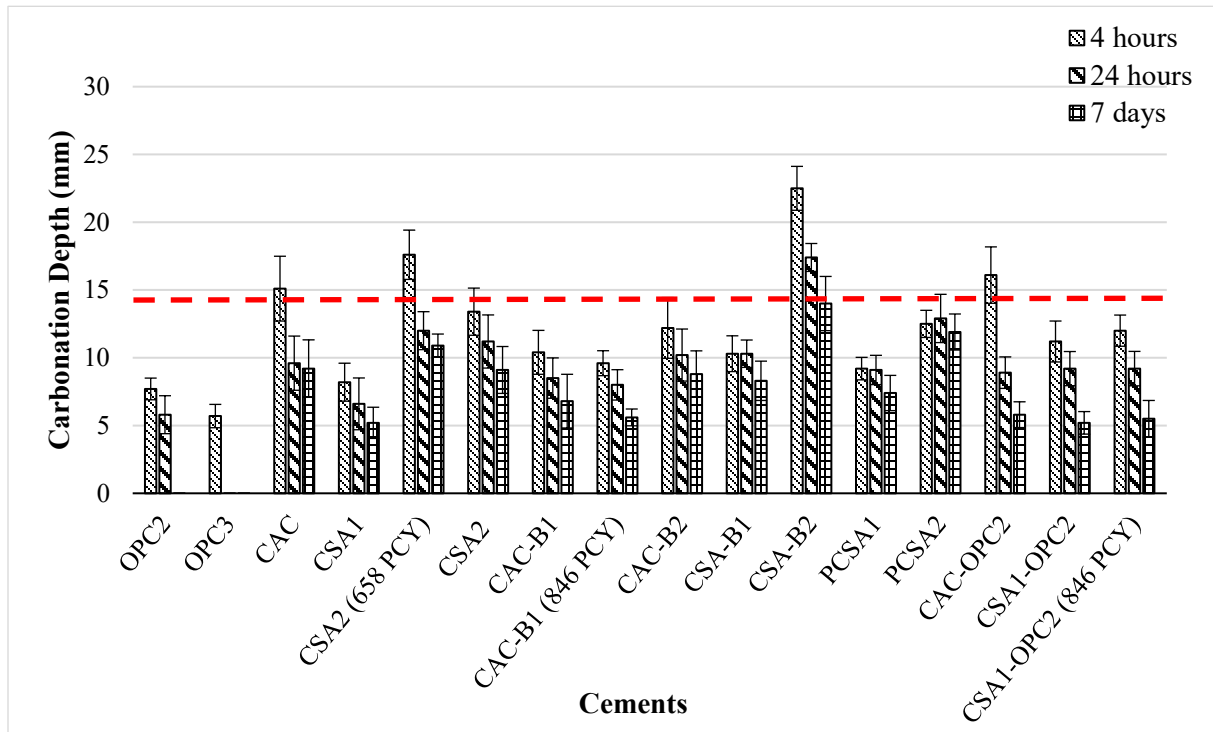
Figure 6.4: Accelerated carbonation depth of binders on day 28
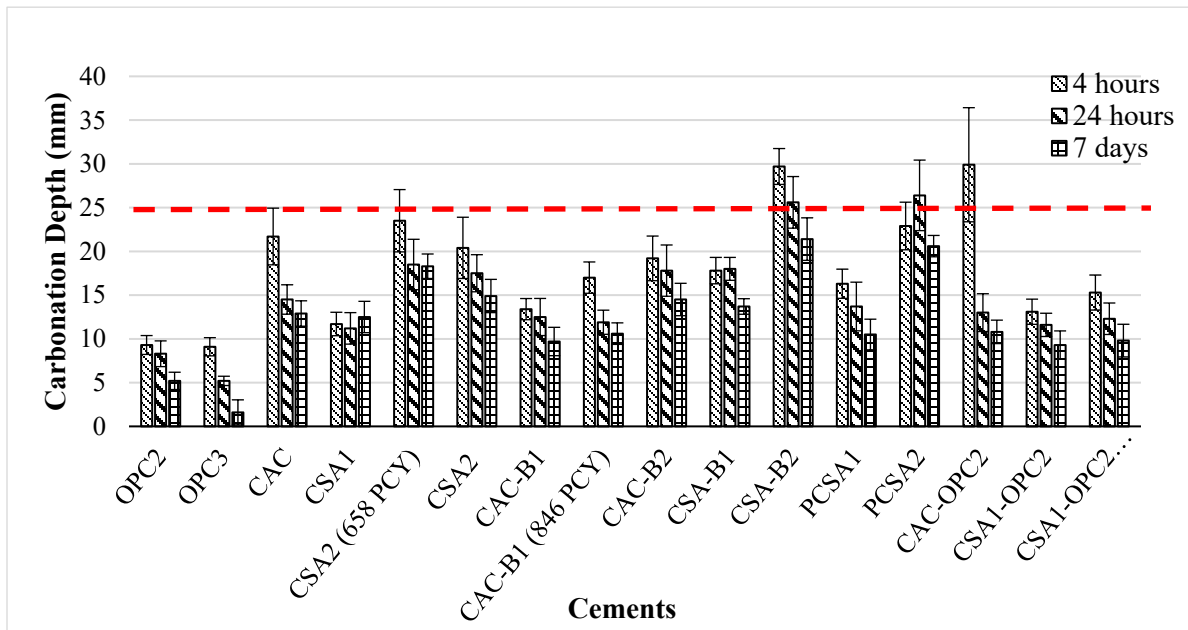
Figure 6.5: Accelerated carbonation depth of binders on day 105
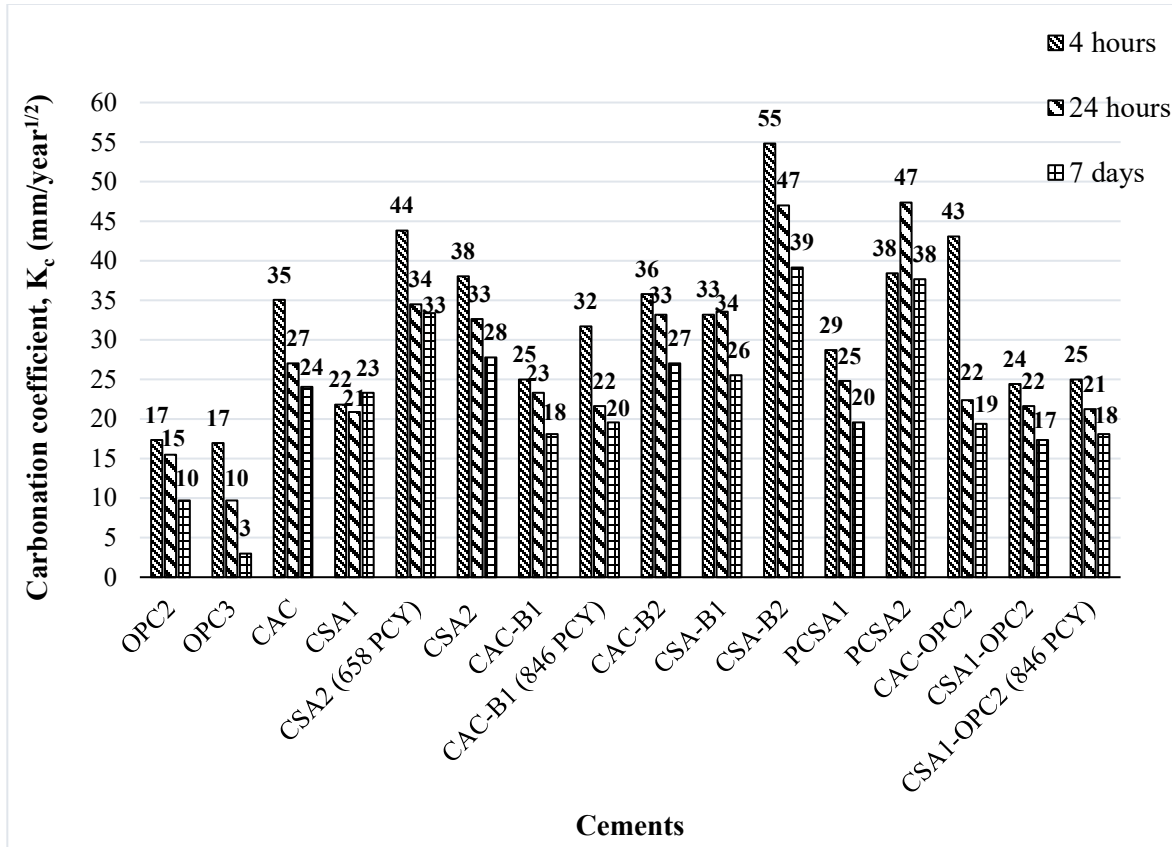
Figure 6.6: Carbonation coefficient of the cement mixtures

Figures 6.4 and 6.5 show that the mixtures exhibited a higher carbonation depth for samples cured for 4-6 hours than those cured for 24 hours and 7 days. However, comparing the 24-hour and 7 days cured samples, there is not much resistance to carbonation offered for the 6 days of additional curing. This difference in carbonation depth due to the different curing regimes can further be supported by considering the carbonation coefficients of the cement mixtures shown in Figure 6.6. The carbonation coefficients shown in Figure 6.6 indicate a higher carbonation rate for the 4-6 hour cured samples compared to the 24 hours and 7 days cured samples. Also, comparing the carbonation coefficients of the 24-hour and 7 days cured samples in Figure 6.6, the additional 6 days of curing did not significantly reduce the carbonation rate, especially in the CAC and CSA cement mixtures.

Most mixtures shown in Figure 6.4 showed moderate carbonation depths in the first 28 days of accelerated carbonation exposure, well below the assumed 25 mm (1 inch) cover thickness. However, the proprietary blended cement CSA-B2 exhibited the least carbonation resistance at day 28, with the carbonation depth of its 4-hour, 24-hour, and 7 days cured samples reaching 22.5 mm, 17.4 mm, and 14 mm, respectively.

In Figure 6.5, the carbonation depths of some mixtures were either close to or exceeded the assumed cover of 25mm (1 inch) after 105 days of exposure. Among the pure cement (OPC2, OPC3, CAC, CSA1, CSA2 (658PCY), and CSA2), CSA2 (658PCY) showed the least resistance to carbonation followed by the CSA2 produced with a total binder content of 446 Kg/m^3 (752 lb/yd^3). CSA1 and CAC showed moderate resistance to carbonation compared to the controls (OPC2 and OPC3), which had the highest resistance to carbonation. Comparing the high ye'elmite cement CSA1 and the CSA belite cements (CSA2 (658PCY), CSA2, CSA-B1, and CSA-B2), the high ye'elmite cement CSA1 showed more resistance to carbonation compared to the CSA belite cements. However, the resistance to carbonation exhibited by the CSA belite cements appeared to be dependent on the proportion of ye'elmite to belite phases present in the cements (see Table 6.1). This is seen in the higher carbonation depth exhibited by CSA-B2 and CSA2 compared to CSA-B1. However, there was an improvement in carbonation resistance in the CSA belite cement mixtures as curing increased to 7 days.

The proprietary blended cements (CAC-B1, CAC-B1 (846PCY), CAC-B2, CSA-B1, CSA-B2, PCSA1, and PCSA2) exhibited a moderate to low resistance to carbonation as shown in Figure 6.5. Among the proprietary blended cements, CSA-B2 and PCSA2 exhibited the least resistance to carbonation, with their carbonation depths either reaching or exceeding the assumed 25 mm (1 inch) cover mark. Comparing CAC-B1 with CAC-B1 (846PCY), it appears that the increase in cement content did not have much effect on the carbonation resistance of the mixture. However, there was a higher carbonation depth in the 4-hour cured sample of CAC-B1 (846PCY), which could have resulted from inadequate curing.

Due to the addition of OPC to the lab blended cements (CSA1-OPC2, CSA1-OPC2 (846PCY), and CAC-OPC2), carbonation resistance appeared to be slightly improved compared to their pure counterparts (CAC and CSA1), especially in samples that were cured for 24 hours and 7 days. Comparing the carbonation depth of CSA1-OPC2 and CSA-OPC2 (846PCY) in Figure 6.5, CSA-OPC2 (846PCY) with a higher cement content exhibited a slightly higher carbonation depth than CSA1-OPC. Comparing the concrete mixtures that constitute CAC and CSA cements without OPC (CAC, CAC-B2, CSA1, CSA2, CSA-B1, and CSA-B2), and those that constitute a blend of either CAC or CSA cements with OPC (CAC-B1, PCSA1, CAC-OPC2, and CSA1-OPC2), there seems to be an increase in carbonation resistance due to the addition of OPC.

6.3.2 Relationship Between Carbonation Depth and Compressive Strength

Figures 6.7, 6.8, and 6.9 show the relationship between the carbonation depth due to the different curing regimes (4 hours, 24 hours, and 7 days) and the compressive strength on days 1, 7, and 28, respectively.
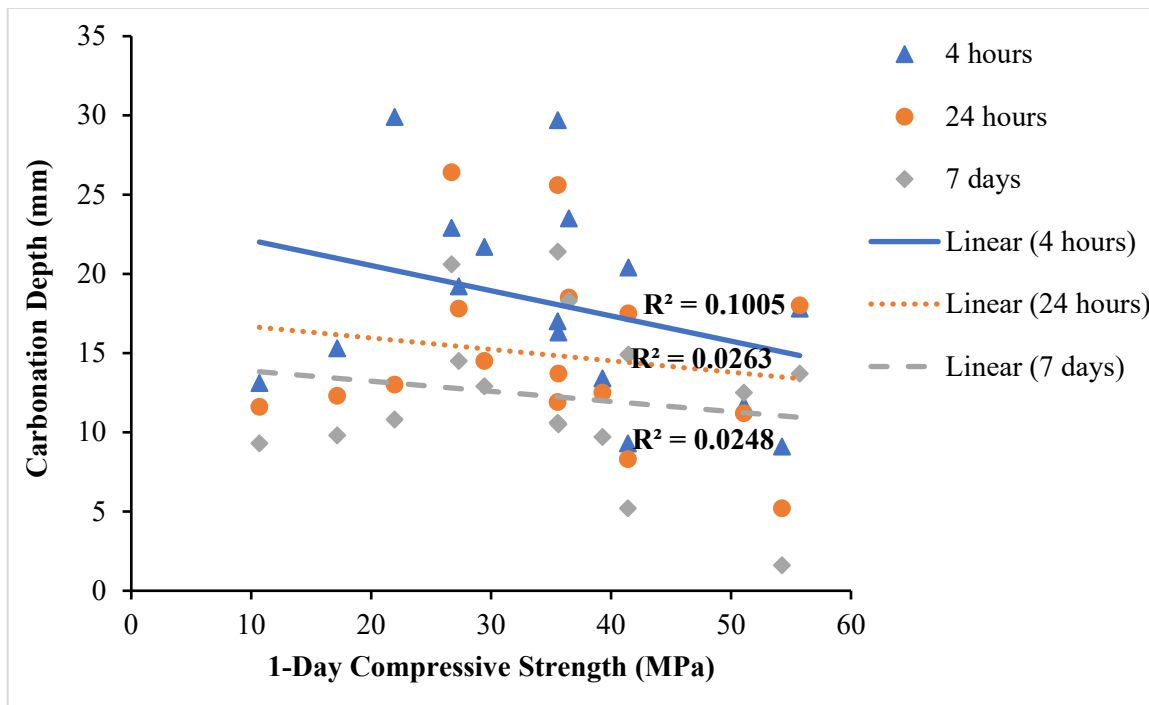
Figure 6.7: Relationship between the carbonation depths after 105 days of accelerated exposure and the 1-day compressive strengths
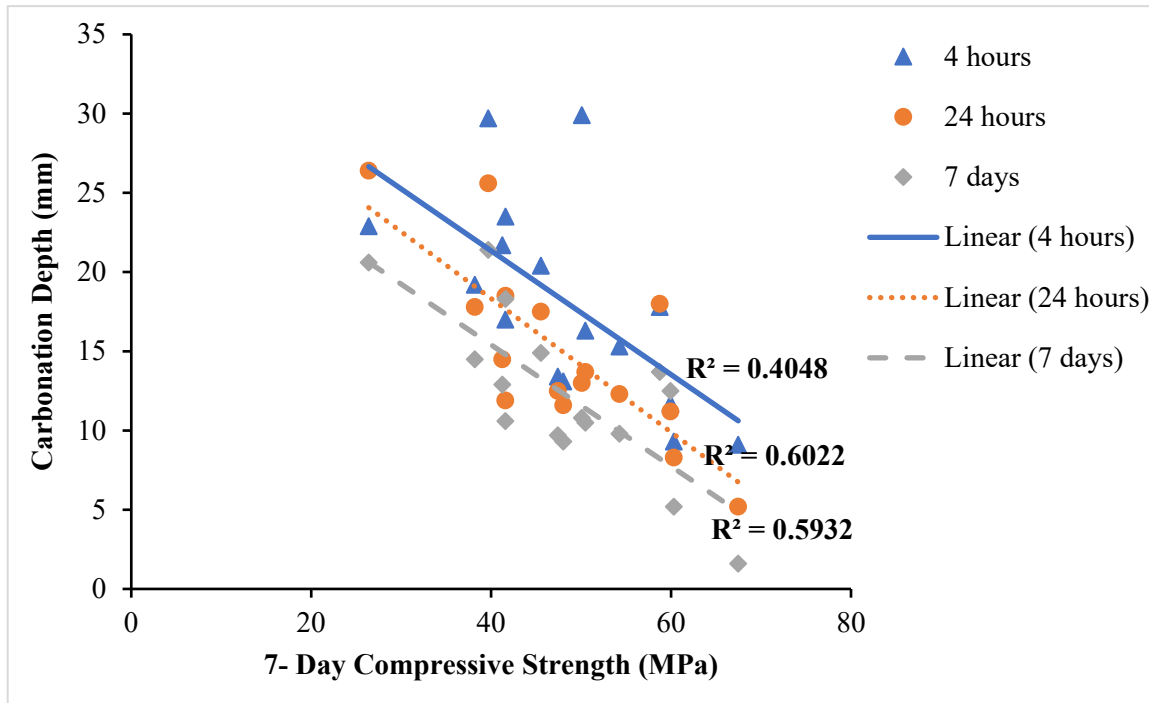
Figure 6.8: Relationship between the carbonation depths after 105 days of accelerated exposure and the 7-day compressive strengths
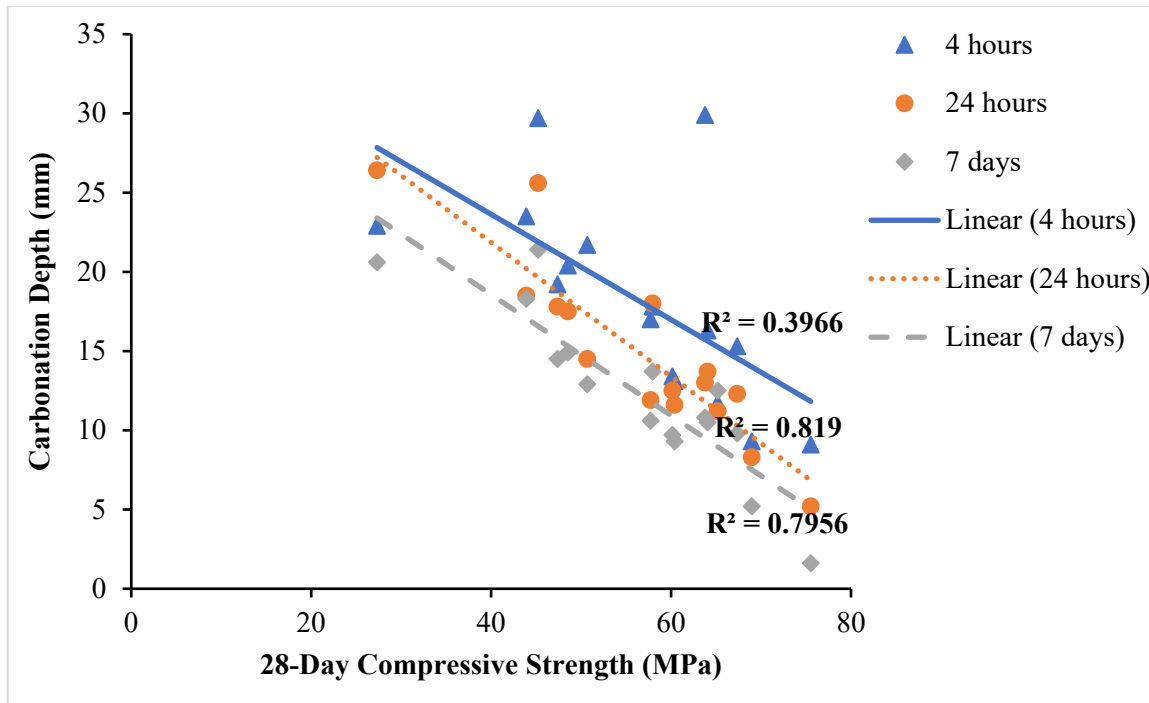
Figure 6.9: Relationship between the carbonation depths after 105 days of accelerated exposure and the 28-day compressive strengths

Figure 6.7 shows a very weak correlation (R^2 values) between the carbonation depths (4 hours, 24 hours, and 7 days) and the 1-day compressive strengths. However, the carbonation depth of the 4-hour cured samples in Figure 6.7 shows more correlation to the 1-day compressive strengths than the 24 hours and 7 days cured samples. Comparing Figures 6.8 and 6.7, Figure 6.8 shows a higher correlation (R^2 values) between the carbonation depths (4 hours, 24 hours, and 7 days) and the 7-day compressive strengths. However, the carbonation depths of the 24-hour and the 7 days cured samples showed a close correlation with the 7-day compressive strengths than the 4-hour cured samples. In Figure 6.9, the carbonation depths of the 24-hour and 7 days cured samples showed a stronger correlation with the 28-day compressive strengths compared to their correlation with the 7-day and 1-day compressive strengths. Also, comparing the R^2 values in Figures 6.7, 6.8, and 6.9, the 24-hour cured sample showed a slightly more correlation with the compressive strengths on days 7 and 28 than the 7 days cured samples. The correlation between the carbonation depth of the 4-hour cured samples and compressive strength declined as compressive strength increased from day 7 in Figure 6.7 to day 28 in Figure 6.9.

6.3.3 Bulk Electrical Resistivity

Figures 6.10 and 6.11 show the bulk electrical resistivity values of the pure and blended cements (proprietary and lab blended), respectively.

142
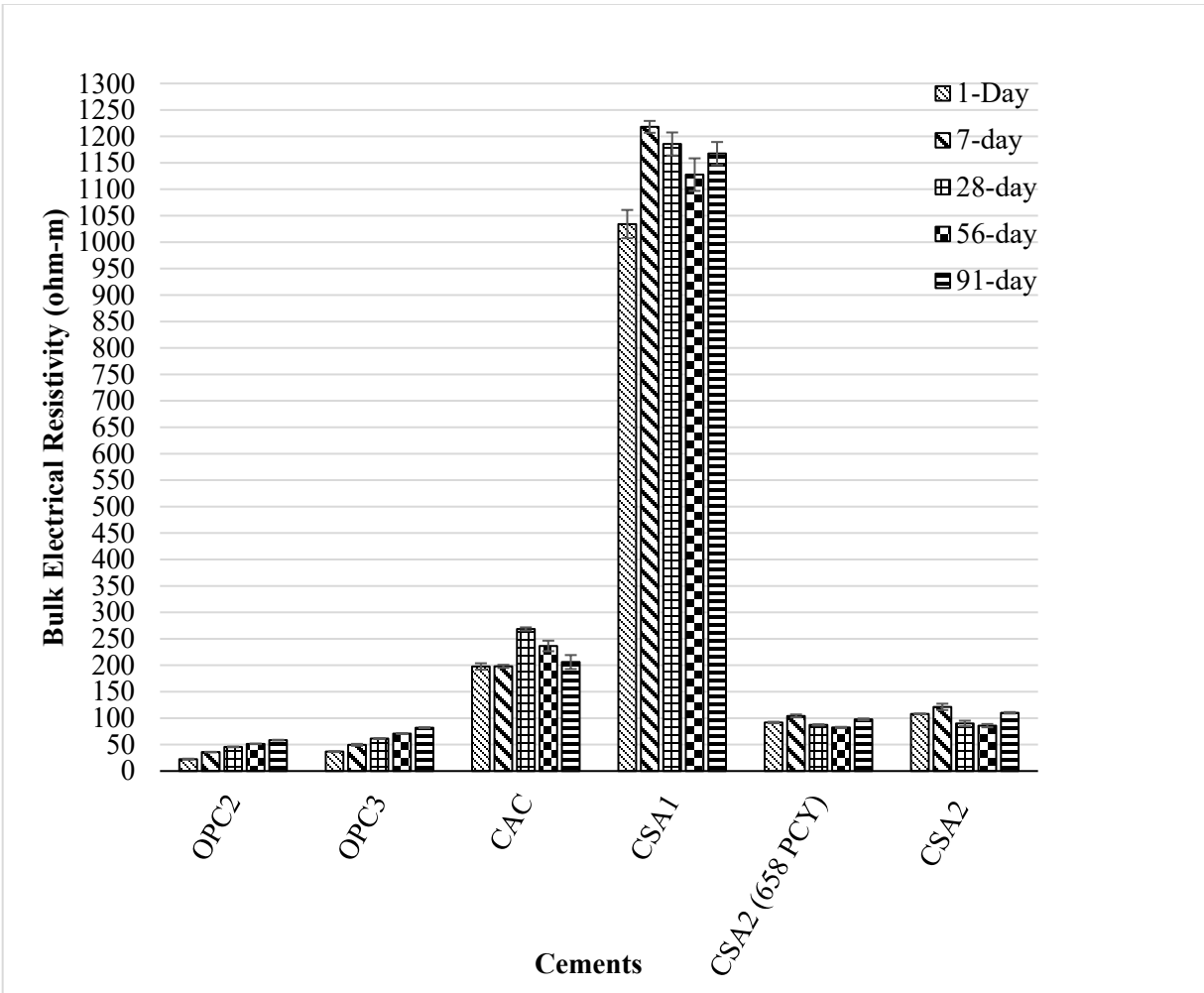
Figure 6.10: Bulk electrical resistivity for pure cements
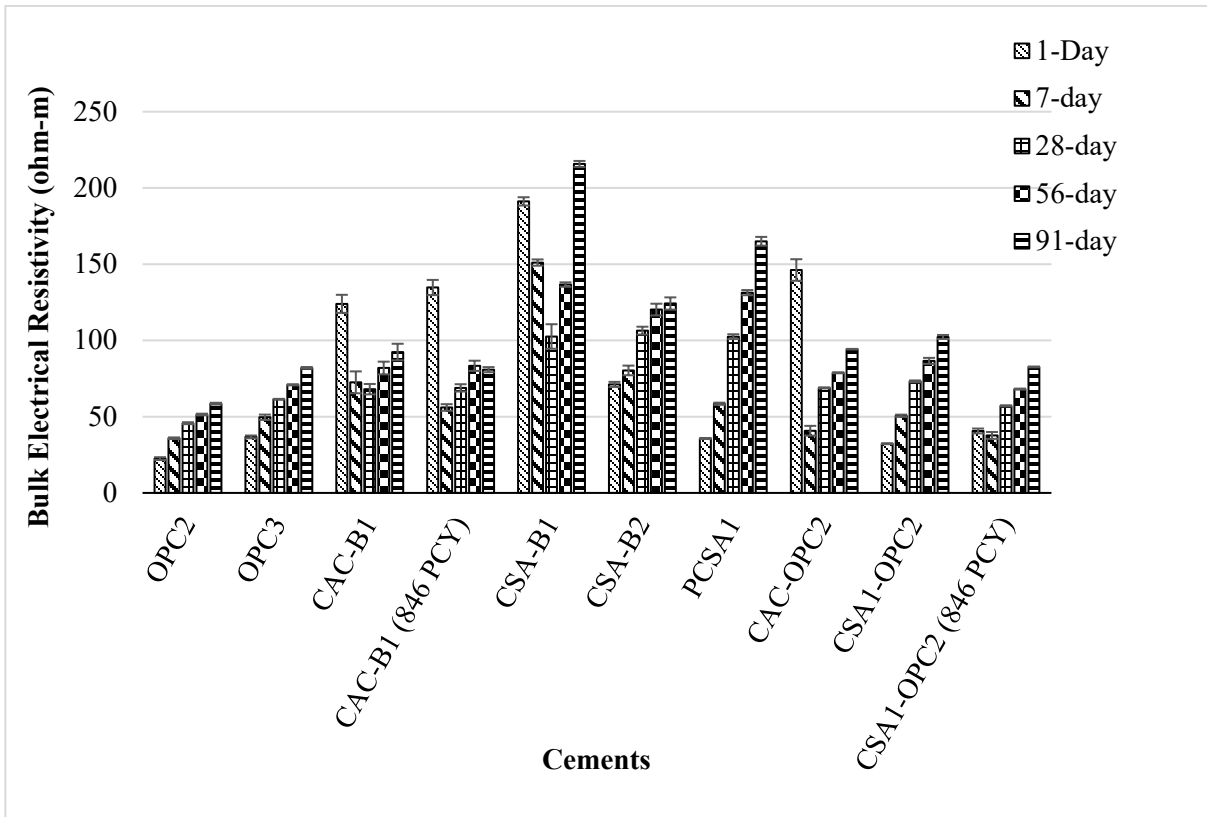
Figure 6.11: Bulk electrical resistivity for blended cements

In Figure 6.10, the pure cements CAC, CSA1, CSA (658PCY), and CSA2 exhibited higher resistivity values from day 1 through 91 compared to the controls OPC2 and OPC3. The pure cement CSA1 showed the highest resistivity of all the cements investigated in this study as shown in Figure 6.10. The resistivity values of CSA1 in ohm-meter from day 1 through 91 were 1034, 1218, 1186, 1128, and 1167, respectively. Following CSA1 was the pure cement CAC with resistivity values in ohm-meter from day 1 through 91 as 197, 198, 269, 237, and 206. CSA2 appears to have lower resistivity values compared to CAC and CSA1, as shown in Figure 6.10.

The lab blended cements (CSA1-OPC2, CSA1-OPC2 (846 PCY), and CAC-OPC2) in Figure 6.11 exhibited higher electrical resistivity compared to the control OPC2 at all ages. The proprietary blended cements also showed higher resistivity values than the controls (OPC2 and OPC3). However, OPC3 showed higher resistivity values than OPC2 due to its high early strength attributes. Comparing the CSA belite cements in Figures 6.10 and 6.11, CSA-B1 showed a higher resistivity, especially on days 1, 7, 56, and 91, than CSA-B2, CSA2, and CSA2 (658PCY).

The CAC-based-cements CAC-B1, CAC-B1 (846 PCY), and CAC-OPC2 exhibited a high resistivity at day 1, implying less porosity and permeability at an early age. However, they all showed a decrease in resistivity on day 7 and then increased again as hydration continued through day 91. Similarly, CAC, CSA1, CSA-B1, CSA2, and CSA2(658PCY) also showed fluctuations in their resistivity from day 1 through 91.

Considering the effect of increasing the total cement content on electrical resistivity, CAC-B1 (846PCY) exhibited slightly higher resistivity values than those of CAC-B1 on days 1, 28, and 56, as shown in Figure 6.11. However, CAC-B1 exhibited slightly higher resistivity values than CAC-B1 (846PY) on days 7 and 91. In Figure 6.11, CSA1-OPC exhibited higher resistivity values than CSA1-OPC2 (86PCY) on days 7, 28, 56, and 91. However, CSA1-OPC2(86PCY) showed higher resistivity than CSA1-OPC on day 1. Also, Figure 6.10 shows that CSA2 exhibited higher resistivity than CSA2 (658PCY) on days 1, 7, 28, 56, and 91.

6.3.4 Relationship Between Carbonation Depth and Bulk Electrical Resistivity

Figures 6.12, 6.13, and 6.14 show the relationship between the carbonation depth due to the different curing regimes (4 hours, 24 hours, and 7 days) and the bulk electrical resistivities on days 1, 7, and 28, respectively.
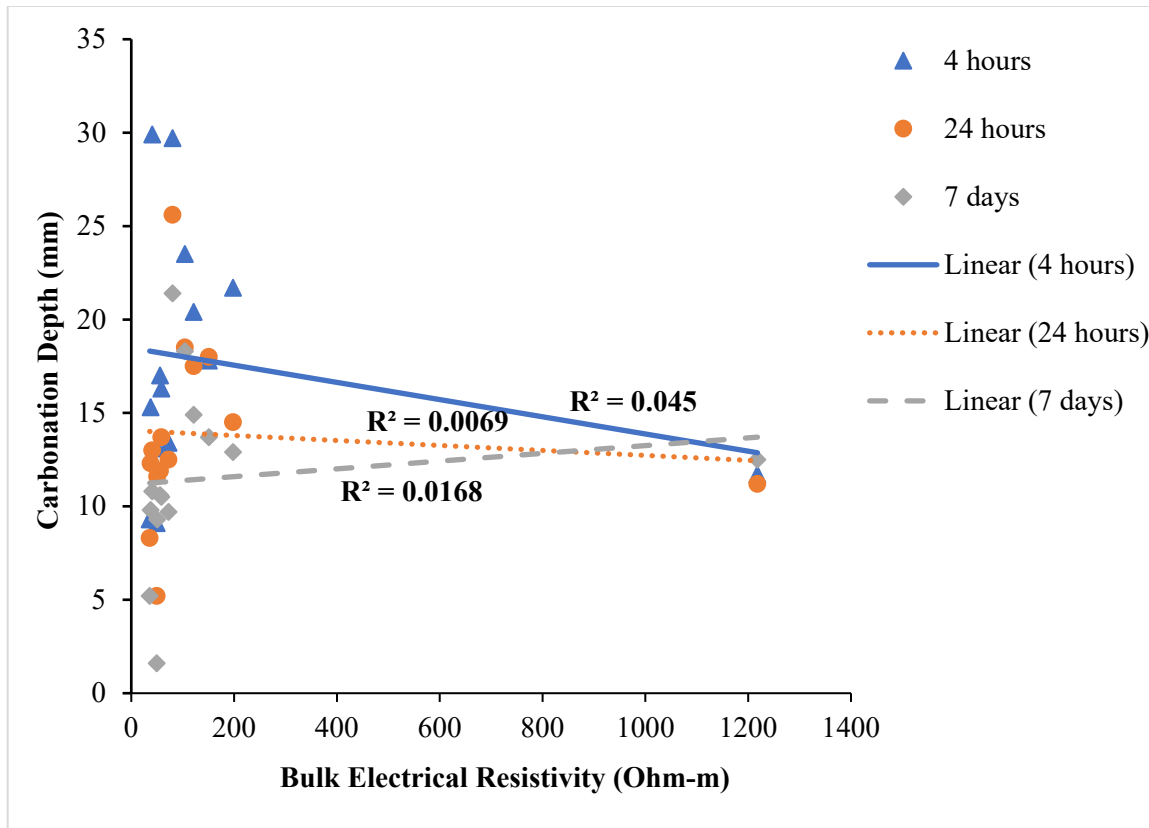
Figure 6.12: Relationship between the carbonation depths after 105 days of accelerated exposure and the bulk electrical resistivities at day 1
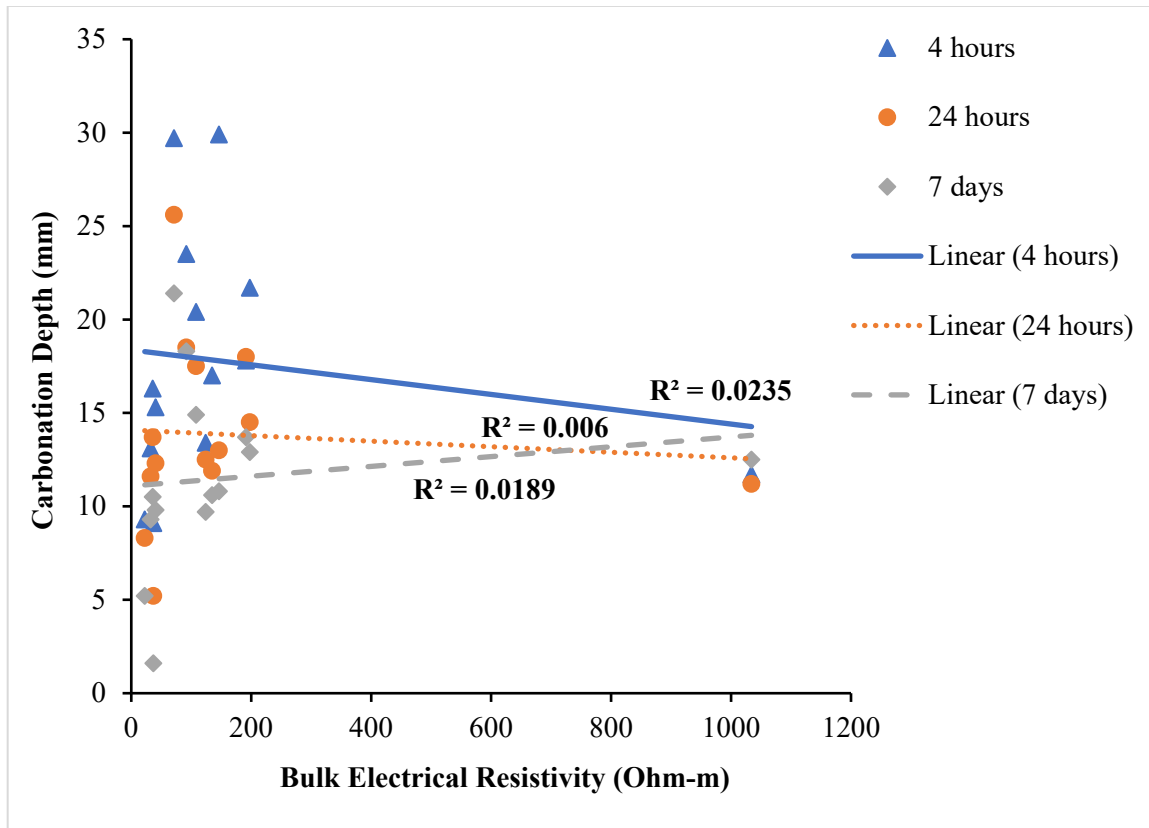
Figure 6.13: Relationship between the carbonation depths after 105 days of accelerated exposure and the bulk electrical resistivities at day 7
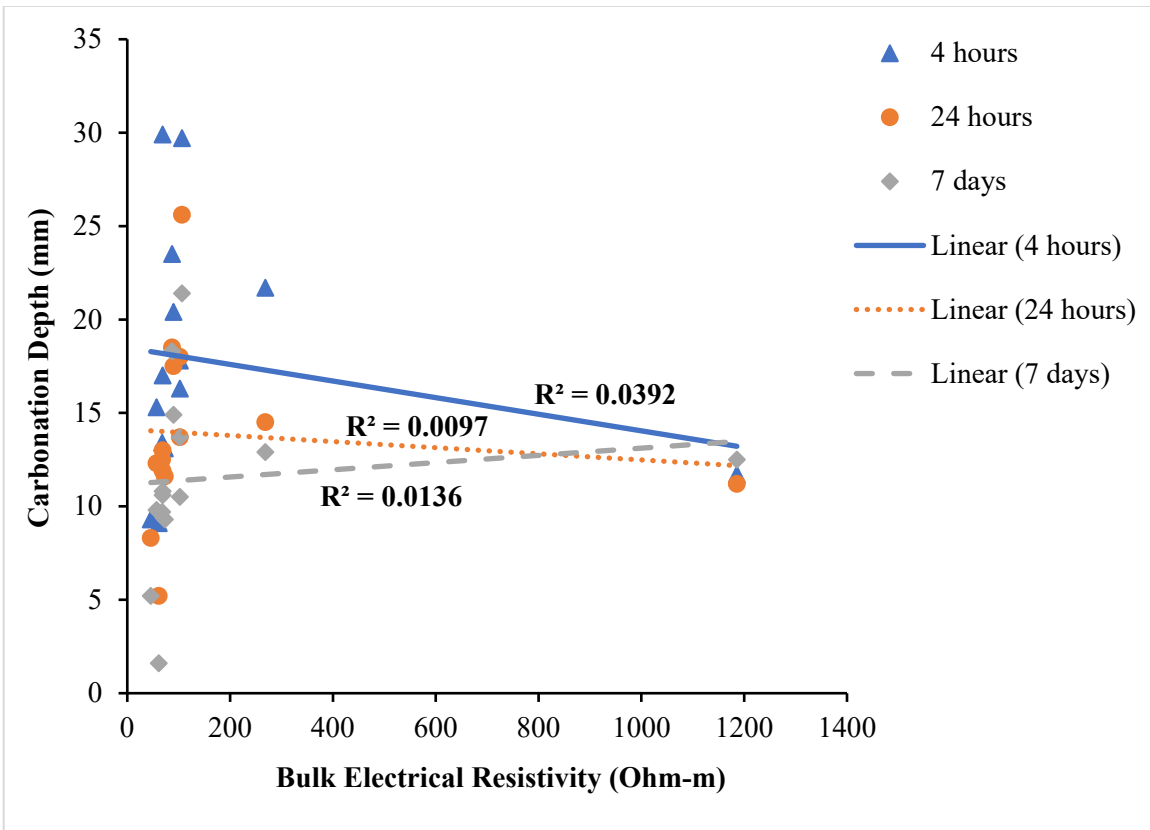
Figure 6.14: Relationship between the carbonation depths after 105 days of accelerated exposure and the bulk electrical resistivities at day 28

Curing enhances the microstructure of concrete and reduces penetrability to harmful chemicals. This implies that concrete properties such as electrical resistivity and carbonation resistance that depend on the pore structure of concrete should also be influenced by curing. However, Figures 6.12, 6.13, and 6.14 show a very weak correlation (R^2 values) between the carbonation depths due to the different curing regimes (4 hours, 24 hours, and 7 days) and the bulk electrical resistivities on days 1, 7, and 28, respectively.

6.4 DISCUSSION

6.4.1 Accelerated Carbonation

The observed increase in resistance to carbonation as the curing duration increases from 4 hours to 24 hours and then to 7 days can be attributed to the microstructural development of the concrete over time. Curing ensures the continuous hydration of cementitious materials in concrete, hence improving the strength and durability of concrete [9, 10]. Although the expectation was to have a substantial increase in

carbonation resistance in the 7 days cured samples compared to those cured for 24 hours, the carbonation depths exhibited by the majority of the concrete mixtures showed that there was not much resistance to carbonation offered for the 6 days of additional curing. This can be attributed to the rapid early strength gain and microstructural development peculiar to CAC and CSA cements, especially those with high ye'elmite content [4, 5, 17, 20]. Since the majority of the strength and microstructural configuration of concrete produced with these cements are attained in the early hours of their hydration, extended curing wouldn't contribute so much to their strength and microstructural development. However, due to the later strength gain and microstructural development attributes of the CSA belite cements (CSA2, CSA-B1, and CSA-B2), OPC2 and the blended mixtures of CAC and CSA cement with OPC [4, 19], they exhibited improved resistance to carbonation due to the additional six days of curing compared to CSA1 and CAC in Figures 6.5. This implies that in order to improve the carbonation resistance in concrete, adequate curing is required for concrete produced with OPC, blended systems of OPC with either CAC or CSA cement, and CSA belite cement. However, a minimum of 24 hours of curing should provide significant improvement in the carbonation resistance of concrete produced with CAC and high ye'elmite CSA cement.

The low resistance to carbonation exhibited by the pure cements CAC, CSA1, CSA2 (658PCY), and CSA2 and the proprietary blended cements CSA-B1, CSA-B2, and CAC-B2 can be attributed to their low alkalinity or lack of CH compared to OPC2 and OPC3. The presence of CH in OPC concrete helps to provide a buffer to CO_2 ingress in OPC concrete [24, 25]. During the carbonation reaction in OPC concrete, the dissolved CO_2 and CH in OPC concrete react to produce $CaCO_3$ which clogs the pore network and prevents further diffusion of CO_2 into the concrete, thus reducing the rate of further carbonation [3, 4]. Another possible reason for the low carbonation resistance exhibited by these cements is the breakdown of their main hydration products due to carbonation. The carbonation reaction in CAC and CSA cement concrete results in the breakdown of their main hydration products, hydrogarnet, and ettringite hence increasing porosity and the rate of further carbonation in CAC and CSA cement concrete [4, 5]. Although OPC2 and OPC3 showed the highest resistance to carbonation compared to the other cements, OPC3 still showed higher carbonation resistance than OPC2 due to its fineness and rate of hydration [10]. The increased fineness of the OPC3 increases the surface area in contact with water during hydration, hence resulting in early strength gain and microstructure development [10].

Comparing the concrete mixtures that constitute CAC and CSA cements without OPC (CAC, CAC-B2, CSA1, CSA2, CSA2 (658PCY), CSA-B1, and CSA-B2), and those that constitute a blend of either CAC or CSA cements with OPC (CAC-B1, PCSA1, CAC-OPC2, CSA1-OPC2, and CSA1-OPC2(846PCY)), it can be observed that the addition of OPC increased CH content and CO_2 buffer capacity of the mixtures

[24, 25]. This explains the higher carbonation resistance exhibited by the CAC and CSA cement mixtures blended with OPC compared to those without OPC. The highest carbonation depth exhibited by PCSA2 compared to other cement mixtures in this study could be attributed to the presence of fly ash (see Table 2.1) [26-28]. The combined effect of hydraulic cement replacement with fly ash and the consumption of CH due to the pozzolanic reaction of fly ash could have affected the early age strength and microstructural development of PCSA2 as well as its buffer to CO_2 ingress, hence the reason for its low resistance to carbonation [26, 28].

The ye'elmite phase in CSA cements is responsible for their rapid early strength gain and microstructural development, while the belite phase is responsible for later strength gain and microstructural development [4, 19, 21]. This implies that CSA cements with high ye'elmite content will produce a less porous and more dense microstructure at an early age compared to CSA cements with high belite. The higher carbonation depth exhibited by the pure cements CSA2 (658PCY) and CSA2, especially the 4-hour and 24-hour cured samples, can be attributed to their high belite content compared to CSA1, which has a high ye'elmite content (see Table 6.1). The same applies to the proprietary cement blends CSA-B1 and CSA-B2. Although both cements have high belite content, as indicated in Table 6.1, the ratio of the ye'elmite phase to the belite phase in CSA-B1 (0.8) is higher compared to that in CSA-B2 (0.6). This could be the reason for the higher carbonation depth exhibited in CSA-B2 compared to CSA-B1. Also, the improvement in carbonation depth in CSA2, CSA-B1, and CSA-B2 as curing extended from 24 hours to 7 days can be attributed to the hydration of the belite phase and the consequent development of microstructure [19, 29].

Increasing cement content can help improve the concrete microstructure and carbonation resistance [30]. This could be seen in the improved resistance to carbonation in CSA2 at all curing ages compared to CSA (658PCY), as shown in Figure 6.5. However, the improvement in carbonation resistance due to the increase in cement content was not clearly evident in CAC-B1 and CAC-B1 (846PCY). The same applies to CSA1-OPC2 and CSA1-OPC2 (846PCY), where CSA1-OPC2 (846PCY) exhibited slightly higher carbonation depth than CSA1-OPC2 at all curing ages in Figure 6.5. This disparity in performance is unusual and unexpected and might need further investigation to ascertain the reason for the lesser resistance to carbonation despite the increase in cement content.

6.4.2 Relationship Between Carbonation Depth and Compressive Strength

The compressive strength and durability properties of concrete strongly depend on the proper curing of concrete [10]. The curing of concrete provides the moisture required to sustain hydration and develop concrete microstructure. Hence, as the duration of curing increases, concrete properties such as

compressive strength and carbonation resistance also improve [15, 26]. The weak correlation (R^2 values) between the carbonation depths of the 4 hours, 24 hours, and 7 days cured samples and the 1-day compressive strength in Figure 6.7 can be attributed to a poorly developed microstructure due to inadequate curing. However, comparing the same carbonation depths with the compressive strengths on days 7 and 28 in Figures 6.8 and 6.9, the correlation increased from a moderate correlation (R^2 values) with the 7-day compressive strengths to a strong correlation (R^2 values) with the 28-day compressive strengths, especially for the carbonation depths of the 24 hours and 7 days cured samples. This increase in correlation could be attributed to the improvement of microstructure as the duration of curing increased [15, 26]. The close R^2 values for the 24 hours and 7 days cured samples, as shown in Figures 6.7, 6.8, and 6.9, can be attributed to the rapid early strength and microstructural development exhibited by the CAC and CSA cements [4, 11, 29]. Due to this development of microstructure at early age, the carbonation depths of the 24-hour and 7 days cured samples appeared to have a close correlation (R^2 values) to the compressive strengths.

6.4.3 Bulk Electrical Resistivity

The higher resistivity values from day 1 through 91 exhibited by the CAC and CSA cement mixtures (pure, proprietary, and lab-blended) compared to the controls (OPC2 and OPC3) in Figures 6.10 and 6.11 can be attributed to the rapid early strength gain and microstructural development of CAC and CSA cements [4, 11, 29]. Similarly, the high resistivity values exhibited by OPC3 from days 1 through 91 compared to OPC2 can be attributed to the early strength gain and microstructural development characteristics peculiar to OPC3. Type III cement (OPC3) is more finely ground compared to Type I/II cement (OPC2) [10]. The fineness of Type III cements increases the surface area that comes in contact with water during hydration leading to faster hydration and microstructural development [10].

The cement CSA1 which is in the pure cement category, exhibited the highest resistivity values at all ages compared to all other cement mixtures because of its high ye'elmite content. The ye'elmite phase accounts for the rapid early strength gain and microstructural development of CSA cement concrete [21, 29]. Comparing the low resistivity values of CSA2(658PCY), CSA2, CSA-B1, and CSA-B2 to the high resistivity values of CSA1 at all ages, it is possible to associate the performance of CSA2(658PCY), CSA2, CSA-B1, and CSA-B2 to their high belite phase content compared to the ye'elmite phase. This is because the belite phase accounts for later strength gain and microstructural development in CSA cement concrete [19]. The higher resistivity values exhibited by the belite cement CSA-B1 on days 1, 7, 56, and 91 compared to the other belite cements CSA2 (658PCY), CSA2, and CSA-B2 can be attributed to its proportion of ye'elmite phase to belite phase.

151

The improvement in resistivity exhibited by the lab-blended cement mixtures (CAC-OPC2, CSA1-OPC2, and CSA1-OPC2 (846PCY)) and the proprietary blended cement containing OPC (PCSA1, CAC-B1 (846PCY), and CAC-B1) can be attributed to the increase in the rate of hydration and microstructure development due to the blending of CAC and CSA cement with OPC. The rapid early strength and microstructure development properties of CAC and CSA cement are usually harnessed by blending them with OPC to accelerate the hydration of OPC as well as its microstructural development [4, 11, 19, 20].

The drop in resistivity exhibited by the CAC mixtures in Figures 6.10 and 6.11 could be attributed to the conversion of the metastable hydrates (CAH_{10} and C_2AH_8) to stable hydrates (C_3AH_6 and AH_3), resulting in increased porosity and loss of strength [11]. Aside from conversion, another factor that could have caused the fluctuation in resistivity, as observed in the aforementioned CAC-based cement mixtures as well as CSA1, CSA2, and CSA-B1, as shown in Figures 6.10 and 6.11 is the leaching of ions [31]. The samples for this study were cured with water in a wet curing room instead of a simulated pore solution with a similar concentration to the concrete's pore solution. Hence, allowing the possibility of leaching of ions from the pore solution of the concrete due to a concentration gradient [31].

As stated earlier, the increase in cement content can help improve the concrete microstructure and decrease penetrability in concrete [30]. This is exemplified in the higher resistivity values exhibited by CSA2 compared to CSA2 (658PCY) on days 1, 7, 28, 56, and 91. However, CAC-B1 (846PCY) and CAC-B1 did not show any clear difference in resistivity due to increased cement content. Also, CSA1-OPC exhibited higher resistivity values than CSA1-OPC2 (86PCY) on days 7, 28, 56, and 91, except for day 1. This performance of CAC-B1 (846PCY) and CSA1-OPC2 (86PCY), despite the increased cement content and extended curing, is an aberration and would require more investigation to ascertain the reason for the disparity.

6.4.4 Relationship Between Carbonation Depth and Bulk Electrical Resistivity

Bulk electrical resistivity measurements are used to assess the permeability of concrete by subjecting the concrete to an electric field and ascertaining the resistance of the flow of current through the pores of the concrete [31, 32]. This implies that the higher the resistivity value of a concrete sample, the less permeable it will be to harmful chemicals such as the dissolved CO_2 that causes carbonation. Despite the high resistivity exhibited by the CAC and CSA categories (pure, proprietor, and lab blended) compared to the controls (OPC2 and OPC3), their resistance to carbonation was observed to be lesser than the controls. This could be the reason why there was no correlation between the carbonation depths and bulk electrical resistivity in Figures 6.12, 6.13, and 6.14. A good explanation for this disparity in performance is the low CO_2 buffer capacity of the CAC and CSA cement mixtures compared to OPC [24, 25] as well as the

breakdown of hydration products of CAC and CSA during carbonation [4, 5]. Since the concrete samples used in the study were not exposed to carbonation before bulk electrical resistivity measurement, the effect of CO_2 buffer capacity and the changes in microstructure during carbonation was not captured. Hence, the reason for the low resistance to carbonation despite the low permeability indicated by the high resistivity values.

6.5 CONCLUSIONS

The 4-hour cured samples showed higher carbonation depth compared to 24-hour cured and 7-days cured samples. However, there was not much difference in carbonation resistance between the 24-hour cured and 7-day cured samples due to rapid early strength gain and microstructural development of the CAC and CSA cements. It follows that adequate curing should take place for at least 7 days for OPC based cement concrete and 24 hours for CAC and CSA cement concrete to increase their carbonation resistance.

The lab blended cements (CSA1-OPC2, CSA1-OPC2 (846 PCY), and CAC-OPC2) exhibited higher electrical resistivity compared to the control OPC2 at all ages. This was attributed to the addition of CSA and CAC, considering their higher rate of hydration and microstructural development. Also, the lab blended cements showed a slight improvement in carbonation resistance compared to their pure counterparts due to the presence of CH produced from the hydration of the OPC constituent.

The pure and proprietary blended CAC and CSA cements showed moderate to high carbonation depths compared to the controls (OPC2 and OPC3), which showed the least carbonation depths of all the cements under investigation. The higher carbonation depth exhibited by the pure and proprietary blended CAC and CSA cements was attributed to their low alkalinity or lack of CH and the increase in porosity due to the decomposition of their hydrates during carbonation.

The pure and proprietary blended CAC and CSA cements exhibited high resistivity values that indicated a low porosity and permeability. However, their low permeability did not reflect in their ability to resist carbonation. This disparity in performance exhibited by the CAC and CSA cements was attributed to a low CO_2 buffer capacity and changes in microstructure during the carbonation reaction, which was not captured by the bulk electrical resistivity measurements.

The CSA cements with high ye'elmite content showed higher carbonation resistance and electrical resistivities than the CSA belite cements due to their rapid early strength gain and microstructural development characteristics.

The carbonation depths of the 4 hours, 24 hours, and 7 days cured samples showed a very weak correlation (R^2 values) with the 1-day compressive strengths. However, as the compressive strengths increased from days 7 to 28, the correlation (R^2 values) with carbonation depths increased from moderate to strong (R^2 values), especially for the carbonation depths of the 24 hours and 7 days cured samples. This increase in correlation was attributed to the improvement of pore structure as the duration of curing increased.

6.6 REFERENCES

[1]   M. Yu, J. Lee, and C. Chung, "The Application of Various Indicators for the Estimation of Carbonation and pH of Cement Based Materials," *Journal of Testing and Evaluation,* vol. 38, pp. 534-540, 2010. [Online]. Available: www.astm.org.

[2]   A. V. Saetta, B. A. Schrefler, and R. V. Vitaliani, "The carbonation of concrete and the mechanism of moisture, heat and carbon dioxide flow through porous materials," *Cement and Concrete Research,* vol. 23, no. 4, pp. 761-772, 1993.

[3]   V. Shah and S. Bishnoi, "Understanding the Process of Carbonation in Concrete using Numerical Modeling," *Journal of Advanced Concrete Technology,* vol. 19, no. 11, pp. 1148-1161, 2021.

[4]   S. Lamberet, "Durability of ternary binders based on Portland cement, calcium aluminate cement and calcium sulfate," EPFL, 2004.

[5]   E. T. G. Moffatt and M. D. Thomas, "Effect of Carbonation on the Durability and Mechanical Performance of Ettringite-Based Binders," *ACI Materials Journal,* vol. 116, no. 1, 2019.

[6]   J. Newman and B. S. Choo, *Advanced concrete technology set*. Elsevier, 2003.

[7]   D. N. Katpady, H. Hazehara, M. Soeda, T. Kubota, and S. Murakami, "Durability assessment of blended concrete by air permeability," *International Journal of Concrete Structures and Materials,* vol. 12, no. 1, pp. 1-11, 2018.

[8]   B. Liu, G. Luo, and Y. Xie, "Effect of curing conditions on the permeability of concrete with high volume mineral admixtures," *Construction and Building Materials,* vol. 167, pp. 359-371, 2018.

[9]   S. H. Kosmatka, W. C. Panarese, and B. Kerkhoff, *Design and control of concrete mixtures*. Portland Cement Association Skokie, IL, 2002.

[10]   S. Mindess, F. J. Young, and D. Darwin, *Concrete*. New Jersey: Prentice Hall, 2003.

[11]   K. L. Scrivener and A. Capmas, "13-Calcium Aluminate Cements," *Lea's Chemistry of Cement and Concrete (Fourth Edition). Butterworth-Heinemann, Oxford,* pp. 713-782, 2003.

[12]   J. Kaufmann, F. Winnefeld, and B. Lothenbach, "Stability of ettringite in CSA cement at elevated temperatures," *Advances in Cement Research,* vol. 28, no. 4, pp. 251-261, 2016.

[13]   L. Li, R. Wang, and S. Zhang, "Effect of curing temperature and relative humidity on the hydrates and porosity of calcium sulfoaluminate cement," *Construction and Building Materials,* vol. 213, pp. 627-636, 2019.

[14]   *Standard practice for curing concrete. ACI 308-2016*, A.-A. C. Institute, 2016.

[15]   J. Balayssac, C. H. Détriché, and J. Grandet, "Effects of curing upon carbonation of concrete," *Construction and Building Materials,* vol. 9, no. 2, pp. 91-95, 1995.

[16]   L. Xu, K. Wu, C. Rößler, P. Wang, and H. Ludwig, "Influence of curing temperatures on the hydration of calcium aluminate cement/Portland cement/calcium sulfate blends," *Cement and Concrete Composites,* vol. 80, pp. 298-306, 2017.

[17]   J. H. Ideker, C. Gosselin, and R. Barborak, "An Alternative Repair Material," *Concrete International,* Article vol. 35, no. 4, pp. 33-37, 04// 2013. [Online]. Available: http://libproxy.txstate.edu/login?url=http://search.ebscohost.com/login.aspx?direct=true&db=aps&AN=86652443&login.asp&site=eds-live&scope=site.

[18]   M. Dornak, J. Zuniga, A. Garcia, T. Drimalas, and K. J. Folliard, "Development of Rapid, Cement-Based Repair Materials for Transportation Structures," 2015.

[19]   E. Moffatt, "Durability of rapid-set (ettringite-based) concrete," University of New Brunswick., 2016.

[20]   M. P. E. Moses and B. Perumal, "Latest Advances in Alternative Cementations Binders than Portland cement," *IOSR Journal of Mechanical and Civil Engineering,* vol. 13, no. 5, pp. 45-53, 2016.

[21]   Y. Tao, A. Rahul, M. K. Mohan, G. De Schutter, and K. Van Tittelboom, "Recent progress and technical challenges in using calcium sulfoaluminate (CSA) cement," *Cement and Concrete Composites,* p. 104908, 2022.

[22]   R. I. Iacobescu, Y. Pontikes, D. Koumpouri, and G. Angelopoulos, "Synthesis, characterization and properties of calcium ferroaluminate belite cements produced with electric arc furnace steel slag as raw material," *Cement and Concrete Composites,* vol. 44, pp. 1-8, 2013.

[23]   K. Tuutti, *Corrosion of steel in concrete*. Cement-och betonginst., 1982.

[24]   A. Leemann and F. Moro, "Carbonation of concrete: the role of CO_2 concentration, relative humidity and CO_2 buffer capacity," *Materials and Structures,* vol. 50, pp. 1-14, 2017.

[25]   A. Leemann, H. Pahlke, R. Loser, and F. Winnefeld, "Carbonation resistance of mortar produced with alternative cements," *Materials and Structures,* vol. 51, no. 5, p. 114, 2018.

[26]   J. Khunthongkeaw, S. Tangtermsirikul, and T. Leelawat, "A study on carbonation depth prediction for fly ash concrete," *Construction and building materials,* vol. 20, no. 9, pp. 744-753, 2006.

[27]   M. Thomas and J. Matthews, "Carbonation of fly ash concrete," *Magazine of Concrete Research,* vol. 44, no. 160, pp. 217-228, 1992.

[28]   D. Ho and R. Lewis, "Carbonation of concrete and its prediction," *Cement and Concrete Research,* vol. 17, no. 3, pp. 489-504, 1987.

[29]   E. G. Moffatt and M. D. Thomas, "Durability of Rapid-Strength Concrete Produced with Ettringite-Based Binders," *ACI Materials Journal,* vol. 115, no. 1, pp. 105-115, 2018.

[30]   N. Buenfeld and E. Okundi, "Effect of cement content on transport in concrete," *Magazine of Concrete Research,* vol. 50, no. 4, pp. 339-351, 1998.

[31]   R. Spragg, Y. Bu, K. Snyder, D. Bentz, and J. Weiss, "Electrical testing of cement-based materials: Role of testing techniques, sample conditioning, and accelerated curing," 2013.

[32]   I. Mariani. "Evaluating Concrete Quality with Electrical Resistivity." Giatec. https://www.giatecscientific.com/education/evaluating-concrete-quality-with-electrical-resistivity/ (accessed 18th March, 2022).

CHAPTER 7: ACCELORATED CARBONATION TESTING (EFFECT OF RELATIVE HUMIDITY AND CO$_2$ CONCENTRATION)

7.1 INTRODUCTION

Carbonation is one of the environmental factors that influence concrete durability. It occurs when CO$_2$ from the atmosphere reacts with hydration products such as calcium hydroxide (CH) [1]. The CH combined with other alkalies such as sodium hydroxide (NaOH) and potassium hydroxide (KOH) resulting from hydration, produces a concrete pH of 13-14 [1]. This high alkalinity plays an important role in reinforced concrete by forming a passive protective film around the steel reinforcement bars, which prevents them from being attacked by chemicals [1-3]. As CO$_2$ from the atmosphere permeates into the concrete, the CO$_2$ begins to react with the alkali hydroxides (CH, NaOH, and KOH) in concrete, which lowers the pH of the concrete. As the pH near the vicinity of the steel rebars drops below 9, the passive film protecting the steel rebars becomes unstable and breaks down hence exposing the steel to a general form of corrosion [1, 4, 5]. Due to the high CH content in ordinary Portland cement (OPC) based concrete, the carbonation process in OPC produces calcium carbonate (CaCO$_3$). The precipitation of CaCO$_3$ results in the clogging of the pore network of OPC concrete and prevents further diffusion of CO$_2$ into the concrete, thus reducing the rate of further carbonation [1, 3]. On the contrary, cement with low alkali content, such as CAC, CSA, and other ettringite-based systems, tend to carbonate faster. The carbonation reaction in these alternative cements also results in the breakdown of their main hydration product hence resulting in a significant loss of strength and an increase in porosity [3, 6].

Among other factors, relative humidity (RH) and CO$_2$ concentration play a significant role in concrete's carbonation rate. The diffusion of CO$_2$ into concrete is enabled by its dissolution in the concrete's pore solution. Therefore, at very low RH the pores could be dry, thus not providing the medium required for dissolution. While a very high RH could lead to the filling of the pores hence greatly reducing the dissolution of CO$_2$ and the carbonation process. The optimum outdoor humidity required to promote carbonation is in the range of 55-75% RH [3]. In the same vein, an increase in CO$_2$ concentration can increase the rate of carbonation in concrete [7]. This influence of RH and CO$_2$ concentration on the carbonation rate of concrete has been reported by several authors. Leeman and Moro [7] investigated the role of CO$_2$ concertation and RH in the carbonation of concrete. The results showed that the carbonation rate increased with increased CO$_2$ concentration. Also, as the RH increased from 57% to 70% and then to 80% the carbonation rate decreased due to pore saturation. Chen et al. [8] investigated the effect of

temperature, RH, and CO_2 concentration on concrete carbonation depth and compressive strength. The results showed that carbonation depth increased as RH increased from 40% to 70%, however, RH beyond 70% showed a reduction in carbonation depth. Also, the depth of carbonation increased with the increase in CO_2 concentration. Aguayo et al. [9] also investigated the effect of high-volume fly ash on the carbonation of concrete. The concrete samples produced using varying cement and fly ash contents were cured for 1 and 7 days and then subjected to accelerated carbonation conditions of 4% CO_2 concentration and 57% RH. The test results showed that increasing the addition of fly ash increases the depth of carbonation. Also, moist curing from 1 through 7 days reduced carbonation depth for both plain and blended fly ash concrete. Elsalamawy et al. [10] investigated the role of RH and cement type on the carbonation resistance of concrete. The results showed that carbonation depth increased with RH and reached a peak in the range of 60-70%RH where it began to decline. Also, the carbonation depth increased in a high slag cement type used in the study compared to OPC.

The goal of this chapter is to ascertain the effect of low and high CO_2 concentrations and RH on the accelerated carbonation of concrete produced using CSA, CAC, and the blended systems of OPC with CAC and OPC with CSA.

7.2 EXPERIMENTAL

7.2.1 Materials

This study involves testing various cement systems categorized as pure cements (i.e. cements that are not blended with any other material), proprietary blends (i.e. cements pre-blended with other materials during production), and lab blends (i.e. laboratory blended cements, 25% CAC + 75% PC and 25% CSA + 75% PC). The reason for the various categories is to depict the current practice in the use of CAC and CSA cements. Due to the high cost of pure CAC and CSA cements, (i.e. CAC and CSA cements that are not blended with any other materials), their use is currently limited to niche areas where their special qualities are required [11, 12]. However, there are also cases where CAC and CSA cements are blended with OPC to accelerate the hydration of OPC and reduce the high cost of using CAC and CSA cements only [3, 13-15]. CAC and CSA cements are also blended with supplementary cementitious materials (SCM) such as fly ash to improve their durability performance and with other chemical admixtures that are used to control their workability [11-13]. The blending of CAC and CSA cements with other materials such as OPC, SCMs, and other chemical admixtures is usually carried out during cement production or in the process of mixing concrete. Therefore, having the proprietary blended and laboratory blended cement categories in our study was reasonable. The 25%/75% proportion for the laboratory blended cements was

adopted because it was the optimum blend that satisfied both economy and mechanical performance. A description of these cements and their chemical compositions are shown in Tables 7.1 and 7.2, respectively. In Table 7.1, the controls OPC Type I/II (labeled as OPC2) and OPC Type III (labeled as OPC3) were used due to their different rates of hydration and strength development. OPC Type III has finely ground cement particles, which hydrate faster than OPC Type I/II and thereby show greater strength and microstructural development at an early age [16]. Also, in Table 7.1, the terms CSA ye'elmite cement and CSA belite cement were used to indicate the main phases in the CSA cements and to assess the impact of the hydration rate of these phases and their hydration products on the carbonation resistance of the CSA cements. The ye'elmite phase is responsible for rapid early strength gain and microstructural development in CSA cements, while the belite phase is responsible for later strength gain and microstructural development in CSA cements [17, 18]. The phase compositions for the CSA cements in Table 7.1 were calculated using modified Bogue equations adapted from Iacobescu et al. [18].

Table 7.1: Description of individual cement

Cement Category	Cement Type	Description
Pure Cements	OPC2	OPC Type I/II
	OPC3	OPC Type III
	CAC	Standard CAC cement
	CSA1	CSA Ye'elmite cement (40% Ye'elmite and 26% belite)
	CSA2	CSA belite cement (58% belite and 30% ye'elmite)
Proprietary Blended Cements	CAC-B1	CAC blend with OPC
	CAC-B2	CAC blended with set accelerating admixture
	CSA-B1	CSA belite cement (39% belite and 30% ye'elmite)
	CSA-B2	CSA belite cement (42% belite and 27% ye'elmite)
	PCSA1	CSA blend with OPC
	PCSA2	CSA blend with OPC and Fly ash
Lab Blends	CAC-OPC2	CAC blend with OPC
	CSA1-OPC2	CSA blend with OPC

Table 7.2: Chemical composition of the individual cements

Cement Type	Cement ID	SiO_2	Al_2O_3	Fe_2O_3	CaO	MgO	SO_3	Na_2O	K_2O	Na_2O_e	LOI
Pure Cements	OPC2	21.06	4.02	3.19	63.91	1.08	2.89	0.14	0.61	0.53	2.29
	OPC3	19.67	5.34	1.76	63.41	0.99	5.27	0.10	0.44	0.39	4.06
	CAC	4.34	38.65	15.09	38.37	0.39	0.16	0.05	0.14	0.14	1.55
	CSA1	9.07	21.61	2.26	45.26	0.94	20.26	0.07	0.30	0.27	1.05
	CSA2	20.56	16.14	1.35	45.31	1.23	14.73	0.77	0.72	1.24	4.74
Proprietary Blended Cements	CAC-B1	13.46	12.23	2.67	56.65	2.86	9.90	0.20	0.79	0.72	1.21
	CAC-B2	12.71	32.94	12.95	35.09	1.79	0.84	0.50	0.24	0.65	1.23
	CSA-B1	13.63	15.82	0.75	51.28	1.14	16.62	0.29	0.62	0.69	3.06
	CSA-B2	14.72	14.37	1.22	53.85	1.23	14.40	0.10	0.59	0.49	3.39
	PCSA1	17.38	11.06	2.98	55.82	1.25	10.68	0.43	0.52	0.77	2.26
	PCSA2	20.14	15.73	3.52	43.90	1.55	12.88	0.59	0.52	0.93	1.95
Lab Blends	CAC-OPC2	16.53	10.79	2.71	58.07	0.89	7.43	0.14	0.50	0.47	2.19
	CSA1-OPC2	18.06	8.42	2.96	59.25	1.04	7.23	0.12	0.53	0.47	1.98

Well-graded limestone rocks and siliceous river sand were used as coarse and fine aggregates, respectively. Other materials used in this study are a liquid polycarboxylate-ether-based superplasticizer and a set retarder, citric acid, which was used for slump control and to delay setting and allow time for mixing and casting. A total of 16 mixtures were produced for this study. Out of the 16 mixtures, 11 were produced with a total cement content of 446 kg/m^3 (752 lb/yd^3) and a W/CM ratio of 0.35. To determine the effect of increased binder content, 2 mixtures out of the previously mentioned 11 were produced with a total cement content of 502 kg/m^3 (846 lb/yd^3). The remaining 3 mixtures were produced with a total cement content of 390 kg/m^3 (658 lb/yd^3) and W/CM ratio of 0.38 based on manufacturers recommendation. The total cement content of 502 kg/m^3 (846 lb/yd^3) and 390 kg/m^3 (658 lb/yd^3) were represented in this study as 846PCY and 658PCY, respectively. The "PCY" stands for pounds per cubic yard. Table 7.3 shows the concrete mixture proportions and compressive strengths on days 1, 7, and 28.

Table 7.3: Concrete mixture proportions and compressive strengths

Cement Type	W/CM	Total Binder Kg/m^3(lb/yd^3)	Replacement Level of Cement with Second Cement Blend (% of Control Cement Type by Mass)		Strength MPa (PSI)		
			Control Binder	Type I/II	1-Day	7-Day	28-Day
OPC2	0.35	446 (752)	100%	-	41 (6005)	60 (8746)	69 (10003)
OPC3	0.35	446 (752)	100%	-	54 (7868)	67 (9785)	76 (10954)
CAC	0.35	446 (752)	100%	-	29 (4269)	41 (5982)	51 (7353)
CSA1	0.35	446 (752)	100%	-	51 (7409)	60 (8692)	65 (9454)
CSA2	0.38	390 (658)	100%	-	36 (5291)	42 (6034)	44 (6370)
CSA2	0.38	446 (752)	100%	-	41 (6011)	46 (6605)	49 (7040)

CAC-B1	0.35	446 (752)	100%	-	39 (5698)	47 (6876)	60 (8726)
CAC-B1	0.35	502 (846)	100%	-	36 (5157)	42 (6032)	58 (8374)
CAC-B2	0.30	446 (752)	100%	-	27 (3960)	38 (5539)	47 (6873)
CSA-B1	0.38	390 (658)	100%	-	56 (8082)	59 (8519)	58 (8405)
CSA-B2	0.38	390 (658)	100%	-	36 (5158)	40 (5755)	45 (6559)
PCSA1	0.35	446 (752)	100%	-	36 (5165)	50 (7322)	64 (9293)
PCSA2	0.35	446 (752)	100%	-	27 (3874)	26 (3829)	27 (3962)
CAC-OPC2	0.35	446 (752)	25%	75%	22 (3185)	50 (7265)	64 (9251)
CSA1-OPC2	0.35	446 (752)	25%	75%	11 (1549)	48 (6964)	60 (8761)
CSA1-OPC2	0.35	502 (846)	25%	75%	17 (2490)	54 (7871)	67 (9768)

7.2.2 Sample Preparation

Three concrete prisms of dimension 100 x 100 x 350 mm (4 x 4 x 14 in) and six concrete cylinders of dimension 100 x 200 mm (4 x 8 in) were produced for each of the mixtures in Table 7.3. The samples were cured with wet burlap and plastic sheet covers after casting. Out of the three prisms, one was demolded after curing for 4-6 hours, depending on the time to achieve the final set. The remaining two concrete prisms were cured for 24 hours before demolding. However, one of the 24-hour cured prisms was transferred into a curing room at 23°C (73°F) and 100% RH for an additional 6 days of curing after demolding. The concrete cylinders were also demolded and transferred into the curing room for further curing. The concrete prisms (4 hours, 24 hours, and 7 days cured prisms) were placed in a drying room at 23°C (73°F) and 50% RH after curing for 14 days before accelerated carbonation exposure. This was to reduce the level of saturation from curing that could hinder the carbonation process as well as to more easily maintain the RH within the chamber.

7.2.3 Testing

Two concrete cylinders were tested for compressive strength on days 1, 7, and 28. The results of the compressive strength test are shown in Table 7.3. The accelerated carbonation exposure was carried out in a sealed chamber fitted with equipment such as a dehumidifier for maintaining RH, a CO_2 cylinder to supply CO_2, CO_2 monitors to regulate the supply of CO_2, and an internal sensor to monitor the RH of the system. Figure 7.1 shows the accelerated carbonation chamber.

Figure 7.1: Accelerated carbonation chamber

The testing was carried out at two CO_2 concentrations of 1% and 4%. Whereas the RH was 57% and 75%. This was to enable the evaluation of the effect of low and high CO_2 concentrations as well as low and high RH. Considering the size of the mixtures and the limited space available in the accelerated carbonation chamber, this study was broken down into 4 phases encompassing the conditions of exposure as shown in Table 7.4.

Table 7.4: Accelerated carbonation test phases

Phases	Conditions
Phase 1	1% CO_2 concentration and 57% RH
Phase 2	1% CO_2 concentration and 75% RH
Phase 3	4% CO_2 concentration and 57% RH
Phase 4	4% CO_2 concentration and 75% RH

During each testing phase, carbonation depth measurements were carried out before exposure and then on days 28, 56, 63, 70, and 105. To measure carbonation depth, a 50 mm (2-inch) thick sample was cut out

of the concrete prism and then sprayed with phenolphthalein to reveal carbonated (colorless) and uncarbonated (purple color) regions. The exposed surface of the cut concrete prism was coated with carbonation-resistant paint and returned to the accelerated carbonation chamber to prevent carbonation from the cut surface. Measurements were taken with the aid of a steel scale (0.5 mm accuracy) by measuring the distance from the edge of the sample to the point where the uncarbonated (purple color) region begins on the sample. This was done on five different points on each of the four edges of the sample. However, there was a 25 mm (1 inch) offset from the corners to avoid any "corner effects" of CO_2 ingression during measurements. The final carbonation depth was the average depth measured from all four edges. Figure 7.2 illustrates the carbonation depth measurement procedure.

(a)   (b)   (c)   (d)
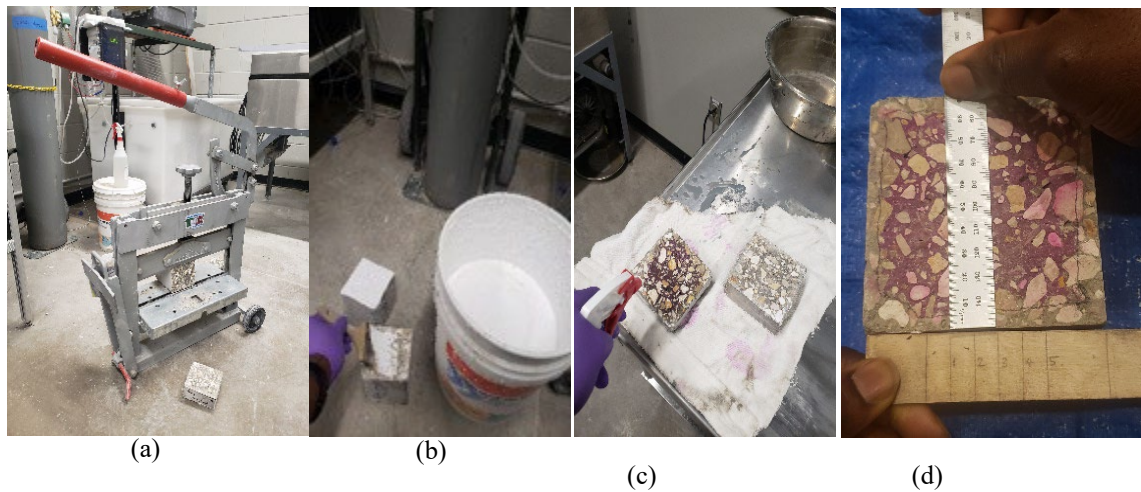
Figure 7.2: Carbonation depth measurement procedure. (a) cutting out the 50 mm thick sample, (b) coating the exposed surface of the concrete prism with carbonation-resistant paint, (c) spraying the 50 mm cut sample with phenolphthalein, (d) measurement with steel scale

7.3 RESULTS AND DISCUSSION

7.3.1 Carbonation depth at 57% RH and 75% RH with a low CO_2 concentration (1%)

Figure 7.3 shows the accelerated carbonation depths of all mixtures (4-hour, 24-hour, and 7-day cured samples) after 105 days of exposure at 1% CO_2 concentration and 57% and 75% RH. The dashed line in Figure 7.3 represents a line of equality which signifies the point where the depth of carbonation at 57% RH equals that at 75% RH. The regions above the line indicate areas of higher carbonation depth influenced by a high RH (75% RH). Whereas the region below the line indicates areas of higher carbonation depth influenced by a low RH (57% RH). Figure 7.3 shows that nearly all the data points lie below the dashed line indicating higher carbonation depths influenced by the low RH (57% RH). This

high carbonation depth exhibited by most of the mixtures can be attributed to the partial filling of pores at such low RH (57% RH), which in turn enables the dissolution of CO_2 and the consequent increase in the rate of carbonation. However, at high RH (75% RH), the pores are mostly filled, reducing the dissolution of CO_2 and the rate of carbonation [3, 7]. Figure 7.3 also shows that aside from the RH, the curing duration also influences the depth of carbonation. This is evident in the distribution of the data points with the 7-days cured samples near the bottom of the equality line, followed by the 24-hour cured samples at the middle and the 4-hour cured samples at the top.
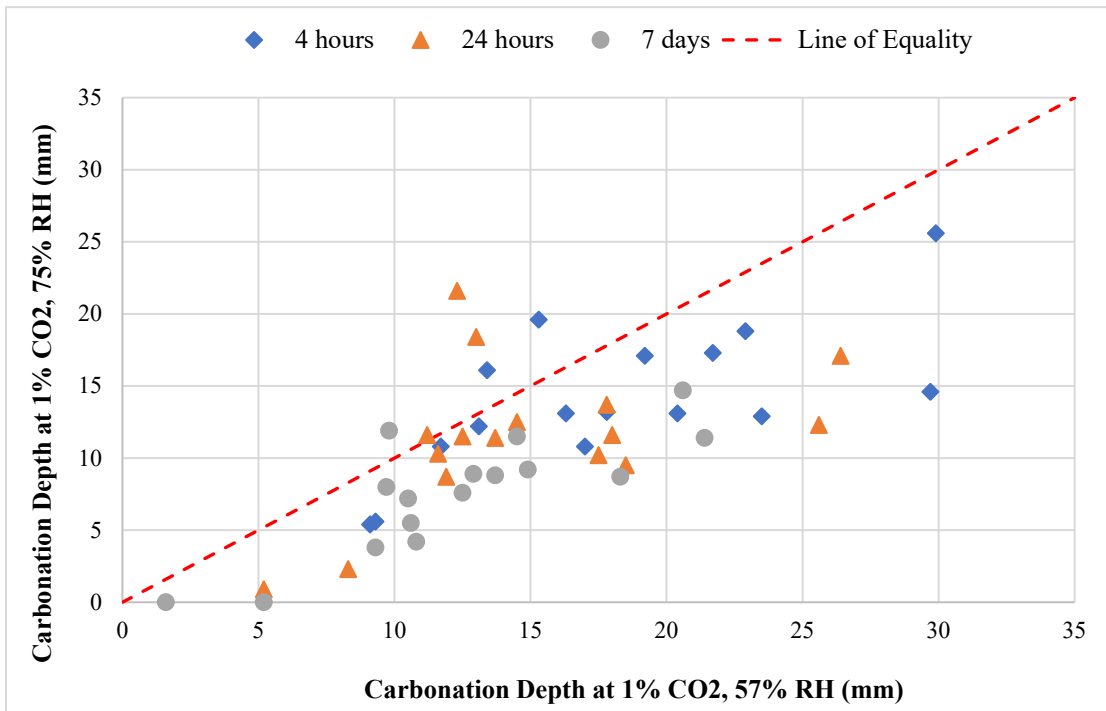
Figure 7.3: Carbonation depths at 1% CO2, 57% RH and 1% CO2, 75% RH

Figure 7.4 shows the carbonation resistance of the mixtures at high and low RH while maintaining a low CO_2 concentration. As the study focuses on evaluating RH and CO_2 concentration rather than curing duration, Figure 7.4 shows only the 7-day cured samples for all mixtures.
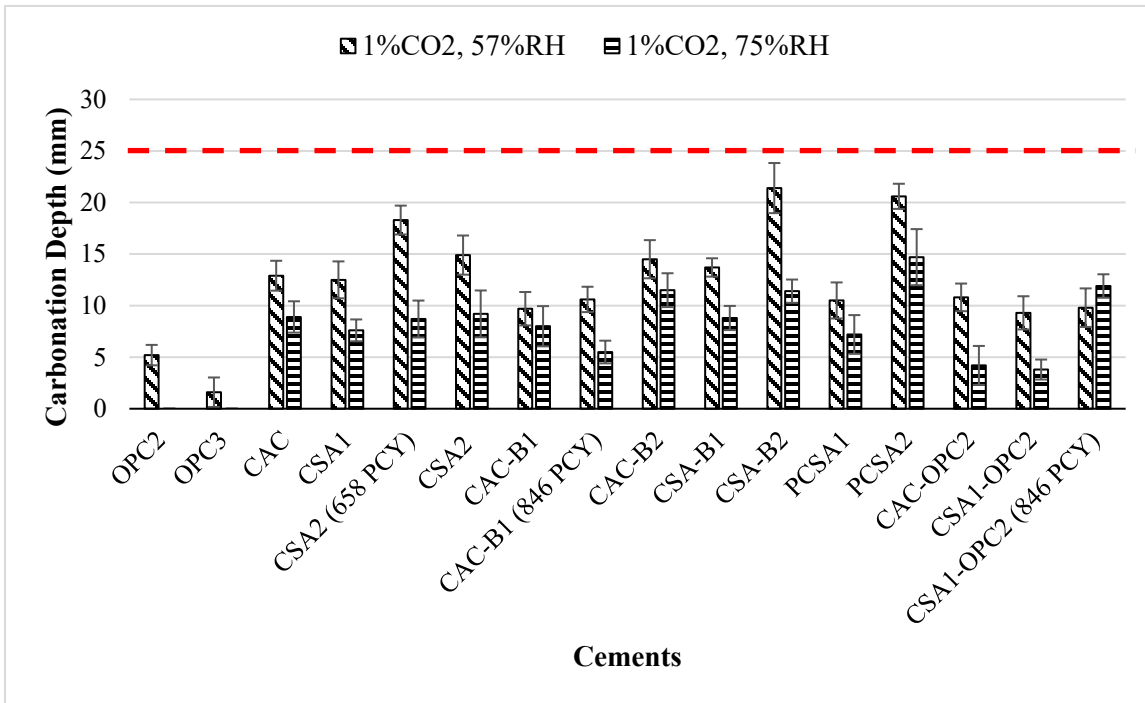
Figure 7.4: Carbonation depth of the 7-days cured samples at 1% CO2, 57% RH and 1% CO2,75% RH

The dashed line in Figure 7.4 was included to assess the potential of corrosion due to carbonation by assuming a 25 mm (1 inch) cover thickness to steel reinforcement. Figure 7.4 shows that all the mixtures except for CSA1-OPC2 (846PCY) exhibited a higher carbonation depth at low RH (57% RH) compared to a high RH (75% RH). However, high carbonation depths closer to the assumed 25 mm (1 inch) thickness line was exhibited by the pure cement CSA2 (658 PCY) and the proprietary blended cements PCSA2 and CSA-B2 at 57% RH. Again, the high carbonation depth exhibited by the mixtures at low RH (57% RH) can be attributed to the partial filling of pores at low RH, which promotes the dissolution of CO_2 and increases the carbonation rate in concrete [3, 7]. The controls OPC2 and OPC3 showed the highest resistance to carbonation compared to all other cements, especially at 75% RH, where they had no carbonation. This could be due to a combined effect of the high CO_2 buffer capacity peculiar to OPC [7, 19] and the filling of concrete pores at high RH (75% RH) [3, 7]. Furthermore, carbonation in CSA and CAC concrete could lead to the decomposition of their main hydrates, resulting in increased porosity and increased rate of carbonation [1, 3, 6].

Considering the pure cement CAC and the proprietary blended cements CAC-B1, CAC-B1(846PCY), and CAC-B2, the proprietary blended cements CAC-B1 and CAC-B1(846PCY) exhibited lower carbonation depth at 57% and 75%RH compared to the pure cement CAC and proprietary blended cement CAC-B2. A good explanation for the higher carbonation resistance exhibited by CAC-B1 and CAC-

B1(846PCY) at 57% and 75%RH would be the presence of CH as a result of the addition of OPC during production (see Table 7.1). The presence of CH helps to produce $CaCO_3$ during the carbonation reaction. This helps to clog the pore network and provides a buffer for the ingress of CO_2 into the concrete, thus reducing the rate of further carbonation [2, 3]. Comparing CAC-B1(846PCY) and CAC-B1, CAC-B1(846PCY) exhibited a slightly higher carbonation depth than CAC-B1 at 57% RH, but CAC-B1 exhibited a significantly higher carbonation depth than CAC-B1(846PCY) at 75% RH. This high resistance to carbonation exhibited by CAC-B1(846PCY) could be due to a combined effect of filled pores at high RH [7] and a more developed microstructure due to the increased cement content [20].

Comparing the lab blended cement, CAC-OPC2, CSA1-OPC2, and CSA1-OPC2 (846PCY) with the pure cements (CSA1 and CAC), the lab blended cements showed an improvement in carbonation resistance at 57%RH and 75%RH. The only exception, in this case, is the lab-blended cement CSA1-OPC2 (846PCY) exposed at 75%RH. This improvement in carbonation resistance exhibited by the lab-blended cements is also a result of the addition of OPC2. The addition of OPC helps to increase the buffer capacity of the lab blended cements, thus improving their resistance to carbonation [2, 3]. The higher carbonation depth exhibited by CSA1-OPC2 (846PCY) compared to CSA1-OPC2 at 57%RH and 75%RH is unusual and unexpected. The increase in cement content was expected to provide a more dense microstructure leading to an improved carbonation resistance [20]. However, there is a need to conduct more investigations to ascertain the reason for the aberrant performance.

The proprietary blended cement PCSA1, a blend of CSA and OPC, showed higher resistance to carbonation at low and high RH (57% and 75% RH) compared to the CSA cements without OPC due to an increased CO_2 buffer capacity. The higher carbonation depth exhibited by PCSA2, a blend of CSA, OPC, and fly ash, at 57%RH could be attributed to the combined effect of low RH (57%RH), cement replacement with fly ash, and the consumption of CH due to the pozzolanic activity of fly ash leading to reduced CO_2 buffer capacity [21-23].

The high ye'elmite CSA, CSA1, showed a higher carbonation resistance than the CSA belite cements CSA2, CSA2 (658PCY), CSA-B1, and CSA-B2 at 57% and 75% RH. This performance of CSA1 can be attributed to the ye'elmite phase, which is responsible for the rapid early strength gain and microstructural development of CSA cement [17, 24]. The belite phase, on the other hand, is responsible for later strength gain and microstructural development in CSA cement [17, 24]. Among the CSA belite cements, CSA-B1 showed the highest resistance to carbonation at 57% and 75% RH due to its higher proportion of ye'elmite to belite phase compared to the other belite cements.

7.3.2 Carbonation depth at 57% RH and 75% RH with a high CO_2 concentration (4%)

Figure 7.5 shows that the majority of the mixtures exhibited higher carbonation depths after 105 days of exposure at 57%RH compared to their exposure at 75%RH. However, due to the high CO_2 concentration (4%), the data points appear to be closer to the line of equality compared to their position at 1% CO_2 concentration as shown in Figure 7.3. This implies that the increase in CO_2 concentration must have resulted in an increase in carbonation at both RH (57% and 75%RH) [7].
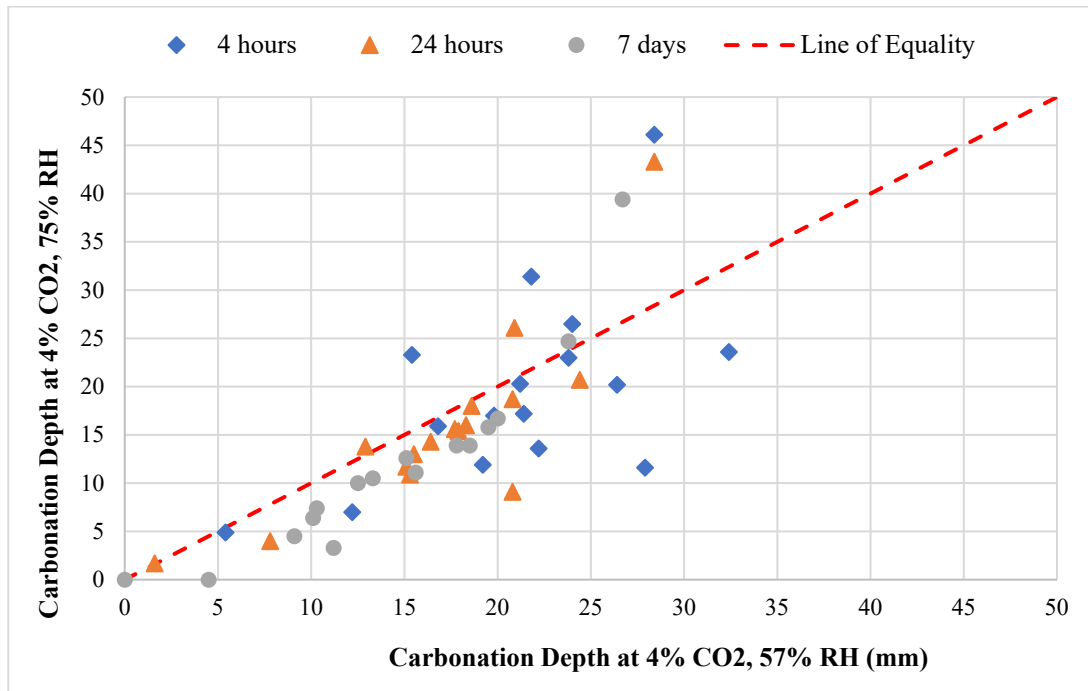
Figure 7.5: Carbonation depth at 4% CO2, 75% RH and 4% CO2, 57% RH
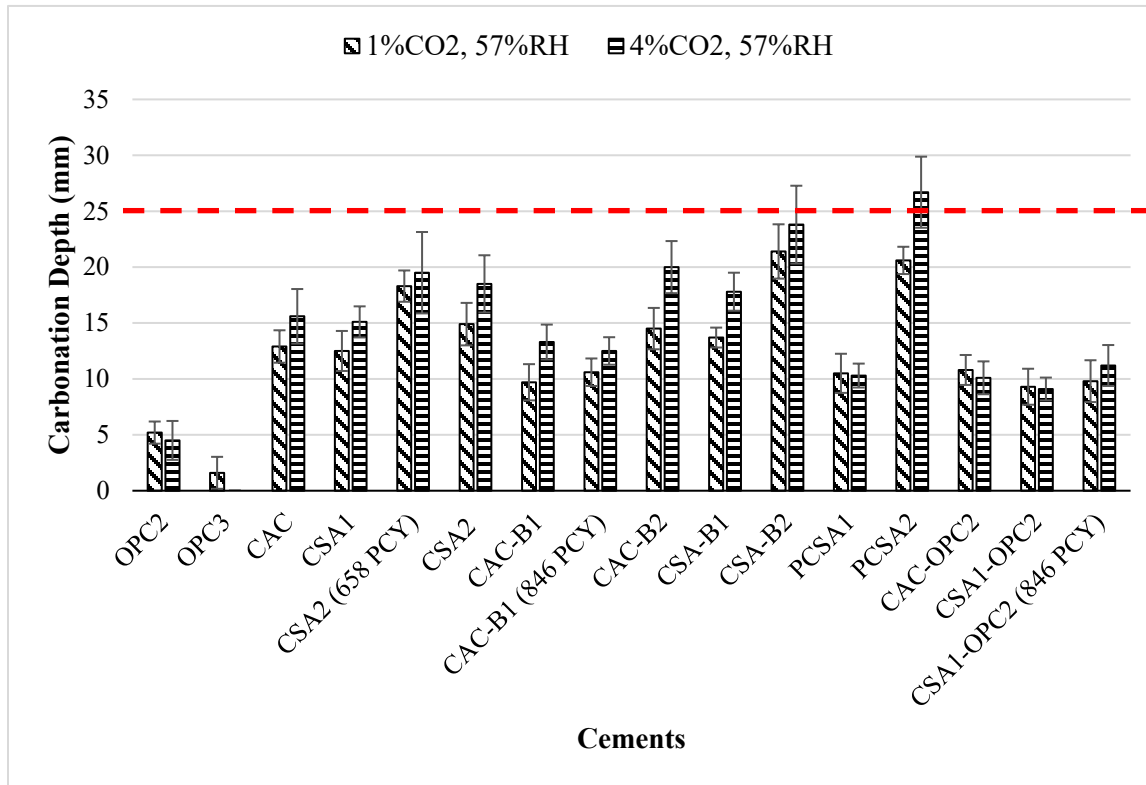
Figure 7.6: Carbonation depth of the 7-days cured samples at 1% CO2, 57% RH and 4% CO2, 57% RH

Figure 7.6 shows that the CAC and CSA cements categories (pure, proprietary, and lab-blended cements) exhibited moderate to high carbonation depths, which are either close to or beyond the assumed 25 mm (1 inch) cover thickness due to the influence of increased CO_2 concentration (4% CO_2) and low RH (57%RH). This observed effect of increased CO_2 concentration and low RH on the carbonation rate of concrete is consistent with the results published by Leeman and Moro [7].

Considering the effect of increasing the CO_2 concentration from 1% to 4% at low RH (57%RH) by the categories of cement considered (pure, proprietary, and lab-blended cements), Figure 7.6 shows that among the pure cements, the carbonation depth of the controls OPC2 and OPC3 reduced as the CO_2 concentration increased. Whereas other cements under the pure cements category (CAC, CSA1, CA2(658PCY), and CSA2) showed an increase in carbonation depth as the CO_2 concentration increased. This reduction in carbonation depth exhibited by the controls (OPC2 and OPC3) despite the increase in CO_2 concentration can be attributed to an increased buffer caused by the production of more $CaCO_3$ from the carbonation reaction [7]. However, the increased carbonation depth exhibited by the pure CAC and CSA cements could have been a result of the combined effect of low buffer capacity, increased CO_2 concentration, and the decomposition of main hydrates during carbonation [1, 3, 6]. The pure cements CAC and CSA1 seem to have similar carbonation resistance that is higher than that of CSA2 and CSA2

(658PCY). This can be attributed to the rapid early development of strength and microstructure peculiar to pure CAC and high ye'elmite CSA [24]. This early improvement of microstructure improves the carbonation resistance of these cements. However, the other pure cements CSA2 and CSA2 (658PCY), exhibited the highest carbonation depth within the pure cement category. This could be attributed to the high belite content of CSA2 and CSA2 (658PCY) and the lower hydration rate of the belite phase [17]. The belite phase in CSA2 and CSA2 (658PCY) is responsible for later strength and microstructural development and hence can contribute to increased carbonation resistance with time [25]. Furthermore, CSA2 seems to have a higher carbonation resistance than CSA2 (658PCY), probably due to a more dense microstructure provided by the higher cement content in CSA2 [20].

The lab-blended cements (CAC-OPC2, CSA1-OPC2, CSA1-OPC2(846PCY)) exhibited a moderate carbonation depth despite the increase in CO_2 concentration at low RH compared to the pure cements CAC and CSA1. This improvement in carbonation resistance exhibited by lab-blended cements can be attributed to the addition of OPC2. The OPC constituent must have helped to provide an increased buffer to CO_2 for the lab blended cements as the CO_2 concentration increased [7]. However, unlike the other lab-blended cements, CSA-OPC2 (846PCY) showed a slight increase in carbonation depth as the CO_2 concentration increased. Increasing cement content is supposed to help provide a dense microstructure, thus decreasing penetrability. Despite the higher cement content of CSA1-OPC2 (846PCY) compared to CSA1-OPC2, the carbonation depth of CSA1-OPC2 (846PCY) was observed to be slightly higher than CSA1-OPC. Again, this performance of CSA1-OPC2 (846PCY) compared to CSA1-OPC2 in resisting carbonation is unusual and unexpected. Hence, there is a need for further investigation to ascertain the reasons for the discrepancy.

As shown in Figure 7.6, the proprietary blended cement PCSA1 exhibited a moderate carbonation depth similar to the lab-blended cements despite the increase in CO_2 concentration to 4% at low RH (57%RH). This performance of PCSA1 results from blending CSA and OPC during production, thus increasing the CH content and CO_2 buffer capacity of PCSA1 [19]. In contrast, the proprietary blended cement PCSA2 exhibited the highest carbonation depth of all the cement mixtures shown in Figure 7.6. This high carbonation exhibited by PCSA2 compared to PCSA1 must have been due to the combined effect of increased CO_2 concentration and the presence of fly ash which consumes CH emanating from the hydration of OPC during its pozzolanic reaction, hence reducing the alkalinity and buffer capacity of PCSA2 [7].

The belite cements, CSA-B1 and CSA-B2, showed an increase in carbonation depth as the CO_2 concentration increased from 1% to 4%. However, the CSA belite cement CSA-B1 still showed higher

resistance to carbonation than CSA-B2 and the other belite cements (CSA2 and CSA2 (658PCY)) due to its high proportion of ye'elmite to the belite phase.

Comparing the pure cement CAC with the proprietary blended cements CAC-B1, CAC-B1 (846PCY), and CAC-B2, it can be observed that all 4 cements showed an increase in carbonation depth due to the increase in CO_2 concentration. However, the proprietary blended cements CAC-B1 and CAC-B1 (846PCY) seemed to have exhibited a higher carbonation resistance than CAC and CAC-B2. This could be a result of the increased buffer capacity due to more CO_2 being available to react with the CH emanating from the OPC constituent in CAC-B1 and CAC-B1 (846PCY) [7, 19].

Figure 7.7 shows a moderate to low carbonation depth for nearly all mixtures as the CO_2 concentration increases to 4% at high RH (75%RH). The only exceptions are the proprietary cements PCSA2 and CSA-B2 with carbonation depths that are within or beyond the assumed 25 mm (1 inch) cover thickness.
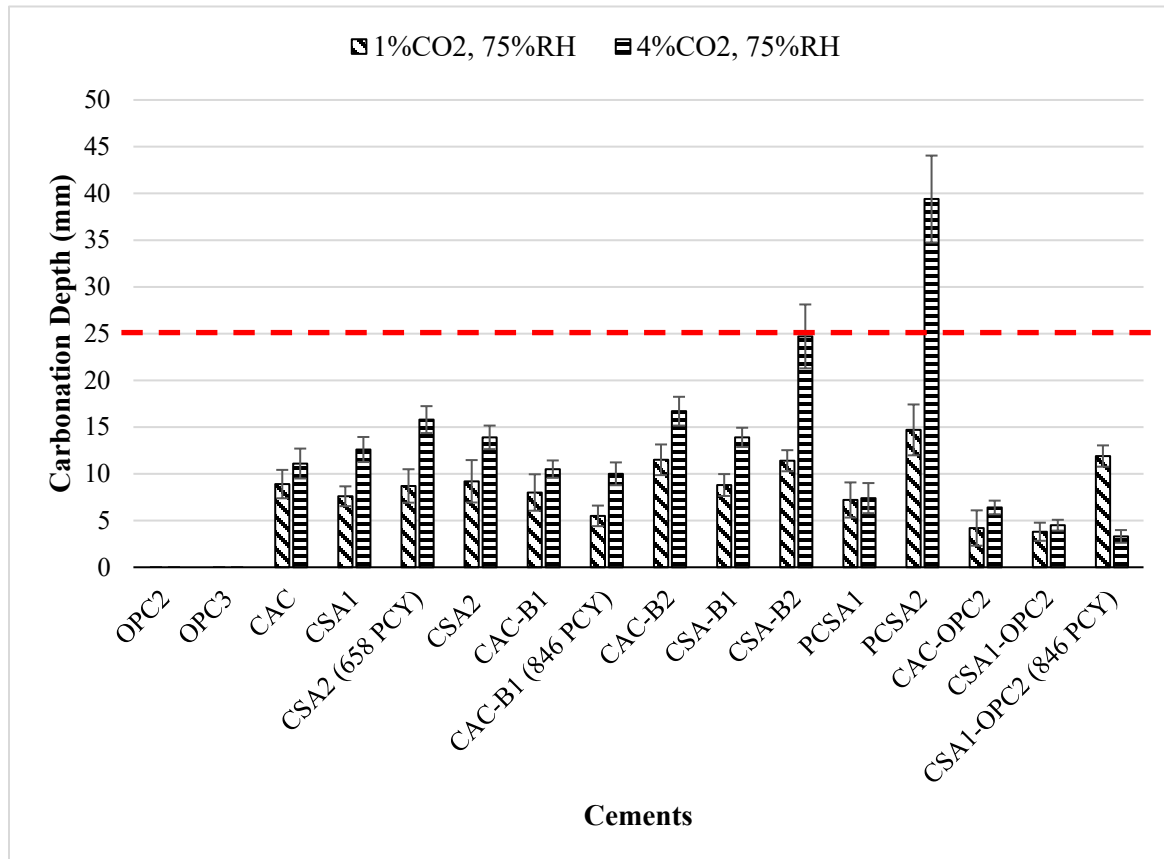
Figure 7.7: Carbonation depth of the 7-days cured samples at 1% CO_2, 75% RH and 4% CO_2, 75% RH

Despite the increase in CO_2 concentration, as shown in Figure 7.7, the control samples showed the highest resistance to carbonation with no carbonation at high RH (75%RH). In the same manner, the lab-blended

cement (CAC-OPC2, CSA1-OPC2, CSA1-OPC2(846PCY)) showed low carbonation depths despite the increased CO_2 concentration compared to the CAC and CSA cements in the other categories (pure and proprietary blended cements). The only exception among the lab blended cements is CSA1-OPC2(846PCY), with a higher carbonation depth at 1% CO_2 concentration compared to 4%.

The improved performance in carbonation resistance exhibited by most of the cement, in this case, is a result of the high RH (75%), which impedes the dissolution of CO_2 despite the increase in CO_2 concentration. However, the control mixtures (OPC2 and OPC3), the lab-blended cements, and the proprietary blended cement containing OPC showed more resistance to carbonation due to the combined effect of high RH (75%RH) and increased production of $CaCO_3$ resulting from the elevated CO_2 concentration (4% CO_2) [7, 19].

7.3.3 Relationship Between The Carbonation Coefficient and Compressive Strength

The carbonation coefficient for the 7 days cured samples at the different accelerated exposure conditions considered in this study was determined using the square root of time model [26], as shown in Equation 7.1.

$$X_f - X_i = K_c \times t^{1/2} \qquad \text{Eq. 7.1}$$

X_f is the final carbonation depth, X_i is the initial carbonation depth, t is the exposure time, and K_c is the carbonation coefficient or carbonation rate. Figures 7.8, 7.9, and 7.10 show the carbonation coefficients at the different accelerated carbonation test conditions (1% CO_2/57% RH, 4% CO_2/57% RH, 1% CO_2/75% RH, and 4% CO_2/75% RH) plotted against the compressive strengths at days 1, 7, and 28, respectively. Table 7.3 shows the compressive strength.
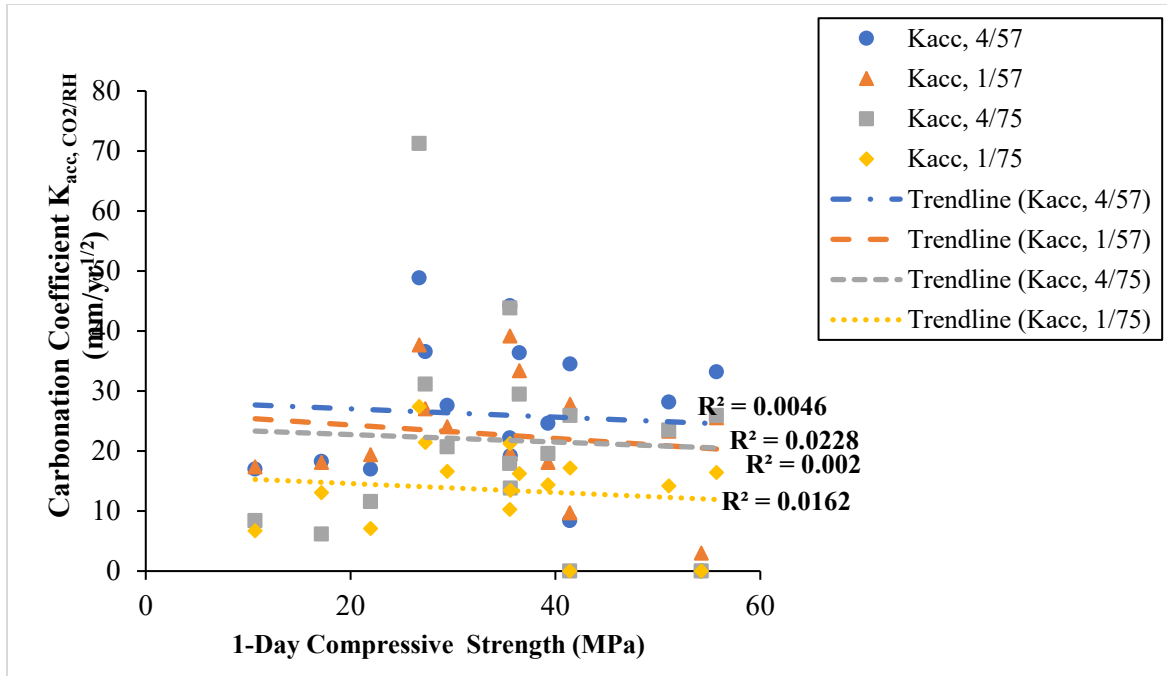
Figure 7.8: Relationship between the carbonation coefficients after 105 days of accelerated exposure and the 1-day compressive strengths
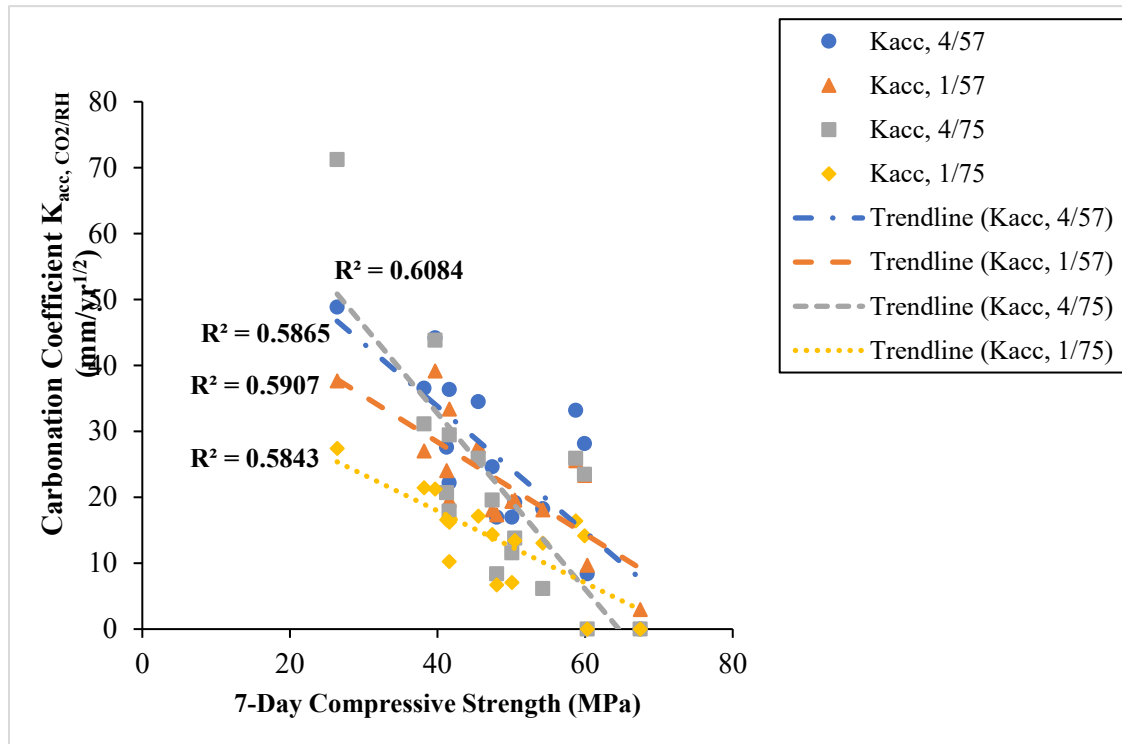
Figure 7.9: Relationship between the carbonation coefficients after 105 days of accelerated exposure and the 7-day compressive strengths

171
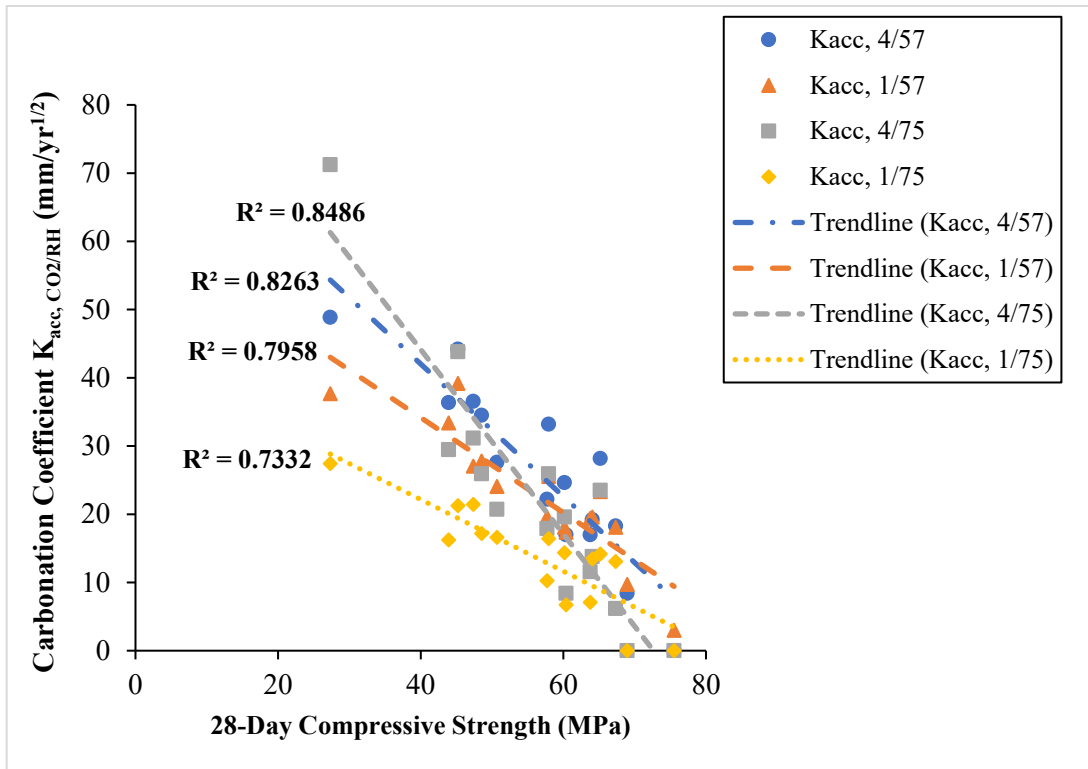
Figure 7.10: Relationship between the carbonation coefficients after 105 days of accelerated exposure and the 28-day compressive strengths

Figure 7.8 shows a very weak correlation (R^2 values) between the carbonation coefficients and the 1-day compressive strength. However, Figures 7.9 and 7.10 show a moderate and strong correlation (R^2 values) between the carbonation coefficients and the 7-day and 28-day compressive strengths, respectively. This increase in correlation (R^2 values) between the carbonation coefficients and the compressive strength, as the compressive strengths increase from day 1 to day 7 and then to day 28, can be attributed to the improved microstructure due to curing. Curing provides the moisture necessary to sustain hydration in the concrete leading to improved strength and microstructural development [16]. This improvement of microstructure due to curing influences both carbonation resistance and compressive strength [16, 27]. This emphasizes the need for adequate curing to improve the carbonation resistance of concrete, notwithstanding the carbonation exposure conditions.

7.4 CONCLUSIONS

1. Practically all the cement systems investigated, except for CSA1-OPC2 (846PCY) exhibited a higher carbonation depth at 1% CO_2 concentration and 57% RH compared to that at 1% CO_2 concentration and 75%RH. This was attributed to the partial filling of pores at such low RH (57%

172

RH), which in turn enables the dissolution of CO_2 and the consequent increase in the rate of carbonation. Whereas, at high RH (75% RH) the pores are mostly filled hence reducing the dissolution of CO_2 and the rate of carbonation.

2. Aside from the controls, PCSA1, CAC-OPC2, and CSA1-OPC2 cements, all other cement systems showed a higher carbonation depth as the CO_2 concentration increased to 4% at 57% RH. This was attributed to the combined effect of increased carbonation due to the increased CO_2 concentration and the partial filling of pores at low RH (57% RH). However, due to the filing of pores at high RH (75% RH), the carbonation depths at 4% CO_2 and 75% RH were lesser than 4% CO_2 and 57% RH.

3. The control mixtures (OPC2 and OPC3), lab blended cements (CAC-OPC2, CSA1-OPC2 (846PCY), and CSA1-OPC2) and the proprietary blended cements containing OPC showed higher resistance to carbonation resistance compared to other mixtures at the different conditions considered. This was attributed to the high CO_2 buffer capacity provided by OPC.

4. The high ye'elmite CSA cements, CSA1, showed more carbonation resistance than the CSA belite cements (CSA2, CSA2(658PCY), CSA-B1, and CSA-B2) at all the exposure conditions considered due to the rapid early strength gain and microstructural development provided by the ye'elmite phase. However, the belite cement, CSA-B1, showed more resistance to carbonation than the other belite cements due to its high proportion of ye'elmite to the belite phase.

5. The carbonation coefficients obtained for the different exposure conditions show an increasing correlation (R^2 values) to the compressive strengths from days 1 to 7 and 28. This was attributed to the improvement of microstructure due to curing, which influences both carbonation resistance and compressive strength.

7.5 REFERENCES

[1]   M. Yu, J. Lee, and C. Chung, "The Application of Various Indicators for the Estimation of Carbonation and pH of Cement Based Materials," *Journal of Testing and Evaluation,* vol. 38, pp. 534-540, 2010. [Online]. Available: www.astm.org.

[2]   V. Shah and S. Bishnoi, "Understanding the Process of Carbonation in Concrete using Numerical Modeling," *Journal of Advanced Concrete Technology,* vol. 19, no. 11, pp. 1148-1161, 2021.

[3]   S. Lamberet, "Durability of ternary binders based on Portland cement, calcium aluminate cement and calcium sulfate," EPFL, 2004.

[4]   A. Fahim, "Corrosion of reinforcing steel in concrete: monitoring techniques and mitigation strategies," University of New Brunswick., 2018.

[5]   D. Zhang, D. Xu, X. Cheng, and W. Chen, "Carbonation resistance of sulphoaluminate cement-based high performance concrete," *Journal of Wuhan University of Technology-Mater. Sci. Ed.,* vol. 24, no. 4, pp. 663-666, 2009.

[6]   E. T. G. Moffatt and M. D. Thomas, "Effect of Carbonation on the Durability and Mechanical Performance of Ettringite-Based Binders," *ACI Materials Journal,* vol. 116, no. 1, 2019.

[7]   A. Leemann and F. Moro, "Carbonation of concrete: the role of CO 2 concentration, relative humidity and CO 2 buffer capacity," *Materials and Structures,* vol. 50, pp. 1-14, 2017.

[8]   Y. Chen, P. Liu, and Z. Yu, "Effects of environmental factors on concrete carbonation depth and compressive strength," *Materials,* vol. 11, no. 11, p. 2167, 2018.

[9]   F. Aguayo, A. Torres, Y.-J. Kim, and O. Thombare, "Accelerated carbonation assessment of high-volume fly ash concrete," *Journal of Materials Science and Chemical Engineering,* vol. 8, no. 3, pp. 23-38, 2020.

[10]   M. Elsalamawy, A. R. Mohamed, and E. M. Kamal, "The role of relative humidity and cement type on carbonation resistance of concrete," *Alexandria Engineering Journal,* vol. 58, no. 4, pp. 1257-1264, 2019.

[11]   J. H. Ideker, C. Gosselin, and R. Barborak, "An Alternative Repair Material," *Concrete International,* Article vol. 35, no. 4, pp. 33-37, 04// 2013. [Online]. Available: http://libproxy.txstate.edu/login?url=http://search.ebscohost.com/login.aspx?direct=true&db=aps&AN=86652443&login.asp&site=eds-live&scope=site.

[12]   M. Dornak, J. Zuniga, A. Garcia, T. Drimalas, and K. J. Folliard, "Development of Rapid, Cement-Based Repair Materials for Transportation Structures," 2015.

[13]   E. Moffatt, "Durability of rapid-set (ettringite-based) concrete," University of New Brunswick., 2016.

[14]   K. L. Scrivener and A. Capmas, "13-Calcium Aluminate Cements," *Lea's Chemistry of Cement and Concrete (Fourth Edition). Butterworth-Heinemann, Oxford,* pp. 713-782, 2003.

[15]   M. P. E. Moses and B. Perumal, "Latest Advances in Alternative Cementations Binders than Portland cement," *IOSR Journal of Mechanical and Civil Engineering,* vol. 13, no. 5, pp. 45-53, 2016.

[16]   S. Mindess, F. J. Young, and D. Darwin, *Concrete*. New Jersey: Prentice Hall, 2003.

[17]   Y. Tao, A. Rahul, M. K. Mohan, G. De Schutter, and K. Van Tittelboom, "Recent progress and technical challenges in using calcium sulfoaluminate (CSA) cement," *Cement and Concrete Composites,* p. 104908, 2022.

[18]   R. I. Iacobescu, Y. Pontikes, D. Koumpouri, and G. Angelopoulos, "Synthesis, characterization and properties of calcium ferroaluminate belite cements produced with electric arc furnace steel slag as raw material," *Cement and Concrete Composites,* vol. 44, pp. 1-8, 2013.

[19]   A. Leemann, H. Pahlke, R. Loser, and F. Winnefeld, "Carbonation resistance of mortar produced with alternative cements," *Materials and Structures,* vol. 51, no. 5, p. 114, 2018.

[20]   N. Buenfeld and E. Okundi, "Effect of cement content on transport in concrete," *Magazine of Concrete Research,* vol. 50, no. 4, pp. 339-351, 1998.

[21]   J. Khunthongkeaw, S. Tangtermsirikul, and T. Leelawat, "A study on carbonation depth prediction for fly ash concrete," *Construction and building materials,* vol. 20, no. 9, pp. 744-753, 2006.

[22]   M. Thomas and J. Matthews, "Carbonation of fly ash concrete," *Magazine of Concrete Research,* vol. 44, no. 160, pp. 217-228, 1992.

[23]   D. Ho and R. Lewis, "Carbonation of concrete and its prediction," *Cement and Concrete Research,* vol. 17, no. 3, pp. 489-504, 1987.

[24]   E. G. Moffatt and M. D. Thomas, "Durability of Rapid-Strength Concrete Produced with Ettringite-Based Binders," *ACI Materials Journal,* vol. 115, no. 1, pp. 105-115, 2018.

[25]   K. Quillin, "Performance of belite–sulfoaluminate cements," *Cement and concrete research,* vol. 31, no. 9, pp. 1341-1349, 2001.

[26]   K. Tuutti, *Corrosion of steel in concrete*. Cement-och betonginst., 1982.

[27]   S. H. Kosmatka, W. C. Panarese, and B. Kerkhoff, *Design and control of concrete mixtures*. Portland Cement Association Skokie, IL, 2002.

CHAPTER 8: EFFECT OF NATURAL CARBONATION OF RAPID SETTING HYDRAULIC CEMENT CONCRETE SYSTEMS

8.1 INTRODUCTION

Concrete carbonation is a natural phenomenon that involves the reaction between atmospheric carbon dioxide (CO_2) and cement hydration products such as calcium hydroxide (CH) [1]. When extreme levels of carbonation are present in reinforced concrete, the passive film protection on steel reinforcement may be depleted, exposing the steel to corrosion [2]. Several atmospheric factors are believed to influence the natural carbonation of concrete. For instance, at high temperatures, the diffusion of CO_2 and the carbonation chemical reactions are accelerated. However, the solubility of CO_2 is reduced, and the stability of the products of carbonation, such as $CaCO_3$, is affected at high temperatures [3]. The concentration of CO_2 in the atmosphere also influences the rate of natural carbonation. Cities with high CO_2 emissions could experience a higher depth of carbonation that could reduce the life span of reinforced concrete structures in such cities [4, 5]. Another important factor that influences the natural carbonation of concrete is precipitation. When structural elements are exposed to precipitation, their pores can get fully saturated, preventing the dissolution of atmospheric CO_2 required for natural carbonation.

To ascertain the level of influence these factors have on the natural carbonation of concrete, concrete samples are usually exposed to natural conditions and are assessed at intervals to ascertain the depth of natural carbonation. The samples are sometimes either sheltered from precipitation or left unsheltered. The idea behind this act is to depict the effect of natural carbonation on unsheltered structural elements, such as retaining walls and the external wall of buildings with intermittent pore saturation periods due to rain or wet conditions and sheltered structural elements that are constantly partially saturated [6]. Aguayo et al. [7] investigated the carbonation resistance of various concrete mixtures containing supplementary cementitious materials (SCMs) exposed to sheltered and unsheltered natural carbonation conditions in Austin, Texas, USA. The test results showed that the carbonation depths measured after 730 days increased as the SCMs replacement level increased. Also, the sheltered samples showed a higher depth of carbonation than the unsheltered samples. Vu et al. [5] investigated the resistance to carbonation of concrete exposed to sheltered and unsheltered natural carbonation in four different climates (Lyon (France), Chennai (India), Austin (USA), and Changsha (China)). The samples were prepared with different SCMs and exposed for 5 years. The results showed that the extent of natural carbonation in sheltered conditions was similar in the different climates considered. However, the impact of precipitation

on the natural carbonation of unsheltered samples was significant, and the degree of impact depended on the climatic condition as well as the number of rainy days per year. Rathnarajan et al. [8] evaluated the carbonation resistance of concrete samples produced with mineral admixtures and exposed to sheltered and unsheltered natural carbonation for 5 years. The results showed that the carbonation resistance of samples exposed to sheltered natural conditions was 10-20% less than those exposed to unsheltered natural conditions.

The natural carbonation of concrete is a slow process and takes a long time to show a significant effect. As a result, accelerated carbonation studies are commonly used in laboratories to assess concrete quickly under controlled conditions [9]. Also, several models have been developed to predict the carbonation depth in concrete [10-12]. One of those models is that proposed by Tuutti, which asserts that the depth of carbonation over time is proportional to the square root of time [10]. This is illustrated as shown in Equation 8.1:

$$X_c = K_c \times t^{1/2}$$ Eq. 8.1

Where X_c is the carbonation depth, t is the exposure time, and K_c is the carbonation coefficient. The transferability of accelerated carbonation results to natural conditions can be achieved by comparing the carbonation coefficients of both to see if there is a correlation between the results [13, 14].

This study focuses on investigating the effect of natural carbonation in concrete produced using CSA, CAC, and blended systems of OPC with CSA and OPC with CAC and placed in sheltered and unsheltered conditions. Also presented in this study is the comparison of the carbonation coefficients of the sheltered and unsheltered natural concrete samples produced with the cement systems investigated in this study with that of accelerated carbonation from a different study on the same cement systems to see if any correlation exists.

8.2 EXPERIMENTAL

8.2.1 Materials

This study involved 16 cement systems categorized as pure cements (i.e. binders that are not blended with any other material), proprietary blends (i.e. cements pre-blended with other materials during production), and lab blends (i.e. laboratory blended binders, 25% CAC + 75% PC and 25% CSA + 75% PC). The reason for the various categories is to depict the current practice in the use of CAC and CSA cements. Due to the high cost of pure CAC and CSA cements, (i.e. CAC and CSA cements that are not blended

176

with any other materials), their use is currently limited to niche areas where their special qualities are required [15, 16]. However, there are also cases where CAC and CSA cements are blended with OPC to accelerate the hydration of OPC and reduce the high cost of using CAC and CSA cements only [17-20]. CAC and CSA cements are also blended with supplementary cementitious materials (SCM) such as fly ash to improve their durability performance and with other chemical admixtures that are used to control their workability [15, 16, 18]. The blending of CAC and CSA cements with other materials such as OPC, SCMs, and other chemical admixtures is usually carried out during cement production or in the process of mixing concrete. Therefore, having the proprietary blended and laboratory blended cement categories in this study was reasonable. The 25%/75% proportion for the laboratory blended cements was adopted because it was the optimum blend that satisfied both economy and mechanical performance. A description of these cements and their chemical compositions are shown in Tables 8.1 and 8.2, respectively. In Table 8.1, the controls OPC Type I/II (labeled as OPC2) and OPC Type III (labeled as OPC3) were used due to their different rates of hydration and strength development. OPC Type III has finely ground cement particles, which hydrate faster than OPC Type I/II and thereby show greater strength and microstructural development at an early age [21]. Also, in Table 8.1, the terms CSA ye'elmite cement and CSA belite cement were used to indicate the main phases in the CSA cements and to assess the impact of the hydration rate of these phases and their hydration products on the carbonation resistance of the CSA cements. The ye'elmite phase is responsible for rapid early strength gain and microstructural development in CSA cements, while the belite phase is responsible for later strength gain and microstructural development in CSA cements [22, 23]. The phase compositions for the CSA cements in Table 8.1 were calculated using modified Bogue equations adapted from Iacobescu et al. [23].

Table 8.1: Description of individual cement

Cement Category	Cement Type	Description
Pure Cements	OPC2	OPC Type I/II
	OPC3	OPC Type III
	CAC	Standard CAC cement
	CSA1	CSA Ye'elmite cement (40% Ye'elmite and 26% belite)
	CSA2	CSA belite cement (58% belite and 30% ye'elmite)
Proprietary Blended Cements	CAC-B1	CAC blend with OPC
	CAC-B2	CAC blended with set accelerating admixture
	CSA-B1	CSA belite cement (39% belite and 30% ye'elmite)
	CSA-B2	CSA belite cement (42% belite and 27% ye'elmite)
	PCSA1	CSA blend with OPC

Lab Blends	PCSA2	CSA blend with OPC and Fly ash
	CAC-OPC2	CAC blend with OPC
	CSA1-OPC2	CSA blend with OPC

Table 8.2: Chemical composition of the individual cements

Cement Type	Cement ID	SiO_2	Al_2O_3	Fe_2O_3	CaO	MgO	SO_3	Na_2O	K_2O	Na_2O_e	LOI
Pure Cements	OPC2	21.06	4.02	3.19	63.91	1.08	2.89	0.14	0.61	0.53	2.29
	OPC3	19.67	5.34	1.76	63.41	0.99	5.27	0.10	0.44	0.39	4.06
	CAC	4.34	38.65	15.09	38.37	0.39	0.16	0.05	0.14	0.14	1.55
	CSA1	9.07	21.61	2.26	45.26	0.94	20.26	0.07	0.30	0.27	1.05
	CSA2	20.56	16.14	1.35	45.31	1.23	14.73	0.77	0.72	1.24	4.74
Proprietary Blended Cements	CAC-B1	13.46	12.23	2.67	56.65	2.86	9.90	0.20	0.79	0.72	1.21
	CAC-B2	12.71	32.94	12.95	35.09	1.79	0.84	0.50	0.24	0.65	1.23
	CSA-B1	13.63	15.82	0.75	51.28	1.14	16.62	0.29	0.62	0.69	3.06
	CSA-B2	14.72	14.37	1.22	53.85	1.23	14.40	0.10	0.59	0.49	3.39
	PCSA1	17.38	11.06	2.98	55.82	1.25	10.68	0.43	0.52	0.77	2.26
	PCSA2	20.14	15.73	3.52	43.90	1.55	12.88	0.59	0.52	0.93	1.95
Lab Blends	CAC-OPC2	16.53	10.79	2.71	58.07	0.89	7.43	0.14	0.50	0.47	2.19
	CSA1-OPC2	18.06	8.42	2.96	59.25	1.04	7.23	0.12	0.53	0.47	1.98

Well-graded limestone rocks and siliceous river sand were used as coarse and fine aggregates, respectively. Other materials used in this study are a liquid polycarboxylate-ether-based superplasticizer and a set retarder, citric acid used to control slump, and delay setting to allow time for mixing and casting. Out of the 16 mixtures produced in this study, 11 were produced with a total cement content of 446 kg/m^3 (752 lb/yd^3) and a W/CM ratio of 0.35. In order to determine the effect of increased binder content, 2 mixtures were produced with a total binder content of 502 kg/m^3 (846 lb/yd^3). Based on the manufacturer's recommendation, the remaining 3 mixtures were produced with a total binder content of 390 kg/m^3 (658 lb/yd^3) and a W/CM ratio of 0.38. The total cement content of 502 kg/m^3 (846 lb/yd^3) and 390 kg/m^3 (658 lb/yd^3) were represented in this study as 846PCY and 658PCY, respectively. The "PCY" stands for pounds per cubic yard. Table 8.3 shows the concrete mixture proportions used in this study.

Table 8.3: Concrete mixture proportions

Cement Type	W/CM	Total cement kg/m³(lb/yd³)	Replacement Level of Cement with Second Cement Blend (% of Control Cement Type by Mass)	
			Control Cement	Type I/II
OPC2	0.35	446 (752)	100%	-

OPC3	0.35	446 (752)	100%	-
CAC	0.35	446 (752)	100%	-
CSA1	0.35	446 (752)	100%	-
CSA2	0.38	390 (658)	100%	-
CSA2	0.38	446 (752)	100%	-
CAC-B1	0.35	446 (752)	100%	-
CAC-B1	0.35	502 (846)	100%	-
CAC-B2	0.30	446 (752)	100%	-
CSA-B1	0.38	390 (658)	100%	-
CSA-B2	0.38	390 (658)	100%	-
PCSA1	0.35	446 (752)	100%	-
PCSA2	0.35	446 (752)	100%	-
CAC-OPC2	0.35	446 (752)	25%	75%
CSA1-OPC2	0.35	446 (752)	25%	75%
CSA1-OPC2	0.35	502 (846)	25%	75%

8.2.2 Sample Preparation and Testing

Two concrete prisms of dimension 100 x 100 x 350 mm (4 x 4 x 14 in) were produced for each of the mixtures in Table 8.3. The samples were cured with wet burlap and plastic sheet covers after casting for 24 hours. Out of the two prisms, one was demolded after 24-hour curing and transferred to an unsheltered natural environment. While the other was demolded at the same time and transferred to a sheltered natural environment. The unsheltered environment is an outdoor environment at Texas State University where the samples were placed vertically on their squared face and exposed to precipitation and other natural weather conditions. In contrast, the sheltered environment was an indoor environment where the samples were placed standing vertically on their squared face and protected from precipitation and other outdoor weather conditions. Figure 8.1 shows the natural unsheltered carbonation environment.

Figure 8.1: Natural unsheltered carbonation environment.

Table 8.4: Weather data in the unsheltered natural environment during exposure [24]

Average Temperature, °C (°F)	14°C - 27°C (57°F -80°F)
Average Relative Humidity, (%)	71 - 64
Average Precipitation, mm (inches)	911 (35.9)

Carbonation depth measurements were carried out at 6 months intervals in the first 2 years and a year interval afterward. In order to measure carbonation depth, a 50 mm (2-inch) thick sample was cut out of the concrete prism and then sprayed with phenolphthalein to reveal carbonated (colorless) and uncarbonated (purple color) regions. The exposed surface of the cut concrete prism was coated with carbonation-resistant paint and returned to the natural exposure location. Measurements were taken with the aid of a steel scale (0.5 mm accuracy) by measuring the distance from the edge of the sample to the point where the uncarbonated (purple color) region begins on the sample. This was done on five different points on each of the four edges of the sample. However, there was a one-inch offset from the corners to avoid any "corner effects" of CO_2 ingression during measurements. The final carbonation depth was the average depth measured from all four edges. Figure 8.2 illustrates the carbonation depth measurement procedure.

<div align="center">(a)   (b)   (c)   (d)</div>
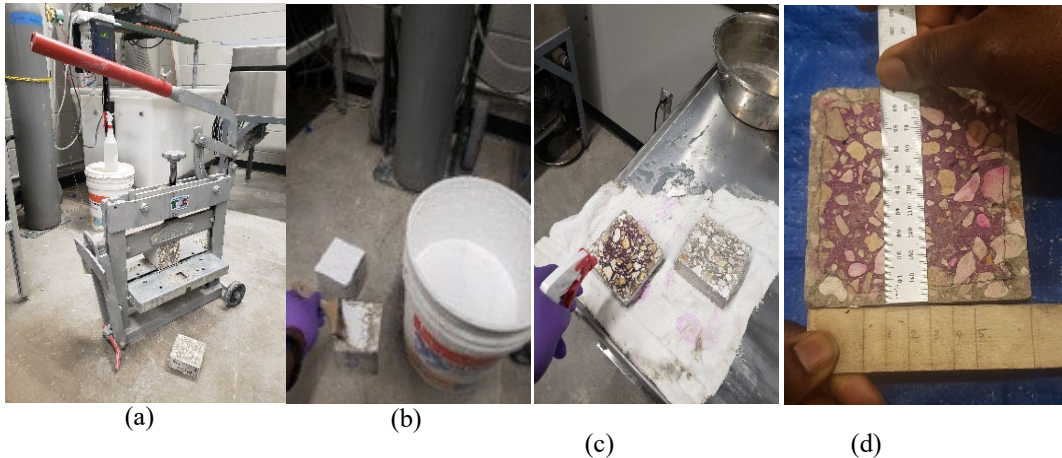
Figure 8.2: Carbonation depth measurement procedure. (a) cutting out the 50 mm thick sample, (b) coating the exposed surface of the concrete prism with carbonation-resistant paint, (c) spraying the 50 mm cut sample with phenolphthalein, (d) measurement with steel scale

8.3 RESULTS AND DISCUSSION

8.3.1 Carbonation Depth Due To Unsheltered and Sheltered Natural Exposure

The result in Figure 8.3 shows the natural carbonation depths for all mixtures after 3 years of exposure to carbonation in both sheltered and unsheltered natural conditions. The blue arrows in Figure 8.3 indicate four cement mixtures (CSA2, CSA2 (658PCY), CSA-B1, and CSA-B2) that are yet to be measured for carbonation at year 3. While the red dashed line indicates an assumption of 25 mm (1-inch) cover thickness to aid the analysis of the different cements.
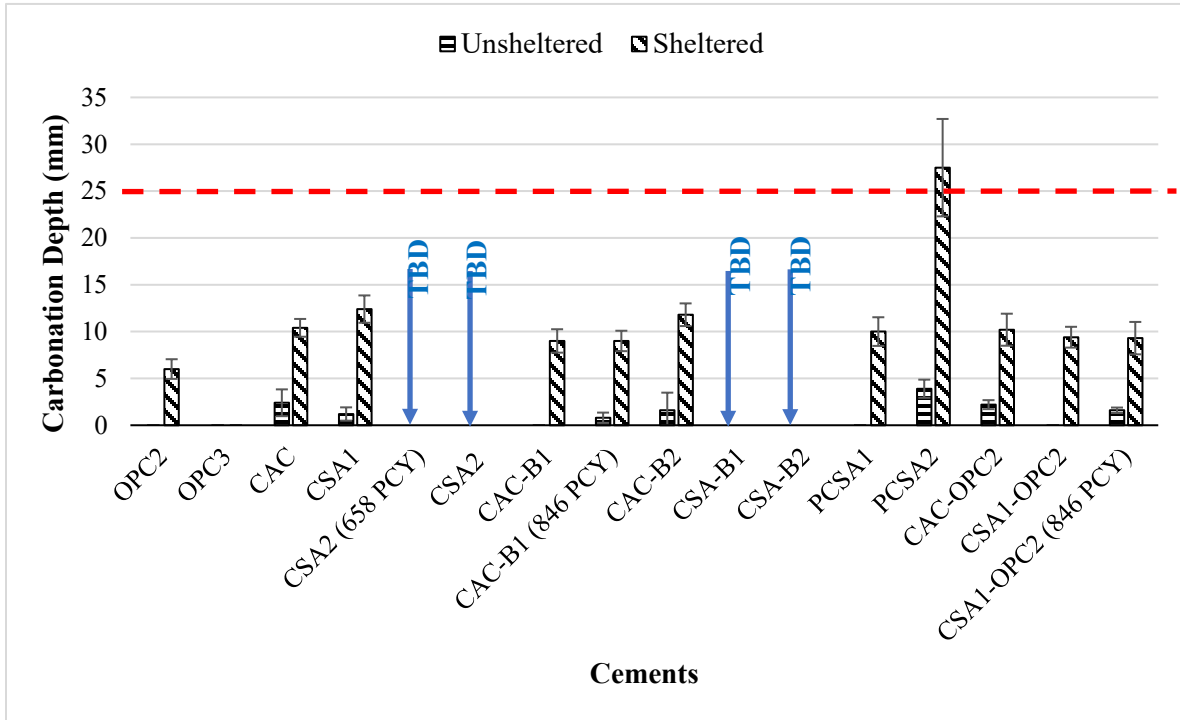
Figure 8.3: Natural carbonation depth in year 3 for sheltered and unsheltered exposure

Figure 8.3 shows a higher carbonation depth for practically all samples exposed to the sheltered natural condition compared to those in the unsheltered natural condition. The only exception is OPC3 which had no carbonation in both exposure conditions (sheltered and unsheltered). Compared to all other cement in this study, the controls (OPC2 and OPC3) showed the highest resistance to unsheltered and sheltered natural carbonation. This is due to their CH content and ability to form $CaCO_3$, which helps reduce porosity and carbonation rate [14, 25]. The higher carbonation depth exhibited by the sheltered samples compared to the unsheltered samples can be attributed to the constant partially saturated pores peculiar to sheltered environments, which can promote the dissolution of CO_2 and the rate of carbonation [6, 7]. Also, the low or no carbonation exhibited by the unsheltered samples can be attributed to the intermittent pore saturation periods experienced during outdoor exposure, which could have impeded the dissolution of CO_2 and the carbonation rate in the concrete [6, 7].

Comparing the carbonation depth of the mixtures in Figure 8.3 based on their categories, it can be observed that within the pure cement category, the sheltered sample for CSA1 showed a higher carbonation depth than the sheltered samples for CAC, OPC2, and OPC3. However, the unsheltered samples for CSA1 and CAC showed a little carbonation depth after natural exposure for 3 years. The unsheltered samples for OPC2 and OPC3 showed no carbonation after 3 years of natural exposure. The higher carbonation depths exhibited by CSA1 and CAC compared to the controls can be attributed to the

lack of CH, which helps to provide a buffer to CO_2 ingress in the controls (OPC2 and OPC3) [2, 18]. In addition, the increase in porosity and loss of strength due to the breakdown of the main hydrates of CAC and CSA cement concrete during carbonation [2, 18] could also have contributed to the low resistance to carbonation exhibited by CSA1 and CAC compared to the controls.

The sheltered samples for the lab-blended cements (CAC-OPC2, CSA-OPC2, and CSA-OPC2 (846PCY)) exhibited a moderate carbonation depth after 3 years of exposure to natural carbonation. As for their unsheltered samples at year 3, CSA1-OPC2 showed no carbonation, while CAC-OPC2 and CSA1-OPC2 (846PCY) showed little carbonation. Comparing the lab-blended cements with their pure counterpart (CAC and CSA1), it can be observed that the lab-blended cements showed a slight improvement in resisting carbonation due to the CO_2 buffer provided by the OPC2 constituent [14].

The sheltered samples for the proprietary blended cements CAC-B1, CAC-B1 (846PCY), CAC-B2, and PCSA1 showed a moderate carbonation depth after 3 years of exposure. However, the sheltered samples for CAC-B1, CAC-B1 (846PCY), and PCSA1 showed more resistance to carbonation than CAC-B2 due to the blending with OPC during production. The sheltered sample for PCSA2 showed the highest carbonation depth of all the cements under study, with its depth of carbonation exceeding the assumed 25 mm cover mark. This high carbonation depth in the sheltered sample for PCSA2 compared to other proprietary blended cements can be attributed to the presence of fly ash (See Table 8.1). The fly ash constituent might have caused the high carbonation depth due to a combined effect of hydraulic cement replacement and the consumption of the CH emanating from the OPC constituent during the pozzolanic reaction [11, 26]. The fly ash inclusion should have improved carbonation resistance over time. However, that comes with adequate curing, and the samples for this study were cured for only 24 hours with wet burlap and plastic sheets before transferring them to the sheltered and unsheltered sites. As for their unsheltered samples, CAC-B1 (846PCY) and PCSA2 showed little carbonation, while CAC-B1 and PCSA1 showed no carbonation after 3 years of exposure.

In order to analyze the performance of the cements missing in Figure 8.3 (CSA2, CSA2(658PCY), CSA-B1, and CSA-B2) as regards natural carbonation, the carbonation depth results after 2 years of natural exposure are presented in Figure 8.4.
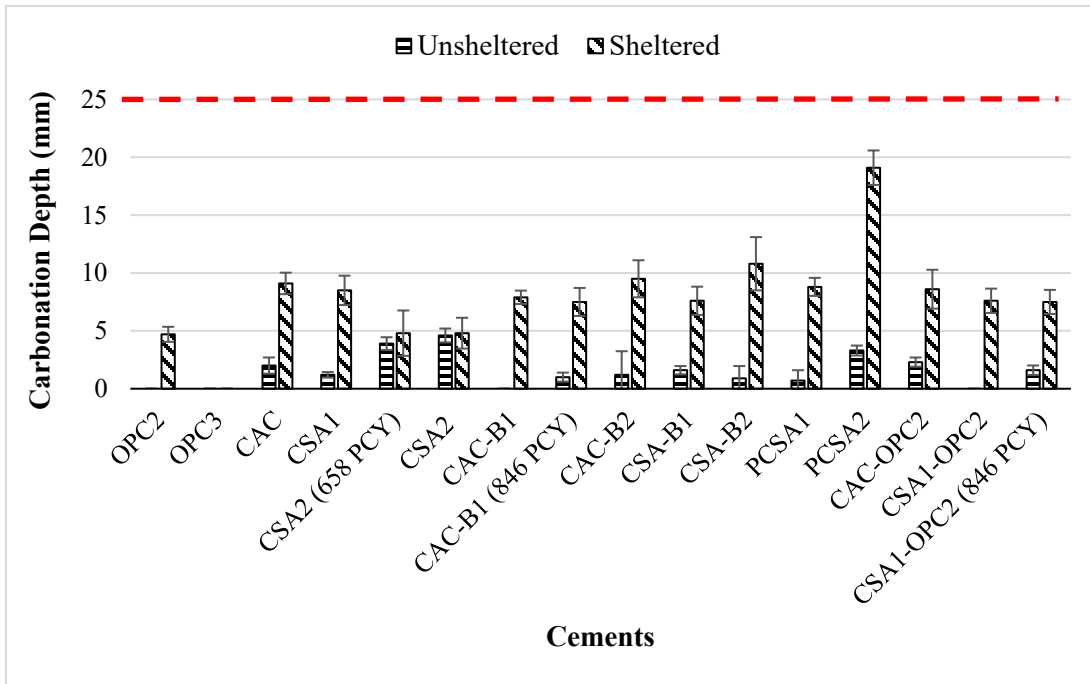
Figure 8.4: Natural carbonation depth in year 2 for sheltered and unsheltered exposure

Figure 8.4 shows that in year 2, the sheltered samples for the pure cements CSA2 and CSA2 (658PCY) showed a lower carbonation depth than the sheltered samples of all other CAC and CSA cement categories (pure, proprietary, and lab-blended cements) considered in this study. However, the unsheltered samples for CSA2 and CSA2 (658PCY) seemed to have a higher carbonation depth than those of other CSA and CAC categories considered in year 2. There is also not much difference in the carbonation depth of unsheltered and sheltered samples of CSA2 and CSA2 (658PCY) as shown in Figure 8.4. There could be several reasons for this similar performance of the sheltered and unsheltered samples of CSA2 and CSA2 (658PCY) in year 2; however, one good reason could be the presence of coarse pores, which creates a constant partial saturation situation despite the wet and dry periods peculiar to outdoor environments.

Additionally, the sheltered samples of CSA-B1 and CSA-B2 showed a moderate carbonation depth in year 2. However, the carbonation depth exhibited by the sheltered sample for CSA-B2 appeared to be second to the highest in Figure 8.4. This high carbonation depth exhibited by the CSA-B2 can be attributed to its high belite content compared to ye'elmite. The ye'elmite phase reacts very fast and contributes to early strength gain and microstructural development in CSA cements [2]. However, the belite phase is slow in reaction; hence it only contributes to later strength gain and microstructural development [2, 27]. Therefore, the high belite content in CSA-B2 might have resulted in a poorly developed microstructure leading to higher CO_2 ingress and carbonation depth.

8.3.2 Carbonation Coefficient Due to Exposure to Natural and Accelerated Carbonation

As stated earlier, the square root of time model is one of many models that has been used to predict the carbonation depth at a future time. In order to understand if there is any correlation between the rate of natural carbonation of the different cement systems considered in this study and their rate of accelerated carbonation, this study compares the carbonation coefficients of a previous accelerated carbonation study on these cement systems and their carbonation coefficient in this study. The carbonation coefficient was obtained by calculating the regression of carbonation depth with respect to the square root of time, as shown in Equation 8.1. This study considered samples cured for 24 hours and 7 days in the previous study and exposed to accelerated carbonation at CO_2 concentrations of 1% and 4% and RH of 57% and 75%. Tables 8.5 and 8.6 show the calculated carbonation coefficients at year 3 for the different mixtures exposed to natural carbonation and the previous accelerated carbonation exposure of the 24-hour and 7 days cured samples, respectively. The 24-hour cured samples were chosen from the accelerated study because the natural carbonation samples in this study were also cured for 24 hours. Whereas the 7 days cured samples were included to see the effect of extended curing in the carbonation coefficients due to accelerated exposure compared to natural exposure.

Table 8.5: Carbonation coefficients due to accelerated carbonation on 24-hour cured samples and 3 years of natural carbonation

Cement Type	Carbonation Coefficients (mm/year$^{1/2}$)					
	Accelerated Carbonation				Natural Carbonation	
	$K_{acc, 4/57}$	$K_{acc, 1/57}$	$K_{acc, 4/75}$	$K_{acc, 1/75}$	$K_{N, sh}$	$K_{N, ush}$
OPC2	14.5	15.5	7.5	4.3	3.5	0.0
OPC3	3.0	9.7	3.2	1.7	0.0	0.0
CAC	34.1	27.0	33.6	23.3	6.0	1.4
CSA1	32.8	20.9	27.8	21.6	7.2	0.7
CAC-B1	30.4	23.3	25.4	19.8	5.2	0.0
CAC-B1 (846 PCY)	27.4	21.6	23.3	14.9	5.2	0.0
CAC-B2	43.4	33.2	37.5	25.5	6.8	0.9
PCSA1	24.1	24.8	25.4	19.8	5.8	0.0
PCSA2	52.4	47.4	76.3	30.0	15.9	2.3
CAC-OPC2	26.7	22.4	19.9	19.2	5.9	1.3
CSA1-OPC2	28.3	21.6	20.3	30.9	5.4	0.0
CSA1-OPC2 (846 PCY)	37.5	21.3	17.0	38.8	5.4	0.9

Table 8.6: Carbonation coefficients due to accelerated carbonation on 7 days cured samples and 3 years of natural carbonation

| Cement Type | Carbonation Coefficients (mm/year$^{1/2}$) | | | | | |
| | Accelerated Carbonation | | | | Natural Carbonation | |
	$K_{acc, 4/57}$	$K_{acc, 1/57}$	$K_{acc, 4/75}$	$K_{acc, 1/75}$	$K_{N, sh}$	$K_{N, ush}$
OPC2	8.4	9.7	0.0	0.0	3.5	0.0
OPC3	0.0	3.0	0.0	0.0	0.0	0.0
CAC	27.6	24.1	20.7	16.6	6.0	1.4
CSA1	28.2	23.3	23.5	14.2	7.2	0.7
CAC-B1	24.6	18.1	19.6	14.4	5.2	0.0
CAC-B1 (846 PCY)	22.2	19.6	17.9	10.3	5.2	0.0
CAC-B2	36.5	27.0	31.1	21.4	6.8	0.9
PCSA1	19.2	19.6	13.8	13.4	5.8	0.0
PCSA2	48.8	37.7	71.2	27.4	15.9	2.3
CAC-OPC2	17.0	19.4	11.6	7.1	5.9	1.3
CSA1-OPC2	17.0	17.3	8.4	6.7	5.4	0.0
CSA1-OPC2 (846 PCY)	18.3	18.1	6.2	13.1	5.4	0.9

In Tables 8.5 and 4.6, "K" stands for carbonation coefficient, "acc" stands for accelerated, "x/y" stands for %CO_2/%RH, "N" stands for natural, "sh" stands for sheltered, and "ush" stands for unsheltered. Figure 8.5 shows the carbonation coefficients ($K_{N, sh}$) of the samples exposed to sheltered natural carbonation plotted against the carbonation coefficients ($K_{acc, CO2/RH}$) of the 24-hour cured samples exposed to accelerated carbonation at CO_2 concentrations of 1% and 4%, and RH of 57% and 75%. In the same vein, Figure 8.6 shows the carbonation coefficients ($K_{N, ush}$) of the samples exposed to unsheltered natural carbonation plotted against the carbonation coefficients ($K_{acc, CO2/RH}$) of the 24-hour cured samples exposed to accelerated carbonation at CO_2 concentrations of 1% and 4%, and RH of 57% and 75%.
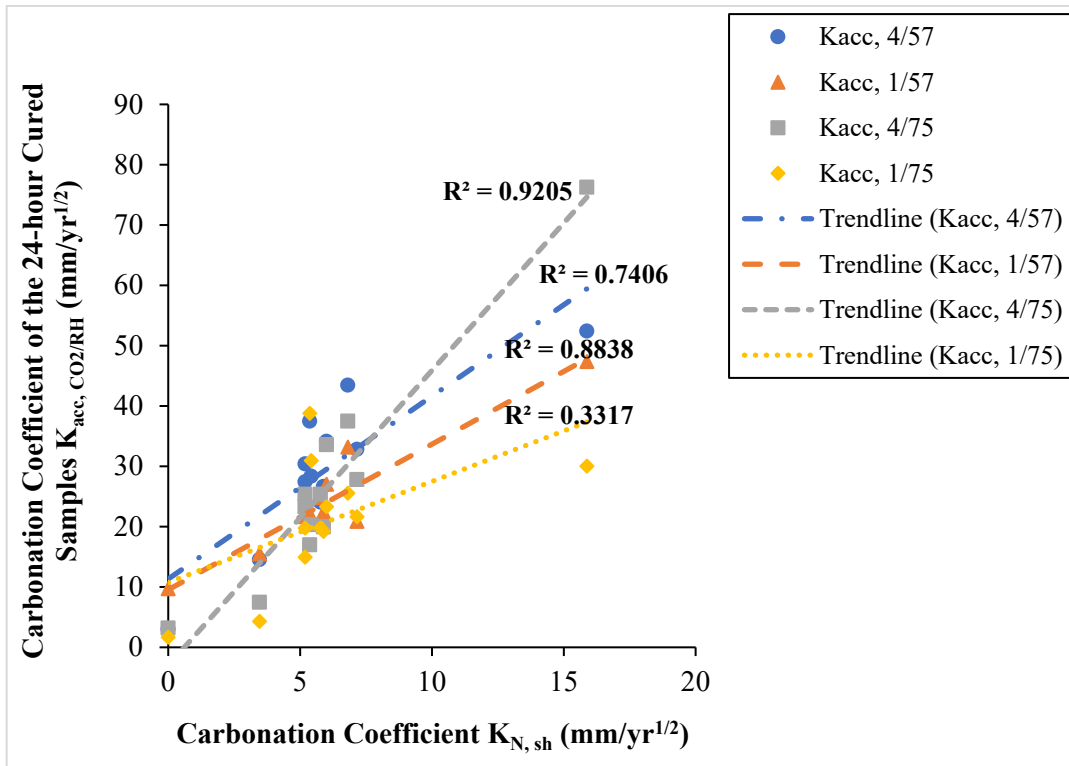
Figure 8.5: Carbonation coefficient for sheltered natural versus accelerated carbonation for 24-hour cured samples
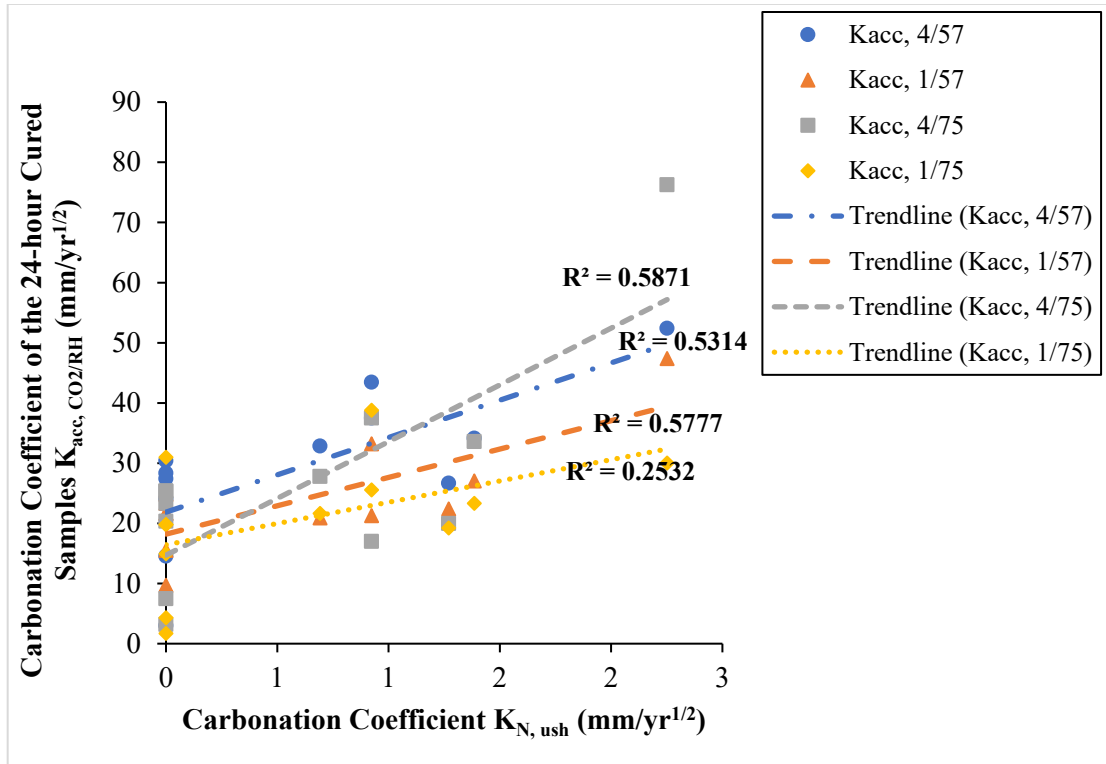
Figure 8.6: Carbonation coefficient for unsheltered natural versus accelerated carbonation for 24-hour cured samples

Figure 8.5 shows a strong correlation (R^2 values) between the carbonation coefficients under sheltered natural conditions ($K_{N, sh}$) and the carbonation coefficients of the 24-hour cured samples under accelerated conditions ($K_{acc, CO2/RH}$). However, the correlation is more pronounced when CO_2 is high (4%) or RH is low (57%), but not when neither of those conditions is present (1%CO2/75%RH). The strong correlation (R^2 values) in Figure 8.5 could be related to the constant partial saturation of pores peculiar to sheltered natural environments [6], which is likely to occur at low RH (57%RH) as used in the accelerated carbonation study. Also, the closeness of the 4%CO_2 concentration to values reported to produce similar reaction products in natural carbonation could also contribute to the strong correlation (R^2 values) in Figure 8.5 [14]. The high correlation increases the transferability of the accelerated results to sheltered natural conditions.

In Figure 8.6, the carbonation coefficients under unsheltered natural conditions ($K_{N, ush}$) appeared to be moderately correlated (R^2 values) with those of the 24-hour cured samples under accelerated conditions ($K_{acc, CO2/RH}$). However, the moderate correlation applies to accelerated conditions with high CO_2 concentrations (4%) or low humidity (57%RH), but not when neither of those conditions is present (1%CO2/75%RH). The moderate correlation (R^2 values) at high CO_2 concentrations (4%) and low

humidity (57%RH) could be explained by the less probability of experiencing such conditions in an unsheltered natural environment. With the high RH (75%) used in the accelerated carbonation study, the correlation (R^2 values) was expected to be high in such cases considering the likelihood of such high RH in unsheltered natural conditions. However, the complexity of factors at play in unsheltered natural conditions might have influenced the disparity in correlation observed in Figure 8.6.

Figure 8.7 shows the carbonation coefficients ($K_{N, sh}$) of the samples exposed to sheltered natural carbonation plotted against the carbonation coefficients ($K_{acc, CO2/RH}$) of the 7 days cured samples exposed to accelerated carbonation at CO_2 concentrations of 1% and 4%, and RH of 57% and 75%. In the same vein, Figure 8.8 shows the carbonation coefficients ($K_{N, ush}$) of the samples exposed to unsheltered natural carbonation plotted against the carbonation coefficients ($K_{acc, CO2/RH}$) of the 7 days cured samples exposed to accelerated carbonation at CO_2 concentrations of 1% and 4%, and RH of 57% and 75%.
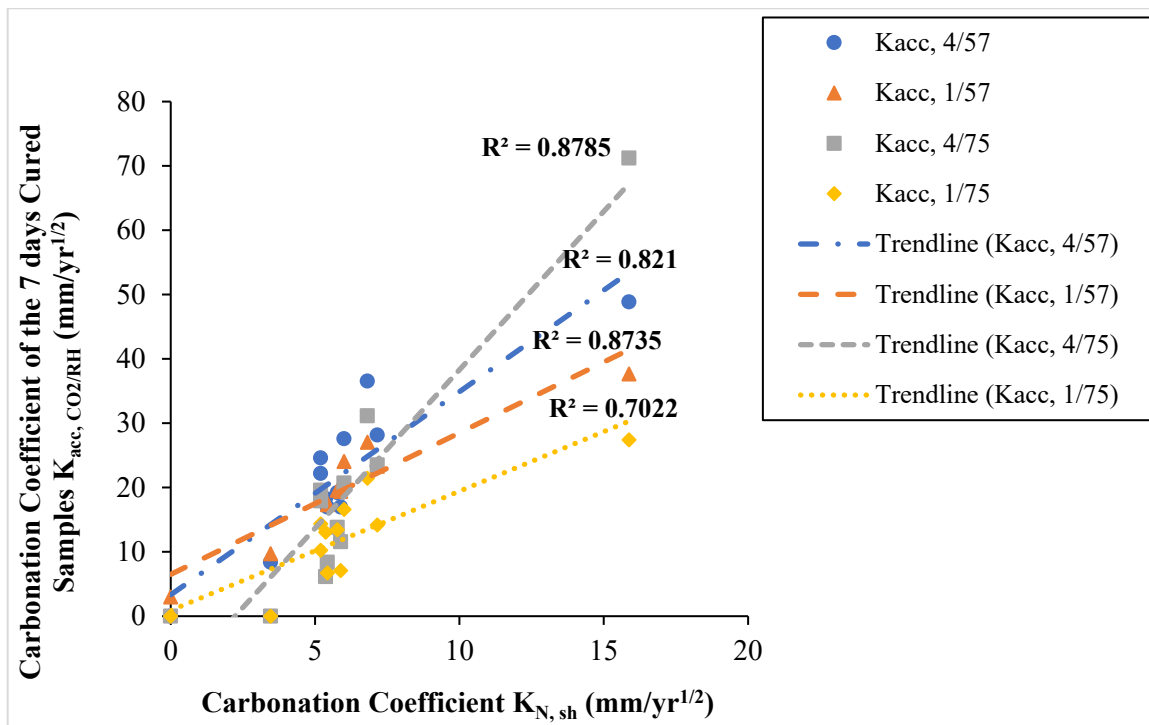
Figure 8.7: Carbonation coefficient for sheltered natural versus accelerated carbonation for 7 days cured samples

189
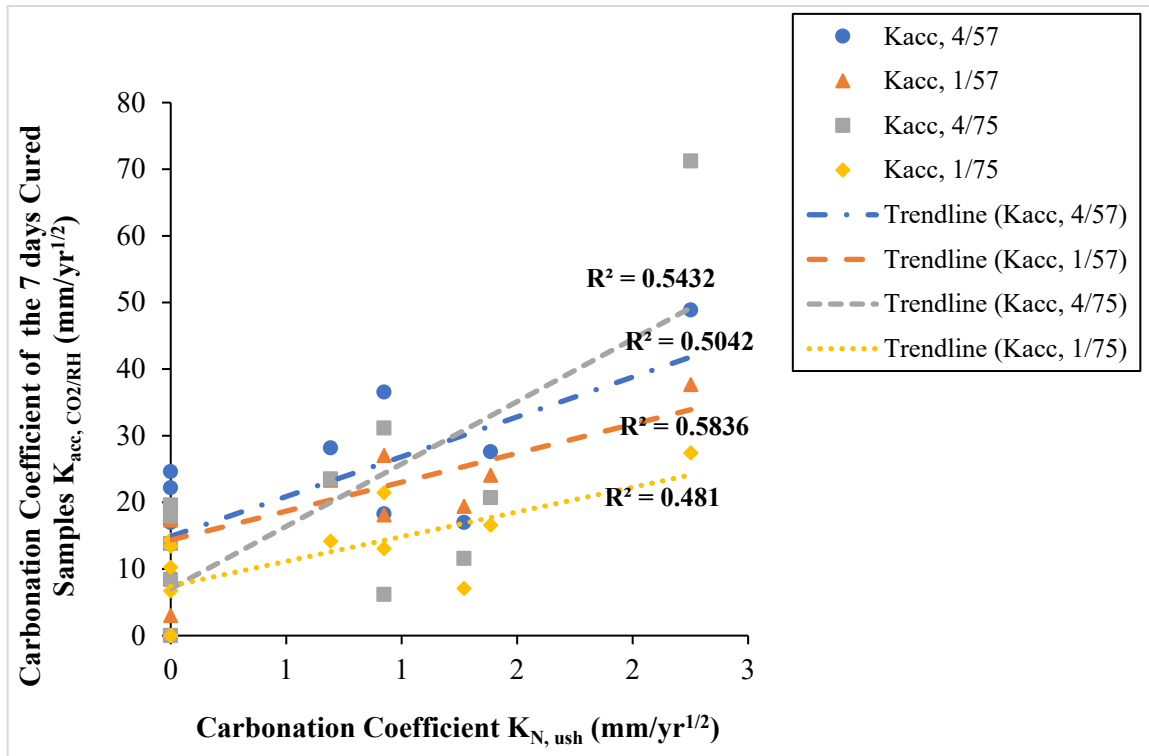
Figure 8.8: Carbonation coefficients for unsheltered natural versus accelerated carbonation for 7 days cured samples

In Figure 8.7, the correlation (R^2 values) between the carbonation coefficients under sheltered natural conditions ($K_{N, sh}$) and the carbonation coefficients of the 7 days cured samples under accelerated conditions ($K_{acc, CO2/RH}$) appears to be similar to that of the sheltered natural conditions and 24-hour cured samples under accelerated conditions in Figure 8.5. However, the carbonation coefficients under sheltered natural conditions showed a strong correlation (R^2 values) with the carbonation coefficients of the 7 days cured samples under accelerated conditions at $1\%CO_2/75\%RH$. This could be attributed to the improvement of microstructure due to extended curing. Meanwhile, the carbonation coefficients of the other accelerated conditions at either a high CO_2 concentration (4%) or low RH (57%) as shown in Figure 8.7, exhibited a stronger correlation (R^2 values) to the carbonation coefficients of the sheltered natural conditions. This could still be attributed to the constant partial filling of pores which is likely to occur in a sheltered natural environment and at low RH (57% RH) as used in the accelerated carbonation study [7, 28]. Also, the strong correlation at $4\%CO_2$ concentration could be attributed to the closeness of the $4\%CO_2$ concentration used in the accelerated carbonation study to the values reported to produce similar reaction products in natural carbonation [14]. This strong correlation (R^2 values) between the carbonation coefficients due to the sheltered and accelerated conditions increases the transferability of the accelerated results to sheltered natural conditions.

In Figure 8.8, the carbonation coefficients under unsheltered natural conditions ($K_{N, ush}$) appear to be moderately correlated (R^2 values) with those of the 7 days cured samples under accelerated conditions ($K_{acc, CO2/RH}$). This correlation between the carbonation coefficients in unsheltered natural conditions and the 7 days cured samples under accelerated conditions is as well similar to those of unsheltered natural conditions and the 24-hour cured samples under accelerated conditions. Again, the moderate correlation (R^2 values) at high CO_2 concentrations (4%) and low RH (57%RH) could be explained by the less probability of experiencing such conditions in an unsheltered natural environment. Also, the moderate correlation (R^2 values) at 75%RH, despite the likelihood of having a high RH (75%) in unsheltered natural conditions, can be attributed to the complexity of factors at play in unsheltered natural conditions.

8.4 CONCLUSIONS

1. Practically all samples exposed to sheltered natural carbonation showed higher carbonation depth after 3 years compared to samples exposed to unsheltered natural carbonation. The only exception was OPC3 which had no carbonation in both sheltered and unsheltered natural conditions. The higher carbonation depth exhibited by the sheltered samples compared to the unsheltered samples can be attributed to the constant partially saturated pores of the sheltered samples that promote the dissolution of CO_2 and the rate of carbonation. Whereas the intermittent pore saturation periods experienced during unsheltered natural exposure must have impeded the dissolution of CO_2 and the rate of carbonation in the concrete samples exposed to unsheltered natural environments.

2. The control mixtures (OPC2 and OPC3) showed the highest resistance to unsheltered and sheltered natural carbonation compared to all other cement in this study. This is due to their high CH content and ability to form $CaCO_3$ which helps to reduce porosity and rate of carbonation.

3. The sheltered samples for the lab-blended cements (CAC-OPC2, CSA-OPC2, and CSA-OPC2(846PCY)) exhibited a moderate carbonation depth after 3 years of exposure to natural carbonation. Comparing the lab-blended cements with their pure counterpart (CAC and CSA1), it can be observed that the lab-blended cements showed a slight improvement in resisting carbonation due to the presence of OPC2.

4. The majority of the CAC and CSA cements in the categories considered in this study (pure, proprietary, and lab blended) exhibited moderate carbonation depths in sheltered natural conditions coupled with little or no carbonation in unsheltered conditions. The only exception was the sheltered samples of PCSA2 with high carbonation depths beyond the assumed 25 mm (1

inch) cover mark. This performance of PCSA2 was attributed to the effect of hydraulic cement replacement and the pozzolanic activity of the fly ash constituent.

5. The carbonation coefficients of the 24-hour and 7 days cured samples exposed to accelerated carbonation at CO_2 concentrations of 1% and 4%, and RH of 57% and 75% showed a strong correlation (R^2 values) to the carbonation coefficients due to sheltered natural exposure, especially when accelerated conditions were either at high CO_2 concentration (4%) or low RH (57%). The unsheltered natural carbonation coefficient showed a moderate correlation (R^2 values) to the carbonation coefficients of 24-hour and 7 days cured samples exposed to accelerated conditions. The strong correlation (R^2 values) between the carbonation coefficients due to the sheltered natural conditions and the accelerated conditions increases the transferability of the accelerated results to sheltered natural conditions.

8.5 REFERENCES

[1]   M. Yu, J. Lee, and C. Chung, "The Application of Various Indicators for the Estimation of Carbonation and pH of Cement Based Materials," *Journal of Testing and Evaluation,* vol. 38, pp. 534-540, 2010. [Online]. Available: www.astm.org.

[2]   E. T. G. Moffatt and M. D. Thomas, "Effect of Carbonation on the Durability and Mechanical Performance of Ettringite-Based Binders," *ACI Materials Journal,* vol. 116, no. 1, 2019.

[3]   S. von Greve-Dierfeld *et al.*, "Understanding the carbonation of concrete with supplementary cementitious materials: a critical review by RILEM TC 281-CCC," *Materials and structures,* vol. 53, no. 6, pp. 1-34, 2020.

[4]   M. Elsalamawy, A. R. Mohamed, and E. M. Kamal, "The role of relative humidity and cement type on carbonation resistance of concrete," *Alexandria Engineering Journal,* vol. 58, no. 4, pp. 1257-1264, 2019.

[5]   Q. H. Vu *et al.*, "Impact of different climates on the resistance of concrete to natural carbonation," *Construction and Building Materials,* vol. 216, pp. 450-467, 2019.

[6]   S. Ekolu, "A review on effects of curing, sheltering, and CO2 concentration upon natural carbonation of concrete," *Construction and Building Materials,* vol. 127, pp. 306-320, 2016.

[7]   F. M. Aguayo, T. Drimalas, and K. J. Folliard, "Natural Carbonation Of Concrete," *Special Publication,* vol. 305, pp. 2.1-2.12, 2015.

[8]   S. Rathnarajan, B. Dhanya, R. G. Pillai, R. Gettu, and M. Santhanam, "Carbonation model for concretes with fly ash, slag, and limestone calcined clay-using accelerated and five-year natural exposure data," *Cement and Concrete Composites,* vol. 126, p. 104329, 2022.

[9]   F. Aguayo, A. Torres, Y.-J. Kim, and O. Thombare, "Accelerated carbonation assessment of high-volume fly ash concrete," *Journal of Materials Science and Chemical Engineering,* vol. 8, no. 3, pp. 23-38, 2020.

[10]   K. Tuutti, *Corrosion of steel in concrete*. Cement-och betonginst., 1982.

[11]   D. Ho and R. Lewis, "Carbonation of concrete and its prediction," *Cement and Concrete Research,* vol. 17, no. 3, pp. 489-504, 1987.

[12]   L. Jiang, B. Lin, and Y. Cai, "A model for predicting carbonation of high-volume fly ash concrete," *Cement and concrete research,* vol. 30, no. 5, pp. 699-702, 2000.

[13]   G. N. Malysz, V. G. Cappellesso, L. Silvestro, D. C. C. Dal Molin, and A. B. Masuero, "Natural and Accelerated Carbonation in Concrete Associated with Recycled Coarse Aggregate Treated by

Air Jigging Technology," *Journal of Materials in Civil Engineering,* vol. 34, no. 7, p. 04022133, 2022.

[14]   A. Leemann and F. Moro, "Carbonation of concrete: the role of CO 2 concentration, relative humidity and CO 2 buffer capacity," *Materials and Structures,* vol. 50, pp. 1-14, 2017.

[15]   J. H. Ideker, C. Gosselin, and R. Barborak, "An Alternative Repair Material," *Concrete International,* Article vol. 35, no. 4, pp. 33-37, 04// 2013. [Online]. Available: http://libproxy.txstate.edu/login?url=http://search.ebscohost.com/login.aspx?direct=true&db=aps&AN=86652443&login.asp&site=eds-live&scope=site.

[16]   M. Dornak, J. Zuniga, A. Garcia, T. Drimalas, and K. J. Folliard, "Development of Rapid, Cement-Based Repair Materials for Transportation Structures," 2015.

[17]   S. Lamberet, "Durability of ternary binders based on Portland cement, calcium aluminate cement and calcium sulfate," EPFL, 2004.

[18]   E. Moffatt, "Durability of rapid-set (ettringite-based) concrete," University of New Brunswick., 2016.

[19]   K. L. Scrivener and A. Capmas, "13-Calcium Aluminate Cements," *Lea's Chemistry of Cement and Concrete (Fourth Edition). Butterworth-Heinemann, Oxford,* pp. 713-782, 2003.

[20]   M. P. E. Moses and B. Perumal, "Latest Advances in Alternative Cementations Binders than Portland cement," *IOSR Journal of Mechanical and Civil Engineering,* vol. 13, no. 5, pp. 45-53, 2016.

[21]   S. Mindess, F. J. Young, and D. Darwin, *Concrete*. New Jersey: Prentice Hall, 2003.

[22]   Y. Tao, A. Rahul, M. K. Mohan, G. De Schutter, and K. Van Tittelboom, "Recent progress and technical challenges in using calcium sulfoaluminate (CSA) cement," *Cement and Concrete Composites,* p. 104908, 2022.

[23]   R. I. Iacobescu, Y. Pontikes, D. Koumpouri, and G. Angelopoulos, "Synthesis, characterization and properties of calcium ferroaluminate belite cements produced with electric arc furnace steel slag as raw material," *Cement and Concrete Composites,* vol. 44, pp. 1-8, 2013.

[24]   "Climate in San Marcos (Texas, United States of America)." https://weather-and-climate.com/average-monthly-Rainfall-Temperature-Sunshine,san-marcos-texas-us,United-States-of-America (accessed March 17, 2023).

[25]   A. Leemann, H. Pahlke, R. Loser, and F. Winnefeld, "Carbonation resistance of mortar produced with alternative cements," *Materials and Structures,* vol. 51, no. 5, p. 114, 2018.

[26]   J. Khunthongkeaw, S. Tangtermsirikul, and T. Leelawat, "A study on carbonation depth prediction for fly ash concrete," *Construction and building materials,* vol. 20, no. 9, pp. 744-753, 2006.

[27]   K. Quillin, "Performance of belite–sulfoaluminate cements," *Cement and concrete research,* vol. 31, no. 9, pp. 1341-1349, 2001.

[28]   S. Roy, K. Poh, and D. Northwood, "Durability of concrete—accelerated carbonation and weathering studies," *Building and environment,* vol. 34, no. 5, pp. 597-606, 1999.

CHAPTER 9: EVALUATION OF CORROSION OF RAPID SETTING HYDRAULIC CEMENT CONCRETE SYSTEMS

9.1 INTRODUCTION

Chloride-ion-induced corrosion is one major cause of corrosion of reinforcing steel in concrete. Corrosion due to chloride-ion ingress occurs when the concentration of chloride ions in the vicinity of reinforcing steel exceeds the chloride threshold necessary for the steel rebar to remain protected by a passive film formed around its surface. Chloride-ion can be introduced into the concrete matrix through various means such as exposure to a marine environment, application of deicing salts, use of chloride-contaminated aggregate or water for mixing, and use of chloride set accelerators [1]. The ingress of chloride ions into concrete can take place in several ways. These include diffusion due to a concentration gradient, capillary sorption, permeation, dispersion, etc. [2]. In the case of a fully saturated concrete cover, ionic diffusion is expected to have the most dominant effect. Due to a concentration gradient between the exposed surface and the pore solution within the concrete, chloride ions enter the concrete by ionic diffusion. This process is often described by Fick's second law of diffusion, as shown in equation 9.1.

$$\frac{\partial C}{\partial t} = D \frac{\partial}{\partial x}\left(\frac{\partial C}{\partial x}\right)$$ Eq 9.1

Fick's second law of diffusion defines the chloride concentration as a function of time and distance under non-steady state conditions. This accounts for the change in concentration relative to time as is the case of chloride-ion diffusion in concrete [2]. However, the solutions to Fick's second law are only possible when physical boundary conditions are specified. The standard test method for determining the apparent coefficient of diffusion of cementitious mixtures by bulk diffusion is stipulated in ASTM C1556 [3].

The ingress of chlorides in concrete is influenced by several materials and environmental factors, including cover thickness, chloride resistivity, chloride binding capacity of concrete, damage to concrete cover due to loads, the water-binder ratio of the concrete mixture, curing conditions, age of concrete, cement type, cement composition, surface chloride concentration, relative humidity, and ambient temperature [4]. Considering the porous nature of concrete, it is certain that chlorides will get to the vicinity of steel reinforcement if exposed to a chloride-rich environment [5]. However, several measures can be taken to slow the rate of chloride ingress and prevent the concentration of the chloride ion in the vicinity of the steel from reaching the threshold that could destroy the passive layer [5].

Concrete's resistance to chloride penetration is mainly determined by its pore structure (i.e. size, connectivity, and tortuosity of pores) and the thickness of concrete cover to reinforcement [4, 5]. The higher the porosity of concrete, the easier it is for chlorides to penetrate hence increasing the likelihood of premature corrosion of reinforcing steel. The porosity of concrete can be reduced by reducing the W/CM ratio, appropriate use of SCMs, proper compaction, adequate curing, and other practices that ensure the production of durable concrete. Likewise, an adequate cover thickness will help provide more lasting protection to steel reinforcement [5]. The chloride binding capacity of concrete is another important factor to consider when evaluating the rate of chloride ingress in concrete. Chloride binding may be defined as the interaction between the porous concrete matrix and chloride ions, which results in their effective removal from the pore solution [1, 6]. The total amount of chloride in concrete is the sum of bound chloride and free chloride. However, it is the free chloride that is responsible for the corrosion of reinforcing steel in concrete [2]. The bound chloride either reacts chemically with hydration products or gets physically adsorbed within pores [2]. Chemical binding occurs as a chemical reaction between the chloride ion and certain cement phases that are abundant in ordinary portland cement (OPC) concrete, such as CH, AFm, tetracalcium aluminate ferrite (C_4AF), and tricalcium aluminate (C_3A), to form chloroaluminate hydrate ($C_3A.CaCl_2.10H_2O$) also known as Friedel's salt [2]. The amount of C_3A in the cement plays a major role in determining chloride binding capacity [6]. Friedel's salt has a less porous structure and helps to slow down the transport of chloride ions [2]. However, binders with a high amount of AFt such as CSA and CAC + CS have shown to exhibit a low binding ability and low Friedel's salt content [7]. The pH reduction due to carbonation has also been found to reduce the ability of both OPC and ettringite-based systems to bind external chloride due to the solubility of Friedel's salt and its ferrite equivalent ($3CaO.FeO_3.CaCl_2.10H_2O$) at low pH [7]. However, this effect of carbonation on binding ability is more pronounced in ettringite-based binders than in OPC because of the higher pH content [7]. There are also reports on the ability of the CAC hydrates to bind chlorides, thus removing them from the pore solution [8, 9]. The binding capability of CACs increases as the alumina (Al_2O_3) content increases [8, 9]. The physical binding of chloride ions occurs as a result of van der Waals forces between cations on the negatively charged hydrated cement particles and the negatively charged chloride ions in pore solution [5]. Generally, the process of chloride binding reduces the pore solution concentration, which is the driving force of the chloride diffusion process, hence reducing the chloride transport process and prolonging the time for corrosion to initiate. [2]. Another important factor that can affect the rate of chloride ingress in concrete is the presence of damage and cracks in the concrete cover due to loads. The formation of cracks in concrete provides easy access to chloride ions, oxygen, and water in the vicinity of steel reinforcement hence accelerating its corrosion [10, 11].

Chloride-induced corrosion initiation tends to be localized and follows the model of pitting corrosion. Pits start to form at some point on the steel surface, usually where there is a steel-concrete interface defect or a passive film defect. The breakdown of the passive layer at those defective points leads to a local dissolution of the metal. Two types of corrosion occur in reinforced concrete, namely microcell and macrocell corrosion. Microcell corrosion is said to be the dominant corrosion type in chloride-contaminated concrete [12, 13]. It occurs when both the anodic half-cell reaction (dissolution of iron) and the cathodic half-cell reaction (reduction of the dissolved oxygen) are taking place in adjacent locations on the same steel reinforcement [12, 13]. Whereas macrocell corrosion, which is also known as galvanic corrosion, occurs when an actively corroding steel reinforcement is connected to another steel reinforcement that is in a passive state because of its composition or environmental conditions. The half-cell reactions on both steel reinforcements introduce a potential difference resulting in the flow of electrons from the actively corroding steel through the connection to the cathodic site on the passive steel reinforcement. A good example is in structural elements with top and bottom reinforcement connected with stirrups, where the cover to the top reinforcement is exposed to a harsh chloride environment, and the bottom is free from chloride [12, 13]. Macrocell and microcell corrosion can be measured using the test method ASTM G109 "Standard Test Methods for Determining Effects of Chemical Admixtures on Corrosion of Embedded Steel Reinforcement in Concrete Exposed to Chloride Environments" with few modifications [14].

This study is focused on assessing the susceptibility of cracked, carbonated, and normal concrete produced with alternative cementitious binders such as CAC and CSA cement to corrosion due to chloride ingress using a modified ASTM G109 method. In addition, the apparent chloride diffusion coefficient of concrete produced with CAC and CSA cement was determined per ASTM C1556 "Standard Test Method for Determining the Apparent Chloride Diffusion Coefficient of Cementitious Mixtures by Bulk Diffusion", while the bulk resistivity measurements from a previous study involving these cements were assessed.

9.2 EXPERIMENTAL

9.2.1 Materials

This study involves testing various cement systems categorized as pure cements (i.e. cements that are not blended with any other material), proprietary blends (i.e. cements pre-blended with other materials during production), and lab blends (i.e. laboratory blended cements, 25% CAC + 75% PC and 25% CSA + 75% PC). The reason for the various categories is to depict the current practice in the use of CAC and CSA

cements. Due to the high cost of pure CAC and CSA cements, (i.e. CAC and CSA cements that are not blended with any other materials), their use is currently limited to niche areas where their special qualities are required [15, 16]. However, there are also cases where CAC and CSA cements are blended with OPC to accelerate the hydration of OPC and reduce the high cost of using CAC and CSA cements only [17-20]. CAC and CSA cements are also blended with supplementary cementitious materials (SCM) such as fly ash to improve their durability performance and with other chemical admixtures that are used to control their workability [15, 16, 18]. The blending of CAC and CSA cements with other materials such as OPC, SCMs, and other chemical admixtures is usually carried out during cement production or in the process of mixing concrete. Therefore, including the proprietary blended and laboratory blended cement categories in this study was reasonable. The 25%/75% proportion for the laboratory blended cements was adopted because it was the optimum blend that satisfied both economy and mechanical performance. A description of these cements and their chemical compositions are shown in Tables 9.1 and 9.2, respectively. In Table 9.1, the controls OPC Type I/II (labeled as OPC2) and OPC Type III (labeled as OPC3) were used due to their different rates of hydration and strength development. OPC Type III has finely ground cement particles, which hydrate faster than OPC Type I/II and thereby show greater strength and microstructural development at an early age [21]. Also, in Table 9.1, the terms CSA ye'elmite cement and CSA belite cement were used to indicate the main phases in the CSA cements and to assess the impact of the hydration rate of these phases and their hydration products in resisting corrosion due to chloride-ion ingress. The ye'elmite phase is responsible for rapid early strength gain and microstructural development in CSA cements, while the belite phase is responsible for later strength gain and microstructural development in CSA cements [22, 23]. The phase compositions for the CSA cements in Table 9.1 were calculated using modified Bogue equations adapted from Iacobescu et al. [23].

Table 9.1: Description of individual cement

Cement Type	Cement ID	SiO_2	Al_2O_3	Fe_2O_3	CaO	MgO	SO_3	Na_2O	K_2O	Na_2O_e	LOI
Pure Cements	OPC2	21.06	4.02	3.19	63.91	1.08	2.89	0.14	0.61	0.53	2.29
	OPC3	19.67	5.34	1.76	63.41	0.99	5.27	0.10	0.44	0.39	4.06
	CAC	4.34	38.65	15.09	38.37	0.39	0.16	0.05	0.14	0.14	1.55
	CSA1	9.07	21.61	2.26	45.26	0.94	20.26	0.07	0.30	0.27	1.05
	CSA2	20.56	16.14	1.35	45.31	1.23	14.73	0.77	0.72	1.24	4.74
Proprietary Blended Cements	CAC-B1	13.46	12.23	2.67	56.65	2.86	9.90	0.20	0.79	0.72	1.21
	CAC-B2	12.71	32.94	12.95	35.09	1.79	0.84	0.50	0.24	0.65	1.23
	CSA-B1	13.63	15.82	0.75	51.28	1.14	16.62	0.29	0.62	0.69	3.06
	CSA-B2	14.72	14.37	1.22	53.85	1.23	14.40	0.10	0.59	0.49	3.39
	PCSA1	17.38	11.06	2.98	55.82	1.25	10.68	0.43	0.52	0.77	2.26
	PCSA2	20.14	15.73	3.52	43.90	1.55	12.88	0.59	0.52	0.93	1.95
Lab Blends	CAC-OPC2	16.53	10.79	2.71	58.07	0.89	7.43	0.14	0.50	0.47	2.19
	CSA1-OPC2	18.06	8.42	2.96	59.25	1.04	7.23	0.12	0.53	0.47	1.98

Table 9.2: Chemical composition of the individual cement

Cement Type	Cement ID	SiO_2	Al_2O_3	Fe_2O_3	CaO	MgO	SO_3	Na_2O	K_2O	Na_2O_e	LOI
Pure Cements	OPC2	21.06	4.02	3.19	63.91	1.08	2.89	0.14	0.61	0.53	2.29
	OPC3	19.67	5.34	1.76	63.41	0.99	5.27	0.10	0.44	0.39	4.06
	CAC	4.34	38.65	15.09	38.37	0.39	0.16	0.05	0.14	0.14	1.55
	CSA1	9.07	21.61	2.26	45.26	0.94	20.26	0.07	0.30	0.27	1.05
	CSA2	20.56	16.14	1.35	45.31	1.23	14.73	0.77	0.72	1.24	4.74
Proprietary Blended Cements	CAC-B1	13.46	12.23	2.67	56.65	2.86	9.90	0.20	0.79	0.72	1.21
	CAC-B2	12.71	32.94	12.95	35.09	1.79	0.84	0.50	0.24	0.65	1.23
	CSA-B1	13.63	15.82	0.75	51.28	1.14	16.62	0.29	0.62	0.69	3.06
	CSA-B2	14.72	14.37	1.22	53.85	1.23	14.40	0.10	0.59	0.49	3.39
	PCSA1	17.38	11.06	2.98	55.82	1.25	10.68	0.43	0.52	0.77	2.26
	PCSA2	20.14	15.73	3.52	43.90	1.55	12.88	0.59	0.52	0.93	1.95
Lab Blends	CAC-OPC2	16.53	10.79	2.71	58.07	0.89	7.43	0.14	0.50	0.47	2.19
	CSA1-OPC2	18.06	8.42	2.96	59.25	1.04	7.23	0.12	0.53	0.47	1.98

Other materials used in this study are well-graded limestone rocks, siliceous river sand, a liquid polycarboxylate-ether-based superplasticizer, and a set retarder, citric acid, which was used to delay setting and allow time for mixing and casting. A total of 10 different cement mixtures were produced for the laboratory corrosion study (ASTM G109), as shown in Table 9.3, excluding PCSA1 and PCSA2. However, the chloride penetration test (ASTM C1556 and ASTM C1152) was carried out with all the cement mixtures in Table 9.3. A total cement content of 446 kg/m^3 (752 lb/yd^3) and a W/CM ratio of 0.35 was used for all mixtures except CSA2, CSA-B1, and CSA-B2 which were produced with a total cement content of 390 kg/m^3 (658 lb/yd^3) and W/CM ratio of 0.38 based on manufacturers recommendation.

Table 9.3: Concrete mixture proportions

Cement Type	W/CM	Total Cement kg/m^3(lb/yd^3)	Replacement Level of Cement with Second Cement Blend (% of Control Cement Type by Mass)	
			Control Cement	Type I/II
OPC2	0.35	446 (752)	100%	-
OPC3	0.35	446 (752)	100%	-
CAC	0.35	446 (752)	100%	-
CSA1	0.35	446 (752)	100%	-

CSA2	0.38	390 (658)	100%	-
CAC-B1	0.35	446 (752)	100%	-
CSA-B1	0.38	390 (658)	100%	-
CSA-B2	0.38	390 (658)	100%	-
PCSA1	0.35	446 (752)	100%	-
PCSA2	0.35	446 (752)	100%	-
CAC-OPC2	0.35	446 (752)	25%	75%
CSA1-OPC2	0.35	446 (752)	25%	75%

9.2.2 Sample Preparation

Six reinforced concrete samples of dimension 280 x 115 x 153 mm (11 x 4.5 x 6 in) were produced for each of the ten mixtures used in laboratory corrosion investigation according to ASTM G109 (see Figure 9.1). The steel reinforcements were sandblasted to remove any existing corrosion product before casting. While casting the samples, a crack depth of 10 mm and width of 1.0 mm was introduced in two samples out of the six samples produced for each mix using a plastic shim, as shown in Figure 9.2. The plastic shims were removed after the samples attained the final set, thus leaving the desired crack. Initial curing was done with wet burlap and plastic sheet covers after casting for 24 hours. At the end of the 24-hour cure, the samples were removed from the molds and transferred to a curing room at 23°C and 100% RH where they were cured for an additional six days. To reduce saturation levels after curing, the samples were placed in a drying room at 23°C and 50% RH for 14 days. At the end of the drying period, two more laboratory corrosion samples out of the six for each mix were placed in an accelerated carbonation chamber at 4% CO_2 concentration and 57% RH for 28 days, as shown in Figure 9.3. The depth of carbonation of the corrosion samples at 28 days (Table 9.4) was obtained by measuring accelerated carbonation samples of dimensions 100 x 100 x 350 mm (4 x 4 x 14 in), which were produced from the same mix as the corrosion samples and treated the same way as the corrosion samples. A plastic dam of dimension 150 x 75 x 75 mm (6 x 3 x 3 in) was fixed at the top of each corrosion sample, as shown in Figure 9.1, and all the surfaces of the corrosion samples were coated with a two-part epoxy except the surface inside the dam. To make connections between the top and bottom reinforcement as prescribed in ASTM G109, 16-gauge copper wires and 100-ohm resistors were soldered together and attached to the end of the rebars with the aid of threaded screws. Going into the testing phase, they were 2 cracked, 2 carbonated, and 2 normal corrosion samples for each of the ten mixtures for the laboratory corrosion studies.
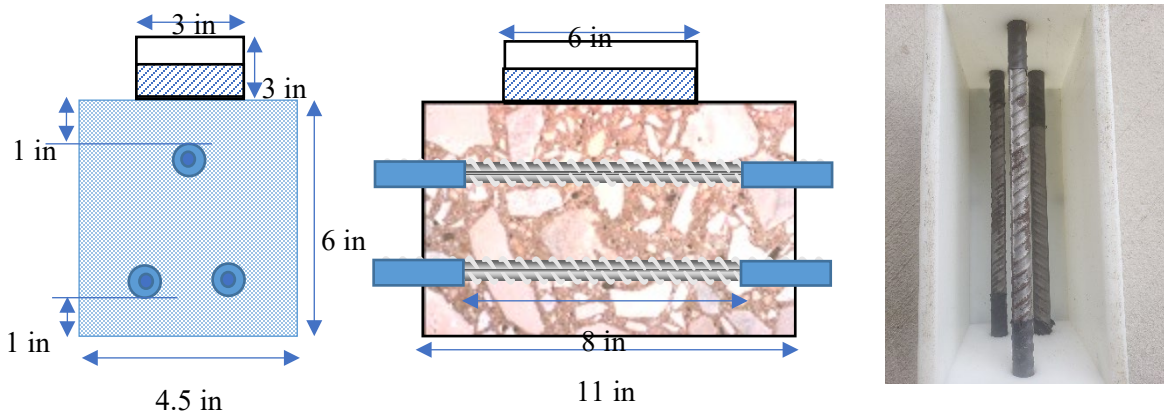
Figure 9.1: Schematic representation of ASTM G109 samples

Figure 9.2: Set-up for crack introduction

Table 9.4: Carbonation depth at day 28 for carbonated corrosion samples

Cement Type	Depth (mm)	Deviation (mm)
OPC2	0	± 0
OPC3	0	± 0
CAC	7	± 1.04
CSA1	6.9	± 0.86
CSA2	8.8	± 1.30
CAC-B1	7.9	± 1.66
CSA-B1	9.2	± 1.04
CSA-B2	10.3	± 1.50
CAC-OPC2	5.4	± 2.29
CSA1-OPC2	4.4	± 0.62

Figure 9.3: Accelerated carbonation chamber.

Aside from the corrosion samples, one concrete cylinder of dimensions 100 x 200 mm (4 x 8 in) were produced for each of the mixtures in Table 9.3. The concrete cylinder was transferred into the same curing room as the corrosion samples after the initial 24-hour cure with wet burlap. The concrete cylinder was used in the chloride penetration test per ASTM C1556. The concrete cylinder was cut to obtain the top 75 mm from the finished surface as the test specimen, while an additional 20 mm slice cut from the remainder of the sample was used to determine the initial chloride content. The test specimen was coated with a two-part epoxy except for the sawn surface. Following the epoxy coating, the test specimens were immersed in a saturated calcium hydroxide water bath and weighed every 24 hours until their mass change was not more than 0.1% in 24 hours. Finally, the sample was soaked for 6 months in NaCl solution prepared by dissolving 165 grams of NaCl in a liter of de-ionized water.

9.2.3 Testing

All laboratory corrosion samples (cracked, carbonated, and normal) were placed in the drying room at 23°C and 50% RH before ponding with NaCl. The test samples were ponded with 3% NaCl (30g/ liter of de-ionized water) for 2 weeks, after which they were allowed to dry for another 2 weeks before the process was repeated. During the wet cycles, the top of the dams was covered with aluminum foils to reduce evaporation. The wet and dry cycles allowed for the ingress of chlorides as well as oxidizing agents (oxygen). Macrocell corrosion measurements were done at the end of the first week of each wet

cycle. The macrocell corrosion for all samples was measured by determining the voltage drop across the resistor in millivolts using a voltmeter. The measurement with the voltmeter was done by connecting the negative terminal of the voltmeter to the top bar and the positive terminal to the bottom bar. The voltage drop obtained was used in calculating the microcell current in micro Ampere (μA) using Equation 9.2 [14].

$$I = \frac{V}{R}$$
<div align="right">Eq. 9.2</div>

Where V is the voltage drop between the top and bottom bars in (μV), and R is the resistance of the resistor (100 ohms).

Microcell corrosion measurements were done at the end of each two-week wet cycle. The measurements were carried out with Gamry testing equipment and software using the Linear Polarization Resistance (LPR) technique. Before each microcell corrosion measurement, the wire connection at the top rebar of every sample was disconnected and allowed to stay for 1-2 hours. Afterward, the NaCl solution in the dam was removed with the aid of a vacuum cleaner. A stainless-steel apparatus was used as the counter electrode. This apparatus was built to have a vertical hollow and base that can fit into the dam and make contact with the surface of the concrete via a damp sponge. A silver/silver chloride (Ag/AgCl) reference electrode was passed through the hollow and made contact with the concrete surface via the damp sponge. The top rebar, which is nearer to the pond surface and potentially susceptible to microcell corrosion, served as the working electrode. The electrodes were connected to the Gamry instrument and computer system, as shown in Figure 9.4.

Figure 9.4: Configuration for microcell corrosion measurement

The LPR technique executed by the Gamry instrument helped to measure the half-cell potential (E_{corr}) of the top rebar (working electrode) relative to the reference electrode (Ag/AgCl electrode) and the microcell corrosion current (I_{corr}). In the LPR technique, the equipment first measures the open circuit potential, also known as the half-cell potential (E_{corr}) of the rebar under study, and then shifts the potential $\pm$ 10mV from the E_{corr}. The current due to the shift in potential and the consequent resistance is known as the corrosion current (I_{corr}), and polarization resistance (R_p), respectively. The I_{corr} is given by Equation 9.3 [24]:

$$I_{corr} = \frac{\beta_a \beta_c}{2\cdot303(\beta_a + \beta_c)} \left(\frac{1}{R_p}\right) \qquad \text{Eq. 9.3}$$

Where R_p is the polarization resistance, β_a is the anodic Beta coefficient in volts/decade, and β_c is the cathodic Beta coefficient in volts/decade. The Beta coefficients, also known as Tafel coefficients, were assumed to be 120 mV which is the value usually used for reinforcing steel actively corroding in concrete [18]. Since the perturbation current applied during the potential shift was done via the counter electrode, the corrosion current density was calculated using Equation 9.4:

$$i_{corr} = \frac{I_{corr}}{A} \qquad \text{Eq. 9.4}$$

Where A is the base area of the counter electrode in cm^2, I_{corr} is the corrosion current in μA, and i_{corr} is the corrosion current density in $\mu A/cm^2$. The half-cell potential and corrosion current density were used in analyzing the rate of microcell corrosion in the laboratory corrosion samples.

The specimens for the chloride penetration test were removed from the NaCl solution after 6 months of exposure. The edges of the specimen were cut off to remove the epoxy coating before profile grinding. The profile grinding process was done in eight increments. The first was about 1mm, followed by three 3 mm increments and four 5 mm increments. Due to the difficulty in attaining the precise mentioned increments, a digital caliper was used to measure the exact depth during the grinding process. The chloride content of each layer was determined by performing potentiometric titration with the aid of an automated titrator which is connected to a 0.1M silver nitrate source and an Ag/AgCl reference electrode. To carry out the titration, 2g of the profiled concrete powder was weighed in a 100 mL beaker. The concrete powder was dissolved by adding 2 mL of 50% v/v nitric acid to the beaker. The mixture was stirred with a glass rod and allowed to stand for 1 hour. Afterward, 2 mL of 0.5M sodium acetate was added, followed by de-ionized water up to the 80 mL mark on the beaker. A magnetic stirrer was dropped in the beaker before placing it on the titrator stir table to enable stirring during titration. The titrator dispensed silver nitrate into the beaker until an equivalence point was reached. The equivalence point was used in calculating the total chloride percent by mass of concrete.

9.3 RESULTS AND DISCUSSION

9.3.1 Macrocell Corrosion

Figures 9.5, 9.6, and 9.7 show the average macrocell current of the cracked, carbonated, and normal corrosion samples, respectively.
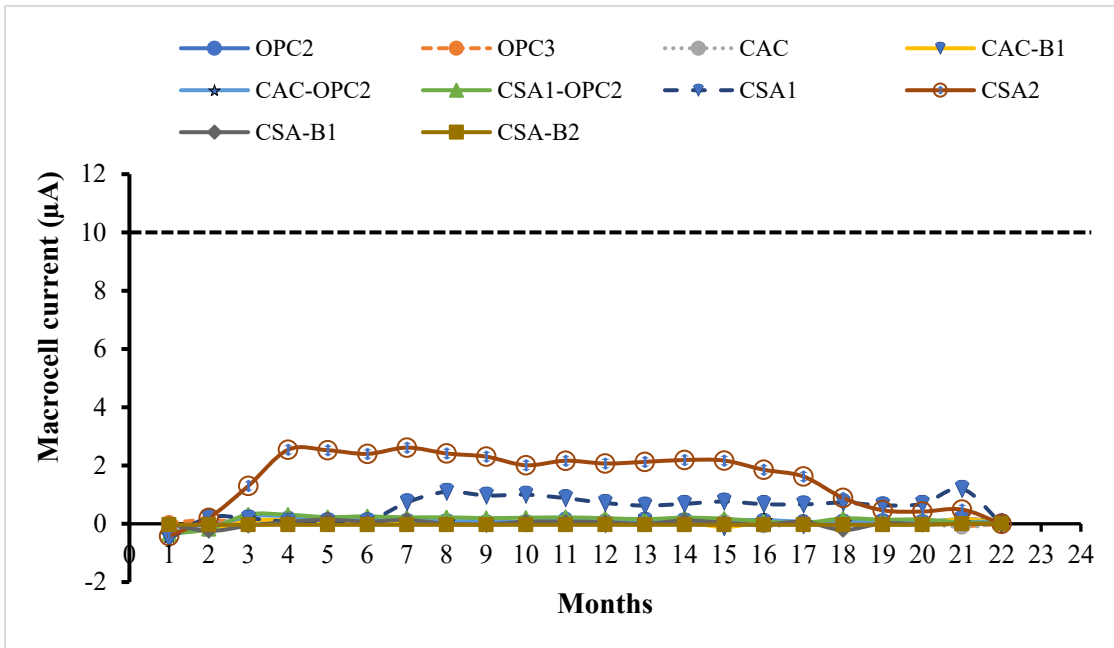
Figure 9.5: Macrocell corrosion current for cracked samples
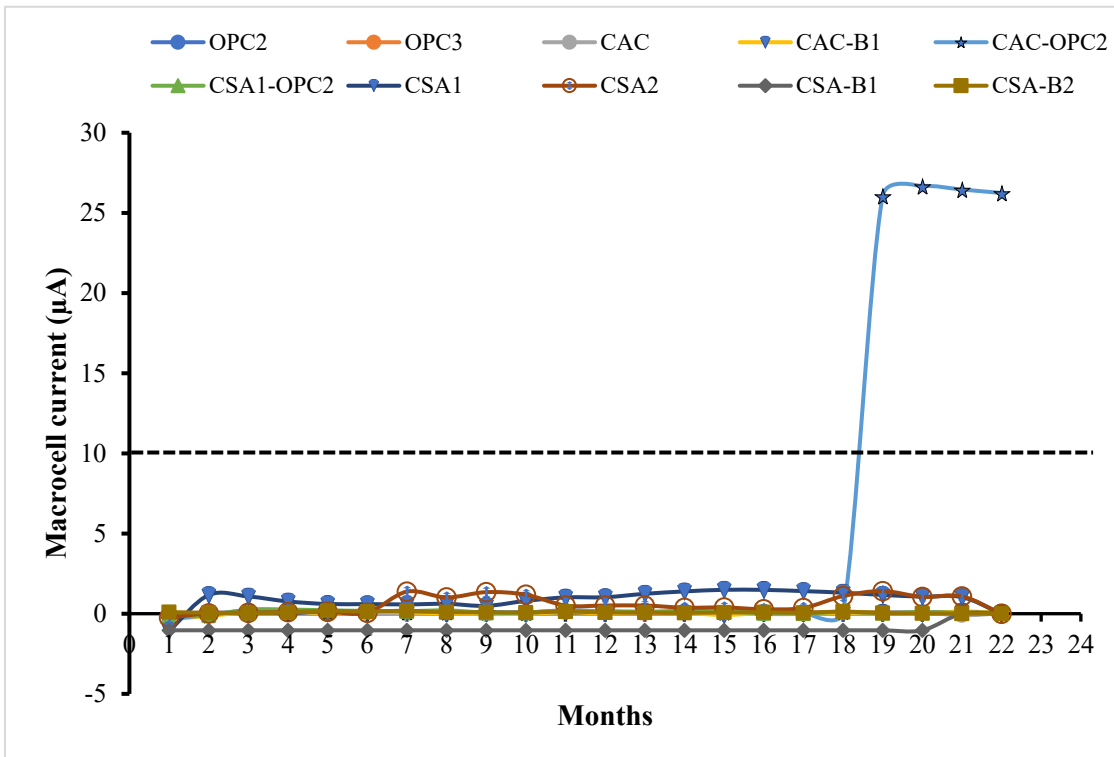
Figure 9.6: Macrocell corrosion current for carbonated samples
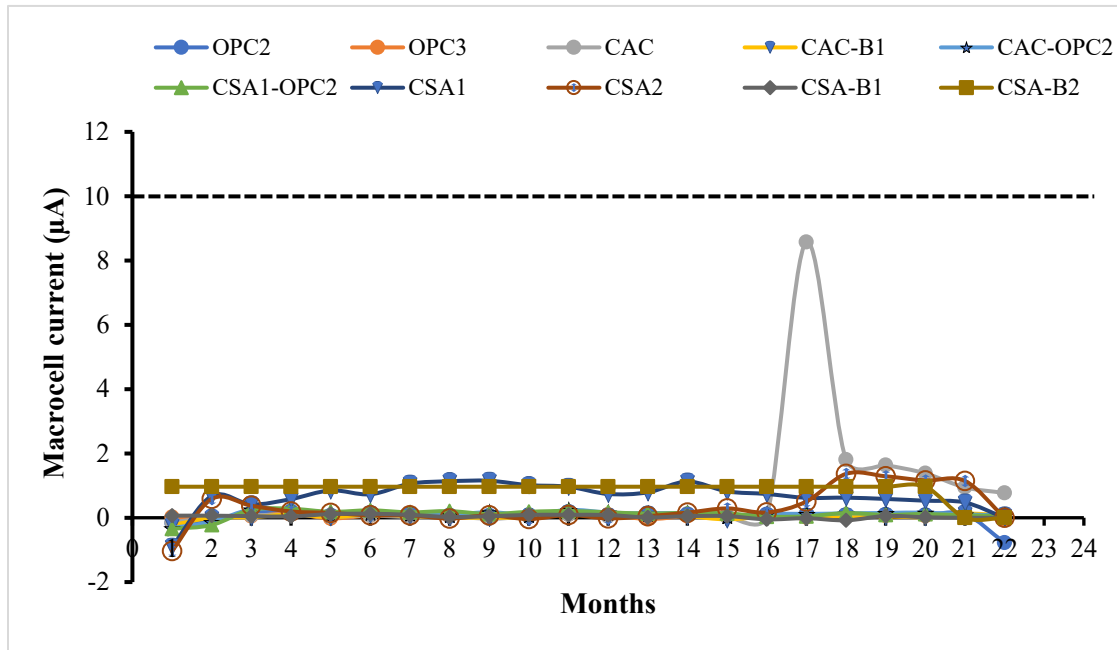
Figure 9.7: Macrocell corrosion current for normal samples

According to ASTM G109, the current due to macrocell corrosion should be monitored every four weeks until the average macrocell current reaches 10 µA and at least half of the samples show a current greater than 10 µA. This is to ensure sufficient corrosion before visual evaluation. The black dashed lines in Figure 9.5, 9.6, and 9.7 was added to indicate the 10 µA limit per ASTM G109. In Figure 9.5, the majority of the cracked samples showed little macrocell current far below the 10 µA limit throughout the monitoring period. This could imply that the rebars are not actively corroding. However, the samples for the pure cement CSA1 and CSA2 showed an increase in macrocell current compared to other samples. This performance of CSA1 and CSA2 could be a result of their low binding capacity and low Friedel salt content [7], which is further worsened by the presence of the introduced crack. The combined effect of binding capacity and crack could increase the number of free chlorides in the CSA samples and reduce the time to reach the chloride threshold necessary to initiate corrosion.

Figure 9.6 shows that the measurements so far on the carbonated samples indicate a relatively low macrocell current below the 10 µA limit except for the CAC-OPC2 blend. This high current produced by CAC-OPC2 over a consecutive 4-month period could imply that the rebar is actively corroding. However, this performance of CAC-OPC2 compared to other cement was unexpected. OPC2 is known to produce $CaCO_3$ during carbonation, which helps to clog pore networks hence reducing porosity and chloride ingress [17, 25]. So, the CAC-OPC2 was expected to show more resistance than the performance in Figure 9.6. There is a need to compare the performance of CAC-OPC2 with the results of other

206

monitoring techniques as well as visual evaluation of the sample upon attaining the ASTM G109 requirement. Figure 9.7 also shows a relatively low macrocell current below the 10 µA limit for all normal samples throughout the monitoring period. The sudden spike and decline in macrocell current by CAC in the 18th month could be due to the repassivation of a damaged passive film on the rebar due to chloride ions.

9.3.2 Microcell Corrosion

Figures 9.8, 9.9, and 9.10 show the half-cell potential of the cracked, carbonated, and normal samples over 21 months, respectively.
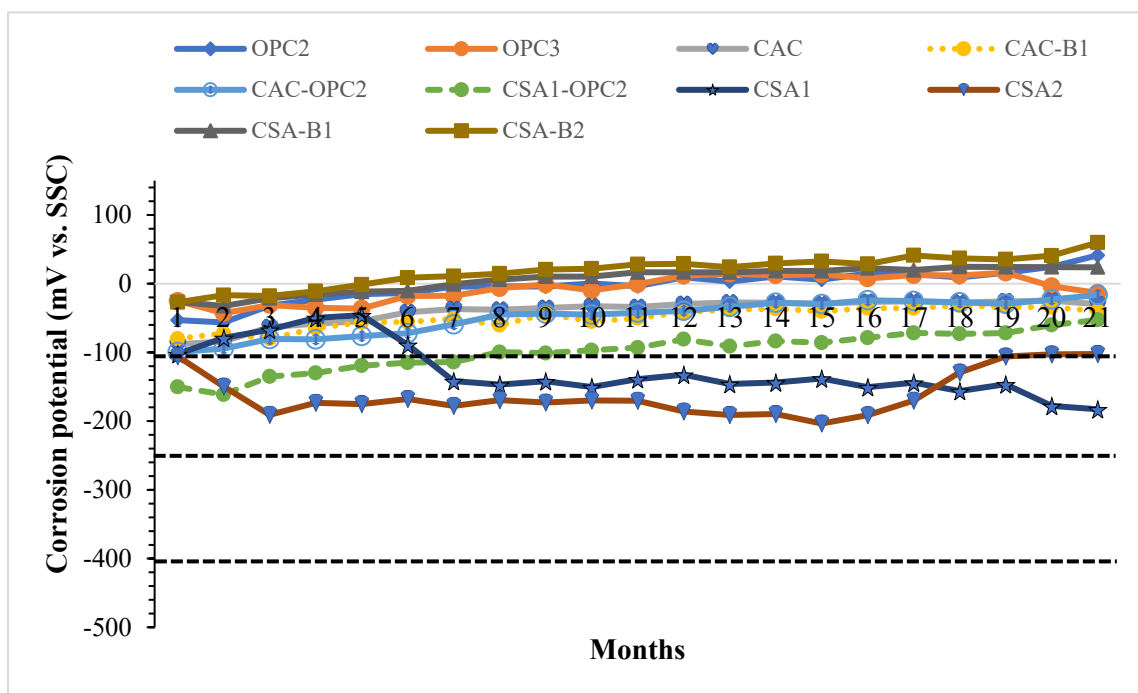
Figure 9.8: Half-cell measurements relative to Ag/AgCl for cracked samples
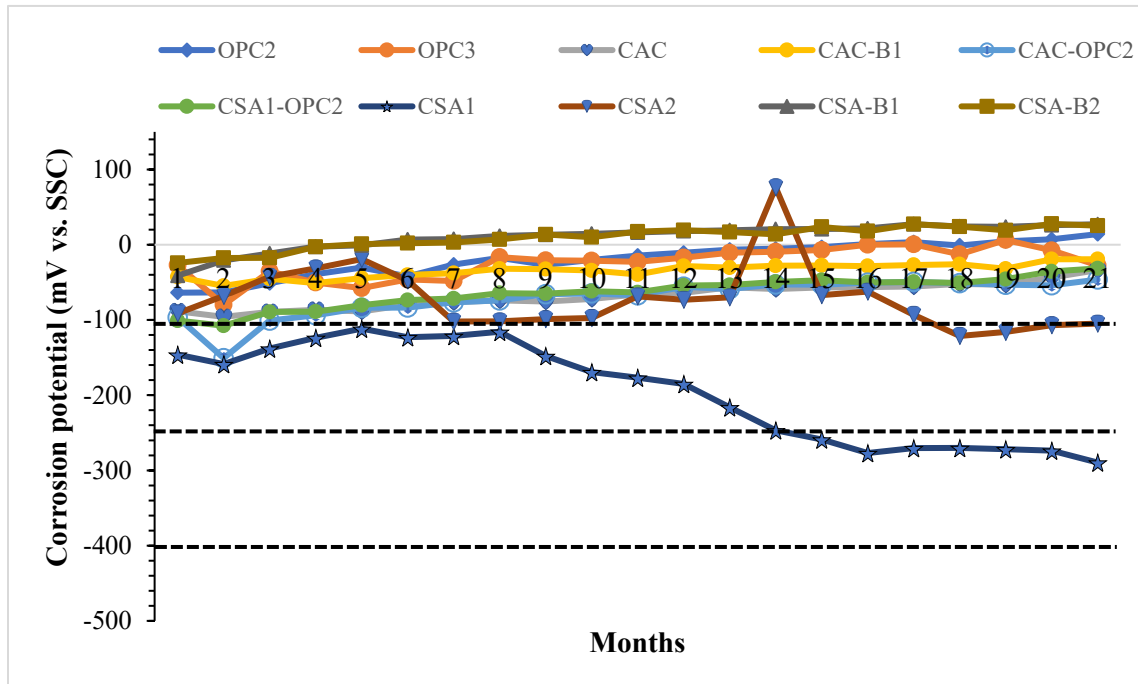
Figure 9.9: Half-cell measurements relative to Ag/AgCl for carbonated samples
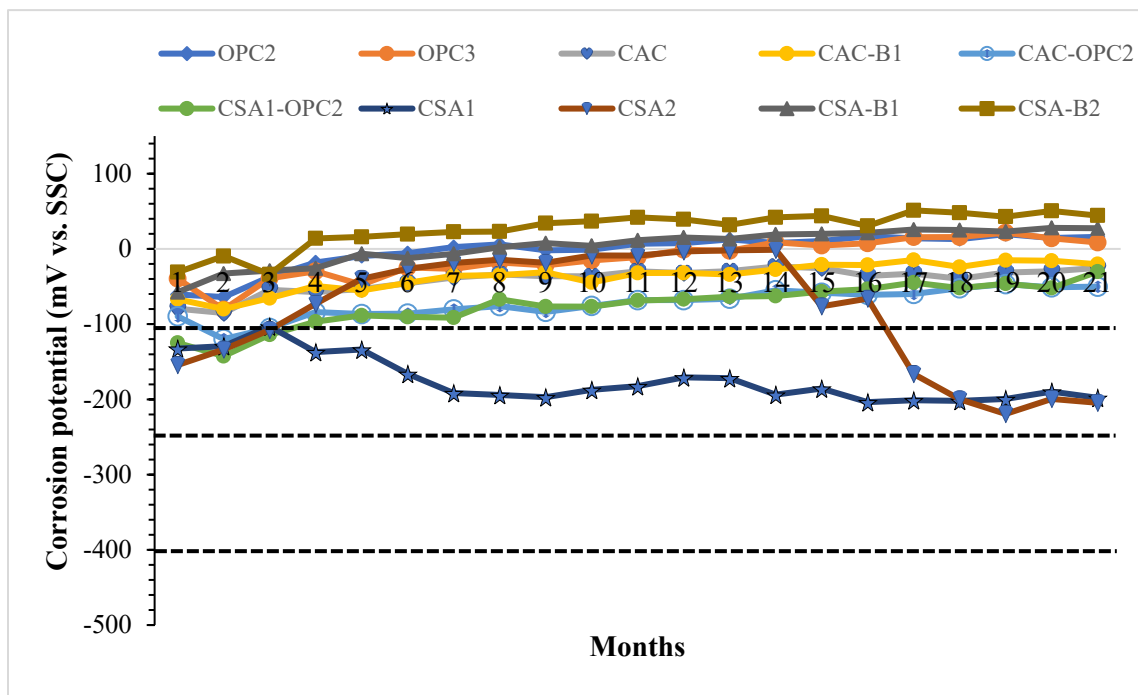
Figure 9.10: Half-cell measurements relative to Ag/AgCl for normal samples

In using half-cell potential for monitoring the corrosion activity on the rebar, an increasing negative value is assumed to indicate an increase in corrosion activity. However, this depends on the propensity of the

iron (rebar) to dissolve and the availability of oxygen [24]. To analyze the corrosion activities in the samples using their measured potentials, reference was made to Table 9.5, which was developed based on ASTM C876 criteria for classifying corrosion activity within a system. Though ASTM C876 was developed for a $Cu/CuSO_4$ reference electrode [26], Table 9.5 presents the equivalent Ag/AgCl potentials.

Table 9.5: Risk of corrosion using Half-cell potential [27]

Corrosion potential (mV vs Ag/AgCl)	Condition
> -106	Low (< 10% risk of corrosion)
-106 to -256	Intermediate (50% risk of corrosion)
-256 to -406	High (> 90% risk of corrosion)
< -406	Severe corrosion

The black dashed lines in Figures 9.8, 9.9, and 9.10 were added to indicate the limits shown in Table 9.5. In Figure 9.8, the majority of the cacked samples showed a low risk of corrosion as they all started from a negative potential, probably due to passivation, and increased towards a positive potential. The few exceptions in Figure 9.8 are the cracked samples produced with CSA1 and CSA2. The CSA1 and CSA2 samples appear to fall within the intermediate region, as described in Table 9.5. This means that there is a 50% chance risk of corrosion in those samples. This performance of the cracked cement mixtures using their half-cell potential is in agreement with that inferred by comparing their macrocell current in Figure 9.5. Again, the performance of CSA1 and CSA2 based on their half-cell potential can be attributed to their low binding capacity and low Friedel salt content. The CSA1-OPC2 blend in Figure 9.8 showed an improvement in resisting corrosion as it started with a high potential like CSA1 and CSA2 but later continued to increase towards a positive potential with time.

Figure 9.9 shows that the majority of the carbonated samples produced potential that indicated a low risk of corrosion. However, CSA1 and CSA2 exhibited the least resistance to corrosion. Though this time, CSA1 appeared to have exhibited higher negative potentials considered in Table 9.5 as a high risk of corrosion due to carbonation. CSA cement concrete has low alkali content; hence they tend to carbonate faster than OPC. The carbonation process also breaks down the AFt phases in CSA concrete, thus increasing porosity and chloride-ion ingress [7].

Figure 9.10 also shows a low risk of corrosion for most of the normal samples except for CSA1 and CSA2, which showed high negative potentials considered intermediate (50% chance of corrosion), as shown in Table 9.5. However, CSA2 appears to have shown a higher resistance to corrosion than CSA1 considering its increase toward a positive potential until the 14th month, when it declined toward a more negative potential. The difference in resisting corrosion due to chloride-ion ingress observed among the

samples (cracked, carbonated, and normal) could be attributed to factors such as porosity, chloride binding capacity, and the effect of carbonation in the concrete microstructure.

Figures 9.11, 9.12, and 9.13 show the current density of the cracked, carbonated, and normal samples, respectively.
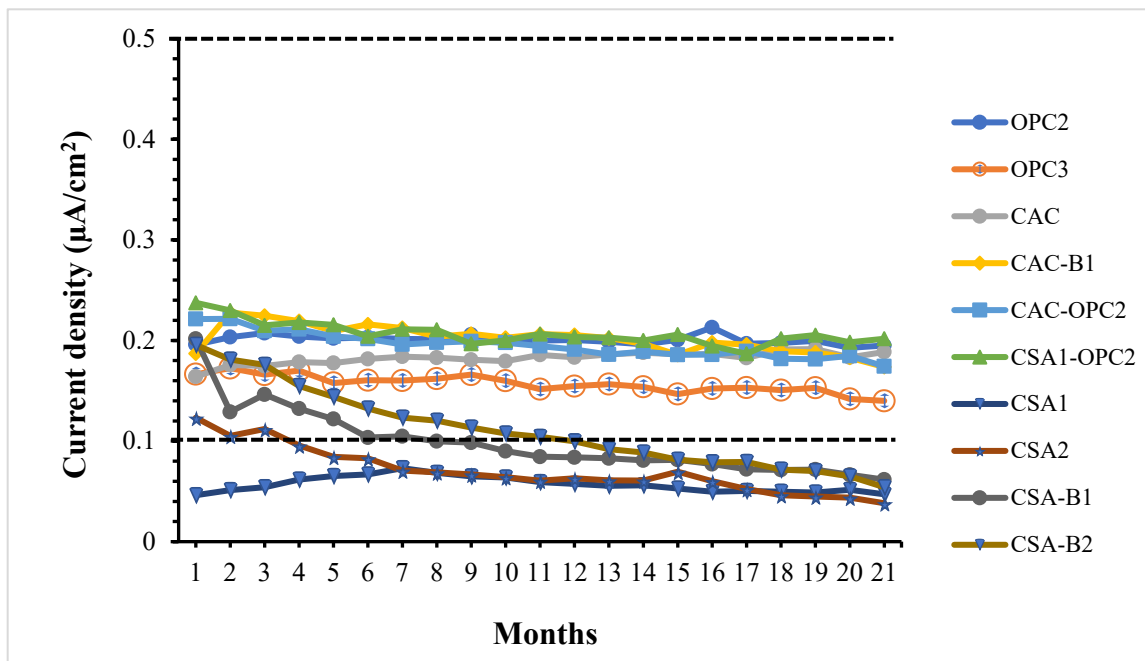
Figure 9.11: Current density from LPR measurements for cracked samples
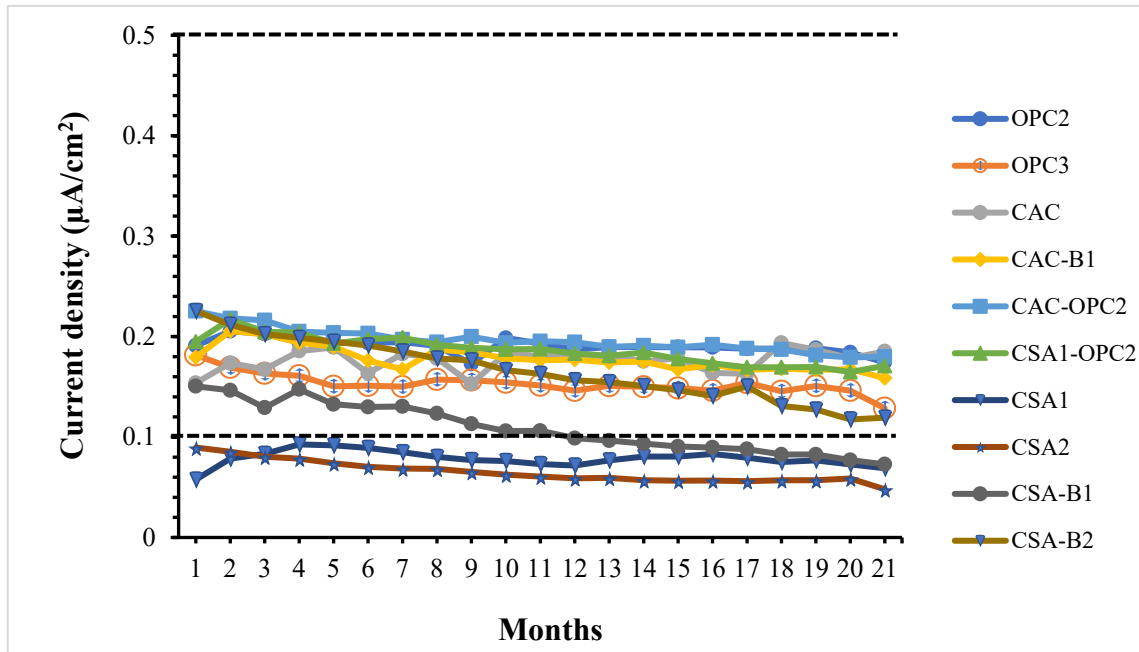
Figure 9.12: Current density from LPR measurements for carbonated samples
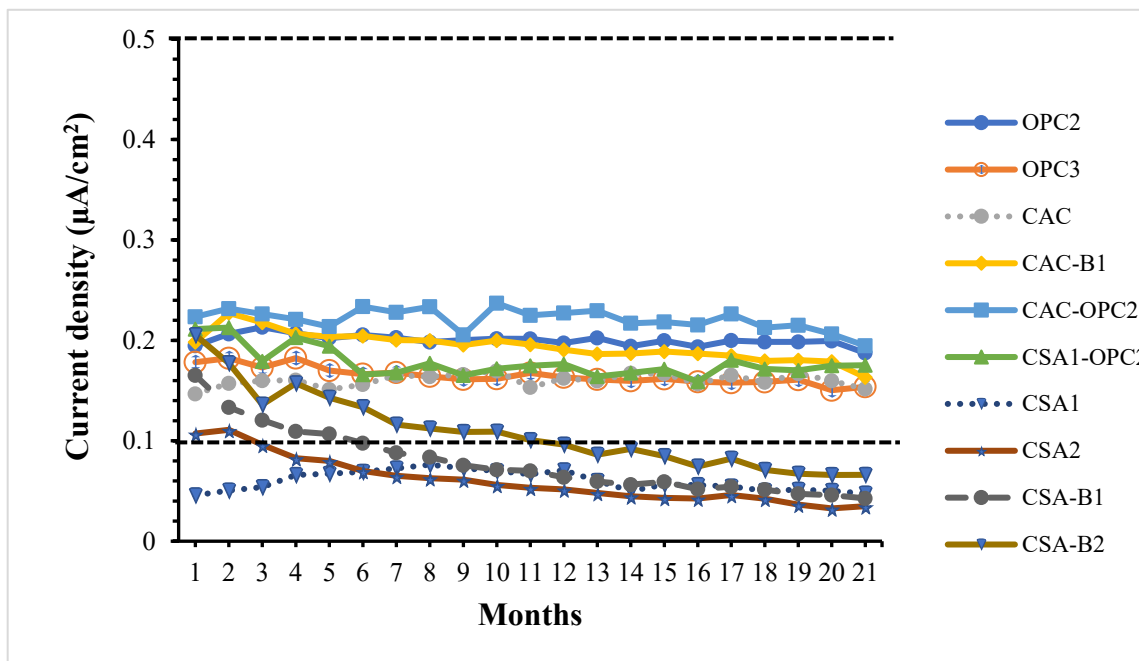
Figure 9.13: Current density from LPR measurements for normal samples

Table 9.6: Risk of corrosion using corrosion current density [18, 27, 28]

Corrosion current density ($\mu A/cm^2$)	Corrosion classification
Up to 0.1	Passive condition
0.1 – 0.5	Low to moderate corrosion
0.5 – 1	Moderate to high corrosion
More than 1	High corrosion rate

The increase in corrosion activity is expected to increase the corrosion current density. Hence, the LPR current densities measured in this study are analyzed by comparing the values with corrosion current density ranges that have been used by several authors in classifying the corrosion rate in reinforced concrete based on the LPR technique. The ranges of corrosion current density are presented in Table 9.6. Also, the black dashed lines in Figures 9.11, 9.12, and 9.13 are included to indicate the current density ranges in Table 9.6. Figures 9.11, 9.12, and 9.13 show that the cracked, carbonated, and normal samples showed current density values that classified them under the passive to moderate corrosion category, as shown in Table 9.6. This performance of the samples (cracked, carbonated, and normal) based on their current density appears to be consistent with that of the macrocell current and half-cell potential.

9.3.3 Chloride Penetration

Figure 9.14 presents the chloride profiles of the concrete mixtures in Table 9.3 after immersion in 165g/L NaCl for 6 months. While Table 9.7 shows their diffusion coefficients and surface concentrations. In the presence of a chloride concentration gradient, chlorides ingress into saturated concrete through the process of diffusion. Hence, diffusion coefficients and surface concentrations are important for comparing the performance of concrete as it relates to chloride ingress [18]. The diffusion coefficient values in Table 9.6 were determined per ASTM C1556 by fitting the chloride profiles to Fick's second law using a non-linear regression analysis and the least square method.
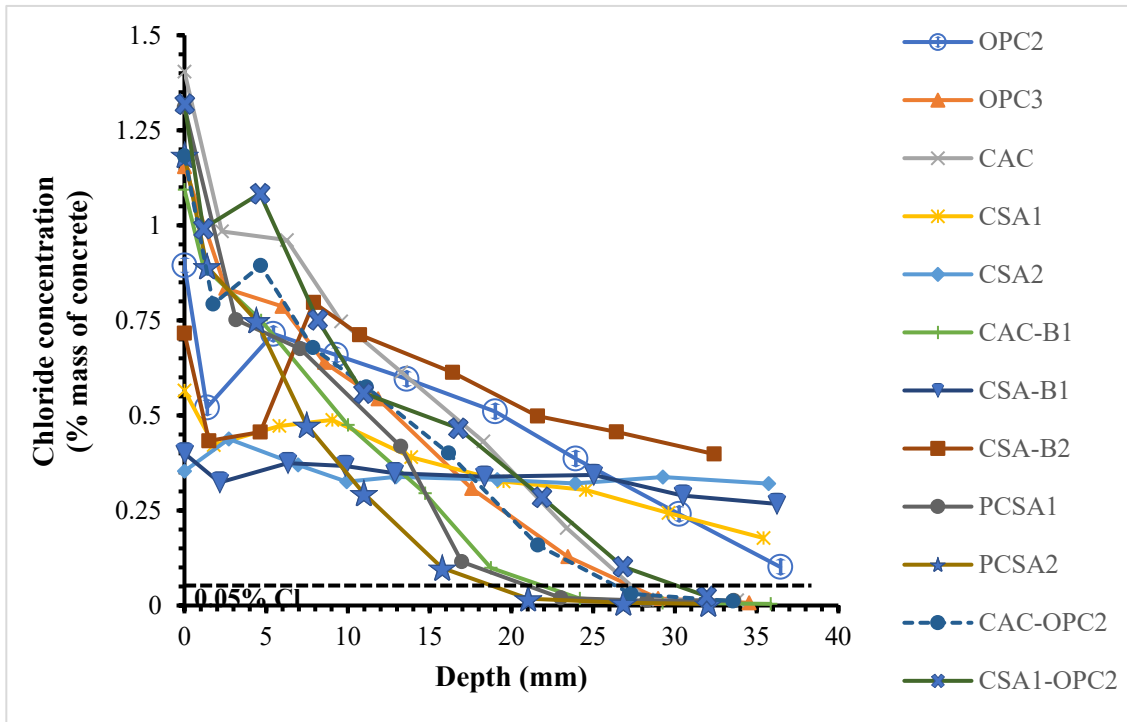
Figure 9.14: Chloride penetration for the cement mixtures

Table 9.7: Diffusion coefficient and surface concentration after 6 months of ponding

Cement Type	Surface concentration, C_S (%)	Diffusion coefficient, D_C (m²/s)
OPC2	0.89	6.25E-12
OPC3	1.15	1.78E-12
CAC	1.40	2.00E-12
CSA1	0.57	1.04E-11
CSA2	0.35	6.75E-10
CAC-B1	1.09	1.16E-12
CSA-B1	0.40	6.41E-11
CSA-B2	0.72	2.94E-11
PCSA1	1.31	1.00E-12
PCSA2	1.18	6.46E-13
CAC-OPC2	1.18	1.79E-12
CSA1-OPC2	1.32	2.00E-12

The corrosion of steel rebar due to chloride-ion occurs only when the amount of free chlorides near the surface of the steel reaches a threshold that can destroy the passive protective film on the rebar [24]. To analyze the chloride penetration of each cement mixture, a chloride threshold of 0.05% by mass of

concrete was assumed, as indicated by the black dashed line in Figure 9.14. This assumed value of the threshold is a commonly used value for assessing the ingress of chloride in standard steel-reinforced concrete [18, 24]. However, there is no one generally accepted chloride threshold due to the various measuring techniques for chloride and the complexity of reinforced concrete chemistry [29].

In Figure 9.14, based on a chloride threshold of 0.05% by mass of concrete, the proprietary blended cement PCSA2 showed the highest resistance to chloride-ion ingress with penetration of approximately 19 mm. PCSA2 also showed the least diffusion coefficient, as shown in Table 9.7. Following PCSA2 are PCSA1, CAC-B1, CAC-OPC2, OPC3, CAC, and CSA1-OPC2 with penetrations of approximately 21 mm, 22mm, 26 mm, 27 mm, 27mm, and 30 mm, respectively. The diffusivity of chloride in the above-mentioned mixtures, as represented by their diffusion coefficients in Table 9.7, also follows the same order. Also, the surface concentration of the above-mentioned mixtures is in the range of 1 - 1.4%, with CAC having the highest surface concentration. The high surface concentration exhibited by these mixtures can be attributed to a high binding capacity which reduces the available free chloride in these mixtures.

Figure 9.14 also showed that CSA2, CSA-B1, CSA-B2, CSA1, and OPC2 showed higher chloride content beyond the assumed 0.05% threshold in the total depth assessed during grinding. However, CSA2 showed the highest diffusion coefficient, followed by CSA-B1, CSA-B2, and CSA1, as shown in Table 9.6. The surface concentrations of CSA2, CSA-B1, CSA-B2, and CSA1 are 0.35, 0.4, 0.72, and 0.57, respectively. This low surface concentration and high diffusion coefficients exhibited by these CSA cements confirm their low binding capacity and low Friedel salt content, which consequently increases the number of free chlorides in the CSA samples and reduces the time to reach the chloride threshold necessary to initiate corrosion.

The control OPC3 showed more resistance to chloride ingress compared to the control OPC2. This can be attributed to the higher amount of C_3A in OPC3 compared to OPC2. C_3A is necessary for producing Friedel salt, which helps to slow the transport of chlorides in concrete [2]. Also, the lab-blended cements CAC-OPC and CSA1-OPC2 showed improved performance in resisting chloride ingress due to the presence of OPC compared to CAC and CSA1. Comparing CAC and CAC-B1 with CSA2, CSA-B1, CSA-B2, and CSA1 in Figure 9.14 and Table 9.7, it can be seen that the CACs outperformed the CSAs in resisting chloride-ion ingress. This is attributed to the chloride binding capability of CAC hydrates which increases as alumina (Al_2O_3) content of the CAC increases [8]. The outstanding performance of the proprietary blended cement PCSA1, PCSA2, and CAC-B1 in resisting chloride penetration can be attributed to the blended materials by the proprietors during production. The performance of PCSA1 and

PCSA2 could have been a result of blending OPC, CSA, and permeability-reducing admixtures. Since PCSA2 contains fly ash, the filler effect of fly ash might have been the reason for the low penetrability exhibited by PCSA2 compared to the other cements [30]. CAC-B1 chloride penetrability can be attributed to the blending of OPC and CAC, thus harnessing the chloride binding capabilities of both cements [9]. However, there is a need for microstructural analysis to ascertain other possible reasons for the variation in chloride-ion penetration resistance exhibited by these cements.

9.3.4 Bulk Resistivity

Figures 9.15 and 9.16 show the bulk resistivity measurements from a previous study on 100 x 200 mm (4 x 8 inches) concrete cylinders produced with the cements listed in Table 9.3, except PCSA2, which was not available during the study. The bulk resistivity samples were cured in a curing room at 23°C and 100%RH and were tested on days 1,7, 28, 56, ad 91. The samples were tested in a saturated surface dry state with the Gamry instrument using the Electrochemical Impedance Spectroscopy (EIS) technique.
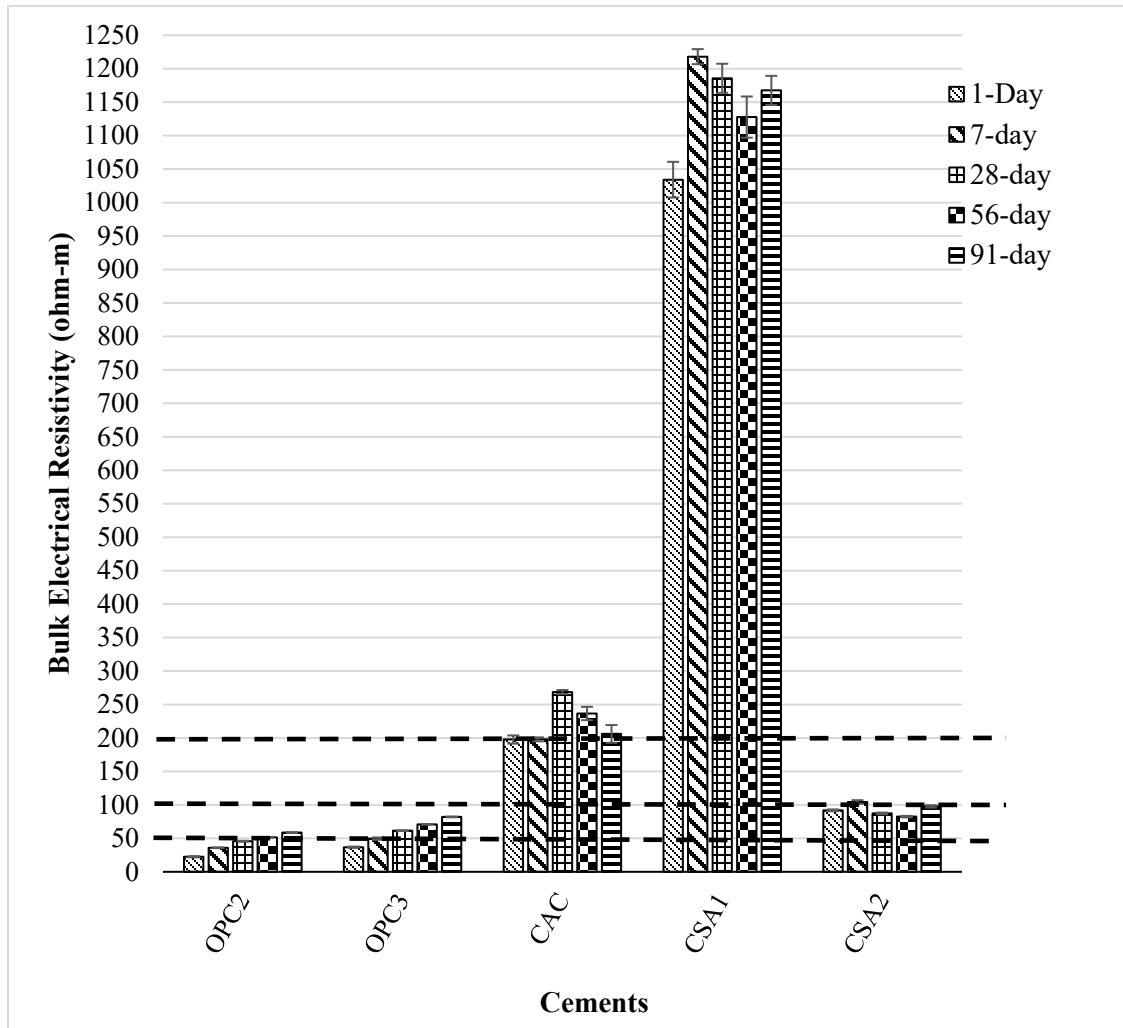
Figure 9.15: Bulk electrical resistivity for pure cements
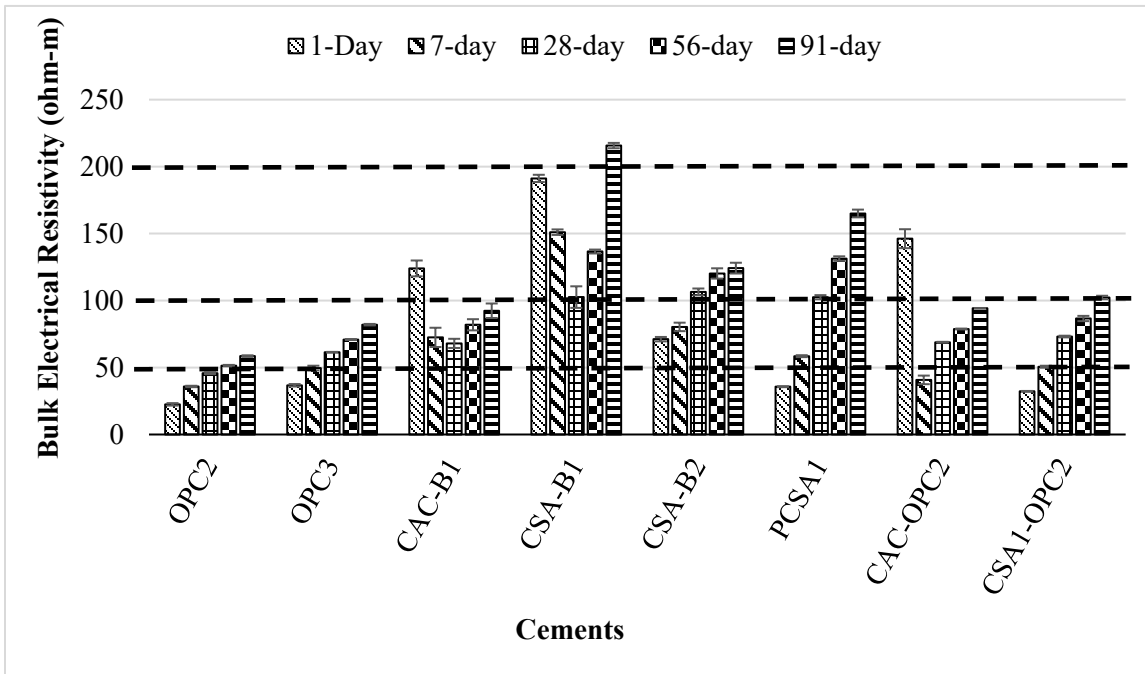
Figure 9.16: Bulk electrical resistivity of blended cements

Figure 9.15 shows a comparison of the controls (OPC2 and OPC3) with the pure cements, while Figure 9.16 shows a comparison of the controls with the blended cements (proprietary and lab blended cements). To aid the analysis, reference will be made to Table 9.8, which shows the equivalent bulk electrical resistivity ranges to the coloumb ranges prescribed in ASTM C1202 for determining chloride penetrability. The black dashed lines in Figures 9.15 and 9.16 indicate the limits in Table 9.8.

Table 9.8: Chloride-ion penetrability based on bulk electrical resistivity [31]

Chloride Penetration	Bulk Electrical Resistivity (ohm-m)
High	<50
Moderate	50 – 100
Low	100 – 200
Very Low	200 – 2000
Negligible	>2000

Comparing CSA1 with other cements in Figures 9.15 and 9.16, CSA1 showed the highest resistivity from day 1 through 91. This is due to its high ye'elmite content resulting in rapid strength and microstructural development. Based on the high resistivity value of CSA1, it could be considered as having a very low chloride penetrability following the information in Table 9.8. The pure CSA2 cement in Figure 9.15 did not exhibit as high resistivity as CSA1 due to its high belite content compared to ye'elmite. However, based on its resistivity values, it can be considered as having moderate chloride penetrability. Other CSA-based cements in Figure 9.16 (CSA-B1, CSA-B2, PCSA1, and CSA1-OPC2) exhibited resistivity values

as they aged, placing them in the category of very low to moderate chloride penetrability. Despite the outstanding performance attributed to CSA1, CSA2, CSA-B1, and CSA-B2 from bulk electrical resistivity assessment, their performance seems not to be consistent with that from the chloride penetration test and the modified ASTM G109 test. This is because bulk electrical resistivity measurements are designed to determine concrete permeability, not chloride binding capacity, which is also an important determinant of chloride penetrability.

In Figure 9.16, OPC2 showed low resistivity values that classified it as having high chloride penetrability until day 91. Whereas by day 28, OPC3 was already showing moderate chloride penetrability. This performance of OPC3 can be attributed to its high C_3A content compared to OPC2. Also, in Figure 9.16, the lab-blended cement (CAC-OPC2 and CSA1-OPC2) showed moderate chloride penetrability as they aged. Whereas, CAC and CAC-B1 showed moderate to very low chloride penetrability all through. Unlike the CSA-based cements (CSA1, CSA2, CSA-B1, and CSA-B2) the chloride penetrability of the controls, lab-blended cements, CAC, and CAC-B1 based on bulk resistivity measurements appear to be consistent with the chloride penetration and modified ASTM G109 tests. This means that close attention must be paid to the type of cement when using bulk resistivity in assessing the chloride penetrability of concrete.

9.4 CONCLUSIONS

1. The results of the microcell and macrocell corrosion monitoring techniques employed in this study show low to moderate corrosion activity in the ASTM G109 corrosion samples. However, the CSA cements CSA1 and CSA2 appear to be showing a higher corrosion activity compared to other mixtures due to low chloride binding capacity.

2. Based on an assumed chloride threshold of 0.05 %, the chloride penetration of PCSA2, PCSA1, CAC-B1, CAC-OPC2, OPC3, CAC, and CSA1-PCSA2 was 19 mm, 21 mm, 22mm, 26 mm, 27 mm, 27mm, and 30 mm, respectively. Whereas CSA2, CSA-B1, CSA-B2, CSA1, and OPC2 showed higher chloride content beyond the assumed 0.05% threshold in the total depth assessed during grinding. Also, the CSA cements (CSA2, CSA-B1, CSA-B2, CSA1) showed higher diffusion coefficients and surface concentrations than the other cements due to a low chloride binding capacity and low Friedel salt content.

3. The CAC mixtures (CAC and CAC-B1) showed higher resistance to chloride penetration compared to the CSA mixtures (CSA2, CSA-B1, CSA-B2, and CSA1). This is attributed to the ability of CAC to bind chlorides compared to CSA cement.

4. The lab-blended cements CAC-OPC and CSA1-OPC2 showed improved performance in resisting chloride ingress due to the presence of OPC compared to CAC and CSA1.

5. The proprietary blended cements PCSA1, PCSA2, and CAC-B1 showed an outstanding performance in resisting chloride penetration. This performance was attributed to the blending of CAC and CSA cement with OPC or other permeability reducing admixtures during production.

6. The bulk electrical resistivity was not effective in ascertaining the chloride penetrability of the CSA-based cements (CSA1, CSA2, CSA-B1, and CSA-B2). However, the chloride penetrability of the other cements based on bulk electrical resistivity measurements was consistent with other test methods in this study.

9.5 REFERENCES

[1] G. Glass and N. Buenfeld, "Chloride-induced corrosion of steel in concrete," *Progress in Structural Engineering and Materials,* vol. 2, no. 4, pp. 448-458, 2000.

[2] M. U. Khan, S. Ahmad, and H. J. Al-Gahtani, "Chloride-induced corrosion of steel in concrete: an overview on chloride diffusion and prediction of corrosion initiation time," *International journal of corrosion,* vol. 2017, 2017.

[3] *ASTM C1556-11a Standard Test Method for Determining the Apparent Chloride Diffusion Coefficient of Cementitious Mixtures by Bulk Diffusion*, ASTM International, 2016. [Online]. Available: https://compass.astm.org/document/?contentCode=ASTM%7CC1556-11AR16%7Cen-US

[4] Y. Zhou, B. Gencturk, K. Willam, and A. Attar, "Carbonation-induced and chloride-induced corrosion in reinforced concrete structures," *Journal of Materials in Civil Engineering,* vol. 27, no. 9, p. 04014245, 2015.

[5] E. G. Moffat, "Durability of Rapid-Set (Ettringite-Based) Concrete," Doctor of Philosophy Dissertation, Civil Engineering, University of New Brunswick, 2016.

[6] G. Glass and N. Buenfeld, "The influence of chloride binding on the chloride induced corrosion risk in reinforced concrete," *Corrosion Science,* vol. 42, no. 2, pp. 329-344, 2000.

[7] E. T. G. Moffatt and M. D. Thomas, "Effect of Carbonation on the Durability and Mechanical Performance of Ettringite-Based Binders," *ACI Materials Journal,* vol. 116, no. 1, 2019.

[8] G. Kim, S. Park, and S. Park, "Chloride removal of calcium aluminate cements: Reaction and physicochemical characteristics," *Case Studies in Construction Materials,* p. e01975, 2023.

[9] K. Y. Ann and C.-G. Cho, "Corrosion resistance of calcium aluminate cement concrete exposed to a chloride environment," *Materials,* vol. 7, no. 2, pp. 887-898, 2014.

[10] Y. Ji, Y. Hu, L. Zhang, and Z. Bao, "Laboratory studies on influence of transverse cracking on chloride-induced corrosion rate in concrete," *Cement and Concrete Composites,* vol. 69, pp. 28-37, 2016.

[11] F. Du, Z. Jin, W. She, C. Xiong, G. Feng, and J. Fan, "Chloride ions migration and induced reinforcement corrosion in concrete with cracks: a comparative study of current acceleration and natural marine exposure," *Construction and Building Materials,* vol. 263, p. 120099, 2020.

[12] C. Hansson, A. Poursaee, and S. Jaffer, "Corrosion of reinforcing bars in concrete," *R&D Serial,* vol. 3013, pp. 106-124, 2007.

[13] C. Hansson, A. Poursaee, and A. Laurent, "Macrocell and microcell corrosion of steel in ordinary Portland cement and high performance concretes," *Cement and concrete research,* vol. 36, no. 11, pp. 2098-2102, 2006.

[14]   *ASTM G109-21 Standard Test Methods for Determining Effects of Chemical Admixtures on Corrosion of Embedded Steel Reinforcement in Concrete Exposed to Chloride Environments*, ASTM International, 2021. [Online]. Available: https://compass.astm.org/document/?contentCode=ASTM%7CG0109-21%7Cen-US

[15]   J. H. Ideker, C. Gosselin, and R. Barborak, "An Alternative Repair Material," *Concrete International,* Article vol. 35, no. 4, pp. 33-37, 04// 2013. [Online]. Available: http://libproxy.txstate.edu/login?url=http://search.ebscohost.com/login.aspx?direct=true&db=aps&AN=86652443&login.asp&site=eds-live&scope=site.

[16]   M. Dornak, J. Zuniga, A. Garcia, T. Drimalas, and K. J. Folliard, "Development of Rapid, Cement-Based Repair Materials for Transportation Structures," 2015.

[17]   S. Lamberet, "Durability of ternary binders based on Portland cement, calcium aluminate cement and calcium sulfate," EPFL, 2004.

[18]   E. Moffatt, "Durability of rapid-set (ettringite-based) concrete," University of New Brunswick., 2016.

[19]   K. L. Scrivener and A. Capmas, "13-Calcium Aluminate Cements," *Lea's Chemistry of Cement and Concrete (Fourth Edition). Butterworth-Heinemann, Oxford,* pp. 713-782, 2003.

[20]   M. P. E. Moses and B. Perumal, "Latest Advances in Alternative Cementations Binders than Portland cement," *IOSR Journal of Mechanical and Civil Engineering,* vol. 13, no. 5, pp. 45-53, 2016.

[21]   S. Mindess, F. J. Young, and D. Darwin, *Concrete*. New Jersey: Prentice Hall, 2003.

[22]   Y. Tao, A. Rahul, M. K. Mohan, G. De Schutter, and K. Van Tittelboom, "Recent progress and technical challenges in using calcium sulfoaluminate (CSA) cement," *Cement and Concrete Composites,* p. 104908, 2022.

[23]   R. I. Iacobescu, Y. Pontikes, D. Koumpouri, and G. Angelopoulos, "Synthesis, characterization and properties of calcium ferroaluminate belite cements produced with electric arc furnace steel slag as raw material," *Cement and Concrete Composites,* vol. 44, pp. 1-8, 2013.

[24]   P. R. Roberge, *Corrosion engineering*. McGraw-Hill Education, 2008.

[25]   M. Yu, J. Lee, and C. Chung, "The Application of Various Indicators for the Estimation of Carbonation and pH of Cement Based Materials," *Journal of Testing and Evaluation,* vol. 38, pp. 534-540, 2010. [Online]. Available: www.astm.org.

[26]   *ASTM C876-22 Standard Test Method for Corrosion Potentials of Uncoated Reinforcing Steel in Concrete*, ASTM International, 2022. [Online]. Available: https://compass.astm.org/document/?contentCode=ASTM%7CC0876-22B%7Cen-US

[27]   J. Broomfield, *Corrosion of steel in concrete: understanding, investigation and repair*. Crc Press, 2003.

[28]   A. Fahim, "Corrosion of reinforcing steel in concrete: monitoring techniques and mitigation strategies," University of New Brunswick., 2018.

[29]   Z. Yang and M. Knight, "Acceptable Chloride Ion Limit in Concrete," Tennessee. Department of Transportation, 2018.

[30]   S. von Greve-Dierfeld *et al.*, "Understanding the carbonation of concrete with supplementary cementitious materials: a critical review by RILEM TC 281-CCC," *Materials and structures,* vol. 53, no. 6, pp. 1-34, 2020.

[31]   I. Mariani. "Evaluating Concrete Quality with Electrical Resistivity." Giatec. https://www.giatecscientific.com/education/evaluating-concrete-quality-with-electrical-resistivity/ (accessed 18th March, 2022).

CHAPTER 10: EVALUATION OF MARINE EXPOSURE CORROSION OF RAPID SETTING HYDRAULIC CEMENT CONCRETE SYSTEMS

10.1 INTRODUCTION

Marine concrete structures are exposed to harsh conditions that could lead to the physical and chemical degradation of such structures. A good example is the physical weathering of concrete due to wave actions and suspended objects [1]. The chemical degradation of concrete is a result of the interaction between chemical substances in seawater and those in concrete. One major attribute of seawater is its high salt content. Seawater salt content is estimated to be around 35 parts per thousand [2] and constitutes mainly sodium chloride (NaCl), magnesium chloride ($MgCl_2$), calcium chloride ($CaCl_2$), and potassium chloride (KCl) [1, 3]. Corrosion in marine concrete structures is largely attributed to the ingress of chloride ions originating from these salts. Although other sources of chlorides exist, such as deicing salt, the use of chloride set accelerators, and chloride-contaminated aggregate or mixing water [4].

Considering the oxidizing role of oxygen in the corrosion process, its availability is consequential to the corrosion of rebar in concrete [2]. Structural elements that are exposed to wet and dry cycles due to high and low tides levels are likely to have a high corrosion rate compared to those constantly submerged in seawater [1, 5]. This is because the wet and dry cycles due to high and low tides ensure the availability of chlorides and oxygen necessary to initiate and sustain corrosion [5].

The initiation of corrosion due to chloride ingress depends on the concentration of chloride ions near the vicinity of reinforcing steel. The steel reinforcement remains protected by a passive film until the concentration of chloride in the vicinity of the steel reinforcement reaches a threshold that can breakdown the passive film and initiate corrosion [6, 7]. Considering the porous nature of concrete, it is certain that chlorides will reach the vicinity of steel rebar in concrete if exposed to a chloride-rich environment [8]. However, measures can be taken to slow the rate of chloride ingress hence preventing the chloride concentration in the vicinity of steel from reaching the threshold that could destroy the passive layer during the service life of the structure [8]. To provide more lasting protection to steel reinforcement, adequate concrete cover to reinforcement must be provided coupled with other measures such as low W/CM ratio, appropriate use of SCMs, proper compaction, adequate curing, and other practices that ensure the production of durable concrete [8, 9].

The rate at which chlorides ingress into concrete also depends on the chloride binding capacity of the concrete. In concrete, there is a combination of bound and free chlorides. However, the corrosion of reinforcing steel in concrete is caused by free chlorides [10]. The chloride binding process occurs when chloride ions react chemically with hydration products or get physically adsorbed within pores resulting in their removal from the pore solution [4, 10, 11]. A good illustration of a chemical interaction is the reaction between chloride ions and cement phases such as calcium hydroxide (CH) and tricalcium aluminate (C_3A) to form chloroaluminate hydrate ($C_3A.CaCl_2.10H_2O$), also known as Friedel's salt [10]. Friedel's salt slows down the transport of chloride ions due to its less porous structure [10]. The formation of Friedel's salt is prevalent in ordinary portland cement (OPC) concrete because of the high C_3A content. However, binders with a high amount of ettringite (AFt), such as CSA and CAC + calcium sulfate (CS), have shown low chloride binding ability and low Friedel's salt content [12].

This study is focused on assessing the corrosion rate due to long-term field exposure in a harsh chloride environment of reinforced concrete produced with alternative cementitious materials such as CSA, CAC, and blended systems of OPC with CSA and OPC with CAC. In addition, the effect of cover thickness on the corrosion rate of the rebars was also assessed.

10.2 EXPERIMENTAL

10.2.1 Materials

This study involved cement systems categorized as pure cements (i.e. cements that are not blended with any other material), proprietary blended cements (i.e. cements pre-blended with other materials during production), and lab blended cements (i.e. cements blended in the laboratory, 25% CAC + 75% PC and 25% CSA + 75% PC). The reason for the various categories is to depict the current practice in the use of CAC and CSA cements. Due to the high cost of pure CAC and CSA cements, (i.e. CAC and CSA cements that are not blended with any other materials), their use is currently limited to niche areas where their special qualities are required [13, 14]. However, there are also cases where CAC and CSA cements are blended with OPC to accelerate the hydration of OPC and reduce the high cost of using CAC and CSA cements only [5, 15-17]. The blending of CAC and CSA cements with OPC is usually carried out during cement production or in the process of mixing concrete. Therefore, including the proprietary blended and laboratory blended cement categories in this study was reasonable. The 25%/75% proportion for the laboratory blended cements was adopted because it was the optimum blend that satisfied both economy and mechanical performance. A description of these cements and their chemical compositions are shown in Tables 10.1 and 10.2, respectively. In Table 10.1, the OPC Type I/II (labeled as OPC2) was

used as the control mixture. Also, the terms CSA ye'elmite cement and CSA belite cement were used to indicate the main phases in the CSA cements and to assess the impact of the hydration rate of these phases and their hydration products in resisting corrosion due to long-term field exposure in a harsh chloride environment. The ye'elmite phase is responsible for rapid early strength gain and microstructural development in CSA cements, while the belite phase is responsible for later strength gain and microstructural development in CSA cements [18, 19]. The phase compositions for the CSA cements in Table 10.1 were calculated using modified Bogue equations adapted from Iacobescu et al. [19].

Table 10.1: Description of individual cement

Cement Category	Cement Type	Description
Pure Cements	OPC2	OPC Type I/II
	CAC	Standard CAC cement
	CSA1	CSA Ye'elmite cement (40% Ye'elmite and 26% belite)
	CSA2	CSA belite cement (58% belite and 30% ye'elmite)
Proprietary Blended Cements	CAC-B1	CAC blend with OPC
	CSA-B1	CSA belite cement (39% belite and 30% ye'elmite)
	CSA-B2	CSA belite cement (42% belite and 27% ye'elmite)
Lab Blends	CAC-OPC2	CAC blend with OPC
	CSA1-OPC2	CSA blend with OPC

Table 10.2: Chemical composition of the individual cement

Cement Type	Cement ID	SiO_2	Al_2O_3	Fe_2O_3	CaO	MgO	SO_3	Na_2O	K_2O	Na_2O_e	LOI
Pure Cements	OPC2	21.06	4.02	3.19	63.91	1.08	2.89	0.14	0.61	0.53	2.29
	CAC	4.34	38.65	15.09	38.37	0.39	0.16	0.05	0.14	0.14	1.55
	CSA1	9.07	21.61	2.26	45.26	0.94	20.26	0.07	0.30	0.27	1.05
	CSA2	20.56	16.14	1.35	45.31	1.23	14.73	0.77	0.72	1.24	4.74
Proprietary Blended Cements	CAC-B1	13.46	12.23	2.67	56.65	2.86	9.90	0.20	0.79	0.72	1.21
	CSA-B1	13.63	15.82	0.75	51.28	1.14	16.62	0.29	0.62	0.69	3.06
	CSA-B2	14.72	14.37	1.22	53.85	1.23	14.40	0.10	0.59	0.49	3.39
Lab Blends	CAC-OPC2	16.53	10.79	2.71	58.07	0.89	7.43	0.14	0.50	0.47	2.19
	CSA1-OPC2	18.06	8.42	2.96	59.25	1.04	7.23	0.12	0.53	0.47	1.98

Other materials used in this study are well-graded limestone rocks, siliceous river sand, a liquid polycarboxylate-ether-based superplasticizer, and a set retarder, citric acid used for slump control and to delay setting and allow time for mixing and casting. A total of 9 cement mixtures were used for the field

corrosion investigation, as shown in Table 10.3. The majority of the mixtures were produced with a total cement content of 446 kg/m^3 (752 lb/yd^3) and a W/CM ratio of 0.35 except CSA2, CSA-B1, and CSA-B2, which were produced with a total cement content 390 kg/m^3 (658 lb/yd^3) and W/CM ratio of 0.38 based on manufacturers recommendation.

Table 10.3: Concrete mixture proportions

Cement Type	W/CM	Total cement kg/m^3 (lb/yd^3)	Replacement Level of Cement with Second Cement Blend (% of Control Cement Type by Mass)	
			Control cement	Type I/II
OPC2	0.35	446 (752)	100%	-
CAC	0.35	446 (752)	100%	-
CSA1	0.35	446 (752)	100%	-
CSA2	0.38	390 (658)	100%	-
CAC-B1	0.35	446 (752)	100%	-
CSA-B1	0.38	390 (658)	100%	-
CSA-B2	0.38	390 (658)	100%	-
CAC-OPC2	0.35	446 (752)	25%	75%
CSA1-OPC2	0.35	446 (752)	25%	75%

10.2.2 Sample Preparation

Two concrete samples of dimensions 150 x 150 x 525 mm (6 x 6 x 21 in) were produced for each of the nine mixtures in Table 10.3. One of the samples was reinforced with steel, and the other was not reinforced in order to carry out forensic studies following long-term exposure. The reinforced sample had two steel reinforcements which were sandblasted to remove any existing corrosion product before casting. The samples were cast with molds designed to ensure that the reinforcements were located to have 25 mm (1 inch) and 50 mm (2 inches) covers from opposite surfaces along the squared cross-section. Initial curing was done with wet burlap and plastic sheet covers after casting for 24 hours. At the end of the 24-hour cure, the samples were removed from the molds, and the protruding rebars at the end of the samples were sealed with a plastic material and rubber band to prevent corrosion. Afterward, the samples were transferred to a curing room at 23°C and 100% relative humidity (RH), where they were cured for an additional six days. At the end of curing, the samples were transferred to a simulated marine site located at an outdoor location at Texas State University. Figure 10.1 shows the marine site configuration.
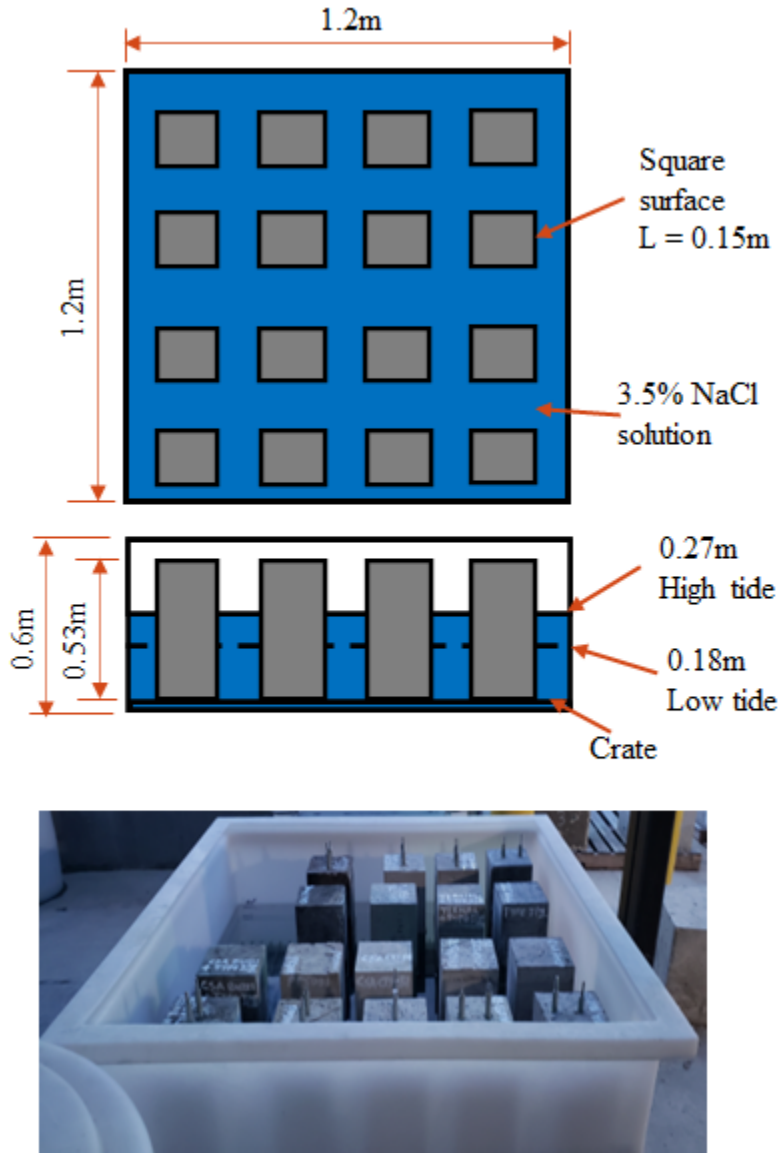
Figure 10.1: Outdoor marine site configuration

10.2.3 Testing

The simulated marine site constitutes a polyethylene tank of dimension 1.2 x 1.2 x 0.6 m (48 x 48 x 24 in) containing 3.5% NaCl solution. The tank was marked to locate the point 0.27 m (10.5 in) from the top of a crate at the bottom of the tank where the samples rested. This mark served as the high tide mark. Another mark was made to locate a height of 0.18 m (7 in) from the same point as the initial. This served as the low tide mark. The NaCl solution was made by dissolving 132.4 g of NaCl in 1 gallon of water at room temperature 23°C (73°F). With the samples inside the tank, the tank was filled with the 3.5% NaCl solution to the high tide mark. A submersible pump was also placed in the tank to keep the saltwater in

circulation. Frequent checks were made to fill the tank up to the high tide level when it dropped to the low tide level due to evaporation.

Microcell corrosion measurements were carried out at one-month intervals for the first three months and three months intervals afterward. Before each microcell corrosion measurement, the samples are removed from the exposure site and transferred to the laboratory which is at room temperature (23°C (73°F)) for 16 ± 2 hours. This allows for the condition (e.g. temperature) of the sample to stabilize before measurement. The measurements were carried out with Gamry testing equipment and software using the Linear Polarization Resistance (LPR) technique. In carrying out the measurement, a stainless-steel apparatus was used as the counter electrode. This apparatus was built to have a vertical hollow and a rectangular base that made contact with the surface of the concrete via a damp sponge. A silver/silver chloride (Ag/AgCl) reference electrode was passed through the hollow and made contact with the concrete surface via the same damp sponge. The counter electrode was always positioned at the center of the surface and aligned in the direction of the measured reinforcement, as shown in Figure 10.2. This positioning of the counter electrode was adopted because it lies between the low and high tide line implying that it had both the supply of chloride and oxygen necessary for corrosion initiation. To ascertain the effect of cover thickness on the ingress of chloride-ion, measurements were done on the 25 mm (1 inch) and 50 mm (2 inches) cover surfaces, with the rebars serving as the working electrode in each case. The electrodes were connected to the Gamry instrument and computer system, as shown in Figure 10.2.

Figure 10.2: Microcell measurement set up for outdoor corrosion samples

The LPR technique executed by the Gamry instrument helped to measure the half-cell potential (E_{corr}) of the rebars (working electrode) relative to the reference electrode (Ag/AgCl electrode) and the microcell

corrosion current (I_{corr}). In the LPR technique, the equipment first measures the open circuit potential, also known as the half-cell potential (E_{corr}) of the rebar under study, and then shifts the potential $\pm$ 10mV from the E_{corr}. The current due to the shift in potential and the consequent resistance is known as the corrosion current (I_{corr}), and polarization resistance (R_p), respectively. The I_{corr} is given by Equation 10.1 [20]:

$$I_{corr} = \frac{\beta_a \beta_c}{2 \cdot 303(\beta_a + \beta_c)}\left(\frac{1}{R_p}\right) \qquad \text{Eq. 10.1}$$

Where R_p is the polarization resistance, β_a is the anodic Beta coefficient in volts/decade, and β_c is the cathodic Beta coefficient in volts/decade. The Beta coefficients, also known as Tafel coefficients, were assumed to be 120 mV which is the value usually used for reinforcing steel actively corroding in concrete [5]. Since the perturbation current applied during the potential shift was done via the counter electrode, the corrosion current density was calculated using Equation 10.2:

$$i_{corr} = \frac{I_{corr}}{A} \qquad \text{Eq. 10.2}$$

Where A is the base area of the counter electrode in cm^2, I_{corr} is the corrosion current in μA, and i_{corr} is the corrosion current density in $\mu A/cm^2$. The half-cell potential and corrosion current density were used in analyzing the rate of microcell corrosion in the outdoor corrosion samples.

10.3 RESULTS AND DISCUSSION

10.3.1 Half-cell potential for the 25 mm (1 inch) and 50 mm (2 inches) covered rebars

Figures 10.3 and 10.4 show the half-cell potential for the 1-inch and 2-inch covered rebars of each sample, respectively.

Figure 10.3: Half-cell potential relative to Ag/AgCl electrode for the 25 mm (1 inch) covered rebars

Figure 10.4: Half-cell potential relative to Ag/AgCl electrode for the 50 mm (2 inches) covered rebars
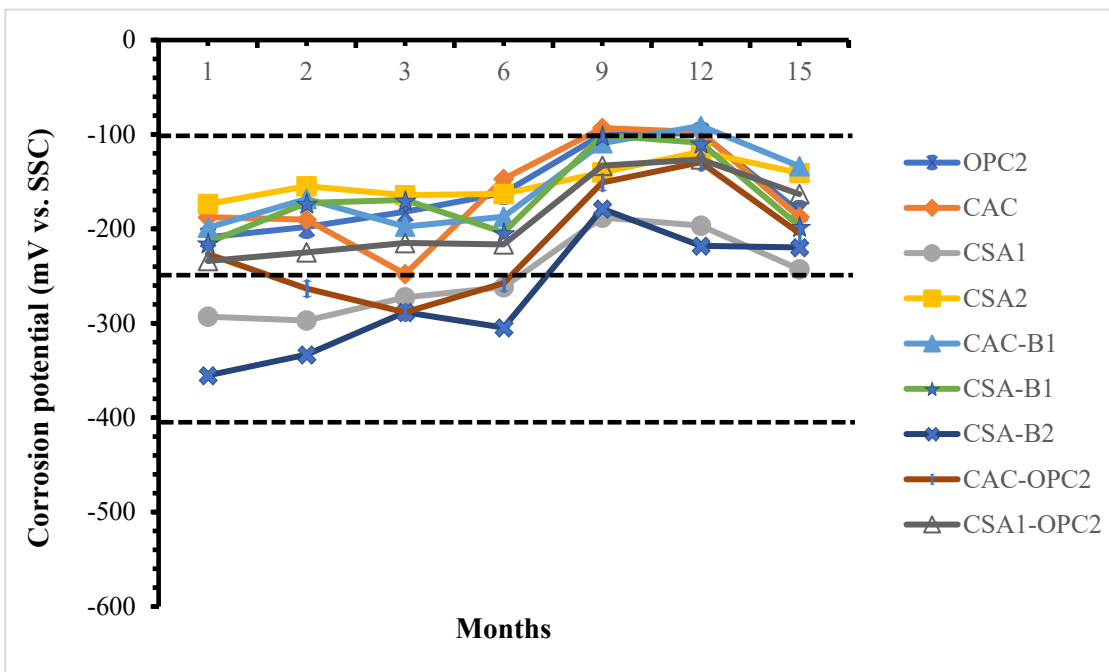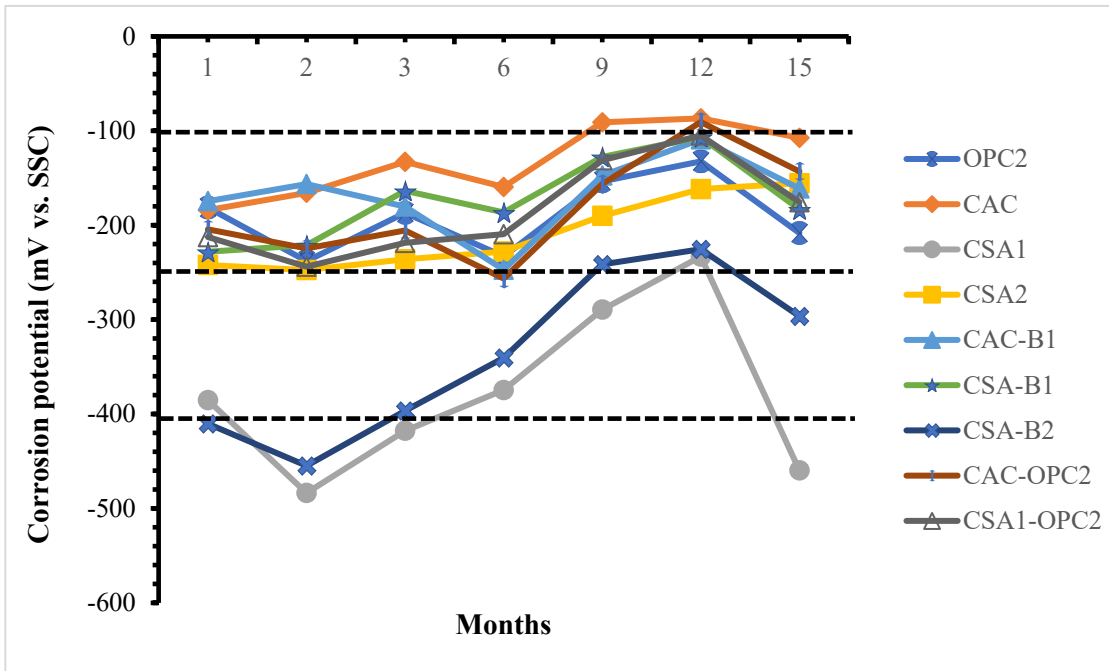
In using half-cell potential for monitoring the corrosion activities on the rebars, it is assumed that an increasing negative value indicates an increase in corrosion activity. However, this depends on the propensity of the iron (rebar) to dissolve and the availability of oxygen [20]. To analyze the corrosion activities in the samples using their measured potentials, reference was made to Table 10.4, which was developed based on ASTM C876 "Standard Test Method for Corrosion Potentials of Uncoated Reinforcing Steel in Concrete" criteria for classifying corrosion activity within a system. Though ASTM C876 was developed for a $Cu/CuSO_4$ reference electrode [21], Table 10.4 presents the equivalent Ag/AgCl potentials.

Table 10.4: Risk of corrosion using half-cell potential [22]

Corrosion potential (mV vs Ag/AgCl)	Condition
> -106	Low (< 10% risk of corrosion)
-106 to -256	Intermediate (50% risk of corrosion)
-256 to -406	High (> 90% risk of corrosion)
< -406	Severe corrosion

The black dashed lines in Figures 10.3 and 10.4 indicate the limits shown in Table 10.4. In Figure 10.3, the majority of the samples appear to fall within the intermediate region, as described in Table 10.4. This means there is a 50% risk of corrosion occurring on the 25 mm (1 inch) covered rebars of those samples. The only exceptions in Figure 10.3 are CSA-B2 and CSA1. Both increased from a high negative potential in the 2nd month to a low negative potential in the 12th month, probably due to passivation. However, there was a decline in potential beyond the 12th month, with CSA1 showing severe corrosion at 15 months while the potential of CSA-B2 indicated high corrosion. The low resistance to corrosion due to chloride ion ingress exhibited by CSA1 and CSA-B2 compared to the other cement mixtures can be attributed to a low chloride binding capacity. In Figure 10.4, all the samples showed an intermediate (50%) risk of corrosion on their 50 mm (2 inches) covered rebar. Although CSA1 and CSA-B2 showed a high negative potential at the unset, they increased afterward, and by the 15th month, they showed potential values that categorized them as having an intermediate risk of corrosion. Comparing the mixtures in Figures 10.3 and 10.4, especially CSA1 and CSA-B2, it is seen that the 2-inch cover thickness reduced the rate of corrosion of the rebars due to chloride-ion ingress compared to the 1-inch cover thickness.

10.3.2 Corrosion current density for the 25 mm (1 inch) and 50 mm (2 inches) covered rebars

Figures 10.5 and 10.6 show the corrosion current density for the 25 mm (1 inch) and 50 mm (2 inches) covered rebars in each concrete sample. The increase in corrosion activity is expected to increase the corrosion current density. In this study, the measured current densities were analyzed by comparing the

values with corrosion current density ranges that several authors have used in classifying the corrosion rate in reinforced concrete based on the LPR technique. The ranges of corrosion current density are presented in Table 10.5. Also, the black dashed lines in Figures 10.5 and 10.6 indicate the current density ranges in Table 10.5.
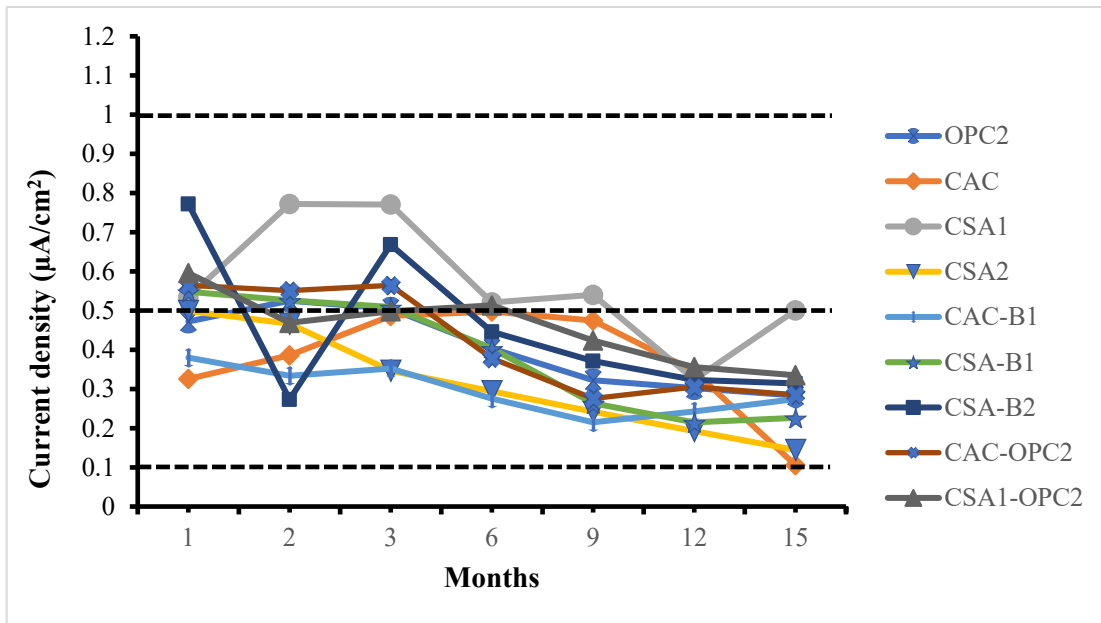
Figure 10.5: Corrosion current density for the 25 mm (1 inch) covered rebars
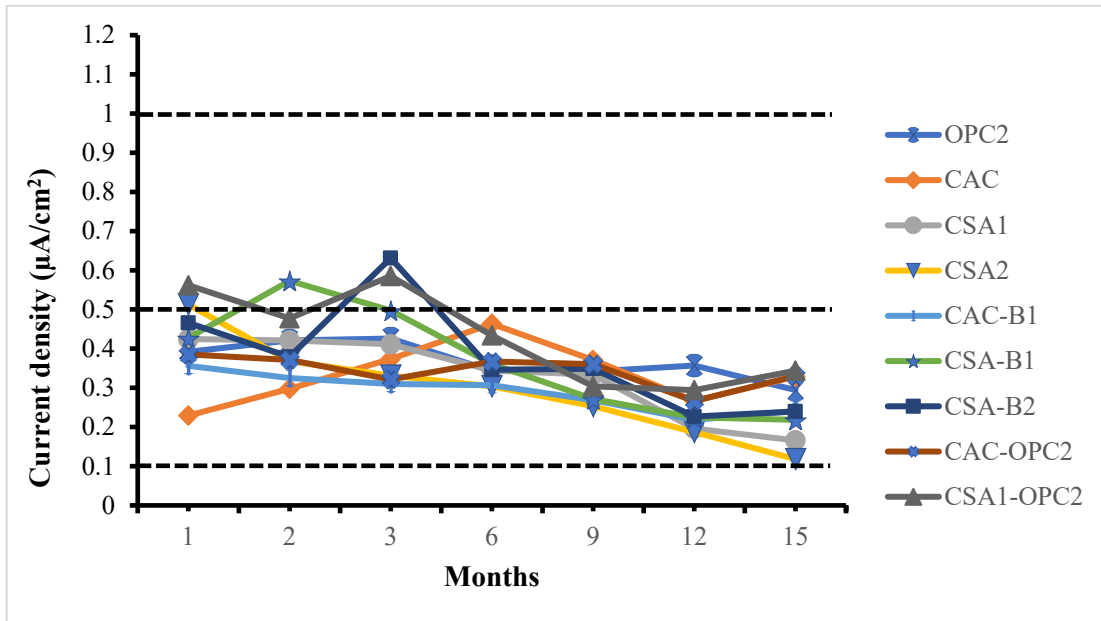
Figure 10.6: Corrosion current density for the 50 mm (2 inches) covered rebars

Table 10.5: Risk of corrosion using corrosion current density [5, 7, 22]

Corrosion current density (μA/cm^2)	Corrosion classification
Up to 0.1	Passive condition
0.1 – 0.5	Low to moderate corrosion
0.5 – 1	Moderate to high corrosion
More than 1	High corrosion rate

Based on the current densities of the samples in Figure 10.5, it appears that all the samples exhibit a low to moderate corrosion rate on their 25 mm (1 inch) covered rebar. Comparing the current densities for all samples in the 1st month and 15th month, it can be seen that all samples exhibited a decrease in current density with time. This reduction in current density could be attributed to the formation of a passive layer on the 25 mm (1 inch) covered rebar. CSA1 showed the highest corrosion rate compared to the rest of the mixtures. Again, this could be attributed to its low resistance to chloride ingress due to a low chloride binding capacity. Figure 10.6 shows that all the samples exhibited a low to moderate rate of corrosion on the 50 mm (2 inches) covered rebar. Again, comparing the mixtures in Figures 10.5 and 10.6, especially CSA1 and CSA-B2, it is seen that the 50 mm (2 inches) cover thickness reduced the corrosion rate of the rebars compared to the 25 mm (1 inch) cover thickness. The performance of the samples, as indicated by the current density, seem to be consistent with the half-cell corrosion measurement except for the 25 mm (1 inch) covered rebar of CSA1 and CSA-B2, which showed a severe and high corrosion rate, respectively, as indicated by their half-cell potentials in the 15th month (see Figure 10.3).

The variation in corrosion activity exhibited by the concrete mixtures in the half-cell potential and current density results can result from their porosity level and ability to bind chlorides. OPC is known to have good chloride binding capacity due to the formation of Friedel's salt, a compound that is capable of trapping chlorides and removing them from the pore solution [10]. CAC hydrates are also known to bind chlorides [23]. However, blending CAC and OPC, which is the case for CAC-B1 and CAC-OPC2, could further increase chloride binding since both cements have their individual chloride binding capacities [24]. The hydration products of CSA, such as ettringite and aluminum hydroxide, cannot bind chloride, thus increasing their susceptibility to corrosion due to chloride-ion ingress [25]. This could be the reason for the high corrosion activity observed in CSA1 and CSA-B1. The other CSA-based cement concrete might have performed differently due to other reasons such as pore structure, the interaction of chloride ions with charged cement particles, the ability of the belite phase to hydrate and form calcium-silicate-hydrate capable of binding chlorides, and the blending of CSA with OPC [4, 11, 26]. Blending CSA with OPC, which is the case in CSA1-OPC2, can provide the C$_3$A necessary for forming Friedel's salt, thus increasing the chloride binding capacity of the blend.

The less corrosion activity observed in the half-cell potential and current density results for the 50 mm (2-inch) covered rebar compared to the 25 mm (1 inch) covered rebar emphasizes the need to provide adequate cover to steel reinforcement as a way to reduce the rate of corrosion in reinforced concrete due to chloride ingress.

10.4 CONCLUSIONS

1. Based on the half-cell potential and current density values, the 25 mm (1 inch) and 50 mm (2 inches) covered rebars in the concrete samples showed a low to moderate corrosion rate except for the 25 mm (1 inch) covered rebar in CSA1 and CSA-B2 which showed a severe and high corrosion rate respectively as indicated by their half-cell potentials in the 15th month.

2. Comparing the half-cell potential and current density values for the 25 mm (1 inch) and 50 mm (2 inches) covered rebars, it is observed that the 50 mm (2 inches) cover thickness reduced the rate of corrosion of the rebars due to chloride-ion ingress compared to the 25 mm (1 inch) cover thickness.

3. The cement mixture CSA1 appeared to have exhibited the highest corrosion rate, followed by CSA-B2, especially in the 1-inch covered rebar. This low resistance to corrosion due to chloride-ion ingress exhibited by CSA1 and CSA-B2 compared to the other cement mixtures can be attributed to a low chloride binding capacity.

10.5 REFERENCES

[1]   F. Qu, W. Li, W. Dong, V. W. Tam, and T. Yu, "Durability deterioration of concrete under marine environment from material to structure: A critical review," *Journal of Building Engineering,* vol. 35, p. 102074, 2021.

[2]   K. A. Chandler, *Marine and offshore corrosion: marine engineering series*. Elsevier, 2014.

[3]   *ASTM D1141- 98 Standard Practice for Preparation of Substitute Ocean Water*, ASTM International, 2021. [Online]. Available: https://compass.astm.org/document/?contentCode=ASTM%7CD1141-98R21%7Cen-US

[4]   G. Glass and N. Buenfeld, "Chloride-induced corrosion of steel in concrete," *Progress in Structural Engineering and Materials,* vol. 2, no. 4, pp. 448-458, 2000.

[5]   E. Moffatt, "Durability of rapid-set (ettringite-based) concrete," University of New Brunswick., 2016.

[6]   R. E. Melchers and C. Q. Li, "Reinforcement corrosion initiation and activation times in concrete structures exposed to severe marine environments," *Cement and concrete research,* vol. 39, no. 11, pp. 1068-1076, 2009.

[7]   A. Fahim, "Corrosion of reinforcing steel in concrete: monitoring techniques and mitigation strategies," University of New Brunswick., 2018.

[8]   E. G. Moffat, "Durability of Rapid-Set (Ettringite-Based) Concrete," Doctor of Philosophy Dissertation, Civil Engineering, University of New Brunswick, 2016.

[9]   Y. Zhou, B. Gencturk, K. Willam, and A. Attar, "Carbonation-induced and chloride-induced corrosion in reinforced concrete structures," *Journal of Materials in Civil Engineering,* vol. 27, no. 9, p. 04014245, 2015.

[10]   M. U. Khan, S. Ahmad, and H. J. Al-Gahtani, "Chloride-induced corrosion of steel in concrete: an overview on chloride diffusion and prediction of corrosion initiation time," *International journal of corrosion,* vol. 2017, 2017.

[11]   G. Glass and N. Buenfeld, "The influence of chloride binding on the chloride induced corrosion risk in reinforced concrete," *Corrosion Science,* vol. 42, no. 2, pp. 329-344, 2000.

[12]   E. T. G. Moffatt and M. D. Thomas, "Effect of Carbonation on the Durability and Mechanical Performance of Ettringite-Based Binders," *ACI Materials Journal,* vol. 116, no. 1, 2019.

[13]   J. H. Ideker, C. Gosselin, and R. Barborak, "An Alternative Repair Material," *Concrete International,* Article vol. 35, no. 4, pp. 33-37, 04// 2013. [Online]. Available: http://libproxy.txstate.edu/login?url=http://search.ebscohost.com/login.aspx?direct=true&db=aps&AN=86652443&login.asp&site=eds-live&scope=site.

[14]   M. Dornak, J. Zuniga, A. Garcia, T. Drimalas, and K. J. Folliard, "Development of Rapid, Cement-Based Repair Materials for Transportation Structures," 2015.

[15]   S. Lamberet, "Durability of ternary binders based on Portland cement, calcium aluminate cement and calcium sulfate," EPFL, 2004.

[16]   K. L. Scrivener and A. Capmas, "13-Calcium Aluminate Cements," *Lea's Chemistry of Cement and Concrete (Fourth Edition). Butterworth-Heinemann, Oxford,* pp. 713-782, 2003.

[17]   M. P. E. Moses and B. Perumal, "Latest Advances in Alternative Cementations Binders than Portland cement," *IOSR Journal of Mechanical and Civil Engineering,* vol. 13, no. 5, pp. 45-53, 2016.

[18]   Y. Tao, A. Rahul, M. K. Mohan, G. De Schutter, and K. Van Tittelboom, "Recent progress and technical challenges in using calcium sulfoaluminate (CSA) cement," *Cement and Concrete Composites,* p. 104908, 2022.

[19]   R. I. Iacobescu, Y. Pontikes, D. Koumpouri, and G. Angelopoulos, "Synthesis, characterization and properties of calcium ferroaluminate belite cements produced with electric arc furnace steel slag as raw material," *Cement and Concrete Composites,* vol. 44, pp. 1-8, 2013.

[20]   P. R. Roberge, *Corrosion engineering*. McGraw-Hill Education, 2008.

[21]   *ASTM C876-22 Standard Test Method for Corrosion Potentials of Uncoated Reinforcing Steel in Concrete*, ASTM International, 2022. [Online]. Available: https://compass.astm.org/document/?contentCode=ASTM%7CC0876-22B%7Cen-US

[22]   J. Broomfield, *Corrosion of steel in concrete: understanding, investigation and repair*. Crc Press, 2003.

[23]   G. Kim, S. Park, and S. Park, "Chloride removal of calcium aluminate cements: Reaction and physicochemical characteristics," *Case Studies in Construction Materials,* p. e01975, 2023.

[24]   K. Y. Ann and C.-G. Cho, "Corrosion resistance of calcium aluminate cement concrete exposed to a chloride environment," *Materials,* vol. 7, no. 2, pp. 887-898, 2014.

[25]   G. Paul, E. Boccaleri, L. Buzzi, F. Canonico, and D. Gastaldi, "Friedel's salt formation in sulfoaluminate cements: a combined XRD and 27Al MAS NMR study," *Cement and Concrete Research,* vol. 67, pp. 93-102, 2015.

[26]   K. Quillin, "Performance of belite–sulfoaluminate cements," *Cement and concrete research,* vol. 31, no. 9, pp. 1341-1349, 2001.

CHAPTER 11: ALKALI SILICA REACTIVITY AND DELAYED ETTRINGITE FORMATION IN RAPID SETTTING HYDRAULIC CEMENT CONCRETE SYSTEMS

11.1 INTRODUCTION

Alkali-silica reaction is a chemical interaction between siliceous constituents found in concrete aggregates and hydroxyl ions. Hydroxyl ions are found within concrete mainly because of the concentration of sodium and potassium [1]. The reactive silica found in the aggregates of most concrete mixes produces a reaction called alkali-silica gel. Once this gel absorbs moisture, it expands which creates internal pressure in the concrete. The internal pressure can reach the point to exceed the tensile strength and crack the concrete. Therefore, potential ASR in concrete is studied, tested, and inspected to avoid deleterious cracking and degradation of the infrastructure.

ASR has visual indicators, such as map cracking, closed joints, and spalling. ASR has been widely known as one of the more prevalent deterioration mechanisms affecting concrete worldwide [2]. These problems were originally identified by Thomas Stanton in the State of California in the 1930s [3] as shown in Figure 11.1.
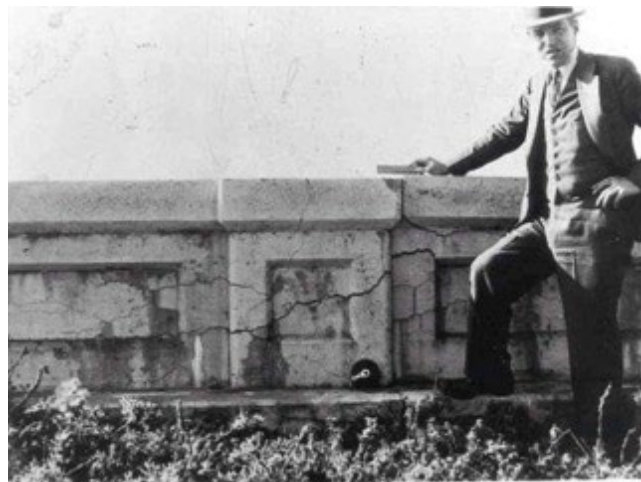
Figure 11.1: Thomas E. Stanton showing structure affected by ASR [3]

Stanton discovered that the expansion of concrete structures was directly subjective to the alkali content of each concrete mixture, the magnitude of the reactive silica in the aggregates, and the exposure to different temperatures and moisture. Shortly after Thomas' [3] findings were distributed around the

construction industry the diagnosis of ASR turned out to be more common. This discovery also led to the initiation of studies and deep investigations sponsored by agencies such as the Army Corps of Engineers, Bureau of Public Roads, Portland Cement Association, and others [2].

11.1.1 Mechanisms and Essential Components

To have ASR damaging reaction occur, there are certain requirements that need to be present. First, there must be a sufficient quantity of reactive silica within the aggregates. Secondly, there must be a sufficient concentration of alkali which is mainly characterized to be generated from portland cements, however, may also come from other constituents (i.e., SCMs, admixtures, and other powder-based binders). Lastly, plenty of moisture must be present in the environment where the structure is located [2]. Figure 11.2 displays the three requirements for concrete to subjected to ASR in the field as discussed by REF [2].
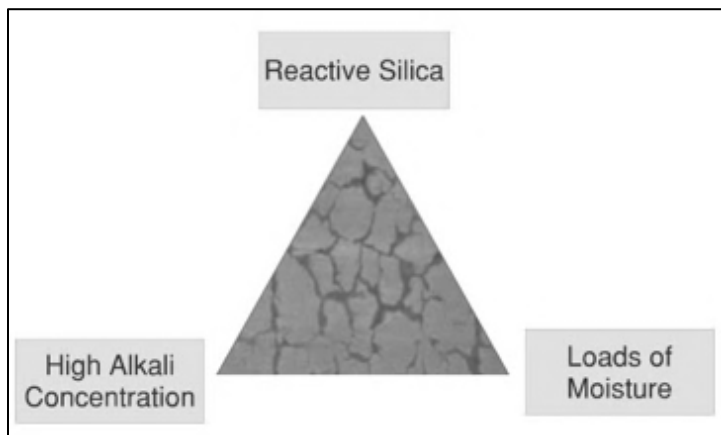
Figure 11.2: ASR components [2]

Although ASR has been identified to be affecting many of the world's concrete structures for over 75 years, its mechanisms to spot haven't yet been fully developed or proved. Its mechanisms start with the formation of alkali-silica gel which is mainly composed of sodium, potassium, hydroxyl, and some amounts of calcium [4]. Therefore, this gel absorbs water from the cement past which it surrounds. Once the gel absorbs a certain amount of water from the surrounding cement paste, the structure expands. The expansion of this water and gel absorption causes internal stress in the structure which ultimately leads to cracking (see Figure 11.3).
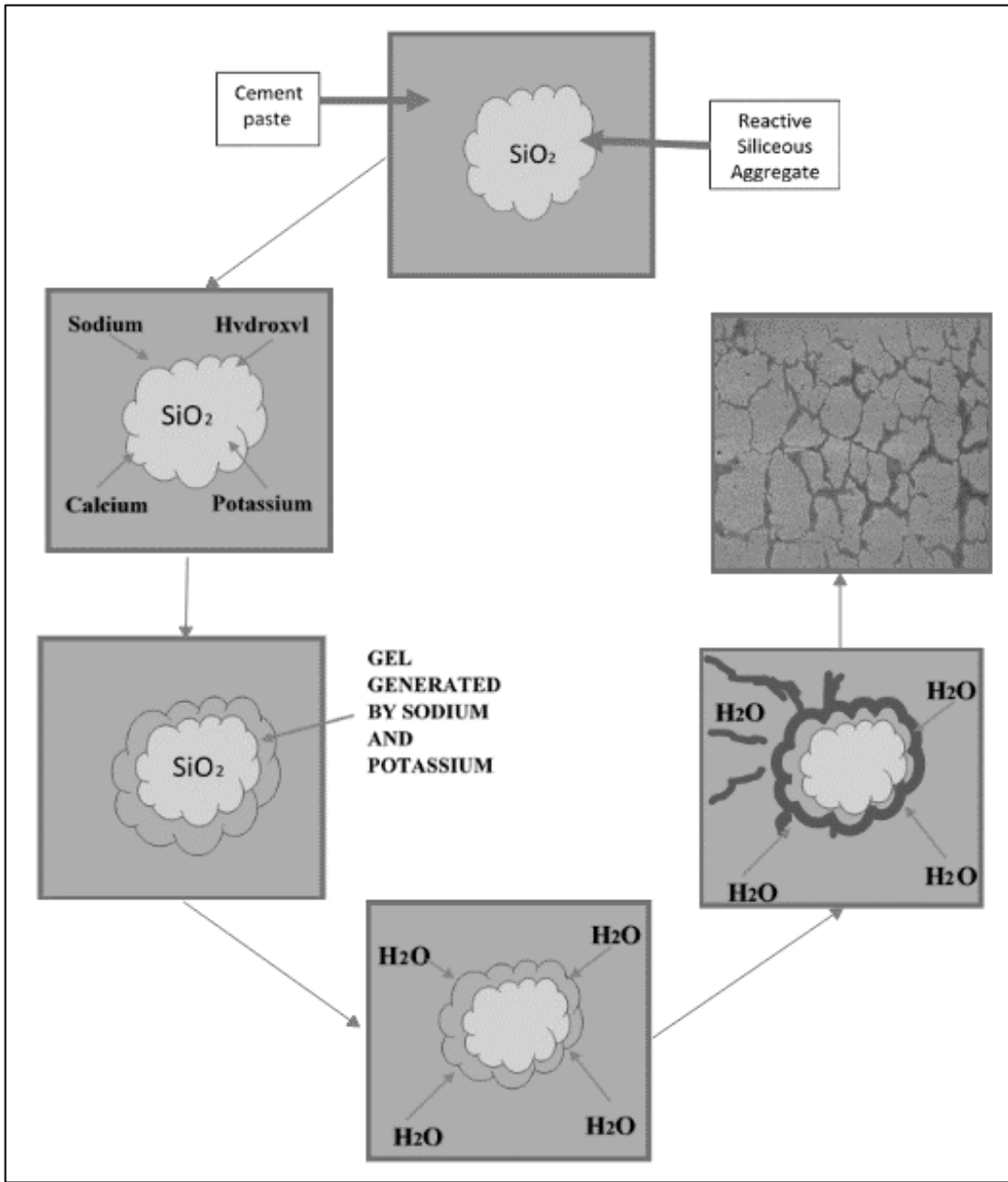
Figure 11.3: ASR Mechanism

As previously mentioned, ASR is characterized for generating cracks in concrete structures. Although with time, many types of cracks can be seen in concrete constructions due to their normal deterioration. The cracks of ASR typically lean more to look like map shapes. In addition to producing cracks, ASR also generates expansion which can be restrained in one or more directions [2].

Even though the signs of deterioration in concrete generated by the ASR manifest 5 to 10 years after construction, they can usually be identified during a routine site inspection which is performed regularly

in job sites [5]. Structures located in cold and dry weather, might not show any ASR symptoms until the construction reaches an age of 15 years or more. The influence of temperature and weather conditions for ASR to react becomes a concern for the Texas infrastructures as the temperatures tend to be high and the weather is very humid almost all year long. According to the ASR field identification book published by the Federal Highway Administration, some of the common visual symptoms of ASR can range from surface pop-outs, cracking, crushing of concrete, discoloration on surfaces, gel production, expansion causing deformation and displacement of structures [6].

The major symptom of ASR is a map cracking pattern which surfaces on concrete structures that are unrestrained [2]. Added to the cracks, discoloration can also occur. As shown below in Figure 11.4 the cracks take place in a randomly oriented form. These cracks are distinctive and can be seen in a variety of structures such as in concrete pavement and concrete columns of bridges.
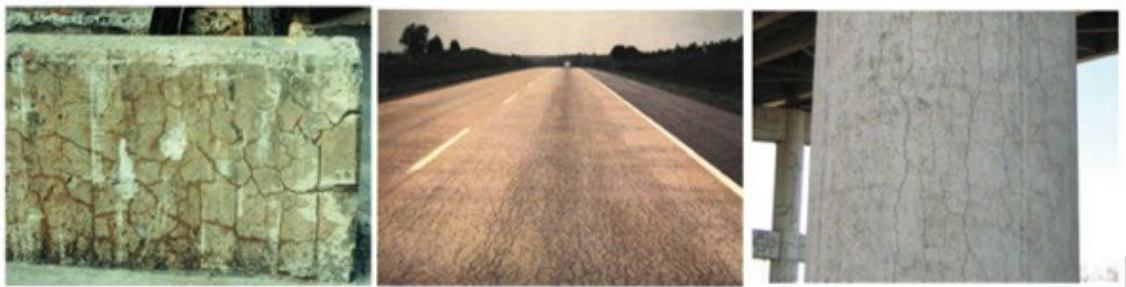
Figure 11.4: Concrete Structures Affected by ASR [2]

11.1.2 Laboratory and Field-testing Methods

11.1.3 Accelerated Mortar Bar Test (ASTM C1260)

This method was developed by Oberholster and Davies in 1986 at the National Building Research Institute in South Africa [7]. It provides a tool to identify the potential cause of ASR due to the utilization of a determined type of aggregate. Initially, ASTM C1260 "Standard Test Method for Potential Alkali Reactivity of Aggregates (Mortar-Bar Method)" [8] was dedicated to only test the aggregate reactivity, but it had been found to be a great method to assess the levels of efficacy of supplementary cementing materials (SCMs) to reduce ASR expansion. The ASTM C1260 is used to determine whether an aggregate is potentially reactive.

The test is composed by a process involving the casting of mortar bars containing either coarse or fine aggregates. The following step in this test is to demold the mortar bars after 24 hours and place them in

water at room temperature. The temperature of the water must be raised to 80°C in the oven, and the mortar bars specimens are stored in this new temperature and condition for another 24 hours. The bars are then removed from the water and measured to keep track of any length changes. After this process, the specimens are submersed in a 1 normal NaOH solution at 80 C to be stored for 14 days. The specimens are stored toward the soaking of the solution while periodically length measurements are taken.

In addition, the ASTM C1778 [9] provides guidance on the expansion criteria for ASTM C1260. This criterion defines whether the specimen is innocuous, potentially reactive, and reactive referred in Table 11.1.

Table 11.1: Mortar Bar Expansion Values.

Expansion %	Considered as:
< 0.10 %	Harmless
0.10 to 0.20 %	Potentially reactive
> 0.20 %	Reactive

Even though the ASTM C1260 is suitable for aggregate reactivity testing, it is not a reliable source to assess alkalinity in cements. The solution used to soak the samples in this test method has a very high alkaline content that can cover any effect caused by alkalinity in the cement. According to the Portland Cement Association [10], it is often more reliable and more common for researchers to use the ASTM C1293, "Standard Test Method for Determination of Length Change of Concrete Due to Alkali-Silica" Reaction [11], which is also known as the concrete prism test or CPT. Though, ASTM C1260 has been used as a guidance for the creation of the mixture design this standard is used to determine whether an aggregate is potentially reactive.

11.1.4 Concrete Prism Test (ASTM C1293)

The ASTM C1293 [11] concrete prism test (CPT) is one of the most suitable and reliable methods to evaluate potential responses that will eventually lead to ASR. The ASTM C1293 provides researchers a strong similarity that connects to the performance of specimens in the field. Additionally, this test is used to determine the susceptibility of an aggregate in expansive alkali-silica reaction by providing a way to measure the length changes of concrete prisms.

ASTM C1293 concrete prism test is utilized as the main method to evaluate potential responses that will eventually lead to ASR. ASTM C1293 is a long-term test as it can take a year or up to 24 months if SCMs are incorporated for assessing performance.. The standard is meant to show the level of deleteriousness

that the different mixtures could reach, referred in Table 11.2. It is well-thought-out for the specimen to fail the CPT expansion test if it expands more than 0.040% in one year.

Table 11.2: CPT Expansion Values (ASTM C1293)

Specimen to be considered as:	CPT Expansion %
Non-reactive	<0.040
Moderately reactive	0.040-0.120
Highly reactive	0.120-0.240
Very highly reactive	>0.240

11.1.5 Outdoor Field Concrete Blocks

The purpose of developing concrete exposure blocks is to have a field trial to offer a more realistic sized element to evaluate ASR effects on different types of binder systems. Additionally, the concrete blocks are considered as a field trial to analyze the effects of ASR in respect to real-world environmental conditions. Fournier et al. [5] determined that interpreting the reactivity of aggregates in laboratory conditions is faster to obtain results but not as reliable as actually exposing the specimen to outdoor conditions. Thomas et al [2] also investigated that a specimen could fail ASTM C1293 in two years of age, nonetheless, it could take 10 years for an exposure block to surpass the 0.04% limit.

11.2 DELAYED ETTRINGITE FORMATION (DEF)

11.2.1 Historical Background

Ettringite is the mineral name for calcium sulfoaluminate that is usually found in OPC concretes. Ettringite stands as the mineral name for calcium sulfoaluminate [10]. According to the Portland Cement Association (PCA), delayed ettringite formation (DEF) is referred to be a potential deleterious reformation of ettringite in moist concrete, mortar, or paste after the destruction of primary ettringite by high temperature. Ettringite that begins forming at early stages is known as "primary ettringite". The formation at early stages is part of an important component of portland cement systems. Following, ettringite is formed by the dissolution, and recrystallization in cracks is referred to as "secondary ettringite" and does not harm the performance of concrete [10].

DEF can affect large-scale elements of precast elements as shown in Figure 11.5. The secondary ettringite formation is the result of the continuous dissolution of ettringite in fine cracks and cavities [12]. DEF is

perceived as a complex phenomenon that never affects the entire structure [13]. This structural deficiency has been seen around the world for many years, and it has been noted to be related to the exposure of the elements to high temperatures and the presence of water. Dayarathne [14] explained DEF is defined as the result of a modification of the chemical reactions during hydration.

Figure 11.5: Concrete Structures Affected by DEF. [12]

11.2.2 Mechanisms and Essential Components

DEF is a heat-induced internal sulfate attack. This deficiency occurs when concrete is exposed to high temperatures at early stages such as curing. This internal sulfate attack directly affects durability and strength of the concrete in a similar way to Alkali-Silica Reaction. Dayarathne [14] also explained, besides the existing sulfate within the aggregate, there must be two important conditions for DEF to happen. The first condition is that the specimen's internal temperature must exceed 158°F / 70°C. The second condition is that there must be sufficient moisture available in the environment where the concrete exists, as shown in Figure 11.6. DEF is often connected with ASR; therefore, the use of potentially reactive aggregates can also exacerbate DEF.
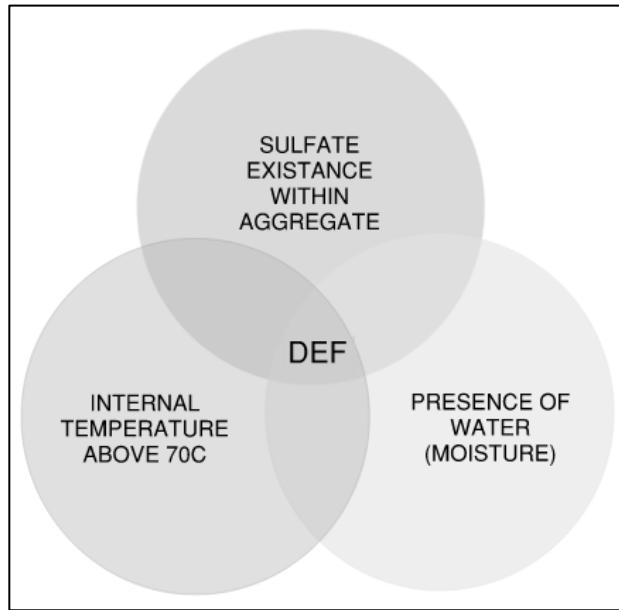
Figure 11.6: DEF Components

The absence of any of the conditions depicted in Figure 11.6 prohibits the formation of late ettringite. Rising temperatures can also alter the conditions of the equilibrium of the already existing sulfate within the aggregate. The sulfate content and sulfate/alumina ratio of the cements are contributing factors for DEF. In addition, for DEF to develop, temperature alterations must happen within the first 12 to 24 hours after mixing. DEF will not occur if the temperature of the specimen stays high for numerous days.

Figure 11.7 depicts the mechanism DEF as described by REF [15]. Sulfate and alumina get confined rapidly leading them to form inner C-S-H sulfate when exposed to high temperatures. Sulfate and alumina slowly get released over time allowing pores to generate the formation of ettringite at later ages.
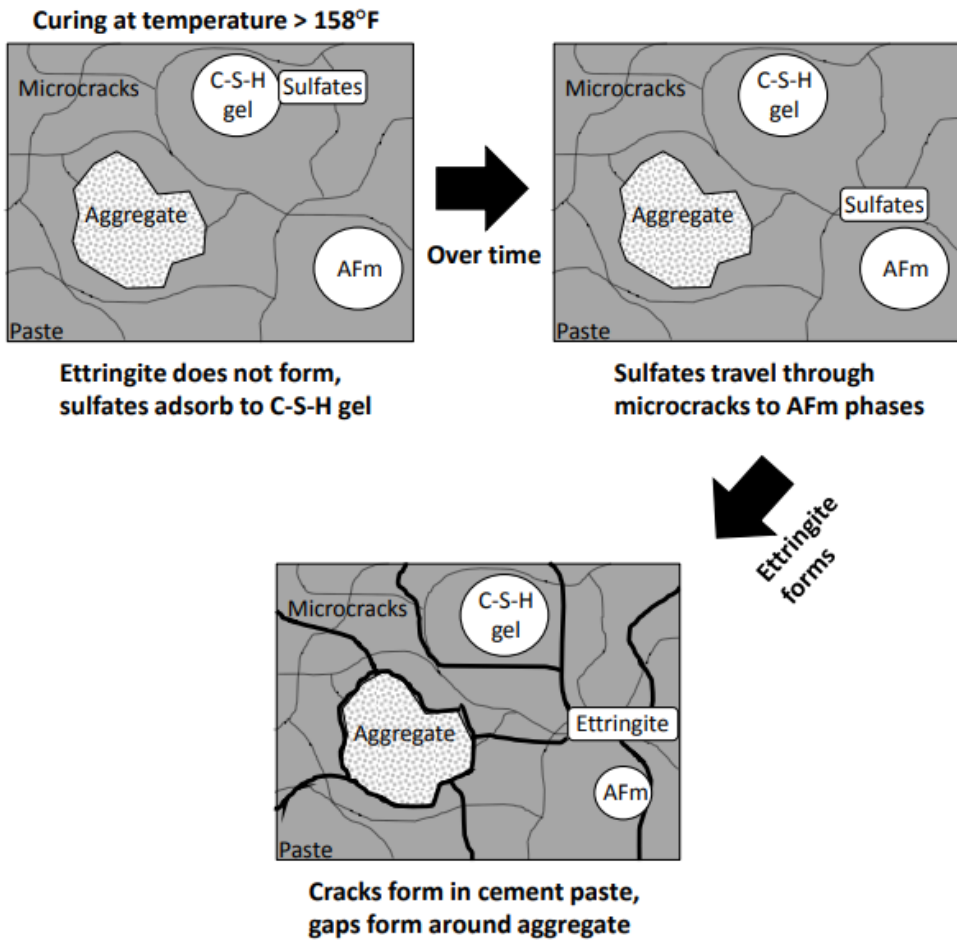
Figure 11.7: DEF Mechanism [15]

11.2.3 Testing Methods

Presently, there are no accepted standard ASTM or AASHTO test methods to assess the performance of DEF in cementitious materials in a laboratory setting. The contributions of DEF are difficult to separate from the effects of distinct mechanisms such as ASR. However, the Kelham method [16] as often been used to accelerate how DEF could affect various cementitious material.

This project applied the reasoning from Kelham [16] to cover molds with a water-soaked cloth to ensure 100% RH during curing. Samples were maintained at 23°C then subjected to a heat curing cycle. The curing regime according to the Kelham method reached 95°F. The Kelham Method differs from the Fu Method [17]in the way that specimens are cured and the maximum temperature reached.

Fu developed a study in 1997 to define whether aggregates could cause reactivity generating expansion in specimens. Fu's study was based on thermal cycling to generate reactivity. His study was later referred as the Fu Method which was helpful for Kelham to acquire more knowledge in ettringite formation. Fu Method utilizes a curing method of oven drying the specimens, whereas, the Kelham Method only dries the specimens in a moist environment. The Kelham method is more reliable to expand the knowledge on DEF due to the management of the moisture conditions that can assimilate the most to the Texas environment. In the REF [18], Fu indicated that ettringite formation can be found in cement paste exposed to temperatures higher than 65°C when its drying, nonetheless the cement paste starts decomposing when drying occurs at 93°C.

11.2.4 DEF Performance of RSHC's

Currently, there are no studies that can be a tool of understanding how DEF reacts on CAC and CSA cements. RSHC's are known for reaching high temperatures at early stages of curing. Pavoine et al [13] exposed the application of a method that can accelerate the impact of DEF in cementitious materials that heat at temperatures over 65°C during curing. Pavoine et al [13] took into count the sulphate content and the alkali content of the cements and concluded that the risk of DEF can be limited by reducing the amount of sulphate and alkali content.

11.3 MATERIALS

11.3.1 Aggregates

Various aggregates were incorporated in this experimental work and are listed in Table 11.3 Three fine aggregates were used for accelerated mortar bar testing (AMBT). Two fine aggregates are classified as "highly reactive" and "moderately reactive" in accordance with ASTM C1778, based on their ASTM C1293 expansion values. The high reactive fine aggregate was obtained from a source in El Paso, TX and is labeled FA1. The moderately reactive aggregate was obtained from Eagle Pass, TX and is labeled FA2. A third fine aggregate was also included and is a non-reactive crushed limestone sand from San Antonio, TX and is labeled FA3.

ASR testing involving concrete specimens including the concrete prism test and outdoor exposure blocks, incorporated a combination of one source of non-reactive limestone coarse aggregate from San Antonio, TX (labeled as CA) and a the highly reactive river sand (FA1). It should be noted that both CA and FA3 are identical aggregate materials and come from the same source in San Antonio, TX.

Table 11.3: Aggregates: Types, Categories and Origins

Aggregates	Description	Category	Source
CA	Crushed Limestone Rock	Non-reactive	San Antonio, TX
FA1	Natural River Sand	Highly reactive	El Paso, TX (Jobe)
FA2	Natural River Sand	Moderately reactive	El Endio, TX
FA3	Manufactured Limestone Sand	Non-reactive	San Antonio

11.3.2 Cements

In this experimental program, a total of 10 rapid setting hydraulic cements (RSHCs) were investigated. The majority of RSCHs were either a calcium aluminate (CAC) or calcium sulfoaluminate cement (CSA) as the primary base binder, with several of them produced as proprietary blended products containing other supplementary cementing materials and/or mineral admixtures (e.g., water reducer, retarder, etc.) to enhance fresh and hardened properties. All proprietary blends of CAC and CSA cements with other materials was carried out during cement production by the manufacturer.

Additionally, two laboratory blends of either CAC or CSA combined with a local Type I/II cement prior to the process of mixing concrete were also investigated. The blended CSA binder, designated as CSA-OPC2, contained a mixture of calcium sulfoaluminate in which the main phases were ye'elimite and calcium sulfate (CSA1) blended with a Type I/II cement procured locally in central Texas at a 25% replacement level (by total mass). Similarly, the blended CAC binder, designated as CAC-OPC2, utilized a combination of calcium aluminate cement and calcium sulfate at a ratio of 2.2:1. This blend was then combined with a Type I/II cement at a 25% replacement level. It should be noted that the proprietary blend cement, CAC-B1, is an equivalent ternary system to CAC-OPC1 containing equal parts of calcium aluminate, calcium sulfate, and Type I/II. However, the type I/II used in the blend was from a different source procured by the manufacturer, and all constituents were blended during cement production. The reason for investigating both proprietary and laboratory blended RSHC systems was to provide a performance comparison between each variation depicting what is often done in current practice in the field with CAC and CSA cements.

Finally, besides CACs and CSAs, three ASTM C150 [19] portland cements procured locally in central Texas were chosen for this study including a high-early strength Type III for comparison to the RSHCs.

Table 11.4 outlines all the cements investigated in this study along with their identification (ID) codes, followed by a short description. Table 11.5 outlines the chemical composition of all the cements investigated in this study given by X-ray flurorescence (XRF) analysis. It should be noted that the equivalent alkali content (Na_2O_e) for RSHCs was calculated using the same expression for equivalent alkalis in portland cement ($\%Na_2O + 0.658*\%K_2O$).

Cement or Blend Type	Cement ID	Cement Category	Description
Straight Cements	OPC1	Portland	Type I OPC, high C_3A, high alkali,
	OPC2	Portland	Type I/II OPC, moderate C_3A, and low alkali
	OPC3	Portland	High-early strength Type III OPC
	CAC	Calcium Aluminate	100% Plain CAC, main phase monocalcium aluminate
	CSA1	Calcium Sulfoaluminate	100% Plain CSA, main phases ye'elimite and calcium sulfate
	CSA2	Calcium Sulfoaluminate	100% Plain CSA, main phases belite, ye'elimite and calcium sulfate
Proprietary Blended Cements	CAC-B1	Calcium Aluminate	Ternary blend of CAC, calcium sulfate, and Type I/II
	CAC-B1*	Calcium Aluminate	Blend of CAC and calcium sulfate, used in combination with Type I/II to produce laboratory ternary blend (CAC-OPC2)
	CAC-B2	Calcium Aluminate	Blend of CAC and fly ash
	CSA-B1	Calcium Sulfoaluminate	Proprietary pre-blend of CSA with mineral admixtures (powder additives)
	CSA-B2	Calcium Sulfoaluminate	Proprietary pre-blend of CSA with mineral admixtures (powder additives)
	PCSA1	Calcium Sulfoaluminate	Proprietary pre-blend not reported by manufacturer
	PCSA2	Calcium Sulfoaluminate	Proprietary pre-blend not reported by manufacturer
Lab Blends	CAC-OPC2	Calcium Aluminate with portland cement	A lab blended cement containing 25% of a calcium aluminate/calcium sulfate blend and 75% of OPC2
	CSA1-OPC2	Calcium sulfoaluminate with portland cement	A lab blended cement containing 25% of CSA1 and 75% of OPC2

Table 11.5: Chemical composition of all sets of cement in this study

Cement Type	Cement ID	SiO$_2$	Al$_2$O$_3$	Fe$_2$O$_3$	CaO	MgO	SO$_3$	Na$_2$O	K$_2$O	Na$_2$O$_e$	LOI
Pure Cements	OPC1	19.60	5.19	2.06	64.01	1.12	3.86	0.12	0.91	0.72	3.80
	OPC2	21.06	4.02	3.19	63.91	1.08	2.89	0.14	0.61	0.53	2.29
	OPC3	19.67	5.34	1.76	63.41	0.99	5.27	0.10	0.44	0.39	4.06
	CAC	4.34	38.65	15.09	38.37	0.39	0.16	0.05	0.14	0.14	1.55
	CSA1	9.07	21.61	2.26	45.26	0.94	20.26	0.07	0.30	0.27	1.05
	CSA2	20.56	16.14	1.35	45.31	1.23	14.73	0.77	0.72	1.24	4.74
Proprietary Blended Cements	CAC-B1	13.46	12.23	2.67	56.65	2.86	9.90	0.20	0.79	0.72	1.21
	CAC-B1*										
	CAC-B2	12.71	32.94	12.95	35.09	1.79	0.84	0.50	0.24	0.65	1.23
	CSA-B1	13.63	15.82	0.75	51.28	1.14	16.62	0.29	0.62	0.69	3.06
	CSA-B2	14.72	14.37	1.22	53.85	1.23	14.40	0.10	0.59	0.49	3.39
	PCSA1	17.38	11.06	2.98	55.82	1.25	10.68	0.43	0.52	0.77	2.26
	PCSA2	20.14	15.73	3.52	43.90	1.55	12.88	0.59	0.52	0.93	1.95
Lab Blends	CAC-OPC2	16.53	10.79	2.71	58.07	0.89	7.43	0.14	0.50	0.47	2.19
	CSA1-OPC2	18.06	8.42	2.96	59.25	1.04	7.23	0.12	0.53	0.47	1.98

11.4 ALKALI-SILICA REACTIVITY EXPERIMENTAL PROCEDURES

Laboratory and field investigations were carried out to investigate the susceptibility of various RSHCs to ASR. This study included several standardized and modified test methods to assess ASR performance including ASTM C1293 (concrete prism test, CPT), ASTM C1260/C1567 (accelerated mortar bar test, AMBT), AASHTO TP 142 (accelerated concrete cylinder test, ACCT), and large scale concrete exposure blocks to provide more realistic information on the behavior of these systems in real-world exposure under Texas conditions. The sections below present details on the testing procedure for each ASR mortar and concrete testing condition.

11.4.1 Accelerated Mortar Bar Test (ASTM C1260/C1567)

Two different series of accelerated mortar bar tests (AMBT) were performed in study including the standardized ASTM C126/C1567 and a modified method. Detailed are provided of each are provided in the sections below.

11.4.1.1 Standardized ASTM C1260/1567 (Series 1)

Each RSHC was evaluated for their ASR susceptibility following ASTM C1260 in which standard mortars are cast and immersed in a 1 M sodium hydroxide (NaOH) solution at 176 °F (80 °C). To evaluate the sensitivity of each RSHC to ASR, three fine aggregates (FA1, FA2, and FA3) with known reactivity with regard to ASR from Texas was selected in this study. More details on the aggregates are provided in the section above. All aggregates were brought to an oven-dry condition and were

subsequently sieved, washed, and graded based on the requirements in ASTM C1260. Four mortar bars with dimensions of 25x25x250 mm (1 x 1 x 11.25 in) were cast for each RSHC system. Sample proportions for a four mortar mixture are included in Table 11.6. It should be noted that ASR mixtures evaluating lab blended cements were proportioned according to their replacement level (see Table 11.7).

After casting, the mortar bars were covered with wet burlap and plastic at 23°C (73 °F) for 24 hours. Subsequently, the bars were demolded and placed in ambient water temperature and stored at 80 °C (176 °F) for 24 hours. After this conditioning, initial length measurements were taken, and the bars were placed in 1 M NaOH solution at 80 °C (176 °F). Length measurements were recorded four times between 1 and 14 days. In addition, 21- and 28-day measurement were taken. The expansion limit of 0.10% at 14 days was selected as the criteria to compare the different systems. Table 11.7 shows the experimental matrix of all RSHC mixtures evaluated following ASTM C1260. It should be noted that no admixtures (e.g., set retarders or water reducers) were used in the fabrication of RSHC mortars for testing in this series.

Table 11.6: ASTM C1260 sample proportions

	Gradation for ASR testing for 4 mortar bars		
	Retained on Sieve #	**Mass, %**	**Quantity, g**
Fine Aggregate	#8	10%	132.0
	#16	25%	330.0
	#30	25%	330.0
	#50	25%	330.0
	#100	15%	198.0
	Total Fina Aggregate FA1/FA2/FA3		1,320.0
		Cement	587.7
		Water	299.25

Table 11.7: Standard accelerated mortar bar test (AMBT) mixture matrix

Cement ID	W/C	Aggregate	Replacement level of RSHC with OPC2 Lab Blend (% of RSHC by mass	
			RSHC Binder	OPC2 Lab Blend
OPC2	0.47	FA1/FA2/FA3	100%	-
OPC3	0.47	FA1/FA2/FA3	100%	-
CAC	0.47	FA1/FA2/FA3	100%	-
CSA1	0.47	FA1/FA2/FA3	100%	-
CSA2	0.47	FA1/FA2/FA3	100%	-
CAC-B1	0.47	FA1/FA2/FA3	100%	-
CAC-B2	0.47	FA1/FA2/FA3	100%	-
CSA-B1	0.47	FA1/FA2/FA3	100%	-
CSA-B2	0.47	FA1/FA2/FA3	100%	-
PCSA1	0.47	FA1/FA2/FA3	100%	-
PCSA2	0.47	FA1/FA2/FA3	100%	-
CAC-OPC2 (B1)	0.47	FA1/FA2/FA3	25%	75%
CAC-OPC2 (B2)	0.47	FA1/FA2/FA3	75%	25%
CSA1-OPC2 (B1)	0.47	FA1/FA2/FA3	25%	75%
CSA1-OPC2 (B2)	0.47	FA1/FA2/FA3	75%	25%

11.4.1.2 Modified ASTM C1260/1567 (Series 2)

While each RSHC was evaluated for their ASR susceptibility following ASTM C1260, it was of interest to identify potential influences in performance and whether standard laboratory methods can accurately determine reactivity with respect to ASR. Thus, a modified approach to the ASTM C1260 standard was also included in which RSCH mortar mixtures were evaluated using a low W/C ratio of 0.35 as commonly used in practice for RSHCs. In this series of test, only the highly-reactive fine aggregate (FA1) was used to evaluate ASR performance. Besides the low W/C used in this series of tests, all other procedures including casting, storage conditions, and monitoring remained identical to ASTM C1260. Table 11.8 shows the experimental matrix of all RSHC mixtures evaluated following a modified ASTM C1260. In these mixtures, high range water reducer was incorporated as needed to achieve suitable workability in the fabrication of RSHC mortars for testing however, no set retarder were incorporated.

Cement ID	W/C	Aggregate	Replacement level of RSHC with OPC2 Lab Blend (% of RSHC by mass	
			RSHC Binder	OPC2 Lab Blend
OPC2	0.35	FA1	100%	-
OPC3	0.35	FA1	100%	-
CAC	0.35	FA1	100%	-
CSA1	0.35	FA1	100%	-
CSA2	0.35	FA1	100%	-
CAC-B1	0.35	FA1	100%	-
CAC-B2	0.35	FA1	100%	-
CSA-B1	0.35	FA1	100%	-
CSA-B2	0.35	FA1	100%	-
PCSA1	0.35	FA1	100%	-
PCSA2	0.35	FA1	100%	-
CAC-OPC2 (B1)	0.35	FA1	25%	75%
CAC-OPC2 (B2)	0.35	FA1	75%	25%
CSA1-OPC2 (B1)	0.35	FA1	25%	75%
CSA1-OPC2 (B2)	0.35	FA1	75%	25%

11.4.2 Concrete Prism Test (ASTM C1293)

Three different series of concrete prism tests (CPT) were performed in study including the standardized ASTM C1293 and modified approaches. Detailed are provided of each are provided in the sections below. Table 11.9 summarizes the various mixture designs used in each series of tests.

11.4.2.1 Standardized ASTM C1293 (Series 1)

Each RSHCs were evaluated following ASTM C1293 in which a single highly-reactive fine aggregate (FA1) and non-reactive coarse aggregate (CA) were used in all concrete mixtures. To prepare for concrete specimens, the coarse aggregate was sieved using a fractionator machine into three equal parts of the three gradation sizes.: 1/2 in, 3/8 in, and 1/5 in (or No. 4) and proportioned according to ASTM C1293. All concrete mixtures had a constant W/C ratio equal to 0.42 and a total cement content of 705 lb/yd^3. Finally, all concrete mixtures were boosted to contain a total equivalent alkali content of 1.25% by mass

of total cement as specified in ASTM C1293. The alkalinity of each concrete mixture was boosted with the addition of a 50/50 NaOH solution in the mixing water. As mentioned previously, the calculated total equivalent alkali (Na_2Oe) was based on the assumption that the same expression for equivalent alkalis in portland cement ($\%Na_2O + 0.658*\%K_2O$) would also apply to RSHCs. Thus, there is some uncertainty in the actual total alkali content that is available from each RSHC for alkali silica reactivity. More information on the alkalis of each cement is provided in Chapter 2.

For each mixture four concrete prisms with dimensions of 3 x 3 x 11.25 in. were cast. After casting, the concrete prisms were covered with wet burlap and plastic at 73°F (23 °C) for 24 hours. Subsequently, the prisms were demolded and were cured for 6 additional days in moist curing room. After this conditioning, initial length measurements were taken, and the bars were stored upright in 5-gallon pails above tap water and stored at 100 °F (38 °C) where length measurements were recorded periodically. A layer of felt fabric was placed in contact with the interior surface of the bucket in order to facilitate wicking of the water from the bottom and create a high RH environment (> 90% RH) as shown in Figure 11.8. Expansion measurements were obtained as indicated in ASTM C1293. Table 11.7 shows the experimental matrix of all RSHC mixtures evaluated following the standardized ASTM C1293 method.

Figure 11.8: Container storing prisms for ASTM C1293

11.4.2.2 Modified ASTM C1293 (Series 2 & 3)

Similar to the ASR mortar bar testing, in order to identify potential influences in performance, variation in the standard ASTM C1293 test method were also evaluated. In this program series, the following two additional series were determined to be of interest for concrete ASR evaluations:

1. **Series 2** – Modified ASTM C1293 using a low W/C ratio of 0.35, a total cementitious content of 752 lb/yd^3, and a total equivalent alkali content of 1.25% with the addition of a 50/50 NaOH solution (boosted).

2. **Series 3** – Modified ASTM C1293 using a low W/C ratio of 0.35, a total cementitious content of 752 lb/yd^3, and with no additional alkalis into the mixtures (Unboosted).

As can be seen, the primary difference between the standardized ASTM C1293 method and the two modified series is the change in mixture designs including using a low W/C ratio and higher total binder content (752 lb/yd^3). Additionally, Series 3 testing did not involve the addition of alkalis (unboosted). This was done to ideally keep conditions as realistic as possible but kept in controlled laboratory conditions to provide valuable ASR performance data on RSHC binder systems. Besides these changes, all other procedures including casting, storage conditions, and monitoring remained identical to ASTM C1293.

Table 11.9: Mixture proportions for the three ASTM C1293 testing series

Series	W/C	Total Binder Kg/m^3(lb/yd^3)	Coarse Aggregate (CA) Kg/m^3(lb/yd^3)	Fine Aggregate (FA1) Kg/m^3(lb/yd^3)	Water Kg/m^3(lb/yd^3)	Boosted
1	0.42	418 (705)	1094 (1844)	684 (1152)	156 (263)	✓
2	0.35	446 (752)	1094 (1844)	684 (1152)	156 (263)	✓
3	0.35	446 (752)	1094 (1844	684 (1152)	156 (263)	X

11.4.2.3 Sample and Measurement Complication for ASTM C1293 Testing (Series 1-3)

Prior to diving into the ASTM C1293 performance results, it should be noted that the ASR measurements in this experimental program produced extreme expansions for all mixtures that is generally not typical when performing ASTM C1293 testing. The researchers believe that this may have been attributed to a change in length comparator device/equipment during the early measurements and consequently, led to an abrupt change in the initial "0-day" length of the samples that was not accounted. While the level of measured expansion was extreme and likely artificial, the behavior of expansion for each mixture over time is consistent with that of ASR (i.e., expansion with eventual exhaustion of alkalis in the system due

to leaching). Thus, sample preparation and fabrication were determined to not be a factor in the observed results. Additionally, petrographic imaging and assessment of each mixture using the Damage Rating Index (DRI) assisted with confirming the damage was due to ASR (See section 11.6.1.7).

11.4.3 Accelerated Concrete Cylinder Test (AASHTO TP 142)

The accelerated concrete cylinder test (ACCT, AASHTO TP 142) is intended to detect the alkali-silica reactivity of an aggregate or assess the effectiveness of SCMs in mitigating alkali-silica reaction (ASR) in terms of measuring the length change of a cylindrical concrete specimen 3 x 6 in immersed in a soak solution with chemistry equal to the pore solution chemistry (PSC) of the tested concrete specimen at 140ºF (60ºC). SCMs from a specific source can be tested individually or in combination with SCMs from other sources. In this project, the ACCT was used to further assess the ASR performance of RSHC systems.

To perform this testing, Texas State University (TSU) used the support and resources from the Texas Transportation Institute (TTI). TTI conducted the ACCT (AASHTO TP 142) testing for 7 RSHC mixtures shown in Table 11.10. It should be noted that the fine aggregate used in this testing series was FA2. Texas State University (TSU) fabricated the samples (3 x 6 inches cylinders) and transported them to TTI's lab. For each mix, one cylinder was tested. The ACCT test needs soak solution chemistry equals pore solution chemistry (PSC) of the tested specimens. TSU provided TTI with average pore solution concentrations shown in Table 11.11 and obtained in [20]. Table 11.11 and a representative PSC [i.e., 0.14 mol/L Na^+, 0.22 mol/L K^+ and saturated with $Ca(OH)_2$] was used to prepare soak solution for all the mixtures.

Table 11.10: Mixture proportions for AASTHO TP 142

Mix No.	Cement Type	W/C	Total Binder $Kg/m^3(lb/yd^3)$	Coarse Aggregate (CA) $Kg/m^3(lb/yd^3)$	Fine Aggregate (FA2) $Kg/m^3(lb/yd^3)$	Water $Kg/m^3(lb/yd^3)$
1	CSA1	0.35	446 (752)	1094 (1844)	684 (1152)	156 (263)
2	CSA2	0.38	446 (752)	1114 (1914)	710 (1196)	170 (286)
3	CAC-B1	0.35	446 (752)	1094 (1844)	684 (1152)	156 (263)
4	CSA-B1	0.38	446 (752)	1114 (1914)	710 (1196)	170 (286)
5	CSA-B2	0.38	446 (752)	1114 (1914)	710 (1196)	170 (286)
6	PCSA1	0.35	446 (752)	1094 (1844)	684 (1152)	156 (263)
7	PCSA2	0.35	446 (752)	1094 (1844)	684 (1152)	156 (263)

Table 11.11: Suggested pore solution chemistry

Potential Cement Type	Concentration (mmol/L)					
	Na^+	K^+	Ca^{2+}	$Al(OH)_4^-$	SO_4^{2-}	OH^-
CSA1	155	250	2.60	178	55	55
CSA2	105	179	2.50	N/A	27	60

11.4.4 Concrete Exposure Blocks

For each concrete mixture, one large-scale exposure block was cast. The exposure block was chosen to have 400 mm (16 in) cubic shape. Figure 11.9 shows various views of the molds for the ASR blocks. Concrete blocks were kept at outdoor exposure with the aim of evaluating ASR performance of RSHC concrete in real-world conditions (i.e., temperatures and humidity fluctuations in San Marcos, TX). Moreover, to apply the most realistic conditions all concrete blocks were fabricated following Series 3 mixture designs (see Section 11.4.2.2). That is, all concrete mixtures were fabricated following a modified ASTM C1293 using a low W/C ratio of 0.35, a total cementitious content of 752 lb/yd^3, and with no additional alkalis into the mixtures (Unboosted). All Series 3 concrete prisms and exposure blocks were cast on the same date.

To fabricate the exposure blocks, each concrete mixture was cast in the mold in two lifts and consolidation was achieved with a portable vibrating rod after each lift. Each block was instrumented with 20 cast-in-place stainless steel bolts that were later used to measure expansion. Each 9.5 mm (3/8 in) diameter bolt was screwed into wood inserts located within each side and top face of the exposure block mold. After concrete was cast within the mold only the tip of the bolt remained visible on the exterior of the block. Prior to casting, a 1 mm (0.04 in) "demec" hole was machined into the end of each bolt using a drill press with a 1 mm (0.04 in) diameter drill bit. Twelve expansion measurements were collected using these "demec" points. Figure 11.10 shows the location of the pins and their measuring diagram. Each exposure block was covered in burlap and wet cured for seven days at ambient temperature prior to taking initial expansion measurements. Once initial measurements were obtained the block was placed outside on the exposure site (See Figure 11.11). Subsequent measurements were taken when outside temperatures are approximately 23 °C (73 °F). To monitor temperature in the blocks for the most accurate measurements, temperature and relative humidity sensor was embedded into large concrete blocks at the moment of casting as shown in Figure 11.11 in each concrete block. Besides monitoring the long-term temperature, the short-term time-temperature history for each mixture was captured through the use embedded sensor and results are reported in Chapter 3. Figure 11.12 shows the finished results of each concrete block sample. Each block was properly labeled marking 5 sides with 4 pins each to allow

tracking of measurements. The vertical sides of steel pins were labeled as to A0-A1 and the horizontal steel to as B0-B1.

Figure 11.9: (1) Exterior View of 16 x 16 x 16 in Wooden Mold (2) Side View of Wooden Mold (3) Interior View of Wooden Mold.
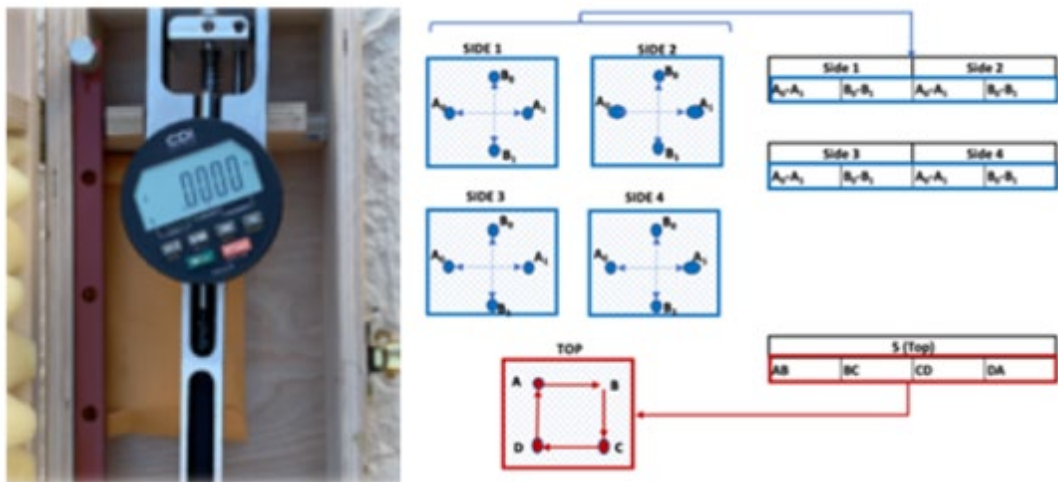

Figure 11.10: (1) Gauge Measurement Device (2) Pin Measurements Diagram

Figure 11.11: Exposure Concrete Block Site at Texas State University - February 15, 2021

Hilti
Temperature
and Humidity
Sensor
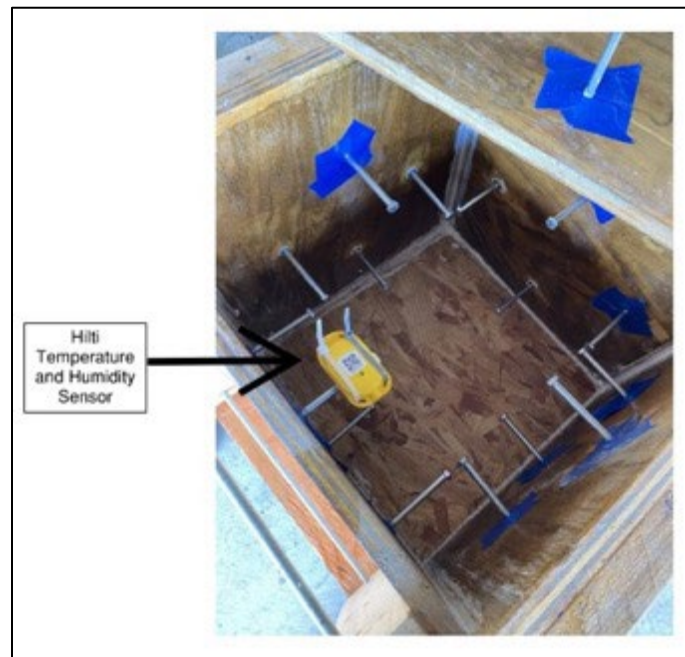
Figure 11.12: Interior view of 16 x 16 x 16 in wooden mold with temperature and humidity sensor attached

Figure 11.13: Completed concrete exposure block – CSA2

11.4.5 Damage Rating Index (DRI)

The Damage Rating Index (DRI) is a semi-quantitative petrographic method designed to evaluate concrete damaged by ASR. With this method polished concrete samples are visually assessed under a stereomicroscope and certain features associated with ASR damage are identified and counted. The total count for each feature is then multiplied by a weighting factor. The weighting factors were chosen to accurately assess each feature according to its importance in relation to ASR damage.

In this experimental matrix, only concrete specimens subjected to Series 3 concrete prism testing were evaluated for their DRI. At the end of the 2 year testing, one concrete prism was removed from each container and prepared for evaluation. To prepare the sample for petrographic analysis, a 50 mm (2 in) slice was taken from the concrete prism. The 50 mm samples were then polished with SiC papers of increasing fineness (#120, #400, #600, #800, and #1200) until a mirror-like surface was achieved. Next a 1 cm2 (0.4 in2) grid was drawn on each sample with permanent marker.

Using a stereomicroscope with a camera attached each 1cm (0.4 in.) square was visually examined at a magnification ranging between 15-18x. The following petrographic features were identified and counted in each square:

- Closed cracks in coarse aggregate particle
- Open cracks in coarse aggregate particle
- Cracks with reaction product in coarse aggregate
- Coarse aggregate debonded
- Disaggregated/Corroded aggregate particle
- Cracks in cement paste
- Cracks with reaction product in cement paste

Once all features were counted for the entire sample they were summed and multiplied by the corresponding weighting factor. The modified weighting factors proposed by Villenueve [21] and Fournier [22] are used in this study and summarized in Table 11.10. Once all the factors were weighted, the summation of the factored counts provided the DRI value for each sample. Finally, the DRI values were divided into four groups which are summarized in Tables 11.11 and 11.12.

Table 11.12: Weighting factors used to determine damage rating index

Petrographic Features	Weighting Factors
Closed cracks in coarse aggregate particle	0.25
Open cracks in coarse aggregate particle	2
Cracks with reaction product in coarse aggregate	2
Coarse aggregate debonded	3
Disaggregated/Corroded aggregate particle	2
Cracks in cement paste	3
Cracks with reaction product in cement paste	3

Table 11.13: Description of DRI Damage Groups [21, 22]

Damage Group	DRI Values	Key Characteristics
1	<200/250	Concrete is in good condition with no signs of deterioration visible at macro level and limited signs of deterioration at micro level (15x magnification). Signs of ASR of samples in this group are generally considered to be at trave level.
2	200/250-400	Concrete is in generally good condition with fair signs of deterioration visible at the macro level, but fair to moderate signs of deterioration at the microlevel. Signs of ASR of samples in this group are generally considered to be at fair to moderate level.
3	400-700/750	Concrete with moderate signs of deterioration visible at the macro level and important signs of damage visible at the micro level. Signs of ASR of samples in this group are generally considered moderate to severe.

4	>700/750	Concrete with severe signs of deterioration visible both at the macro and micro levels and important signs of damage visible at the micro level. Signs of ASR of samples in this group are generally considered severe to very severe.

Table 11.14: Summary of DRI Values Relative to Degree of ASR

DRI	Degree of ASR
<200/250	Trace
200/250-400	Fair to Moderate
400-700/750	Moderate to Severe
>700/750	Severe to Very Severe

11.5 DELAYED ETTRINGITE FORMATION EXPERIMENTAL METHODS

11.5.1 Accelerated High Temperature Curing (Kelham Test Method)

For a given DEF-susceptible mixture, the curing temperature threshold needed to trigger DEF will vary, depending on the chemistry of the cement (particularly alkali content, C_3A content, etc.). In general, OPCs require a temperature exceeding 70°C (158 °F) to trigger DEF. To better assess this for RSHC materials, testing was performed to determine the temperature sensitivity of various mixtures under a Kelham [16] testing regime.

Two series of testing were prepared to investigate the effect of temperature threshold in the generation of DEF in rapid setting cements. The curing cycle utilized by Kelham was based on a peak temperature of 95°C (203°F) for 12 hours in order to trigger DEF in mortar samples (see Figure 11.13). The second temperature cycle was done at a peak temperature of 65°C (149°F) (see Figure 11.14). For both sets of testing, the same mixture proportions were used with the difference of their thermal cycling for curing being the primary focus in the investigation.

**Figure 11.14: Series 1: Kelham Method for DEF Curing**

Figure 11.15: Series 1: Kelham Method for DEF Curing

259
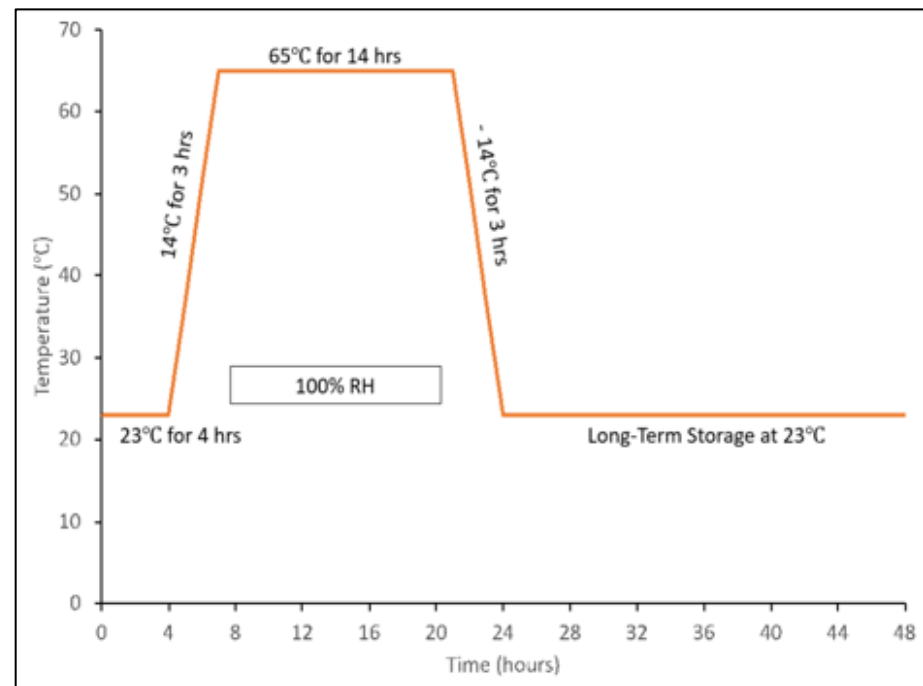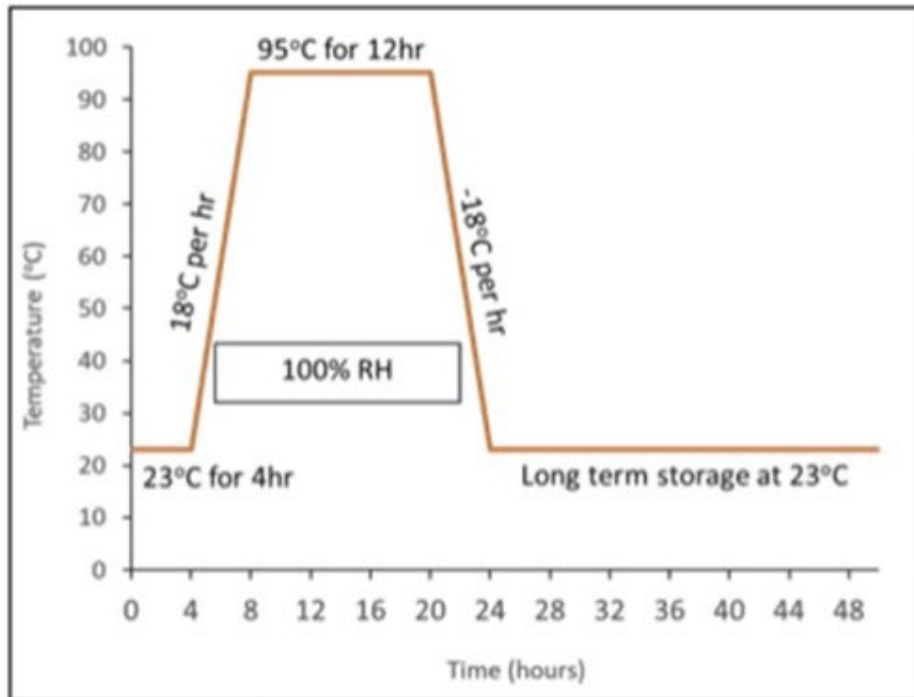
Series 1 and 2 consisted of the exact same set of binders and mixture proportions with the only difference of the curing cycles. Each series was composed of 14 standard mortar mixtures which include (4) 1 x 1 x 11.25 in prism specimens with a W/C ratio of 0.47. Each series were prepared with a highly-reactive fine aggregate (FA1) in terms of alkali silica reactivity. Table 11.13 below summarizes the overall series of mixture included in this program.

Table 11.15: DEF mixture matrix

Cement ID	W/C	Aggregate	Replacement level of RSHC with OPC2 Lab Blend (% of RSHC by mass	
			RSHC Binder	OPC2 Lab Blend
OPC2	0.35	FA1	100%	-
OPC3	0.35	FA1	100%	-
CAC	0.35	FA1	100%	-
CSA1	0.35	FA1	100%	-
CSA2	0.35	FA1	100%	-
CAC-B1	0.35	FA1	100%	-
CAC-B2	0.35	FA1	100%	-
CSA-B1	0.35	FA1	100%	-
CSA-B2	0.35	FA1	100%	-
PCSA1	0.35	FA1	100%	-
PCSA2	0.35	FA1	100%	-
CAC-OPC2	0.35	FA1	25%	75%
CAC-OPC2	0.35	FA1	75%	25%
CSA1-OPC2	0.35	FA1	25%	75%

The mixing procedure was performed in accordance with ASTM C1260/C1567. After molds were filled with mortar, each mold was placed in a container with approximately 25 mm (1 inch) of water at the bottom to achieve >95% RH during the high temperature cycle for triggering DEF. Plastic bases were used to lift each mold to avoid contact of the molds with the water. Once each mixture was subjected to the heat cycle, samples were demolded, left to cool to room temperature and measured for initial length. Thereafter, all samples were maintained an airtight sealed contained in a saturated solution of limewater at 23°C while measurements taken periodically.

11.6 RESULTS AND DISCUSSIONS

11.6.1 Alkali Silica Reaction

11.6.1.1 Standardized ASTM C1260/1567

Table 11.14 below summarize the ASR performance of all RSHC mixtures evaluated with the three fine aggregates (FA1, FA2, and FA3). Additionally, the table includes a key color coding identifying the potential reactivity of each RSHC system based on their average 14-day expansion and guidance from ASTM C1778 [9]. As expected, between the three different aggregates the crushed limestone fine aggregate consistently produced the lowest levels of expansion. Interestingly, the lab blended systems (CAC-OPC2 (B2) & CSA-OPC2 (B2)) containing high proportion of RSHC (75% RSHC and 25% OPC2) observed higher expansion. This was not expected as it was assumed that the expansion due to ASR would be contributed more from the OPC system. Between the moderately (FA2) and highly reactive fine aggregate (FA1), the majority of mixtures showed general agreement in performance. That is, higher and increasing expansion was observed in mixtures containing the highly reactive fine aggregate (FA1) compared to the moderately reactive fine aggregate (FA2). The only exceptions were CSA-B2 and CAC1-OPC2 (B2) which showed contradictory results between the two aggregates. Nonetheless, the outcomes from this test confirmed the correlation between the reactivity level of the aggregate with the type of cement.

Table 11.16: AMBT 14-Day Average Expansion and Performance Criteria for all RSHC Mixtures

Cement ID	Avg Expansion @ 14 Day (%)		
	FA1 (Jobe)	FA2 (El Indio)	FA3 (Limestone)
OPC1	0.61	0.35	0.04
OPC2	0.44	0.33	0.01
OPC3	0.60	0.43	0.02
CAC1	0.09	0.02	0.00
CSA1	0.15	N/A	0.05
CSA2	0.03	0.03	0.01
CAC-B1	0.55	0.15	0.03
CAC-B2	0.12	0.05	0.00
CSA2-B1	0.25	0.17	0.07
CSA2-B2	0.02	0.37	0.06
PCSA1	0.52	0.54	0.02
PCSA2	0.12	0.05	0.00
CAC1-OPC2 (B1)	0.46	0.29	0.06

CAC1-OPC2 (B2)	N/A	0.09	0.07
CSA1-OPC2 (B1)	0.59	0.42	0.12
CSA1-OPC2 (B2)	0.25	0.61	0.13

	Non-reactive	Less than 0.10%
Key	Potentially reactive	0.10% to 0.20%
	Reactive	Greater than 0.20%

Figures 11.15-11.28 illustrates the expansion results of all RSHC systems using the various aggregate types obtained from the AMBT and are analyzed by type of cement. The cements were divided into OPC, CSA1, CAC1, CSA2, and lab blend systems. Between all binder systems, OPC1, OPC2, OPC3, CAC-B1, PCSA1, CAC-OPC2, and CSA-OPC2 consistently measured the most expansion, especially when tested with the highly reactive fine aggregate (FA1). On the other hand, binder systems containing CSA as the primary component showed the least level of expansion.
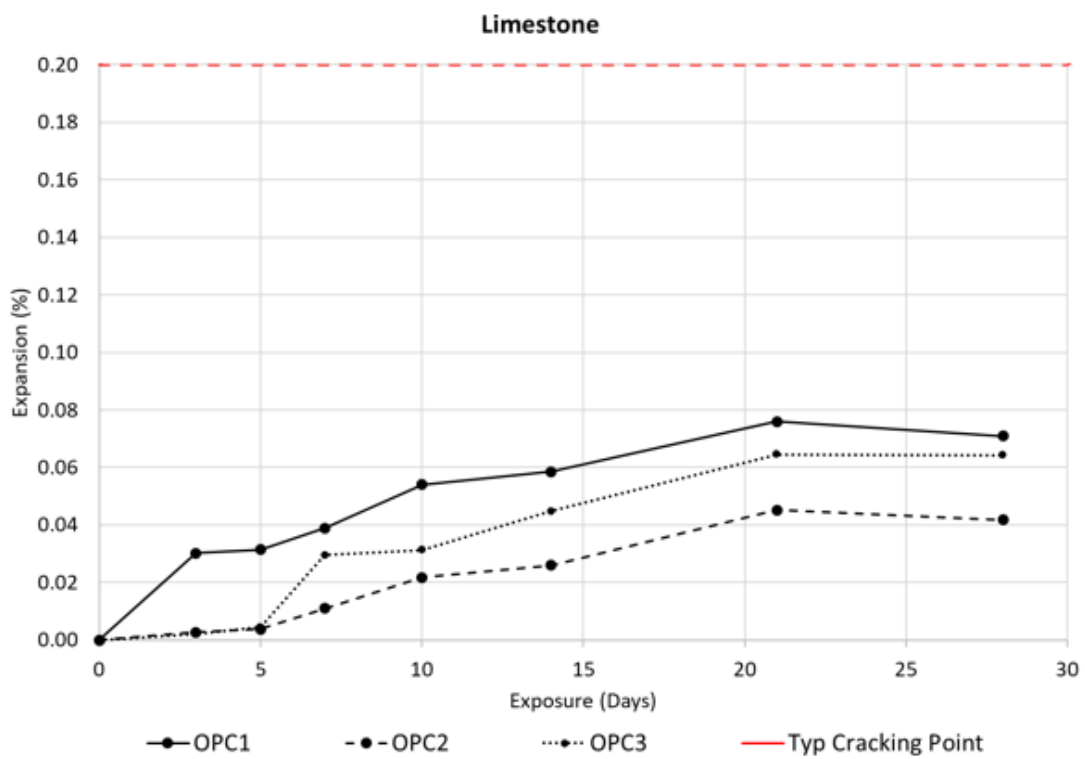
Figure 11.16: AMBT Results for OPC Systems using Non-Reactive Fine Aggregate (FA3)
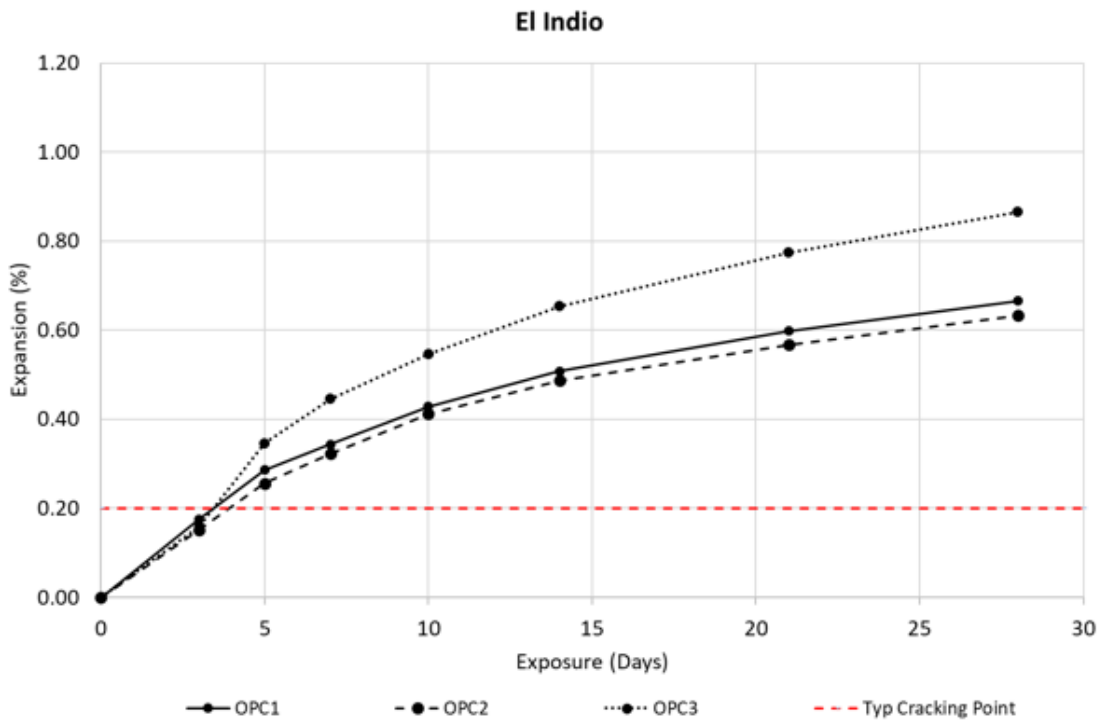
Figure 11.17: AMBT Results for OPC Systems using Moderately-Reactive Fine Aggregate (FA2)
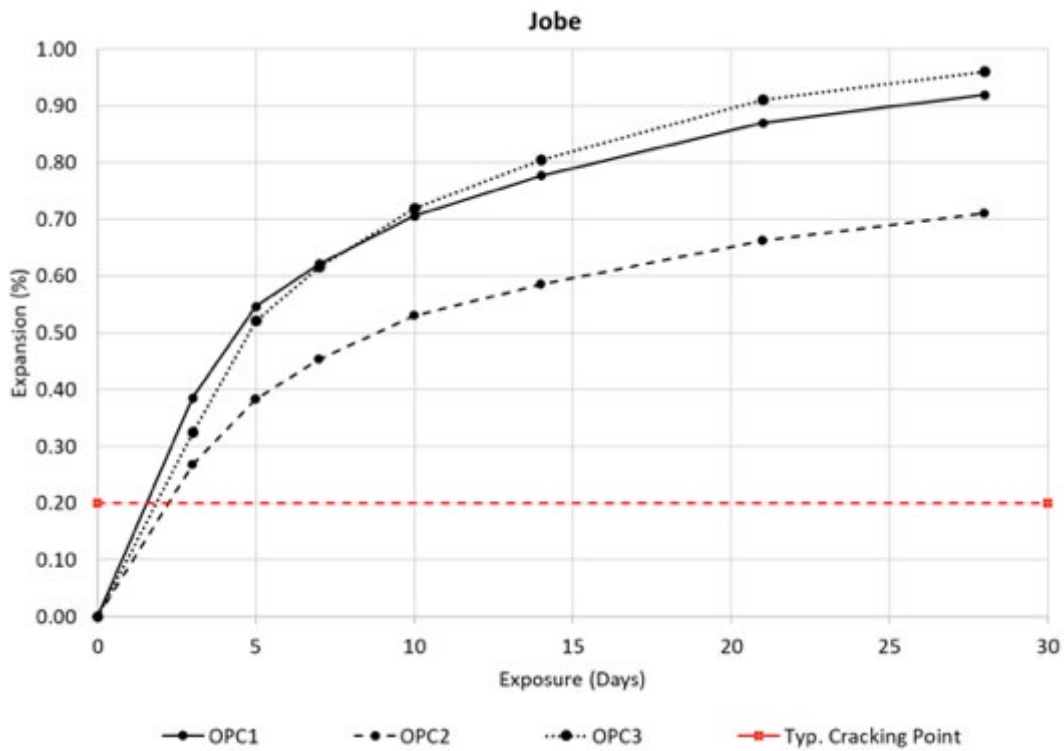

Figure 11.18: AMBT Results for OPC Systems using Highly-Reactive Fine Aggregate (FA1)

263
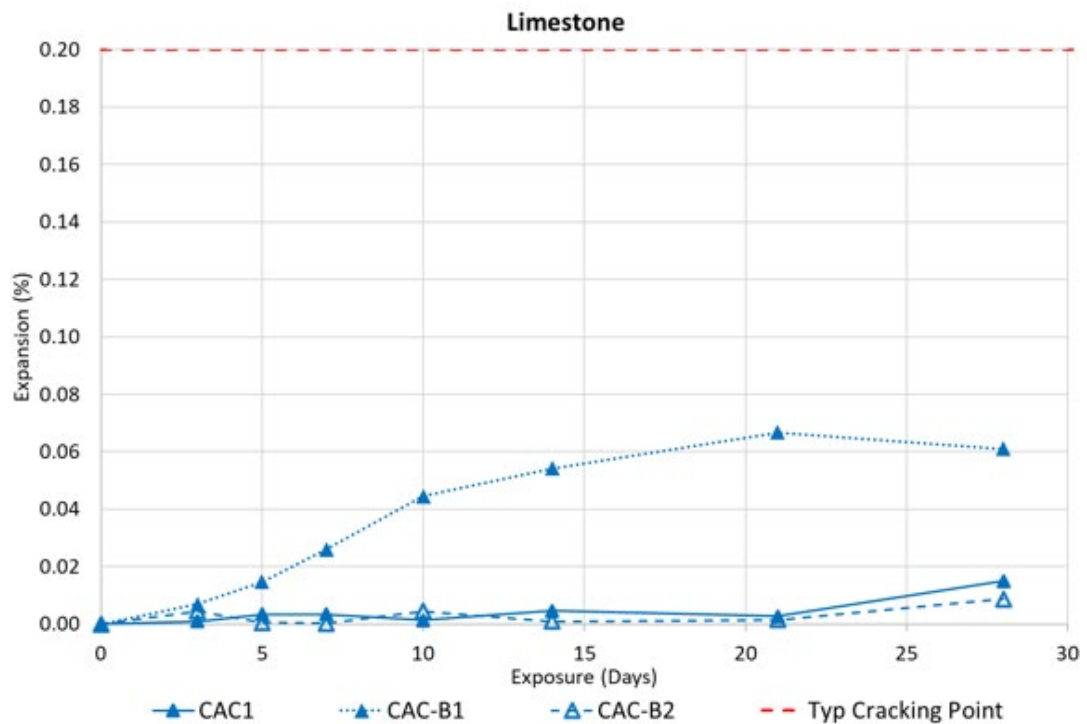
**Figure 11.19: AMBT Results for CAC Systems using Non-Reactive Fine Aggregate (FA3)**
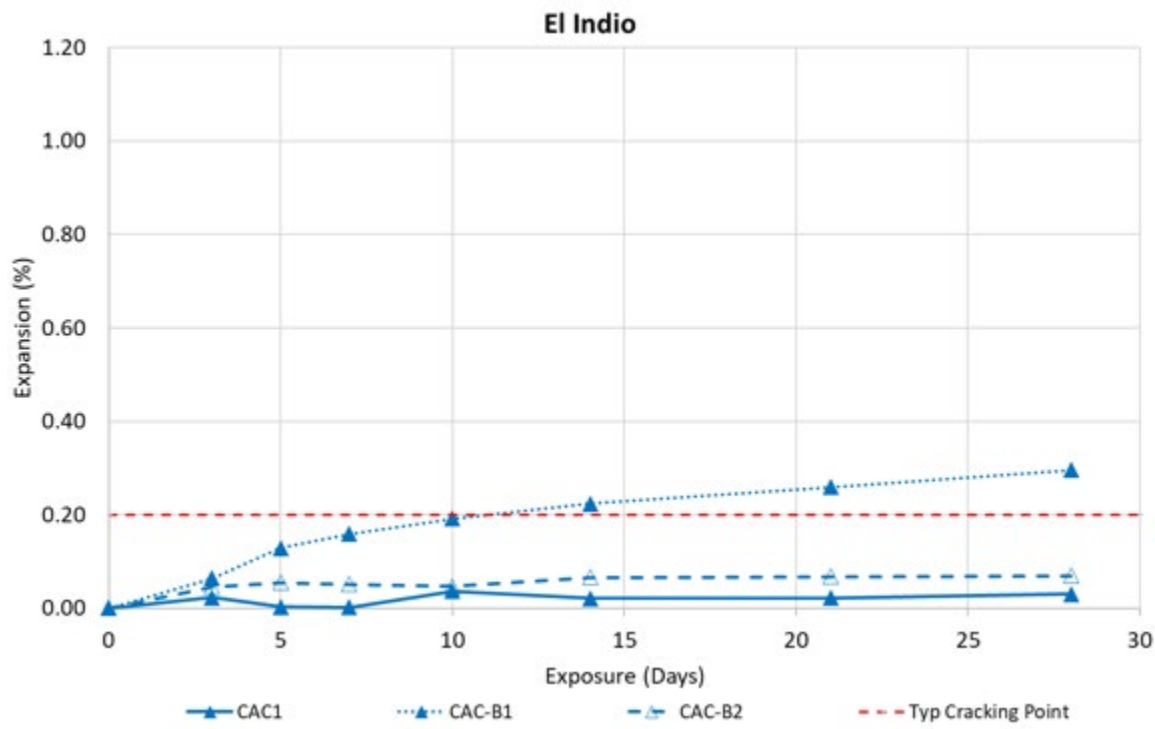
Figure 11.20: AMBT Results for CAC Systems using Moderately-Reactive Fine Aggregate (FA2)

264
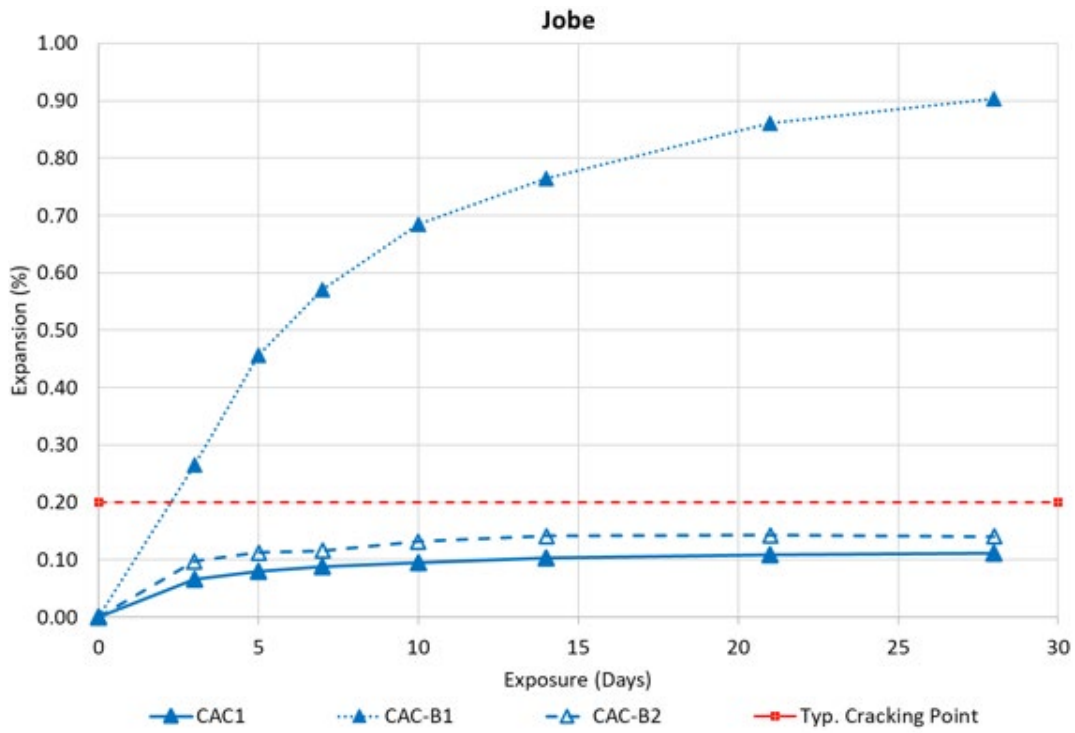
**Figure 11.21: AMBT Results for CAC Systems using Highly-Reactive Fine Aggregate(FA1)**
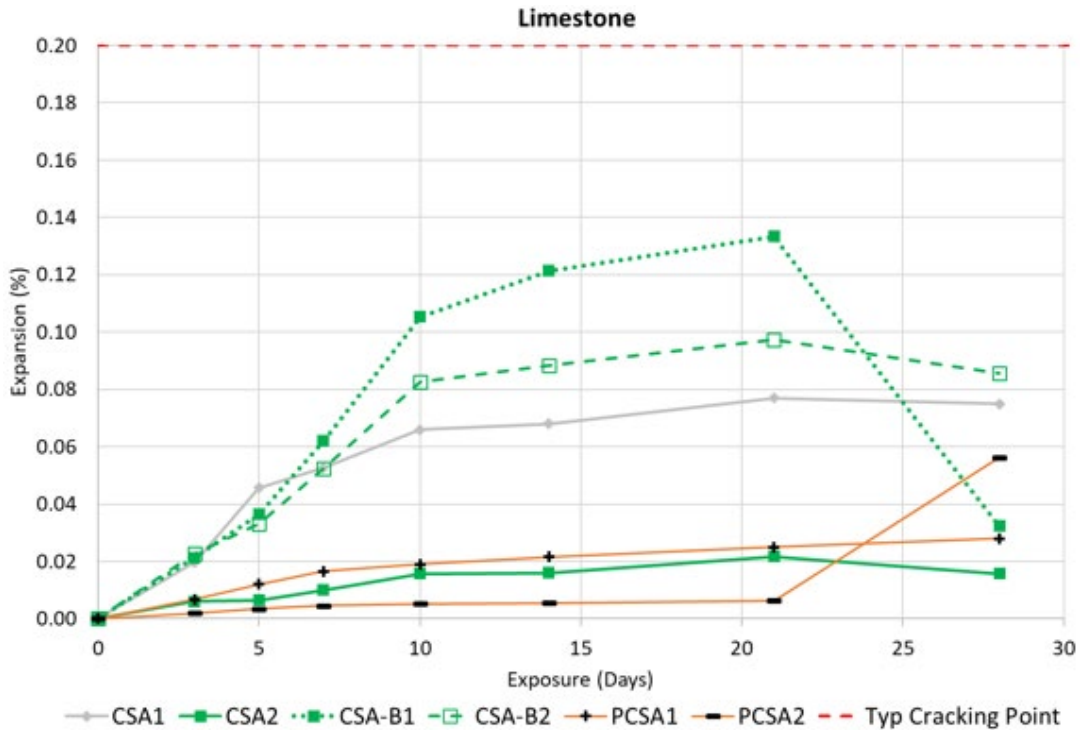
Figure 11.22: AMBT Results for CSA and PCSA Systems using Non-Reactive Fine Aggregate (FA3)

265
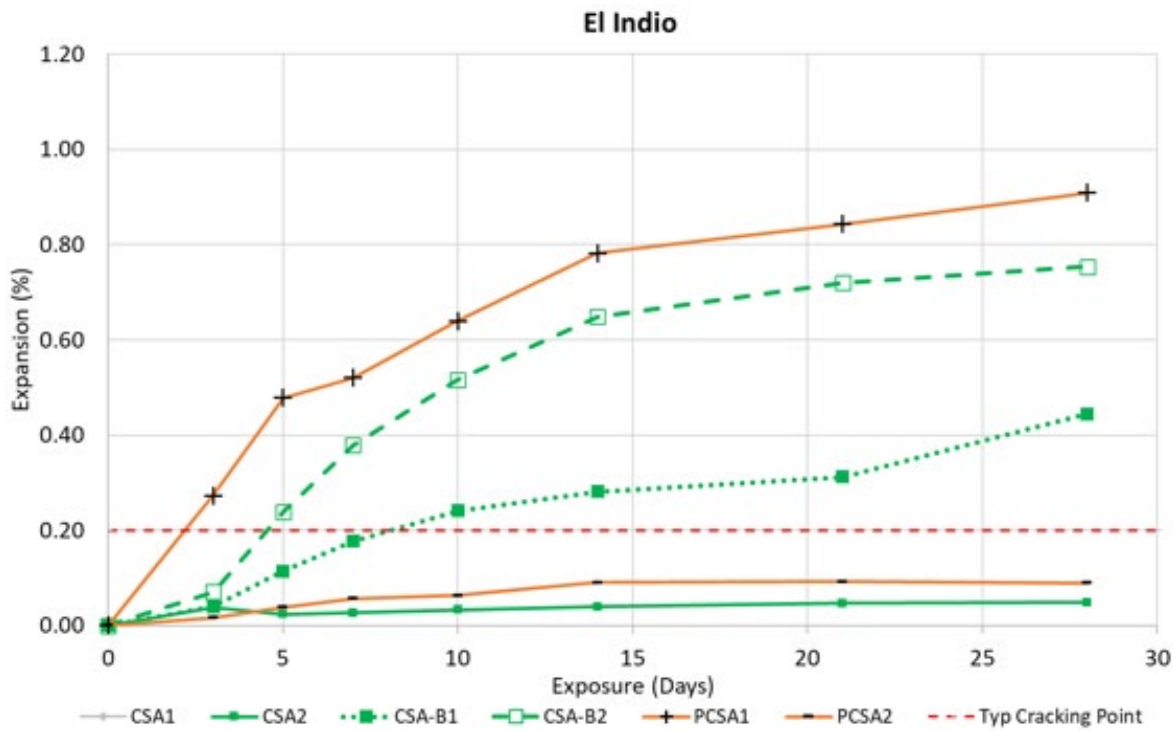
Figure 11.23: AMBT Results for CSA and PCSA Systems using Moderately-Reactive Fine Aggregate (FA2)
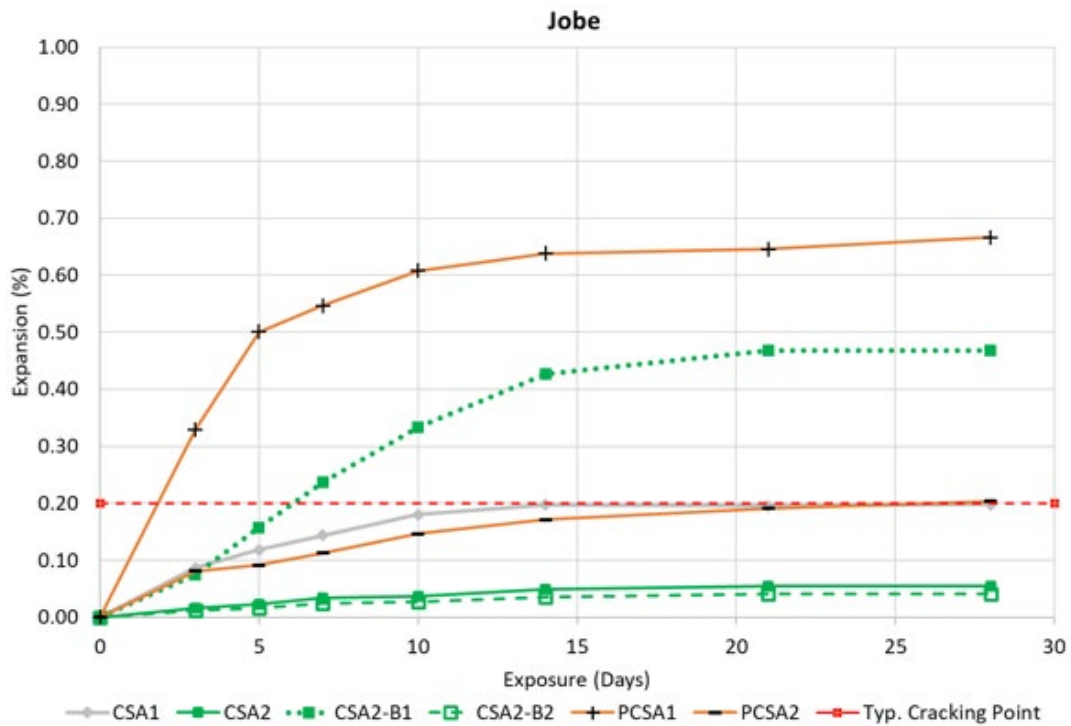

Figure 11.24: AMBT Results for CSA and PCSA Systems using Highly-Reactive Fine Aggregate (FA1)

266
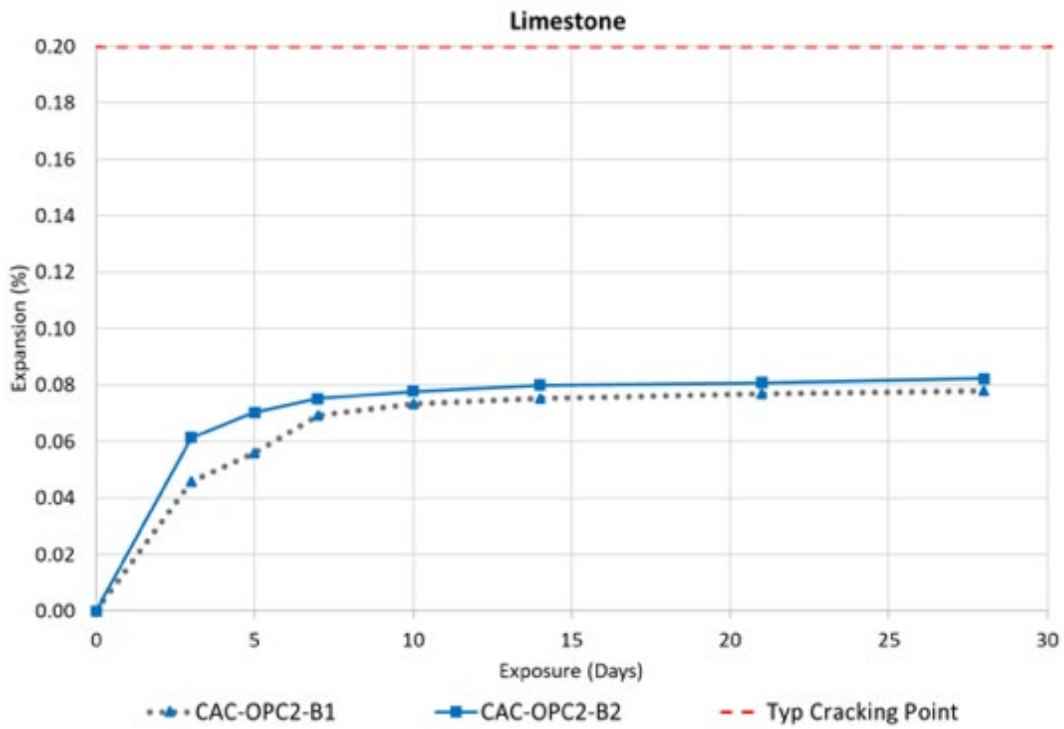
Figure 11.25: AMBT Results for Blended CAC Systems using Non-Reactive Fine Aggregate (FA3)
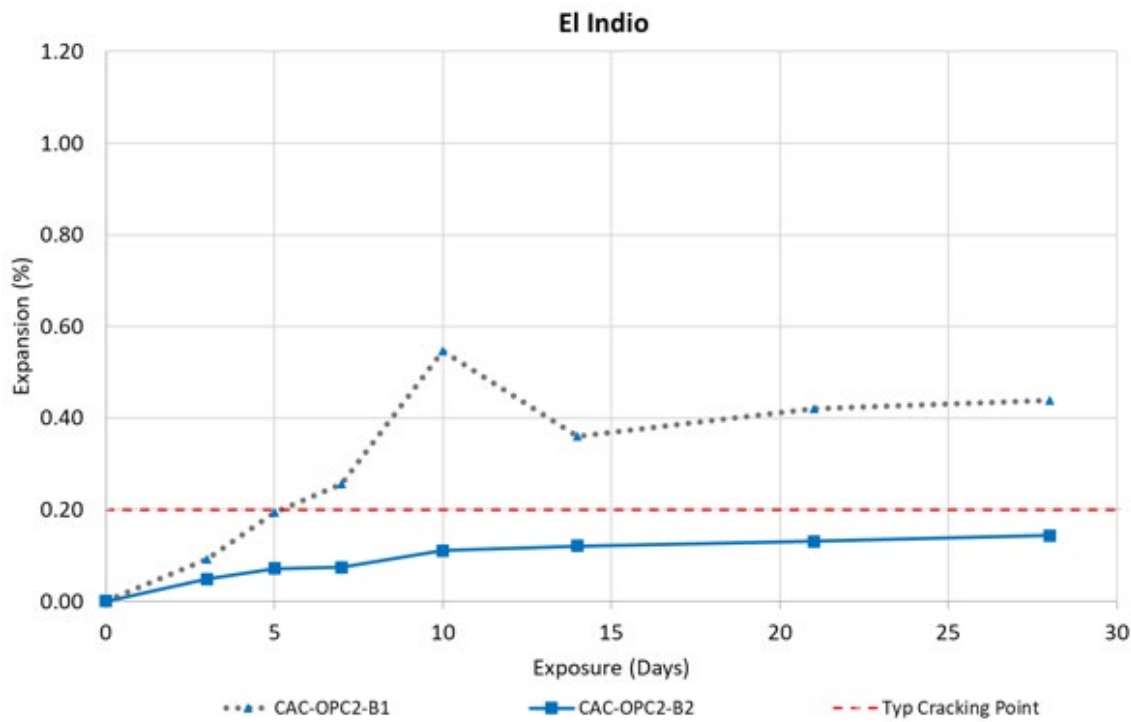
Figure 11.26: AMBT Results for Blended CAC Systems using Moderately-Reactive Fine Aggregate (FA2)
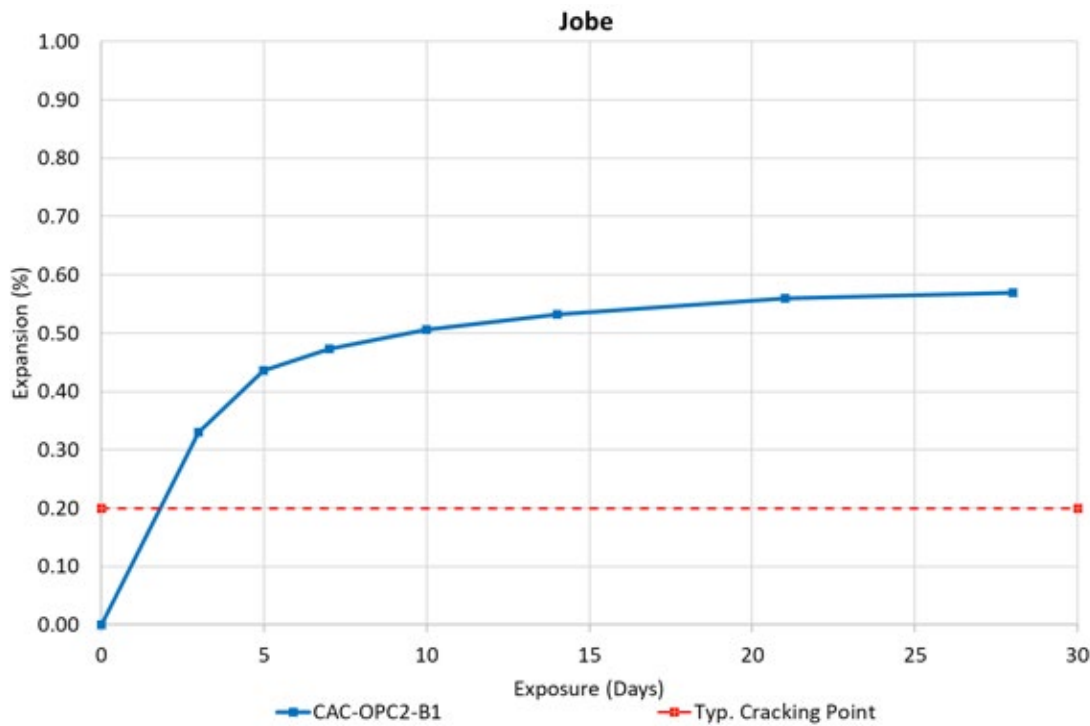
Figure 11.27: AMBT Results for Blended CAC Systems using Highly-Reactive Fine Aggregate (FA1)
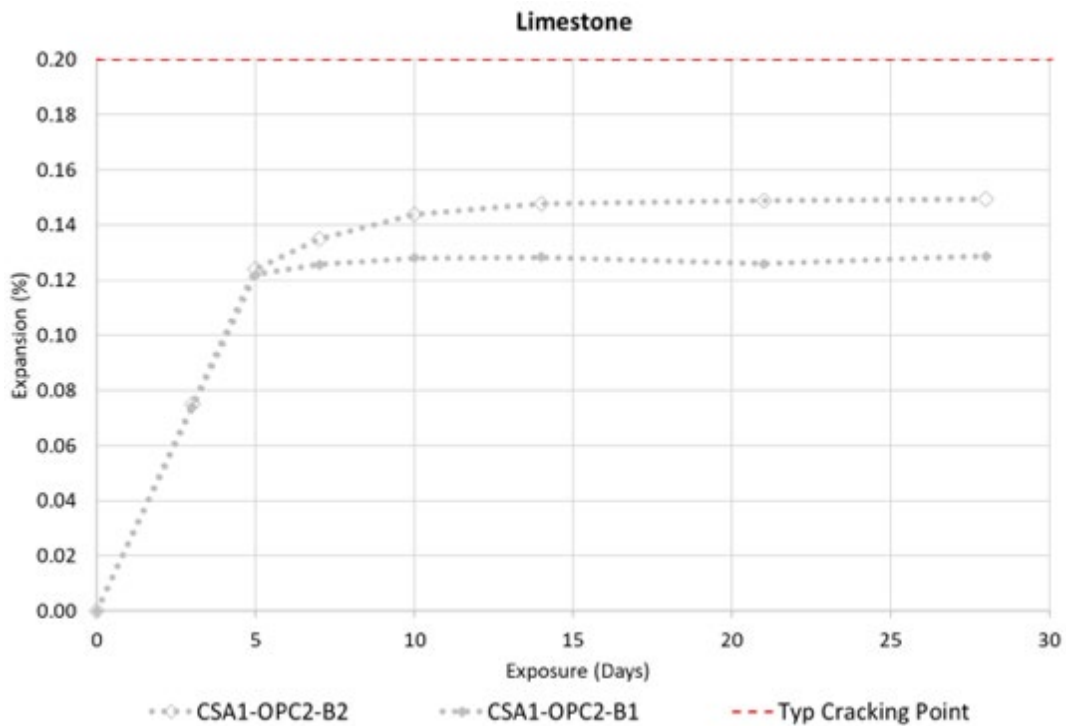
Figure 11.28: AMBT Results for Blended CSA Systems using Non-Reactive Fine Aggregate (FA3)
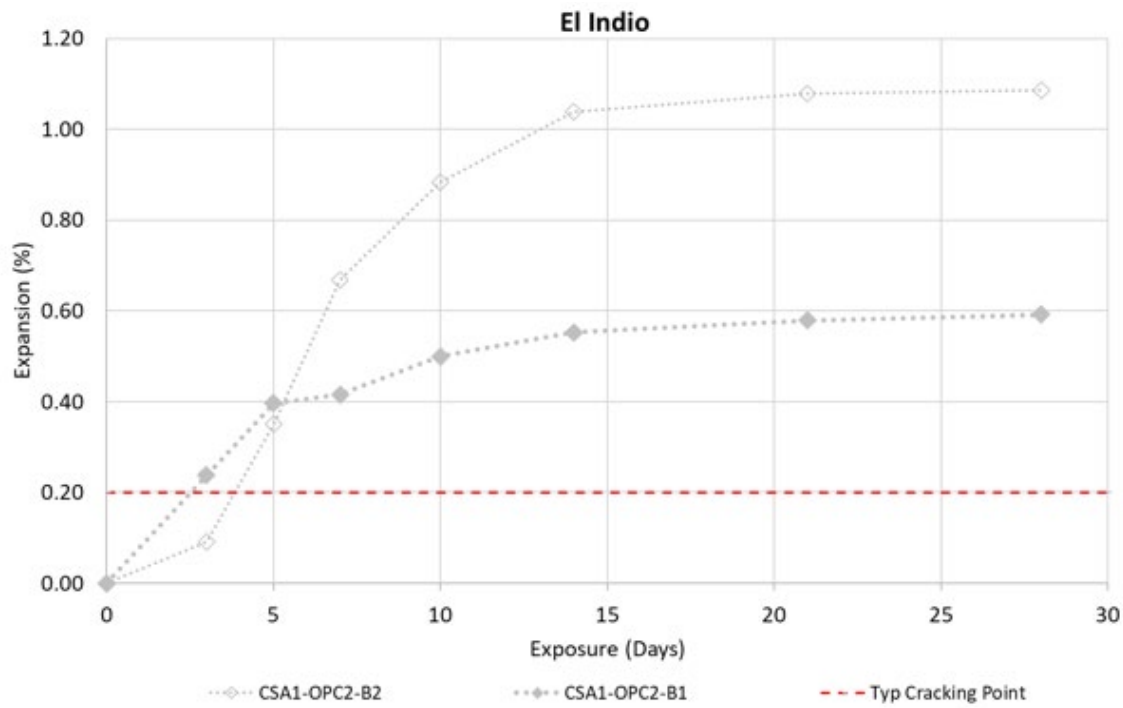
**Figure 11.29: AMBT Results for Blended CSA Systems using Moderately-Reactive Fine Aggregate (FA2)**
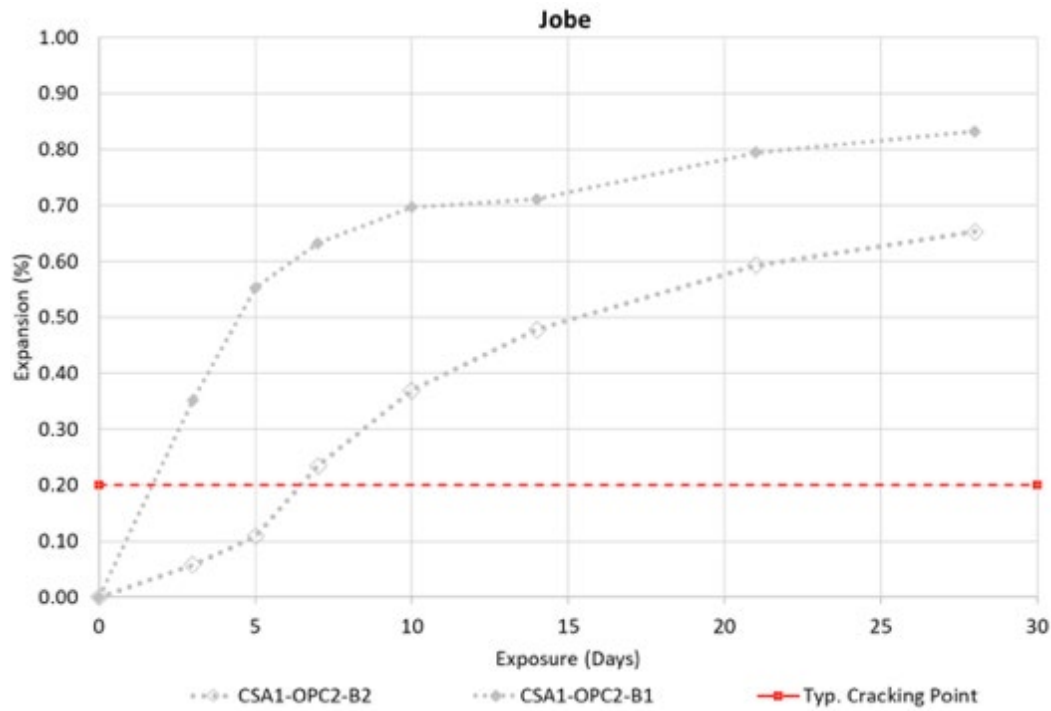
Figure 11.30: AMBT Results for Blended CSA Systems using Highly-Reactive Fine Aggregate (FA1)

11.6.1.2 Modified ASTM C1260/1567

Figure 11.29 shows the expansion curves for the cementitious mixture evaluated following ASTM C1260 at a W/C ratio of 0.47. As a reminder, in this series of test only the highly-reactive fine aggregate (FA1) was used to evaluate ASR performance. The results show that the only mixtures that were able to achieve an expansion less than 0.10% at 14 days were CSA2 (0.05%), CSA2-B2 (0.03%), and CAC1 (0.09%), with three others (CSA1, PCSA2, and CAC-B2) having an expansion less than 0.20% after 14 days of exposure. What appears to be fairly clear in the results is the apparent increase in expansion when mixtures incorporated some amount of OPC in the blend. For example, CSA1 showed moderate expansion at about 0.19% after 14-days exposure but dramatically increased to more than 0.70% when used as a blended system with OPC. Interestingly, the expansion was even greater than the straight OPC2 mixture which showed an expansion of 0.59% at 14-days exposure. Similar behavior is observed in CAC-B1 and CAC1-OPC2 where OPC is incorporated as a pre-blend and lab-blend, respectively.

Figure 11.30 shows the expansion curves for the cementitious mixture evaluated following ASTM C1260 at a W/C ratio of 0.35. As expected, the expansion of all systems decreased from the use of a lower W/C and resulting reduction in permeability in the system. It is also likely that the lower W/C ratio increased the strength of each sample which may have resulted in higher resistance to the observed expansion. With the reduction in W/C ratio, several more binder were able to achieve an expansion less than 0.10% at 14-days including CSA1, CSA2, CSA2-B2, CAC1, CAC-B2, PCSA2. While all mixtures showed a marked reduction in expansion, CAC1-B1 did not seem to improve very much.

Figure 11.31 summarizes the 14-day expansion exhibited by all mixtures in a bar chart form for both series 1 and 2. Here it can be seen the differences in expansion between the two series as well as those mixtures that did not exceed the 0.10% expansion limit.

Figure 11.32-11.34 shows several relationships between 14-day expansion data for all mixtures and various oxide information based on the chemical analysis of each cement. The data used to develop these relationships were collected from XRF analysis performed by TxDOT. It should be noted that there is some level of uncertainty on the results obtained from chemical analysis due to the rarity of XRF information available on the rapid setting binders. In addition, the calculated total equivalent alkali (Na_2O_e) was based on the assumption that the calculation used for ASTM C150 portland cements would also apply to RSHCs. Figures 11.32 and 11.33 show there is clearly no relationship that exists between the observed expansion of each binder and their equivalent alkali or aluminate oxide content. As expected, the equivalent alkali should have very little impact on the reactivity of these binders due to storage of these samples in 1 M sodium hydroxide. In addition, while the expansion does decrease with

increasing aluminate content, the correlation is very weak. However, there does appear to be some indication that expansion does reduce substantially when the alumina content within the binders is great than 20%. On the other hand, there is a more substantial relationship that exists between the observed expansion and the calcium oxide content as measured by the XRF analysis (Figure 11.34). Further evaluation is needed to understand the relationship and alkali silica reactivity of each RSCH binder.
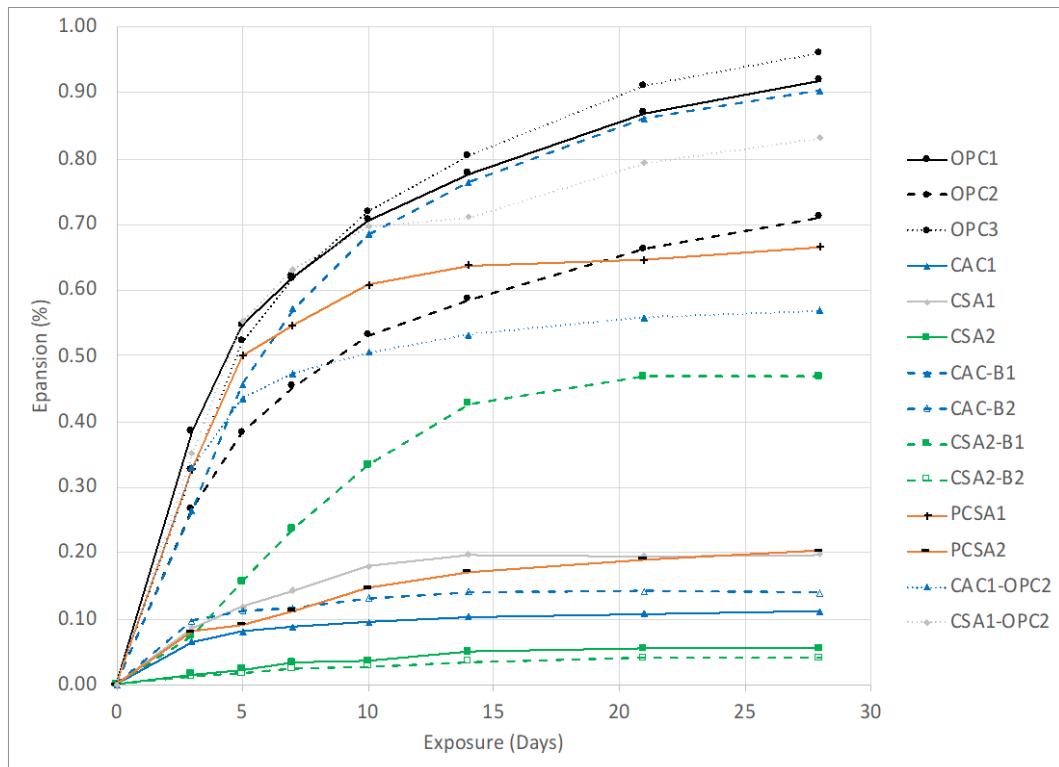

**Figure 11.31: Series 1 Expansion curves for ASR Mortar Samples**
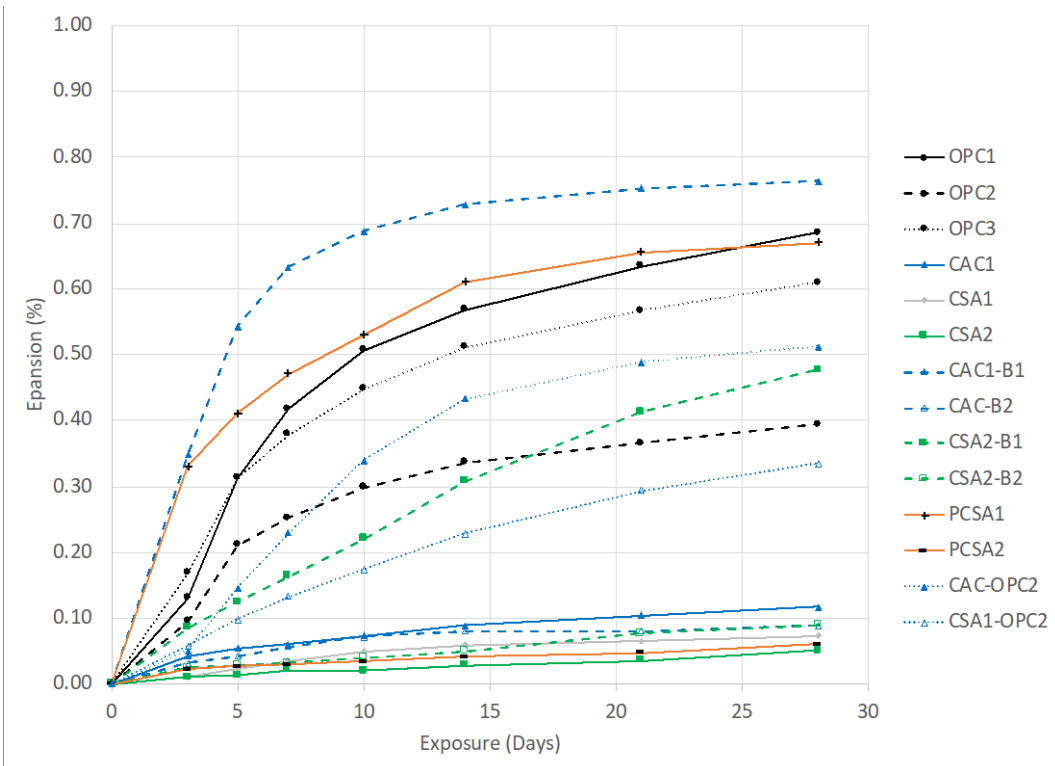
**Figure 11.32: Series 2 Expansion curves for ASR Mortar Samples**
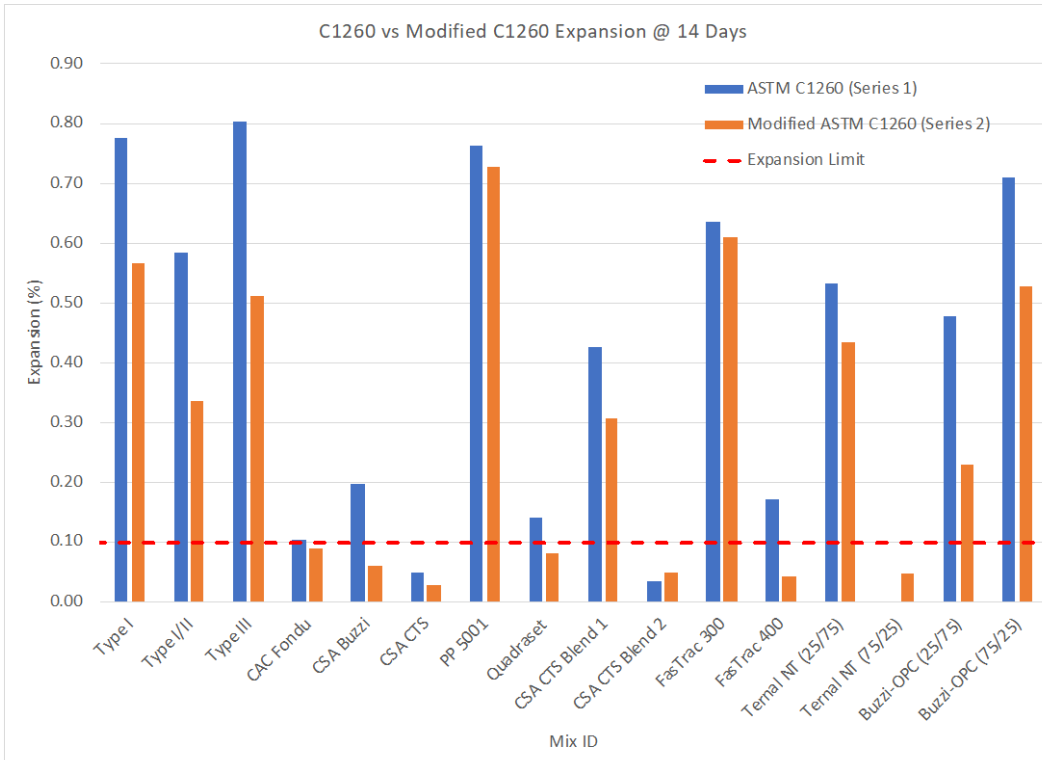
**Figure 11.33: Series 2 Expansion curves for ASR Mortar Samples**
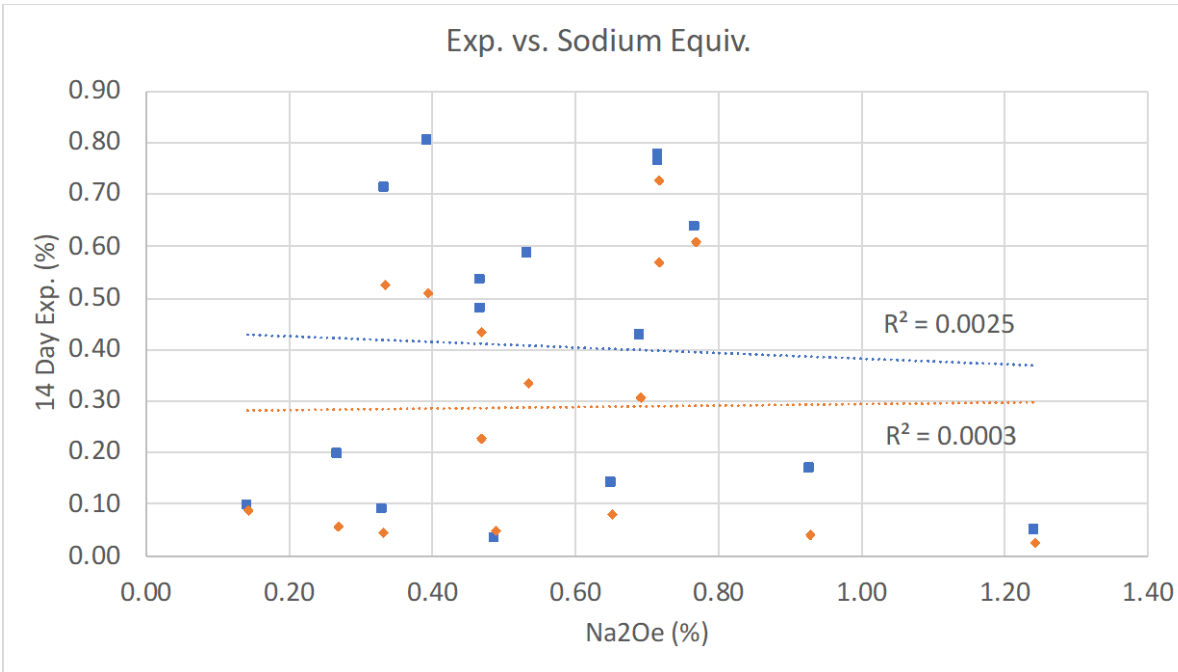
**Figure 11.34: ASR Expansion vs. alkali equivalent Oxide by XRF**
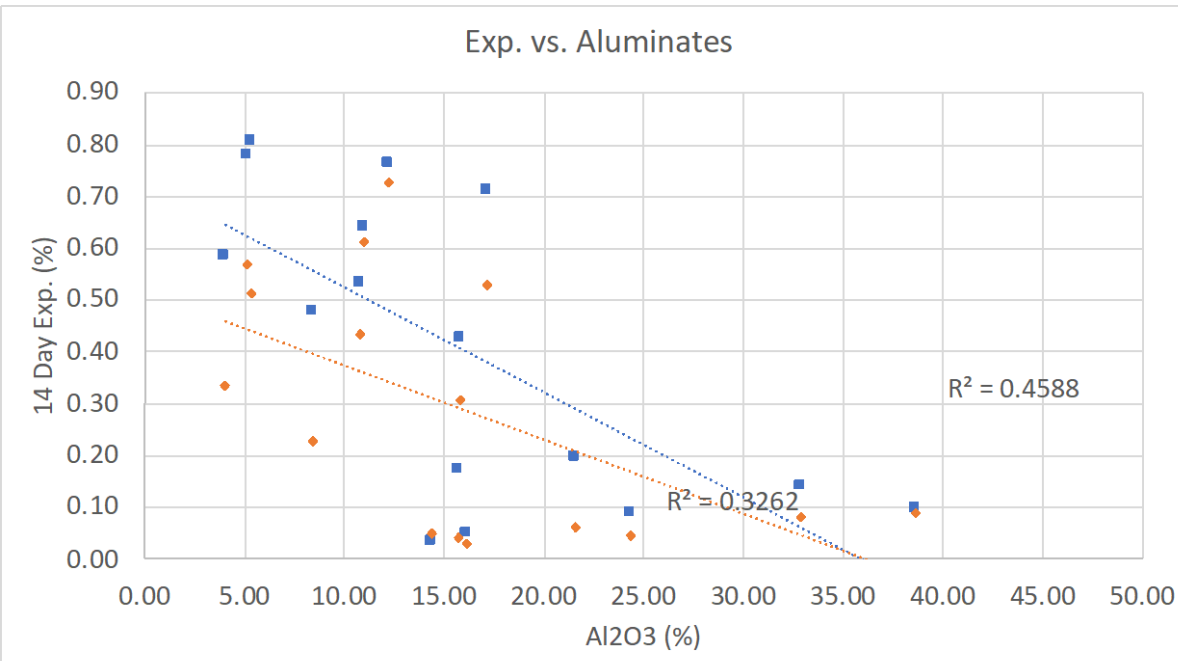
Figure 11.35: ASR Expansion vs. Alumina Oxide by XRF

273
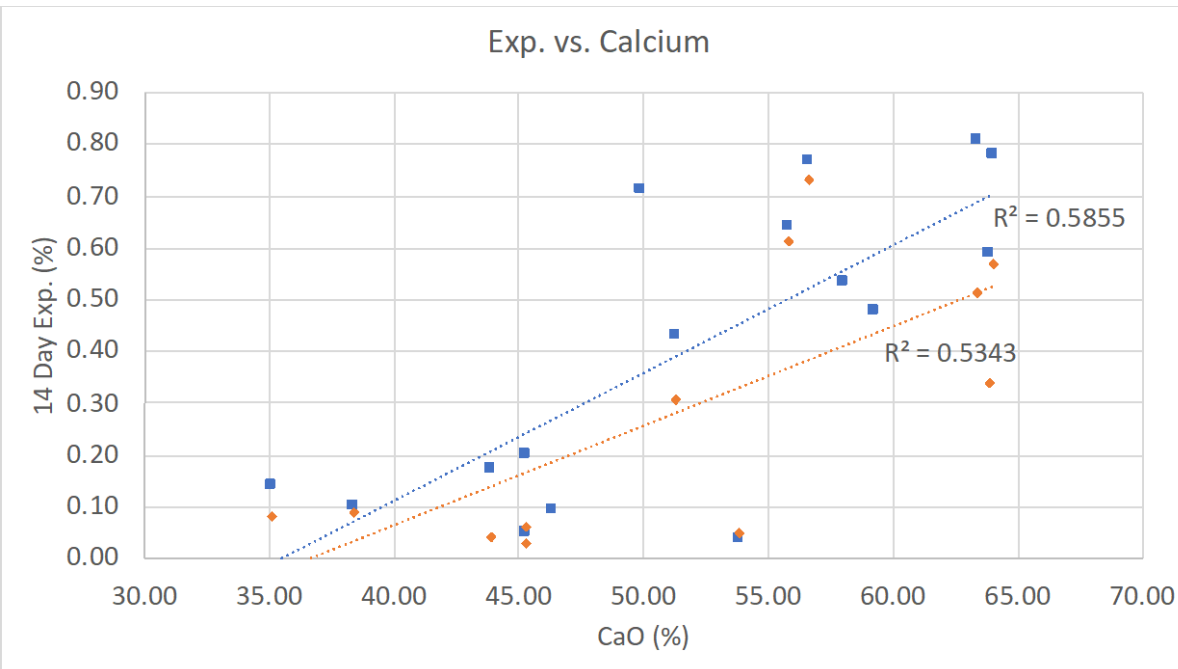
Figure 11.36: ASR Expansion vs. Calcium Oxide by XRF

11.6.1.3 Standardized ASTM C1293 (Series 1)

The alkali silica reactivity (ASR) results for each RSHC following the standardized ASTM C1293 method are presented in Figure 11.37 below. As expected, the OPC1 showed high expansion within 6 months of exposure. On the other hand, there were unexpected expansion results for some RSHCs. In particular, CSA1 showed extreme expansion within four months of testing and was no longer measurable after 6 months due to the excessive expansion and no longer fitting within the length comparator. CSA1 is a high ye'limite cement and is not known to behave deleteriously in ASR environment. However, CSA1 did not show similar behavior when subjected C1293 conditions and not boosted with additional alkalis (See Section 11.6.1.4). Thus, the results clearly showed that the addition of alkalis into the system did not produce realistic expansion and likely triggered a different form of expansion. More worok is needed to understand the sensitivity of alkalis in calcium sulfoalumiante cements.

The results also showed that many RSHCs in which Portland cement was included in the system (whether as a lab blend or intergrinded during production), excessive expansion was also observed. For example, CAC1-B1, CAC1-OPC2, and CSA1-OPC all experienced some of the highest expansions. While these cements were also boosted with the additional of alkalis to achieve an equivalent alkali loading (Na_2O_e) of

1.25%, the results also showed that the addition of Portland cement may have had some impact on the observed expansion.

Besides CSA-B1, all other RSHC showed relatively lower expansion in comparison to the those mentioned above. Additionally, the expansion behavior is generally in agreement with what was observed in the ASTM C1260/C1257 testing (See Section 11.6.1.2). In other words, RSHCs that observed high expansion in the accelerated mortar bar test also observed high expansion in the concrete prism test.
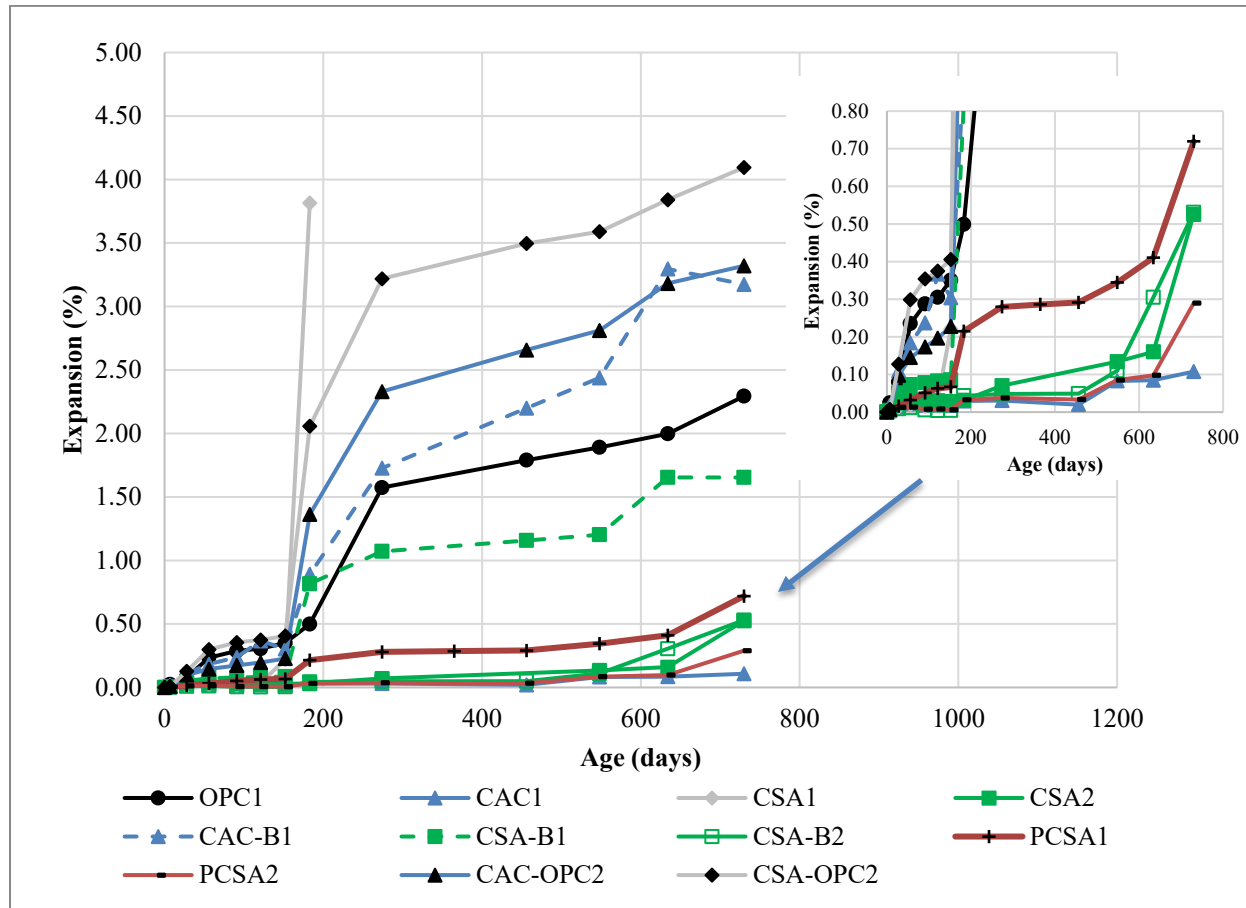
Figure 11.37: Expansion results for standardized ASTM C1293 (Series 1 – Boosted)

11.6.1.4 Modified ASTM C1293 (Series 2 & 3)

The results for Series 2 and Series 3 modified ASTM C1293 tests are shown in Figures 11.38 and 11.39, respectively. To recall, Series 2 are those specimens using a low W/C ratio of 0.35, a total cementitious content of 752 lb/yd³, and a total equivalent alkali content of 1.25% with the addition of a 50/50 NaOH solution (boosted). On the other hand, Series 3 are proportioned identically but have no additional alkalis into the mixture (Unboosted).

Series 2 mixtures showed similar behavior to those mixtures evaluated in Series 1 with the exception that the measured expansion was lower. RSHC mixtures CSA1, CSA1-OPC2, CAC-OPC2, CAC-B1, and CSA-B1 all showed the highest level expansion after 2 years of testing. Additionally, CSA1 showed extreme and unexpected expansion as noted in Series 1 testing. Whereas in the results shown in Series 3, CSA1 showed very little expansion after 2 years of measurements. Thus, it is likely the expansion in CSA1 is being attributed from the addition of alkalis in the system (boosted) as required by ASTM C1293.

Series 3 test results showed some fairly significant differences in behavior compared to Series 1 and 2. For example, CSA-B2 showed a much higher than expected expansion which was also not in agreement with the behavior that observe in the accelerated mortar bar test (See Section 11.6.1.2). Additionally, CAC-OPC2 observe a much lower than expected expansion after 2 years. Based on the behavior in all three series of testing, the results seem to suggest that there is some high sensitivity to the alkalinity of the RSHC system and its impact on ASR performance when the system contains a component of Portland cement. The results seem to further suggest that the impact may be more sensitive to the RSHC system depending on how two components are combined (i.e., lab blend versus intergrinded during production). Further research is needed in this area to understand the impact and subsequent ASR behavior of blended RSHC systems.
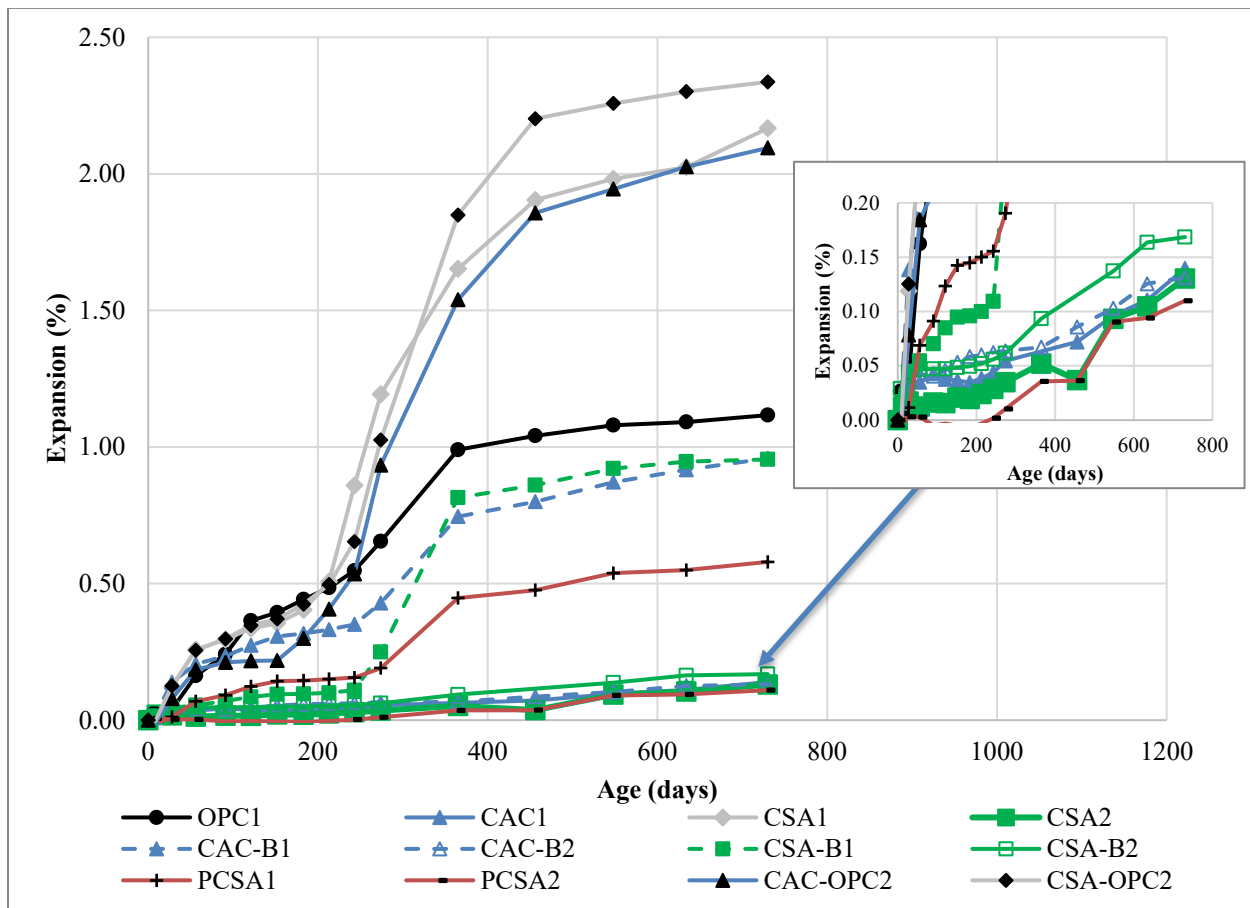
Figure 11.38: Expansion results for modified ASTM C1293 (Series 2 – Boosted)
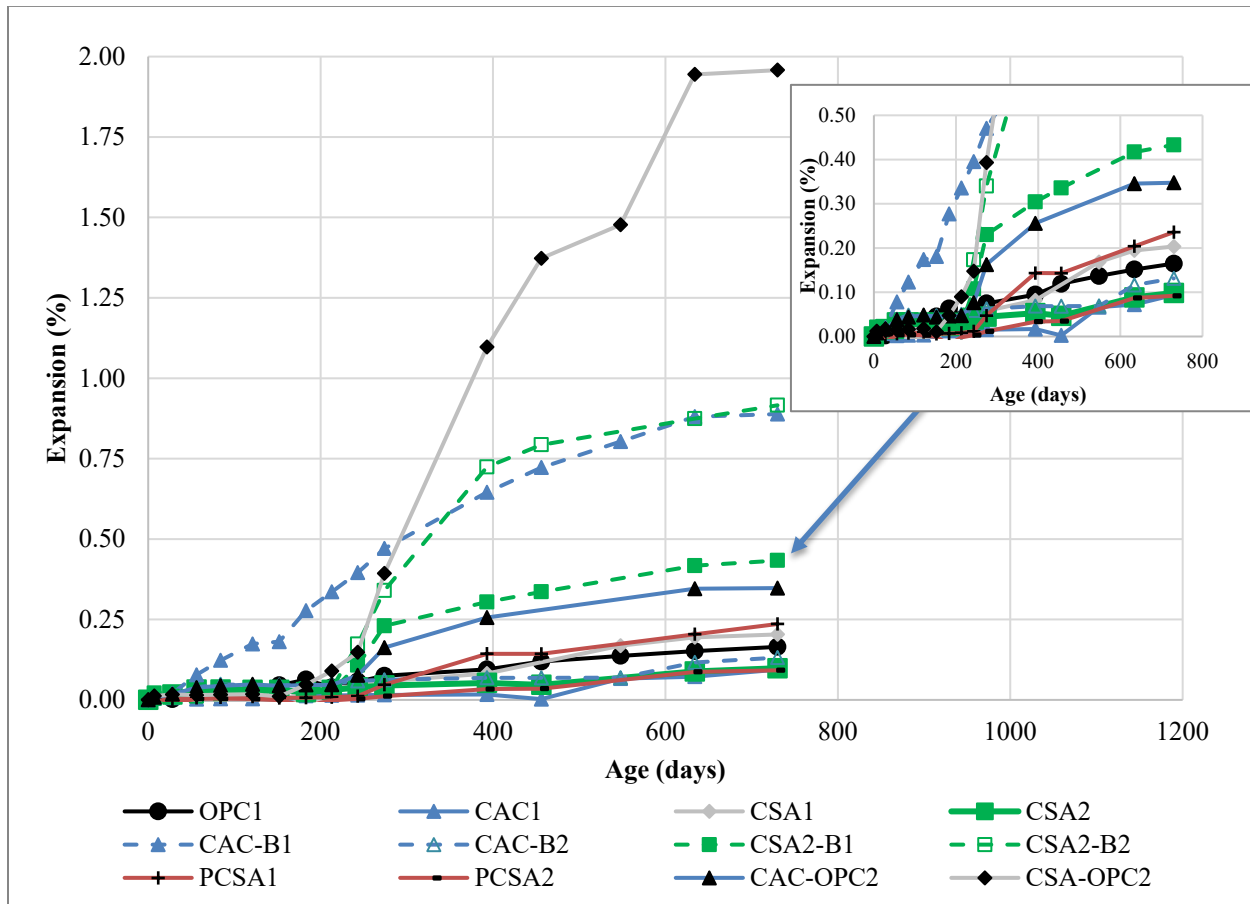
Figure 11.39: Expansion results for modified ASTM C1293 (Series 3 – Unboosted)

11.6.1.5 Accelerated Concrete Cylinder Test (AASHTO TP 142)

The researchers conducted a comprehensive validation of the ASR testing procedure, encompassing a wide array of alternative rapid hardening binders as illustrated in Figure 11.38. Across the spectrum of mixtures examined, which encompassed a diverse range of alternative rapid hardening binders, it was consistently observed that none of the mixes exceeded the expansion limit of 0.04 percent within the 90-day testing period, with the sole exception being mix #3 (CAC-B1). This outcome strongly suggests that the mix design employed for mix #3 (CAC-B1) is not conducive to mitigating ASR-related concerns.
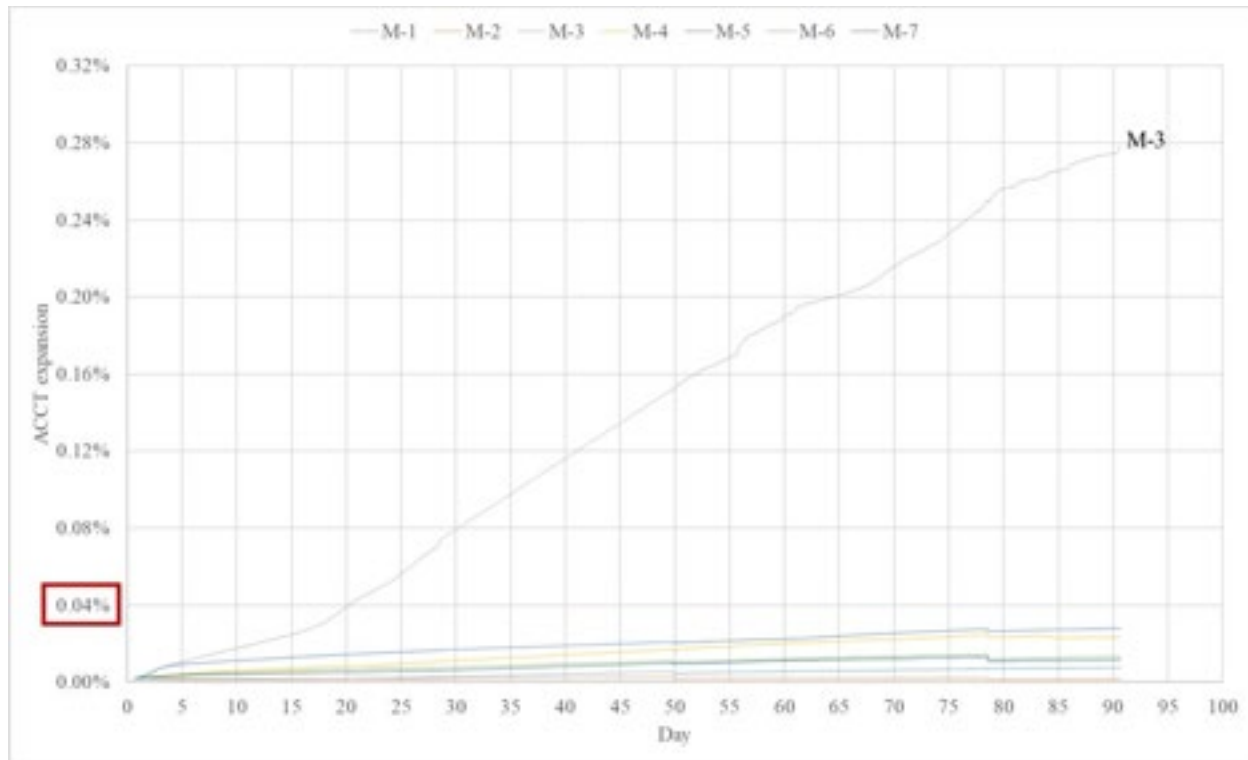
Figure 11.40: Expansion results for accelerated concrete cylinder test (AASHTO TP 142)

11.6.1.6 Concrete Exposure Blocks

Figure 11.41 shows expansion results for the large exposure blocks placed outdoors in San Marcos, TX and subjected to "real-world" conditions. To recall, exposure blocks were cast alongside Series 3 concrete prism specimens in which samples were cast using a low W/C ratio of 0.35, a total cementitious content of 752 lb/yd^3 but no additional alkalis into the mixture (Unboosted)

After three years of exposure, OPC1 and CAC-B1 are the only mixtures displaying relatively high amounts of expansion. Additionally, both mixtures are also displaying sign of distress and cracking on the blocks. Thus, results seem to be in agreement with the performance observed all accelerated laboratory tests.
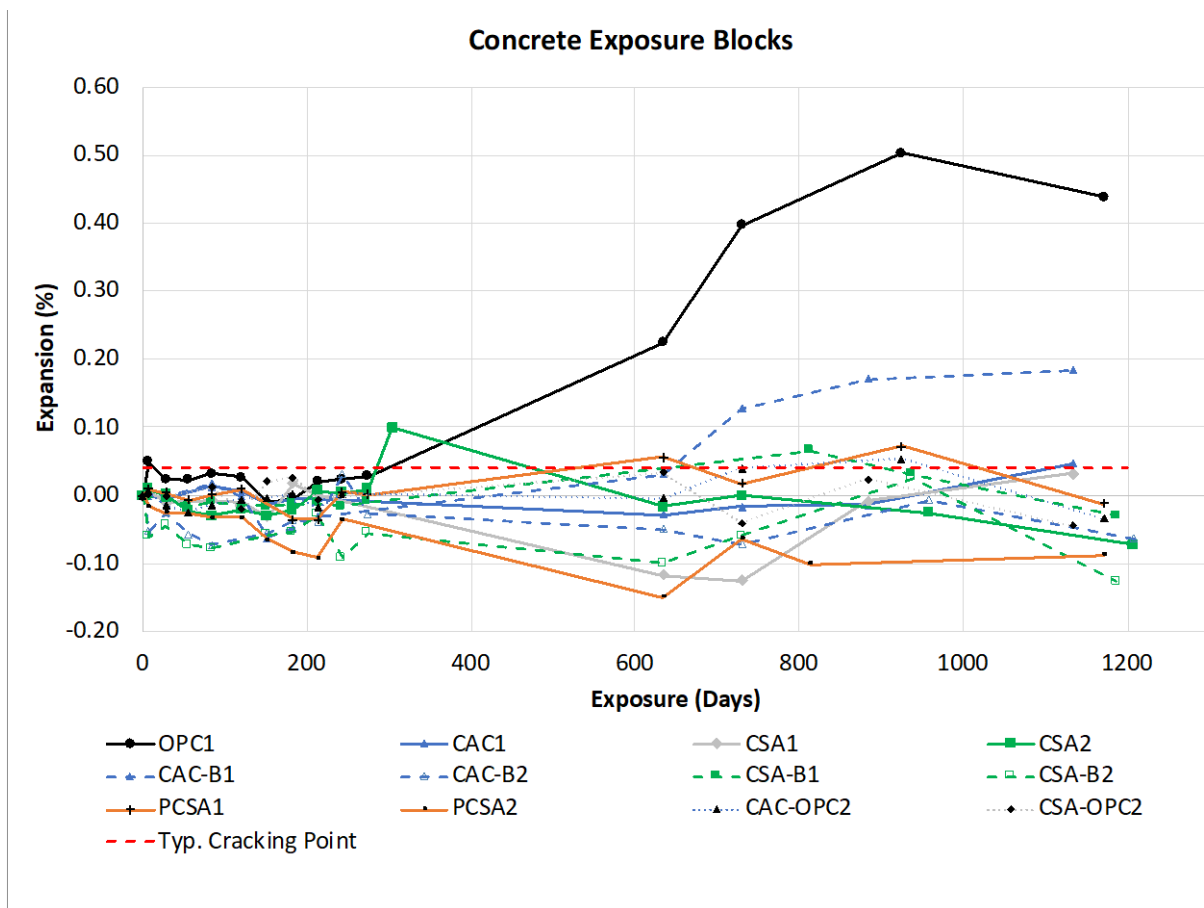
Figure 11.41: Expansion results for concrete exposure blocks

11.6.1.7 Damage Rating Index (DRI)

Damage rating index was only performed on samples in Series 1 were evaluated (See Figure 11.37). One concrete sample was taken from each Series 1 – ASTM C1293 test and visual observations were made of each sample using a stereomicroscope at 15-18x magnifications. The final DRI values for each sample are listed in Table 11.15 below.

Table 11.17: DRI values for Series 1 ASTM C1293 specimens.

Sample ID	DRI	Damage Group	Degree of ASR
OPC1	334	2	Fair to Moderate
CAC	212	1	Trace
CSA1	182	1	Trace
CSA2	142	1	Trace
CAC-B1	684	3	Moderate to Severe

CAC-B2	412	3	Moderate to Severe
CSA2-B1	252	2	Fair to Moderate
CSA2-B2	476	3	Moderate to Severe
PCSA1	328	2	Fair to Moderate
PCSA2	112	1	Trace
CAC-OPC2	564	3	Moderate to Severe
CSA1-OPC2	1050	4	Severe

Overall, the DRI values correlate fairly well with the level of expansion seen in Series 1 ASTM C1293 testing. The laboratory blend composed of CSA-OPC2 showed the highest level of expansion and the DRI examination revealed extensive cracking in the cement paste with many cracks filled with reaction product (see Figure 11.40). On the other hand, mixtures such as CAC, CSA1, CSA2, and PCS2 showed some of the lowest expansion after 2 years and also revealed trace amounts of ASR type damage. However, mixtures that observed moderate amounts of expansion revealed varying degrees of ASR damage based on the DRI method. For example, PCSA1 observed less expansion after 2 years of monitoring than most other RSHCs but revealed a much higher DRI value (see Figure 11.41).

CSA—OPC2
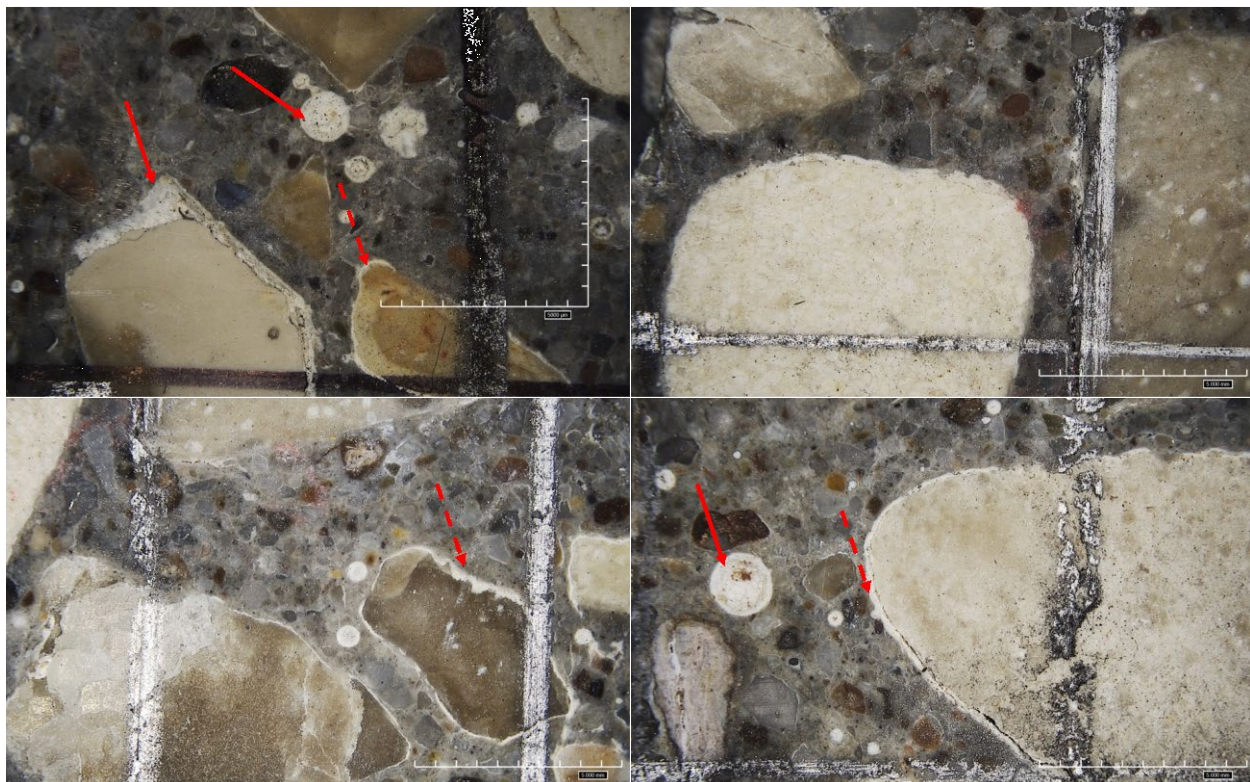
Figure 11.42: Several photos of CSA-OPC2 mixture showing several cracks with reaction products which pass through cement paste (solid arrow and reaction rim noted around aggregate (dashed arrow)

PCSA1
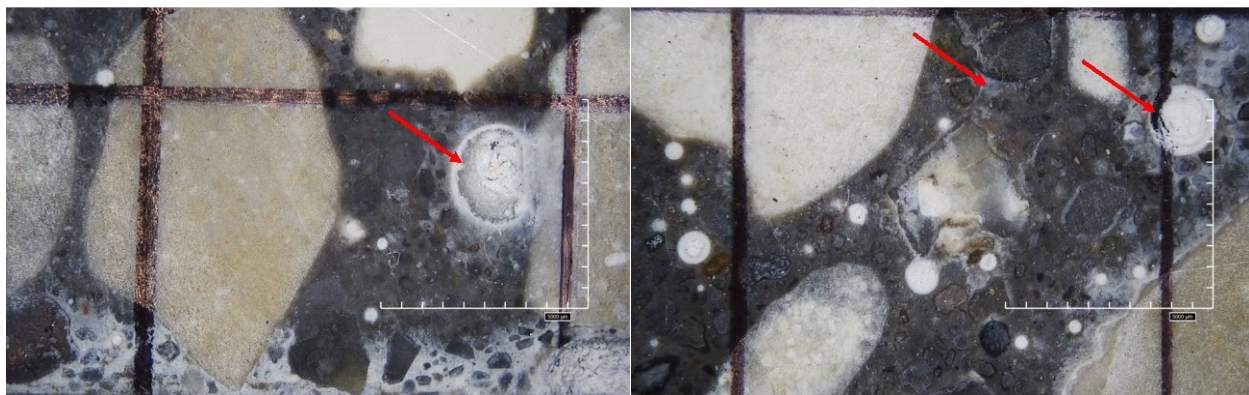
Figure 11.43: Several photos of PCSA1 mixture minor amount reaction products which pass through cement paste.

Very little cracking was observed in CAC mixture as shown in Figure 11.42 and in turn the sample had a very low DRI value. However, CAC-B1showed a much different view with several cracks and reaction product throughout the entire system. As noted before, CAC is straight cement fondu binder and has consistently shown very low alkali silica reactivity in this program. The low alkalinity of the binder and the absence of hydroxyl ions is likely the primary reason for this. On the other hand, CAC-B1 is a ternary blend of CAC1, calcium sulfate, and ordinary portland cement. In the system used in this study, 70-75% of the binder was composed of OPC with the remaining composed of CAC and calcium sulfate. This system allows for the rapid formation of ettringite which can develop early-age strength as well as long-term strength development from the silicates in OPC. Hence, this eliminates the potential for any strength reduction (i.e., conversion) typically common in CAC binders. However, the high OPC content and combination of OPC with CAC has led to the extensive alkali silica reactivity (see Figure 11.43). Interestingly, this binder performed worse than the straight OPC mixture as per the ASTM C1293 expansion results. Further analysis is necessary to identify the primary cause for this abnormal expansion in the ternary CAC systems.

CAC
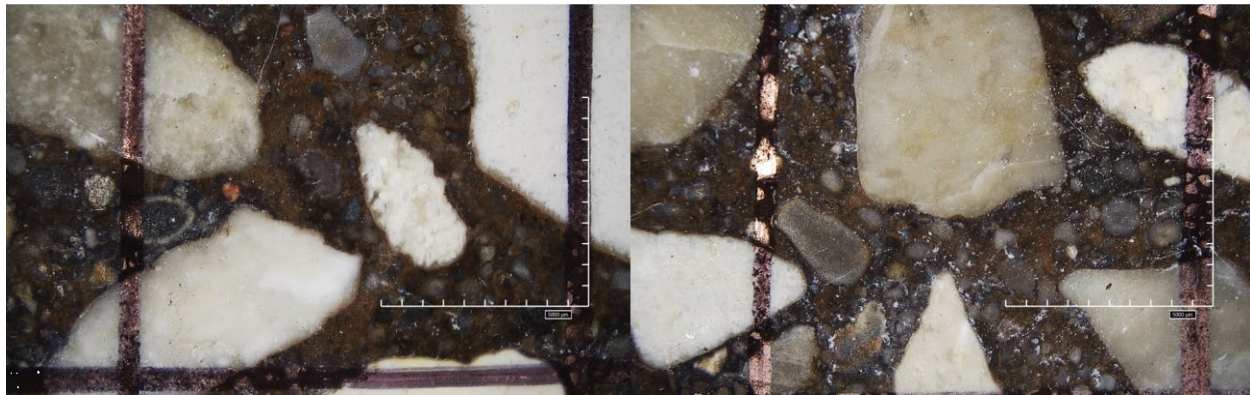
Figure 11.44: Several photos of CAC mixture no apparent degradation noticeable in sample

CAC-B1
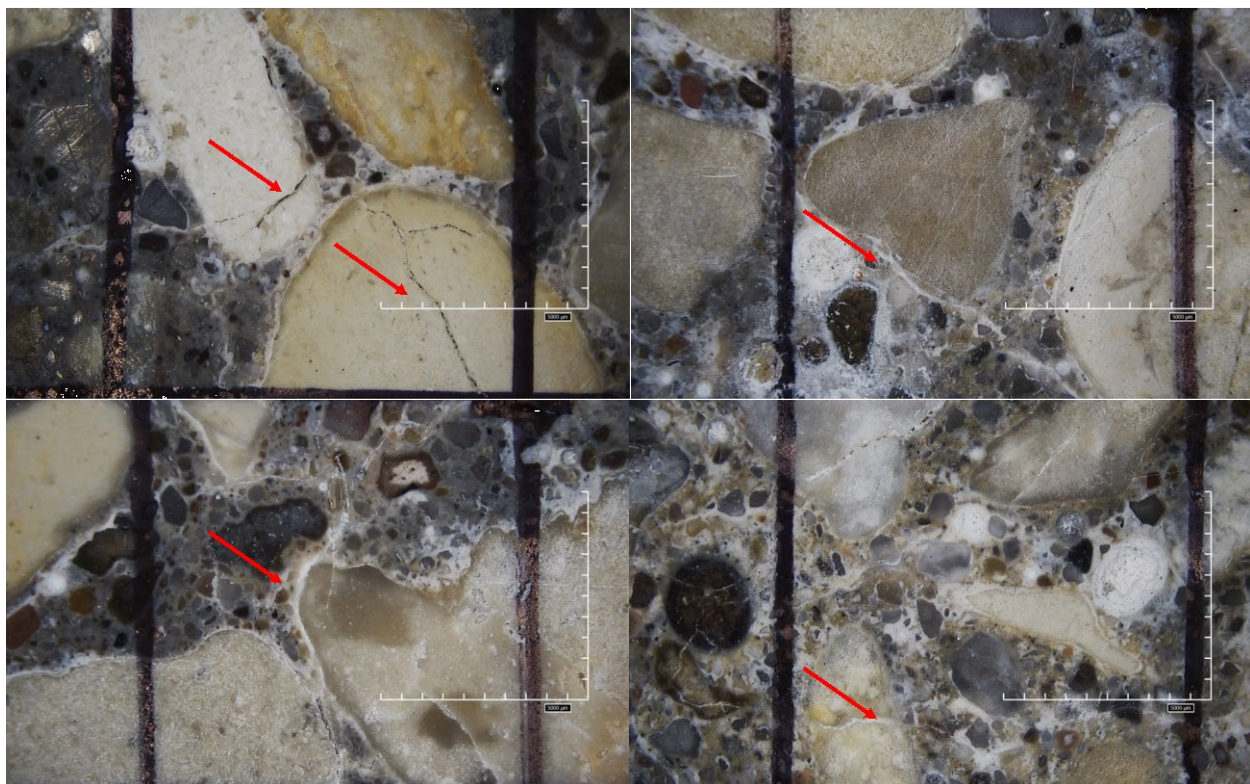
Figure 11.45: Several photos of CAC-B1 mixture showing severe amounts of cracks both in bulk cement paste and aggregates.

The results of the petrographic analysis of ASTM C1293 samples using the Damage Rating Index correlate quite well with the levels of expansion reached in ASTM C1293. In general, those samples with higher levels of expansion also had higher DRI values. The added benefit of using the Damage Rating Index in conjunction with ASTM C1293 is the ability to visually verify the presence of alkali-silica gel, reacted aggregates, and cracks within the cement paste. This is especially useful and necessary when attempting to confirm the presence of ASR in RSCHs. As previously stated, most accelerated laboratory test methods were developed for use with ordinary portland cement; therefore, the employment of additional analytical methods is essential until it is determined that these methods are also suitable for the evaluation of RSHCs.

11.7 DELAYED ETTRINGITE FORMATION

11.7.1 Accelerated High Temperature Curing (Kelham Test Method)

Currently, there are no standard ASTM or AASHTO test methods to obtain the possible effects of DEF in cementitious materials in a laboratory setting. The contributions of DEF are difficult to separate from the effects of distinct mechanisms such as ASR. This project applied the approach provided from Kelham [16] to assess DEF performance. Specifically. samples underwent two heat curing cycle reaching 95°C (203°F) and 65°C (149°F). The Kelham method method were addressed to accelerate the means in which DEF could affect the cementitious material.

Figures 11.44 and 11.45 present the DEF expansion results for Series 1 and 2, respectively. The majority of the test specimens have been in limewater storage for more than 36 months. In comparing the two curing temperatures, significant expansions has only occurred in specimens that were subjected to a 95 °C (203 °F) heat temperature cycle. In fact, most mixture subjected to the lower heat temperature cycler have shown negligible amount of expansion with no signs of damage on any of the bars. On the other hand, for samples subjected to the higher temperature cycle most mixtures observed an immediate trigger to expansion after only 3-6 months of in limewater solution with most having expanded more than 1.0%. The significant expansion is likely attributed to the large amounts of ettringite that traditionally is formed in RSHCs to achieve high early strengths in these binder systems.

It is worth noting the interesting and peculiar behavior of CSA1 cement particularly in DEF and ASR testing. The CSA1 binder used in this program is commonly known as a high Ye'elminite cement. While this binder can be used as the primary cement, it can also be blended in the field with an OPC in varying amounts to control setting and strength development. In this program, both types of mixtures were chosen to be cast to evaluate their behavior (CSA1 and CSA-OPC2). The blend included using a CSA-OPC2

blend at a 25% and 75% ratio, respectively. In both ASR and DEF testing, a significant amount of expansion is experienced in the blended system CSA-OPC2 (see Figures 11.35 and 11.36). Furthermore, while the pure CSA1 mixture has not experienced any significant expansion in DEF testing, expansion is observed in ASR performance testing particularly in mixtures where sodium hydroxide was used to boost the alkali level. In both rounds of durability tests, a high reactive fine aggregate is used in the mixtures. While in ASR testing the fine aggregate is used to accelerate and trigger reactivity, it is very unlikely ASR reactivity would come into play in DEF bars as the alkalis are readily leach into the limewater solution. Thus, the expansion-related effects appear to be due to some instability of CSA under different alkali loading and conditionings. Further research is needed to better understand the role of alkalinity and CSA cements.
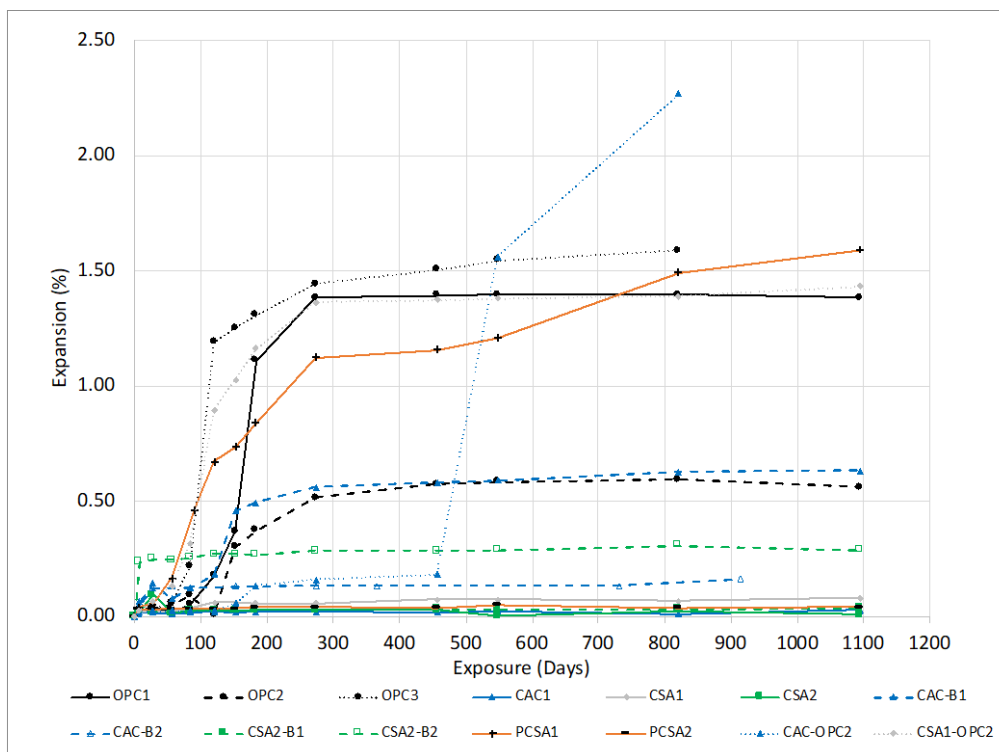
Figure 11.46: Expansion results for DEF subjected Series 1 curing cycle (95 °C)
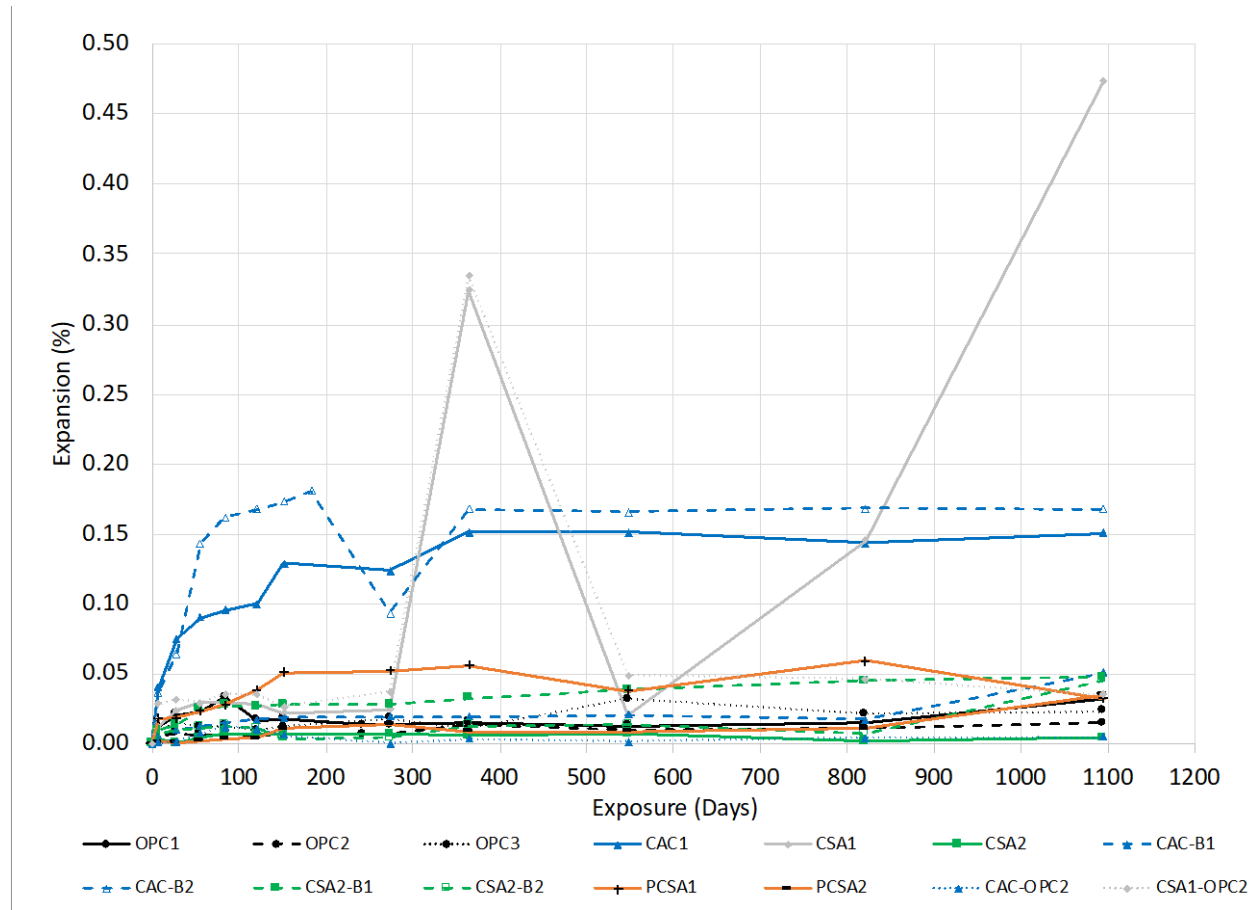
Figure 11.47: Expansion results for DEF subjected Series 2 curing cycle (65 °C)

11.8 CONCLUSIONS

This chapter attempted to achieve a better understanding of the ASR and DEF potential on RSHCs . It provided a better understanding of the mechanisms that CAC, CSA, and laboratory blended binders have with respect to ASR and DEF. The conclusion for each standardized and modified performance test methods on RSHCs related to ASR and DEF are summarized below.

11.8.1 Concrete Exposure Blocks

- Most RSHCs did not observe any substantial amount of expansion in the concrete exposure blocks after three years of exposure. While this may suggest that they are likely not conducive to ASR, more time needed to observe their long-term behavior in real-world conditions.

- CAC-B1 did consistently show some level expansion in both lab and field experimental work. Additionally, cracking was apparent in the exposure block after three years of exposure. Further monitoring is warranted as well as evaluating possible mitigation techniques.

11.8.2 Concrete Prisms

- The results showed that the ASR performance of RSHC was highly sensitive to the addition of alkalis (boosted) as required per ASTM C1293, especially in CSA cements. More work is needed to elucidate this behavior.

- In general, CAC-B1, CAC-OPC2, CSA-OPC2, and CSA-B1 consistently showed the highest amount of expansion in all three series of concrete prism tests.

- Alkali silica reactivity (ASR) results varied among different types of cement, with unexpected expansion observed in some calcium sulfoaluminate cements (CSA1) despite not being known for deleterious behavior in ASR environments.

- RSHCs containing Portland cement exhibited excessive expansion, suggesting a potential impact of Portland cement on observed expansion even when alkalis were added to achieve an equivalent alkali loading.

- Series 2 and Series 3 modified ASTM C1293 tests showed differences in expansion behavior, with Series 3 indicating a higher sensitivity to alkalinity in RSHC systems, particularly when combined with Portland cement.

- The results underscore the need for further research to understand the sensitivity of alkalis in calcium sulfoaluminate cements and the impact of blending RSHC systems on ASR behavior.

11.8.3 Accelerated Mortar Bar

- ASR performance of RSHC mixtures varied based on the type of fine aggregate used, with crushed limestone consistently resulting in the lowest expansion levels.

- Lab-blended systems containing a high proportion of RSHC unexpectedly showed higher expansion, contrary to the assumption that OPC would contribute more to ASR-induced expansion.

- The correlation between aggregate reactivity level and cement type was confirmed, with higher expansion observed in mixtures with highly reactive fine aggregate compared to moderately reactive fine aggregate, though exceptions were noted.

- Lowering the water/cement (W/C) ratio resulted in decreased expansion for all systems, likely due to reduced permeability and increased sample strength, with some mixtures achieving expansions below 0.10% at 14 days.

- Relationships between 14-day expansion data and various oxide content showed no clear correlation with equivalent alkali or aluminate oxide content but indicated a substantial relationship with calcium oxide content, suggesting the need for further evaluation to understand ASR reactivity in RSHC binders.

11.8.4 Damage Rating Index (DRI)

- The Damage Rating Index (DRI) values obtained from visual examinations correlated well with the levels of expansion observed in Series 1 ASTM C1293 testing, providing additional insight into the ASR damage.

- Mixtures with high expansions, such as the laboratory blend composed of CSA-OPC2, exhibited extensive cracking in the cement paste with many cracks filled with reaction product, indicating severe ASR damage.

- Samples with lower expansions, such as CAC, CSA1, CSA2, and PCS2, also showed trace amounts of ASR damage, with varying degrees of cracking observed based on DRI values.

- Ternary blend mixtures like CAC-B1, despite containing components known for low ASR reactivity individually, showed extensive ASR damage likely due to the combination of OPC and CAC, suggesting the need for further analysis to identify the primary cause of abnormal expansion in such systems.

11.8.5 Delayed Ettringite Formation

- The Kelham method, involving heat curing cycles at 95°C (203°F) and 65°C (149°F), was applied to accelerate DEF effects, revealing significant expansions only in specimens subjected to the higher heat cycle, with most expanding over 1.0% within 3-6 months in limewater solution.

- Blended systems containing CSA1 and OPC, such as CSA-OPC2, exhibited significant expansion in DEF testing, while pure CSA1 mixtures showed no significant expansion. However, CSA1 did exhibit expansion in ASR testing, particularly with boosted alkali levels, indicating potential instability under different alkali loading conditions.

- Further research is needed to understand the role of alkalinity and the behavior of CSA cements in DEF conditions, as the expansion-related effects observed appear to be influenced by the alkali loading and conditioning environment.

11.9 REFERENCES

[1]   P. Virmani, "Alkali-silica reaction mechanisms and detection: An advanced understanding," U.S. Department of Transportation, 2014. [Online]. Available: https://www.fhwa.dot.gov/publications/research/infrastructure/structures/bridge/14079/14079.pdf

[2]   M. Thomas, Folliard, K., Fournier, B., Rivard, P., Drimalas, T., "Methods for evaluating and treating ASR-affected structures: Results of field application and demonstration projects – Volume I: Summary of findings and recommendations. ," U.S. Department of Transportation - Federal Highway Administration. , 2013. [Online]. Available: https://www.fhwa.dot.gov/pavement/concrete/asr/pubs/hif14002.pdf

[3]   T. Stanton, "Expansion of concrete through reaction between cement and aggregate," *American Society of Civil Engineers,* 1940. [Online]. Available: https://bit.ly/2Y48hZC.

[4]   I. Sims, Poole, A. , "Alkali-aggregate reaction in concrete," 2016. [Online]. Available: https://bit.ly/2yGJAHQ

[5]   B. Fournier, Bérubé, M., Folliard, K., Thomas, M. , "Report on the diagnosis, prognosis, and mitigation of alkali-silica reaction (ASR) in transportation structures," The Transtec Group, Inc. , 2010.

[6]   S. Diamond, "Alkali Silica Reactions – Some Paradoxes," *Cement and Concrete Composites,* vol. 19, no. 5-6, pp. 391-401, 1997.

[7]   F. H. Administration, "Alkali-Silica Reaction," U.S. Department of Transportation. , 2003. [Online]. Available: https://www.fhwa.dot.gov/publications/research/infrastructure/pavements/pccp/03047/02.cfm

[8]   *ASTM C1260-21 Standard Test Method for Potential Alkali Reactivity of Aggregates (Mortar-Bar Method)*, ASTM International, 2021.

[9]   *ASTM C1778-23 Standard Guide for Reducing the Risk of Deleterious Alkali-Aggregate Reaction in Concrete*, ASTM International, 2023.

[10]   P. C. Association, "Ettringite formation and the performance of concrete," PCA, 2001. [Online]. Available: https://www.cement.org/docs/default-source/fc_concrete_technology/is417-ettringite-formation-and-the-performance-of-concrete.pdf?sfvrsn=412%26sfvrsn=412

[11]   *ASTM C1293-23 Standard Test Method for Determination of Length Change of Concrete Due to Alkali-Silica Reaction*, ASTM International, 2023.

[12]   M. Thomas, Folliard, K., Drimalas, T., & Ramlochan, T. , "Diagnosing delayed ettringite formation in concrete structures. ," *Cement and Concrete Research,* vol. 38, no. 6, pp. 841-847, 2008.

[13]   X. B. Pavoine, L. Divet. , "The impact of cement parameters on Delayed Ettringite Formation," *Cement and Concrete Composites,* vol. 34, no. 4, pp. 521-528, 2012.

[14]   W. Dayarathne, "Evaluation of the potential for delayed ettringite formation in concrete," in *Natural Engineering Conference* University of Moratuwa, 2013. [Online]. Available: https://uom.lk/sites/default/files/eru/files/eru201311.pdf. [Online]. Available: https://uom.lk/sites/default/files/eru/files/eru201311.pdf

[15]   K. L. Kreitman, "NONDESTRUCTIVE EVALUATION OF REINFORCED CONCRETE STRUCTURES AFFECTED BY ALKALI-SILICA REACTION AND DELAYED ETTRINGITE FORMATION," Civil and Environmental Engineering, University of Texas at Austin, 2011.

[16]   S. Kelham, "Effects of Cement Composition and Hydration Temperature on Volume Stability of Mortar," *Cement and Concrete Composites,* vol. 18, no. 3, pp. 171-179, 1996.

[17]   Y. Fu, "Delayed ettringite formation in Portland cement products," University of Ottawa. , 1996.

[18]   Y. Fu, Ding, J., Beaudoin, J. J., , "Expansion of Portland cement mortar due to internal sulfate attack," *Cement and Concrete Research,* vol. 27, no. 9, pp. 1299-1306, 1997.

[19]   *ASTM C150M-19 Standard Specification for Portland Cement*, ASTM International, 2019. [Online]. Available: https://compass.astm.org/document/?contentCode=ASTM%7CC0150_C0150M-19%7Cen-US

[20]   S. Z. Lingbo Wang, Xudong Tang, Qiang, Xu, Kuangliang Qian, "Pore Solution Chemistry of Calcium Sulfoaluminate Cement and Its Effects on Steel Passivation," *Journal of Applied Sciences,* vol. 9, 2019, doi: https://doi.org/10.3390/app9061092.

[21]   V. F. Villenueve, "Determination of the damage in concrete affected by AST - the Damage Rating Index (DRI)." in *14th International Conference of alkali aggregate reaction (AAR) in concrete.*, Austin, TX., 2012.

[22]   B. Fournier, et al., "Description of petrogrpahic features of damage in concrete used in the determination of the Damage Rating Index (DRI).", uebec City, Quebec: Universite Laval, Geology and Geological Department., 2015.

CHAPTER 12: VALUE OF RESEARCH

12.1 INTRODUCTION

The value of research (VoR) for this project can be considered through the production of a cost analysis, considering the cost of the RSHCs and their performance. The research team believes that three economic benefit areas are realized in this project including: 1) Expedited Project Delivery; 2) Reduced Construction, Operations, and Maintenance Cost; and 3) Materials and Pavements. Factors which influence construction time include mobilization of the contractor, site preparation, chosen construction method, lead time for ordering parts, materials, and supplies, sub-contractor availability, sequencing of tasks, weather, and others. Rapid construction considers each factor individually to determine how it's time to completion can be shortened and how that will influence other factors and ultimately the entire construction schedule. For cast-in-place concrete construction, placement of reinforcement, placement of formwork, and strength development of the concrete all take time. Shortening the time to develop strength in concrete is commonly addressed by using Type III cement with relatively high dosages of accelerating admixtures; however, there are now other cements in the market that have rapid setting and strength gain characteristics, such as calcium sulfoaluminate (CSA) and calcium aluminate cement (CAC), and concretes incorporating blends of these cements and ordinary portland cements (OPC), which have been extensively investigated in this research. These cements, while having been successfully used in repair applications for many decades, have far less history of being used in new construction, especially in structural applications as a result of limited long-term durability data. Consequently, literature on the use of these materials in structural application is scarce, especially in regards to the cost considerations of using RSHCs for structural applications. Therefore, the VoR for this project needs to be assessed through a cost analysis as outlined below.

12.2 OBJECTIVE

The objective of this VoR is to produce a cost analysis of using RSHCs in structural applications. There are three distinct questions that result from changes to material and structural design utilizing RSHCs.

1. What is the general cost comparison between OPC based concrete versus RSHC based concrete?
2. How does using RSHC based concrete impact the construction schedule and overall project schedule?
3. How is overall cost impacted by adjustments to material and schedule?

12.3 METHODOLOGY

The cost analysis will begin by first considering just the cost of concrete produced with OPC versus that produced with RSHCs and blends of OPC and RSHCs. Appropriate adjustments will be made to consider the amount of cement and constituents used, as well as equipment for transporting, placing and consolidating the concrete mixture such that a realistic comparison can be made. However, to complete a comprehensive cost analysis, it is important to also consider time using concrete made with RSHCs. Specifically, the timing sequence following final finishing procedures and the curing time required to gain an appropriate strength, sufficient enough to commence the immediate next activity in the project schedule. In other words, the curing time requirement. Therefore, it is important to consider a holistic project schedule (such as a network-based schedule) along with its individual cast-in-place concrete element activities and their corresponding durations. From this, one version of the schedule can be considered in which the cast-in-place concrete activities are produced with OPC and require a conventional duration (on average 8-days) required for appropriate strength gain. For comparison, the same schedule can then be modified considering all cast-in-place concrete activities are produced with a RSHC (or blend) and require a maximum of 1-day duration. From this comparison, not only can the impact on the total project duration be determined, but a project S-curve can be plotted which would

demonstrate the "cash loaded" schedule. A project S-curve will help elucidate how project costs are distributed over the entire project duration.

Since, every project is unique with their own constraints regarding safety, cost, quality, and time it is difficult to create a cost analysis that will be applicable to every structural project. Therefore, a cost analysis of a previous TxDOT bridge project will be used as a "representative" project, in order to demonstrate how an individual project could be impacted by using concrete incorporating RSHCs. This representative TxDOT bridge project cost analysis can then be used as a baseline comparison when completed and a cost/benefit analysis can be used to decide if it is applicable to use OPC concrete versus RSHC concrete. As there are various manufactures producing RSHC, as well as cement blends, this cost analysis will only consider cost associated with the cements and blends that were previously obtained for laboratory investigations in TxDOT 0-7017. However, the accompanying excel file provided with this document can simply be adjusted with different prices as needed. In this representative analysis, only cast-in-place concrete elements will be considered.

12.4 COST ANALYSIS – COST CONSIDERATION

The pure cost analysis consideration was completed by first obtaining an estimated cost per ton of each cement type from the individual manufactures. The individual cost/ton of all materials can be seen in the corresponding excel file. Additionally, a cost analysis excel file from a local ready-mix company was obtained. Their cost analysis sheet contained a conventional (OPC based) concrete mixture design with each material broken down by their cost per ton. Their mixture was a target 3,000psi, 470lb/yd3 (5-sack) cement, 20% fly ash, crushed limestone, river sand, and minor amounts of a water reducing admixture (non-air entrained). The cost for them to produce this mixture, only considering materials, is approximately $41/CY. This cost does not include any overheard (general conditions, infrastructure, transportation, etc.). The local ready-mix supplier sells this concrete mixture for $110/CY, which is an approximate increase of $69, a mark-up of 168%, or a cost multiplier of 2.7. Using this ready-mix cost

analysis excel file, an approximate cost of each RSHC based concrete mixture produced in this study can be obtained. This is done by replacing the amount of cement/CY, cost of cement/CY, reducing the fly ash to 0%, adjusting amount of water reducing admixture, adding cost of retarding admixture, and making appropriate water adjustments to meet the W/C (or W/CM). This excel file can also be used to estimate the cost of the pre-blended, and lab-blended concrete mixtures, as the previous fly ash line can be adjusted to the percent of OPC used and corresponding cost. After doing this for all RSHC based concrete mixtures investigated in this study, a pure cost analysis was produced. This cost analysis only represents the cost of a ready-mix producer to produce these mixtures only considering material costs. The cost analysis can be seen in Figure 12.1.
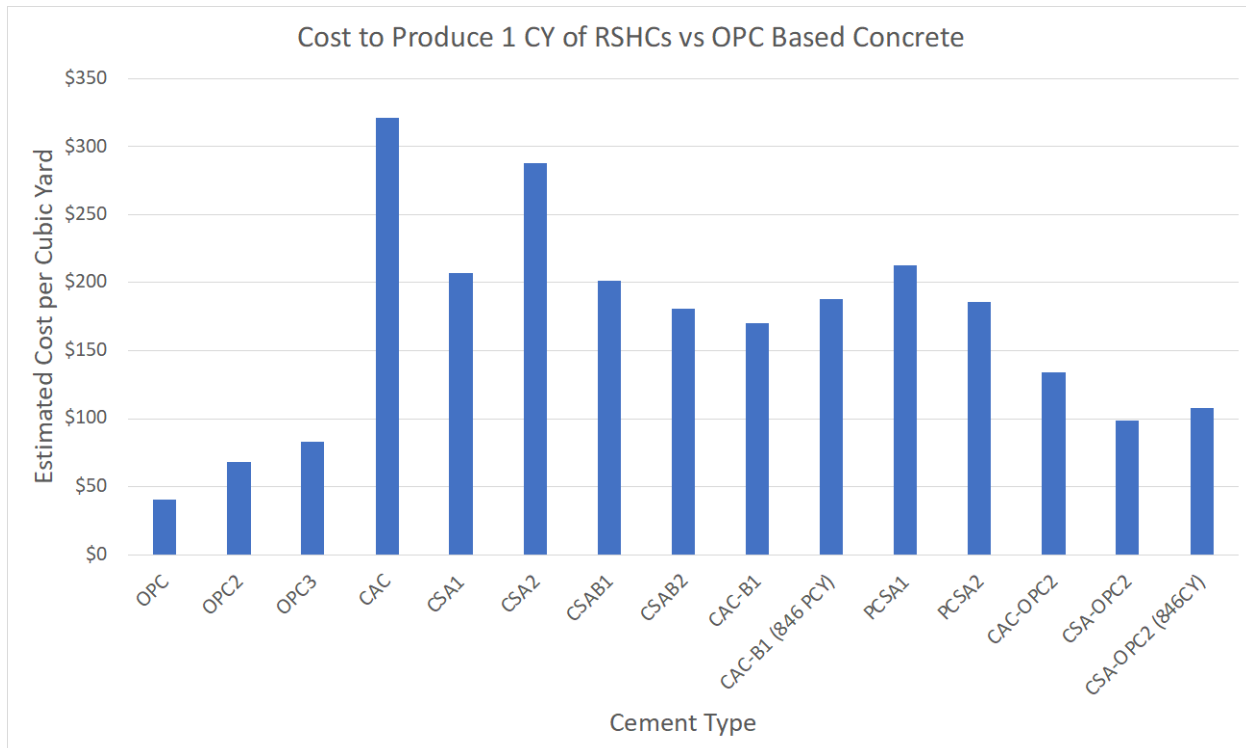

Figure 12.1: Average cost to produce RSHC concrete mixtures for a Ready-Mix producer.

As seen in Figure 12.1, there is an overall significant increase in cost/CY of all RSHC and blended cement systems. The cost of materials to produce the RSHC concrete mixtures (and blends) ranges from $83 – $321, with an average of $183. The price increase of RSHC concrete mixtures ranges of 104% –

690%, with an average increase of 350%. It is important to note that of the RSHCs OPC3, which is a

Type III cement had the overall lowest cost to produce at only $83/CY. The highest costs came from the

CAC and CSA2 cements. However, when considering the CAC/CSA/blended cement systems the lab

blended mixtures cost the least to produce. This due to 75% of the cost being reduced to the cost of OPC,

due the blends being 75% OPC and 25% a RSHCs. Note that there was no significant cost reduction in

the pre-blended cements, although their cements are not pure CAC/CSA, in that they are blended with

OPC. The cost obtained for these materials is what they sell their material, despite it being a blend. It is

also important to note that all of the amounts in Figure 1 do not represent the cost to purchase these

materials and/or have them placed in the field. The values only represent the cost for a ready-mix

company to produce the mixtures. Based on their price multiplier of 2.7 for their conventional concrete

mixture, it is important to consider what the RSHC based (and blends) concrete mixtures would cost if the

ready-mix producer used the same multiplier for all mixtures. This would represent an estimated cost to

purchase the RSHC based (and blends) concrete mixtures, if produced by a ready-mix company, and they

used the same multiplier (or mark-up percentage). This analysis can be seen in Figure 12.2.
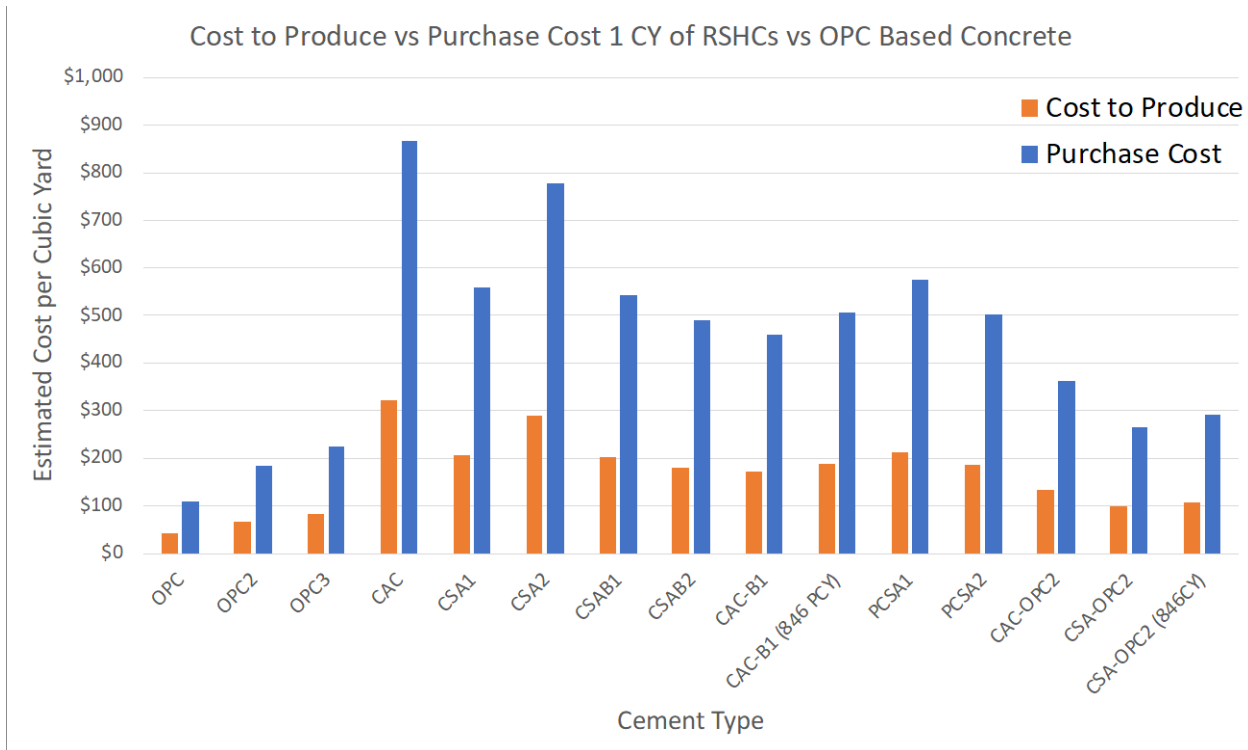
Figure 12.2: Average cost to purchase RSHC concrete mixtures from a Ready-Mix Producer compared to cost to produce.

As seen in Figure 12.2, all values simply increased proportionally by the same 2.7 cost multiplier, however, it is important to also visualize these costs as they are more realistic of what one would have to pay a ready-mix company to produce these concrete mixtures. It is important to consider that the 2.7 cost multiplier may not be the same for these types of mixtures due to many factors, such as the likelihood of increased infrastructure needed at the read-mix plant, extra energy/manpower needed, and insurance due to the possibility of an early set in the truck. These factors could likely increase the mark-up, however, given the already high cost to produce these mixtures, it is also possible that the mark-up could be lower in order to make the mixture more marketable. Another factor to consider is that a ready-mix producer may not be inclined to produce these mixtures, in which a volumetric concrete mixing producer would the other option. Often times, volumetric mixing producers cost more than a ready-mix company simply due to their specialty, cost of equipment/maintenance, and operator training. On the other hand, however, some saving could also be made with volumetric mixing due to their ability to start/stop concrete mixing

296

on demand and purchasing only what is necessary for the project. Due to these factors, the cost multiplier can vary, therefore the provided excel file includes an "cost multiplier" cell, which could be adjusted to consider these variances. For the sake of the VoR analysis, it is important to consider that an increase in cost is needed for initial construction cost if all cast-in place concrete is switched to a RSHC-based concrete. On the low end, a Type III cement costs an estimated $224/yd3 to produce based on the above assumptions. Another assumption that is needed is the volume of cast-in-place concrete required for the project. Insufficient information was available for the representative bridge used in this analysis, but for the sake of analysis and estimation a volume of 1000 yd3 will be used for analysis, resulting in cost of $224,000, which would be compared to $110,000 from using Type I cement. This would be an increase in cost of $114,000 and will be used as a negative value in the VoR excel file for "materials and pavement". However, it is also important to consider that the performance of RSHC-based concrete is superior to that of OPC based concrete, based on the data described in this report, therefore there will be a cost saving in reduced maintenance and increased service life. For the purpose of this analysis an estimation of $50,000 will be used in the "reduced construction, operations, and maintenance cost" category in the VoR excel file to represent the reduced maintenance cost. Although the maintenance cost will vary from year to year and location, this value represents a conservative amount.

12.5 COST ANALYSIS – SCHEDULE CONSIDERATION

As previously stated, a representative TxDOT bridge project will be used for this cost analysis. A network-based schedule for the project titled, "Comal County MH - San Antonio Street - 8408-15-006" along with a corresponding budget breakdown document was used for this analysis. According to the provided project schedule, this project has a total overall duration of 271 days. For the purpose of this analysis, it is only appropriate to consider the cast-in-place concrete activities. An initial and simple analysis can be performed in which all of the cast-in-place concrete activities durations are reduced to 1-day. A 1-day duration can be assumed as, according to the results obtained in this study, an acceptable design strength can be obtained in less than 24-hrs for all RSHCs and blends investigated, often times less

time was sufficient. This also still allows time for formwork to be completed. It is possible that certain activities may have more complex geometries, and may require more than one day for formwork, but for the sake of this representative analysis, the absolute quickest duration of 1-day will be used. Also, only the cast-in-place concrete activities that are on the critical path (i.e., have no float as their early/late start dates and early/late finish dates are the same) will have their duration reduced to 1-day. This is done, as reducing the cast-in-place concrete activities that are not on the critical path (i.e., activities with float) will not affect the rest of the schedule. These particular activities are completed alongside other activities and their early completion will have no effect on subsequent activities. Therefore, it is not necessary to accelerate their durations. This is also acceptable as with these types of activities, the duration beyond 1-day is typically for appropriate strength gain, which requires no manpower. However, external curing should still be provided beyond 1-day for all RSHC concrete to achieve the permeability properties for enhanced durability. Considering these parameters, all cast-in-place concrete activities in the provided network-based schedule that are critical were reduced to 1-day and the results can be seen in Table 12.1.

Table 12.1: Representative Time Saving from Using RSHC on Critical Cast-in-Place Concrete Activities.

	Overall Project Duration (days)
OPC Based Concrete	271
RSHC Based Concrete	202
Time Saved	69

As seen in Table 12.1, reducing all critical path based cast-in-place concrete activities duration to 1-day can accelerate the representative project by a total of 69 days. This results in a statistically significant reduction in the overall project duration. It is important to also consider in this analysis that this is only based on the current arrangement of the schedule, and schedule adjustments were made after the final schedule was produced. However, if the schedule was produced with the idea of using RSHC based concrete with a duration of 1-day ahead of time, the network logic could be adjusted such that more (if not all) of the cast-in-place concrete activities are on the critical path. Although this may not always be possible, it is worth considering how the entire schedule will be affected if all cast-in-place concrete activities had their durations reduced to 1-day. The results of this analysis can be seen in Table 12.2.

Table 12.2: Representative Time Saving from Using RSHC on all Cast-in-Place Concrete Activities.

	Overall Project Duration (days)
OPC Based Concrete	271
RSHC Based Concrete	105
Time Saved	166

As seen in Table 12.2, reducing all cast-in-place concrete activities (both critical and non-critical), will reduce the overall project schedule by more than 50% the original duration. This results in a statistically significant time savings. However, as previously stated, it may not be possible to arrange the network logic in this manner, but this demonstration could be considered prior to developing the network logic such that the use of RSHC in cast-in-place concrete activities is maximized in order to capitalize on their time savings. It is also important to note that both of the above two analysis did not consider an activity in the schedule called "cure bridge deck" with a duration of 21 days. This activity does specify a specific activity (bridge deck) and there were no other activities that specified a period for curing, therefore, it is assumed that the curing period was built into the individual cast-in-place concrete activities. Since the analysis in the above activities did not consider curing, it is important to note that this specific curing activity could also be reduced to 1-day (or ignored completely) if the bridge deck was produced using a RSHC, since sufficient strength gain is achieved in that time frame. In other words, a deck produced using RSHC would not require a curing period of 21-days, therefore, the time savings shown in Table 1 and 2 could possibly be increase by a minimum of 20-days.

Based on the cost analysis (schedule consideration) an estimation can be made based on the overall cost of the specific bridge used in this example. According to the document provided, the overall cost of this bridge was $4,518,896 and took a total of 462 workdays, which corresponds to a cost per work day of $9,781. The number of days saved from the analysis in Table 1 (cast in-place critical activities) is 69 days, which would result in a savings of $674,900. The number of days saved from the analysis in Table 2 (all cast-in place concrete activities) is 166, which results in a savings of $1,623,672. For the purpose of the VoR analysis an average of these two numbers will be used in order to produce a conservative

estimate, which results in a savings from cost alone of $1,149,286. This value has been used in the

provided TxDOT VoR excel template under "expedited project delivery".

Based on the VoR values determined and plotted in the TxDOT VoR excel template, the below figure

(Figure 12.3) is produced which shows a net present value (NPV) of the research relative to the cost of the

four-year project ($572,509).
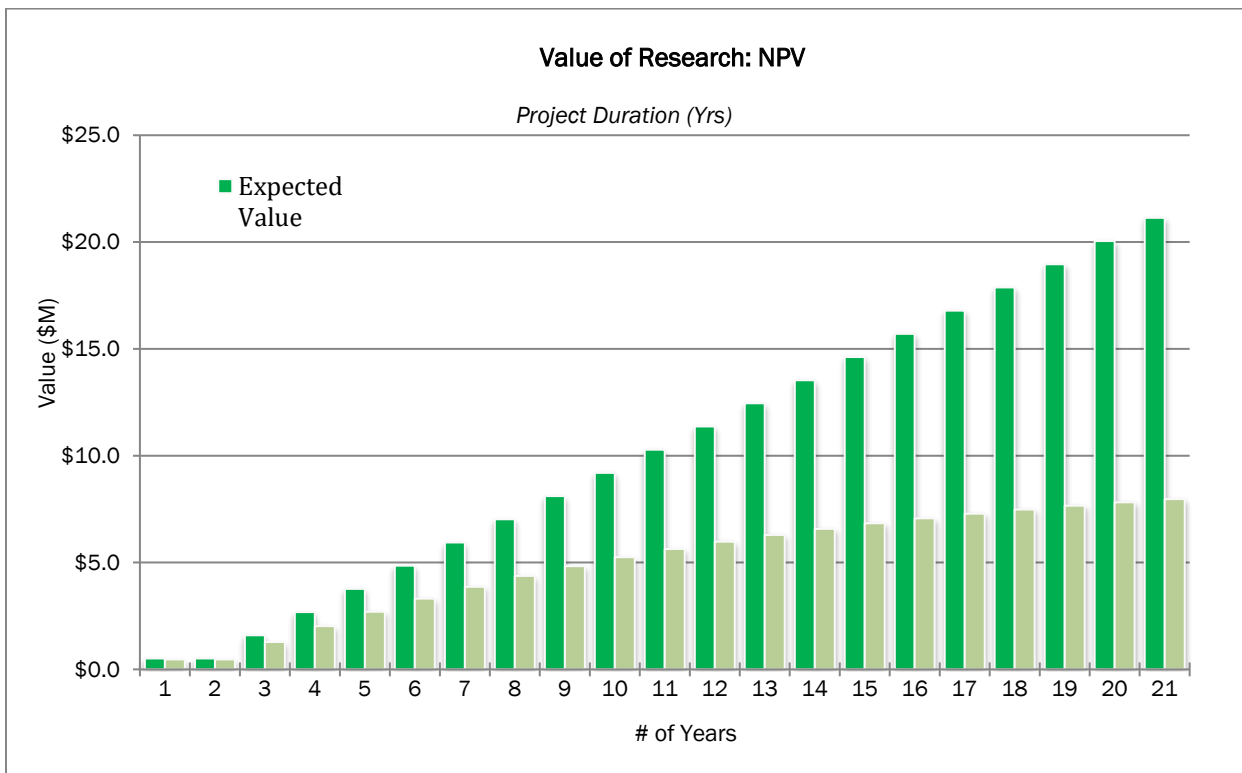
Figure 12.3: Net Present Value Analysis (ref. TxDOT VoR excel template)

To determine the NPV from expected savings from the use of RSHCs in TxDOT assets, an industry

accepted 10% discount rate was applied over a 20 year expected value duration. The results suggest a

NPV of nearly $8M over the 20 year duration providing a cost benefit ratio (CBR) of $13.9. That TxDOT

could expect $13.9 in benefit for each $1. This assumption, however, considers only a one type of bridge

construction and cost over the 20 year duration. These estimated benefit can vary significantly based on

the type of construction project and duration of that project.

12.6 COST ANALYSIS – COST AND SCHEDULE CONSIDERATIONS

As previously stated, it is important to also consider both the individual cost of the concrete made with either cement system, but also the affect it will have on the schedule timing. This analysis considered multiple factors beyond the previous VoR analysis. In order to accomplish this a cash loaded schedule can be created from the provided network-based schedule, which links the activity duration to the cost of that activity. This is first accomplished by producing a Gantt chart from the network diagram. It is important to create a Gantt chart based on the network schedule as appropriate activity overlaps will be considered based off of the network logic. Additionally, since this analysis is only focused on the cast-in-place concrete activities, it is only imperative to create the Gantt focusing on those activities. Following the creation of the Gantt chart, the individual activities can be linked with their original costs per day. The cost used in this analysis is the cost to purchase the material from the producer. In this case the values used are the cost to purchase concrete per CY, thus the 2.7 cost multiplier is included. For the sake of comparison this does not include the cost of placing and finishing, as each activity may require different placing/finishing techniques, which will result in different costs. After loading the Gantt chart with the costs, a cost histogram can be plotted demonstrated the overall cost per workday. Following this, each cost per workday can be sequentially added to each other to determine the cumulative costs per workday. This information can be plotted over the entire span of the project to create a project S-curve. Following the creation of the original Gantt chart and S-curve using OPC based concrete mixtures, the Gantt chart can be adjusted, such that all of the activities now only take 1-day to complete. After doing this, the updated cost of each RSHC mixture can be included and a new histogram and S-curve can be created representing those mixtures. The histogram of cost per workday when using OPC based concrete can be seen in Figure 4 and the corresponding S-curve can be seen in Figure 12.5.
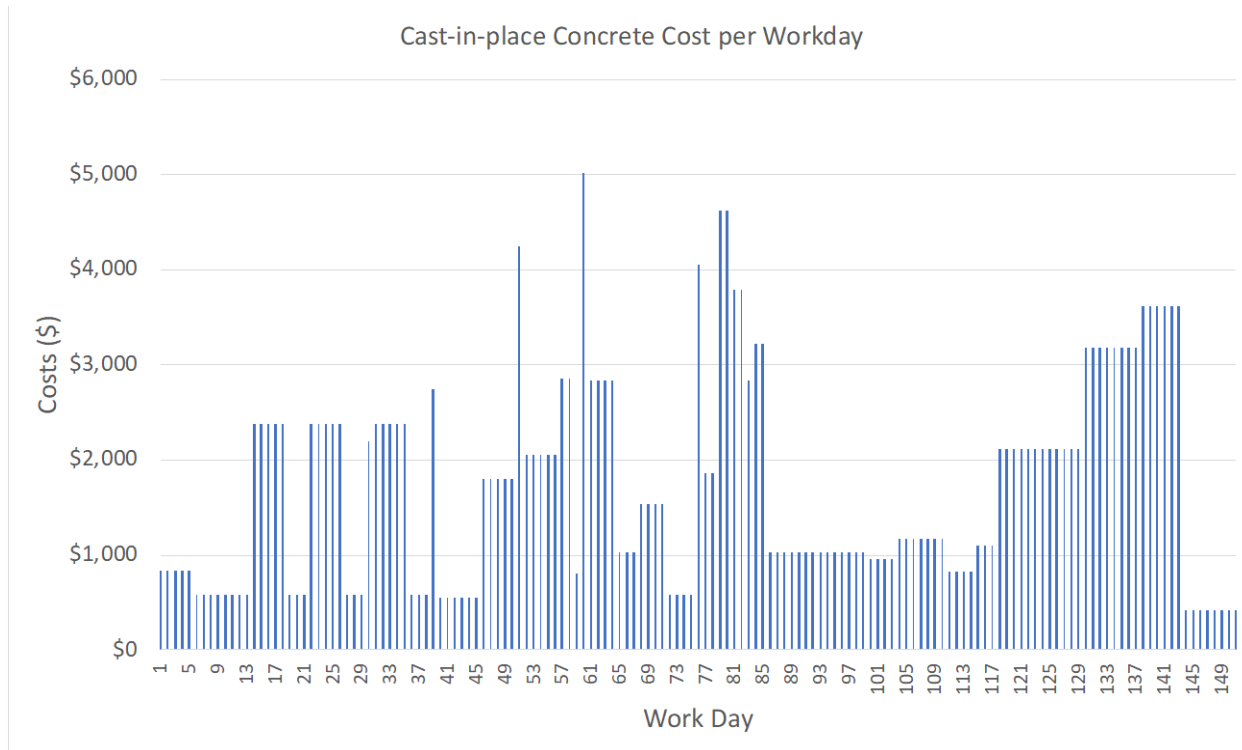
**Figure 12.4: Cost histogram using OPC based concrete.**
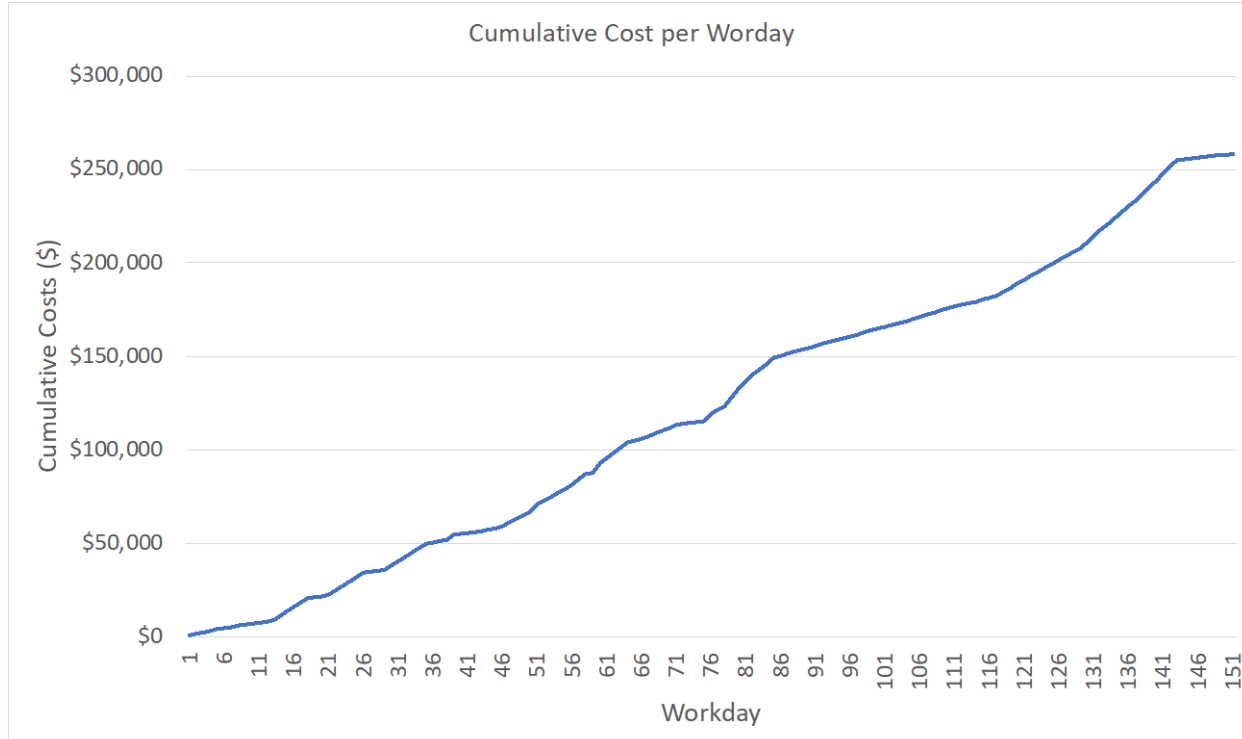
Figure 12.5: Project S-curve using OPC based concrete.

As seen in Figures 12.4, the cost histogram can be used as a project management tool to determine average costs per workday as the project commences. Additionally, the histogram could be used to determine which workday(s) will yield the highest cost for these particular activities. This is quite useful as there may be contractual limitations that could prevent payments from exceeding a certain amount per a certain period, therefore there will need to be adjustments to the schedule and/or costs during that particular problem area. Additionally, the project S-curve shown in Figure 12.4 could be used to visualize how costs may increase (or reduce) as the project moves from along, as well as the total overall cost per a set of individual activities (in this case OPC based concrete).

As previously discussed, the same analysis was completed using the costs of each RSHC (and blends) and added to the altered Gantt chart to produce a histogram and project S-curve. For the purpose of this analysis the same cost multiplier (2.7) from the pure cost analysis was used. Recall this cost does not equate to pure profit, it merely represents the difference between the cost of the materials in the mixture to what the mixture is sold, therefore the multiplier could vary depending on where it is sold, who it is sold to, and how it is placed and finished. For the sake of comparison, the 2.7 multiplier was used throughout the RSHC (and blends) based mixtures. Displaying a combined histogram of all mixtures, results in an illegible graph, therefore only a combined project S-curve is shown in Figure 12.6. Figure 12.7 shows a project S-curve for just the RSHCs for better visualization. The original histograms for each RSHC and blends can be seen in the accompanying excel file.
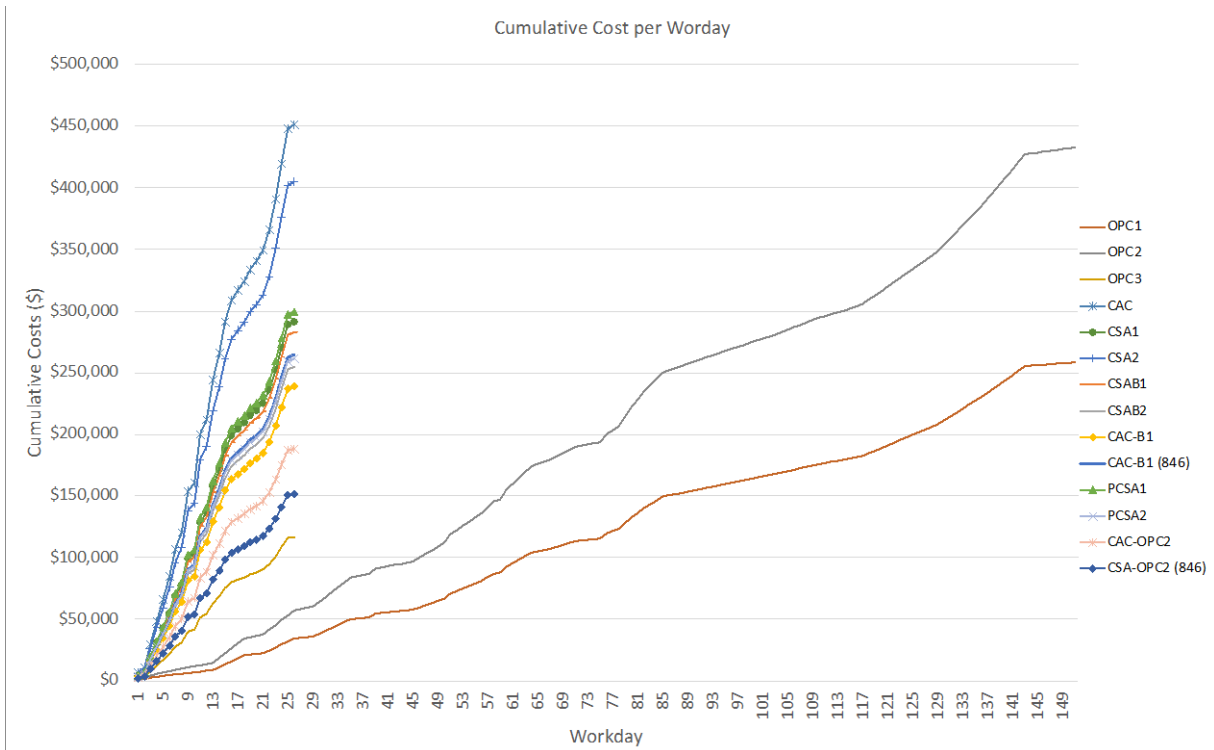
**Figure 12.6: Project S-curve for all cement systems.**
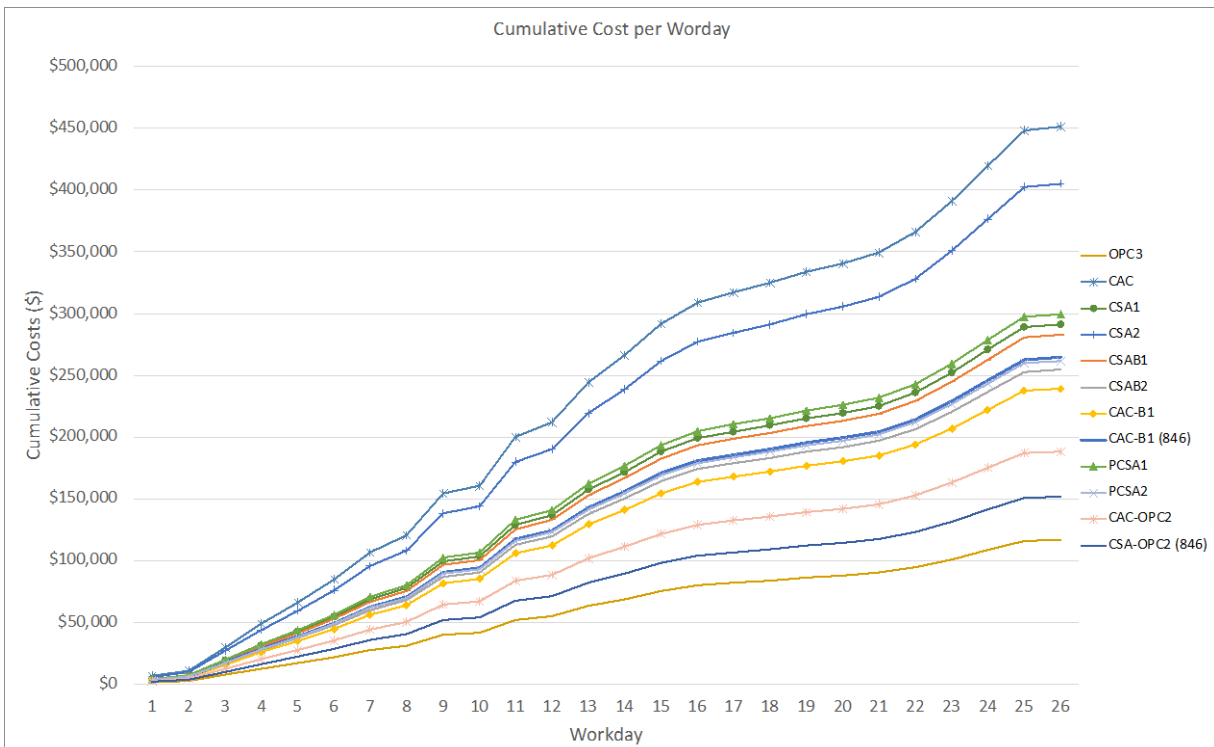
Figure 12.7: Project S-curve for just the RSHC (and blends) based concretes.

304

As seen in Figures 12.6 and 12.7 is a method to compare both cost and schedule considerations of using RSHCs as one can see the time reduction and the cost to obtain such a time reduction. Considering these two factors alone (and not concrete performance or longevity of the material), OPC3, which is a Type 3 cement is the top performing cement, as it costs the least while significantly reducing the schedule. However, if only considering a CAC/CSA/Blended cement system, the top performing cement system is the CSA-OPC2 (846), which is a laboratory blended cement of 75% OPC and 25% CSA (buzzi) using 846lb/yd^3 of cement. Therefore, this demonstrates that this type of analysis can be used to assess these types of concretes.

12.7 CONCLUSIONS

Through this analysis the three objective questions have been answered. The general cost comparison that only considers the costs between each material revealed a significant for using RSHC based concrete over OPC based concrete. The pure cost analysis also demonstrated the likelihood of a significant markup for these materials, which could easily vary due to many circumstances. However, the provided excel file can be used as a tool in future decision making, as it is easily editable.

The schedule analysis revealed that using RSHC based concrete instead of OPC based concrete in only cast-in-place concrete activities can have a significant decrease in the overall project duration. This is not considering the fact that the representative schedule used did not anticipate using RSHC based concretes, therefore, there is the possibility that using RSHC based concrete can further reduce the overall project duration if the scheduler knows this ahead of time.

Lastly, the cash-loaded analysis demonstrated a method to analysis both costs and project schedule. This analysis produces both a histogram of costs per workday and project S-curves that plot the cumulative costs over the entire duration of the project. By comparing all of the S-curves together, the impact on both cost and schedule are realized.

CHAPTER 13: CONCLUSIONS AND FUTURE RESEARCH VALUE NEEDS

13.1 CONCLUSIONS

Significant laboratory and field data were generated during the course of this project. Although some of the tests are ongoing and may require additional time to fully elucidate the behavior and performance of RSHC concretes, some general observations can be made at this time:

- Performing simple fresh and hardened property tests on RSHC mortars such as flow, slump flow, compressive strength, and shrinkage can provide meaningful information such as admixture requirements, characterizing short- and long-term strength development, and shrinkage potential. A robust mortar testing standard would help screen the potential of RSHC for structural applications. However, RSHC mortar behavior were particularly sensitive to changes in mixture proportions including cement to sand (C/S) ratio, and water to cement (W/C) ratio, and water reducer dosage to achieve suitable workability. These influences are not addressed in ASTM C1600 and requires future testing to determine appropriate proportion for comparison to concrete scale-structural class mixtures.

- The fresh and hardened performance of RSHC concretes were found to be comparable to that of ordinary portland cement mixtures in terms of workability and mechanical strength. While working time (i.e., setting) remained a challenge in some mixtures, short- and long-term strengths were suitable for structural class concrete in Texas. Additionally, the temperature sensitivity of RSHC concrete from high (38 °C) and low (10 °C) curing temperatures were not found to severely impact the short-and long-term strengths in this study.

- Practically all RSHC concretes exhibited higher carbonation depth than OPC based cements, and this was consistently observed across lab and field samples. Additionally, while laboratory samples showed higher carbonation with increasing CO_2 concentration, the carbonation rate did not slow significantly when exposed to a higher relative humidity (75%). On the other hand, field samples showed more sensitivity to the type of exposure conditions. Practically all samples exposed to sheltered natural carbonation (i.e., protected from precipitation) showed higher carbonation depth after 3 years compared to samples exposed to unsheltered natural carbonation. In fact, very little carbonation (if any) was observed in samples placed in unsheltered natural carbonation after 3 years indicating that there may not be a concern with concrete carbonation in particular environments.

- Laboratory specimens exposed to accelerated carbonation highlighted the impact of curing on carbonation ingress. Curing dramatically improved carbonation performance of RSHC concretes with a minimum 1-day cured recommended. The only exception to this was CSA1 which showed no improvement with extended curing time.

- The carbonation coefficients of the 24-hour and 7 days cured samples exposed to accelerated carbonation at CO_2 concentrations of 1% and 4%, and RH of 57% and 75% showed a strong correlation (R^2 values) to the carbonation coefficients due to sheltered natural exposure, especially when accelerated conditions were either at high CO_2 concentration (4%) or low RH (57%). The unsheltered natural carbonation coefficient showed a moderate correlation (R^2 values) to the carbonation coefficients of 24-hour and 7 days cured samples exposed to accelerated conditions. The strong correlation (R^2 values) between the carbonation coefficients due to the sheltered natural conditions and the accelerated conditions increases the transferability of the accelerated results to sheltered natural conditions.

- The results from the laboratory corrosion monitoring techniques employed in this study show low to moderate corrosion activity in the ASTM G109 corrosion samples up to 2 years of exposure. However, the CSA cements CSA1 and CSA2 appear to be showing a higher corrosion activity compared to other mixtures due to low chloride binding capacity. More time is needed to elucidate the corrosion behavior of outdoor field specimens.

- Based on an assumed chloride threshold of 0.05 %, the chloride penetration of PCSA2, PCSA1, CAC-B1, CAC-OPC2, OPC3, CAC, and CSA1-PCSA2 was 19 mm, 21 mm, 22mm, 26 mm, 27 mm, 27 mm, and 30 mm, respectively. Whereas CSA2, CSA-B1, CSA-B2, CSA1, and OPC2 showed higher chloride content beyond the assumed 0.05% threshold in the total depth assessed during grinding. Also, the CSA cements (CSA2, CSA-B1, CSA-B2, CSA1) showed higher diffusion coefficients and surface concentrations than the other cements due to a low chloride binding capacity and low Friedel salt content. The CAC mixtures (CAC and CAC-B1) showed higher resistance to chloride penetration compared to the CSA mixtures (CSA2, CSA-B1, CSA-B2, and CSA1). This is attributed to the ability of CAC to bind chlorides compared to CSA cement. The lab-blended cements CAC-OPC and CSA1-OPC2 showed improved performance in resisting chloride ingress due to the presence of OPC compared to CAC and CSA1.

- The bulk electrical resistivity was not effective in ascertaining the chloride penetrability of the CSA-based cements (CSA1, CSA2, CSA-B1, and CSA-B2). However, the chloride penetrability of the other cements based on bulk electrical resistivity measurements was consistent with other test methods in this study.

- ASR performance testing varied significantly depending on the conditioning of the samples. For example, there was a clear impact on the addition of alkalis (i.e., boosted) to the expansion on the concrete system due to alkali silica reactivity. Mixtures evaluated in Series 3 with no additional alkalis showed the least expansion, with mixtures in Series 2 and 3 observing a dramatic increase in expansion The ASR testing highlight how current standardized test methods as performed do not suitably characterize ASR in RSHCs. While ATM C1260 seems to show consistency in performance, current ASTM methods for assessing ASR performance in RSHC concretes are not recommended. ACCT may be more appropriate tests for determining ASR performance but is more challenging and costly to implement.

13.2 RECOMMENDATION FOR FUTURE RESEARCH

Based on the findings to date from this project, the following recommendations are made for future research that is needed for the implementation of RSHC concrete in Texas bridge and highway structural applications:

- Research should continue to build a testing program focused on RSHC mortars that can help in screening the potential of an RSHC binder system for its use in structural application. In particular, flowability, working time, and characterizing strength development should be key factors that should be assessed.
- While the research presented in this study showed suitable engineering properties for structural class concrete can be achieved, more work is needed to characterize engineering properties using other aggregate types, sizes, and proportions.
- Continue to monitor laboratory and outdoor exposure site specimens cast and evaluated under this project including ASR, corrosion, and concrete carbonation tests. This is especially critical for field samples that have not yet exhibited expansion or degradation.
- More work is needed to understand the disconnect between permeability test methods (e.g., RCPT and resistivity) and chloride penetration results. Additionally, more work is needed to evaluate the ingress of chlorides in RSHC concrete, especially in the case of carbonated and cracked samples.
- More work is needed to understand alkali silica reactivity of RSHC concrete. In particular, the boosting of alkalis seems to have a negative and erratic impact on RSHC binder system do not seem to accurately reflect performance observed in field exposure blocks and the accelerated concrete cylinder test (AASHTO TP 142). Additionally, the blending of RSHC with OPC in the

lab further exacerbates this issue. More work is needed to understand blended systems (CSA or CAC with OPC).